AD Number	Date 5/3/2007	DTIC ACCESSION NOTICE
1. Report Identifying Information		
A. Originating Agency USAMRMC		
B. Report Title and/or Number HONG, LOTAN and STEWART		
C. Monitor Report Number ANNUAL (JAN 2007)		
D. Prepared Under Contract Number W81XWH-04-1-0142		
2. Distribution Statement DISTRIBUTION STATEMENT A Approved for public release; distribution unlimited		

SEND REPORT AS ATTACHMENT

AD_____

AWARD NUMBER: W81XWH-04-1-0142

TITLE: VITAL: Vanguard Investigations of Therapeutic Approaches to Lung Cancer

PRINCIPAL INVESTIGATOR: Waun Ki Hong, M.D.
Reuben Lotan, Ph.D.
David Stewart, M.D.

CONTRACTING ORGANIZATION: The University of Texas
M.D. Anderson Cancer Center
Houston, Texas 77030

REPORT DATE: January 2007

TYPE OF REPORT: Annual

PREPARED FOR: U.S. Army Medical Research and Materiel Command
Fort Detrick, Maryland 21702-5012

DISTRIBUTION STATEMENT: Approved for Public Release;
Distribution Unlimited

The views, opinions and/or findings contained in this report are those of the author(s) and should not be construed as an official Department of the Army position, policy or decision unless so designated by other documentation.

REPORT DOCUMENTATION PAGE

Form Approved
OMB No. 0704-0188

Public reporting burden for this collection of information is estimated to average 1 hour per response, including the time for reviewing instructions, searching existing data sources, gathering and maintaining the data needed, and completing and reviewing this collection of information. Send comments regarding this burden estimate or any other aspect of this collection of information, including suggestions for reducing this burden to Department of Defense, Washington Headquarters Services, Directorate for Information Operations and Reports (0704-0188), 1215 Jefferson Davis Highway, Suite 1204, Arlington, VA 22202-4302. Respondents should be aware that notwithstanding any other provision of law, no person shall be subject to any penalty for failing to comply with a collection of information if it does not display a currently valid OMB control number. **PLEASE DO NOT RETURN YOUR FORM TO THE ABOVE ADDRESS.**

1. REPORT DATE *(DD-MM-YYYY)*	2. REPORT TYPE	3. DATES COVERED *(From - To)*
01-01-2007	Annual	15 Dec 2005 – 14 Dec 2006

4. TITLE AND SUBTITLE

VITAL: Vanguard Investigations of Therapeutic Approaches to Lung Cancer

5a. CONTRACT NUMBER

5b. GRANT NUMBER
W81XWH-04-1-0142

5c. PROGRAM ELEMENT NUMBER

6. AUTHOR(S)

Waun Ki Hong, M.D., Reuben Lotan, Ph.D. and David Stewart, M.D.

E-Mail: Whong@mdanderson.org

5d. PROJECT NUMBER

5e. TASK NUMBER

5f. WORK UNIT NUMBER

7. PERFORMING ORGANIZATION NAME(S) AND ADDRESS(ES)

The University of Texas
M.D. Anderson Cancer Center
Houston, Texas 77030

8. PERFORMING ORGANIZATION REPORT NUMBER

9. SPONSORING / MONITORING AGENCY NAME(S) AND ADDRESS(ES)
U.S. Army Medical Research and Materiel Command
Fort Detrick, Maryland 21702-5012

10. SPONSOR/MONITOR'S ACRONYM(S)

11. SPONSOR/MONITOR'S REPORT NUMBER(S)

12. DISTRIBUTION / AVAILABILITY STATEMENT
Approved for Public Release; Distribution Unlimited

13. SUPPLEMENTARY NOTES
Original contains colored plates: ALL DTIC reproductions will be in black and white.

14. ABSTRACT

The VITAL Research Program will provide a better understanding of the cellular and molecular processes that drive lung tumorigenesis so that an accurate risk model for recurrence and/or the development of the second primary tumor can be developed, and the biologic agents most effect in reducing these events in the group of high-risk patients can be identified. Until this time,our clinical trails (Vanguard and Celecoxib trials) are ongoing and Tarceva trial will be opened in January 2007. The research projects are proceeding well as proposed, producing valuable findings with cell lines, and will validate these results using the clinical samples obtained from the VITAL trials in the coming years.

15. SUBJECT TERMS
lung cancer, risk model, cancer recurrence, clinical trials

16. SECURITY CLASSIFICATION OF:			17. LIMITATION OF ABSTRACT	18. NUMBER OF PAGES	19a. NAME OF RESPONSIBLE PERSON
a. REPORT	b. ABSTRACT	c. THIS PAGE			USAMRMC
U	U	U	UU	340	19b. TELEPHONE NUMBER *(include area code)*

TABLE OF CONTENTS

INTRODUCTION

Smoking-related cancers such as lung and head and neck cancers are a major cause of cancer death in the United States. About 25% of lung cancer patients are diagnosed with stage I or II disease and undergo surgery with curative intent, but the 5-year survival for the group of patients is only 30%-70%. Patients with a strong history of smoking and prior early-stage cancer are found to be at high risk for cancer recurrence or development of second primary tumors (SPTs). An effective adjuvant therapy after surgery in this group of patients is not well established yet. The survival benefit of adjuvant chemotherapy was uncertain until recent findings reported by Winton and colleagues (Winton et al., 2005). They found that adjuvant chemotherapy (vinorelbine and cisplatin) increases the 5-year survival of surgically resected non-small cell lung cancer (NSCLC) patients, resolving the debate over the benefit of adjuvant chemotherapy. Thus, better-designed clinical trials and basic research are needed to establish the standard of care for these patients after surgery.

The program VITAL (Vanguard Trial of Investigational Therapeutics in Adjuvant Treatment of Lung Cancer) developed in 2003 leads to this direction. It aims to develop a risk assessment model for cancer recurrence and development of smoking-related SPT based on the understanding of molecular events in pre-malignant tissues that underlie progression to malignancy in the high-risk population, and to identify effective preventive agents for this group of patients. Specifically, our objectives are

- To identify biologically-based treatments for prevention of cancer recurrence and development of second primary tumors in high-risk patients
- To understand molecular events in premalignant tissues that contribute to progression or malignancy
- To develop a risk prediction model for disease recurrence and development of second primary tumors in high-risk patients by combining clinical treatment outcomes with molecular and imaging data.

PROGRESS REPORT (BODY)

Project 1: Biologic Approaches for Adjuvant Treatment of Aerodigestive Tract Cancer

(PI and co-PIs: Drs. Waun Ki Hong, Edward S. Kim, Rodolfo C. Morice, David J. Stewart)

Aim 1 Assess the smoking-related disease-free survival in patients who are current or former smokers with a prior definitively-treated stage I/II lung or head and neck cancer.

The main objective was to open the Vanguard study at MDACC as well as the 2 other participating sites. A total of 300 patients with definitively treated stage I/II lung or head and neck cancer and at least a 20-pack-year smoking history will be enrolled in the trials. Enrolled patients will undergo baseline testing including chest x-ray, CT scan, labs, bronchoscopy, and other specimen collections (i.e., sputum, saliva, serologies). Bronchoscopies and specimen collection will be performed at baseline and at months 12, 24 and 36. White-light alone or white light and autofluorescence modalities will be used. Abnormal areas detected by bronchoscopy will also be biopsied. Histologic assessment will be performed to determine whether malignant changes will occur during the time period. If severe dysplasia, carcinoma in situ or carcinoma is discovered, patients will go for the plans outlined in the clinical protocol. Once patients have completed 3-years of testing, they will be followed for until the study is completed.

Update

In the past year, we have continued enrolling patients in the VITAL/Vanguard trials. A total of 34 patients have been enrolled in Vanguard trial. Patient clinical data and tissues have been and continue to be collected and will be distributed to investigators of VITAL research projects through the VITAL Pathology Core. (For details, please refer to the Pathology Core update, pg. 33.) The adjuvant Tarceva (erlotinib) protocol will be reviewed by our Clinical Research Committee (CRC) on January 23, 2007, and by our IRB on February 7, 2007. The protocol was forwarded to the DOD for simultaneous review on January 18, 2007. One patient is enrolled in the celecoxib trial.

Due to a change in the climate for treatment plans in which patients are followed more closely by their local medical oncologist, our patient accrual has been lower than expected. To enhance the patient accrual, we have taken several important actions in the last year. We conducted a review of the trial in our lung NCI program project which initially had similar difficulties to learn and adopt important measures which were successful in improving patient accrual. We have made several small but important modifications to this protocol that we expect to improve accrual with higher risk patients balanced with the ability to accrue sufficient numbers of patients to obtain statistical significance with this trial. These changes include lessening the number of follow-up visits to allow for the climate change for patients to be seen by their local oncologist, opening the trial to stage III patients, and decreasing the pack years required to 10. The higher risk stage III patients offset the decrease in pack years but allows for more patients to be eligible for these trials. In addition, we have increased the personnel, such as research nurses, entirely dedicated to just the trials in this program.

We have worked to increase the visibility for our program and clinical trials. We have distributed patient brochures and advertised the trials on the radio in order to enhance the awareness of the trials locally and on our website (www.mdanderson.org/lung) to increase awareness nationally and internationally to improve the patient accrual. For our lung NCI program project, these measures were successful in increasing accrual and expect to see similar increases for this program. The majority (462/683; 67.5%) of candidates came from these ads. We will be monitoring the success of these measures, which were developed this past year and just released last month, and adjusting as necessary to accomplish our goals.

In addition, we have invited the local Methodist Hospitalto participate in the VITAL/Vanguard trials which would increase our accrual of early stage lung, head and neck cancer patients. Dr. Shanda Blackmon would be the Surgery Principal Investigator and has expressed great interest in participating. Contract negotiations are currently underway.

Although the Vanguard trial was activated at the Eisenhower Medical Center, the patient accrual was very poor; we thus closed the trial at this Center. Conemaugh Memorial Medical Center had delayed activation pending several clarifications which were resolved via conference call. The revised protocol was resubmitted to their IRB and received their full approval on November 16, 2006. Currently, the DOD is reviewing the approved protocol and informed consent for implementation at Conemaugh. Upon the DOD approval, Conemaugh Memorial Medical Center will activate the study.

Aim 2 Evaluate effects of biologic agents as adjuvant therapy on the modulation of histology and specific biomarkers in this high-risk population.

Current adjuvant chemotherapy offers some benefits in the high-risk patients, but is not a long-term preventive strategy. We plan to open several biologic adjuvant clinical trials with novel

agents such as celecoxib, erlotinib, lonafarnib, and possibly others. Considerable preclinical data exist for these agents for cancer as well as normal or precancerous bronchial epithelium.

Update
The Vanguard study has been activated and is accruing patients as described above. The first biologic adjuvant trial using celebrex was opened on September 29, 2005, and 1 patient is enrolled. The second biologic adjuvant trial using erlotinib will be reviewed by our IRB the first week of February, as mentioned above. The pharmaceutical company, Genentech, has agreed to supply erlotinib for this study. The protocol is pending review (January 31, 2007) by the company. This aim will be completed at the end of the study period.

Aim 2 Evaluate effects of biologic agents as adjuvant therapy on the modulation of histology and specific biomarkers in this high-risk population.

Current adjuvant chemotherapy offers some benefits in the high-risk patients, but is not a long-term preventive strategy. We plan to open several biologic adjuvant clinical trials with novel agents such as celecoxib, erlotinib, lonafarnib, and possibly others. Considerable preclinical data exist for these agents for cancer as well as normal or precancerous bronchial epithelium.

Update
The Vanguard study has been activated and is accruing patients as described above. The first biologic adjuvant trial using celebrex was opened on September 29, 2005, and 1 patient is enrolled. The second biologic adjuvant trial using erlotinib will be reviewed by our IRB the first week of February, as mentioned above. The pharmaceutical company, Genentech, has agreed to supply erlotinib for this study. This aim will be completed at the end of the study period.

Aim 3 Develop a lung cancer risk model to help predict the likelihood of development utilizing imaging and biologically-based information in this high-risk population.

Patients with a history of smoking and a prior surgically resected stage I/II head and neck or lung cancer are at high risk for cancer recurrence or SPTs. There are no standard interventions, which have been proven to help reduce the risk of cancer occurrence. A Gail risk model implemented in the initial management of breast cancer screening has proven useful and has helped with early detection and more stringent follow-up in the higher risk cohorts. Patients enrolled in the Vanguard trial will have aggressive post-operative follow-up with analysis including frequent serologies, bronchial specimens and CT scanning. Trends in these multiple biomarkers would be analyzed and used to develop a predictive model. Establishing a risk model will eventually help identify patients who may be at higher risk for lung cancer development and promote earlier interventions for prevention.

Update
This aim will be completed at the end of the study period.

Key Research Accomplishments

- 36 patients were enrolled in Vanguard trial.
- Patient clinical data and tissues have been and continue to be collected and will be distributed to support research projects in the VITAL grant.
- The adjuvant celecoxib trial is open and has enrolled 1 patient.

- The adjuvant erlotinib protocol was submitted to our IRB and the DOD for review.
- New recruitment strategies have been implemented to increase patient accrual, including protocol changes, distributing patient brochures, actively contacting potential patients, advertising the trials on our website (www.mdanderson.org/lung) and local radio, and negotiating the addition of Methodist Hospital.

Conclusions
The completion of the VITAL/Vanguard trials is the key to this grant. We have implemented a number of actions that we expect to increase the accrual and ensure the high quality of clinical data and patient samples to be collected and distributed to the research investigators in the VITAL program. This is a top priority for our program.

Project 2: Identification of Biomarkers of Response to Chemoprevention Agents in Lung Epithelium

(PI and co-PIs: Li Mao, M.D., Reuben Lotan, Ph.D., John Minna, M.D.)

We proposed to use genomic and proteomic analysis to identify changes in gene expression and proteins which correlate/associate with cancer risk in the carcinogen damaged aerodigestive tract field and also use these signatures to monitor the response of this field to chemoprevention. We will determine modifications of these changes by chemopreventive agents in premalignant cells *in vitro* and to use probes for the modified genes and proteins to analyze tissue specimens from individuals participating in the chemoprevention clinical trials.

Aim 1 Develop immortalized human bronchial epithelial cell cultures using a subset of patient tissue specimens collected in Project 1 and characterize the expression profiles of these cells using oligonucleotide based microarrays.

The main goal of this aim of this project is to establish these cultures from the patients entered onto the clinical trial described in Project 1 and to characterize their gene expression profiles.

Update
This year, we continued our efforts to develop additional immortalized human bronchial cell strains (HBECs), and have made considerable progress in generating immortalized HBECs from now 36 different individuals that were collected on various tissue procurement protocols at The University of Texas Southwestern and at M. D. Anderson Cancer Center as summarized in Table 1. These represent males, females, a spectrum of smoking status, as well as persons with and without lung

Table 1. Summary of all Immortalized Human Bronchial Epithelial Cell (HBEC) Strains Started from Patient Specimens

Total Number of HBEC Lines	**36**
Female	21
Male	15
Smokers	9
Ex-smokers	15
Non-smokers	4
Smoking Status TBD	8
<50 years old	3
50-60 years old	8
60-70 years old	11
>70 years old	9
Age TBD	5
Lung Cancer	20
Other cancer	5
No cancer	4
Cancer Status TBD	7
E/KT pairs*	19
HBEC/Tumor pairs**	2

* same bronchial epithleial cells immortalized with hTERT and cdk4 or with oncogenic HPV E6, E7
** HBEC line made along with companion lung cancer cell line from the same patient.

cancer. We have also immortalized 15 of these same bronchial epithelial specimens with oncogenic HPV E6 and E7. Finally, we have made two pairs of immortalized HBECs and lung cancer cell lines from the same patient. We have performed Affymetrix gene expression profiles on these HBECs and representative results are presented in Project 2, Aim 3 below.

Aim 2 Characterize effects of the chemopreventive agents used in Project 1 on cell proliferation and apoptosis in the immortalized human bronchial epithelial cell cultures developed in Specific Aim 1.

We will determine the potential role of different chemopreventive agents [e.g., celecoxib, N-[4-hydroxyphenyl]retinamide (4-HPR), Iressa (gefitinib), and SCH63663] alone or in combination with one another for their effects on cell proliferation and apoptosis in cell cultures established in Aim 1. We will also determine the relative sensitivity among the various cell cultures to each of the agents by determining the 50% growth inhibitory concentration (IC_{50}). Results from this Specific Aim will be the basis to identify molecular signatures proposed in Specific Aim 3.

Update

We have analyzed the effects of several agents on the growth of premalignant human bronchial epithelial cells most of which have been developed in Aim 1. Figure 1 shows the dose response curves for the inhibition of the immortalized HBE cell series by Iressa, 4HPR, celecoxib and SCH66336. The responses of the different cell lines varied by as much as several fold with respect to the IC_{50} concentration. The same cell line could be more sensitive to one agent and less sensitive to another relative to the other cell lines perhaps reflecting the different mechanism of action of the different agents and the intrinsic properties of the cell lines.

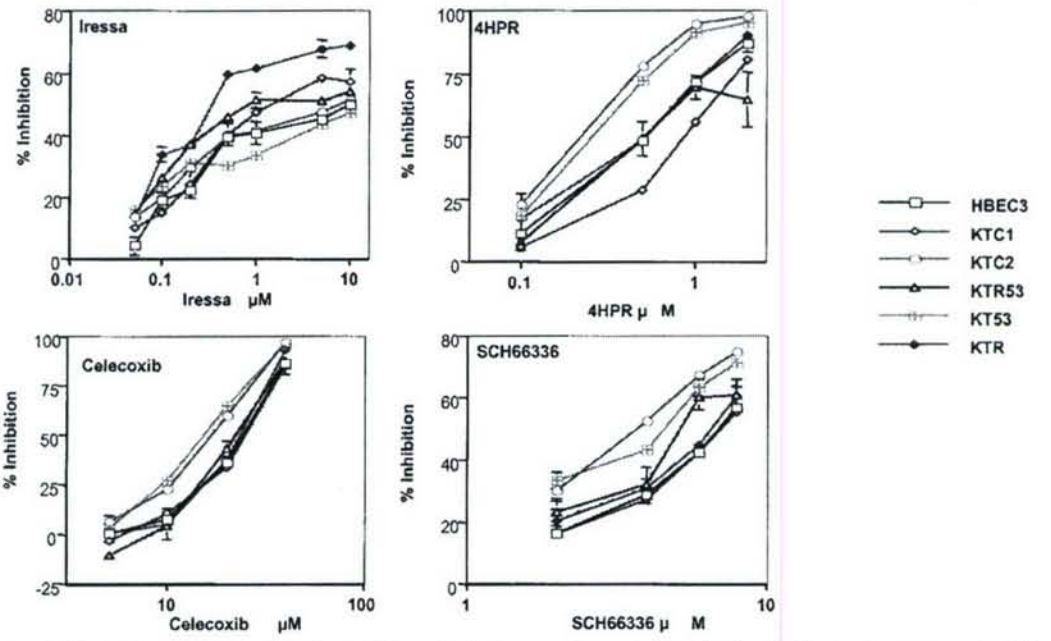

Figure 1. HBE cells were cultured on 96-well plates and treated with the indicated agents at different concentrations. After 3 days, the cell numbers in triplicate wells were estimated using the sulforhodamine B assay and % of growth inhibition was calculated by comparing the optical density of treated cultures to control cultures. The data are presented as the mean ± SD.

Further studies were performed with 13 HBE cell lines using the EGFR inhibitor Tarceva (Figure 2). This inhibitor was as effective in inhibiting the tumorigenic 1170-I cells as it was in inhibiting the less progressed cell lines of the BEAS-2B family including the immortalized 1799 and the transformed 1198. Since the 1170-I and the 1198 cell lines were reported to express more EGFR than 1799 and BEAS-2B, it follows that the sensitivity to Tarceva among these cell lines is not affected by the difference in receptor expression as had been reported in human lung cancer cell lines by others. The results of inhibition of the HBEC cell series indicate that whereas Tarceva inhibited all cell lines, the degree of inhibition was lowest for the KT53 cell line (no more than 45% inhibition at any dose compared to 60-80% for some others).

Figure 2. The indicated cell lines were cultured in wells of a 96-well plate and treated in triplicates with control medium or the indicated concentrations of Tarceva. The treatments were terminated after 1, 2, or 3 days and cell numbers at these times were estimated using the sulforhodamine B assay. % Growth inhibition was calculated from the absorbencies of treated cultures relative to untreated controls. The data are presented as the mean ± SD.

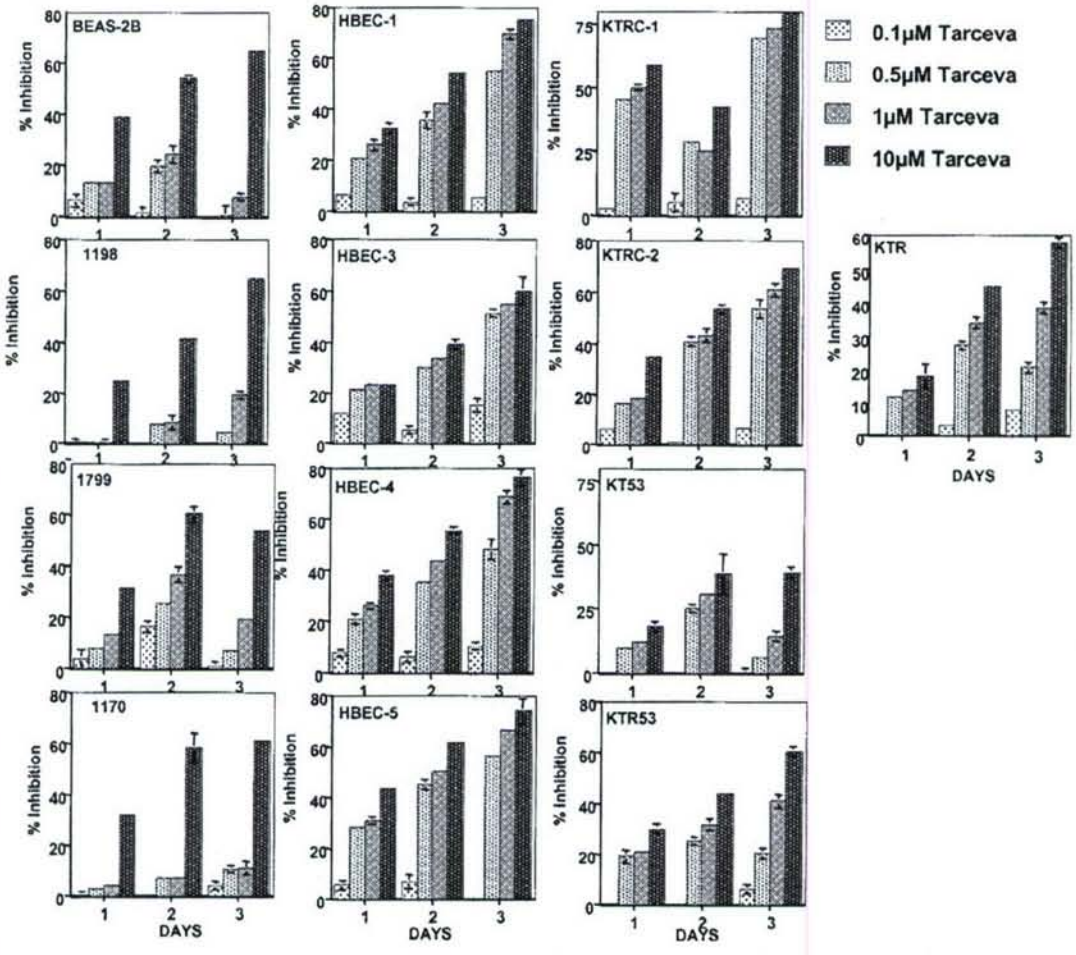

Aim 3 Identify gene expression and protein "signatures" which reflect lung tumorigenesis and sensitivity or resistance to chemopreventive regimens proposed in Project 1, and to validate the signatures and to determine their biological importance in precancer cell models of lung cancer.

Update

1) Detection of genes upregulated or downregulated by insertion of oncogenic changes into HBECs

As described in prior reports, we have generated HBECs oncogenically manipulated to contain oncogenic $KRAS^{V12}$, stable knockdown (by shRNA) of p53 or the combination of these two changes. In addition, we have made multiple other oncogenic changes (e.g. mutant EGFR, CMYC, BCL2, PTEN knockdown). The expression profiles for these HBEC lines with preneoplastic changes have been determined using Affymetrix U133 2 plus arrays as well as using quantitative RT PCR for selected genes. We have identified a series of genes specifically upregulated or downregulated in these manipulated HBECs (see Tables 2 and 3 for genes upregulated or down regulated by the combination of $KRAS^{V12}$ and p53 knockdown). These gene expression changes will be some of those used to analyze preneoplastic specimens from patients.

Table 2. Genes upregulated >4 fold by KRASV12 and p53 knockdown in HBECs

Symbol	Gene	Log_2
DNAJB9	DnaJ (Hsp40) homolog, subfamily B, member 9	3.24
AGR2	anterior gradient 2 homolog (Xenopus laevis)	3.21
LCN2	lipocalin 2 (oncogene 24p3)	3.09
GDF15	growth differentiation factor 15	2.97
TSLP	thymic stromal lymphopoietin	2.62
HERPUD1	homocysteine-inducible, endoplasmic reticulum stress-inducible, ubiquitin-like domain member 1	2.61
TRIB3	tribbles homolog 3 (Drosophila)	2.59
UPP1	uridine phosphorylase 1	2.54
ARRDC3	arrestin domain containing 3	2.48
HSD11B1	hydroxysteroid (11-beta) dehydrogenase 1	2.34
CTGF	connective tissue growth factor	2.27
IL1RL1	interleukin 1 receptor-like 1	2.26
P8	p8 protein (candidate of metastasis 1)	2.25
TACSTD1	tumor-associated calcium signal transducer 1	2.24
DTR	diphtheria toxin receptor (heparin-binding epidermal growth factor-like growth factor)	2.24
STC2	stanniocalcin 2	2.22
DAF	decay accelerating factor for complement (CD55, Cromer blood group system)	2.21
SLITRK6	SLIT and NTRK-like family, member 6	2.15
RDH-E2	retinal short chain dehydrogenase reductase	2.14
SDF2L1	stromal cell-derived factor 2-like 1	2.12
PMAIP1	phorbol-12-myristate-13-acetate-induced protein 1	2.11
PRG1	proteoglycan 1, secretory granule	2.07
ABCG1	ATP-binding cassette, sub-family G (WHITE), member 1	2.06
BEX2	brain expressed X-linked 2	2.03
CCNA1	cyclin A1	2.01

Table 3. Genes downregulated >4 fold by KRASV12 and p53 knockdown in HBECs

Symbol	Gene	Log_2
ANGPTL4	angiopoietin-like 4	-3.03
TXNIP	thioredoxin interacting protein	-2.91
ARRDC4	arrestin domain containing 4	-2.91
GSTM3	glutathione S-transferase M3 (brain)	-2.63
ODZ2	odz, odd Oz/ten-m homolog 2 (Drosophila)	-2.45
IGFBP3	insulin-like growth factor binding protein 3	-2.42
CHST2	carbohydrate (N-acetylglucosamine-6-O) sulfotransferase 2	-2.32
PI3	protease inhibitor 3, skin-derived (SKALP)	-2.30
MCM6	MCM6 minichromosome maintenance deficient 6 (MIS5 homolog, S. pombe) (S. cerevisiae)	-2.28
UHRF1	ubiquitin-like, containing PHD and RING finger domains, 1	-2.24
MAGEE1	melanoma antigen, family E, 1	-2.09
KCNJ15	potassium inwardly-rectifying channel, subfamily J, member 15	-2.05
MCM5	MCM5 minichromosome maintenance deficient 5, cell division cycle 46 (S. cerevisiae)	-2.04
SERPINB3	serine (or cysteine) proteinase inhibitor, clade B (ovalbumin), member 3	-2.00
ZNF367	zinc finger protein 367	-2.00

2) Oncogenic manipulation and biologic selection for complete tumorigenic transformation of immortalized normal human bronchial epithelial cells

As reported previously, to develop an *in vitro* model system to study the multi-step pathogenesis of lung cancer, we established a series of cdk4/hTERT-immortalized human bronchial epithelial cell lines (HBECs) which can be genetically manipulatedthat are able to differentiate into mature airway cells in organotypic cultures, but do not form colonies in soft agar or tumors in nude mice (Vaughan et al., 2006). We observed that combinations of p53 knockdown with mutant EGFR or with physiological levels of oncogenic $KRAS^{V12}$ in our HBECs showed partial progression towards malignancy. These cells formed colonies in soft agar, but failed to form tumors in nude mice. The detailed findings have been published in *Cancer Research* (Sato et al., 2006) as attached in the Appendix 2.

3) Oncogenic manipulation and biologic selection for complete tumorigenic transformation of immortalized normal human bronchial epithelial cells

As reported previously, to develop an *in vitro* model system to study the multi-step pathogenesis of lung cancer, we established a series of cdk4/hTERT-immortalized human bronchial epithelial cell lines (HBECs) which can be genetically manipulatedthat are able to differentiate into mature airway cells in organotypic cultures, but do not form colonies in soft agar or tumors in nude mice (Vaughan et al., 2006). We observed that combinations of p53 knockdown with mutant EGFR or with physiological levels of oncogenic $KRAS^{V12}$ in our HBECs showed partial progression towards malignancy. These cells formed colonies in soft agar, but failed to form tumors in nude mice. The detailed findings have been published in *Cancer Research* (Sato et al., 2006) as attached in the Appendix 2.

In the present study, we evaluated various combinations of oncogenic manipulation, higher levels of expression of oncogenic KRASV12, and the biologic behavior of clones selected to grow to large size in soft agar. We found that without oncogenic manipulation, soft agar colony forming efficiency (CFE) was approximately ≤ 0.1%; With various oncogenic manipulations, including higher expression of KRAS ^{V12} alone, soft agar colony CFEs were approximately 3%, and the combination of higher KRAS ^{V12} and p53 knockdown increased CFE to 8%. None of these changes were tumorigenic. However, the combination of higher KRAS ^{V12} and p53 knockdown but not high KRAS ^{V12} alone led to development of a subset of very large soft agar colonies (0.1-0.2%). These large colonies were isolated and found to have CFE of 10 -15% with large colony numbers increased 10-fold. Five of the large colonies were expanded and tested for tumorigenicity and 2 were capable of forming subcutaneous and orthotopic (bronchus) tumors. Of interest, one was an adenocarcinoma and the other was a squamous cell carcinoma. In addition, the adenocarcinoma expressed high levels of KRAS ^{V12} but the squamous carcinoma expressed normal levels of KRAS ^{V12}. Thus, we conclude that multiple oncogenic changes found in lung cancer (telomerase expression, p16 bypass, p53 ablation, mutant EGFR, oncogenic KRAS) introduced into HBECs are still not capable of full oncogenic transformation. However, a subset of cells selected for the ability to form large colonies in soft agar is capable of tumor formation and tend to differentiate into two non-small cell lung cancer phenotypes (adenocarcinoma and squamous cell cancer). An abstract of the results was presented in the 2006 AACR meeting (Sato et al., 2006 AACR).

The expression, genetic, and epigenetic changes as well as the stem cell like characteristics of these subsets of cells are being investigated to delineate the key final steps in lung cancer pathogenesis.

4) Detecting low-abundant proteins in human plasma proteome by using multi-lectin affinity chromatography and two-dimensional gel electrophoresis

One of initiatives in this Aim is the identification of protein signatures in plasma, which would be used as effective surrogate markers for lung tumorigenesis and sensitivity or resistance to chemopreventive regimens.

Glycosylation is one of the most common post-translational protein modifications and plays a fundamental role in a diverse set of biologic processes. Plasma glycoproteins can be enriched using lectins, which bind to specific sugar structures. To determine the utility of a multi-lectin column, we analyzed two independent sets of plasma samples, each consisting of 400μl mixture of plasma from five healthy controls. Captured proteins in the column were released sequentially using inhibitory carbohydrates and collected stepwise. The total glycoprotein bound to the column was 10.9% of total plasma proteins including 2.3% to jacalin, 3.7% to conconavalin A (ConA), and 4.9% to wheat germ agglutin (WGA). Therefore, this column provides 20-44 folds enrichment of plasma glycoproteins in each fractionation. We further performed two-dimensional gel electrophoresis (2-DE) and generated reproducible profiles of enriched plasma glycoproteins. Several major plasma proteins, such as albumin, transferrin, immunoglobulin G, and α1-antitrypsin, were largely removed by the enrichment strategy. In the areas of high molecular weight proteins on the 2-DE gels, substantially more protein spots were visible in the sample with enrichment than its un-enriched counterpart (289 spots vs. 117 for WGA fractionation as an example). Our results demonstrate that the multi-lectin affinity–2-DE approach can help visualize lower-abundant plasma proteins and may improve the identification of plasma protein markers. This strategy has potential to be used to identify plasma protein markers associated with cancer. An abstract was presented in the 2006 AACR Meeting (Kawaguchi et al., 2006 AACR).

5) Identification of proteins associated with lung cancer progression using the novel protein enrichment strategy

As we reported last year, we have developed a novel 2-DE-based strategy to enrich moderately abundant and low-abundance proteins. The strategy takes advantage of the specific binding capability of certain chemicals or ions (baits) to specific protein structures to pull down a subset of cellular proteins and their binding partners before 2-DE analysis. Using this strategy, we are able to achieve enrichment of total cellular proteins by as much as 100-fold in each selection and specifically allow to determine the potential functions of the proteins.

In this grant period, we used MS-MS to analyze sequence properties of 65 protein spots differentially presented on the 2-DE gels between the immortalized HBE cells established in Aim 1 and NSCLC cell lines using the enrichment strategy. Many of the proteins were expressed at moderate or low abundant levels in these samples, validating our previous claim that the strategy will allow identification of low abundant cellular proteins in the 2-DE based assays. It is an important improvement because the identification of this class of proteins has been a major bottleneck in identifying relevant protein markers using the proteomics approach. Among the proteins, we identified that CDK4 is highly expressed in all but 1 of 5 immortalized HBE cell lines as expected, but not expressed in any of the NSCLC cell lines tested. This difference in expression may be due the fact that most NSCLC cell lines are defective in p16 and do not require CDK4 for immortalization. A previous study has demonstrated that the normal bronchial epithelial cells can become immortalized only when both hTERT and CDK4 are activated. The immortalized HBE line not expressing CDK4 might provide a tool to determine an alternative mechanism by which the cell line maintains its immortality without activation of CDK4. An abstract was presented in the 2006 AACR meeting (Ren et al., 2006 AACR).

Aim 4 Develop techniques to assess these molecular signatures in tissue specimens and serum obtained in Project 1, and assess the relevance of these molecular signatures as *in vivo* biomarkers using baseline and post-treatment specimens.

Update

We have collected bronchial brush specimens from all the participants of VITAL trial in Project 1. These specimens will be used for biomarker analyses. Also, we have developed qRT-PCR assays for a series of genes relevant to lung cancer pathogenesis and used these to profile various HBEC cells. One set of these genes of particular interest is the set with the stem cell proliferation signature. We have found significant differences in the expression of these genes in a panel of HBECs isogenic with each other except for oncogenic manipulation (Figure 3).

Key Research Accomplishments

- Established additional immortalized human bronchial epithelial cell (HBEC) strains from multiple donors
- Genetically manipulated the HBECs to derive isogenic strains that expressed oncogenic KRAS, mutant EGFR, and/or loss of p53 expression as well as HBECs with various EGFR tyrosine kinase domain mutations alone or with p53 knockout, and characterized their biologic and gene expression behavior showing they had partial progression towards malignancy
- Identified gene expression signatures associated with the introduction of oncogenic changes into the HBEC cells
- Determined IC_{50}s for Tarceva on all 13 HBE cell lines

- Demonstrated progression of oncogenically manipulated HBECs to full malignancy after biologic selection in soft agar
- Determined protein profiles related to lung tumorigenesis using immobilized metal ion adsorption chromatography
- Detected low-abundant proteins in human plasma proteome by using multi-lectin affinity chromatography and two-dimensional gel electrophoresis

Conclusion and Future Work

We can conclude that clonal selection of some cells with the combination of higher levels of $KRAS^{V12}$ and p53 knockdown are capable of full progression to tumorigenesis whereas others were not. The identification of the differential factors involved is important. Methods have been developed for the identification of protein profiles, including proteins of low abundance that are related to lung cancer tumorigenesis and will be used with patient samples to identify key protein signatures. In the next year, we will also continue to establish new immortalized HBEC cultures when patient samples become available from the VITAL trials and test new chemoprevention agents on the HBECs with and without oncogenic manipulation.

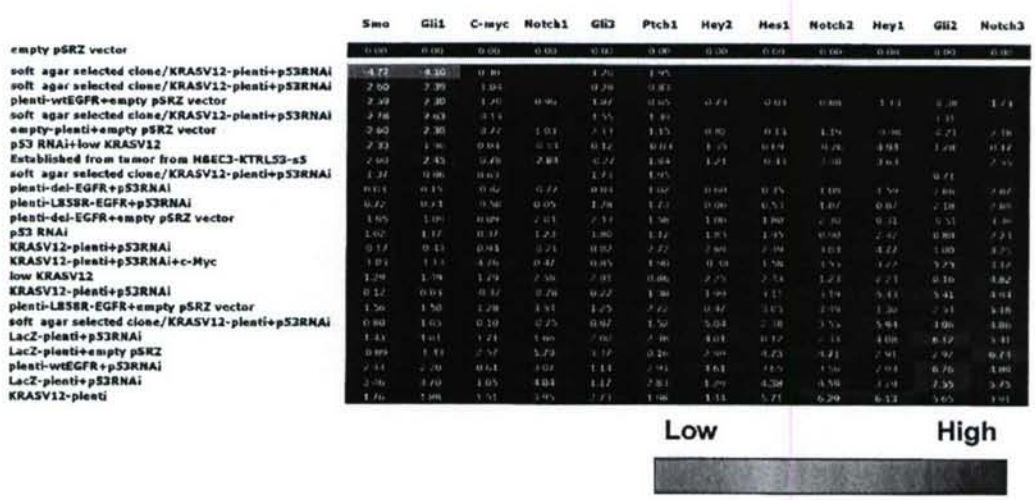

Figure 3: Isogenic HBECs with various oncogenic manipulations vary in their expression (qRT-PCR) of stem cell proliferation signature genes. Vector control is set to 1 (black or dark) and the changes in gene expression are made relative to this (green down regulated, red upregulated). We now have a panel of 25 stem cell proliferation genes, 12 of which are shown here. (Collaboration with Neil Watkins at Johns Hopkins Cancer Center).

Project 3: Premalignant Bronchial Epithelia: Molecular and Cellular Characterization of Lung Tumorigenesis

(PI and co-PIs: Walter Hittelman, Ph.D., Ja Seok Koo, Ph.D., Rodolfo C. Morice, M.D.)

Aim 1 Identify and characterize differentially expressed genes in the LIFE bronchoscopy-identified abnormal areas of the bronchial epithelia of of enrolled subjects in VITAL trials.

Previous studies have shown that bronchial regions that appear abnormal by LIFE bronchoscopy show increased genetic changes when compared to normal appearing sites,

even if there are no differences in histological appearance. Since LIFE-positive lesions are at increased risk for cancer development, especially when they contain particular genetic alterations, we hypothesize that these LIFE-positive sites represent lesions at an early stage of tumorigenesis and may differentially express genes important for driving tumorigenesis. Thus, comparative gene expression analyses between LIFE-positive and LIFE-negative sites within the same individual may provide a filter for identifying genes whose levels of expression are important for driving tumorigenesis.

Update

1) LIFE Bronchoscopy

Since the autofluorescence bronchoscopy system became available on Aug 16, 2005, collection of Vanguard samples guided by light-induced fluorescence endoscopy (LIFE) technology has been possible. Our initial plan was to obtain 30 bronchial brush and 30 biopsy specimens from 10 subjects entered onto the VITAL trial. Each subject was to undergo white-light and LIFE bronchoscopy and three biopsies and three bronchial brushings would be obtained, one from a light normal/LIFE normal region, one from a light normal/LIFE abnormal lesion, and one from light abnormal/LIFE abnormal region.

The case information we obtained so far is listed in Table 4. Among them, 7 cases matched our eligibility criteria and the samples of both biopsy and bronchial brushing from each of them have been collected (Table 4).

Table 4: Status of specimen collection (Wn, white light normal; Wab, white light abnormal; Ln, LIFE normal; Lab, LIFE abnormal

Case No.	Date	MDA#	Sample ID
1	1/18/2006	651359	not match criteria
2	2/16/2006	646661	K1-Wn/Ln K1-Wab/Lab
3	3/2/2006	625985	not match criteria
4	3/14/2006	662005	K2-Wn/Ln K2-Wab/Lab
5	3/24/2006	662690	not match criteria
6	4/18/2006	662601	not match criteria
7	5/1/2006	642687	not match criteria
8	5/2/2006	664477	not match criteria
9	6/14/2006	672121	K3-Wn/Ln K3-Wn/Lab K3-Wab/Lab
10	6/27/2006	662526	not match criteria
11	6/29/2006	662306	not match criteria
12	7/13/2006	631954	K4-Wn/Ln K4-Wn/Lab
13	7/19/2006	635849	not match criteria
14	7/19/2006	648151	K5-Wn/Ln (RML) K5-Wab/Lab (RML) K5-Wab/Lab (RUL) K5-Wab/Lab (LUL) K5-Wab/Lab (MC)
15	7/25/2006	638463	not match criteria
16	9/13/2006	318113	not match criteria
17	10/10/2006	644050	not match criteria
18	10/13/2006	667484	K6-Wn/Ln K6-Wab/Lab
19	10/25/2006	686663	not match criteria
20	10/31/2006	519391	K7-Wn/Ln K7-Wab/Lab

The biopsies collected were cultured to get the primary tracheobronchial epithelial cells. Cell lysis, RNA, secretion, cytospin slides and paraffin-embedded histology blocks have been collected at day 15 and day 22 after culturing cells, respectively. The cells from the brushes were used to extract RNA for further microarray analysis. Table 5 lists the cell number and the RNA quality and quantity we obtained from these samples.

Table 5. Status of the isolation of epithelial cells from biopsy and brush specimens.

Sample ID	Cell number (Yield)	RNA quality	RNA quantity (μg)	Gene Expression Profiling
K1-Wn/Ln	250x10^4	good	3396.9	Completed
K1-Wab/Lab	200x10^4	good	1822.5	Completed
K2-Wn/Ln	400x10^4	good	2130	ongoing
K2-Wab/Lab	400x10^4	good	2700	ongoing
K3-Wn/Ln	120x10^4	good	3614.4	ongoing
K3-Wn/Lab	120x10^4	good	2913	ongoing
K3-Wab/Lab	760x10^5	good	2730	ongoing
K4-Wn/Ln	440x10^4	good	5516.4	ongoing
K4-Wn/Lab	480x10^4	good	4343.7	ongoing
K5-Wn/Ln (RML)	280x10^4	poor		
K5-Wab/Lab (RML)	640x10^4	poor		
K5-Wab/Lab (RUL)	200x10^4	N.D.		
K5-Wab/Lab (LUL)	280x10^4	N.D.		
K5-Wab/Lab (MC)	280x10^4	N.D.		
K6-Wn/Ln	920x10^4	good	5250	
K6-Wab/Lab	920x10^4	poor		
K7-Wn/Ln		good	2180	ongoing
K7-Wab/Lab		good	3384	ongoing

2) Reconstruction of bronchial epithelium *in vitro* using the VITAL biopsies.

Using an organotypic, air-liquid interface (ALI) culture method (ad described in more detail under Aim 2 below), we successfully reconstructed bronchial epithelium using bronchial epithelial cells isolated from biopsies of LIFE normal and LIFE abnormal. Briefly, tissue specimens containing bronchial epithelium were plated onto 60 mm dishes with BEGM media (Clonetics, San Diego, CA) containing insulin (5 μg/ml), hydrocortisone (0.072 μg/ ml), transferrin (10 μg/ml), epinephrine (0.5 μg/ml), triiodothyronine (6.5 ng/ml), epidermal growth factor (0.5 ng/ml), bovine pituitary extract (1% v/v), gentamicin (50 μg/ml), amphotericin B (50 ng/ml), and retinoic acid (5×10^{-8} M). Epithelial cells were harvested by enzymatic detachment and seeded onto the porous membrane filter of the Transwell-clear (Corning) 6 well plates. An ALI was created on day 7. The cultures were maintained in the above media for total 15 and 22 days. Cell lysis, RNA, secretion, cytospin slides and paraffin-embedded histology blocks have been collected at day 15 and day 22 cultured cells separately. Cell lysis, RNA, secretion, cytospin slides and paraffin-embedded histology blocks have been collected at day 15 and day 22 cultured cells separately.

3) Global gene expression analysis using microarray.

According to previous report (Spira, A et al. 2004), bronchial brushings yielded 90% epithelial cells, as determined by cytokeratin staining, with the majority being ciliated cells. To identify genes differentially expressed in LIFE abnormal versus LIFE normal bronchial epithelial cells, we extracted RNA from brushing and compared global gene expression profiles using Agilent oligonucleotide array Genechip that represents 40,000 human genes. Currently, we have completed the microarray analysis for K1 samples (see Table 4) and the others are in progress.

We found 2588 over-expressed genes and 3384 down-expressed genes with statistical significance in K1 LIFE abnormal brushings compared with K1 LIFE normal brushings. These deregulated genes are demonstrated to be involved in many pathways by KEGG pathway analysis (Kanehisa, 1997). We are especially interested in MAPK signaling pathway and cytokine-cytokine receptors interaction, and we are validating the expression of several genes using cultured bronchial epithelial cells isolated from VITAL biopsies.

To globally evaluate how close our organotypically cultured bronchial epithelial cells originated from biopsies of LIFE normal and LIFE abnormal bronchial epithelium reflects the expression profile of bronchial epithelial cells *in vivo*, we performed microarray using cultured epithelial cells and determined the overall gene expression pattern of brush samples. The results were compared. Gene expression levels were ranked in each microarray and the rank was plotted for every gene. Correlation coefficients were calculated. The results (Figure 4) show a good correlation between the gene expression pattern of brush sample and biopsy culture. Importantly, the culture did not induce any significant changes in gene expression as indicated by the few dots distributed in the upper left corner of the plot. It also indicates that cultured sample is from a more homogeneous population of cells as compared with brush sample.

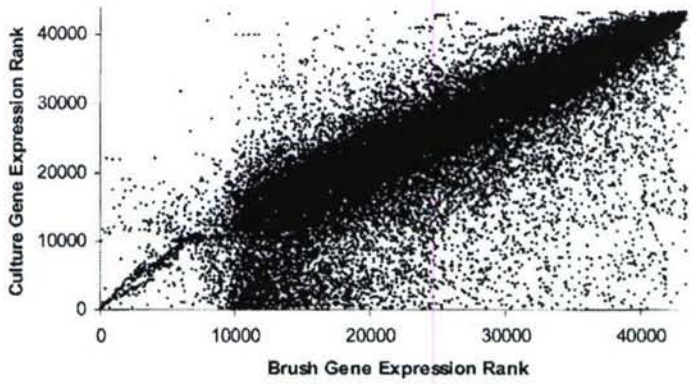

a. Normal brushing vs. normal culture cells (r= 0.874)

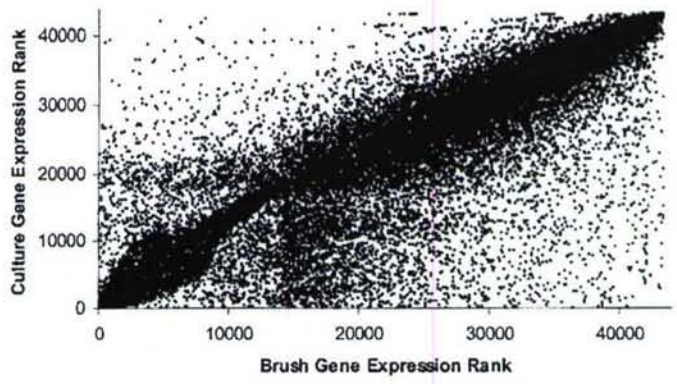

b. Abnormal brushing vs. abnormal culture cells (r= 0.859)

Figure 4. Correlation between brushing and biopsy cultured cells in gene expression pattern

4) Invasion analysis of LIFE normal and LIFE abnormal bronchial epithelial cells.
To investigate if LIFE abnormal cells have higher invasive tendency than LIFE normal cells, invasion assay was performed using cultured epithelial cells from three cases. Briefly, Transwell chambers (BD Biosciences, CA) were coated with 0.1% gelatin (or with matrigel, for comparison) and plated with VITAL cells (5×10^4) were plated. Following incubation (24-48 hrs) and fixation of the cells, noninvasive cells on the upper surface of the filter were removed, and the cells that had invaded onto the filter were quantitated using Image J (NIH program). Figure 5 shows the representative images of the invasive cells and the quantitative results. The assay was also performed using Transwell chambers coated with matrigel with the same outcome. These early results suggest that LIFE abnormal cells are more aggressive than LIFE normal cells. The genes related to the higher malignant characteristic of the cells identified through microarray analysis are being studied.

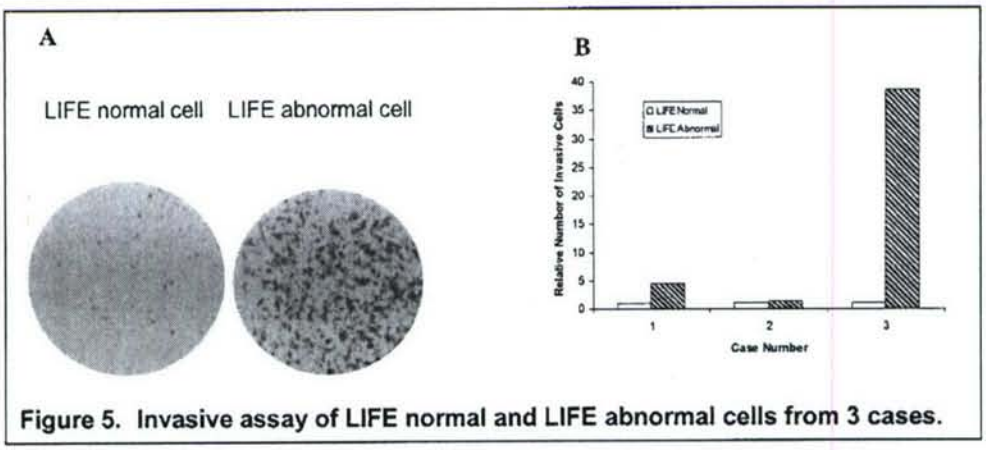

Figure 5. Invasive assay of LIFE normal and LIFE abnormal cells from 3 cases.

Aim 2 Establish an organotypic model system that mimics *in vivo* interactions between normal, premalignant, and malignant bronchial epithelial cells in the lung using cells derived from bronchial biopsies and immortalized bronchial cells.

Our prior studies using chromosome in situ hybridization to visualize genetic changes in the bronchial epithelium of current and former smokers suggested that, over years of tobacco smoke exposure, the combination of accumulating genetic damage, ongoing tissue damage, and wound healing results in a mosaic of evolving clonal outgrowths throughout the bronchial epithelium. To better understand the molecular basis of preferential outgrowth of more advanced bronchial epithelial clones, we proposed to utilize a cell culture model whereby normal and abnormal bronchial epithelial cells are grown on collagen or stoma cell-coated, suspended filters and exposed to an air-liquid interface. This organotypic culture environment mimics lung stratified epithelium, complete with basal cells, ciliated columnar cells, and mucus-producing goblet cells. Our group has extended this model system by tagging cell populations with fluorescent probes (e.g., green fluorescence protein) that allows us to carry out live cell imaging of mixed clonal populations. This model system permits characterization of the ability of more advanced bronchial epithelial cell populations to expand on the growth surface at the expense of less advanced bronchial epithelial cell populations.

Update
Due to the delays of the initiation of the clinical trial of Project 1 and the implementation of fluorescence bronchoscopy, we have focused our organotypic studies by using already

established bronchial epithelial cell strains. We previously described studies, which examined the cell cycle regulation of these different bronchial cell strains representing different stages of lung tumorigenesis in the organotypic culture model. Using BrdU pulse labeling (to label cells in DNA synthesis phase) or phospho-Histone H3 labeling (to mark cells in mitosis), immunofluorescence staining, and laser confocal microscopic analysis of these organotypic cultures, we found that both the NHBE cells and the immortalized HccBE cells (three different lines tested) preferentially proliferate in the basal layer of the culture; however, the immortalized cells (HCC-BE cells) also showed some proliferation in the parabasal layers. In contrast, the more advanced cells (BEAS2B, 1799, 1198, and 1170) proliferated throughout all cell layers of the three dimensional cultures.

In order to examine competitive interactions between different cell populations, we previously reported that we had modified the lung organotypic culture model in such a way that different cell types could be plated as distinct colonies on the same collagen VI-coated growth filter and then allowed to compete with each other for the growth surface. In order to distinguish the different competing cell populations, we have stably transfected and obtained clonal outgrowths of the different cell types labeled with fluorescent living color vectors (containing green fluorescence protein (GFP), yellow fluorescence protein (YFP), red fluorescence protein (RFP), or cyano fluorescence protein (CFP). In this way, we can directly view the competitive interaction between different cell strains in real time using fluorescence microscopy and live cell imaging. At the completion of the experiment, we then would fix the culture filters and visualize the interactions at higher magnification and in three dimensional space using laser scanning confocal microscopy and fluorescence counterstains for DNA or other molecular entities.

An example of a three dimensional interaction between two cell types (NHBE and 1170 cells) is shown in Figure 6 where one XY plane of interaction is shown as well as its orthogonal views (i.e., from the sides). Through these types of studies, we observed four types of ways that one more aggressive cell type could preferentially take over the growth surface from a less aggressive cell type. Figure 6 illustrates three takeover pathways (i.e., under, over, or through). In some interactions between less advanced populations, we observed a generalized pushing mechanism where the whole population would move forward as a tight group without individual cells breaking away from the group.

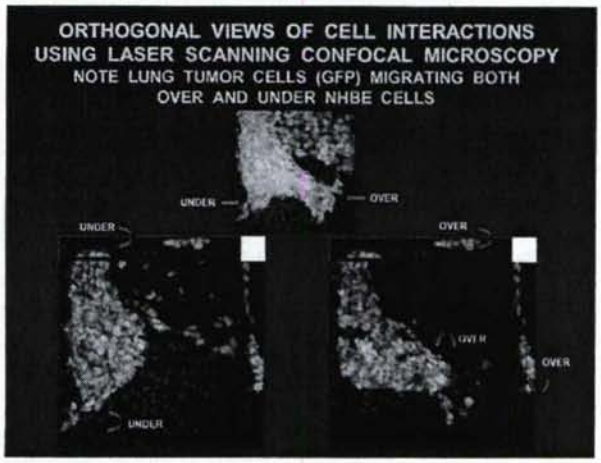

Figure 6: Visualization of modes of epithelial takeover in three dimensions by confocal microscopy.

To first screen the differential ability of different cell types to take over the growth surface of the organotypic culture, we used multiple small cloning rings to place different cell types on the culture filter and then, after the different cell types had attached in a confluent manner, we removed the cloning rings and observed the cultures as the cell populations grew out radially and came into competition with the other cell types.

We previously described the results of interactions between NHBE cells and the SV40-immortalized cell types BEAS2B, 1799, 1198, and 1170 cells. During this last project period, we

used a modified arrangement of this same system to focus on interactions between NHBE cells and three cdk4/h-TERT- immortalized bronchial cell populations (HCC-BE1, HCC-BE2, and HCC-BE3) that had been derived from the bronchial biopsies of three different participants in a lung chemoprevention trial. In particular, we created a thick wall cloning ring where we would place one cell type in the center and another cell type in the area outside the cloning ring, allowed the cells to become confluent while separated. We then lifted the cloning ring to permit the cells to grow, migrate, and compete with each other over time. We chose this alternative, radial arrangement so that we could easily obtain biologically identical interaction zones for subsequent characterization of the molecular underpinnings of preferential competition for the growth surface simply by cutting pie-shaped crescents from the filter.

An example of a time course for one such interaction between YFP-labeled HCC-BE2 cells (inside) and unlabeled (phase-contrast but pseudo-colored red) HCC-BE1 cells is shown in Figure 7. In this case, after removing the cloning ring from the filter (day 1), the two cell populations grew toward each other and initiated contact (day 4), and then competed for the growth surface. In this case, HCC-BE2 cells appeared to have a competitive advantage for the growth surface over HCC-BE1 cells. The areas occupied by each colony were recorded each day using live cell microscopy, digital imaging, and image analysis software. At the end of the experiment (usually after at least 10 days of interaction), the cultured filters were pulse labeled with BrdU (to identify the cells in S phase), fixed in 4% cold buffered paraformaldehyde, washed, and stored for later molecular and three-dimensional characterization. In the first sets of experiments, we observed a rank order of preferential takeover abilities of the cell types: HCC-BE2 > HCC-BE3 > HCC-BE1 > NHBE cells. Interestingly, we found that the HCC2-YFP subclone had preferential ability to take-over its unlabeled HCC2 parent population (non-clonal). This latter finding was a surprise and suggested that a more aggressive subclone had been isolated following YFP transfection. This finding will prove useful for carrying out differential expression analysis to identify candidate genes that may underlie the ability to preferentially expand in this organotypic culture model system.

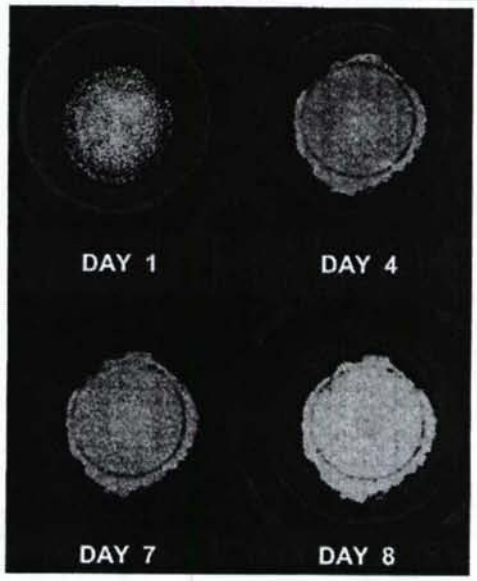

Figure 7: Competitive interactions between HCC-BE2 YFP and HCC-BE1 (red) cells in organic culture over time.

To verify these observations and to obtain a better view of the dynamics of the interactions, we obtained overnight live cell movies of various interaction regions by capturing digital phase and fluorescent images with our inverted, live cell imaging microscope every 20 minutes and then stitched the images into a movie. Figure 8 shows example individual frames (viewed in two dimensional space) that occurred over a period of 750 minutes of one such competitive interaction where the YFP labeled population appeared to have a competitive edge for the growth surface. We are now repeating these experiments to determine if the results are reproducible.

One problem that we will face with fresh bronchial cell outgrowths (obtained from biopsies from different lung sites from the same individual and initiated by Dr. Koo's laboratory) is that the cells will not contain living color markers. Since these bronchial epithelial cells will not have been immortalized *ex vivo* and have a limited number of culture passages, it would be difficult to transfect these cells and then select for cells that have been stably transfected using antibiotic selection. Also, fresh normal cells are known to have low transfection frequencies. We have therefore decided to utilize lentiviral infection technologies to generate bronchial epithelial populations containing living color genes. Lentiviral infection strategies have the advantage of high infection rates, and gene expression does not require that the cell populations be rapidly proliferating. We are now developing separate lentiviral vectors that will allow us to label these bronchial epithelial cells with GFP, YFP, monoRFP, or CFP in these freshly generated cultures. We are also generating lentiviral vectors that will allow us to infect cells with color-tagged genes or siRNAs of interest to better characterize the molecular underpinnings of preferential clonal outgrowth.

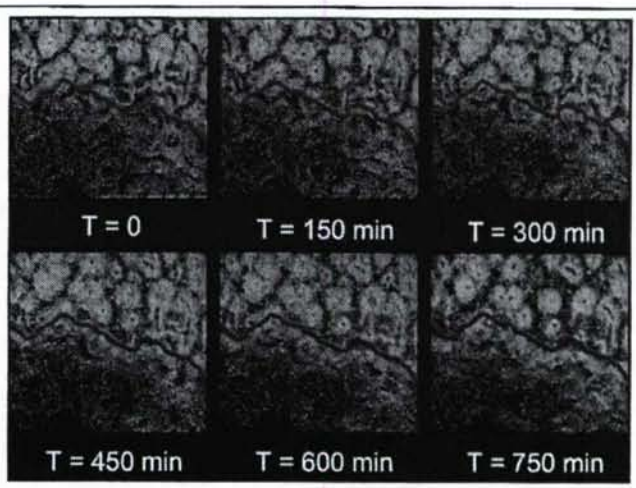

Figure 8. Still images from a live cell-imaging movie following the competitive interaction between bronchial epithelial cell strains in organotypic culture.

Aim 3 Determine the mechanisms of genetic instability and elucidate the signaling pathways associated with clonal outgrowth of premalignant and malignant bronchial epithelial cells using the organotypic model system.

Our prior studies using chromosome *in situ* hybridization to visualize genetic changes in the bronchial epithelium of current and former smokers suggested that current tobacco exposure was associated with increased levels of ongoing genetic instability (i.e., chromosome polysomy). Upon smoking cessation, while the initiated clonal outgrowths appeared to be maintained over tens of years, the levels of ongoing genetic instability appeared to decrease gradually during the first year following smoking cessation, but, in some cases, we observed evidence for ongoing genetic instability in the bronchial epithelial cells even 10-20 years following smoking cessation. Since nearly half of the newly diagnosed lung cancer cases occur in former smokers, we felt that this finding suggested that an ongoing intrinsic process of genetic instability might exist in the lungs of some former smokers that drives continued genetic evolution toward lung cancer even after cessation of extrinsic carcinogenic exposure. Our working hypothesis is that years of tobacco exposure induces a chronic damage and wound healing cycle that results both in the accumulation of genetic alterations in the epithelial cells that influences both chromosome stability mechanisms (e.g., loss of cell cycle checkpoint and cell loss mechanisms through loss of p16 expression, p53 mutations, cyclin D1 overexpression, etc) and creates a poor growth environment (e.g., altered stromal signals). The goal of this aim was to utilize the lung organotypic model to address this hypothesis *in vitro* utilizing bronchial epithelial cells derived from LIFE bronchoscopically identified "abnormal" and "normal" regions of the lung of current and former smokers participating in the clinical trial of Project 1.

Update

Previously, we provided data that suggested that ongoing genetic instability could be detected in these bronchial epithelial cells and led to the development of subclonal outgrowths. We had also observed that while NHBE cells showed little genetic instability and subclonal outgrowth, bronchial epithelial cells representing more progressed stages of lung tumorigenesis exhibited increased levels of genetic instability and subclonal outgrowth. In the three dimensional organotypic lung cultures, we had found that HCC-BE1 cells showed slightly higher levels of mitotic infidelity (aberrant anaphases containing chromosome bridges, lagging chromosome fragments, and multipolar spindle arrangements) than NHBE cells and that BEAS2B and more progressed cells showed significantly higher levels of genetic instability. Moreover, we found that the degree of genetic instability was related to the location of cell division, i.e., cells that divided at the basal layer showed lower levels of instability than cells that divided away from the basal layer.

We then initiated studies to determine whether these cell populations exhibited the markings of a stress reaction in association with the mitotic instability. To do this, we immunostained fixed organotypic culture filters with an antibody to phosphorylated Histone H2AX. This histone is described to be phosphorylated in response to either DNA double strand breaks or chromatin alterations associated with stalled DNA replication forks. In agreement with our mitotic aberration results, we found that HCC-BE1 cells showed the highest frequency of cells with high levels of phosphorylated H2AX when compared to HCC-BE2 and HCC-B3 cells.

We also found that the cells decorated with phospho-H2AX were preferentially located away from the basal layer (Figure 9).

Figure 9. Three-dimensional spatial location of bronchial epithelial cells staining positive (blue, green, orange, and red) for phospho-H2AX in organotypic cultures of HCC-BE1 (left), HCC-BE2 (middle), and HCC-BE3 (right) cells.

These results therefore suggest that cells that divide away from the basal layer have an increased incidence of mitotic instability and the H2AX-phosphorylation stress reaction. We will continue to examine the molecular basis for increased chromosome instability in cells that divide away from the basal layer in this model system.

Another goal of this project is to better understand the molecular pathways involved in epithelial cell outgrowth. Since EGFR is frequently found to be overexpressed and molecularly altered in lung cancer and is thought to play a role in the regulation of lung growth and migration, we decided to examine the status of EGFR expression and post-translational modification in this three dimensional, bronchial cell organotypic culture model. We hypothesized that the EGFR status would be spatially regulated in the organotypic culture according to what functions the cells were carrying out in that region (e.g., proliferating versus migrating). We decided to examine different phosphorylated EGFR sites for two reasons. First, it is suspected that different

sites on EGFR might be phosphorylated when cells are carrying out different functions (e.g., proliferation, migration, etc.) through different signaling pathways. Second, it is suspected that EGFR phosphorylated at different sites may localize at different subcellular locations depending on the particular signaling/functional pathway being elicited. For example, phosphorylation of EGFR at tyr1173 has been reported to create a SHC docking site and may be involved in activation of the MAP kinase signaling, while phosho-tyr992 is reported to play a role in activation of PLC-γ-mediated signaling.

The results of these studies are still preliminary and need to be repeated. However, early studies of HCC-BE2 cells migrating radially outward from a clonal focus demonstrated that the cells showing the highest EGFR levels were located on the outside of the colonies (the leading edge) and the cells showing the lowest EGFR levels were preferentially located in the center of the colonies where there was little ongoing cell migration or proliferation (Figure 10). Interestingly, cells showing the tyr1173 phosphorylated form of EGFR were also preferentially found on the outer regions of the colonies, and cells showing an elongated cellular appearance (typical of a cell undergoing active migration) showed nuclear location of this phosphorylated EGFR form. Cells labeled for the tyr992 phosphorylated EGFR site also showed stronger staining in cells near the outer edge of the colony, however the subcellular pattern was cytoplasmic and speckled in appearance. These studies might suggest that different phosphorylated forms of EGFR might be involved in different cellular functions. We have initiated similar EGFR staining studies in the organotypic cultures; however the studies need to be repeated prior to reporting.

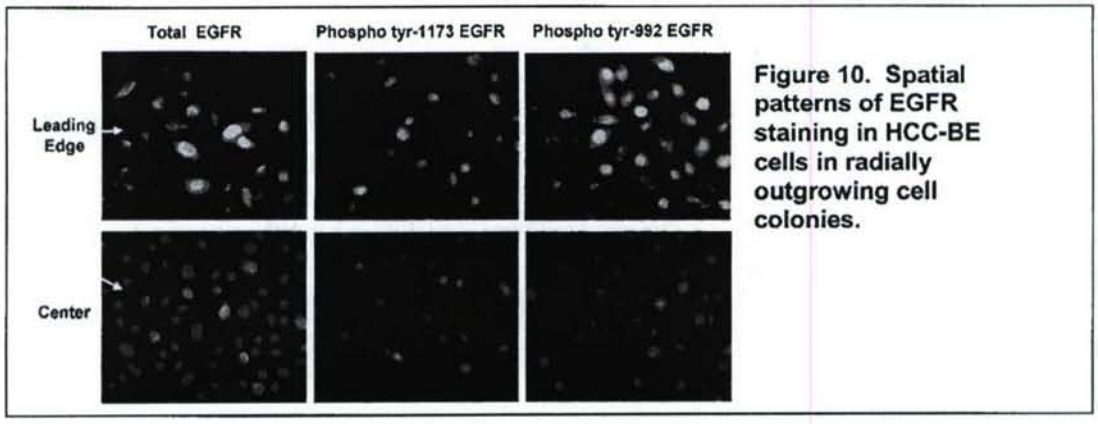

Figure 10. Spatial patterns of EGFR staining in HCC-BE cells in radially outgrowing cell colonies.

Aim 4 Characterize the impact of chemopreventive and/or chemotherapeutic agents on early lung tumorigenesis events in reconstructed bronchial epithelium and in the bronchial biopsies of subjects entered onto the clinical trials in Project 1.

The goal of the first three specific aims of this project is essentially to develop and utilize the lung organotypic culture model to identify the factors that control ongoing clonal expansion and genetic instability in the lungs of current and former smokers. The goal of the fourth specific aim is to integrate the information garnered from the first three specific aims to identify targeted strategies to slow preferential outgrowth of more advanced bronchial epithelial cells and to decrease the levels of ongoing genetic instability. We also proposed to determine whether treatment of these organotypic cultures with the chemopreventive agents used in the clinical trial of Project 1 would slow these aberrant properties *in vitro* and whether results obtained in the organotypic culture model reflected the observations seen in the lungs of the participants in the clinical trial.

Update

Due to the delays in acquiring the fluorescence bronchoscopy apparatus and accrual of subjects with fluorescence abnormalities in their bronchial epithelium, this aim remains to be done. However, with our recent development of lentiviral vectors to differentially mark (i.e., induce live cell fluorescence) primary bronchial epithelial cultures from different biopsy sites, we are prepared to carry out the proposed studies efficiently.

Key Research Accomplishments

- Collected high quality RNA from brushings and isolated bronchial epithelial cells from biopsies of LIFE normal and LIFE abnormal. Successfully set up culture to reconstitute bronchial epithelium in these specimens.
- Demonstrated that our organotypically cultured bronchial epithelial cells isolated from biopsies of LIFE normal and LIFE abnormal bronchial epithelium reflects expression profile of bronchial epithelial cells *in vivo*, which provided a useful model for our future work using cultured bronchial epithelial cells.
- Demonstrated that LIFE normal and LIFE abnormal bronchial epithelial cells had differences at the molecular level, although they didn't show obvious morphological differences in histologic evaluation of cultures, which might reflect the gene expression difference in the early stage of tumorigenesis.
- Demonstrated that LIFE abnormal epithelial cells appear to have higher aggressive tendency than LIFE normal cells. The genes responsible for this character might play an important role in lung tumorigenesis and tumor development.
- Demonstrated that chromosome instability in bronchial epithelial cells occurred in cells proliferating away from the basal layer and was associated with a stress response in the cells associated with phosphorylation of Histone H2AX.
- Demonstrated that immortalized HBECs derived from different individuals show differential takeover ability when placed in competition with normal bronchial epithelial cells and with each other.
- Demonstrated that EGFR expression and phosphorylation patterns may be spatially regulated in two-dimensional and three-dimensional culture conditions, perhaps reflective of specific cellular processes including proliferation and migration.

Conclusions and Future Studies

We have improved our ability to reconstruct bronchial epithelium *in vitro* by culturing bronchial epithelial cells isolated from biopsies of LIFE normal and LIFE abnormal areas. The *in vitro* cultured bronchial epithelial cells properly reflect expression profile of bronchial epithelial cells *in vivo*. The cultured bronchial epithelial cells derived from LIFE abnormal areas shows higher invasive tendency than those from LIFE normal areas and we are studying the molecular mechanism to better understand lung tumorigenesis in premalignant bronchial epithelial cells. Also, we have been studying the molecular mechanisms underlying the preferential takeover advantage of one bronchial epithelial cell strain over another strain.

We will continue to process and analyze the expression patters of brushing and biopsies of patients on our clinical trial that meet the eligibility criteria for LIFE bronchoscopy and to create the organotypic cell cultures from the biopsies for this purpose as well. Further evaluation of the invasiveness of abnormal and normal LIFE bronchial epithelial cells is also needed and will continue. We will complete the lentiviral vector development or siRNA development as needed for completion of this project. We will continue investigation of the molecular basis for increased

chromosomal instability and of EGFR phosphorylation status and spatial patterns. Finally, we will complete Aim 4 studies as soon as the samples and results are available.

Project 4: Modulation of Death Receptor-Mediated Apoptosis for Chemoprevention

(Project Leader and co-leader: Shi-Yong Sun, Ph.D.; Fadlo R. Khuri, M.D.)

The objective is to understand the role of death receptor (DR)-mediated apoptotic pathways in lung carcinogenesis, cancer prevention, and therapy in order to develop mechanism-driven combination regimens by modulating DR-mediated apoptosis for chemoprevention and therapy of lung cancer.

Aim 1 To determine whether decoy receptor (DcR) and tumor necrosis factor-related apoptosis-inducing ligand (TRAIL) expression are reduced or lost while DR remains largely expressed and whether procaspase-8 and FLIP expression and Akt activity are increased during lung carcinogenesis.

Update

As reported last time, we planned to examine the expression of the proposed proteins, particularly death receptor 5 (DR5), DR4, caspase-8, c-FLIP and p-Akt, in normal lung tissue, primary and metastatic lung cancer tissues using immunohistochemistry (IHC), but we met some difficulty in obtaining premalignant lung cancer tissues. We thus purchased commercial tissue microarrays (TMAs; Accurate Chemical & Scientific Corp, Westbury, NY) that contain these tissues and re-optimized the staining conditions of these proteins in TMAs, finding that DakoCytomation EnVision+Dual Link System-HRP (DAB+ (Dako, Carpinteria, CA) substantially enhances the signals and quality of the IHC. We now have optimal conditions for staining caspase-8, DR5, DR4, c-FLIP and p-Akt. In the coming year, we will focus on staining the proposed proteins in human lung tissues, including lung cancer tissue.

Aim 2 To establish TRAIL-resistant cell lines from a TRAIL-sensitive lung cancer cell line and determine whether levels of DcRs, DRs, procaspase-8, TRAIL and FLIPs and Akt activity are altered and are associated with cell resistance to TRAIL and DR-inducing agents.

Update

As reported last year, the TRAIL-resistant lung cancer cell lines did not exhibit cross-resistance to some DR-inducing agents such as celecoxib, PS-341, CDDO-Me, PPARγ ligands, and FTIs (SCH66336 and R115777). Since then, we investigated whether these agents modulate the death receptor-mediated apoptotic pathways and if yes, whether and how the modulations impact cell apoptosis. The findings are summarized below.

1) Modulation of DR5 and c-FLIP expression and enhancement of TRAIL-induced apoptosis by celecoxib and its derivative dimethyl celecoxib (DMC)

Our previous work demonstrates that celecoxib induces DR5 expression, resulting in induction of apoptosis and enhancement of TRAIL-induced apoptosis in human lung cancer cells (Liu et al., 2005). Recently, we found that celecoxib downregulated the expression of c-FLIP, a major negative regulator of the death receptor-mediated extrinsic apoptotic pathway, through an ubiquitin/proteasome-dependent mechanism independent of COX-2 in human lung cancer cells. Overexpression of c-FLIP, particularly $FLIP_L$, inhibited not only celecoxib-induced apoptosis, but

also apoptosis induced by the combination of celecoxib and TRAIL. These results thus indicate that c-FLIP downregulation also contributes to celecoxib-induced apoptosis and enhancement of TRAIL-induced apoptosis, which complement our previous finding that the extrinsic apoptotic pathway plays a critical role in celecoxib-induced apoptosis in human lung cancer cells. Collectively, we conclude that celecoxib induces apoptosis in human lung cancer cells through activation of the extrinsic apoptotic pathway, primarily by induction of DR5 and downregulation of c-FLIP. The detailed findings can be reviewed in the article published in *Cancer Research* (Liu et al., 2006) as attached in the Appendix 2.

Celecoxib exhibits anticancer activity in both preclinical studies and clinical practice. However, celecoxib has relatively weak apoptosis-inducing activity and modest cancer therapeutic efficacy. Therefore, efforts have been made to develop derivatives of celecoxib with superior anticancer activity. Dimethyl-celecoxib (DMC) is just such a derivative that lacks COX-2-inhibitory activity, but demonstrates better apoptosis-inducing activity than celecoxib albeit with undefined mechanisms in vitro and exhibits anticancer activity in animal models. In this study, we examined the effects of DMC on the growth of human lung cancer cells as well as its cooperative effect with TRAIL on induction of apoptosis and the underlying mechanisms. By comparing the effects of DMC and celecoxib on the growth of a group of human lung cancer cell lines, we found that DMC decreased cell survival with IC_{50}s ranging from 10 μM to 20 μM, whereas celecoxib did so with IC_{50}s ranging between 20 and 30 μM, indicating that DMC is slightly more effective than celecoxib in decreasing the survival of lung cancer cells. When cells were treated with the combination of DMC and TRAIL, enhanced or synergistic effects in reduction of cell survival and induction of apoptosis including activation of caspases were observed in comparison with the effects in cells exposed to each agent alone. To understand the mechanisms underlying this synergy, we also analyzed the effects of DMC on modulation of several apoptosis-related genes. We found that DMC rapidly increased DR5 levels and reduced c-FLIP (both $FLIP_L$ and $FLIP_S$) levels starting from 2 h post treatment while having limited effects on modulating the levels of other proteins including DR4, Bcl2, Bcl-X_L and Bax. Importantly, enforced expression of $FLIP_L$ or silencing of DR5 expression using DR5 small interfering RNA (siRNA) partially abrogated the enhanced effects on induction of apoptosis by the combination of DMC and TRAIL, indicating that both DR5 upregulation and c-FLIP reduction contribute to cooperative induction of apoptosis by the combination of DMC and TRAIL. Collectively, we conclude that DMC sensitizes TRAIL-induced apoptosis in human lung cancer cells via induction of DR5 and downregulation of c-FLIP. An abstract of the work was submitted to the 2007 AACR meeting (Chen et al., 2007 AACR) as attached in the Appendix 2. A manuscript is in preparation.

2) The proteasome inhibitor PS-341 (Bortezomib) upregulates death receptor 5 expression, leading to induction of apoptosis and enhancement of TRAIL-induced apoptosis despite increased c-FLIP and survivin in human lung cancer cells

The proteasome inhibitor PS-341 (Bortezomib or Velcade), an approved drug for treatment of patients with multiple myeloma, is currently being tested in clinical trials against various malignancies including lung cancer. Preclinical studies have demonstrated that PS-341 induces apoptosis and enhances TRAIL-induced apoptosis in human cancer cells with undefined mechanisms. In the present study, we found that PS-341 increased cleavage of caspase-8 and apoptosis. Prevention of caspase-8 activation by silencing caspase-8 expression using caspase-8 small interfering RNA (siRNA) abrogated PS-341-induced apoptosis. These results indicate that PS-341 induces caspase-8-dependent apoptosis. PS-341 induced the expression of death receptor 5 (DR5) and demonstrated cooperativity with TRAIL to induce apoptosis in human lung cancer cells. Importantly, DR5 induction by PS-341 correlated with the ability of PS-

341 to induce apoptosis, whereas blockage of PS-341-induced DR5 upregulation using DR5 siRNA rendered cells less sensitive to apoptosis induced by either PS-341 or its combination with TRAIL. These results demonstrate that DR5 upregulation mediates PS-341-induced apoptosis and enhancement of TRAIL-induced apoptosis in human lung cancer cells. Meanwhile, we exclude the involvement of c-FLIP and survivin in mediating these events because c-FLIP (i.e., $FLIP_S$) and survivin protein levels were actually elevated upon exposure to PS-341. Reduction of c-FLIP with c-FLIP siRNA sensitized cells to PS-341-induced apoptosis, suggesting that c-FLIP elevation protects cells from PS-341-induced apoptosis. Thus, the study highlights the important role of DR5 upregulation in PS-341-induced apoptosis and enhancement of TRAIL-induced apoptosis. An abstract was submitted to the 2007 AACR meeting (Liu et al., 2007 AACR) (Appendix 2). A manuscript is under peer review in *Cancer Research* (Liu et al., 2006).

3) c-Jun N-terminal kinase (JNK)-independent c-FLIP downregulation contributes to induction of apoptosis by the novel synthetic triterpenoid methyl-2-cyano-3, 12-dioxooleana-1, 9-dien-28-oate (CDDO-Me) in human lung cancer cells

The novel synthetic triterpenoid methyl-2-cyano-3, 12-dioxooleana-1, 9-dien-28-oate (CDDO-Me) induces apoptosis of cancer cells, enhances TRAIL-induced apoptosis, and exhibits potent anticancer activity in animal models with a favorable pharmacokinetic profile. Thus, CDDO-Me is being tested in Phase I clinical trials. In an effort to understand the mechanism by which CDDO-Me induces apoptosis, particularly in human lung cancer cells, we demonstrated that CDDO-Me induced apoptosis in human lung cancer cells involving c-Jun N-terminal kinase (JNK)-dependent upregulation of death receptor 5 (DR5) expression. In the current work, we further show that CDDO-Me downregulates the level of c-FLIP, a major inhibitor of death receptor-mediated caspase-8 activation, which contributes to induction of apoptosis by CDDO-Me in human lung cancer cells. CDDO-Me rapidly and potently decreased c-FLIP levels including both long ($FLIP_L$) and short ($FLIP_S$) forms of c-FLIP in multiple human lung cancer cell lines. The presence of the proteasome inhibitor MG132, but not the JNK inhibitor SP600125 or JNK siRNA, prevented CDDO-Me-induced c-FLIP reduction. Thus, CDDO-Me induces proteasome-dependent c-FLIP degradation independently of JNK activation. Importantly, overexpression of c-FLIP (e.g., $FLIP_L$) in both A549 and H157 cell lines protected cells from CDDO-Me-induced apoptosis, indicating that c-FLIP downregulation is involved in CDDO-Me-initiated apoptosis. Given our previous finding that CDDO-Me induces apoptosis involving DR5 upregulation, we collectively conclude that the activation of the extrinsic apoptotic pathway via DR5 induction and c-FLIP downregulation plays a pivotal role in CDDO-Me-induced apoptosis in human lung cancer cells. An abstract of this work was submitted to the 2007 AACR meeting (Zou et al., 2007 AACR) (Appendix 2).

4) PPARγ ligands enhance TRAIL-induced apoptosis through DR5 upregulation and cFLIP downregulation in human lung cancer cells

Peroxisome proliferator-activated receptor γ (PPARγ) ligands are potential chemopreventive agents. Many studies have shown that PPARγ ligands induce apoptosis in various types of cancer cells including lung cancer cells. Some PPARγ ligands have been shown to downregulate c-FLIP expression and thus enhance TRAIL-induced apoptosis in some cancer cell lines. In the current study, we further showed that PPARγ ligands induced the expression of DR5 and increased DR5 distribution at the cell surface in addition to reducing c-FLIP levels in human lung cancer cells. These agents demonstrated cooperativity with TRAIL to enhance induction of apoptosis in human lung cancer cells. Both overexpression of c-FLIP and

knockdown of DR5 abrogated PPARγ ligand's ability to enhance TRAIL-induced apoptosis. Thus, it appears that not only c-FLIP downregulation but also DR5 upregulation contribute to PPARγ ligand-mediated enhancement of TRAIL-induced apoptosis in human lung cancer cells. Both the PPARγ antagonist GW9662 and silencing PPARγ expression failed to diminish PPARγ ligand-induced DR5 upregulation or c-FLIP downregulation, indicating that PPARγ ligands modulate the expression of DR5 and c-FLIP through a PPARγ-independent mechanism. Collectively, we conclude that PPARγ ligands exert PPARγ -independent effects on inducing DR5 expression and downregulating c-FLIP levels, leading to enhancement of TRAIL-induced apoptosis. For more detail, please review the manuscript accepted in *Cancer Biology and Therapy* (Zou et al., 2006) as attached in Appendix 2.

5) Farnesyltransferase inhibitors (FTIs) induce apoptosis via CHOP/GADD153-dependent upregulation of death receptor 5 expression in human lung cancer cells

In an effort to explore their mechanisms of action, we demonstrated that the FTIs (SCH66336 and R115777) induced DR5 expression, including the cell surface DR5 level, which contributes to FTI-induced apoptosis in human lung cancer cells. Moreover, SCH66336 induces CHOP/GADD153 expression, leading to an increase in DR5 transactivation and expression. Therefore, we conclude that FTIs induce DR5 expression through a CHOP/GADD153-dependent mechanism, contributing to induction of apoptosis in human lung cancer cells. In addition, the combination of an FTI with TRAIL exerts synergistic effects on induction of apoptosis in human lung cancer cells. Our new findings reveal a novel mechanism by which FTIs induce apoptosis and suggest a novel therapeutic strategy for enhancing the efficacy of FTIs in combination of TRAIL. In addition, we recommend monitoring the modulation of CHOP/GADD153 and DR5 expression in FTI-based lung cancer therapy. These findings were summarized in two manuscripts and are under peer review in *Molecular & Cellular Biology* (Sun et al., 2006) and *Cancer Research* (Qiu et al., 2006) respectively.

In summary, some small molecules indeed modulate the death receptor-mediated apoptotic pathway, which even participated in apoptosis induced by these molecules. However, cells resistant to TRAIL are still sensitive to these small molecules. Taken together, we suggest that DR-inducing agents induce apoptosis through different mechanisms in addition to modulation of the death receptor- mediated apoptotic pathway.

Aim 3 To determine whether suppression of PI3K/Akt activity sensitizes premalignant and/or malignant airway epithelial cells to apoptosis induced by DR-induced agents via enhancement of TRAIL/DR-mediated mechanism.

Update

1) Modulation of p-Akt and COX-2 by celecoxib and its derivative dimethyl-celecoxib (DMC)

In the last report, we presented that celecoxib increased p-Akt levels in some lung cancer cell lines. We then examined the effects of the celecoxib derivative, DMC that lacks COX-2 inhibitory activity, on Akt phosphorylation. We found that DMC also increased p-Akt levels in a time dependent fashion while inducing DR5 and down-regulating c-FLIP levels in some lung cancer cells (Figure 11A). The increase in p-Akt levels occurred at 2 h, reached a peak at 4 h and then declined to basal levels at 16 h post DMC treatment. Thus, it appears that the increase

of Akt phosphorylation is an early event induced by DMC. Similar to celecoxib, DMC increased only in some of the tested lung cancer cell lines (Figure 11B). Given that DMC exerted two phases of modulation of c-FLIP expression including the early reduction of c-FLIP levels (2-8 h) followed by late increase of $FLIP_L$ levels (after 12 h) in H460 cells, we questioned whether the late $FLIP_L$ upregulation by DMC in H460 cells is due to Akt activation because Akt positively regulates c-FLIP expression. Although the PI3K inhibitor LY294002 alone decreased c-FLIP levels and abolished DMC-induced Akt phosphorylation, it failed to prevent DMC-induced increase in $FLIP_L$ expression (Figure 11C). Thus, we conclude that the increase in Akt phosphorylation is not responsible for DMC-induced late upregulation of $FLIP_L$ expression. However, in H157 cells, the combination of DMC and LY294002 enhanced the reduction of c-FLIP (Figure 11C). It appears that prevention of Akt phosphorylation with LY294002 exerts a cell line-dependent effect on DMC-induced modulation of c-FLIP in human lung cancer cell. Future work will clarify the issue.

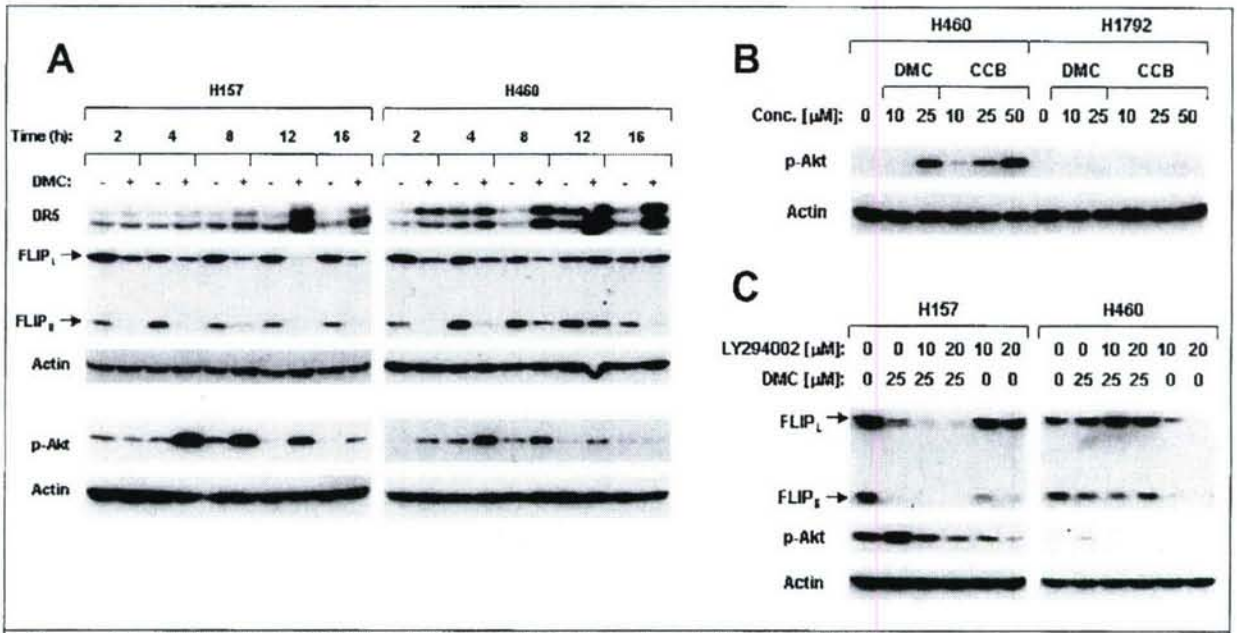

Figure 11. Modulation of DR5, c-FLIP and Akt phosphorylation by DMC in human lung cancer cells. *A*, The indicated cell lines were treated with and without 25 uM DMC for the given times; *B*, The given cell lines were treated with indicated concentrations of DMC or celecoxib (CCB) for 8 h; and *C*, The indicated cell lines were treated with the indicated concentrations of DMC, LY294002 or their combinations for 8 h (H157) or 14 h (H460). After the aforementioned treatments, the cells were subjected to preparation of whole-cell protein lysates and subsequent Western blot analysis for the indicated proteins.

Another surprising finding was that both celecoxib and DMC increased COX-2 expression at concentrations that induce apoptosis. DMC or celecoxib induced DR5 expression accompanying COX-2 induction (Figure 12). The biological role of COX-2 induction during DMC- or celecoxib-induced apoptosis is currently unclear. Given recent findings that COX-2 can function as a proapoptotic protein, we will further pursue the implication of COX-2 induction in DMC- or celecoxib-induced apoptosis with resources including antisense COX-2 cell lines and lentiviral COX-2 siRNAs in hand.

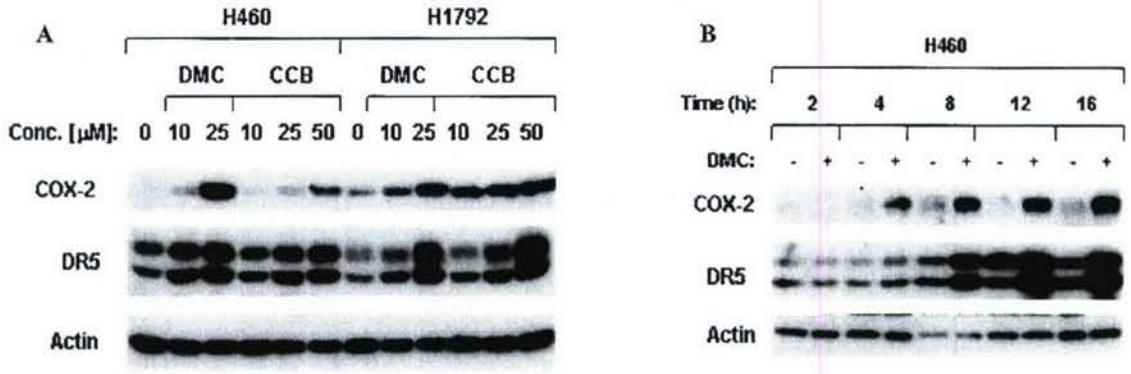

Figure 12. Induction of COX-2 and DR5 expression by DMC and celecoxib (CCB) in human lung cancer cells. *A*, The given cell lines were treated with indicated concentrations of DMC or celecoxib (CCB) for 8 h; and *A*, The indicated cell lines were treated with and without 25 μM DMC for the given times. After the aforementioned treatments, the cells were subjected to preparation of whole-cell protein lysates and subsequent Western blot analysis for the indicated

Aim 4 To determine whether DRs, DcRs, c-FLIP, and procaspase-8 serve as biomarkers for lung cancer chemoprevention and therapy.

Conditions have already been optimized and we will begin Aim 4 in the coming year once we receive the tissue samples obtained through Project 1 and Pathology Core.

Key Research Accomplishments

- Determined that several groups of compounds with cancer therapeutic potential including celecoxib and its derivative, DMC, proteasome inhibitors, triterpenoids, PPARγ ligands, and FTIs, modulated DR5 expression and/or c-FLIP levels (predominantly by downregulation), contributing to the induction of apoptosis and/or enhancement of TRAIL-induced apoptosis.
- Determined that celecoxib and DMC increased p-Akt levels in a time-dependent fashion while inducing DR5 and downregulating cFLIP in some lung cancer cell lines but not all and that LY294002 blocks this phosphorylation in a cell-dependent effect.
- Found that CHOP/GAD153 mediated FTI (SCH66336)-induced DR5 expression.

Conclusions and Future Plans

Appropriate modulation of the extrinsic death receptor-mediated apoptotic pathway such as upregulation of DR5 and/or reduction of c-FLIP levels by small molecules (e.g., celecoxib, lonafarnib, bortezomib) may eliminate premalignant or malignant lung epithelial cells via promoting apoptotic cell death to achieve cancer chemopreventive and therapeutic goals. Moreover, the potential of the modulation of DR5 and c-FLIP as predictive biomarkers for certain drugs in the clinic warrants further investigation. We will continue to study the role of Akt phosphorylation and the implication of COX-2 induction in DMC- or celecoxib-induced apoptosis using antisense COX-2 cell lines and lentiviral COX-2 siRNAs in hand. Finally, when samples are avaliable, we will determine whether DRs, DcRs, c-FLIP, and procaspase-8 can serve as biomarkers for lung cancer chemoprevention and therapy.

Project 5: Molecular Strategies Targeting the AKT Signaling Pathway for Lung Cancer Chemoprevention and Therapy

(PI and co-PI: Ho-Young Lee, Ph.D., Edward S. Kim, M.D.)

Our gaol is to find novel chemopreventive/therapeutic agents that can prevent lung carcinogenesis effectively. Results from our work and others' have demonstrated that Akt, which has a clear role in cellular survival and transformation, is constitutively active in premalignant and malignant HBE cells and in NSCLC cell lines. These findings suggest an importance of PI3K/Akt signaling pathway in lung carcinogenesis. The purpose of our project is to determine whether activation of Akt induces malignant transformation of HBE cells and to develop novel agents to inhibit Akt activity as a strategy of preventing lung carcinogenesis.

For the past 3 years, we have focused on the work proposed in the first part of Aim 1 and Aim 2.

Aim 1 Develop a retroviral vector expressing constitutively active Akt and characterize the *in vitro* and *in vivo* effects of Akt activation on the malignant transformation of HBE cells.

Update

As we reported last year, we finished constructing retroviral vectors expressing constitutively active or dominant negative Akt 1, 2, or 3. The Akt constructs were confirmed by sequencing and western blot analysis. Viral titers have been determined by the colony formation analysis. We have been analyzing the roles of Akt 1, 2 or 3 in the survival of HBE cells under stress conditions (UV, growth factor withdrawal, cigarette carcinogens). We are planning animal experiments to investigate the impact of Akt 1, 2, or 3 in lung tumorigenesis.

Aim 2 Evaluate the ability of chemopreventive agents used in VITAL trials alone and in combination to inhibit Akt activity and induce apoptosis in transformed human bronchial epithelial cells (HBE) and NSCLC cell lines.

Last year, we reported the results of the studies to test the potential of Akt as a target for chemopreventive and therapeutic strategies in NSCLC by using IGFBP-3, a major IGF-binding protein, FTI (Lee et al., 2004), and deguelin, a natural product that inhibits Akt activation in HBE cells and NSCLC cells (Lee et al., 2005). We found that overexpression of a constitutively active Akt rescued the H460 cells from apoptosis induced by single or combined treatment of Ad-IGFBP3 and a farnesyltransferase inhibitor SCH66336. In H1299 tumor xenografts, Ad-IGFBP3 and SCH66336 were associated with decreased tumor volume, increased apoptosis, and decreased Akt levels. We also found that deguelin suppressed Akt activation *in vivo*, and statistically significantly reduced NNK/BaP-induced lung tumor multiplicity, volume, and load in transgenic mice in which Akt expression was induced by tamoxifen and in 4-(methylnitrosoamino)-1-(3-pyridyl)-1-butanone (NNK)/benzo(a)pyrene (BaP)-treated A/J mice, with no detectable toxicity. In addition, we presented some preliminary results of the effects of erlotinib, gefitinib, FTI (SCH66336), and celecoxib on the proliferation of the normal, premalignant (1799 and 1198), and malignant (1170-1) HBE cells.

Update

This year, we have further investigated the chemopreventive/therapeutic activities and action mechanism of erlotinib, gefitinib, FTI (SCH66336), and retinoids on NSCLC or head and neck squamous cell carcinoma (HNSCC) cells. We found that treatment with EGFR TKI, erlotinib, increased the levels of EGFR:IGF-1R heterodimer localized on cell membrane, activated IGF-

1R and its downstream signaling mediators, and stimulated mammalian target of rapamycin (mTOR)-mediated de novo protein synthesis of EGFR and survivin in NSCLC cells. Inhibition of IGF-1R activation, suppression of mTOR-mediated protein synthesis, or knockdown of survivin expression abolished resistance to the EGFR TKIs and induced apoptosis in NSCLC cells *in vitro* and *in vivo*. Our data suggest that enhanced synthesis of survivin protein mediated by the IGFR/EGFR heterodimer counteracts the antitumor action of the EGFR TKIs, indicating the need to integrate IGF-1R-targeted agents into the treatment regimens with EGFR TKI for patients with lung cancer. Detailed findings have been published in *Cancer Research* (Morgillo et al., 2006) as attached in the Appendix-Publications. Similar results were observed when the EGFR TKI, gefitinib, was applied. Currently, we are revising a manuscript of these new findings to be published in *Clinical Cancer Research.*

Moreover, we have conducted mechanistic studies for the FTI SCH66336 that shows antitumor activities in HNSCC *in vitro* and *in vivo*. We found that IGFBP-3 mediates antitumor activities of SCH66336 in HNSCC by inhibiting angiogenesis. SCH66336 significantly suppressed HNSCC tumor growth and angiogenesis via mechanisms that are independent of H-Ras and RhoB. By inducing IGFBP-3 secretion from HNSCC cells, this compound suppresses angiogenic activities of endothelial cells, including vessel formation in chorioallantoic membranes of chick, endothelial cell sprouting from chick aorta, and capillary tube formation of human umbilical vascular endothelial cells (HUVEC). Knockdown of IGFBP-3 expression in HNSCC cells by RNA interference or depletion of IGFBP-3 in HUVECs by neutralizing antibody effectively blocked the effects of IGFBP-3 secreted from SCH66336-treated HNSCC cells on HUVECs. These findings suggest that IGFBP-3 could be a primary target for antitumor activities of FTIs and that IGFBP-3 may be an effective therapeutic approach against angiogenesis in HNSCC. Detailed results can be reviewed in the article published in *Clinical Cancer Research* (Oh et al., 2006) attached in Appendix-Publications.

We have also investigated whether insulin-like growth factor (IGF) axis, which plays a major role in Akt activation, is involved in lung cancer chemopreventive activities of retinoids, well-known chemopreventive agents. We evaluated the effects of the retinoid, 9-*cis*-RA, on IGF axis in former smokers and found that 9-*cis*-RA treatment decreased serum levels of IGF and increased serum levels of IGFBP-3 in former smokers. Detailed results can be reviewed in the articles published in *Journal of Clinical Oncology* (Lee H-Y et al., 2005) attached in Appendix-Publications. As reported last year, we also studied the influence of 9-*cis*-RA on α-tocopherol, an antioxidant, which has shown to reverse the high glucose-induced resistance to the mitogenic activities of IGF-1, and found increased serum levels of α-tocopherol in former smokers treated with 9-*cis*-RA (Han J-Y et al., 2005). Taken together, our findings suggest that the IGF axis is a potential target for the chemopreventive activities of 9-*cis*-RA and that the serum concentrations of IGF, IGFBP-3, and IGF-1/IGFBP-3 could serve as surrogate end point biomarkers of 9-*cis*-RA treatment.

In the coming year, we will continue to test the chemopreventive/therapeutic activities of EGFR inhibitors (erlotinib and gefitinib) alone or in combination with an Akt inhibitor.

Aim 3 Determine whether Akt is activated in bronchial specimens from enrolled patients in VITAL trials and whether treatment with chemopreventive agents suppresses Akt level or activity in these patients.

Project 1 and the Pathology Core are continuing to accrue patients and collecting samples. When more tissue and serum samples are available from the clinical trails, we will perform the correlative studies proposed in this Aim.

Key Research Accomplishments

- EGFR TKIs, including erlotinib and gefitinib, were found to increase the levels of EGFR:IGF-1R heterodimer localized on cell membrane, activate IGF-1R and its downstream signaling mediators, and stimulate mammalian target of rapamycin (mTOR)-mediated de novo protein synthesis of EGFR and survivin in NSCLC cells. Inhibition of IGF-1R activation, suppression of mTOR-mediated protein synthesis, or knockdown of survivin expression abolished resistance to the EGFR TKIs and induced apoptosis in NSCLC cells *in vitro* and *in vivo*.
- Determined that SCH66336 significantly suppressed HNSCC tumor growth and angiogenesis via mechanisms that are independent of H-Ras and RhoB. By inducing IGFBP-3 secretion from HNSCC cells, this compound suppressed angiogenic activities of endothelial cells.
- Determined that the combination of IGFB3 and SCH66336 produced synergistic antiproliferative effects *in vitro* and *in vivo* by inducing apoptosis. A greater combined efficacy was observed in the downregulation of the antiapoptotic Bcl-xL and prosurvival kinase Akt protein expression and increase in the level of proapoptotic IGFBP-3 protein in comparison to each drug alone.
- Discovered that the IGF axis is a potential target for chemoprevention by 9-*cis*-retinoic acid and IGF-1/IGFBP3 may serve as surrogate markers.

Conclusion and Future Plans

We conclude that 1) integration of IGF-1R-targeted agents is required when EGFR TKIs are used to treat lung cancer patients; 2) IGFBP-3 mediates antitumor activities of SCH66336 in HNSCC by inhibiting angiogenesis; 3) the combination of IGFB3 and SCH66336 produces synergistic antiproliferative effects; and 4) the IGF axis is a potential target for the chemopreventive activities of 9-*cis*-RA. We will continue studying the role of Akt, EGFR, and the IGF axis in NSCLC and HNSCC tumorigenesis.

Core B: Biostatistics & Data Management Core

(Core Director: J. Jack Lee, Ph.D.)

Core Goals:

1. To provide statistical design, sample size/power calculations, and integrated, comprehensive analysis for each basic science, pre-clinical, and clinical study.
2. To develop a data management system that provides tracking, quality control, and integration of clinical, pathological, and basic science data.
3. To provide statistical and data management support for genomic and imaging studies including microarray, proteomics, protein antibody array, and spiral CT.
4. To develop and adapt innovative statistical methods pertinent to biomarker-integrated translational lung cancer studies.
5. To generate statistical reports for all projects.
6. To collaborate and assist all project investigators in the publication of scientific results.

The Biostatistics and Data Management Core has continued to work actively with all the VITAL Projects in their research efforts, especially in the area of biostatistical support and consulting in the clinical trial design, implementation, conduct, and analysis of experimental results.

Update

In the third year, our major effort has been in the area of providing statistical/data management support for Project 1, for both the Vanguard trial and the randomized Phase II trials. Biostatistical Core was involved in the protocol design, submission and revision process. We have interacted with study PI, IRB, and regulatory agencies to address critiques and provide revisions. The celecoxib trial has been opened. We have also submitted the protocol of the erlotinib trial for review. In addition, we have met with investigators and research coordinators and provided assistance in designing the Case Report Forms (CRFs) for these trials.

We have developed and continue to provide enhancement of a web-enabled database system to facilitate the conduct of the Vanguard Trial. The database allows remote data capture from any computer with a web browser. It is secure, password protected, and is within our institutional firewall. The database also allows the research nurse to schedule patient visits and print labels for tissue acquisition. It can track the tissue distribution in both sending and receiving. The integrated reporting system provides real-time inventory reports based on the most up-to-date data. We have added the patient randomization module for the celecoxib phase II trial portion of the clinical trials. Histopathology reports have been revised with an easier to read diagnosis and can be emailed directly from within the application. The specimen sample labels have been revised to include more information including the protocol number and timeframe. Selected screen shots are provided in the Appendix 1. The database is fully functional and has captured 34 patients registered in the trial as of December 2006.

We have also worked on statistical methods for the evaluation of the interactions for combination therapy to determine whether the effect is synergistic, additive, or antagonistic. One method was published and attached in the Appendix 2 (Kong and Lee, 2006). Three manuscripts have been submitted. The current available methods require strong assumptions such as the drug interaction follows the same pattern at all doses. It is possible that the combination may produce synergistic effect in certain dose range but additive or antagonistic in other dose ranges. We are developing two new statistical methods – one parametric generalized response surface model and one semi-parametric model, which allow more general interaction patterns for the drug interaction and ease the restriction of the existing methods. Methods for constructing confidence interval for the estimate were also developed. Two S-PLUS codes are available for download from http://biostatistics.mdanderson.org/SoftwareDownload/ .

Key Research Accomplishments

- Provided statistical/data management support for Project 1, for both the Vanguard trial and the randomized Phase II trials (Celecoxib and Tarceva trials)
- Continued to provide enhancement of a web-enable database system to facilitate the conduct of the Vanguard Trial
- Worked on statistical methods for evaluating interaction for combination therapy to determine whether the effect is synergistic, additive, or antagonistic

Conclusion and Future Plans

Biostatistics and Data Management Core has continued to work actively with all the VITAL Projects in their research efforts, especially in the area of biostatistical support and consulting in the clinical trial design, implementation, and analysis of experimental results. In addition, the Core continued to enhance the web-enabled database system to facilitate the conduct of the trials and develop statistical methods for evaluating the interaction of the combination therapy. All project support and database management will continue as well as the development of new statistical methods as described above.

Core C: Pathology and Specimen Procurement Core

(Core and co-Core Director: Ignacio Wistuba, M.D.Adel K. El-Naggar, M.D.)

Aim 1 Develop and maintain a repository of tissue and other biologic specimens from patients enrolled on the clinical trials in Project 1.

Update

Using the procedures and system established for sample collection, processing, banking and distribution, we have acquired, processed and banked a total of 486 specimens from 34 patients enrolled in Vanguard clinical trial (Project 1). Samples from 34 baseline bronchoscopies have been obtained, processed and banked in the Core tissue bank (Table 6). In addition, resected specimens from lung cancer and head/neck tumors have been obtained, reviewed and banked.

Table 6. Summary of specimens collected and banked in the Pathology Core (34 baseline bronchoscopies)

Type of Specimen	Number
Sputum	40
Buccal Brush	40
Bronchial Brush	79
Bronchial Wash	41
Tissue Specimens	245
Total	**486**

A plan of bronchial brush and tissue specimen collection for Project 3 has been developed. Drs. Koo and Hittelman in Project 3 are interested in identifying the molecular abnormalities in the bronchial mucosa examined under the fluorescent bronchoscopy (LIFE instrument). They have obtained bronchial brush and tissue specimens from 7 bronchoscopies from patients having normal white light and abnormal LIFE bronchoscopy features (Table 7).

Table 7. Specimens collected for Project 3.

Case No.	Date	Sample ID
1	2/16/2006	K1-Wn/Ln
		K1-Wab/Lab
2	3/14/2006	K2-Wn/Ln
		K2-Wab/Lab
3	6/14/2006	K3-Wn/Ln
		K3-Wn/Lab
		K3-Wab/Lab
4	7/13/2006	K4-Wn/Ln
		K4-Wn/Lab
5	7/19/2006	K5-Wn/Ln (RML)
		K5-Wab/Lab (RML)
		K5-Wab/Lab (RUL)
		K5-Wab/Lab (LUL)
		K5-Wab/Lab (MC)
6	10/13/2006	K6-Wn/Ln
		K6-Wab/Lab
7	10/31/2006	K7-Wn/Ln
		K7-Wab/Lab

Note: Wn means white light normal; Wab means white light abnormal, Ln means LIFE normal, Lab mean LIFE abnormal.

Aim 2 Maintain a comprehensive database of tissue and specimen characteristics from patients enrolled in the clinical trials of Project 1, including pathologic characteristics of each specimen, inventory and distribution

Update

The Biostatistics Core has developed a web-based database, which has been used to catalogue all the specimens obtained and banked in the Pathology Core, and to report pathology diagnosis. From 34 enrolled patients, 750 biological specimens have been obtained, including 251 bronchial biopsies, 251 bronchial brushes, 42 bronchial washings, 41 buccal brushings, 42 broncoalveolar lavage, 82 NPBL and 41 sputum specimens. All have been tracked and inventoried using the web-site database. As LIFE bronchoscopy biopsies have been performed in all these patients, LIFE abnormalities have been entered in the database to be correlated with histopathological features.

Aim 3 Provide comprehensive pathologic characterization of all tissues and other biologic specimens and assist in preparation and evaluation of studies involving these tissues

Update

Using the comprehensive list of histology diagnoses for bronchoscopy biopsies prepared at the beginning of this project, we have processed and histopathologically diagnosed 218 tissue specimens from 34 baseline bronchoscopies in a timely fashion (Table 8). Two H&E-stained tissue sections have been examined per bronchial biopsy. Although normal bronchial epithelium has been detected in at least one site examined in most (94.6%) subjects, a number of histopathological changes have been detected. The most frequent abnormalities detected were goblet cell metaplasia and basal cell hyperplasia, both detected in 37.8% of patients. Of interest, squamous metaplasia and dysplasia were detected in 6 (16.2%%) and 3 (8.1%) of subjects, respectively. One patient had mild dysplasia only, one patient had mild and moderate dysplasia in two different sites, and one patient had only moderate dysplasia. No severe dysplasia, carcinoma *in situ* and invasive carcinoma have been detected to date. Histopathological analysis of the resected lung, and head/neck cancer samples has also been performed, in which squamous metaplastic and dysplastic lesions have been not detected. Tissue blocks from all these samples are available for future biomarker analysis.

Table 8. Summary of histopathology diagnosis of bronchial biopsies obtained from clinical trial (Project 1).

Diagnosis	Frequency by Site N (%)	Frequency by Patient N (%)
No Tissue/Denuded Epithelium	5 (2.1)	5 (13.5)
Normal Epithelium	167 (70.5)	35 (94.6)
Goblet Cell Metaplasia (GCM)	26 (10.9)	14 (37.8)
Basal Cell Hyperplasia (BCH)	22 (9.3)	14 (37.8)
Combined GCM/BCH	6 (2.5)	3 (8.1)
Squamous Metaplasia	7 (2.9)	6 (16.2)
Mild Dysplasia	4 (1.7)	3 (8.1)

Aim 4 Provide centralized immunohistochemistry and laser capture microdissection services, nucleic acid extractions and assistance with construction and evaluation of tissue arrays.

Update

As part of the Pathology Core, a centralized immunohistochemistry (IHC) laboratory with manual and automated immunohistochemical techniques and *in situ* tissue-based methodologies, such as FISH and laser capture microdissection available for investigators, is in place. Tissue microarray (TMA) construction is also in place (Figure 13), and a complete set of lung cancer specimens (N = 400) and corresponding bronchial and peripheral lung preneoplastic lesions N = 300) are available. A priority sample distribution list for VITAL individual projects is in place for IHC biomarker analysis using formalin-fixed and paraffin-embedded bronchial tissues. The samples obtained from the Clinical Trial (Project 1) have not been processed and distributed yet, because of the relatively small number of specimens obtained so far. Considering the slow patient accrual and limited specimens obtained from the Clinical Trial, the Pathology Core has developed the following strategy to compensate for the limits, and make specimens available for biomarkers validation to VITAL project investigators:

1) We are in the process of reviewing approximately 400 early stages (I to IIIA) lung cancer surgically resected specimens from our Institution from January 1/2003 to December 31/2005 to obtain archival formalin-fixed paraffin embedded specimens to identify tumor and adjacent normal or preneoplastic bronchial and bronchiolar epithelia. Detailed demographic and clinical information will be obtained in all these cases, including follow up for recurrence, secondary primary tumor development and survival.

Figure13. Examples of tissue microarrays (TMA) including preneoplastic lesion

2) From a subset of early lung cancer surgically resected cases in our Institution from 1997 to 2002, we have identified and selected 504 histologically normal and abnormal bronchial, bronchiolar and alveolar epithelium specimens (Table 9) to be examined for molecular marker expression using immunohistochemistry. All these specimens have been placed in tissue microarrays (TMAs). In collaboration with VITAL project investigators and collaborators , we have examined 21 immunohistochemistry markers (Table 10), most of which are related to potential targets for chemoprevention strategies. Survivin is exemplified of our effort in Project 5 below.

Table 9. Respiratory epithelium specimens placed in TMAs for IHC marker analysis.

Diagnosis	Number of Samples
Normal Epithelium	146
Hyperplasia	174
Squamous Metaplasia	28
Squamous Dysplasia	39
Squamous *Carcinoma In Situ*	47
Atypical Adenomatous Hyperplasia	70
Total	**504**

Table 10. Summary of immunohistochemistry markers examined in respiratory epithelium specimens placed in TMAs.

Markers examined by IHC in respiratory epithelium	
E-Cadherin	FGF
Caspase-8	FGFR1
STAT-5	FGFR2
P70S6K	Syndecan-1
NF-κB	Survivin (VITAL Project 5)
IRAK-1	SCC-1 (VITAL Project 3)
IGF (VITAL Project 5)	SCC-2 (VITAL Project 3)
IGFR1 (VITAL Project 5)	pCREB
EGFR (VITAL Project 5)	CREB
Caveolin-1	PTTG
FUS-1	

Survivin IHC Expression in the Early Pathogeneis of Lung Cancer.
One of the objectives of Project 5 was to assess the difference in the survivin expression among different lesion bronchial epithelium histologies obtained form lung cancer patients. Survivin expression was examined in normal tissue, atypical adenomatous hyperplasia (AAH) lesion, basal cell hyperplasia (BCH), squamous metaplasia (SQM), low- and high-grade (including carncinoma *in situ*) dysplasia lesions. A total of 379 lesions were obtained out of 94 lung cancer patients. Survivin expression levels were presented in the form of cytoplasm scores and nuclei scores (Figure 14). The main findings are summarized as the follows:

a) Survivin expression correlated with patient's smoking status. The survivin nuclei scores were marginally significantly correlated with patients' smoking status (p-value: 0.070). Non-smokers tended to have higher survivin expressions at the nuclei level than smokers.

b) Survivin nuclear and cytoplasmic expression is an early event in the pathogenesis of lung cancer and correlated with increasing severity of histopathologic changes. Survivin nuclei scores in normal lesions were significantly lower than those in the AAH lesions and the high-grade dysplasia lesions with the p-values of 0.030 and <0.0001, respectively. The high-grade dysplasia lesions had significantly higher survivin nuclei scores than the hyperplasia lesions, the low-grade dysplasia lesions and the SQM lesions (p-values: <0.0001, 0.002, 0.0004). The survivin cytoplasm scores in the high-grade dysplasia lesions were statistically significantly higher than those in the hyperplasia lesions, the normal lesions, and the SQM lesions with the p-values of <0.0001, 0.0001, and 0.010. The survivin cytoplasm scores in the low-grade dysplasia lesions were also significantly higher than those in the normal lesions, the hyperplasia lesions and the SQM lesions (p-values: 0.014, 0.004, 0.050).

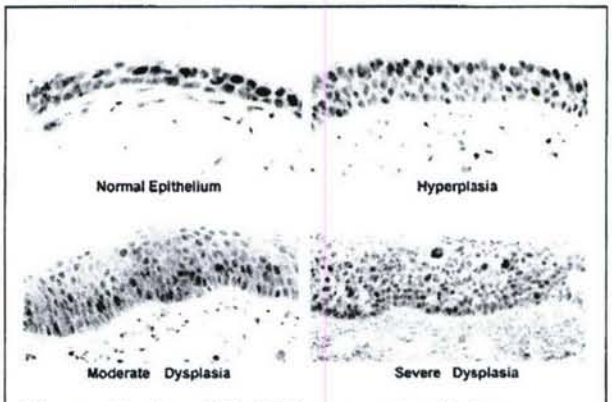

Figure 14. Survivin IHC expression in lung cancer preneoplastic lesions

In addition, we have helped Dr. John Minna on his three-dimensional organotypic culture of HBECs (Project 2.1 of VITAL). We have developed technology for histology and in situ techniques (IHC and FISH) to process and

evaluate the 3D cultures of immortalized HBECs developed by Dr. Minna's lab. The results were submitted to the 2006 AACR (Sato et al., #14261, 2006) (refer to Project 2). We have also examined histological and cytological characteristics of 130 of H&E stained sections from 3-D cultured developed by Dr. Minna's lab (Figure 15). We are in the process of setting up IHC markers to study the cell differentiation and molecular characteristics of cells present in those bronchial cells 3D cultures.

Key Research Accomplishments

- The Core has processed all patients' specimens and reported histology abnormalities of all bronchial biopsies of patients enrolled in Vanguard Trial in a timely fashion.
- The Core has significantly helped research projects by examining HBEC 3-dimensional cell cultures and helping to establish HBEC organotypic cultures from patients enrolled in Vanguard trial.
- Utilizing archival tissue specimens, the Core has helped to identify molecular abnormalities involved in the early pathogenesis of lung cancer, including those with survivin and IGF/R markers.
- The Core has identified molecular abnormalities involved in the early pathogenesis of EGFR mutated lung adenocarcinomas.

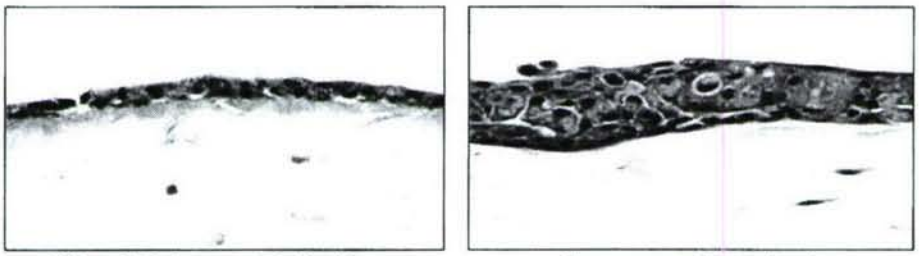

Ciliated Columnar Epithelium Squamous Metaplasia

Figure 15. 3-D organotypic cultures of human normal bronchial epithelial cell immortalized showing two types of histology characteristics

Conclusion and Future Plans

We have acquired and banked specimens from 251 bronchoscopy biopsies and 750 specimens from lung cancer and head/neck tumor patients, and used the web-enabled database developed by the Biostatistics Core to track and inventory bronchoscopy specimens and report histopathological features of the bronchial mucosa from the bronchoscopy biopsy. We have selected, prepared and examined a number of molecular markers in a large series (N = 504) of respiratory epithelium specimens by immunohistochemistry, which have been used to examine several IHC markers related to VITAL projects. We will continue to support all projects with pathology and cytology efforts and to perform molecular marker analysis and development as needed.

Additional Research Activities: Molecular Pathogenesis of Lung Cancer

The main goal of the VITAL research program is to provide a better understanding of the cellular and molecular events that drive lung tumorigenesis. Thus, using a molecular pathology approach, we have attempted to understand the early molecular pathogenesis of lung cancer.

We selected lung adenocarcinoma, the most frequent (~50%) histological type of lung cancer, which has a limited knowledge early molecular pathogenesis. Recent data suggest that at least two molecular pathways (*KRAS* and *EGFR*) are involved in the development of invasive lung adenocarcinomas in smokers and non-smokers, respectively.

Activity 1: Identify the abnormalities of *EGFR* in the pathogenesis of lung adenocarcinomas.

Update

We found that gene mutation and over-expression of *EGFR*, but not gene copy number, are early events in the pathogenesis of lung adenocarcinoma. A manuscript of detailed findings is in preparation for publication, and briefly summarized below.

Patterns of *EGFR* mutation in histologically normal epithelium. We have previously reported mutations in exon 19 and 21 of *EGFR* in at least one sample of microdissected normal small bronchial or bronchiolar epithelia obtained from lung cancer specimens from 9 of 21 (43%) patients with *EGFR* mutant adenocarcinomas, and none in 26 respiratory epithelia from 16 patients without mutation in the tumors (Tang et al., 2005). In the present study, we report mutation analysis of normal epithelium obtained from an additional 3 *EGFR* mutant and 10 wild-type lung adenocarcinomas this year, totaling 24 *EGFR* mutant cases and 26 wild type cases. Whereas the final overall rate of mutation in normal epithelium from mutant tumors is similar (12/24 cases, 50%; 23/85 sites, 27%), we detected *EGFR* exon 19 (15bp, 746-750) deletions in 6 sites of small bronchial (N = 4) and bronchiolar (N = 2) epithelium sites obtained from 3 wild-type tumors (Table 11). Thus, *EGFR* mutation has been found in normal epithelium in 3/26 (12%) wild-type adenocarcinomas and in 6/57 (11%) of the microdissected epithelial sites. Consistent with our previously reported data (Tang et al., AACR 2005), *EGFR* mutants in normal epithelia were detected in small bronchus (14/65, 30%) and bronchiole (15/77, 19%) in both mutant and wild-type tumor cases.

Table 11. Summary of EGFR abnormalities in normal bronchial epithelium from lung adenocarcinoma patients.

EGFR Abnormality	Sites N	Mutant Tumors	Wild-Type Tumors
Mutation	142	23/85 (27%)	6/57 (11%)
Copy Number	22		
Disomy		14 (64%)	ND
Low Trisomy		7 (32%)	ND
High Trisomy		1 (5%)	ND
Polysomy/Amplification		0	ND
EGFR IHC Expression Positive[1]	128	42/80 (53%)	30/48 (63%)
pEGFR IHC Expression Positive[1]	124	27/77 (33%)	15/47 (32%)

[1] Positive immunohistochemical expression score >200 (range 0-400)

TTF-1 immunohistochemical expression and *EGFR* mutation in normal epithelium. A higher level of immunohistochemical expression of nuclear transcriptional thyroid factor (TTF)-1, a crucial transcription factor of the lung, was recently reported in *EGFR* mutant lung adenocarcinomas than in wild-type tumors, suggesting that *EGFR* mutant in lung

adenocarcinoma originates from the terminal respiratory unit (TRU) (Yatabe et al., 2005). The TRU is composed of alveolar cells and nonciliated bronchiolar epithelium, and its characteristics are highlighted by the expression of TTF-1. We thus investigated the correlation between *EGFR* mutation and TTF-1 nuclear expression in tumor and normal epithelium sites. *EGFR* mutant adenocarcinomas (18/20 cases, 90%) demonstrated higher expression of TTF-1 compared to wild-type tumors (10/26 cases, 38%; $P < 0.001$). However, no significant difference ($P = 0.273$) in the frequency of TTF-1 immunohistochemical expression was detected comparing *EGFR* mutant (11/25 sites, 44%) and wild-type (34/105 sites, 33%) respiratory epithelia. Our findings indicate that normal bronchial epithelial cells expressing TTF-1 is not the exclusive precursors of EGFR mutant adenocarcinomas, and therefore, these tumors do not originate exclusively from TRU structures.

***EGFR* copy number in normal epithelium.** To determine the morphological stage in which *EGFR* copy abnormalities start in *EGFR*-mutant adenocarcinomas, we performed a precise mapping strategy and examined *EGFR* copy number in 22 normal bronchial epithelium sites obtained from 9 *EGFR*-mutant adenocarcinomas by FISH. These epithelial sites were also examined for *EGFR* mutation analysis. Of those, 4 normal epithelium sites had *EGFR* mutations in exons 19 (15bp-deletion) and 21 (L858R mutation). Most (14/22, 64%) of normal epithelia demonstrated no *EGFR* abnormalities (disomy), including 2 *EGFR* mutant sites. We did not identify any normal epithelia having *EGFR* amplification or high level of polysomy, which have been defined as increased gene copy number. All 9 tumor cases demonstrated at least one area of increased copy number. Our findings indicate that *EGFR* mutation precedes copy number abnormalities in the sequential pathogenesis of *EGFR*-mutant lung adenocarcinomas.

EGFR immunohistochemical expression in normal epithelium. Using a published (Hirsch et al., 2003) score system for EGFR IHC assessment of tumors and preneoplastic lesions of the lung, we evaluated the level of EGFR and pEGFR membrane expression in normal bronchial epithelia adjacent to *EGFR*-mutant and *EGFR* - wild-type lung adenocarcinomas. Overall, a relatively high level of EGFR (72/128, 56%) and pEGFR (42/124, 34%) expression was detected in normal respiratory epithelium sites. No significant differences were detected in the EGFR and pEGFR expression between normal epithelium and samples obtained from *EGFR*-mutant and *EGFR*-wild-type tumors (Table 12), structures of origin (small bronchus vs. bronchiole), or distance from the tumor. pEGFR positive expression in normal epithelium, but not EGFR, correlated with patients' smoking status, being higher in non- smokers than smokers (18/55, 25% vs. 6/54, 10%; $P = 0.0287$). Twenty-five normal epithelium sites adjacent to 9 *EGFR*- mutant adenocarcinomas were examined for *EGFR* mutation and EGFR and pEGFR immunohistochemcal expression. Of those, 19 (75%) and 10 (40%) epithelial sites were positive for EGFR and pEGFR expression, respectively (Table 12). Seven normal epithelium sites had *EGFR* mutation, and the level of EGFR and pEGFR expression was not significantly higher than wild-type epithelial sites. Thus, overexpression of EGFR and pEGFR is a common event in normal bronchial epithelium adjacent to lung adenocarcinomas, including *EGFR*- wild-type tumors, suggesting a mechanism regulating EGFR overexpression independent of increased copy number and mutation of *EGFR*.

Two abstracts (Tang and Bi et al, 2006; Tang and Varella-Garcia et al., 2006) were presented at the 2006 AACR meeting as attached in Appendix 2.

Table 12. Summary of EGFR abnormalities in the sequential pathogenesis and progression of lung adenocarcinoma (N = 9 cases)

Samples Sites	Gene Abnormalities		Protein IHC Expression	
	Mutation Positive	Increased Copy Number[1]	EGFR Positive[2]	pEGFR Positive[1]
Normal Epithelium	4/22 (18%)	0	19/25 (75%)	10/25 (40%)
Primary Tumor	57/59 (97%)	34/42 (81%)	42/65 (65%)[3]	13/52 (20%)[4]
Metastasis	28/30 (93%)	25/29 (86%)	27/31 (87%)[3]	21/31 (68%)[4]

[1] High polysomy and gene amplification
[2] Positive immunohistochemical (IHC) expression score >200 (range 0-400)
[3] Primary tumor vs. metastasis $P = 0.02$
[4] Primary tumor vs. metastasis $P < 0.00001$

Activity 2: Determine gene promoter hypermethylation in the respiratory mucosa field

Some of the molecular changes such as gene mutation, loss of heterozygosity and microsatellite alterations involved in the early pathogenesis of lung cancer have been shown throughout the respiratory mucosa as a field effect, we decided to examine whether gene promoter methylation (a mechanism of tumor suppressor gene inactivation) is also present as a field effect in the respiratory epithelium of lung cancer patients and smokers. We initially selected the Caveolin-1 (CAV1) gene to study.

Update

Caveolin-1 (Cav-1), an essential structural constituent of caveolae that plays an important role in cellular processes such as transport and signaling, has been implicated in the development of several cancers, including lung. Reduction and absence of Cav-1 expression has been reported in almost all small cell lung cancers (SCLC) and a subset of non-small cell lung cancers (NSCLC), mostly due to gene promoter methylation. To better understand the role of CAV1 gene in the early pathogenesis of lung cancers, we investigated its promoter methylation and IHC expression in the lung respiratory field by examining histologically normal respiratory epithelia adjacent to lung tumors. We studied formalin-fixed surgically resected tumor specimens from 100 lung cancers, including 40 SCLCs and 60 NSCLCs (48 adenocarcinomas, AC; 12 squamous cell carcinomas, SCC). For CAV1 methylation analysis, we extracted DNA from 202 precisely microdissected tissue sites, including 101 tumors and 101 normal epithelia (79 small bronchi and 22 bronchioles). Among normal epithelial sites, 30 were located inside tumors (INE), 60 closed to tumors (<1 mm, ONE), and 11 distant to tumors (DNE). The DNA was assessed by methylation specific polymerase chain reaction for CAV1 methylation and the results were confirmed by sequencing. Cav-1 IHC expression was studied in the same tumoral and epithelial sites examined for methylation. A high level of CAV1 methylation rate was detected in tumors, being more frequent in SCLC (100%) compared to AC (49%) and SCC (50%). NSCLCs, but not SCLCs, demonstrated heterogeneity in CAV1 methylation in 6 cases in which multiple tumor sites were examined. CAV1 methylation was also frequently detected in histologically normal respiratory epithelia adjacent to lung tumors, without differences in methylation frequency by lung tumor histology (SCLC 64%, AC 69% and SCC 63%), and type (bronchi 65% and bronchioles 66%) and location (INE 67%, ONE 66% and DNE 64%) of respiratory structures examined. CAV1 gene methylation was highly correlated with protein expression in tumor (90%) and normal epithelium (95%) tissue sites. Our findings indicate that CAV1 methylation is a frequent molecular abnormality in lung tumors, especially SCLC, and high frequency of Cav-1 abnormalities in normal bronchial and bronchiolar epithelia adjacent to

lung cancers suggests that CAV1 may be involved in the early pathogenesis of lung cancer as field effect. An abstract was submitted to the AACR 2007 (Tang et al., 2007).

Activity 3: Determine the role of the Epithelial to mesenchymal transition (EMT) in the early pathogenesis of lung cancer

Epithelial to mesenchymal transition (EMT) is a process where the cells undergo a developmental switch from epithelial to a motile mesenchyma. EMT occurs as key steps during embryonic morphogenesis, and is now implicated in the initiation, progression and metastasis of epithelial tumors. In lung cancer, the expression of individual EMT markers has been extensively studied and correlated with prognosis. EMT is reported to play a potential role as determinant of EGFR activity and predictor of EGFR tyrosine kinase inhibitor sensitivity in lung cancer, but its role has not been addressed in the early pathogenesis of lung cancer. Thus, we decided to begin our studies in this area of focus.

Update

First, we wanted to better define the EMT characteristics in lung cancers and to identify potential correlations with patients' clinicopathologic features. We studied theIHC expression of 8 EMT marker proteins, E-Cadherin, N-Cadherin, β-Catenin, Snail, MMP-9, NF-κB, Integrin-β6 and Vimentin, in 328 NSCLC (209 adenocarcinomas; 119 squamous cell carcinomas) and 38 SCLC, using formalin-fixed specimens placed in TMAs and image analysis. To correlate the expression of EMT markers with EGFR abnormalities, the IHC expression of EGFR and pEGFR was also examined in all tumors. EGFR mutational status was studied in a subset of 81 adenocarcinomas. Different expression patterns of EMT markers were identified in different lung cancer histologies, with sarcomatoid carcinomas showing the lowest expression ($p<0.0001$) of E-Cadherin, N-Cadherin and β-Catenin. SCLC demonstrated the lowest expression of Integrin-β6 ($p=0.0003$) and the highest expression of MMP-9 ($p=0.02$). Squamous cell carcinoma demonstrated significantly ($p<0.0001$) lower levels of E-Cadherin and N-Cadherin expression compared to adenocarcinoma. In NSCLC, tobacco history was statistically associated with higher expression of N-Cadherin ($p=0.03$), but lower expression of Integrin-β6 ($p=0.03$) and β-Catenin ($p=0.04$). We identified a positive correlation between the expression of E-Cadherin with β-Catenin ($p=0.03$) and MMP-9 ($p=0.01$), while E-Cadherin and Integrin-β6 correlated inversely ($p=0.009$). In NSCLC, EGFR and N-Cadherin expression correlated ($p=0.04$) inversely, and in the subset of adenocarcinoma, the presence of *EGFR* mutations correlated with higher intensity of E-Cadherin ($p=0.005$) and nuclear NF-κB ($p=0.03$). Our findings indicate that the EMT process correlates with tumor histology in lung cancer, smoking history, and EGFR abnormalities in NSCLC. We will next study the EMT in NSCLC resected specimens and in the lung cancer histologically normal and abnormal (preneoplastic lesions).

Developmental Research Project (DRP) 2: Biomarkers for Aggressive Lung Carcinomas in African American Men

(PI: Sharon Lobert, Ph.D., University of Mississippi, Jackson, MS)

Biological factors, in addition to health care access, are likely to contribute to the disparity in survival for Caucasian men and African American men diagnosed with lung cancer. Lung tumors are classified into two major categories: small cell lung cancer (SCLC and NSCLC. The heterogeneity of NSCLCs complicates efforts to determine prognosis and select appropriate treatment regimens. β class III tubulin has been identified as a marker of neuroendocrine differentiation in lung cancer and as a potentially important biomarker for aggressive tumors

(SCLC, neuroendocrine type large cell carcinomas, and some adenocarcinomas). Our proposed research focuses on two hypotheses: 1) β class III tubulin levels are higher in NSCLCs from African American men compared to white men; and 2) the expression of proteins that alter microtubule dynamics is increased in NSCLCs from African American men compared to white men. Higher levels of these proteins would reduce the effectiveness of antimitotic agents used in the treatment of NSCLC that stabilize (paclitaxel) or destabilize (vinorelbine) mitotic spindles. Stages IA, IB and IV NSCLCs (n = 80) will be obtained from the NCI Cooperative Human Tissue Network and quantitative real-time RT-PCR will be used to measure tubulin isotype, stathmin and MAP4 mRNA levels. Equal numbers of samples from white and African American males will be examined. Western blotting will be used to verify protein levels.

Update

Year one

Goal: Quantify and compare biomarker levels (7 β-tubulin isotypes, stathmin and MAP4) in NSCLCs from African American and white men using real-time RT PCR. Samples will also be prepared for later protein quantification.

1. **Tissues (n = 80) will be obtained from the NCI Cooperative Human Tissue Network (CHTN).**

   We have obtained 62 samples from Caucasian patients and 20 from African American patients.

2. **Tissues will be processed to extract mRNA and conditions for real-time RT-PCR experiments will be optimized.**

   We have processed 45 tumor samples from Caucasian patients and 20 tumor samples from African American patients to obtain total RNA samples for qRT-PCR, and have designed primers and made standards for all seven β-tubulin istotypes, stathmin and MAP4.

3. **Real-time PCR experiments will be done as sufficient numbers of samples are obtained.**

   We have completed qRT PCR for all 7 β-tubulin isotypes for 28 Caucasian patient tissues and 14 African American patient tissues (Figures 16 and 17). The data were collected as triplicate samples on each qRT-PCR plate and 2-4 plates to demonstrate reproducibility. Quality controls were used on each plate to establish the validity of the standard curves. Thus, for tubulin isotypes we have completed data collection for 882 samples with standard curves in 2-4 individual experiments (50-60 samples/plate x 2-4). Demographic data and data from pathology reports will be used in the analysis: age, race, description (squamous cell, adenocarcinoma, large cell carcinoma), tumor stage, tumor size, differentiation (well, moderately or poorly differentiated). These data has been entered into a spreadsheet with the sample number. We are currently working on qRT-PCR for β-tubulin isotypes for the remaining 6 samples from African American patients and 17 samples from Caucasian patients that we have processed. Figures 16 and 17 show pooled data from NSCLCs sample for African American and Caucasian patients. The sample number so far for each category is too small to separate the two patient groups (African American and Caucasian).

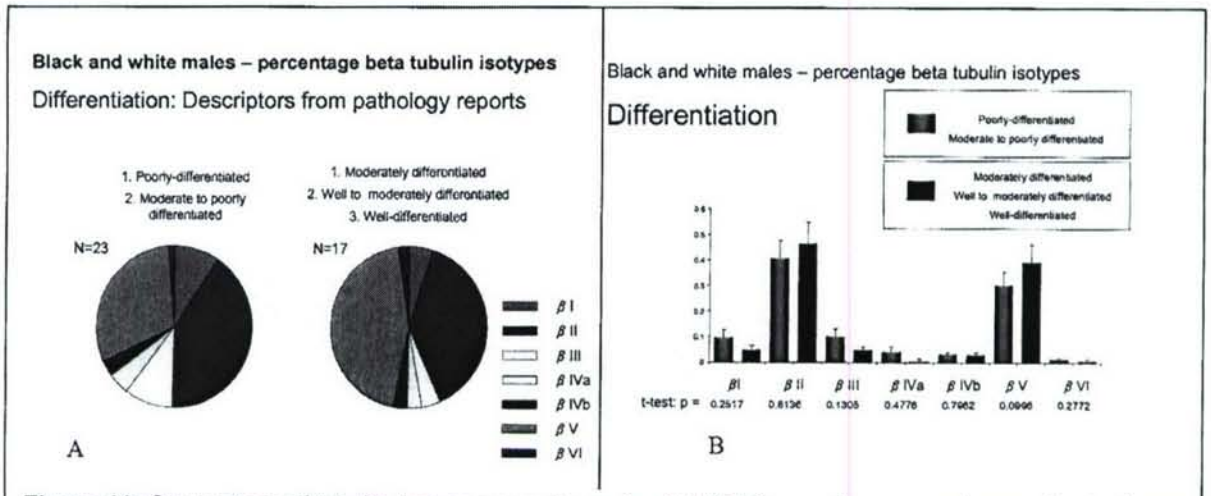

Figure 16. Comparison of tubulin isotype percentages in all NSCLC samples grouped according to tissue differentiation (combined samples from Caucasian and African American patients). Panel A: pie charts. Panel B: bar graph with t-test results showing no significant difference between the two differentiation groupings.

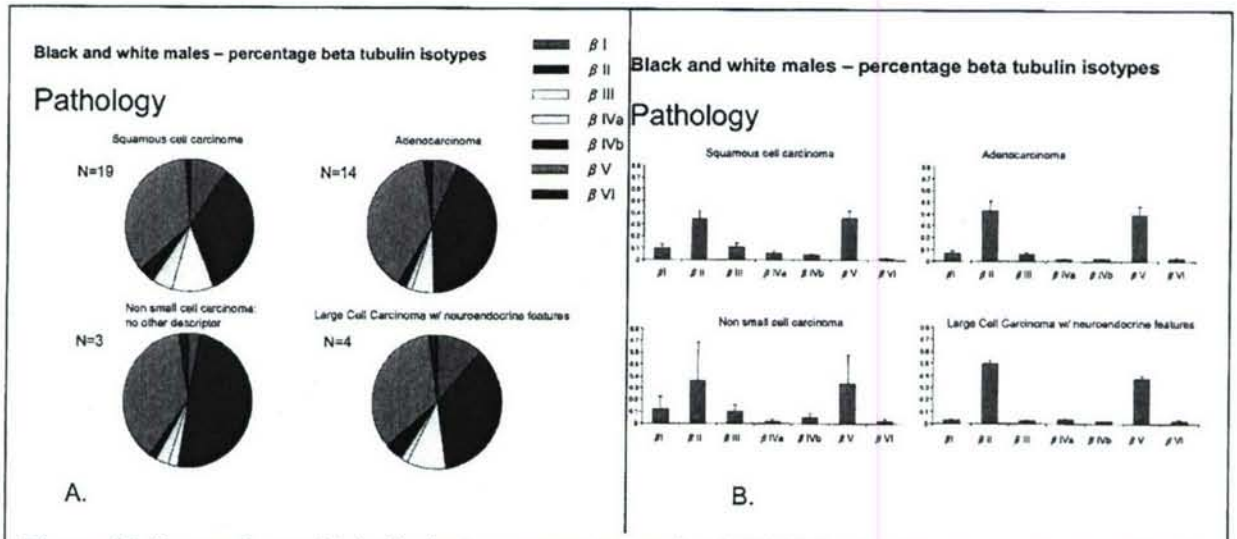

Figure 17. Comparison of tubulin isotype percentages in all NSCLC samples grouped according to pathology report diagnosis (combined samples from Caucasian and African American patients). Panel A: pie charts. Panel B: bar graph with error bars.

We have completed qRT-PCR measurements for MAP4 and stathmin for 20 NSCLC samples from African American patients and 45 NSCLC samples from Caucasian patients (Figure 18). This data set includes 585 total samples (triplicate samples on 3 separate 96 well plates).

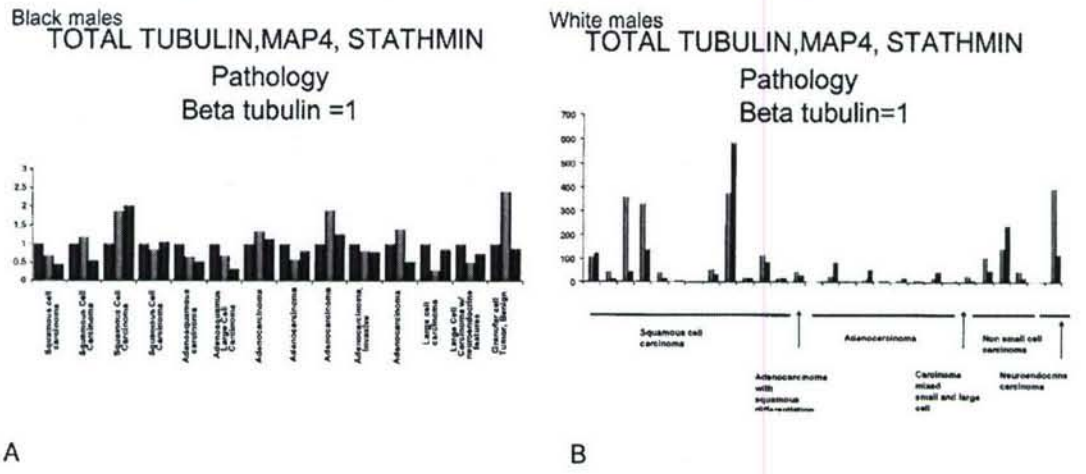

Figure 18. Comparison of total tubulin (red), stathmin (light green) and MAP4 (dark green) levels for NSCLC samples from Panel A: African American patients (n = 14) and Panel B: Caucasian patients (n = 28). The total tubulin, stathmin and MAP4 levels for all 14 samples from African American patients and 8 of the samples from Caucasian patients show close agreement in mRNA copy number, suggesting common regulatory mechanisms may be involved. However 20 of the samples from Caucasian patient do not show close agreement between total tubulin and MAP4 or stathmin. Note that this is a subset of the total samples collected so far. We are completing the measurements of tubulin isotypes in 6 samples from African American patients and 17 samples from Caucasian patients. The stathmin and MAP data collection is complete for 20 samples from African American patients and 45 samples from Caucasian patients.

4. Tissues will also be processed for protein extraction and samples frozen for later Western blotting.

All 45 samples from Caucasian patients and 20 from African American patients have been processed for protein extraction. Samples are kept in SDS sample buffer at -80°C.

Year two

Goal 1: Continue to quantify and compare β-tubulin isotypes, stathmin and MAP4 levels in NSCLCs as in year 1. This continues to be the major focus of the work (see above).

Goal 2: Begin examining protein levels (β-tubulin isotypes, stathmin and MAP4) by quantitative and semiquantitative Western blotting in samples prepared from the NSCLCs.

All the antibodies that will be used in the Western blotting have been tested. The procedure for quantitative Western blotting for tubulin isotypes has been developed (Hiser et al., 2006). We have selected patient samples representing high and low β-tubulin classes II and V. Quantitative Western blotting is currently being done to measure all β-tubulin classes I, II, III, IVa+b, and V. Results from these experiments will be compared with the mRNA levels measured by qRT-PCR. We will also do semi-quantitative Western blotting to measure stathmin and MAP4 levels in these samples.

Year three

Goal: Complete the comparison of β-tubulin isotypes, stathmin, and MAP4 by quantitative and semiquantitative Western blotting.

We plan to continue qRT-PCR experiments on NSCLC tissue samples from African American patients. We anticipate by the end of year three, we will have 8-10 more samples for a total of 28-30 samples from African American patients. Although this falls short of our planned 40 samples, we anticipate we will be able to do comparisons with the 45 samples from Caucasian patients. Further, since we have an abundance of NSCLC samples from Caucasian patients, we plan to continue to process them to add to the pools of well, moderate or poorly differentiated samples. These may allow us to identify trends that indicate whether tubulin, MAP4 and/or stathmin may be useful as biomarkers.

During the final stage of this developmental research grant, we are currently developing a manuscript describing the results of this project and discussing the implications for management of lung cancer, and will submit an abstract to the 2007 Annual Meetings of the American Association for Cancer Research in Los Angeles.

Key Research Accomplishments

- Forty-five NSCLC tissues from Caucasian patients and 20 from African American patients have been processed for RNA and protein samples.
- qRT-PCR experiments have been completed for all 7 β-tubulin isotypes for 28 Caucasian and 14 African American lung tumor samples. Preliminary data analysis has been done.
- qRT-PCR experiments have been completed for 45 NSCLC samples from Caucasian patients and 20 from African American patients for MAP4 and stathmin.
- A spreadsheet with demographic data, pathology data, and experimental data has been created. Data for each sample is entered into the spreadsheet as the tissue is processed. Data analysis is underway. After all data collection is complete and all data have been transferred to the spreadsheet, nonparametric multivariate statistical models will be used to fit the data and assess statistical correlations.
- The procedure for quantitative Western blotting for β-tubulin isotypes has been developed. Western blotting to verify tubulin isotype, stathmin and MAP4 qRT-PCR findings are underway.

Conclusions and Future Plans

- β-tubulin classes II and V are found to be abundant in lung tumor tissues for the first time, which may be important to sequence β-tubulin classes II and V genes for mutations that may be associated with paclitaxel resistance.
- No significant correlation between β-tubulin isotype classes and extent of tissue differentiation as reported in the pathology records for these samples. If our analysis of the remaining samples support this finding, these data will agree with our previous findings suggesting that factors other that tubulin isotype levels are important in tumor or cell culture resistance to antimitotic agents (Hiser et al., 2006; Dozier et al., 2003). It is our hypothesis that proteins that regulate mitotic spindle dynamics or secondary targets for antimitotic drugs may play an important role in tumor response to these drugs. For example, the tumor suppressor protein p53 is thought to regulate stathmin and MAP4 transcription (Zhang et al, 1999; Ali et al., 2002). These two proteins play a role in the

regulation of mitotic spindles and also may impact the tumor response to antimitotic agents (Curmi et al, 2000).

- Stathmin and MAP4 mRNA levels are in close agreement in all samples, suggesting a common regulatory mechanism.
- For 8 of the 28 NSCLC samples from Caucasian patients, the stathmin or MAP4 levels differ from the total tubulin mRNA copy number by > 100-fold. Six of these 8 samples are poorly or moderately - poorly differentiated. Although this observation does not explain differences in disease severity for African American patients with NSCLC compared to Caucasian patients, it does merit further exploration.
- We will perform the Western blotting analyses and compare the results with qRT-PCR.
- We will complete all analyses and determine biomarker trends associated with Caucasian versus African American patients.

KEY RESEARCH ACCOMPLISHMENTS

Project 1: Biologic Approaches for Adjuvant Treatment of Aerodigestive Tract Cancer

- 36 patients were enrolled in Vanguard trial.
- Patient clinical data and tissues have been and continue to be collected and will be distributed to support research projects in the VITAL grant.
- The adjuvant celecoxib trial is open and has enrolled 1patient
- The adjuvant erlotinib protocol was submitted to our IRB and the DOD for review.
- New recruitment strategies have been used to increase patient accrual, including distributing patient brochures, directly contacting potential patients, increasing referrals from other disciplines, and advertising the trials by website and local radio.

Project 2: Identification of Biomarkers of Response to Chemoprevention Agents in Lung Epithelium

- Established additional immortalized human bronchial epithelial cell (HBEC) strains from multiple donors
- Genetically manipulated the HBECs to derive isogenic strains that expressed oncogenic KRAS, mutant EGFR, and/or loss of p53 expression as well as HBECs with various EGFR tyrosine kinase domain mutations alone or with p53 knockout, and characterized their biologic and gene expression behavior showing they had progressed part of the way toward malignancy
- Identified gene expression signatures associated with the introduction of oncogenic changes into the HBEC cells
- Determined IC_{50}s for all 13 HBE cell lines for Tarceva
- Demonstrated progression of oncogenically manipulated HBECs to full malignancy after biologic selection in soft agar
- Determined protein profiles related to lung tumorigenesis using immmobilized metal ion adsorption chromatography
- Detected low-abundant proteins in human plasma proteome by using multi-lectin affinity chromatography and two-dimensional gel electrophoresis

Project 3: Premalignant Bronchial Epithelia - Molecular and Cellular Characterization of Lung Tumorigenesis

- Collected high quality RNA from brushings and isolated bronchial epithelial cells from biopsies of LIFE normal and LIFE abnormal. Successfully set up culture to reconstitute bronchial epithelium in these specimens.
- Demonstrated that our organotypically cultured bronchial epithelial cells isolated from biopsies of LIFE normal and LIFE abnormal bronchial epithelium reflects expression profile of bronchial epithelial cells *in vivo*, which provided a useful model for our future work using cultured bronchial epithelial cells.
- Demonstrated that LIFE normal and LIFE abnormal bronchial epithelial cells had differences at the molecular level, although they didn't show obvious morphological differences in histologic evaluation of cultures, which might reflect the gene expression difference in early stage of tumorigenesis.
- Demonstrated that LIFE abnormal epithelial cells had higher aggressive tendency than LIFE normal cells. The genes responsible for this character might play an important role in lung tumorigenesis and tumor development.
- Demonstrated that chromosome instability in bronchial epithelial cells occurred in cells proliferating away from the basal layer and was associated with a stress response in the cells associated with phosphorylation of Histone H2AX.

- Demonstrated that immortalized HBECs derived from different individuals show differential takeover ability when placed in competition with normal bronchial epithelial cells and with each other.
- Demonstrated that EGFR expression and phosphorylation patterns may be spatially regulated in two-dimensional and three-dimensional culture conditions, perhaps reflective of specific cellular processes including proliferation and migration.

Project 4: Modulation of Death Receptor-Mediated Apoptosis for Chemoprevention

- Determined that several groups of the compounds with cancer therapeutic potential including celecoxib and its derivative, proteasome inhibitors, triterpenoids, PPARγ ligands, and FTIs modulated DR5 expression and/or c-FLIP levels (mostly by downregulation), which contribute to induction of apoptosis and/or enhancement of TRAIL-induced apoptosis.
- Determined that celecoxib and DMC increased p-Akt levels in a time-dependent fashion while inducing DR5 and downregulating cFLIP in some lung cancer cell lines but not all and that LY294002 blocks this phosphorylation in a cell-dependent effect.
- Found that CHOP/GAD153 mediated FTI (SCH66336)-induced DR5 expression.

Project 5: Molecular Strategies Targeting the AKT Signaling Pathway for Lung Cancer Chemoprevention and Therapy

- EGFR TKIs, including erlotinib and gefitinib, were found to increase the levels of EGFR:IGF-1R heterodimer localized on cell membrane, activate IGF-1R and its downstream signaling mediators, and stimulate mammalian target of rapamycin (mTOR)-mediated de novo protein synthesis of EGFR and survivin in NSCLC cells. Inhibition of IGF-1R activation, suppression of mTOR-mediated protein synthesis, or knockdown of survivin expression abolished resistance to the EGFR TKIs and induced apoptosis in NSCLC cells *in vitro* and *in vivo*.
- Determined that SCH66336 significantly suppressed HNSCC tumor growth and angiogenesis via mechanisms that are independent of H-Ras and RhoB. By inducing IGFBP-3 secretion from HNSCC cells, this compound suppresses angiogenic activities of endothelial cells.
- Determined that the combination of IGFB3 and SCH66336 produced synergistic antiproliferative effects *in vitro* and *in vivo* by inducing apoptosis. A greater combined efficacy was observed in the downregulation of the antiapoptotic Bcl-xL and prosurvival kinase Akt protein expression and increase in the level of proapoptotic IGFBP-3 protein in comparison to each drug alone.
- Discovered that the IGF axis is a potential target for chemoprevention by 9-*cis*-retinoic acid and IGF-1/IGFBP3 may serve as surrogate markers.

Core B: Biostatistics & Data Management Core

- Provided statistical/data management support for Project 1, for both the VANGUARD trial and the randomized Phase II trials (Celecoxib and Tarceva trials)
- Continued to provide enhancement of a web-enable database system to facilitate the conduct of the VANGUARD Trial
- Worked on statistical methods for evaluating interaction for combination therapy to determine whether the effect is synergistic, additive, or antagonistic

Core C: Pathology and Specimen Procurement Core

- The Core has processed all patients' specimens and reported histology abnormalities of all bronchial biopsies of patients enrolled in Vanguard Trial in a timely fashion.

- The Core has significantly helped research projects by examining human bronchial epithelial cells (HBEC) 3-dimensional cell cultures and helping to establish HBEC organotypic cultures from patients enrolled in Vanguard trial.
- Utilizing archival tissue specimens, the Core has helped to identify molecular abnormalities involved in the early pathogenesis of lung cancer, including Survivin and IGF/R markers.
- The Core identified molecular abnormalities involved in the early pathogenesis of EGFR mutated lung adenocarcinomas.

DRP-2: Biomarkers for Aggressive Lung Carcinomas in African American Men

- Forty-five NSCLC tissues from Caucasian patients and 20 from African American patients have been processed for RNA and protein samples.
- qRT-PCR experiments have been completed for all 7 β-tubulin isotypes for 28 Caucasian and 14 African American lung tumor samples. Preliminary data analysis has been done.
- qRT-PCR experiments have been completed for 45 NSCLC samples from Caucasian patients and 20 from African American patients for MAP4 and stathmin.
- A spreadsheet with demographic data, pathology data, and experimental data has been developed. Data for each sample is entered into the spreadsheet as the tissue is processed. Data analysis is underway. After all data collection is complete and all data have been transferred to the spreadsheet, nonparametric multivariate statistical models will be used to fit the data and assess statistical correlations.
- The procedure for quantitative Western blotting for β-tubulin isotypes has been developed. Western blotting to verify tubulin isotype, stathmin and MAP4 qRT-PCR findings are underway.

REPORTABLE OUTCOMES

Publications:

Articles *(attached in Appendix 2)*

1. Morgillo F, Woo JK, Kim ES, Hong WK, Lee H-Y. Heterodimerization of IGFR/EGFR and Induction of Survivin Expression Counteracts the Antitumor Action of Erlotinib. *Cancer Res* 66:10100-11, 2006.
2. Oh SH, Kim W-Y, Woo J-K, Kim J-H, Younes MN, Myers JN, Hong WK, Lee H-Y. Identification of insulin-like growth factor binding protein-3 as a farnesyltransferase inhibitor SCH66336-induced negative regulator of angiogenesis in head and neck squamous cell carcinoma. *Clin Cancer Res* 12: 653-61, 2006.
3. Lee H-Y, Chang YS, Han J-Y, Liu D, Lee JJ, Lotan R, Hong WK. Effects of 9-*cis*-retinoic acid on the insulin-like growth factor axis in former smokers. *J Clin Onc* 23:4439-49, 2005.
4. Kong M, Lee JJ. A generalized response surface model with varying relative potency for assessing drug interaction. *Biometrics* 62:986-95, 2006.
5. Liu XG, Yue P, Schonthal AH, Khuri FR, Sun S-Y. Cellular FLICE-Inhibitory Protein Down-regulation Contributes to Celecoxib-Induced Apoptosis in Human Lung Cancer Cells. *Cancer Res* (Priority Report) 66:11115-9, 2006.
6. Zou W, Liu X, Yue P, Khuri RK, Sun S-Y. PPARγ ligands enhance TRAIL-induced apoptosis through DR5 upregulation and c-FLIP downregulation in human lung cancer cells. *Cancer Biol Ther* 6:1, e1-e8, 2006.
7. Wistuba I. Genetics of Preneoplasia: Lessons from Lung Cancer. *Current Mol Med* (in press), 2007.

8. Sato, M., Vaughan, M. B., Girard, L., Peyton, M., Lee, W., Shames, D. S., Ramirez, R. D., Sunaga, N., Gazdar, A. F., Shay, J. W., and Minna, J. D. Multiple oncogenic changes (K-RASV12, p53 knockdown, mutant EGFRs, p16 bypass, telomerase) are not sufficient to confer a full malignant phenotype on human bronchial epithelial cells. *Cancer Res* 66:2116-28, 2006.

Manuscripts submitted, in revision or review

1. Kong M, Lee JJ. A semiparametric model for assessing drug interaction. *Biometrics* (in revision), 2006.
2. Lee JJ, Kong M, Ayers D. A tutorial for determining drug interaction in combination therapy. *J Biopharma Stat* (submitted), 2006.
3. Lee JJ, Kong M. Confidence interval for interaction index for assessing multiple drug interaction. *Stat Biopharm Res* (submitted), 2006.
4. Sun S-Y, Liu X, Yue P, Zhou Z, Zou W, Marcus AI, Khuri FR. The CHOP-dependent upregulation of death receptor 5 expression contributes to farnesyltransferase inhibitor-induced apoptosis in human cancer cells. *Mol Cell Biol* (in review), 2006.
5. Qiu Y, Liu X, Yue P, Lonial S, Khuri RK, Sun S-Y. The farnesyltransferase inhibitor R115777 upregulates DR5 expression and enhances TRAIL-induced apoptosis in human lung cancer cells. *Cancer Res* (in review), 2006.
6. Liu XG, Yue P, Chen S, Hu L, Lonial S, Khuri RK, Sun S-Y. The proteasome inhibitor PS-341 upregulates death receptor 5 expression leading to induction of apoptosis and enhancement of TRAIL-induced apoptosis despite upregulation of c-FLIP and survivin in human lung cancer cells. *Cancer Res* (in review), 2006.

Abstracts *(attached in Appendix 2)*

1. Chen S, Liu X, Yue P, Schönthal AH, Khuri RK, Sun S-Y. Dimethyl-celecoxib, a derivative of the COX-2 inhibitor celecoxib that lacks COX-2 inhibitory activity, sensitizes human lung cancer cells to tumor necrosis factor-related apoptosis-inducing ligand (TRAIL) through induction of DR5 and downregulation of c-FLIP. *AACR*, 2007.
2. Zou W, Chen S, Liu X, Yue P, Sporn MB, Khuri RK, Sun S-Y. c-Jun N-terminal kinase (JNK)-independent c-FLIP downregulation contributes to induction of apoptosis by the novel synthetic triterpenoid methyl-2-cyano-3, 12-dioxooleana-1, 9-dien-28-oate (CDDO-Me) in human lung cancer cells. *AACR*, 2007.
3. Lu T, Wistuba II, Hittelman WN. Existence of clonal and subclonal outgrowths of premalignant and stromal cells in the upper aerodigestive tract of current smokers. *Proceedings of AACR* 47: #462, 2006.
4. Lu T, Wistuba II, Hittelman WN. Increased genetic instability and metastases from spontaneous murine lung adenocarcinomas with K-ras and p53 R172HΔg mutations. *AACR*, 2007.
5. Tang X, Varella-Garcia M, Xavier AC, Bi XQ, Ozburn N, Hong WK, Wistuba II et al. Analysis of EGFR abnormalities in the sequential pathogenesis and progression of lung adenocarcinoma (Poster). *Proceedings of AACR* 47: #69, 2006.
6. Tang X, Bi XQ, Ozburn N, Hong WK, Wistuba II et al. "Field" defect abnormalities in lung adenocarcinoma: KRAS vs. EGFR mutant tumors (Platform Presentation). *Proceedings of AACR* 47: #5683, 2006.
7. Tang X. et al. Caveolin-1 Gene Methylation is a Field Effect Phenomenon in Lung Cancer Patients. *AACR*, 2007.
8. Sato M, Lee W, Girard L, Ramirez RD, Shames DS, Gazdar AF, Shay JW, Minna J D. Oncogenic manipulation and biologic selection for complete tumorigenic transformation of immortalized normal human bronchial epithelial cells. *Proceedings of AACR* 47: #669, 2006.

9. Ren H, Hawke D, Chu Z, Mao L. Protein profiles of lung tumorigenesis using immmobilized metal ion adsorption chromatography. *Proceedings of AACR* 47: #3582, 2006.
10. Kawaguchi H, Ren H, Lang W, Chu Z, Fan Y-H, Mao L. Detecting low-abundant proteins in human plasma proteome by using multi-lectin affinity chromatography and two-dimensional gel electrophoresis. *Proceedings of AACR* 47: #2864, 2006.

Resources:

- Development of immortalized HBEC lines including those with multiple oncogenic changes, which are being made available to multiple collaborators.
- We have also developed additional immortalized HBECs and deposited them in ATCC for worldwide distribution.

CONCLUSIONS

In the third grant year, the VITAL research projects have been proceeding well with respect to their specific aims, and have started to use the patient samples collected from the Vanguard trial, especially Projects 2, 3, and 5 with the support of the VITAL Pathology Core. The Vanguard trial continues to enroll patients and we expect accrual to increase with all the additional efforts to disseminate the trial information and reach patients (e.g. trial brochures, radio ads) and with the participation of Methodist Hospital this coming year.

In 2006, we had 8 publications including 3 in *Cancer Research*, 1 in *Journal of Clinical Oncology*, and 1 in *Clinical Cancer Research*, 10 scientific abstracts submitted to the *AACR* annual meeting, and 6 manuscripts in review, revision, or submitted. We have also developed additional immortalized HBECs and deposited them in ATCC for worldwide distribution. Those cell lines with multiple oncogenic changes will be available to collaborators. Based on the work done at this point, several conclusions can be drawn for the individual projects:

Project 1 continues to make maximum effort to improve the patient accrual and ensure the high quality of the clinical data and patient samples collected and distributed to the research investigators in the VITAL program.

Project 2 continued to establish additional immortalized HBEC lines from donors, which was used to assess the contribution of individual genetic alterations to the tumorigenesis of lung cancer. Specific gene expression signatures are associated with the introduction of oncogenic changes and specific alterations of KRASV12 and p53 induced partial progression to full malignancy, whereas clonal isolation was necessary to induce full malignancy. Methods were developed to characterize the protein profiles, including those of low-abundance, associated with tumorigenesis.

Project 3 improved the ability to reconstruct bronchial epithelium *in vitro* from biopsies of LIFE normal and LIFE abnormal areas. The *in vitro* cultured bronchial epithelial cells accurately reflect expression profile of bronchial epithelial cells *in vivo*. LIFE normal and abnormal bronchial epithelial cells had differences at the molecular level. The cultured bronchial epithelial cells derived from LIFE abnormal areas shows higher invasive tendency than those from LIFE normal areas, as expected.

Project 4 concludes that appropriate modulation of the extrinsic death receptor-mediated apoptotic pathway through such mechanisms as the upregulation of DR5 and/or reduction of c-FLIP levels by small molecules (e.g., celecoxib, lonafarnib, bortezomib) may eliminate premalignant or malignant lung epithelial cells via promoting apoptotic cell death to achieve cancer chemopreventive and therapeutic goals. Moreover, the potential use of the DR5 and c-

FLIP as predictive biomarkers for response to certain drugs in the clinic warrants further investigation.

Project 5 concludes that integration of IGF-1R-targeted agents is required when EGFR TKIs are used to treat lung cancer patients; IGFBP-3 mediates antitumor activities of SCH66336 in HNSCC by inhibiting angiogenesis; the combination of IGFB3 and SCH66336 produced synergistic antiproliferative effects; and the IGF axis is a potential target for the chemopreventive activities of 9-*cis*-RA.

Core B: Biostatistics and Data Management. has continued to work actively with all the VITAL Projects in their research efforts, especially in the area of biostatistical support and consulting in the clinical trial design, implementation, and analysis of experimental results. In addition, the Core continued to enhance the web-enabled database system to facilitate the conduct of the trials and develop novel statistical methods for the evaluation of the interactions in combination therapy.

Core C: Pathology and Specimen Procurement. has acquired and banked specimens from 245 bronchoscopy biopsies and 37 resected specimens from lung cancer and head/neck tumor patients, and used the web-enabled database developed by the Biostatistics Core to track and inventory bronchoscopy specimens and report histopathological features of the bronchial mucosa from the bronchoscopy biopsy. They have selected, prepared and examined a number of molecular markers including several markers related to VITAL projects in a large series (N = 504) of respiratory epithelium specimens by immunohistochemistry.

DRP-2 concludes that β-tubulin classes II and V are abundant in lung tumor tissues, which may be important to sequence β-tubulin classes II and V genes for mutations that may be associated with paclitaxel resistance; there is no significant correlation between β-tubulin isotype classes and extent of tissue differentiation; Stathmin and MAP4 mRNA levels are in close agreement in all samples, suggesting a common regulatory mechanism; the stathmin or MAP4 levels differ from the total tubulin mRNA copy number by > 100-fold as determined from for 8 of the 28 NSCLC samples from Caucasian patients. Six of these 8 samples are poorly or moderately - poorly differentiated.

REFERENCES

- Ali, E., Bash-Bablula, J, Yang, J.-M., and Hait, W.N. Effect of Stathmin on the Sensitivity to Antimicrotubule Drugs in Human Breast Cancer. *Cancer Res* 62, 6964-9, 2002.
- Chun K-H, Lee H-Y, Hassan K, Khuri FR, Hong WK, and Lotan R. Implication of protein kinase B/Akt and Bcl-2/Bcl-xl suppression by the farnesyl transferase inhibitor SCH66336 in apoptosis induction in squamous carcinoma cells. *Cancer Res* 63, 4796–800, 2003.
- Curmi, P.A., Nogues, C., Lachkar, S., Carelle, N., Gonthier, M.-P., Sobel, A., Lidereau, R., and Bieche, I. Overexpression of Stathmin in Breast Carcinomas Points Out to Highly Proliferative Tumours. *Brit J Cancer* 82, 142-50, 2000.
- Dozier, J.H., Hiser, L., Davis, J.A., Stubbs-Thomas, N., Tucci, M.A., Benghuzzi, H.A., Frankfurter, A., Correia, J.J. and Lobert, S. β-Class II Tubulin Predominates in Normal and Tumor Breast Tissues. *Breast Cancer Res* 5, R157-69, 2003.
- Han J-Y, Liu DD, Lee JJ, Kurie JM, Lotan R, Hong WK, Lee H-Y. 9-*cis*-retinoic acid treatment increases serum concentrations of α-tocopherol in former smokers. *Clin Cancer Res* 11:2305-11, 2005.
- Hirsch FR, Varella-Garcia M, Bunn PA, Jr., Di Maria MV, Veve R, Bremmes RM, et al. Epidermal growth factor receptor in non-small-cell lung carcinomas: correlation between

gene copy number and protein expression and impact on prognosis. *J Clin Oncol.* 21:3798-807, 2003.

- Hiser L, Aggarwal A, Young R, Frankfurter A, Spano A, Correia JJ, Lobert, S. Comparison of β-Tubulin mRNA and Protein Levels in 12 Human Cancer Cell Lines. *Cell Motil Cytoskel* 63, 41-52, 2006.
- Kanehisa M. A database for post-genome analysis. *Trends Genet* 13, 375-6, 1997.
- Lee H-Y, Oh SH, Woo J-K, Price R, Cody D, Tran H, Hong WK. Chemopreventive effects of deguelin, a novel Akt inhibitor, on tobacco-induced lung tumorigenesis. *JNCI* 97: 1695-9, 2005.
- Lee H-Y, Moon HJ, Chun K-H, Chang YS, Hassan K, Ji L, Lotan R, Khuri FR, and Hong WK. Effects of insulin-like growth factor binding protein-3 and farnesyl transferase inhibitor SCH66336 on Akt expression and apoptosis in non–small cell lung cancer cells. *JNCI* 96: 1536-48, 2004.
- Liu X, Yue P, Zhou Z, Khuri FR, Sun S-Y. Death receptor upregulation and celecoxib-induced apoptosis in human lung cancer cells. J Natl Cancer Inst, 96:1769-1780, 2004.
- Spira A., J. Beane, et al. "Effects of cigarette smoke on the human airway epithelial cell transcriptome". *PNAS* 101: 10143-8, 2004.
- Tang X, Shigematsu H, Bekele BN, Roth JA, Minna JD, Hong WK, et al. EGFR tyrosine kinase domain mutations are detected in histologically normal respiratory epithelium in lung cancer patients. *Cancer Res* 65:7568-72, 2005.
- Vaughan, M. B., Ramirez, R. D., Wright, W. E., Minna, J. D., and Shay, J. W. A Three-Dimensional Model of Differentiation of Immortalized Human Bronchial Epithelial Cells. *Differentiation* 74:141-8, 2006.
- Yatabe Y, Kosaka T, Takahashi T, Mitsudomi T. EGFR mutation is specific for terminal respiratory unit type adenocarcinoma. *Am J Surg Pathol* 29:633-9, 2005.
- Zhang, C.C., Yang, J-M, Bash-Babula, J., White, E., Murphy, M., Levine, A.J., and Hait, W.N. DNA Damage Increases Sensitivity to Vinca Alkaloids and Decreases Sensitivity to Taxanes through p53–Dependent Repression of Microtubule-Associated Protein 4. *Cancer Res* 59, 3663-70, 1999.

APPENDICES

APPENDIX 1

Core B: Selected Screen Shots

Slide 1

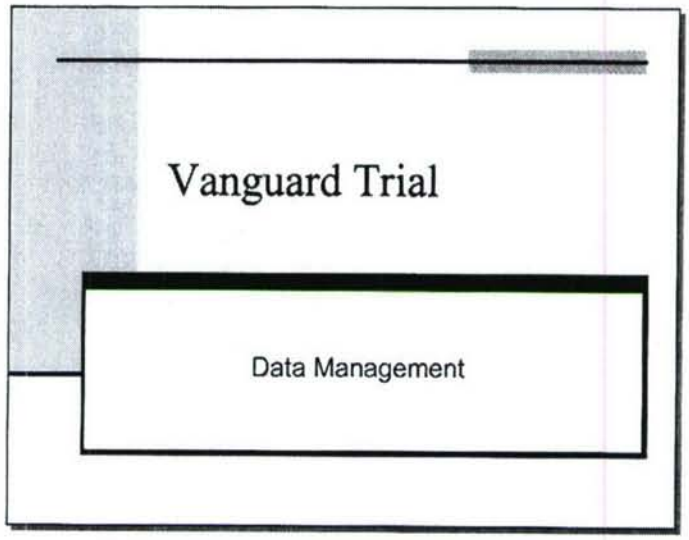

Slide 2

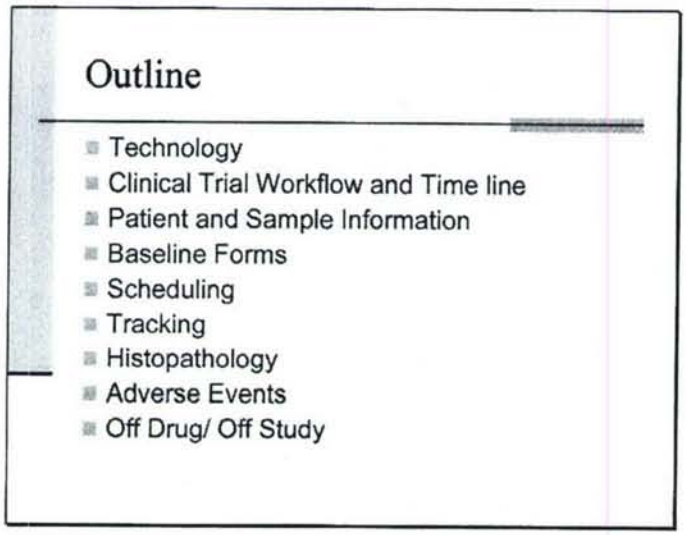

Slide 3

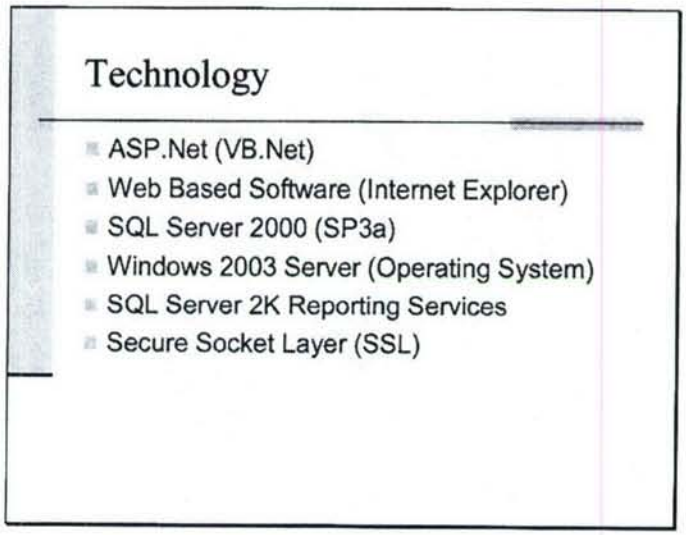

Slide 4

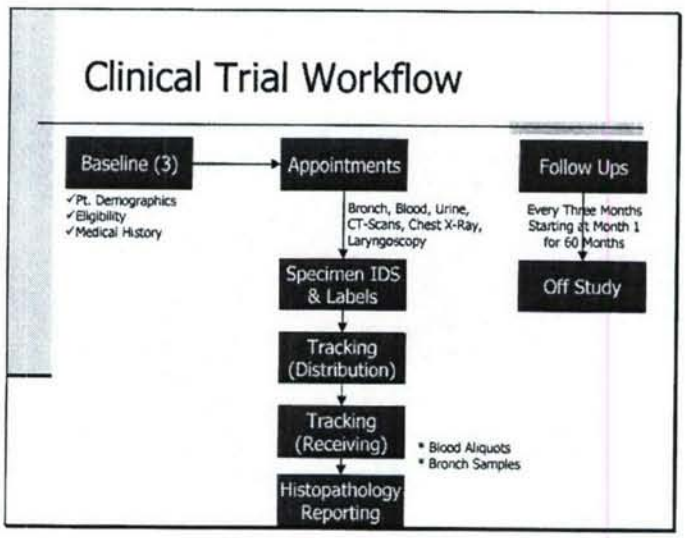

Slide 5

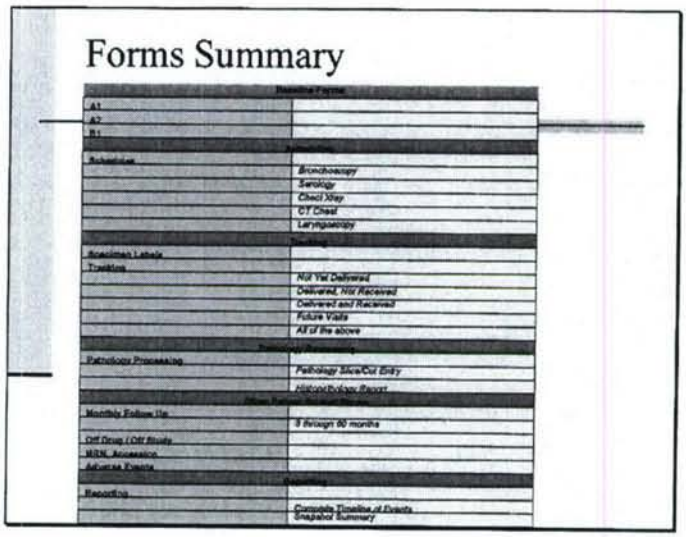

Slide 6

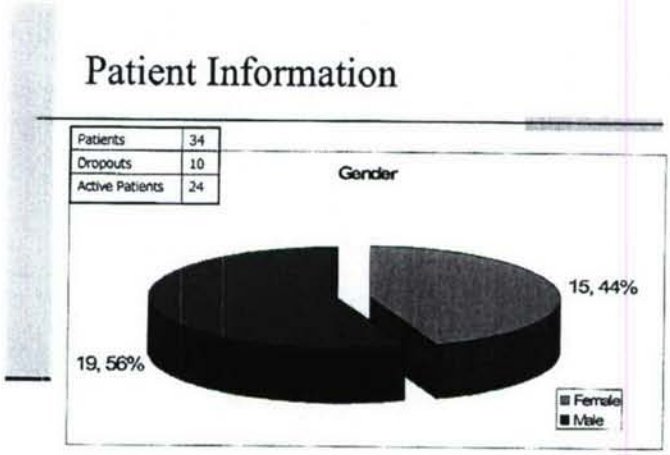

Slide 7

Patient Information

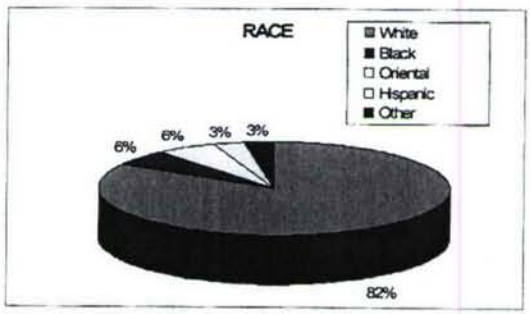

Slide 8

Patient Information

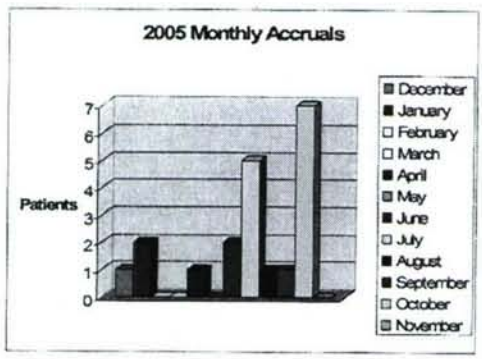

Monthly Accruals		
2004	December	1
2005	January	2
	February	0
	March	0
	April	1
	May	0
	June	2
	July	5
	August	1
	September	1
	October	7
	November	0
	December	0
		20

Slide 9

Patient Information

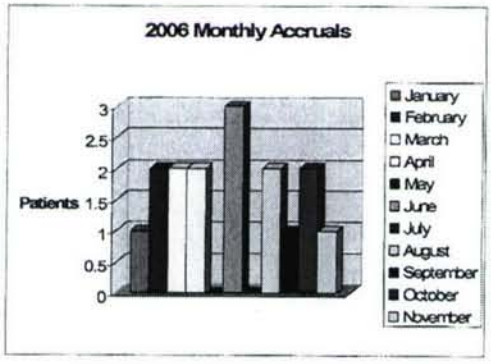

Monthly Accruals		
2006	January	1
	February	2
	March	2
	April	2
	May	0
	June	3
	July	0
	August	2
	September	1
	October	2
	November	1
		16

Slide 10

Patient Information

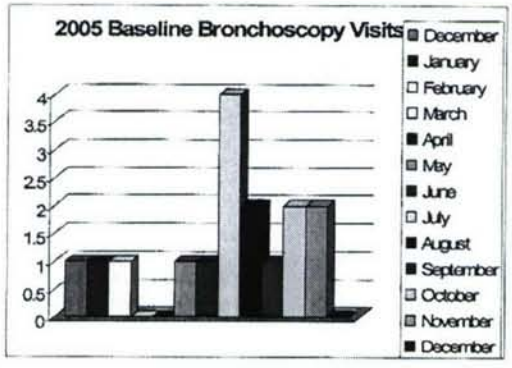

Baseline Bronch Visits		
2004	December	1
2005	January	1
	February	1
	March	0
	April	0
	May	1
	June	1
	July	4
	August	2
	September	1
	October	2
	November	2
	December	0
		16

Slide 11

Patient Information

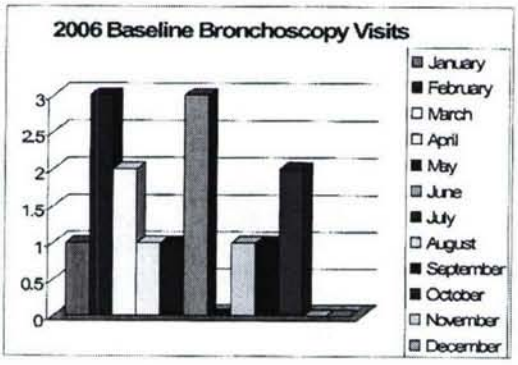

Baseline Bronch Visits		
2006	January	1
	February	3
	March	2
	April	1
	May	1
	June	3
	July	0
	August	1
	September	1
	October	2
	November	0
		15

Slide 12

Sample Information

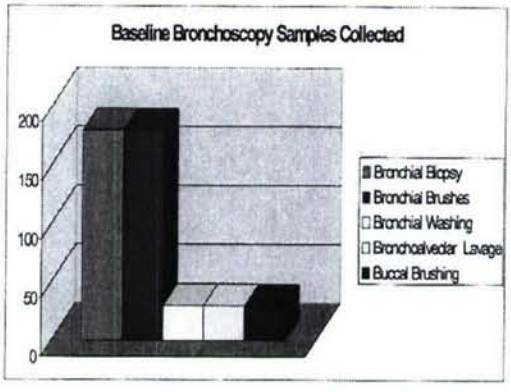

	Count
Bronchial Biopsy	179
Bronchial Brushes	179
Bronchial Washing	30
Bronchoalveolar Lavage	30
Buccal Brushing	29
Total	447

Slide 13

Sample Information

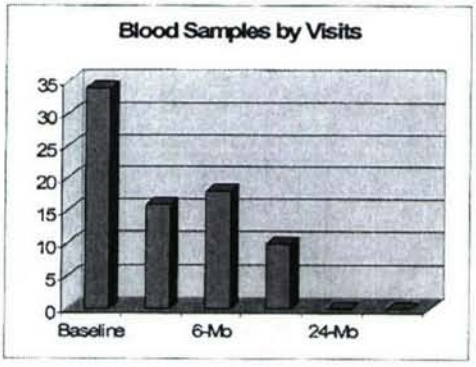

Blood Samples by Visits:	
Baseline	34
3-Mo	16
6-Mo	16
12-Mo	10
24-Mo	0
36-Mo	0
	76

Slide 14

Sample Information

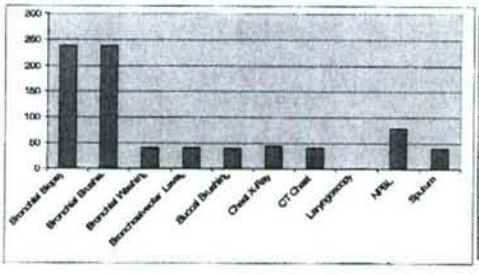

Sample Type	Count
Biopsies	239
Brushes	239
Washings	40
BALs	40
Buccal Brushing	39
Chest X-Ray	44
CT Chest	40
Laryngoscopy	1
NPBL	76
Sputum	39
Total	799

Slide 15

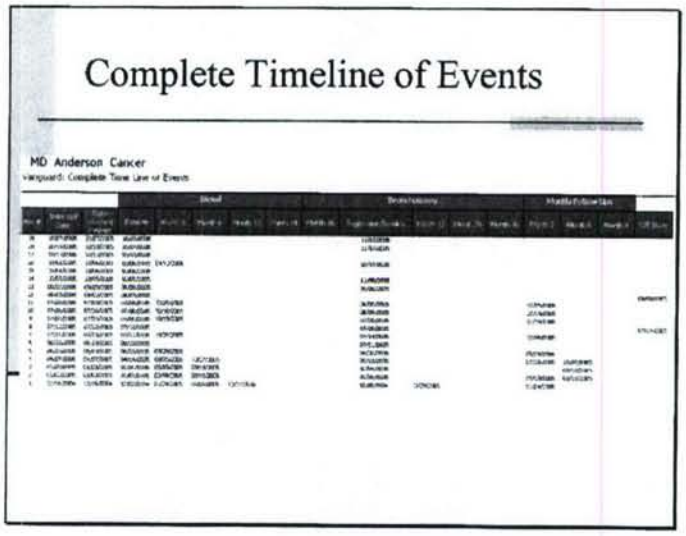

Slide 16

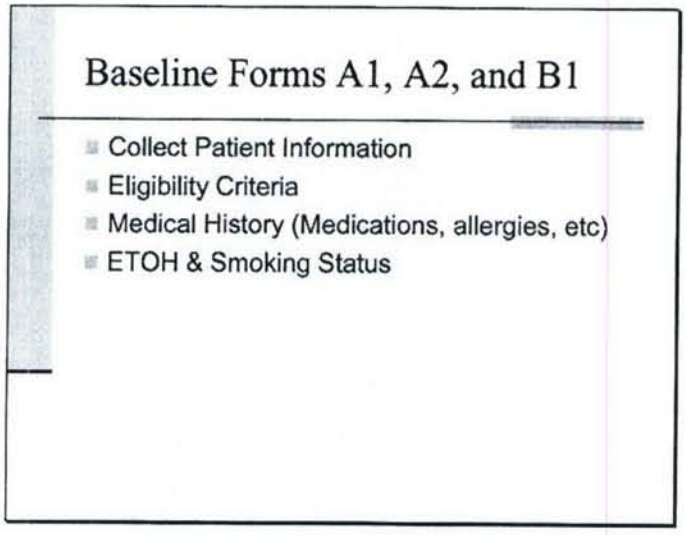

Slide 17

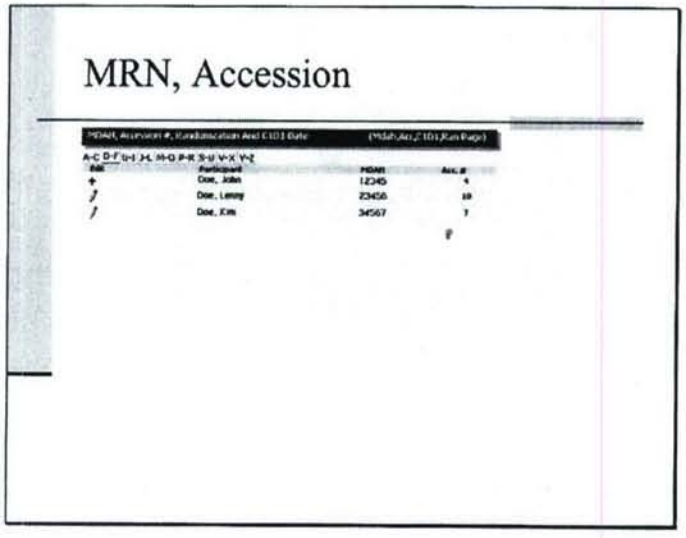

Slide 18

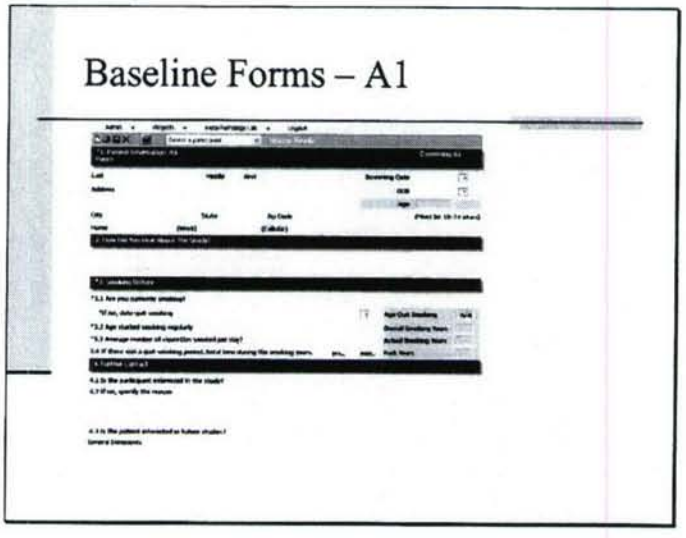

Slide 19

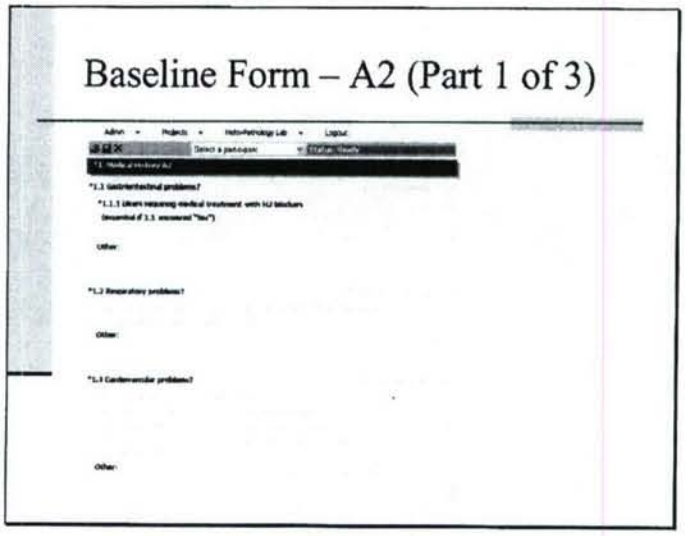

Slide 20

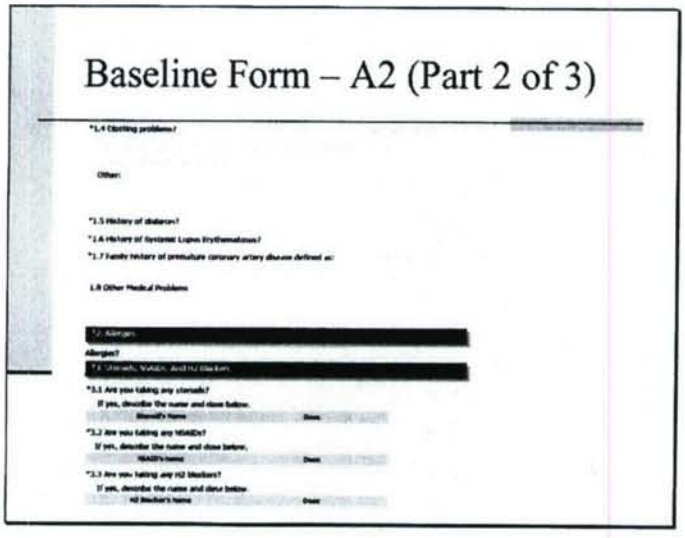

Slide 21

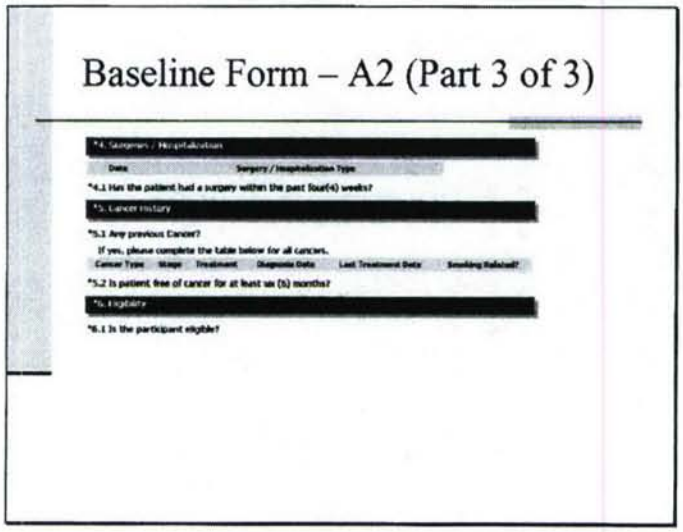

Slide 22

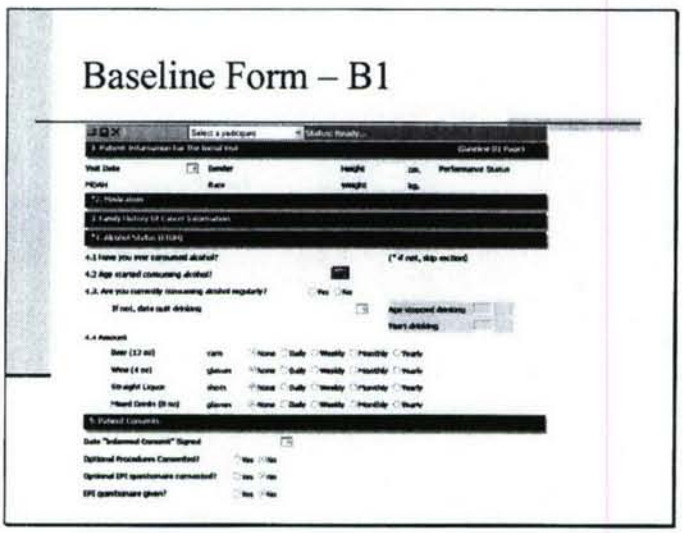

Slide 23

Scheduling

- Database Driven:
  - Visit Types (Bronchoscope)
  - Sample Types (Biopsy)
  - Collection Time Points (Baseline, 1-Month)
  - Scheduler Matrix (Integrates above definitions)
    - Detail (Defines specimen label and collection)
- Specimens' Label Printing

Slide 24

Scheduling Form

Slide 25

Specimen Labels

Slide 26

Tracking

- Five display modes: All, NYD, NYR, DAR, & Future Visits
- Print Tracking Forms

Slide 27

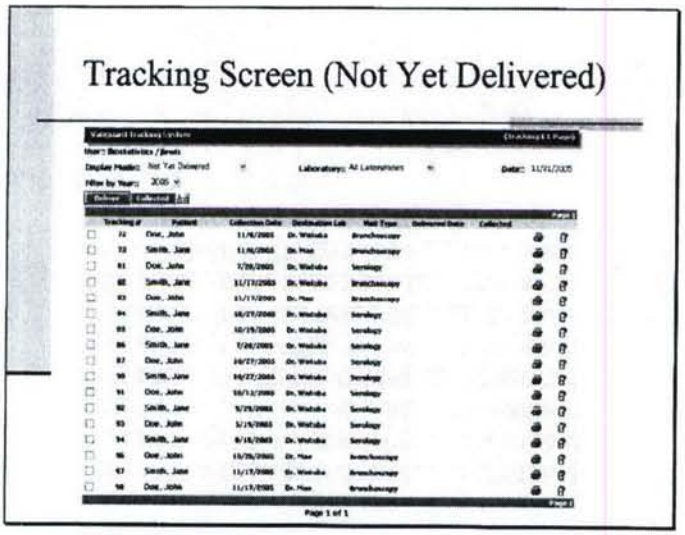

Slide 28

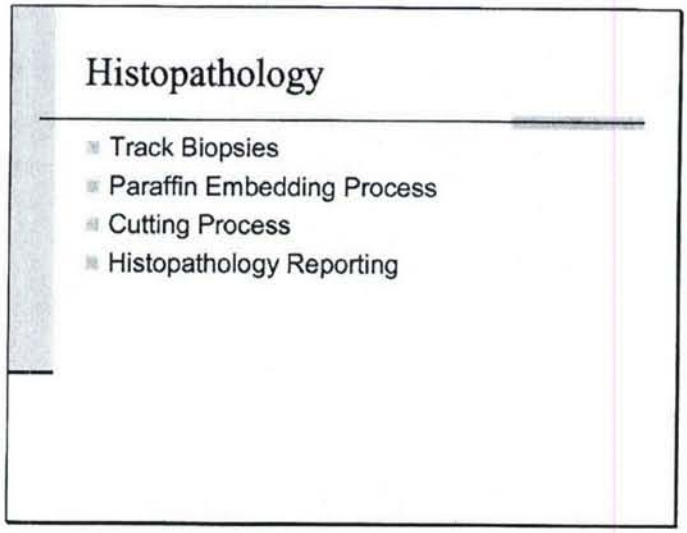

Slide 29

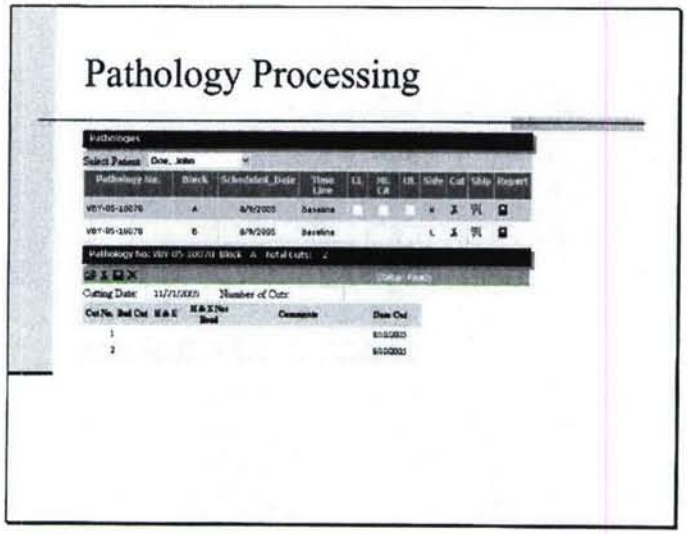

Slide 30

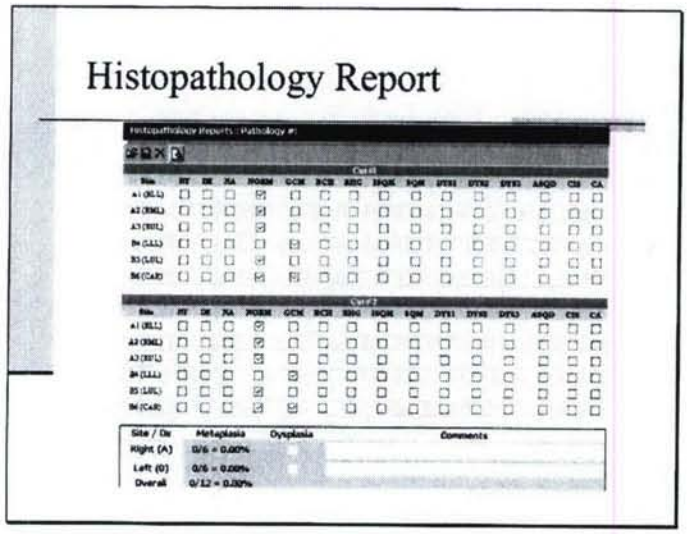

Slide 31

Histopathology Report

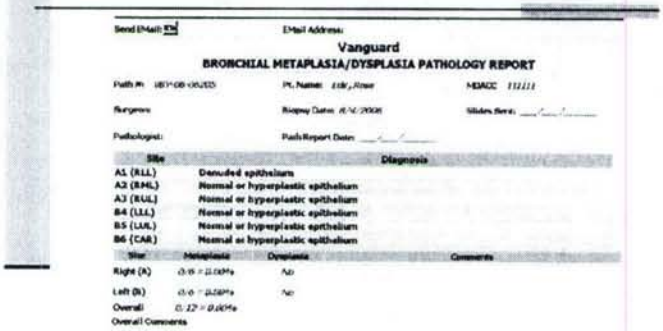

Send EMail: [ ] EMail Address:

Vanguard

BRONCHIAL METAPLASIA/DYSPLASIA PATHOLOGY REPORT

Path #: [illegible] Pt. Name: [illegible] MDACC: [illegible]

Surgeon: Biopsy Date: [illegible] Slides Sent: [illegible]

Pathologist: Path Report Date: [illegible]

Site	Diagnosis
A1 (RLL)	Denuded epithelium
A2 (RML)	Normal or hyperplastic epithelium
A3 (RUL)	Normal or hyperplastic epithelium
B4 (LLL)	Normal or hyperplastic epithelium
B5 (LUL)	Normal or hyperplastic epithelium
B6 (CAR)	Normal or hyperplastic epithelium

Site	Metaplasia	Dysplasia	Comments
Right (A)	[illegible]	No	
Left (B)	[illegible]	No	
Overall	[illegible]		

Overall Comments

Slide 32

Other Forms

- Monthly Follow Ups
- Adverse Events Form
- Off Drug/ Off Study Form

Slide 33

Slide 34

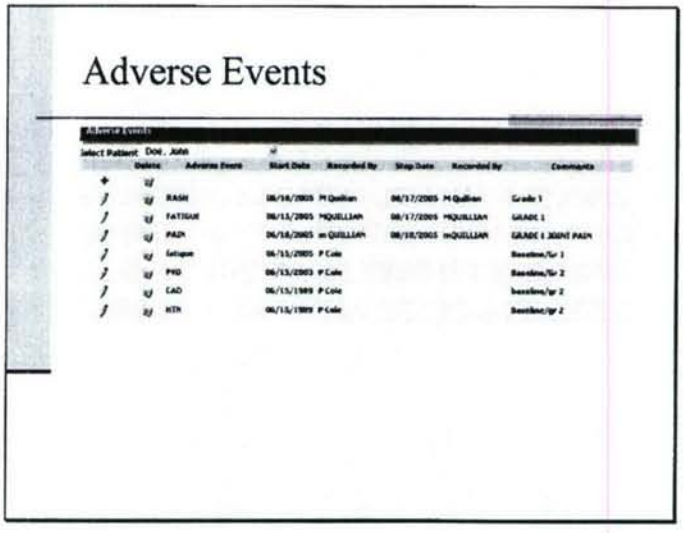

Slide 35

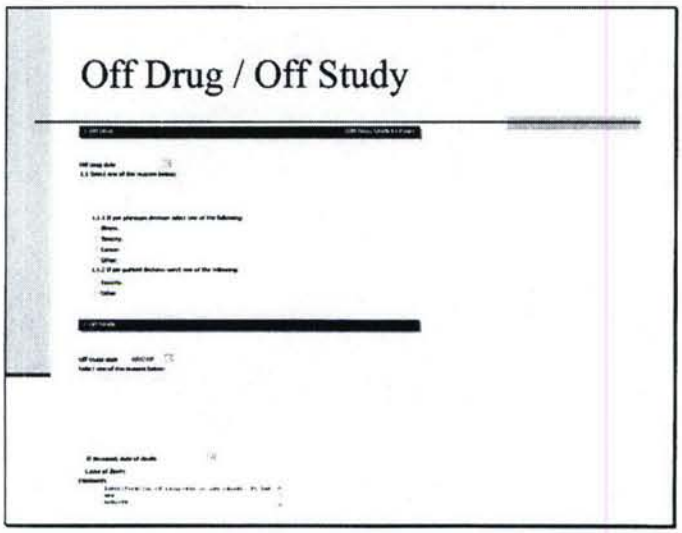

APPENDIX 2

Publications

Heterodimerization of Insulin-like Growth Factor Receptor/Epidermal Growth Factor Receptor and Induction of Survivin Expression Counteract the Antitumor Action of Erlotinib

Floriana Morgillo, Jong Kyu Woo, Edward S. Kim, Waun Ki Hong, and Ho-Young Lee

Department of Thoracic/Head and Neck Medical Oncology, The University of Texas M.D. Anderson Cancer Center, Houston, Texas

Abstract

Epidermal growth factor receptor (EGFR) tyrosine kinase inhibitors (TKIs) have been used to treat non–small cell lung cancer (NSCLC). However, the overall response rate to EGFR TKIs is limited, and the mechanisms mediating resistance to the drugs are poorly understood. Here, we report that insulin-like growth factor-I receptor (IGF-IR) activation interferes with the antitumor activity of erlotinib, an EGFR TKI. Treatment with erlotinib increased the levels of EGFR/IGF-IR heterodimer localized on cell membrane, activated IGF-IR and its downstream signaling mediators, and stimulated mammalian target of rapamycin (mTOR)–mediated *de novo* protein synthesis of EGFR and survivin in NSCLC cells. Inhibition of IGF-IR activation, suppression of mTOR-mediated protein synthesis, or knockdown of survivin expression abolished resistance to erlotinib and induced apoptosis in NSCLC cells *in vitro* and *in vivo*. Our data suggest that enhanced synthesis of survivin protein mediated by the IGFR/EGFR heterodimer counteracts the antitumor action of erlotinib, indicating the needs of integration of IGF-IR–targeted agents to the treatment regimens with EGFR TKI for patients with lung cancer. (Cancer Res 2006; 66(20): 10100-11)

Introduction

The 5-year survival rate for lung cancer patients remains extremely poor (≤15; ref. 1), underscoring the need for more effective treatment strategies. Recently, new therapeutic approaches targeting signaling pathways involved in cell proliferation, apoptosis, angiogenesis, and metastasis have been investigated (2). Among the many potential target pathways, the epidermal growth factor (EGF) receptor (EGFR) signaling pathway has been studied most extensively because EGFR overexpression has been observed in a number of solid tumors, including 40% to 80% of non–small cell lung cancers (NSCLC; ref. 3). The EGFR signaling pathway activates the phosphatidylinositol 3-kinase (PI3K)/Akt and mitogen-activated protein kinase (MAPK) pathways, which play major roles in cell proliferation, survival, and transformation and in therapeutic resistance (4, 5). In addition, the EGFR pathway is implicated in angiogenesis, and cell invasion by its regulation of the expression and activity of matrix metalloproteinases (6, 7).

These findings indicate the therapeutic potential of inhibitors of EGFR tyrosine kinase activation. EGFR tyrosine kinase activity can be inhibited by antibodies against the extracellular domain of EGFR, such as cetuximab, or by small molecules that block the ATP binding site of the cytoplasmic domain, such as gefitinib (ZD1839, Iressa; AstraZeneca Pharmaceuticals, Macclesfield, United Kingdom) and erlotinib (Tarceva®; OSI Pharmaceuticals; Genentech, South San Francisco, CA). Both forms of EGFR inhibition have single-agent antitumor activity against previously treated NSCLC (3, 8–10). Erlotinib exhibits an antiproliferative effect at nanomolar concentrations and has induced apoptosis and reversible cell cycle arrest at G_1 (11). *In vivo* preclinical models have shown that erlotinib administration markedly reduces EGFR autophosphorylation and growth in human head and neck cancer xenografts (HN5 and A431 cells) in nude mice (11, 12). In addition, gefitinib, combined with standard chemotherapeutic agents and/or radiotherapy in preclinical studies, has inhibited EGFR activation, thus causing G_1 cell cycle arrest and contributing to synergistic growth inhibition (13).

Despite a similar chemical structure, these two EGFR tyrosine kinase inhibitors (TKIs) have provided contrasting results in phase III clinical trials, in which only erlotinib showed significantly improved survival compared with placebo (14–16). The response to gefitinib and erlotinib has been suggested to be associated with sex, smoking status, tumor histology, and somatic mutations of the EGFR ATP binding site (17, 18). Recent data have suggested that the insulin-like growth factor-1 receptor (IGF-IR) pathway is also implicated in the resistance of gefitinib and anti-EGFR monoclonal antibody (19, 20). However, to our knowledge, the mechanisms involved in the IGF-IR–mediated acquired resistance to erlotinib in NSCLC cells have not been completely defined. In this article, we report that erlotinib induce EGFR/IGF-IR heterodimerization on the cell membrane, transmitting a survival signal through IGF-IR and its downstream mediators PI3K/Akt and p44/42 MAPK to stimulate mammalian target of rapamycin (mTOR)–mediated synthesis of EGFR and antiapoptotic survivin proteins. Consequently, inactivation of IGF-IR, suppression of mTOR-mediated protein synthesis, or knockdown of survivin protein renders EGFR-overexpressing NSCLC cells sensitive to the erlotinib treatment.

Materials and Methods

Cells, reagents, and animals. The human NSCLC cell lines H596, H226B, H226Br, H460, H1299, A549, H358, H661, and H322 were from the American Type Culture Collection (Manassas, VA) and maintained in RPMI 1640 supplemented with 10% fetal bovine serum (FBS; Life Technologies, Gaithersburg, MD) in a humidified atmosphere with 5% CO_2. IGF and EGF were from R&D Systems (Minneapolis, MN). Erlotinib were prepared as 10 mmol/L stock solution in DMSO and stored at −20°C. LY294002

Note: Supplementary data for this article are available at Cancer Research Online (http://cancerres.aacrjournals.org/).

W.K. Hong is an American Cancer Society Clinical Research Professor. H-Y. Lee is a faculty member at the Graduate School of Biomedical Sciences.

Requests for reprints: Ho-Young Lee, Department of Thoracic/Head and Neck Medical Oncology, The University of Texas M.D. Anderson Cancer Center, Box 432, 1515 Holcombe Boulevard, Houston, TX 77030. Phone: 713-792-6363; Fax: 713-792-0430; E-mail: hlee@mdanderson.org.

©2006 American Association for Cancer Research.

doi:10.1158/0008-5472.CAN-06-1684

(an inhibitor of PI3K), PD98059 (an inhibitor of the MEK1), rapamycin, and AG1024, a TKI of IGF-IR, were from Calbiochem-Novabiochem (Alexandria, New South Wales, Australia); these inhibitors were prepared as 20 mmol/L stock solutions in DMSO and also stored at −20°C. Adenoviral vectors expressing survivin (Ad-survivin; ref. 21) or dnIGF-IR/482 [adenovirus-expressing, dominant-negative IGF-IR (Ad-dnIGF-IR)], a soluble extracellular domain of IGF-IR with an engineered stop codon at amino acid residue 482 (22), and control adenoviral vector [adenovirus-expressing empty vector (Ad-EV)] were amplified as described elsewhere (23). We confirmed increases in the levels of IGF-IR protein by Western blot assay with an antibody for the α-subunit (anti-IGF-IRα N-20, Santa Cruz Biotechnology, Santa Cruz, CA) using medium from the cells that were infected with Ad-dnIGF-IR because IGF-IR/482 has been shown to produce and release the truncated α-subunit of IGF-IR into the medium (22). The effect of the combination of erlotinib and Ad-dnIGF-IR on established s.c. tumor nodules was studied in athymic nude mice (Harlan Sprague-Dawley, Indianapolis, IN) in a defined pathogen-free environment. Six-week-old female mice were used in this study; mice with necrotic tumors or tumors ≥1.5 cm in diameter were euthanized.

Cell proliferation assay. Cells were treated with erlotinib, rapamycin, LY294002, PD98059, AG1024, Ad-dnIGF-IR, Ad-EV, or their combinations in the absence or presence of 10% FBS, EGF (50 ng/mL), or IGF (50 ng/mL). For the experiments with the viruses, cells were infected with 5 and 10 particle forming unit (pfu) for Ad-dnIGF-IR or Ad-EV, in serum-free medium for 2 hours and then incubated for 3 days in RPMI medium supplemented with 10% FBS in the absence or presence of the indicated concentrations of erlotinib. Cell proliferation was measured with the 3-(4,5-dimethylthiazol-2-yl)-2,5-diphenyltetrazolium bromide (MTT) assay. The drug concentrations required to inhibit cell growth by 50% were determined by interpolation from the dose-response curves. For defining the effect of the combined drug treatments, any potentiation was estimated by multiplying the percentage of cells remaining by each individual agent. The synergistic index was calculated as previously described (24). In the following equations, A and B are the effects of each individual agent, and AB is the effect of the combination. Subadditivity was defined as %AB / (%A × %B) < 0.9; additivity was defined as %AB / (%A × %B) = 0.9-1.0; and supra-additivity was defined as %AB / (%A × %B) > 1.0.

Clonogenic growth assay. The anchorage-dependent clonogenic growth assay was done by seeding NSCLC cell lines into six-well plates at low density (≈3×10^3 cells per well). Cells were either left uninfected or infected with 5 or 10 pfu/cell of Ad-dnIGF-IR or Ad-EV, incubated for 72 hours with different concentrations of erlotinib (0.1, 1.0, and 5.0 μmol/L), AG1024 (5 μmol/L), or combinations of the two drugs in serum-free RPMI medium in the absence or presence of IGF (50 ng/mL). Cells were replated in six-well plates and cultured in growth medium for 7 to 10 days, in a humidified atmosphere with 5% CO_2, at 37°C, and then colonies were fixed with 0.1% Coomassie blue (Bio-Rad Laboratories, Hercules, CA) in 30% methanol and 10% acetic acid. We then counted the number of colonies with >50 cells. For the anchorage-independent clonogenic growth assay, $\sim 3 \times 10^3$ cells were suspended in 0.75 mL of 0.22% soft agar that was layered on top of 1 mL of 1% solidified agar in each well of 24-well plates. The plates were then incubated for 10 to 15 days in serum-free RPMI medium containing 0.1 or 1.0 μmol/L concentrations of erlotinib in the absence or presence of 10% FBS or IGF (50 ng/mL). The medium was changed daily during this period, at the end of which tumor cell colonies measuring at least 80 μm were counted under using a dissection microscope.

Cell cycle and apoptosis assays. For cell cycle and apoptosis assays, both adherent and nonadherent cells were harvested, pooled, and fixed with 1% paraformaldehyde and 70% ethanol. For the cell cycle analysis, we stained cells with 50 μg/mL propidium iodide and determined the percentage of cells in specific cell cycle phases (G_1, S, and G_2-M) by using a flow cytometer equipped with a 488 nm argon laser (Epics Profile II; Beckman Coulter, Miami, FL). Approximately 1×10^4 cells were evaluated for each sample. Apoptosis was assessed with a flow cytometry–based terminal deoxyribonucleotide transferase–mediated nick-end labeling (TUNEL) assay processed with an APO-bromodeoxyuridine (APO-BrdUrd) staining kit (Phoenix Flow Systems, San Diego, CA); this assay was modified as previously described (25). Cells treated with DMSO were used as a negative control, and for a positive control, we used the HL-60 leukemic cells treated with camptothecin provided with the kit.

Establishment of resistant cell line. The H460 cell cultures were continuously exposed to erlotinib (10 μmol/L) in routine culture medium that was replaced every day for 5 months. Initially, H460 cell numbers were substantially reduced, and for the next 2 months, the surviving cells were passaged approximately every 10 days with a seeding ratio of 1:2. Cell proliferation slowly increased to allow a passage every 7 days with a seeding ratio of 1:4 over the next 2 months. A stable growth rate was reached after a total of 5 months with routine maintenance of the H460/TKI-R cells involving passage every 4 days with a seeding ratio of 1:8 of the confluent cell number.

Subcellular fractionation. The following procedures were done at 4°C. Cells were scraped into PBS [10 mmol/L sodium phosphate (pH 7.4) and 150 mmol/L NaCl] and then collected by centrifugation. Cell pellets were resuspended with 1 mL of hypotonic buffer [10 mmol/L Tris-HCl (pH 7.5), 1 mmol/L $MgCl_2$, 50 μg/mL leupeptin, 1 mmol/L phenylmethylsulfonyl fluoride, and 1 mmol/L Na_3VO_4]; 10 minutes later, the cells were transferred to a Dounce homogenizer and further disrupted by 25 strokes with a tight-fitting pestle. The homogenate was adjusted to the indicated NaCl concentration from a 5 mol/L stock solution, and nuclei were removed by centrifugation at 1,700 × g for 5 minutes. The postnuclear supernatant was centrifuged again at 10,000 rpm for 20 minutes to remove the mitochondrial fraction; the postmitochondrial supernatant was centrifuged at 45,000 × g for 60 minutes. The supernatant fraction, representing the cytosolic fraction, was adjusted to 1% NP40 from a 10% stock solution. The pellet, representing the plasma membrane fraction, was gently rinsed with 1 mL PBS and then resuspended in 1 mL hypotonic buffer containing 1% NP40.

Immunoblotting and coimmunoprecipitation. NSCLC cells (1×10^6 cells/100 mm^3 dish) were either left uninfected or infected with Ad-EV (50 pfu/cell) or Ad-survivin (50 pfu/cell) and then left untreated or treated with various concentrations of erlotinib (0.1-10.0 μmol/L), AG1024 (5.0 μmol/L), LY294002 (10.0 μmol/L), PD98059 (10.0 μmol/L), rapamycin (1.0 μmol/L), or their combinations in growth medium that was changed daily. When growth factor stimulation was done, cells were cultured in serum-free medium for 1 day and then incubated in EGF (50 ng/mL) or IGF (50 ng/mL) for 15 minutes. For the small interfering RNA (siRNA) transfection, H460 cells in the logarithmic growth phase in six-well plates (5×10^5 cells per well) were transfected with 10 μL of 20 μmol/L survivin siRNA or control scrambled siRNA (Dharmacon Research, Lafayette, CO) using LipofectAMINE 2000 (Invitrogen, Carlsbad, CA), according to the protocol of the manufacturer. After 24 hours of incubation in growth medium, erlotinib was added, and the cells were harvested after 3 days of incubation. Immunoprecipitations were done using 3 mg protein from the total cell lysates and 1 μg mouse monoclonal anti-EGFR antibody, mouse monoclonal anti-IGF-IR antibody (Oncogene Sciences, Uniondale, NY), or healthy preimmune serum anti-mouse for the negative control and by incubating overnight at 4°C. The immunocomplexes were precipitated with protein-G agarose (Pharmacia-LKB Biotechnology, Piscataway, NJ). The immunoprecipitates were resolved on 6% SDS-PAGE gels, followed by Western blotting as described elsewhere (25).

Metabolic labeling. Metabolic labeling was done with H460 and TKI-R cells (5×10^5 in six-well plates). Cells were washed in PBS and incubated in RPMI medium without methionine and cysteine (Sigma, St. Louis, MO) for 2 hours. Next, the medium was replaced with fresh medium containing methionine and cysteine, to final concentrations of 150 mg/L, and the cells were labeled with trans-^{35}S (0.5 mCi; ICN, MP Biomedicals, Irvine, CA). The cells were then treated with 0.1% DMSO or erlotinib (10 μmol/L) for 1, 3, 6, 12, and 24 hours. At harvesting time, the cells were washed in ice-cold PBS and lysed in radioimmunoprecipitation assay buffer. Lysates containing equal amounts of protein (100 μg) were immunoprecipitated using 1 μg of antibody to detect EGFR or 1 μg of antibody to detect survivin (both from Santa Cruz Biotechnology) and 30 μL of 50% slurry of protein G agarose beads (Pharmacia-LKB Biotechnology, Piscataway, NJ). The immunoprecipitates were washed five times with lysis buffer, separated by SDS-PAGE,

and analyzed autofluorographically. Cell extracts were also subjected to Western blot analysis for β-actin to ensure that equal amounts of protein had been used. Two independent experiments were done with similar results; representative results of one experiment are presented.

Northern blot analysis. H460 cells (1×10^6 in 10 mm^3 plates) were treated with erlotinib (10 μmol/L) for different times (0, 24, 48, and 72 hours). The total cellular RNA was isolated by the application of TRIzol. For the Northern blotting, 10 μg of the total cellular RNA prepared from each sample was subjected to electrophoresis on a 1% agarose gel containing 2% formaldehyde and then stained with ethidium bromide, photographed, transferred to a Z probe membrane (Bio-Rad Laboratories), and hybridized to an [α-^{32}P]dCTP-labeled EGFR cDNA probe.

***In vivo* model.** The effect of the combination of erlotinib and Ad-dnIGF-IR on established s.c. tumor nodules was studied in athymic nude mice (Harlan Sprague-Dawley) in a defined pathogen-free environment. Briefly, 6-week-old female nude mice were irradiated with 350 rad from a cesium-137 source and then were injected s.c. with 1×10^7 H1299 cells in 100 μL of growth medium at a single dorsal site. The mice were randomly assigned to one of four treatment groups, with each group containing eight mice. Group 1 (control mice) received 1× PBS and Ad-EV, group 2 received erlotinib and Ad-EV, group 3 received 1× PBS and Ad-dnIGF-IR, and group 4 received erlotinib and Ad-dnIGF-IR. Tumor growth was quantified by measuring the tumors in three dimensions with calipers for a total of 35 days. After the tumor volumes reached ~75 mm^3 (considered day 0), the mice were treated with p.o. administered erlotinib (100 mg/kg of body weight) twice a day. We chose this dosage of erlotinib because it had had no notable effect on H1299 tumor growth in preliminary experiments (data not shown). On day 23, when tumor volumes reached ~125 mm^3, each mouse was given a single intratumoral injection of 2×10^9 particles of Ad-dnIGF-IR or Ad-EV in 100 μL of PBS. Mice with necrotic tumors or tumors ≥1.5 cm in diameter were euthanized immediately. The results were expressed as the mean tumor volume ($n = 5$) with 95% confidence intervals (95% CI). On day 35, all mice were sacrificed and tumor tissues were collected from the xenografts to determine whether the combination of erlotinib and

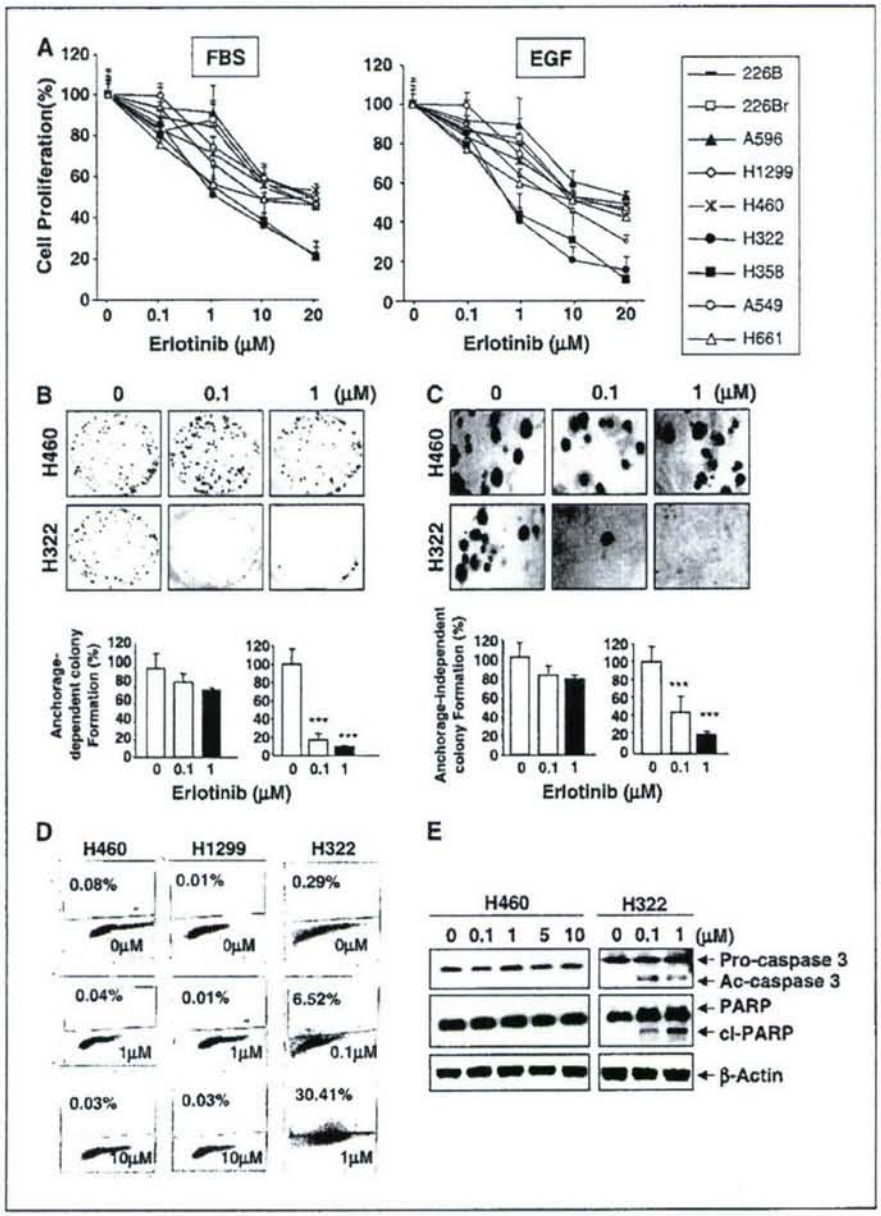

Figure 1. *A*, the MTT assay in NSCLC cell lines (H460, H1299, H661, A596, A549, H226B, H226Br, H322, and H358) treated with the indicated concentrations of erlotinib in RPMI 1640 containing 10% FBS or EGF for 3 days. *B*, clonogenic survival assay of H460 and H322 cells treated with the indicated concentrations of erlotinib. *C*, anchorage-independent growth assay of cells treated with the indicated concentrations of erlotinib. In (*A-C*), independent experiments were repeated thrice. *Columns*, mean of eight (*A*) or three (*B* and *C*) identical wells of a single representative experiment; *bars*, upper 95% CI; **, $P < 0.01$; ***, $P < 0.001$, for comparisons between erlotinib-treated and control cells. *D*, effects of the indicated concentrations of erlotinib on apoptosis in H322, H460, and H1299 NSCLC cells, assessed by a modified TUNEL assay. From a single representative experiment ($n = 2$). *E*, effects of the indicated concentrations of erlotinib on apoptosis-related enzyme expression in H322 and H460 NSCLC cells. The expression of caspase-3, PARP, and β-actin was assessed by Western blotting.

Ad-dnIGF-IR induced apoptosis *in vivo* by Western blot and immunohistochemical analyses as previously described (23).

Statistical analyses. The data acquired from the MTT assay were analyzed using Student's *t* test. All means and 95% CIs from eight samples were calculated using Microsoft Excel software (version 5.0; Microsoft Corporation, Seattle, WA). Cell survival comparisons among groups and statistical significance of differences in tumor growth in the combination treatment group and in the single-agent treatment groups were analyzed by ANOVA for 2 × 2 factorial design. All means from triplicate to eight samples and 95% CIs were calculated using SAS software (release 8.02; SAS Institute, Cary, NC). In all statistical analyses, two-sided *P* values of <0.05 were considered statistically significant.

Results

Differential apoptotic responses of NSCLC cells after treatment with erlotinib. To test the effects of EGFR TKIs on NSCLC cell proliferation, a subset of NSCLC cell lines (H460, H1299, H661, H596, H226B, H226Br, A549, H322, and H358) was treated with erlotinib in regular growth medium containing 10% FBS or in serum-free medium containing EGF. A MTT assay revealed that erlotinib has different levels of antiproliferative activities, depending on cell lines (Fig. 1*A*): Compared with the other NSCLC cell lines, H322 and H358 cells were more sensitive to the erlotinib treatment ($P < 0.001$). Approximately 1 μmol/L erlotinib significantly inhibited proliferation of H322 and H358 cells after 72 hours of treatment. In contrast, the drug concentrations required to inhibit cell growth by 50% for H460, H1299, H661, H596, H226B, H226Br, and A549 cells were 10 to 20 times higher than those needed to inhibit H322 and H358 cells. Consistent with the results from the MTT assay, erlotinib only slightly affected the anchorage-dependent and anchorage-independent colony-forming abilities of H460 and H1299 cells (data not shown) at concentrations <1 μmol/L, a concentration that significantly inhibited those abilities of H322 ($P < 0.001$; Fig. 1*B* and *C*; $P < 0.001$) and H358 (data not shown) cells.

We next asked whether the ability of 1 μmol/L erlotinib to inhibit H322 and H358 cell proliferation was due to decreased cell cycle progression and/or increased apoptosis. Flow cytometric analyses of propidium iodide–stained H460, H1299, and H322 cells revealed that treatment with 1 μmol/L erlotinib for 3 days resulted in no marked change in the cell cycle distribution (data not shown). However, fluorescence-activated cell sorter analysis followed by terminal deoxynucleotidyl transferase–mediated dUTP-biotin nick-end labeling (TUNEL) staining revealed induction of apoptosis in 30.4% of the H322 cells treated with 1 μmol/L erlotinib. In contrast, treatment with up to 10 μmol/L erlotinib did not detectably increase the apoptotic population of H1299 and H460 cells (Fig. 1*D*). In agreement with these findings, the protein levels of the active form of caspase-3 (Ac-caspase-3) and the cleaved form of poly(ADP-ribose) polymerase (PARP; cl-PARP, the 89 kDa fragment) increased in the H322 cells treated with >0.1 μmol/L erlotinib but not in the H460 cells, even after treatment with 10 μmol/L erlotinib (Fig. 1*E*). H358 cells also responded with apoptosis to similar concentrations of erlotinib (data not shown). Together, these findings indicated the presence of mechanisms that affect the response of NSCLC cells to erlotinib-mediated apoptosis.

Role of IGF-IR signaling pathways in the development of resistance to erlotinib treatment in NSCLC cells. To investigate the mechanisms involved in the sensitivity of NSCLC cells to erlotinib, we first tested whether erlotinib successfully blocks activation of EGFR and its downstream mediators in NSCLC cell lines. Figure 2*A* shows that 0.1 to 1.0 μmol/L erlotinib suppressed the levels of phosphorylated EGFR (pEGFR), phosphorylated Akt (pAkt), and phosphorylated p44/42 MAPK (pp44/42 MAPK) in H460 and H1299 cells (cell lines that are weakly sensitive to erlotinib) and H322 and H358 cells (cell lines that are very sensitive to the drug). However, comparable induction of pAkt and p44/42 MAPK was evident in H460 and H1299 cells after treatment with >5.0 μmol/L erlotinib, doses that induce apoptosis in most of the H322 and H358 cells. pAkt and p44/42 MAPK are located in the nodal points of growth factor–mediated cell survival signaling, and the IGF-IR pathway can modulate the action of the erbB family blocking agents in various cancer cells (25–27). Hence, we tested whether IGF-IR was involved in increases in pAkt and p44/42 MAPK. Indeed, erlotinib concentrations >5.0 μmol/L induced phosphorylated IGF-IR (pIGF-IR) in H460 and H1299 cells but not in H322 and H358 cells.

We then studied the influence of IGF-IR signaling pathways on the response of NSCLC cells to erlotinib. H460 cells exhibited significantly decreased proliferation and anchorage-dependent and anchorage-independent colony-forming abilities when the cells were treated with erlotinib in serum-free medium compared with when they were treated in the presence of IGF-I. H322 cells, however, showed statistically significant sensitivity to erlotinib in all conditions (Fig. 2*B*), suggesting that the induced activation of the IGF-IR signaling pathway allows NSCLC cells to survive and proliferate when the EGFR pathway is blocked by erlotinib treatment.

To test our hypothesis, we compare the effects of erlotinib, either single or in combination with AG1024, an IGF-IR TKI, on the proliferation, clonogenic survival ability, and apoptosis of H460 cells. AG1024 has shown significantly lower affinity for the insulin receptor than for the IGF-IR (26). Combined treatment with erlotinib and AG1024 synergistically enhanced the antiproliferative effects of erlotinib on H460 cells compared with single treatment with each drug when cultured in complete (FBS) or serum-free medium in the absence or presence of IGF ($P < 0.001$; Fig. 2*C*; Supplementary Table S1). Erlotinib also showed significantly enhanced antiproliferative properties in H460 cells infected with an Ad-dnIGF-IR compared with the control cells infected with Ad-EV ($P < 0.001$; Fig. 2*D*). Moreover, combined treatment with erlotinib and AG1024 (Fig. 2*E*) or Ad-dnIGF-IR (Fig. 2*F*) significantly suppressed the anchorage-dependent, colony-forming ability of H460 cells ($P < 0.001$; Supplementary Table S2). Furthermore, TUNEL staining and flow cytometric analysis revealed that ~1% of control H460 cells, 1.2% of erlotinib-treated cells, and 26% (95% CI, 14.3-37.6%, $P < 0.05$) of AG1024-treated cells underwent apoptosis. In contrast, combined treatment with both erlotinib and AG1024 significantly enhanced TUNEL staining (77.1%; 95% CI, 64.4-89.8%; $P < 0.001$; Fig. 2*G*) and induced cleavage of the 113-kDa PARP to the 89-kDa fragment in parallel with the concomitant decreases in the levels of pIGF-IR, pAkt, and p44/42 MAPK (Fig. 2*H*). These findings suggest that the IGF-IR pathway provides an alternative proliferation and/or survival mechanism for NSCLC cancer cells in which EGFR is blocked by erlotinib.

Evidence of increased heterodimerization and membrane localization of IGF-IR and EGFR in erlotinib-treated H460 cells. We investigated the mechanism underlying NSCLC cell resistance to erlotinib using *in vitro* model of the H460 cell line (H460/TKI-R) that had been continuously treated with erlotinib. Treatment with >10 μmol/L erlotinib decreased the number of H460 cells, but proliferation of the remaining cells gradually

increased after 3 months of erlotinib treatment. Compared with the parent H460 cells, the H460 cells treated with 10 μmol/L erlotinib for 5 months (H460/TKI-R) had higher levels of pIGF-IR, pAkt, and pp44/42MAPK, with no detectable differences in the expression of IGF-IR, Akt, and p44/42MAPK (Fig. 3*A*). The dose-response curves in Fig. 3*B* revealed no detectable cytotoxicity from erlotinib treatment of the H460/TKI-R cells up to a concentration of 20 μmol/L, whereas inhibition of IGF-IR activation by the AG1024 treatment induced greater antiproliferative effects on the H460/TKI-R cells than it did on the H460 cells. Moreover, compared with a single agent, combined treatment with erlotinib and AG1024 significantly suppressed the anchorage-dependent, colony-forming ability of H460/TKI-R as well as H460 cells ($P < 0.001$; Fig. 3*C*). The effects of combined treatment with erlotinib and AG1024 on colony formation was greater in H460/TKI-R cells than in H460 cells, indicating the dependence of H460/TKI-R cells on the IGF-IR signaling pathway for maintaining cell proliferation and tumorigenic potential.

We investigated the mechanism of erlotinib-mediated activation of IGF-IR in H460 cells. One mechanism by which the growth factor receptor is activated in tumor cells is by receptor dimerization; another is by overwhelming negative regulatory mechanisms that suppress receptor activation. Recent studies have revealed the interaction between the ErbB receptor families and IGF-IR in several tumor models, including breast cancer and oral cancer cell lines (19, 28–32). We, therefore, tested whether EGFR interacts with IGF-IR in H460/TKI-R cells by performing immunoprecipitation. EGFR immunoprecipitates from H460/TKI-R cells showed greater IGF-IR binding compared with that from the parental H460 cells (Fig. 3*D*). Control immunoprecipitates using preimmune serum exhibited no immunoreactive band. The interaction between EGFR and IGF-IR was observed as early as 30 minutes after the erlotinib treatment (Fig. 3*E*). In contrast, no detectable change was observed in the levels of EGFR-EGFR or EGFR-ErbB2 interaction in H460 cells treated with erlotinib for 3 days (Fig. 3*F, top*). Similarly, IGF-IR immunoprecipitates from erlotinib-treated H460 cells showed greater levels of EGFR binding than untreated cells did (Fig. 3*F, bottom*), whereas no detectable binding was observed when the IGF-IR immunoprecipitates were immunoblotted to ErbB2 or ErbB3. Increased EGFR/IGF-IR heterodimerization was also observed in H1299 cells treated with 10 μmol/L erlotinib (Fig. 3*G*). In contrast, the EGFR and control (preimmune serum) immunoprecipitates from untreated or erlotinib-treated H322 cells exhibited no immunoreactive band. These results suggested that erlotinib induces physical contact between EGFR and IGF-IR, which is accumulative.

Erlotinib treatment–induced expression of survivin protein protects NSCLC cells from apoptosis. We next attempted to find evidence connecting erlotinib-induced activation of the IGF-IR with survival of NSCLC cells. Because the inhibitor of apoptosis

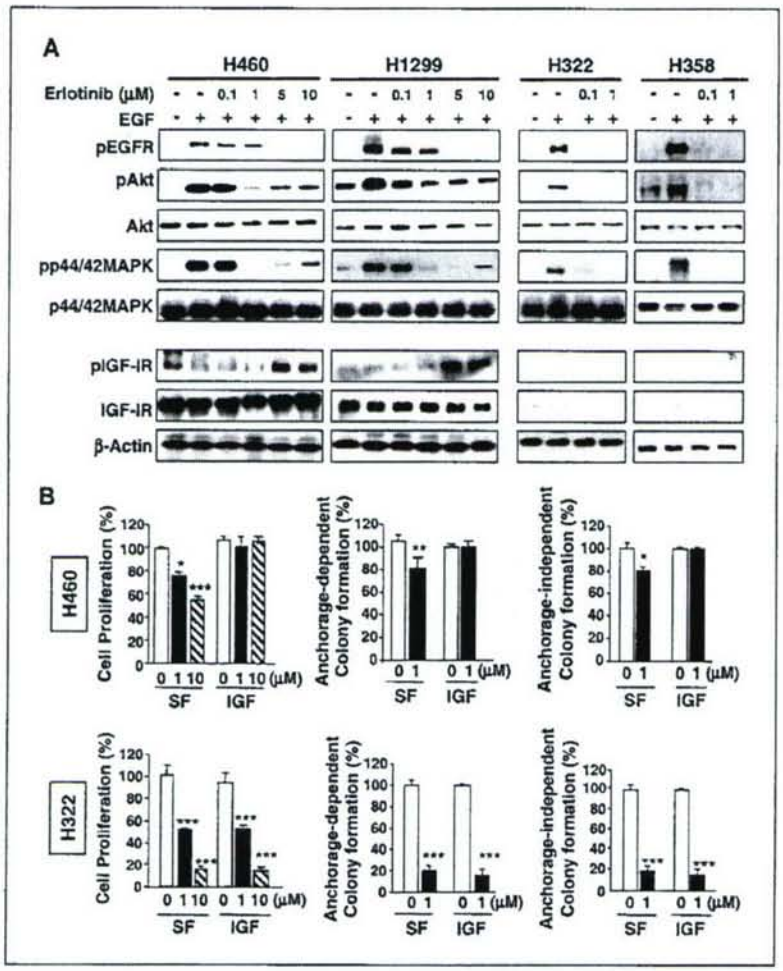

Figure 2. *A*, immunoblotting of the EGFR, IGF-IR, and their downstream signaling components in NSCLC cells treated with indicated concentrations of erlotinib. Western blotting on β-actin is included as a loading control. *B*, role of the IGF-I on the proliferation and survival of NSCLC cells. *Left*, MTT assay in H460 and H322 cells incubated in the serum-free medium without (*SF*) or with IGF-I (50 ng/mL) in the presence of indicated concentrations of erlotinib for 3 days. *Middle* and *right*, efficacy of the indicated concentrations of erlotinib in inhibiting anchorage-dependent and anchorage-independent growth of H460 and H322 cells, respectively, in serum-free and IGF-dependent conditions.

proteins, including survivin and XIAP, decrease the sensitivity of tumor cells to chemotherapeutic drugs, thereby conferring resistance to apoptosis (21, 33), we tested the effects of erlotinib on the expression of these proteins in a subset of NSCLC cells with weak or great sensitivity to erlotinib. We found that expression of survivin but not XIAP markedly increased in H1299, H460, H661, A549, A596, and 226B cells (Fig. 4*A*, *top*) during the time IGF-IR was phosphorylated by the erlotinib treatment (Fig. 4*A*, *bottom*). In contrast, H358 and H322 cells showed no detectable changes in the protein levels of survivin, XIAP, and pIGF-IR during the time EGFR was inactivated by erlotinib treatment. Erlotinib induced survivin expression in a time- and dose-dependent manner (Fig. 4*B*). Interestingly, a similar but less pronounced increase in EGFR expression was observed in H1299, H460, H661, A549, H596 H226Br, and H226B, H460/TKI-R cells but not in H358 and H322 cells. Increases in the survivin and EGFR expression were also observed in H460/TKI-R cells (Fig. 4*C*).

We then tested the response of H460 cells, in which survivin expression was abolished by siRNA transfection. Western blot analysis revealed an obvious increase in PARP cleavage in the 460 cells by the treatment with erlotinib (Fig. 4*D*). Among H322 cells, in which survivin overexpression was induced by the infection with Ad-survivin, the PARP cleavage was substantially reduced after the erlotinib treatment (Fig. 4*E*). These results indicated that increased expression of survivin protein protected NSCLC cells from the erlotinib-induced apoptosis.

mTOR pathway induces *de novo* protein synthesis of EGFR and survivin and protects NSCLC cells from apoptosis. We investigated the mechanisms of erlotinib-mediated increase in survivin and EGFR protein expression. According to Northern blot analysis, exposure of H460 cells to erlotinib resulted in no change in the mRNA levels of survivin (Fig. 5*A*) and EGFR (data not shown). We then determined the effects of erlotinib on the rates of survivin and EGFR protein synthesis. Metabolic labeling of the H460 cells with [^{35}S]Met-Cys revealed that the rate of [^{35}S]labeled survivin (Fig. 5*B*) and EGFR (data not shown) synthesis was remarkably greater in the erlotinib-treated H460 and H460/TKI-R cells than in the untreated parental H460 cells. We then determined whether

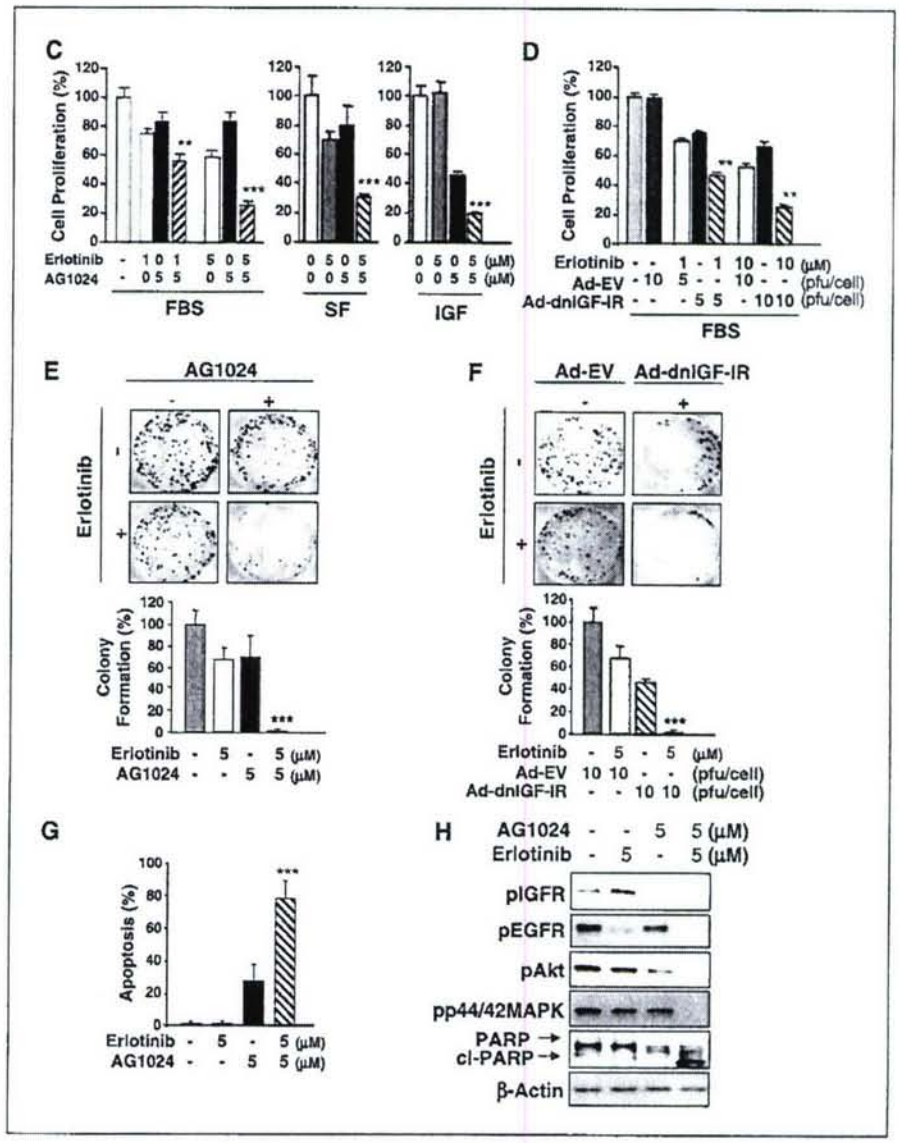

Figure 2 *Continued.* *C* and *D*, effect of targeting both the EGFR and the IGFR-IR on cell proliferation. MTT assay in H460 cells uninfected (*C*) or infected with 5 or 10 infectious forming unit of Ad-EV or Ad-dnIGF-IR (*D*) and treated with indicated concentrations of erlotinib, AG1024, or their combination in serum-free RPMI 1640 containing 10% FBS or IGF (50 ng/mL) for 3 days. *E* and *F*, survival of H460 cells treated with erlotinib (5 μmol/L), AG1024 (5 μmol/L), or their combination (*E*), or cells infected with 10 pfu/cell of Ad-EV or Ad-dnIGF-IR and then untreated or treated with erlotinib (5 μmol/L; *F*) were assessed by counting colonies consisting of >50 cells after 10 days of growth. *G* and *H*, effects of 5 μmol/L erlotinib, 5 μmol/L AG1024, or their combination on apoptosis (*G*) and expression of pEGFR, pIGF-IR, pp44/42MAPK, and pAkt (*H*) were analyzed in H460 cells by a flow cytometry–based TUNEL assay and Western blotting. β-Actin, loading control. *Columns*, mean value of eight (MTT) or three (clonogenic growth assay and TUNEL assay) identical wells of a single representative experiment ($n = 3$); *bars*, upper 95% CI (*B-G*). ***, $P < 0.001$ for comparisons between cells treated with drug combination and cells treated with single agent.

mTOR is involved in the erlotinib-induced protein synthesis of survivin and EGFR by determining the levels of phosphorylated 4E-BP1 and $p70^{s6k}$, downstream mediators of mTOR (27, 34), in the H460 cells treated with erlotinib alone or in combination with rapamycin, an mTOR inhibitor, or AG1024 for 3 days. Western blot analysis revealed that erlotinib up-regulated the protein levels of p4E-BP1, $pp70^{s6k}$ in association with increases in survivin and EGFR expression, all of which were suppressed by

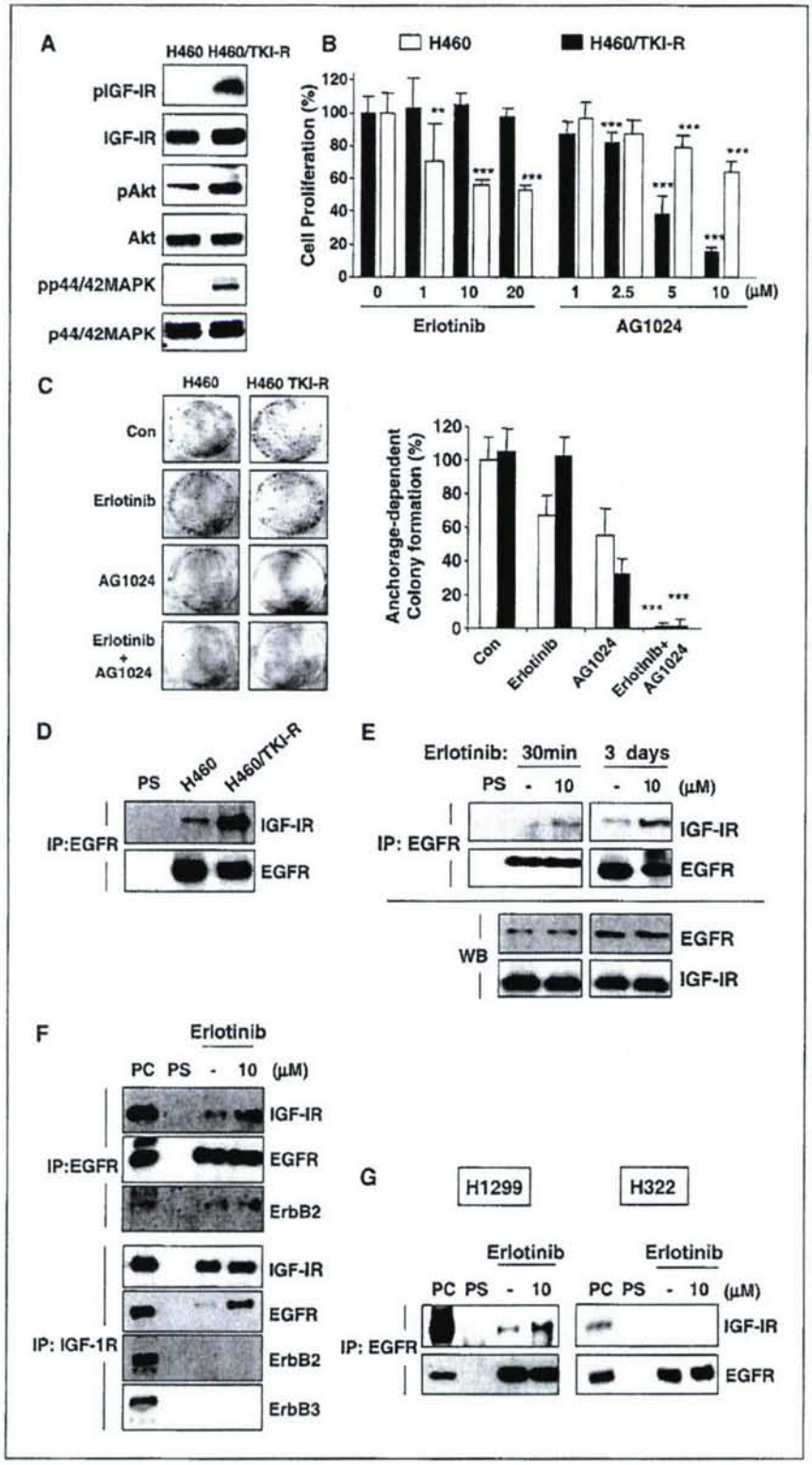

Figure 3. *A*, Western blot analysis of indicated protein expressions in H460 and H460/TKI-resistant (H460/TKI-R) cells. *B*, MTT assay on the proliferation of H460 and H460/TKI-R cells treated with erlotinib (1-20 μmol/L) or AG1024 (1-10 μmol/L). Cells treated with 0.1% DMSO were included as a control (0). *C*, survival of H460 and H460/TKI-R cells treated with erlotinib (5 μmol/L), AG1024 (5 μmol/L), or their combination. *Columns*, mean value of eight (MTT) or three (clonogenic assay) identical wells of a single representative experiment ($n = 3$); *bars*, upper 95% CI (*A* and *B*). ***, $P < 0.001$ compared with control. *D* to *G*, coimmunoprecipitation was done for the interaction between EGFR and IGF-IR. Whole-cell extracts from H460 and H460/TKI-R cells (*D*) or H460 cells, H1299, and H322 cells untreated or treated with erlotinib (10 μmol/L) for 30 minutes (*E*) or 3 days (*E-G*) were immunoprecipitated (*IP*) with anti-EGFR or anti-IGF-IR antibodies. The immunoprecipitates were subjected to Western blot analysis with indicated antibodies. Input (*PC*) represents cell lysates that were not subjected to immunoprecipitation. Control immunoprecipitation was done using control mouse preimmune serum (*PS*).

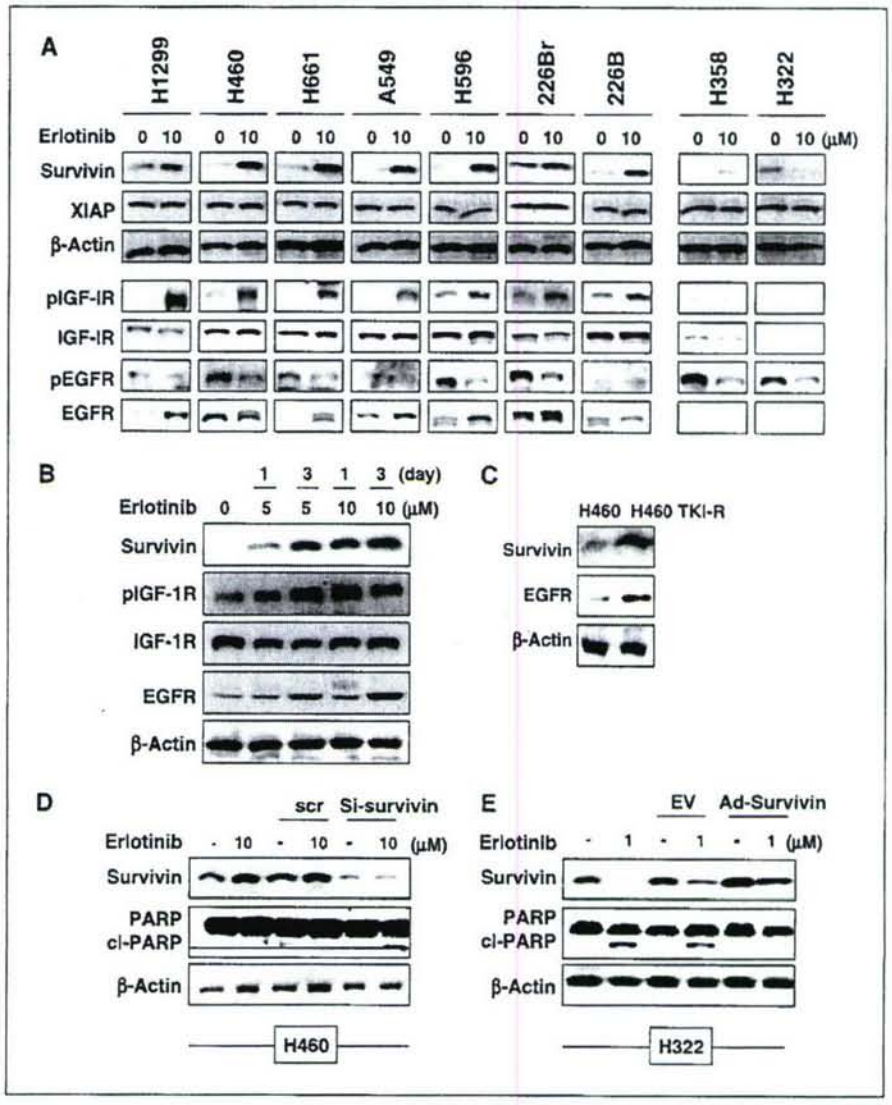

Figure 4. *A* and *B*, Western blot analysis on the survivin, XIAP, pIGF-IR, IGF-IR, pEGFR, EGFR protein expression in indicated NSCLC cell lines treated with erlotinib (1-10 μmol/L) for 1 (*B*) or 3 (*A*, *B*) days. *C*, Western blot analysis on the survivin and EGFR protein in H460 TKI/R cells. *D*, effect of the knockdown of survivin expression on H460 cells in the presence of erlotinib. H460 cells transfected with scramble (*scr*) or survivin siRNA (*si-survivin*), untreated and treated for 48 hours with erlotinib (10 μmol/L), were subjected to protein extraction and Western blotting for evaluation of caspase-3 (pro-caspase-3) and PARP. Loading control: β-actin. *E*, effects of overexpression of survivin in erlotinib-induced apoptosis in H322 cells. H322 cells were infected with 50 pfu/cell of control virus (Ad-EV) or Ad-survivin and incubated for 3 days in the presence of erlotinib (1 μmol/L). Protein extract was subjected to Western blotting for evaluation of survivin, caspase-3 (pro-caspase-3), and PARP. Loading control: β-actin.

treatment with AG1024 or rapamycin (Fig. 5*C*). Moreover, the combined treatment with AG1024, LY294002 (PI3K inhibitor), PD98059 (MEK inhibitor), or rapamycin reduced the levels of membranous EGFR expression (Fig. 5*D*) and of the EGFR and IGF-IR heterodimer (Fig. 5*E*) induced by the 3 days treatment of erlotinib. These findings suggested that the increases in the levels of EGFR/IGF-IR heterodimer on cell membrane and protein expressions of survivin and EGFR were mediated at least in part through translation-dependent events mediated by IGF-IR signaling pathways. We then tested whether inhibitors of the IGF-IR and mTOR pathways sensitize the H460 cells to the erlotinib treatment. H460 cells treated with erlotinib and AG1024 (Fig. 2*G* and *H*) or rapamycin (Fig. 5*F*) showed an increase in the PARP cleavage, suggesting that suppression of IGF-IR and mTOR pathways could restore the apoptotic activities of erlotinib in NSCLC cells.

Antitumor efficacy of dual targeting of EGFR and IGF-IR signaling pathways *in vivo*. To determine whether the inhibition of IGF-IR signaling can enhance the antitumor activities of erlotinib *in vivo*, we tested the effects of erlotinib, Ad-dnIGF-IR, and their combination on the growth of H1299 NSCLC xenograft tumors established in athymic nude mice. The mice treated with erlotinib plus Ad-dnIGF-IR showed synergistically reduced tumor growth compared with the control mice or the mice treated with erlotinib or Ad-dnIGF-IR alone (Fig. 6*A*; Supplementary Table S3). At the end of the study, the mean tumor volume in combined treatment group was 23% ($P < 0.001$) of the mean volume in the control group. Thus, the combination of erlotinib and Ad-dnIGF-IR enhanced the antitumor effects on the growth of NSCLC cells *in vivo*.

We then determined the effects of erlotinib, Ad-dnIGF-IR, and their combination on the activation of the IGF-IR and EGFR, the expression of survivin and EGFR, and the induction of apoptosis *in vivo*. According to Western blot analysis of total protein extracts harvested from the H1299 xenograft tumor tissues, the levels of pEGFR were decreased by erlotinib. In addition, erlotinib treatment induced marked increases in the levels of pIGF-IR, EGFR, and survivin, all of which were effectively blocked by Ad-dnIGF-IR (Fig. 6*B*). Combined treatment with erlotinib and Ad-dnIGF-IR also increased the levels of Ac-caspase-3, which is confirmed by the

immunohistochemical staining of the H1299 xenograft tumor tissues (Fig. 6C). Together, these findings suggested that the combined treatment with erlotinib and Ad-dnIGF-IR exert enhanced *in vivo* antitumor activities by decreased expression of survivin and EGFR and induction of apoptosis.

Discussion

Several preclinical and clinical discoveries have associated EGFR TKIs with antitumor activities. However, the limited response rates of patients to EGFR TKIs, even in patients with high levels of EGFR (15, 16, 35), have been raising questions about the mechanisms leading to the EGFR TKI resistance. Although somatic mutations of the EGFR ATP binding site have been associated with the response to the EGFR TKIs in some cases (17, 18), increasing number of evidence have suggested that the presence of other pathways that mediate the resistance of cancer cells to EGFR TKI therapy (36, 37). In this article, we have shown, to our knowledge for the first time, that erlotinib induces survival of NSCLC cells by inducing heterodimerization of EGFR/IGF-IR, activating IGF-IR pathway and its downstream mediators Akt and p44/42 MAPK, and thus stimulating mTOR-mediated protein synthesis of survivin that plays a crucial role in the blocking apoptosis. We showed here that the blockade of the IGF-IR to mTOR signaling pathway was sufficient to suppress *de novo* survivin protein synthesis and to restore apoptotic activities of erlotinib in NSCLC cells *in vitro* and *in vivo*. Our data present clear evidence that crosstalk between the IGF-IR and the EGFR signaling pathways and consequential survivin expression are involved in the NSCLC cell resistance to erlotinib. The erbB2/Her2/neu, a known preferred coreceptor for the EGFR, has been suggested to play a role in inducing NSCLC cell survival against EGFR TKIs (28). However, we found that the erbB2/Her2/neu was inactivated by the EGFR TKIs in NSCLC cells (data not shown), consistent with previous reports (38). In addition, an interaction between IGF-IR and erbB2 was undetectable, regardless of erlotinib treatment. Therefore, erbB2/Her2/neu is not likely to have a role in inducing EGFR TKI resistance in NSCLC cells.

We investigated the detailed mechanism that mediates IGF-IR activation by erlotinib and the consequent development of drug resistance. Given that gefitinib-resistant DU145/TKI-R prostate cells have shown considerably higher basal levels of IGF-II mRNA than wild-type cells (19), erlotinib might have increased the expression of IGF and conferred resistance to the drug to NSCLC cells. However, in gefitinib-resistant breast cancer cell lines, the IGF II mRNA level did not differ from that of the original clone (19), indicating that autocrine/paracrine production is not entirely responsible for the sensitivity of the cell to EGFR TKIs. Perhaps our most striking finding was that in H460 and H1299 cells, erlotinib induced heterodimerization between IGF-IR and EGFR. The interaction between EGFR and IGF-IR also has been observed in cancer cells (29–31). Given the considerable similarity between EGFR and IGF-IR in the sequence of their extracellular domain (39) and their reliance on EGF and IGF to achieve cell cycle progression and survival, it is plausible that erlotinib-mediated IGF-IR/EGFR heterodimerization can stimulate intracellular signaling components in a distinct pattern and allow NSCLC cells to resist the drug.

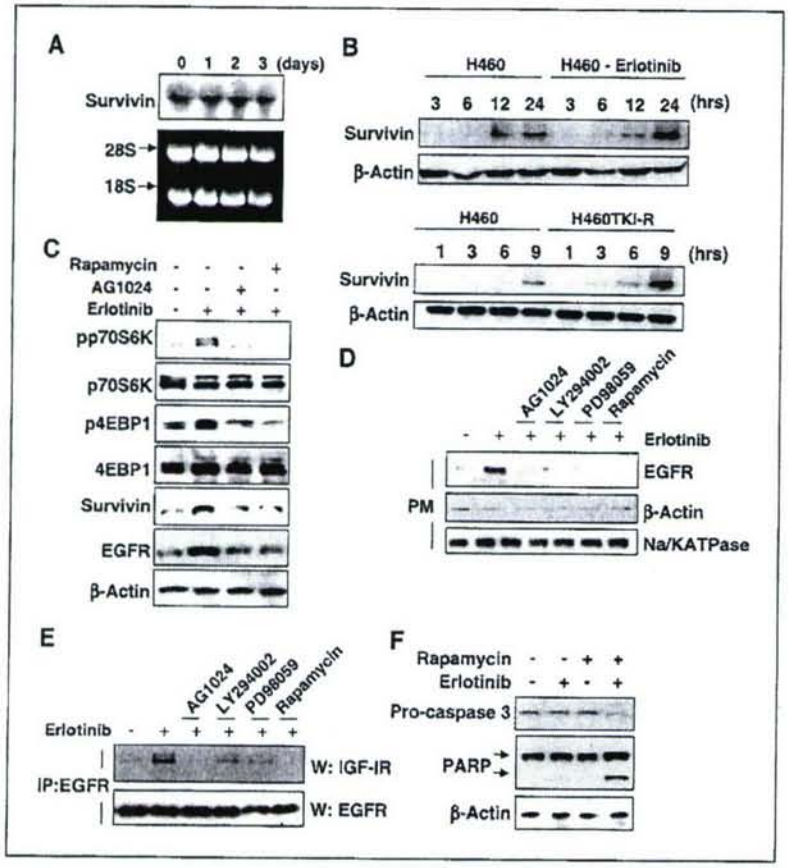

Figure 5. *A*, Northern blot analysis on survivin mRNA in H460 treated with erlotinib (10 μmol/L) for 1, 2, or 3 days. *B*, survivin and EGFR protein synthesis evaluated by metabolic labeling in untreated 460 cells, H460 cells treated with erlotinib (10 μmol/L), and H460TKI-R cells. Cell extracts were also subjected to Western blot analysis for β-actin to ensure that equal amounts of protein were used. *C*, expression of phosphorylated p70S6K (pp70S6K), p70S6K, phosphorylated 4EBP1 (p4EBP1), 4EBP1, survivin and EGFR in H460 cells treated with erlotinib (10 μmol/L), either single or in combination with AG1024 (5 μmol/L) or rapamycin (1 μmol/L), for 3 days. *D* and *E*, effects of erlotinib in combination with AG1024, LY294002, PD98059, or rapamycin on the plasma membrane (*PM*) localization of EGFR (*D*) and on the interaction between EGFR and IGF-IR (*E*). β-Actin, control for cytosol fraction; Na/K ATPase, control for plasma membrane fraction. *F*, effect of combined treatment with erlotinib (10 μmol/L) and rapamycin (1 μmol/L) for 3 days on apoptosis in H460 cells. Protein extract was subjected to Western blotting for the evaluation of pro-caspase-3 and PARP. Loading control: β-actin.

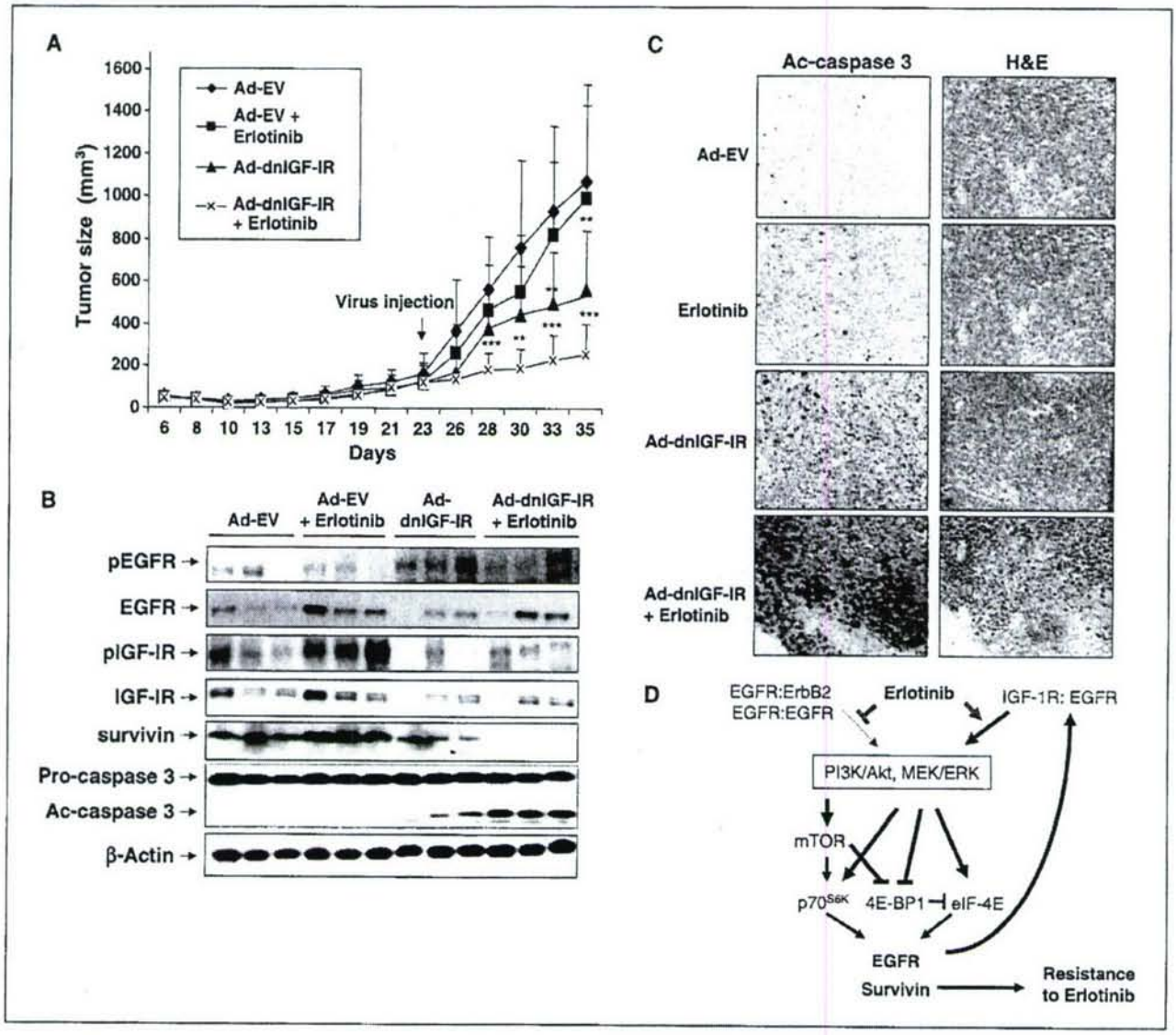

Figure 6. Effects of combined treatment with erlotinib and recombinant Ad-dnIGF-IR on growth of H1299 NSCLC xenograft tumors in athymic nude mice. The mice were randomly assigned to one of four treatment groups, with each group containing five mice. Group 1 (control mice) received 1× PBS and Ad-EV, group 2 received erlotinib and Ad-EV, group 3 received 1× PBS and Ad-dnIGF-IR, and group 4 received erlotinib and Ad-dnIGF-IR. *A*, effect of erlotinib (40 mg/kg body weight, administered p.o. twice daily) on tumor volume. When tumor volume was ~125 mm³, mice were treated with Ad-IGF-IR or Ad-EV (control) in 100 μL PBS. *Points*, mean tumor volume ($n = 5$) with 95% CI; *bars*, SE. **, $P < 0.01$, ***, $P < 0.001$ for comparisons between drug-treated and control cells for each series of experiments. *B*, effects of erlotinib and Ad-dnIGF-IR on the expression of pEGFR, EGFR, pIGF-IR, IGF-IR, survivin, and pro-caspase-3 and Ac-caspase-3 in NSCLC xenograft tumors, assessed by Western blotting. β-Actin = loading control. *C*, effects of combined erlotinib and Ad-IGF-IR on expression of Ac-caspase-3. Tissues were stained with H&E. Representative section from each condition. *D*, schematic model of resistance mechanism to erlotinib.

Previous studies have shown the ability of erlotinib to induce EGFR mRNA and protein expression in the erlotinib-resistant biliary tract cancer cell line HuCCT1 but not in the susceptible A431 epidermoid cell line (40). In current study, we found that erlotinib induces mTOR-mediated *de novo* protein synthesis of survivin and EGFR with no detectable change in their mRNA levels, indicating diverse responses of different cancer cells to erlotinib. Our results may explain some apparently paradoxical findings in several clinical trials (41), in which up-regulation of pEGFR was observed after treatment of breast cancer patients with erlotinib. In another report, modifications of EGFR serum values during treatment of NSCLC seemed to reflect gefitinib activity; responding patients showed decreased serum levels of EGFR relative to those in patients with refractory disease (42). Our data also show the critical role of the induced survivin proteins in the development of resistance to erlotinib; (*a*) survivin expression was induced in NSCLC cell lines with weak sensitivity to the erlotinib treatment; (*b*) overexpression of survivin protected the sensitive NSCLC cells from erlotinib-induced apoptosis; and (*c*) knockdown survivin expression by siRNA provoked apoptosis in NSCLC cells with weak erlotinib sensitivity. mTOR has been known to regulate the translation of subsets of mRNA, many of which encode for proteins involved with driving cell growth, proliferation, and angiogenesis (43). Therefore, resistance and sensitivity to erlotinib in NSCLC may be determined at least in part by the ability of the cancer cells to stimulate mTOR-mediated synthesis of specific proteins that

have key roles in cell proliferation and/or survival and thus to adapt to a stressful environment.

In summary, our findings provide definitive *in vitro* and *in vivo* evidence that erlotinib induces heterodimerization of the EGFR/IGF-IR and stimulates IGF-IR and downstream pathways, including PI3K/Akt, MEK/extracellular signal-regulated kinase (ERK), resulting in the mTOR-mediated increases in EGFR and survivin proteins. On the basis of these findings, it is plausible to suggest that increased EGFR proteins further enhance the interplay between the EGFR and IGFR on the cell membrane, resulting in a further amplification of IGF-IR to mTOR signaling. In addition, the increased survivin proteins seem to provide survival potential to the NSCLC cells against the erlotinib treatment (Fig. 6*D*).

Our findings have direct effect to the treatment of NSCLC with erlotinib. The data showing no detectable interaction between EGFR/IGF-IR in NSCLC cell lines with low levels of IGF-IR expression suggests that the expression of IGF-IR is an important factor for the EGFR and IGF-IR complex and erlotinib sensitivity. Therefore, IGF-IR expression may serve as a predictor for erlotinib resistance in NSCLC. IGF-IR signaling pathway also plays a key role in the resistance to several therapeutic drugs (12, 27, 44–47). Overexpression of IGF-IR has been observed in various human cancers, including lung cancer (48), and is associated with a poor prognosis (49). Importantly, our unpublished data showed that clinical samples from NSCLC patients revealed that the majority of EGFR-overexpressing samples showed correlative increases in IGF-IR protein levels compared with their paired normal counterparts from the same patients. With this prospect, IGF-IR–targeting combination treatment may be required when erlotinib is considered as a therapeutic agent for NSCLC patients. Alternatively, mTOR inhibitors could confer benefit to erlotinib-resistant patients. In light of this notion, we have shown that combined treatment with erlotinib and inhibitors of IGF-IR or mTOR suppressed survivin and EGFR expression, decreased proliferation of NSCLC cells, and induced apoptosis in NSCLC cells *in vitro* and *in vivo*. Further studies are warranted to validate whether the erlotinib combined with inhibitors of IGF-IR or mTOR inhibitors could enhance the objective response and survival rates in NSCLC patients.

Acknowledgments

Received 5/10/2006; revised 7/6/2006; accepted 8/22/2006.

Grant support: NIH grant R01 CA100816 (H-Y. Lee), American Cancer Society grant RSG-04-082-01-TBE 01 (H-Y. Lee), Department of Defense grants W81XWH-04-1-0142-01-VITAL and W81XWH-06-1-0303-BATTLE, and partly by The National Foundation for Cancer Research Fellow grants (W.K. Hong).

The costs of publication of this article were defrayed in part by the payment of page charges. This article must therefore be hereby marked *advertisement* in accordance with 18 U.S.C. Section 1734 solely to indicate this fact.

References

1. Jemal A, Murray T, Samuels A, Ghafoor A, Ward E, Thun MJ. Cancer statistics, 2003. CA Cancer J Clin 2003; 53:5–26.
2. Ferreira CG, Huisman C, Giaccone G. Novel approaches to the treatment of non-small cell lung cancer. Crit Rev Oncol Hematol 2002;41:57–77.
3. Mendelsohn J. The epidermal growth factor receptor as a target for cancer therapy. Endocr Relat Cancer 2001; 8:3–9.
4. Brognard J, Clark AS, Ni Y, Dennis PA. Akt/protein kinase B is constitutively active in non-small cell lung cancer cells and promotes cellular survival and resistance to chemotherapy and radiation. Cancer Res 2001;61:3986–97.
5. Brognard J, Dennis PA. Variable apoptotic response of NSCLC cells to inhibition of the MEK/ERK pathway by small molecules or dominant negative mutants. Cell Death Differ 2002;9:893–904.
6. Khazaie K, Schirrmacher V, Lichtner RB. EGF receptor in neoplasia and metastasis. Cancer Metastasis Rev 1993;12:255–74.
7. Ellerbroek SM, Halbleib JM, Benavidez M, et al. Phosphatidylinositol 3-kinase activity in epidermal growth factor-stimulated matrix metalloproteinase-9 production and cell surface association. Cancer Res 2001;61:1855–61.
8. Sandler A. Clinical experience with the HER1/EGFR tyrosine kinase inhibitor erlotinib. Oncology (Huntingt) 2003;17:17–22.
9. Ready N. Inhibition of the epidermal growth factor receptor in combined modality treatment for locally advanced non-small cell lung cancer. Semin Oncol 2005; 32:S35–41.
10. Hidalgo M. Erlotinib: preclinical investigations. Oncology (Huntingt) 2003;17:11–6.
11. Moyer JD, Barbacci EG, Iwata KK, et al. Induction of apoptosis and cell cycle arrest by CP-358,774, an inhibitor of epidermal growth factor receptor tyrosine kinase. Cancer Res 1997;57:4838–48.
12. Pollack VA, Savage DM, Baker DA, et al. Inhibition of epidermal growth factor receptor-associated tyrosine phosphorylation in human carcinomas with CP-358,774: dynamics of receptor inhibition *in situ* and antitumor effects in athymic mice. J Pharmacol Exp Ther 1999;291: 739–48.
13. Albanell J, Rojo F, Baselga J. Pharmacodynamic studies with the epidermal growth factor receptor tyrosine kinase inhibitor ZD1839. Semin Oncol 2001;28: 56–66.
14. Shepherd FA, Rodrigues Pereira J, Ciuleanu T, et al. Erlotinib in previously treated non-small-cell lung cancer. N Engl J Med 2005;14:123–32.
15. Giaccone G, Herbst RS, Manegold C, et al. Gefitinib in combination with gemcitabine and cisplatin in advanced non-small-cell lung cancer: a phase III trial-INTACT 1. J Clin Oncol 2004;22:777–84.
16. Herbst RS, Giaccone G, Schiller JH, et al. Gefitinib in combination with paclitaxel and carboplatin in advanced non-small-cell lung cancer: a phase III trial-INTACT 2. J Clin Oncol 2004;22:785–94.
17. Lynch TJ, Bell DW, Sordella R, et al. Activating mutations in the epidermal growth factor receptor underlying responsiveness of non-small-cell lung cancer to gefitinib. N Engl J Med 2004;350:2129–39. Epub 2004 Apr 29.
18. Paez JG, Janne PA, Lee JC, et al. EGFR mutations in lung cancer: correlation with clinical response to gefitinib therapy. Science 2004;304:1497–500. Epub 2004 Apr 29.
19. Jones HE, Goddard L, Gee JM, et al. Insulin-like growth factor-I receptor signalling and acquired resistance to gefitinib (ZD1839; Iressa) in human breast and prostate cancer cells. Endocr Relat Cancer 2004;11: 793–814.
20. Liu B, Fang M, Lu Y, Mendelsohn J, Fan Z. Fibroblast growth factor and insulin-like growth factor differentially modulate the apoptosis and G1 arrest induced by anti-epidermal growth factor receptor monoclonal antibody. Oncogene 2001;20:1913–22.
21. Altieri DC. Survivin and apoptosis control. Adv Cancer Res 2003;88:31–52.
22. Lee CT, Park KH, Adachi Y, et al. Recombinant adenoviruses expressing dominant negative insulin-like growth factor-I receptor demonstrate antitumor effects on lung cancer. Cancer Gene Ther 2003;10:57–63.
23. Lee HY, Moon H, Chun KH, et al. Effects of insulin-like growth factor binding protein-3 and farnesyltransferase inhibitor SCH66336 on Akt expression and apoptosis in non-small-cell lung cancer cells. J Natl Cancer Inst 2004;96:1536–48.
24. Goldstein D, Bushmeyer SM, Witt PL, Jordan VC, Borden EC. Effects of type I and II interferons on cultured human breast cells: interaction with estrogen receptors and with tamoxifen. Cancer Res 1989;49: 2698–702.
25. Chun KH, Kosmeder JW II, Sun S, et al. Effects of deguelin on the phosphatidylinositol 3-kinase/Akt pathway and apoptosis in premalignant human bronchial epithelial cells. J Natl Cancer Inst 2003;95:291–302.
26. Parrizas M, Gazit A, Levitzki A, Wertheimer E, LeRoith D. Specific inhibition of insulin-like growth factor-1 and insulin receptor tyrosine kinase activity and biological function by tyrphostins. Endocrinology 1997; 138:1427–33.
27. Peterson RT, Desai BN, Hardwick JS, Schreiber SL. Protein phosphatase 2A interacts with the 70-kDa S6 kinase and is activated by inhibition of FKBP12-rapamycinassociated protein. Proc Natl Acad Sci U S A 1999;96:4438–42.
28. Chakravarti A, Loeffler JS, Dyson NJ. Insulin-like growth factor receptor I mediates resistance to anti-epidermal growth factor receptor therapy in primary human glioblastoma cells through continued activation of phosphoinositide 3-kinase signaling. Cancer Res 2002; 62:200–7.
29. Balana ME, Labriola L, Salatino M, et al. Activation of ErbB-2 via a hierarchical interaction between ErbB-2 and type I insulin-like growth factor receptor in mammary tumor cells. Oncogene 2001;20:34–47.
30. Gilmore AP, Valentijn AJ, Wang P, et al. Activation of BAD by therapeutic inhibition of epidermal growth factor receptor and transactivation by insulin-like growth factor receptor. J Biol Chem 2002;277:27643–50. Epub 2002 May 13.
31. Ahmad T, Farnie G, Bundred NJ, Anderson NG. The mitogenic action of insulin-like growth factor 1 in normal human mammary epithelial cells requires the epidermal growth factor receptor tyrosine kinase. J Biol Chem 2004;279:1713–9. Epub 2003 Oct.
32. Kuribayashi A, Kataoka K, Kurabayashi T, Miura M. Evidence that basal activity, but not transactivation, of the epidermal growth factor receptor tyrosine kinase is required for insulin-like growth factor 1-induced

activation of extracellular signal-regulated kinase in oral carcinoma cells. Endocrinology 2004;145:4976–84. Epub 2004 Jul 22.
33. Holcik M, Gibson H, Korneluk RG. XIAP: apoptotic brake and promising therapeutic target. Apoptosis 2001; 6:253–61.
34. Gingras AC, Gygi SP, Raught B, et al. Regulation of 4E-BP1 phosphorylation: a novel two-step mechanism. Genes Dev 1999;13:1422–37.
35. Herbst RS. Erlotinib (Tarceva): an update on the clinical trial program. Semin Oncol 2003;30:34–46.
36. Amann J, Kalyankrishna S, Massion PP, et al. Aberrant epidermal growth factor receptor signaling and enhanced sensitivity to EGFR inhibitors in lung cancer. Cancer Res 2005;65:226–35.
37. Tracy S, Mukohara T, Hansen M, Meyerson M, Johnson BE, Janne PA. Gefitinib induces apoptosis in the EGFRL858R non-small-cell lung cancer cell line H3255. Cancer Res 2004;64:7241–4.
38. Roskoski R, Jr. The ErbB/HER receptor protein-tyrosine kinases and cancer. Biochem Biophys Res Commun 2004;319:1–11.
39. Garrett TP, McKern NM, Lou M, et al. Crystal structure of the first three domains of the type-1 insulin-like growth factor receptor. Nature 1998;394: 395–9.
40. Jimeno A, Rubio-Viqueira B, Amador ML, et al. Epidermal growth factor receptor dynamics influences response to epidermal growth factor receptor targeted agents. Cancer Res 2005;65:3003–10.
41. Tan AR, Yang X, Hewitt SM, et al. Evaluation of biologic end points and pharmacokinetics in patients with metastatic breast cancer after treatment with erlotinib, an epidermal growth factor receptor tyrosine kinase inhibitor. J Clin Oncol 2004;22:3080–90.
42. Gregorc V, Ceresoli GL, Floriani I, et al. Effects of gefitinib on serum epidermal growth factor receptor and HER2 in patients with advanced non-small cell lung cancer. Clin Cancer Res 2004;10:6006–12.
43. Rao RD, Mladek AC, Lamont JD, et al. Disruption of parallel and converging signaling pathways contributes to the synergistic antitumor effects of simultaneous mTOR and EGFR inhibition in GBM cells. Neoplasia 2005;7:921–9.
44. Gschwind A, Zwick E, Prenzel N, Leserer M, Ullrich A. Cell communication networks: epidermal growth factor receptor transactivation as the paradigm for interreceptor signal transmission. Oncogene 2001;20: 1594–600.
45. Roudabush FL, Pierce KL, Maudsley S, Khan KD, Luttrell LM. Transactivation of the EGF receptor mediates IGF-1-stimulated shc phosphorylation and ERK1/2 activation in COS-7 cells. J Biol Chem 2000; 275:22583–9.
46. Pierce KL, Luttrell LM, Lefkowitz RJ. New mechanisms in heptahelical receptor signaling to mitogen activated protein kinase cascades. Oncogene 2001;20: 1532–9.
47. Marinissen MJ, Gutkind JS. G-protein-coupled receptors and signaling networks: emerging paradigms. Trends Pharmacol Sci 2001;22:368–76.
48. Pollak M. Insulin-like growth factor physiology and cancer risk. Eur J Cancer 2000;36:1224–8.
49. Merrill MJ, Edwards NA. Insulin-like growth factor-I receptors in human glial tumors. J Clin Endocrinol Metab 1990;71:199–209.

Identification of Insulin-Like Growth Factor Binding Protein-3 as a Farnesyl Transferase Inhibitor SCH66336-Induced Negative Regulator of Angiogenesis in Head and Neck Squamous Cell Carcinoma

Seung-Hyun Oh,[1] Woo-Young Kim,[1] Jai-Hyun Kim,[1] Maher N. Younes,[2] Adel K. El-Naggar,[3] Jeffrey N. Myers,[2] Merril Kies,[1] Pinchas Cohen,[4] Fadlo Khuri,[5] Waun K. Hong,[1] and Ho-Young Lee[1]

Abstract The farnesyl transferase inhibitor (FTI) SCH66336 has been shown to have antitumor activities in head and neck squamous cell carcinoma (HNSCC) *in vitro* and *in vivo*. However, its mechanism of action has not been well defined. Here, we report that the insulin-like growth factor (IGF) binding protein (IGFBP)-3 mediates antitumor activities of SCH66336 in HNSCC by inhibiting angiogenesis. SCH66336 significantly suppressed HNSCC tumor growth and angiogenesis via mechanisms that are independent of H-Ras and RhoB. By inducing IGFBP-3 secretion from HNSCC cells, this compound suppresses angiogenic activities of endothelial cells, including vessel formation in chorioallantoic membranes of chick, endothelial cell sprouting from chick aorta, and capillary tube formation of human umbilical vascular endothelial cells (HUVEC). Knockdown of IGFBP-3 expression in HNSCC cells by RNA interference or depletion of IGFBP-3 in HUVECs by neutralizing antibody effectively blocked the effects of IGFBP-3 secreted from SCH66336-treated HNSCC cells on HUVECs. These findings suggest that IGFBP-3 could be a primary target for antitumor activities of FTIs and that IGFBP-3 is an effective therapeutic approach against angiogenesis in HNSCC.

Despite advances in therapy, including surgery, chemotherapy, and radiation, the survival rate of patients with head and neck squamous cell carcinoma (HNSCC) has not improved substantially (1). Conventional treatments have targeted tumor cells alone. In patients with HNSCC, however, the primary tumor has metastasized to regional lymph nodes, distant organs, or both by the time the diagnosis is made (2, 3). Angiogenesis is an essential step in the transition of a tumor from a small cluster of mutated cells to a large, malignant growth and subsequent metastasis to other organs throughout the body (4–6). It has been hypothesized, therefore, that the development of agents targeting tumor angiogenesis could be an effective strategy to control and treat various malignancies.

Increasing number of evidence implicate insulin-like growth factor (IGF) binding proteins (IGFBP) in regulating angiogenesis. IGFBPs modulate the bioactivity of IGFs by sequestering IGFs away from their receptors in the extracellular milieu, thereby regulating the stimulating action of IGF on angiogenesis and invasion (7). Some IGFBPs, however, in particular IGFBP-3, also have exhibited more active, IGF-independent antitumor activities, which are probably mediated by other cell surface receptors, such as the type V transforming growth factor-β receptor (8–11). IGFBP-3 has recently been identified as an IGF-independent inhibitor of vascular endothelial growth factor–induced endothelial cell proliferation (12).

While searching for agents that have antianiogenic activities in HNSCC cells, we found that farnesyl transferase inhibitors (FTI), especially SCH66336 (Lonafarnib, Sarasar) that has shown to induce tumor regression *in vitro* and *in vivo*, inhibit angiogenic activities of HNSCC cells by inducing IGFBP-3 expression. FTIs were originally designed to inhibit posttranslational activation of Ras by blocking farnesylation (13). Recent studies suggest, however, that the cytotoxic actions of FTIs are due not to the inhibition of Ras proteins exclusively but to the modulation of other targets, including RhoB, a G protein that regulates receptor trafficking; the centromere-binding proteins CENP-E and CENP-F; and/or other proteins that have not yet been identified (14). Our results show that SCH66336

Authors' Affiliations: Departments of [1]Thoracic/Head and Neck Medical Oncology, [2]Head and Neck Surgery, and [3]Pathology, The University of Texas M.D. Anderson Cancer Center, Houston, Texas; [4]Department of Pediatrics, University of California, Los Angeles, Los Angeles, California; and [5]The Winship Cancer Institute, Emory University, Atlanta, Georgia

Received 8/8/05; revised 10/7/05; accepted 11/9/05.

Grant support: NIH grants R01 CA100816-01A1 (H-Y. Lee) and R01 CA109520-01 (H-Y. Lee), American Cancer Society grant RSG-04-082-01-TBE 01 (H-Y. Lee), M.D. Anderson Cancer Center Specialized Programs of Research Excellence grant in head and neck cancer P50 CA 97007-01 (W.K. Hong), and Department of Defense grant W81XWH-04-1-0142-01-VITAL (W.K. Hong).

The costs of publication of this article were defrayed in part by the payment of page charges. This article must therefore be hereby marked *advertisement* in accordance with 18 U.S.C. Section 1734 solely to indicate this fact.

Note: W.K. Hong is an American Cancer Society clinical research professor.

Requests for reprints: Ho-Yung Lee, Department of Thoracic/Head and Neck Medical Oncology, Box 432, The University of Texas M.D. Anderson Cancer Center, 1515 Holcombe Boulevard, Houston, TX 77030. Phone: 713-745-0769; Fax: 713-796-8655; E-mail: hlee@mdanderson.org.

©2006 American Association for Cancer Research.

doi:10.1158/1078-0432.CCR-05-1725

induced expression of IGFBP-3 protein, which in turn blocked the PI3K/Akt pathway, resulting in the induction of apoptosis in vascular endothelial cells and regression of HNSCC tumor growth and angiogenesis.

Materials and Methods

Cells, animals, and materials. Human HNSCC cell lines UMSCC38, UMSCC22B, and SqCC/Y1, established originally by Dr. Michael Reiss (Yale University, New Haven, CT) and Dr. Thomas Carey (University of Michigan, Ann Arbor, MI), respectively, were obtained from Dr. Reuben Lotan (M.D. Anderson Cancer Center, Houston, TX). (15). Human non-small cell lung cancer (NSCLC) cell lines H460, Calu1, and H358 were purchased from the American Type Culture Collection (Manassas, VA). These cells were cultured in DMEM supplemented with 10% fetal bovine serum and antibiotics. Human umbilical vascular endothelial cells (HUVEC; Cambrex BioScience, Walkersville, MD) were maintained in a gelatin-coated dish in endothelial cell basal medium (Cambrex BioScience) containing endothelial cell growth supplement at 37°C in a humidified environment with 5% CO_2. HUVECs used in this study were from passages 2 to 7. Female nude mice, 6 weeks of age, were purchased from Harlan-Sprague-Dawley (Indianapolis, IN). Chick eggs were obtained from Charles River Laboratories (Wilmington, MA).

Expression vectors containing pH-ras-V12 or pRhoB-GG were kindly given by Dr. George C. Prendergast (Thomas Jefferson University, Philadelphia, PA). Bovine serum albumin, gelatin, and 3-(4,5-dimethylthiazol-2-yl)-2,5-diphenyltetrazolium bromide were obtained from Sigma-Aldrich (St. Louis, MO). IGF-1 and Des(1-3)IGF were purchased from R&D Systems (Minneapolis, MN). Amicon Ultra-4 was obtained from Millipore Co. (Bedford, MA). Cell culture inserts incorporating PET membranes (6.4-mm diameter, 8-μm pore size) and 24-well plates were from Costar (Cambridge, MA). Anti-pIGF-1R antibodies were purchased from Cell Signaling Technology (Beverly, MA). Antibodies against IGFBP-2, IGFBP-6, IGF-1R, H-Ras, RhoB, α-tubulin, and anti-β-actin were purchased from Santa Cruz Biotechnology, Inc. (Santa Cruz, CA), and anti-CD31 antibody was obtained from BD PharMingen (San Diego, CA). Anti-IGFBP-3 antibody was from Diagnostic Systems Laboratories, Inc. (Webster, TX). SCH66336 was provided by Schering-Plough Research Institute (Kenilworth, NJ). FTI-277 was purchased from Calbiochem (San Diego, CA). SCH66336 and FTI-277 were dissolved in DMSO at various concentrations to establish dose responses. Synthetic small interfering RNAs (siRNA) targeting H-Ras or RhoB were purchased from Ambion (Austin, TX), and IGFBP-3 and nonspecific control siRNA were from Dharmacon (Lafayette, CO).

To test the effects of conditioned medium on proliferation of vascular endothelial cells, HUVECs were plated at 3×10^3 per well in 96-well culture plates, untreated or preincubated with IgG or IGFBP-3 neutralizing antibody, and then treated with conditioned medium (10 μg) from the HNSCC cells. Cell proliferation was measured using the 3-(4,5-dimethylthiazol-2-yl)-2,5-diphenyltetrazolium bromide assay, as previously described (16).

In experiments assessing the effects of SCH66336 on protein and mRNA expression, HNSCC and NSCLC cell lines (1×10^6 in 100-mm^3 dishes) were treated with different concentrations of SCH66336 (0.5, 1, or 5 μmol/L) for indicated time periods in complete medium. When the effects of SCH66336 on pIGF-1R were tested, cells were serum starved for 1 day and stimulated with IGF-I (100 ng/mL, for 30 minutes) before harvest. For siRNA transfection, UMSCC38 cells were plated at concentrations of 1×10^6 per well in 10-cm plates. The next day, the cells were transfected with siRNA using Oligofectamine (Invitrogen, Carlsbad, CA) and cultured in growth medium with or without SCH66336 (5 μmol/L). One day after transfection, cells were changed to serum-free medium containing the same concentration of SCH66336. After 2 days of incubation, cells and conditioned media were collected. When HUVECs were treated with conditioned media from UMSCC38 cells, 1×10^5 per well in six-well plates were treated with conditioned media in endothelial cell basal medium in the absence or presence of IGFBP-3 neutralizing antibody for 12 hours.

Conditioned medium. To collect conditioned media from UMSCC38 cells, UMSCC38 cells (1×10^6 per plate) in 10-cm plates were incubated in growth medium containing SCH66336 (0.5, 1, or 5 μmol/L) for 1 day, washed with PBS, and then resupplied with serum-free medium containing the same concentrations of SCH66336. After 2 days of incubation, conditioned medium was collected and subjected to centrifugation through an Amicon Ultra-4 filter to remove any traces of SCH66336. Concentration of the conditioned medium was measured by the bicinchoninic acid assay (Pierce Biotechnology, Rockford, IL). The molecular mass cutoff of the filter was 5 kDa; the molecular mass of SCH66336 is 0.56 kDa, thus the flow-through containing excess SCH66336 was discarded, and the retentate was collected. Removal of SCH66336 from the conditioned medium was determined as previously described (17). The final filter retentate was concentrated 40-fold for several analyses, including Western blot, HUVEC proliferation and tube formation, chick aortic arch, and chorioallantoic membrane assays.

Animal care and injections. All animal procedures were done in accordance with a protocol approved by the Institutional Animal Care and Usage Committee. Orthotopic sublingual injections of tumor cells were described elsewhere (18). Female nude mice (6-week-old) under anesthesia were injected with UMSCC38 cells (2×10^6) into the lateral tongue ($n = 5$). One week later, when tumors started to develop, 40 mg/kg of SCH66336 or 20% hydroxyl-propyl-β-cyclodexatrin control vehicle was given orally twice a day for 3 weeks. Thirteen days after cell injection, when tumors reached at least 50 mm^3 in volume, tumor size was measured twice a week for 15 days. Tumor growth was quantified by measuring the tumors in two dimensions and calculating volume as described elsewhere (16). One week later, when tumors started to develop, the mouse food was replaced by commercially available soft food (transgenic mice dough; Bio-serv, Frenchtown, NJ), which the mice can ingest even when the oral cavity was blocked by tumor. The mice were humanely killed by CO_2 inhalation when they had lost >20% of their preinjection body weight (average 18.92 g). The tongues were removed and separated into two parts. One part was fixed, embedded in paraffin, and sectioned for active caspase-3 staining. The other part was frozen and sectioned for CD31 staining.

Western blot analysis. Preparation of whole-cell lysates, quantification of the proteins, gel electrophoresis, and Western blotting were done as described elsewhere (19). Equal amounts of proteins in conditioned medium samples were confirmed by Coomassie blue staining of the duplicate gels and Ponceau staining of membrane.

Immunohistochemistry. Immunohistochemical analysis on IGFBP-3 was done using tongue tumor tissues from mice as described elsewhere (17). For CD31 staining, frozen sections of tumor tissues were stained with anti-CD31 antibody (BD PharMingen; 1:100 dilution) and then detected by 3,3′-diaminobenzidine.

Chick aortic arch assay. Chick aortic arch assay was done as described elsewhere (20). Briefly, conditioned media collected from UMSCC38 cells were added to aortic rings from 14-day-old chick embryos. The plates were incubated for 48 hours at 37°C to allow microvessel sprouting from the adventitial layer. Average sprouting was measured with the imageJ program (NIH) after the plates were photographed under the stereomicroscope (Zeiss, Göttingen, Germany). Each condition was tested in six wells. The experiment was repeated thrice with similar results.

Tube formation assay. Tube formation assay was done as described elsewhere (21). HUVECs (5×10^4) were seeded on Matrigel surfaces and grown in the absence or presence of conditioned media from different treatment groups. After 18 hours, images were photographed at ×40 magnification, and tube formation was scored by blinded

observer as follows: a three-branch point event was scored as one tube, as described elsewhere (21). Each condition was tested in six wells. The experiment was repeated thrice with similar results.

Chorioallantoic membrane assay. Chorioallantoic membrane assay was conducted on 9-day-old chick embryos as described elsewhere (21). A coverslip loaded with 50 μg of conditioned medium was applied onto the surface of the chorioallantoic membrane. After 2 days of incubation, a fat emulsion was injected into the chorioallantoic membrane to allow visualization of the blood vessels, and chorioallantoic membranes were photographed with a stereomicroscope.

Reverse transcription-PCR. Total RNA was isolated from cells with the use of Trizol reagent (Invitrogen). cDNA was synthesized as previously described (17). Reverse transcription-PCR was done by coamplification of the genes together with a reference gene (*GAPDH*) using cDNA template generated as already described and corresponding gene-specific primer sets. The primer sequences were as follows: 5′-GAAGGGCGACACTGCTTTTTC-3′ (sense) and 5′-CCAGCTCCAGGAAATGCTAG-3′ (antisense) for *IGFBP-3*; 5′-CAAGAGTGCGCTGACCATCC-3′ (sense) and 5′-CCGGATCTCACGCACCAAC-3′ (antisense) for H-*ras*; 5′-GCGTGCGGCAAGACGTCTG-3′ (sense) and 5′-TCATAGCACCTTGCAGCAGTT-3′ (antisense) for *rho-B*; 5′-GGTGAAGGTCGGTGTGAACGGATTT-3′ (sense) and 5′-AATGCCAAAGTTGTCATGGATGACC-3′(antisense) for *GAPDH*. To avoid amplification of genomic DNA, the primers of each gene were chosen from different exons. Reverse transcription-PCR was done in a total volume of 25 μL containing 1 μL of cDNA solution and 0.2 μmol/L of sense and antisense primers. The reverse transcription-PCR exponential phase was determined on 28 to 38 cycles using cDNAs developed from identical reactions. The thermocycler condition used for amplification was as follows: 6 minutes at 94°C (one cycle), 6 minutes hot start at 94°C, 45 seconds at 56°C to 60°C (25-35 cycles), and 1 minute at 72°C (one cycle). Amplification products (8 μL) were resolved in 2% agarose gel, stained with ethidium bromide, and visualized in a transilluminator and photographed.

Immunoprecipitation. Equal amounts of protein samples were incubated with anti-pTyr antibody and protein A-Sepharose overnight and washed with lysis buffer thrice and 2× PBS twice. Proteins were eluted with 4× SDS loading buffer. Samples were boiled and subjected to electrophoresis on SDS-polyacrylamide gels, and binding was detected by using an enhanced chemiluminescence assay (Amersham Pharmacia Biotech, Piscataway, NJ).

Northern blot analysis. Total cellular RNA was prepared, as previously described (22). Twenty micrograms of total RNA were subjected to electrophoresis in denaturing agarose gels and transferred to a Zeta-probe membrane (Bio-Rad Laboratories, Hercules, CA). Membranes were hybridized with [^{32}P]dCTP random-primed *IGFBP-3* cDNA, washed, and subjected to autoradiography. An equal amount of RNA loading was monitored by ethidium bromide staining of the gels.

Luciferase assay. Cells were seeded in 24-well tissue culture plates and transfected with 500 ng of IGFBP-3 reporter plasmid (pGL2 or pGL2-BP3) and 20 ng of *Renilla* luciferase control vector (pRL-SV40) using LipofectAMINE (Life Technologies/Bethesda Research Laboratories, Grand Island, NY). The total amount of plasmid DNA was equally adjusted with vector DNA. The transfection solution was removed after 6 hours of transfection, and the cells were changed to complete medium with or without different concentrations of SCH66336. Following 2 days of incubation, cells were harvested. The cells were washed with PBS and subjected to lysis in 0.1 mL of 1× passive lysis buffer (Promega, Madison, WI). Cell extracts were assayed for firefly and *Renilla* luciferase activities using the Dual-luciferase reporter assay system according to the manufacturer's instruction (Promega). Firefly luciferase activities were normalized by *Renilla* luciferase activities. Luciferase activities were expressed as the means and SD from three identical wells.

Statistical analysis. Data are shown as means ± SD. For statistical significance between groups, the paired Student's *t* test was done.

Results

SCH66336 inhibits angiogenic activities of HNSCC. We tested the effects of SCH66336 on HNSCC tumor growth by establishing orthotopic tongue tumors of UMSCC38 HNSCC cells in nude mice and treating the mice with SCH66336. Representative tongue tissues from a healthy mouse (*Normal*), and tongue tumors from SCH66336-untreated (*Con*) and SCH66336-treated mice (*SCH66336*) are shown (Fig. 1A). Oral treatment with SCH66336 (40 mg/kg) almost completely suppressed tumor growth ($P < 0.005$). On day 25, the average tumor volume for untreated control mice had increased to 287.86 ± 53.93% (mean ± SD) of the volume on day 13, whereas that for SCH66336-treated mice showed 123.20 ± 14.67% of the volume before the SCH66336 treatment (Fig. 1B, *left*). The average body weight of SCH66336-treated mice was not remarkably changed during the treatment (Fig. 1B, *right*) compared with that of control mice. These findings suggest that FTI SCH66336 is an efficient therapeutic agent in head and neck tumors.

We studied the mechanism of the antitumor activities of SCH66336 in HNSCC. Several HNSCC cell lines treated with as much as 5 μmol/L SCH66336 yielded neither a terminal deoxynucleotidyl transferase–mediated nick end labeling–positive cell population nor changes in expression of caspase-3 and poly (ADP-ribose) polymerase (data not shown), indicating that SCH66336 induces little apoptotic activities in HNSCC cells. Given this finding and the critical role of angiogenesis in tumor growth, we evaluated the effects of SCH66336 on angiogenic activities of HNSCC cells. As shown in Fig. 1C, SCH66336 significantly decreased tumor vascularization ($P < 0.01$) as determined by microvessel density in anti-CD31-stained tongue tumor tissues from control and SCH6636-treated nude mice. We then did a series of *in vitro* and *in vivo* experiments to test the antiangiogenic activities of SCH66336. We directly applied conditioned media from UMSCC38 cells to HUVECs. The proliferation (Fig. 1D) and capillary tube formation (Fig. 1E) of HUVECs were significantly stimulated by conditioned media from the untreated UMSCC38 cells but not by conditioned media from SCH66336 (5 μmol/L)–treated cells ($P < 0.01$). The *ex vivo* chick aortic ring arch assay revealed that conditioned media from untreated UMSCC38 cells also stimulated endothelial cell sprouts ($P < 0.01$), whereas conditioned media from SCH66336-treated cells did not exhibit stimulating effects on endothelial cell sprouting (Fig. 1F). The chorioallantoic membrane assay, an established *in vivo* angiogenesis model, revealed that treatment with conditioned media from untreated UMSCC38 cells but not conditioned media from SCH66336-treated cells significantly induced new vessel formation in chorioallantoic membranes of chick embryos ($P < 0.05$; Fig. 1G). We did not find any signs of toxicity, such as thrombosis, hemorrhage, or egg lethality, in the chorioallantoic membrane assay. Together, this data indicate that SCH66336 can elicit antiangiogenic activities in HNSCC.

Antiangiogenic activities of SCH66336 in HNSCC cells are independent of H-Ras and RhoB. We investigated the mechanisms by which SCH66336 elicits antiangiogenic activities in HNSCC cells. Because FTIs are designed to inhibit Ras farnesylation, the most important step in ras activation (13), we first tested the effects of SCH66336 on Ras in HNSCC cells. Western blot analysis revealed that SCH66336 induced

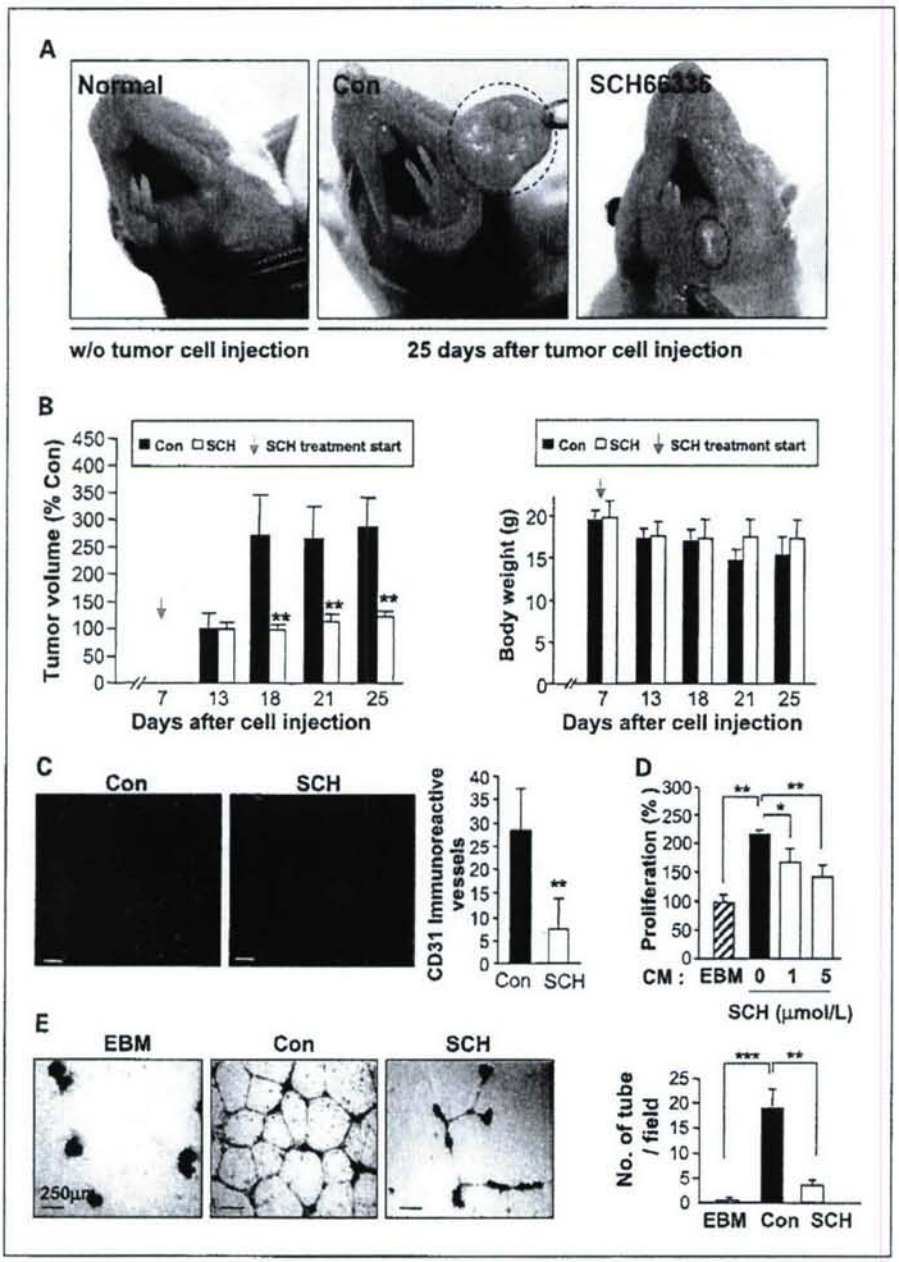

Fig. 1. Antiangiogenic activities of SCH66336 in HNSCC cells. *A*, photograph of normal tongue from nude mice that was not inoculated with UMSCC38 cells (*left*). Nude mice bearing UMSCC38 orthotopic tongue tumors were given 40 mg/kg SCH66336 orally twice a day on days 7 to 25 after tumor cell injection. Orthotopic tongue tumors from vehicle-treated (*middle, Con*) and SCH66336-treated (*right, SCH66336*) nude mice on day 25 after injection of UMSCC38 cells. *B*, effects of SCH66336 (*SCH*) on growth of orthotopic tongue tumors were tested. Relative tumor growth and changes in body weight in the control and the treatment groups compared with control tumor volumes at the time of SCH66336 treatment (day 13). Columns, mean tumor volumes (calculated from five mice); bars, SD. **, $P < 0.01$ compared with control. *C*, orthotopic mouse tongue tissues were stained with an anti-CD31 antibody. The slides were examined at ×100 under fluorescent microscope and analyzed for red (CD31) fluorescence. The number of microvessels per field was counted. Columns, mean of three slides per tumor (calculated from five mice); bars, SD. **, $P < 0.01$ compared with control-treated tumors. *D*, HUVECs were allowed to grow in 100 μL endothelial cell basal medium (*EBM*) containing 10 μL conditioned medium (*CM*) from untreated or SCH66336-treated UMSCC cells. Cell proliferation was analyzed by 3-(4,5-dimethylthiazol-2-yl)-2,5-diphenyltetrazolium bromide assay. Independent experiments were repeated three times. Columns, mean % of eight samples; bars, SD. *, $P < 0.05$; **, $P < 0.01$; ***, $P < 0.001$ compared with negative control. *E*, angiogenic activities of conditioned media from UMSCC38 cells were tested by tube formation assay. Columns, mean of three samples; bars, SD. **, $P < 0.01$; ***, $P < 0.001$ compared with control.

dose-dependent decreases in farnesylated H-Ras (H-Ras-F) in UMSCC38, UMSCC22B, and SqCC/Y1 cells (Fig. 2A). None of these cells have a *ras* mutation (data not shown), suggesting that the antiangiogenic activities of SCH66336 could be traced to proteins other than Ras. One potential target is RhoB, a 21-kDa G-protein, that is both farnesylated and geranylgeranylated by FTase and GGTase I (23), respectively. Recent evidence indicates that RhoB is a mediator of the antitumor activities of FTIs in mouse and rodent model systems and in human cancer cells (24, 25). Indeed, treatment with SCH66336 elicited elevations in the levels of RhoB (Fig. 2A), presumably due to the increased expression of the geranylgeranylated isoform of RhoB (RhoB-GG), as was observed previously (26).

To understand whether decreases in H-Ras-F or induction of RhoB mediated the antiangiogenic activity of SCH66336, we determined whether silencing H-Ras or RhoB expression by siRNA could abolish the activities of SCH66336 in UMSCC38 cells. Transfection with siRNAs targeting H-*ras* or *RhoB* specifically inhibited H-Ras or RhoB protein expression in UMSCC38 cells, whereas control scrambled (*scr*) siRNA did not affect the expression of these genes (Fig. 2B). Two different siRNAs induced similar degrees of gene silencing. These siRNAs also specifically inhibited mRNA expression of target genes regardless of the presence of SCH66336 (Fig. 2C). Cell viability was not specifically altered in any of these cells (data not shown). According to the 3-(4,5-dimethylthiazol-2-yl)-2,5-diphenyltetrazolium bromide assay (Fig. 2D) and

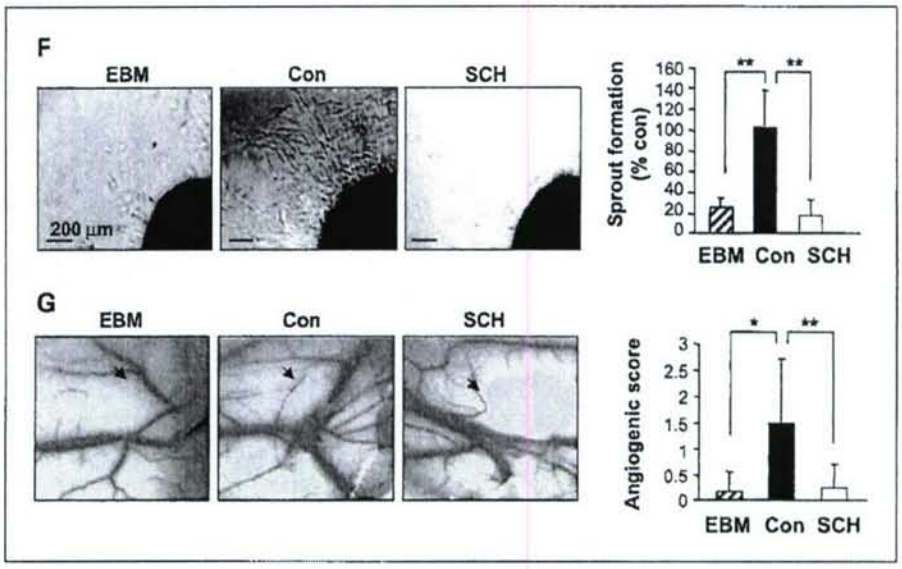

Fig. 1 *Continued.* *F*, endothelial cell sprouting from chick aortic rings that were incubated with conditioned medium from SCH66336-treated or untreated UMSCC38 cells. Columns, means from six samples; bars, SD. Representative group from each condition. Bar, 200 μm. **, $P < 0.01$ compared with negative control. *G*, in a chorioallantoic membrane assay, angiogenesis stimulated by conditioned media from UMSCC38 cells was photographed (*left*) or quantitatively evaluated (*right*). Independent experiments were repeated three times. Columns, mean of >30 eggs; bars, SD/95% confidence intervals. *, $P < 0.05$; **, $P < 0.01$; ***, $P < 0.001$ compared with negative control.

tube formation assays (Fig. 2E), HUVEC proliferation and morphogenesis were stimulated by conditioned media from control UMSCC 38 cells transfected with *scr*. Conditioned media from SCH66336-treated UMSCC38 cells did not show these angiogenic activities. The effects of SCH66336 were still consistent in UMSCC38 cells, which had been transfected with siRNA targeting H-ras or RhoB. Two different siRNAs for H-Ras and RhoB showed similar results (data not shown). All of these findings indicate that SCH66336 suppressed the angiogenic activities of HNSCC cells via H-Ras-independent and RhoB-independent mechanisms.

FTI induces IGFBP-3 expression* in vitro *and* in vivo *via mechanisms that are independent of H-Ras or RhoB. Because the IGF system has an important role in regulating4 proliferation and angiogenesis (27–29), we determined whether SCH66336 treatment stimulates the expression of IGFBPs. An obvious increase in IGFBP-3 protein level was observed in UMSCC38, UMSCC22B, and SqCC/Y1 cells treated with SCH66336 or FTI-277, another FTI (Fig. 3A). Increased levels of the IGFBP-3 protein were also observed in conditioned media from these cells (data not shown). No change was detected in the expression of other IGFBP subfamily members, including IGFBP-2 and IGFBP-6, after SCH66336 treatment (Fig. 3A). Because IGFBP-3 is supposed to control IGF-1–induced IGF-1R activation (30), we next determined the effects of SCH66336 on the levels of phosphorylated IGF-1R (pIGF-1R) in UMSCC38 cells. Western blot analysis revealed that treatment with IGF-1 caused increases in pIGF-1R, which is inhibited by SCH66336 in UMSCC38 cells (Fig. 3B, *left*). Whereas phosphorylation of IGF-1R stimulated by Des(1-3) (10 nmol/L), a mutant IGF-I that has a vastly diminished affinity for the IGFBPs but retains high avidity for IGF-1R (31), was marginally affected by SCH66336 in UMSCC38 cells (Fig. 3B, *middle*), indicating that secretion of functional IGFBP-3 by SCH66336-treated cells down-regulated pIGF-IR. Immunoprecipitation analysis using an antiphosphotyrosine antibody followed by Western blot analysis with an anti-IGF-1Rβ antibody confirmed that SCH66336 inhibited IGF-stimulated IGF-1R phosphorylation (Fig. 3B, *right*). Induction of IGFBP-3 by SCH66336 also found in H460, Calu1, and H358 NSCLC cell lines (Fig. 3C).

We further studied the mechanism by which SCH66336 activates IGFBP-3 expression. Northern and Western blot analyses of UMSCC38 cells revealed that *IGFBP-3* gene expression is induced within 1.5 hours after the SCH66336 treatment, respectively (Fig. 3D). Moreover, a transient transfection experiment done with a luciferase reporter plasmid containing 1.8-kb *IGFBP-3* promoter (pGL2-BP3; ref. 32) indicated that SCH66336 increased *IGFBP-3* promoter activity in UMSCC38 and H460 cells in a dose-dependent manner (Fig. 3E). IGFBP-3 promoter activity was also increased in UMSCC38 cells by the treatment with FTI-277. These findings indicate that SCH66336 induced IGFBP-3 expression at a transcriptional level and that the induction of IGFBP-3 expression is a generic response to FTIs. Blockade of H-Ras or RhoB expression by siRNA (Fig. 3F and G) or overexpression of pH-Ras-V12 or pRhoB-GG (Fig. 3H) did not affect the ability of SCH66336 to induce IGFBP-3 promoter activity and protein expression, indicating that induction of IGFBP-3 expression by SCH66336 is independent of H-Ras or RhoB.

Oral administration of FTI SCH66336 induces IGFBP-3 expression* in vivo *in tongue tumor tissues. We tested whether SCH66336 could increase IGFBP-3 expression *in vivo*. We found obviously higher levels of IGFBP-3 in orthotopic tongue tumor tissues removed from SCH66336-treated mice than in tongue tumor tissues from untreated control mice (Fig. 4A). IGFBP-3 expression was also analyzed in the tissue samples from patients who had received SCH66336. Results are shown from the pretreatment and/or posttreatment matched tumor tissues from three patients. Prominent IGFBP-3 expression was observed in the first patient (33) in histologically normal cells of the anterior tongue (Fig. 4B, *left*), but only focal or no IGFBP-3 expression was found in their squamous carcinoma tumor cells (*SCC*, Fig. 4B, *right*). Tumor tissues from this patient were not available after the SCH66336 treatment. Very low or undetectable levels of IGFBP-3 were also observed in squamous carcinoma tumor cells of the other two patients (patients 2 and 3) who had not been treated with SCH66336 (Fig. 4C, *left*). Three months after

these patients' treatment with SCH66336, however, IGFBP-3 expression was strongly induced in the membranes of the cancer cells undergoing karyolysis (Fig. 4C, *right*). These findings indicate that oral administration of SCH66336 was sufficient to induce IGFBP-3 expression *in vivo*.

IGFBP-3 secreted from SCH66336-treated HNSCC cells inhibits angiogenic activities in HUVECs by blocking Akt activation. To investigate whether IGFBP-3 secreted from SCH66336-treated HNSCC cells inhibited angiogenesis, we determined whether the blockade of IGFBP-3 secretion from SCH66336-treated UMSCC38 cells could restore the angiogenic effects of conditioned media from these cells. To this end, UMSCC38 cells were transfected with *IGFBP-3* siRNA, and the conditioned medium from these cells was applied to HUVECs. *IGFBP-3* siRNA specifically inhibited *IGFBP-3* mRNA expression (Fig. 5A, *left*) as well as protein expression in the untreated and SCH66336-treated UMSCC38 cells (Fig. 5A, *right*). Conditioned media from UMSCC38 cells transfected with *IGFBP-3* siRNA before the SCH66336 treatment (*SCH*) did not show significant effects on tube formation (Fig. 5B) and proliferation (Fig. 5C) of HUVECs compared with conditioned media from *scr*-transfected cells. To mask the effect of IGFBP-3 secreted from UMSCC38 cells on HUVECs, HUVECs were preincubated with IGFBP-3 neutralizing antibody (αBP3) before conditioned medium treatment. Stimulation of HUVECs proliferation by the conditioned media from control UMSCC38 cells was not affected with αBP3 (Fig. 5D). In contrast, proliferation-stimulating activities of conditioned media from SCH66336-treated UMSCC38 cells were almost completely blocked. These findings indicate that IGFBP-3 secreted from SCH66336-treated cells played a major role in inhibiting HUVECs proliferation and morphogenesis.

It has been shown that IGFBP-3 induces apoptosis in endothelial cells by inhibiting activation of Akt, a key enzyme for cell survival (12). Thus, we next tested whether IGFBP-3 secreted from SCH66336-treated HNSCC cells could inhibit activation of Akt. Western blot assays showed that conditioned media from control UMSCC38 cells stimulated phosphorylation of Akt (*pAkt*, Ser^{473}) in HUVECs (Fig. 5E), which was not affected by the αBP3 treatment. Conditioned media from SCH66336-treated UMSCC38 cells marginally stimulated phophorylation of Akt; however, pAkt levels were obviously induced by the incubation of HUVECs with αBP3. Phosphorylation of extracellular signal-regulated kinase (*pERK*) was stimulated in HUVECs by conditioned media from control or SCH66336-treated UMSCC cells but was not affected by the αBP3 (Fig. 5E). These findings suggest that IGFBP-3 secreted from SCH66336-treated HNSCC cells inhibited proliferation of HUVECs by inhibiting Akt activation.

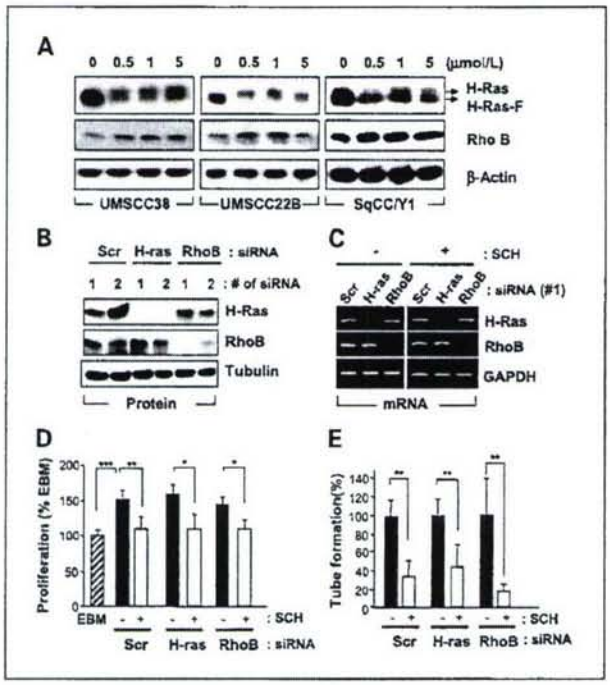

Fig. 2. Role of H-Ras and RhoB in the antiangiogenic and anti-invasive activities of SCH66336 in HNSCC cells. *A*, effects of SCH66336 on levels of unfarnesylated H-Ras and farnesylated H-Ras (H-Ras-F) were examined in UMSCC38, UMSCC22B, and SqCC/Y1 cells treated with indicated doses of SCH66336 for 3 days. *B-C*, effects of scrambled siRNA (*scr*) or siRNA targeting *H-ras* or *RhoB* on protein (*B*) and mRNA (*C*) levels of H-Ras and RhoB were examined. Expression of tubulin or GAPDH was included as loading controls. Lanes 1 and 2, siRNA with different sequence targeting same gene. *D-E*, proliferation (*D*) and morphogenesis (*E*) of HUVECs stimulated by conditioned media from UMSCC38 cells, which were transfected with the indicated siRNA and treated with SCH66336 (5 μmol/L), were tested by 3-(4,5-dimethylthiazol-2-yl)-2,5-diphenyltetrazolium bromide and tube formation assays, respectively. Independent experiments were repeated three times. Columns, means of three samples; bars, SD. *, $P < 0.05$; **, $P < 0.01$; ***, $P < 0.001$ compared with untreated cells from each transfection.

Discussion

In this article, we have shown for the first time that the FTI SCH66336 has antitumor activities, especially those related to angiogenesis, by inducing IGFBP-3 expression. The increased IGFBP-3 in turn induces tumor regression by inhibiting tumor angiogenesis via a mechanism that is independent of H-Ras and RhoB. We were encouraged to pursue this line of research by early observations of tumor regression in a clinical trial in which patients with advanced HNSCC were randomized to receive a short 8- to 14-day course of SCH66336 in the preoperative setting.[6] Our *in vivo* results also clearly show that SCH66336 induces efficient antitumor activities; daily oral administration of SCH66336 (40 mg/kg) was sufficient to suppress growth of implanted UMSCC38 tumors in the tongues of nude mice. SCH66336 was active at a concentration of 1 μmol/L, which is well below the concentration reported to be achievable *in vivo* (about 8 μmol/L) in mice given a single oral dose of 25 mg/kg SCH66336 (34). SCH66336 inhibits proliferation of HNSCC cells (15); similar results have been observed in cell lines derived from breast, colon, pancreas, brain, and lung cancers (35-37).

Despite these promising results, the mechanism of action of FTIs in tumors is still incompletely understood. We did not find evidence of SCH66336-mediated apoptotic activities in most of the HNSCC cell lines used in our study, results which are consistent with previous findings that SCH66336 as a single agent cannot induce apoptosis at doses similar to those we used (38). This led us to investigate the antiangiogenic activities of SCH66336 in HNSCC cells. SCH66336 inhibited the angiogenic activities of HNSCC cells *in vitro* and *in vivo*: (*a*)

[6] Unpublished data.

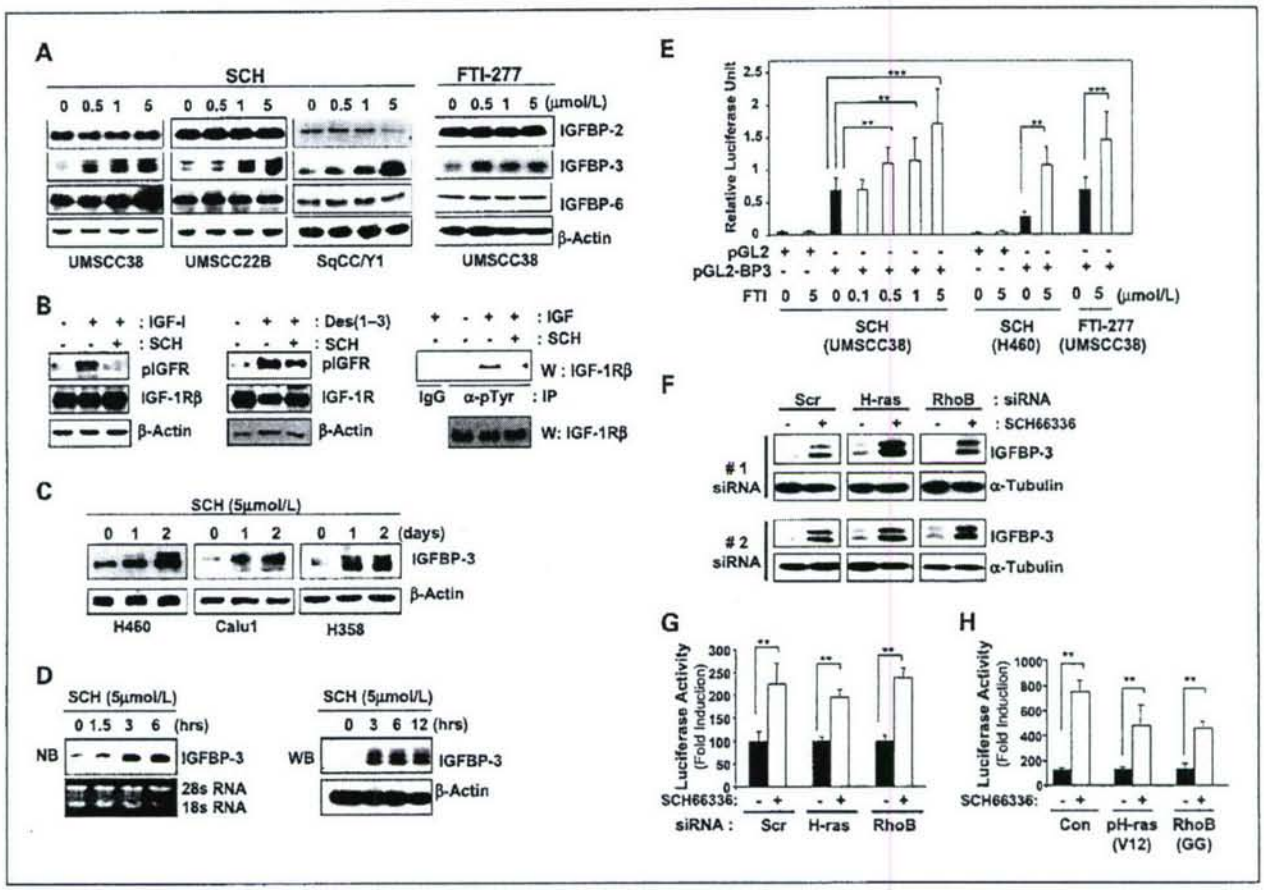

Fig. 3. Effects of FTIs on the expression of IGFBP-3 in HNSCC cells *in vitro* and *in vivo*. *A*, expression of IGFBP-2, IGFBP-3, and IGFBP-6 in UMSCC38, UMSCC22B, and SqCC/Y1 cells, untreated or treated with indicated concentrations of SCH66336 or FTI-277 for 3 days. *B*, Western blot analysis on expression of phosphorylated IGF-1R (Tyr^{1184}; pIGF-1R) and unphosphorylated IGF-1Rβ in UMSCC38 cells that were untreated or treated with SCH66336 and then activated with IGF-I (*left*) or Des(1-3)IGF-I (*middle*). β-Actin was also detected as a loading control. Total protein extracts (500 μg) of UMSCC38 cells that were untreated or treated with SCH66336 before the activation with IGF-1 were subjected to immunoprecipitation (*IP*) with IgG or anti-phosphotyrosine (*pTyr*) antibody. Western blot analysis (*WB*) on immunoprecipitates was done using an anti-IGF-1Rβ antibody (*right*). Equal amount of protein for immunoprecipitation was confirmed by Western blot analysis on IGF-1Rβ expression. *C*, H460, Calu1, and H358 cells treated with 5 μmol/L SCH66336 for 1 or 2 days were also analyzed for IGFBP-3 expression. β-Actin was included as a loading control. *D*, Northern blot (*NB*) and Western blot (*WB*) analyses were done to analyze the effect of SCH66336 on *IGFBP-3* mRNA and protein expression in UMSCC38 cells that were treated with SCH66336 (5 μmol/L) for the indicated time periods. The ethidium bromide–stained RNA gel is illustrated to show the relative amounts of total RNA loaded per well (*top*). *E*, luciferase analysis was done in UMSCC38 and H460 cells that were transiently transfected with pGL2 or pGL2-BP-3 reporter plasmid and then treated with indicated concentrations of SCH66336 or FTI-277. Columns, means of six different samples from three independent experiments; bars, SD. **, $P < 0.01$; ***, $P < 0.001$ compared with pGL2-BP3-transfected cells (*bottom*). *F*, Western blot analysis on expression of IGFBP-3 after transfection H-ras or RhoB siRNA and SCH66336 (5 μmol/L) treatment for 2 days in UMSCC38 cells. *G*, effects of siRNA targeting H-Ras or RhoB on SCH66336-mediated induction of IGFBP-3 promoter activities in UMSCC38 cells that were transfected with scr, H-Ras, or RhoB siRNA. *H*, luciferase analysis in UMSCC38 cells that were transiently cotransfected with reporter plasmid (pGL2 or pGL2-BP3) and expression vector (Control vector, pH-Ras-V12, or pRhoB-GG) and then treated with 5 μmol/L SCH66336. Columns, means of six different wells from three independent experiments; bars, SD. **, $P < 0.01$ compared with untreated control cells.

administration of SCH6636 significantly reduced tumor vascularization in HNSCC orthotopic tongue tumors; (*b*) pretreatment with SCH66336 effectively suppressed angiogenesis-stimulating effects of the conditioned media from HNSCC38 cells on HUVECs in several *in vitro* and *in vivo* angiogenesis assays. The antiangiogenic activities of SCH66336 in HNSCC cells did not correlate with mutation and expression of Ras and RhoB in our study, suggesting that FTIs have mechanisms of action other than inhibiting Ras or RhoB.

We found that FTIs, including SCH66336 and FTI-277, induced expression of IGFBP-3, a major IGFBP in serum (39), in several different cancer cell lines, orthotopic tongue tumor tissues from mice, and a subset of patients with HNSCC. These findings revealed that the effect of FTIs on IGFBP-3 expression is a generic response to FTI treatment, and that oral administration of SCH66336 is sufficient to induce IGFBP-3 expression *in vivo*. Because FTIs up-regulated promoter activities and transcription of the *IGFBP-3* gene, FTIs seemed to induce *IGFBP-3* gene expression at transcription level. The effects of FTIs on IGFBP-3 expression could be mediated by novel farnesylated proteins (37) or by farnesyl transferase–independent off-target activity of FTIs. It is also possible that FTIs may activate various transcription factors that stimulate the IGFBP-3 promoter, such as Sp-1/Sp-3, p53, vitamin D receptor, and retinoid X receptors. A detailed mechanism that is critical for the induction of IGFBP-3 expression by SCH66336 is currently under active investigation in our laboratory.

Perhaps most strikingly, our findings presented here show the role of IGFBP-3 as the functional basis for the use of FTIs in HNSCC targeting tumor angiogenesis; inhibition of

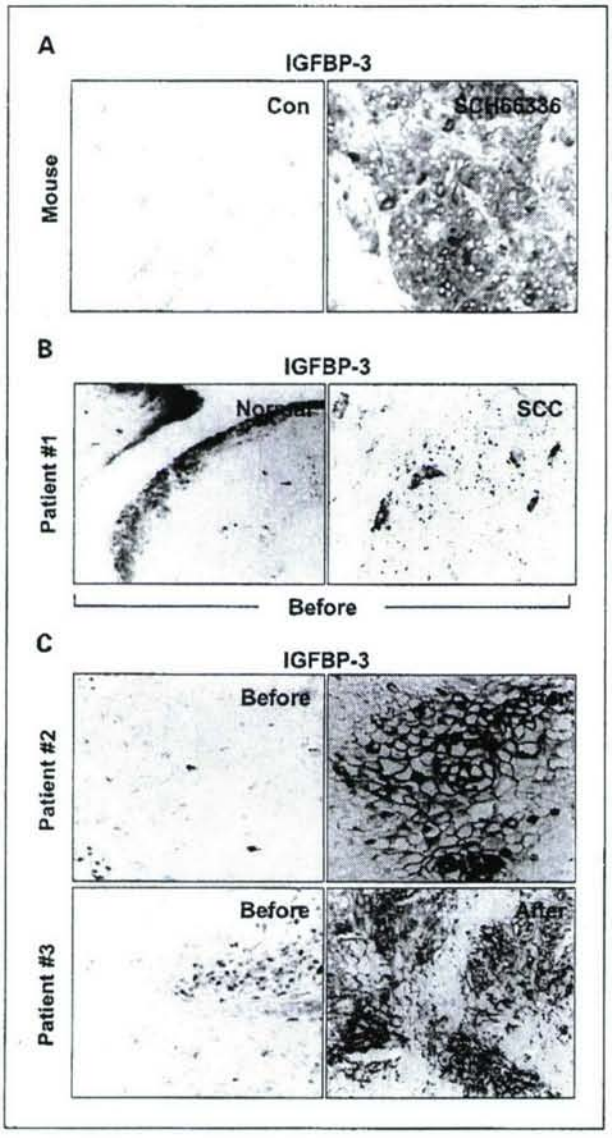

Fig. 4. Immunohistochemical analysis of IGFBP-3 in tongue tumor tissues. *A*, IGFBP-3 expression in orthotopic tongue tumor tissues from control nude mice (*left*) and SCH66336-treated mice (*right*) at 25 days. *B*, IGFBP-3 expression in normal and SCC tissues from a patient with HNSCC. *C*, IGFBP-3 expression was also tested in two patients before (*left*) or after 3 months of treatment with SCH66336 (*right*), ×400.

the secretion of SCH66336-induced IGFBP-3 from UMSCC38 cells by RNA interference or depletion of IGFBP-3 in HUVECs by neutralizing antibody significantly restored angiogenic effects of conditioned media from SCH66336-treated UMSCC38 cells on HUVECs. Consistent with previous findings (12), we also observed that IGFBP-3 secreted from FTI-treated HNSCC cells inhibited endothelial cell proliferation by blocking PI3K/Akt pathways: (*a*) conditioned media from control UMSCC38 cells, but not conditioned media from SCH66336-treated cells, induced phosphorylation of Akt in HUVECs; (*b*) depletion of IGFBP-3 in HUVECs by the IGFBP-3 neutralizing antibody effectively restored mitogenic activities and the levels of pAkt in HUVECs when incubated with conditioned media from SCH66336-treated UMSCC38 cells. Therefore, it is plausible to say that FTIs induce IGFBP-3 expression, which in turn regulate tumor angiogenesis by inhibiting Akt, a key enzyme for cell survival, and thus inducing apoptosis in endothelial cells.

In conclusion, our results reveal, for the first time, that the FTIs have potent antiangiogenic activities in HNSCC cells through the induction of IGFBP-3 expression. Our results could explain the antitumor activities of FTIs in the cancer cells that do not harbor activated Ras oncogene (40–43). IGFBP-3 has been also identified as having antitumor activities in a variety of cancers (16, 44, 45). Several case control studies have shown that serum IGFBP-3 levels inversely correlate with the risk of numerous cancers, including prostate (46), bladder (46), and colon (46). Smoking reduces IGFBP-3 levels (46) and low

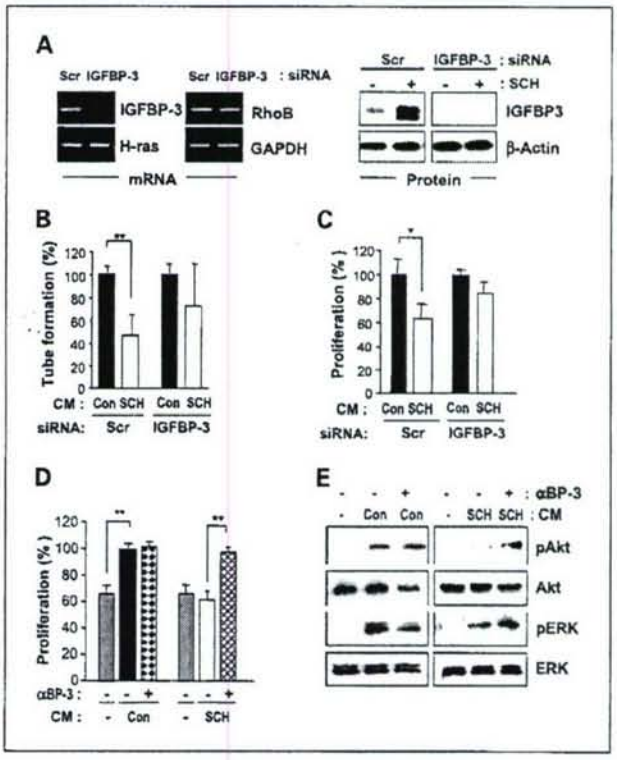

Fig. 5. IGFBP-3 secreted from SCH66336-treated HNSCC cells inhibits angiogenic activities in HUVECs by blocking Akt activation. *A-C*, effects of knock down of IGFBP-3 expression on antiangiogenic activities of SCH66336. *A*, semiquantitative reverse transcription-PCR analysis for *IGFBP-3*, *H-ras*, and *RhoB* mRNA expression (*left*) and Western blot analyses for IGFBP-3 protein expression (*right*) were done in UMSCC38 cells transfected with control (*scr*) or *IGFBP-3* siRNAs for 1 day before the SCH66336 (5 μmol/L) treatment. *GAPDH* mRNA and β-actin protein expression were also detected as controls for reverse transcription-PCR and Western blot analyses, respectively. Effects of conditioned media (*CM*) from these cells on HUVEC morphogenesis (*B*) and proliferation (*C*) were tested by tube formation and 3-(4,5-dimethylthiazol-2-yl)-2,5-diphenyltetrazolium bromide analyses, respectively. Independent experiments were repeated three times. Columns, percentages of eight samples; bars, SD/95% confidence intervals. *, $P < 0.05$; **, $P < 0.01$ compared with control. *D-E*, 3-(4,5-dimethylthiazol-2-yl)-2,5-diphenyltetrazolium bromide (*D*) and Western blot analyses (*E*) were performed in HUVECs, which were untreated or preincubated with IGFBP-3 neutralizing antibody (αBP-3) for 2 hours and then treated with EBM (−) or conditioned media from control UMSCC38 cells (*Con*) or from SCH66336-treated UMSCC38 cells (*SCH*). Independent experiments on cell proliferation were repeated three times. Columns, percentages of eight samples; bars, SD. αBP-3, antibody neutralizing IGFBP-3. **, $P < 0.01$ compared with HUVECs treated with control conditioned media.

IGFBP-3 concentrations are associated with increased risk of head and neck (46) as well as lung cancers (24). Furthermore, a decrease in IGFBP-3 expression due to the methylation or polymorphisms of the IGFBP-3 promoter is associated with an increased risk of lung, breast, and prostate cancers (46). Considering all of these promising results, IGFBP-3 should be critically evaluated in translational clinical trials against pathologic angiogenesis.

References

1. Horiot JC, Bontemps P, van den Bogaert W, et al. Accelerated fractionation (AF) compared to conventional fractionation (CF) improves loco-regional control in the radiotherapy of advanced head and neck cancers: results of the EORTC 22851 randomized trial. Radiother Oncol 1997;44:111–21.
2. Day GL, Blot WJ. Second primary tumors in patients with oral cancer. Cancer 1992;70:14–9.
3. Gupta AK, McKenna WG, Weber CN, et al. Local recurrence in head and neck cancer: relationship to radiation resistance and signal transduction. Clin Cancer Res 2002;8:885–92.
4. Fidler IJ. Critical factors in the biology of human cancer metastasis: twenty-eighth G.H.A. Clowes memorial award lecture. Cancer Res 1990;50:6130–8.
5. Folkman J. Angiogenesis in cancer, vascular, rheumatoid and other disease. Nat Med 1995;1:27–31.
6. Zetter BR. Angiogenesis and tumor metastasis. Annu Rev Med 1998;49:407–24.
7. Moschos SJ, Mantzoros CS. The role of the IGF system in cancer: from basic to clinical studies and clinical applications. Oncology 2002;63:317–32.
8. Leal SM, Liu Q, Huang SS, Huang JS. The type V transforming growth factor β receptor is the putative insulin-like growth factor-binding protein 3 receptor. J Biol Chem 1997;272:20572–6.
9. Valentinis B, Bhala A, DeAngelis T, Baserga R, Cohen P. The human insulin-like growth factor (IGF) binding protein-3 inhibits the growth of fibroblasts with a targeted disruption of the IGF-I receptor gene. Mol Endocrinol 1995;9:361–7.
10. Zadeh SM, Binoux M. The 16-kDa proteolytic fragment of insulin-like growth factor (IGF) binding protein-3 inhibits the mitogenic action of fibroblast growth factor on mouse fibroblasts with a targeted disruption of the type 1 IGF receptor gene. Endocrinology 1997;138:3069–72.
11. Hong J, Zhang G, Dong F, Rechler MM. Insulin-like growth factor (IGF)-binding protein-3 mutants that do not bind IGF-I or IGF-II stimulate apoptosis in human prostate cancer cells. J Biol Chem 2002; 277:10489–97.
12. Franklin SL, Ferry RJ, Jr., Cohen P. Rapid insulin-like growth factor (IGF)-independent effects of IGF binding protein-3 on endothelial cell survival. J Clin Endocrinol Metab 2003;88:900–7.
13. Kohl NE, Mosser SD, deSolms SJ, et al. Selective inhibition of ras-dependent transformation by a farnesyltransferase inhibitor. Science 1993;260:1934–7.
14. Crespo NC, Ohkanda J, Yen TJ, Hamilton AD, Sebti SM. The farnesyltransferase inhibitor, FTI-2153, blocks bipolar spindle formation and chromosome alignment and causes prometaphase accumulation during mitosis of human lung cancer cells. J Biol Chem 2001; 276:16161–7.
15. Chun KH, Lee HY, Hassan K, Khuri F, Hong WK, Lotan R. Implication of protein kinase B/Akt and Bcl-2/Bcl-XL suppression by the farnesyl transferase inhibitor SCH66336 in apoptosis induction in squamous carcinoma cells. Cancer Res 2003;63:4796–800.
16. Lee HY, Chun KH, Liu B, et al. Insulin-like growth factor binding protein-3 inhibits the growth of non-small cell lung cancer. Cancer Res 2002;62:3530–7.
17. Han JY, Oh SH, Morgillo F, et al. Hypoxia-inducible factor 1α and antiangiogenic activity of farnesyltransferase inhibitor SCH66336 in human aerodigestive tract cancer. J Natl Cancer Inst 2005;97:1272–86.
18. Myers JN, Holsinger FC, Jasser SA, Bekele BN, Fidler IJ. An orthotopic nude mouse model of oral tongue squamous cell carcinoma. Clin Cancer Res 2002;8:293–8.
19. Chun KH, Kosmeder JW, Il, Sun S, et al. Effects of deguelin on the phosphatidylinositol 3-kinase/Akt pathway and apoptosis in premalignant human bronchial epithelial cells. J Natl Cancer Inst 2003;95: 291–302.
20. Min JK, Han KY, Kim EC, et al. Capsaicin inhibits *in vitro* and *in vivo* angiogenesis. Cancer Res 2004;64:644–51.
21. Reimer CL, Agata N, Tammam JG, et al. Antineoplastic effects of chemotherapeutic agents are potentiated by NM-3, an inhibitor of angiogenesis. Cancer Res 2002;62:789–95.
22. Chang YS, Wang L, Suh YA, et al. Mechanisms underlying lack of insulin-like growth factor-binding protein-3 expression in non-small-cell lung cancer. Oncogene 2004;23:6569–80.
23. Armstrong SA, Hannah VC, Goldstein JL, Brown MS. CAAX geranylgeranyl transferase transfers farnesyl as efficiently as geranylgeranyl to RhoB. J Biol Chem 1995;270:7864–8.
24. Liu A, Du W, Liu JP, Jessell TM, Prendergast GC. RhoB alteration is necessary for apoptotic and antineoplastic responses to farnesyltransferase inhibitors. Mol Cell Biol 2000;20:6105–13.
25. Du W, Lebowitz PF, Prendergast GC. Cell growth inhibition by farnesyltransferase inhibitors is mediated by gain of geranylgeranylated RhoB. Mol Cell Biol 1999;19:1831–40.
26. Lebowitz PF, Casey PJ, Prendergast GC, Thissen JA. Farnesyltransferase inhibitors alter the prenylation and growth-stimulating function of RhoB. J Biol Chem 1997;272:15591–4.
27. Poulaki V, Mitsiades CS, McMullan C, et al. Regulation of vascular endothelial growth factor expression by insulin-like growth factor I in thyroid carcinomas. J Clin Endocrinol Metab 2003;88:5392–8.
28. Long L, Navab R, Brodt P. Regulation of the *M*, 72,000 type IV collagenase by the type I insulin-like growth factor receptor. Cancer Res 1998;58:3243–7.
29. Zhao WQ, Chen GH, Chen H, et al. Secretion of Annexin II via activation of insulin receptor and insulin-like growth factor receptor. J Biol Chem 2003;278: 4205–15.
30. Devi GR, Yang DH, Rosenfeld RG, Oh Y. Differential effects of insulin-like growth factor (IGF)-binding protein-3 and its proteolytic fragments on ligand binding, cell surface association, and IGF-I receptor signaling. Endocrinology 2000;141:4171–9.
31. Clemmons DR, Dehoff ML, Busby WH, Bayne ML, Cascieri MA. Competition for binding to insulin-like growth factor (IGF) binding protein-2, 3, 4, and 5 by the IGFs and IGF analogs. Endocrinology 1992;131: 890–5.
32. Walker GE, Wilson EM, Powell D, Oh Y. Butyrate, a histone deacetylase inhibitor, activates the human IGF binding protein-3 promoter in breast cancer cells: molecular mechanism involves an Sp1/Sp3 multiprotein complex. Endocrinology 2001;142:3817–27.
33. Carmeliet P, Dor Y, Herbert JM, et al. Role of HIF-1α in hypoxia-mediated apoptosis, cell proliferation and tumour angiogenesis. Nature 1998;394:485–90.
34. Liu M, Bryant MS, Chen J, et al. Antitumor activity of SCH 66336, an orally bioavailable tricyclic inhibitor of farnesyl protein transferase, in human tumor xenograft models and wap-ras transgenic mice. Cancer Res 1998;58:4947–56.
35. Loprevite M, Favoni RE, De Cupis A, et al. *In vitro* study of farnesyltransferase inhibitor SCH 66336, in combination with chemotherapy and radiation, in non-small cell lung cancer cell lines. Oncol Rep 2004; 11:407–14.
36. Shi B, Yaremko B, Hajian G, et al. The farnesyl protein transferase inhibitor SCH66336 synergizes with taxanes *in vitro* and enhances their antitumor activity *in vivo*. Cancer Chemother Pharmacol 2000;46: 387–93.
37. Feldkamp MM, Lau N, Roncari L, Guha A. Isotype-specific Ras.GTP-levels predict the efficacy of farnesyl transferase inhibitors against human astrocytomas regardless of Ras mutational status. Cancer Res 2001; 61:4425–31.
38. Hoover RR, Mahon FX, Melo JV, Daley GQ. Overcoming STI571 resistance with the farnesyl transferase inhibitor SCH66336. Blood 2002;100:1068–71.
39. Baxter RC. Signalling pathways involved in antiproliferative effects of IGFBP-3: a review. Mol Pathol 2001;54:145–8.
40. Ashar HR, James L, Gray K, et al. The farnesyl transferase inhibitor SCH 66336 induces a G(2) → M or G(1) pause in sensitive human tumor cell lines. Exp Cell Res 2001;262:17–27.
41. End DW, Smets G, Todd AV, et al. Characterization of the antitumor effects of the selective farnesyl protein transferase inhibitor R115777 *in vivo* and *in vitro*. Cancer Res 2001;61:131–7.
42. Karp JE, Kaufmann SH, Adjei AA, Lancet JE, Wright JJ, End DW. Current status of clinical trials of farnesyltransferase inhibitors. Curr Opin Oncol 2001;13:470–6.
43. Karp JE, Lancet JE, Kaufmann SH, et al. Clinical and biologic activity of the farnesyltransferase inhibitor R115777 in adults with refractory and relapsed acute leukemias: a phase 1 clinical-laboratory correlative trial. Blood 2001;97:3361–9.
44. Prieur A, Tirode F, Cohen P, Delattre O. EWS/FLI-1 silencing and gene profiling of Ewing cells reveal downstream oncogenic pathways and a crucial role for repression of insulin-like growth factor binding protein 3. Mol Cell Biol 2004;24:7275–83.
45. Ali O, Cohen P, Lee KW. Epidemiology and biology of insulin-like growth factor binding protein-3 (IGFBP-3) as an anti-cancer molecule. Horm Metab Res 2003;35:726–33.
46. Wu X, Zhao H, Do KA, et al. Serum levels of insulin growth factor (IGF-I) and IGF-binding protein predict risk of second primary tumors in patients with head and neck cancer. Clin Cancer Res 2004; 10:3988–95.

VOLUME 23 · NUMBER 19 · JULY 1 2005

JOURNAL OF CLINICAL ONCOLOGY

ORIGINAL REPORT

Effects of 9-*cis*-Retinoic Acid on the Insulin-Like Growth Factor Axis in Former Smokers

Ho-Young Lee, Yoon Soo Chang, Ji-Youn Han, Diane D. Liu, J. Jack Lee, Reuben Lotan, Margaret R. Spitz, and Waun Ki Hong

From The University of Texas Graduate School of Biomedical Sciences at Houston and The University of Texas M.D. Anderson Cancer Center, Houston, TX.

Submitted November 9, 2004; accepted January 24, 2005.

Supported in part by National Institutes of Health Grants U19 CA68437 (W.K.H.), R01 CA109520-01 (H.-Y.L.), CA-100816-01A1 (H.-Y.L), American Cancer Society grant RSG-04-082-01-TBE 01(H.-Y.L), and W81XWH-04-1-0142-01-VITAL from the Department of Defense (W.K.H.). W.K.H. is an American Cancer Society Clinical Research Professor.

Presented in part at the 40th Annual Meeting of the American Society of Clinical Oncology, New Orleans, LA, June 5-8, 2004.

Authors' disclosures of potential conflicts of interest are found at the end of this article.

Address reprint requests to Ho-Young Lee, PhD, Department of Thoracic/Head & Neck Medical Oncology, and the Program in Cancer Biology, Unit 432, The University of Texas M.D. Anderson Cancer Center, 1515 Holcombe Blvd, Houston, TX 77030; e-mail: hlee@mdanderson.org.

© 2005 by American Society of Clinical Oncology

0732-183X/05/2319-4439/$20.00

DOI: 10.1200/JCO.2005.04.572

A B S T R A C T

Purpose
Insulin-like growth factor (IGF) axis has been associated with the risk of lung cancer. 9-*cis*-retinoic acid (9-*cis*-RA) has shown potential chemopreventive activities in former smokers. This study was designed to evaluate the effects of 9-*cis*-RA on IGF axis in former smokers to identify any benefit the retinoid may have in preventing lung cancer.

Patients and Methods
Serum concentrations of IGF-I, IGF binding protein (IGFBP)-3, and their molar ratio (IGF-I/IGFBP-3) were measured with radioimmunoassay kits in stored blood samples from the participants of an original chemoprevention trial. The participants had ceased smoking for at least 12 months and were randomly assigned to receive 3 months of daily oral 9-*cis*-RA (100 mg) or placebo. All statistical tests were two-sided.

Results
A total of 111 samples from the study's baseline and 84 samples from the 3 months treatment were analyzed. The serum concentrations of IGF-I and IGF-I/IGFBP-3 at baseline were significantly lower in female than in male participants. After 3 months of treatment, the serum level of IGF-I and IGF-I/IGFBP-3 were significantly lower in the 9-*cis*-RA group than in the placebo group ($P = .03$ and $P < .01$, respectively), but the IGFBP-3 level was significantly higher ($P = .03$).

Conclusion
9-*cis*-RA treatment modulated the IGF axis in former smokers, suggesting that the IGF axis is a potential target for the chemopreventive activities of 9-*cis*-RA and that the serum concentrations of IGF, IGFBP-3, and IGF-I/IGFBP-3 could serve as surrogate end point biomarkers of 9-*cis*-RA treatment.

J Clin Oncol 23:4439-4449. © 2005 by American Society of Clinical Oncology

Lung cancer is the leading cause of cancer death in men and women in the United States,[1,2] and cigarette smoking is the predominant risk factor for lung cancer. Therefore, smoking cessation campaigns have been a major focus of preventive effort.[3,4] However, the risk for lung cancer does not diminish during the first 5 years after smoking cessation[5,6]; former smokers continue to have an increased risk compared with people who have never smoked.[7] These findings indicate that additional preventive strategies for former smokers are needed. One effective strategy is the administration of agents that suppress the promotion or progression steps of lung carcinogenesis by inhibiting the proliferation and survival of preneoplastic cells that have acquired genomic DNA damage as a result of exposure to cigarette carcinogens.

An increasingly recognized mediator of cell proliferation and survival is insulin-like growth factor (IGF).[8,9] IGFs can also inhibit apoptosis and play an important role in

differentiation of many normal and cancer cell types and in neoplastic transformation and metastasis.[9-11] The IGF system is regulated by IGF binding proteins (IGFBPs), especially IGFBP-3, which bind to IGFs in the extracellular milieu with high affinity and specificity, thus reducing the bioavailability of IGFs; more than 90% of circulating IGF-I is bound within a large complex containing IGFBP-3 and its acid-labile subunit.[9] A growing number of epidemiologic studies have suggested that increased serum concentrations of IGFs, altered concentrations of IGFBP-3, or both, are associated with an increased risk for several types of cancer, including lung cancer, and that high IGFBP-3 concentrations can attenuate this risk.[12-17] We have shown that loss of IGFBP-3 expression, due partly to hypermethylation of its promoter,[18] is a marker of poor prognosis in patients with early-stage non–small-cell lung cancer (NSCLC).[19,20] We have also demonstrated that overexpression of IGFBP-3 inhibits the growth of NSCLC cells in vitro and in vivo by inducing apoptosis.[21] These data indicate that for high-risk patients, the IGF system is a potential target for preventive strategies, for novel antineoplastic therapies, or for both.

An increasing body of evidence has suggested that retinoids, the most frequently studied chemopreventive agents for lung cancer, modulate the IGF axis.[22-24] Results of several in vivo studies in experimental animals have shown that retinoids suppress carcinogenesis in a variety of tissue types, including the lung.[25,26] Of the naturally occurring retinoids, all-*trans*-retinoic acid (all-*trans*-RA) binds to RA receptors (RARs), and 9-*cis*-retinoic acid (9-*cis*-RA) binds to RARs, retinoid X receptors (RXRs), and other nuclear receptor complexes in which the RXR is a ligand-binding partner, such as the vitamin D receptor and the peroxisome proliferator–activated receptor.[27] 13-*cis*-RA binds to RAR and, after stereoisomerization, to either all-*trans*-RA or 9-*cis*-RA in a process that occurs intracellularly.[28]

We demonstrated in a clinical lung cancer chemoprevention trial that 9-*cis*-RA treatment can restore RARβ expression in former smokers after 3 months of treatment.[29] RARβ expression has been implicated in the prevention of tumor development and has shown growth-inhibitory and apoptotic effects on the bronchial epithelia of former smokers.[30] These previous findings thus raised the possibility that 9-*cis*-RA has potential chemopreventive properties in former smokers.

To shed more light on the beneficial effects of 9-*cis*-RA on former smokers, we analyzed the effects of 9-*cis*-RA on the IGF axis, especially on the serum concentrations of IGF-I and IGFBP-3 and on the molar ratio of IGF-I to IGFBP-3, which has been proposed to reflect tissue bioactivity, in a previously studied population of former smokers.[31] We found that 9-*cis*-RA treatment modulated the IGF axis in these former smokers, suggesting that the serum IGF axis is a target of the potential chemopreventive activities of 9-*cis*-RA in former smokers.

Patients

The original study from which we derived our data was a three-arm, randomized, double-blinded, placebo-controlled trial comparing the effects of 9-*cis*-RA (100 mg) with those of 13-*cis*-RA (1 mg/kg) plus α-tocopherol (AT; 1,200 U) administered for 3 months. In this study, a significant increase in RARβ expression and a reduction of metaplasia were observed in individuals treated with 9-*cis*-RA, but not with 13-*cis*-RA plus AT, compared with those treated with placebo. Because antioxidants such as AT can affect the concentrations of the components of the IGF axis,[32] we decided not to include the 13-*cis*-RA plus AT treatment group in our analysis. The eligibility criteria were previously described.[29] Briefly, the study population consisted of former heavy smokers clinically free of any cancer, who were registered in the Departments of Thoracic/Head and Neck Medical Oncology and of Thoracic Surgery at The University of Texas M.D. Anderson Cancer Center. To be eligible, subjects had to have adequate renal, hematologic, and hepatic function and must not have taken more than 25,000 U of vitamin A or other retinoids daily for at least 3 months before study entry. Subjects were allowed to have had a prior smoking-related cancer, but they had to have been tumor free for 6 months before enrollment in the study. Subjects were required to abstain from consuming dietary vitamin supplements while on the study. The treatment duration was 3 months, based on the toxicity data from a previous phase I trial that included 9-*cis*-RA treatment.[33] Subjects were seen monthly and were evaluated for compliance with the trial protocol, drug-related toxic effects, and serum cotinine concentrations.

The clinical trial from which the samples analyzed in this study were derived indicated that 9-*cis*-RA had some side effects. Specifically, subjects in the 9-*cis*-RA group experienced grade 2 (46 subjects) and grade 3 (nine subjects) toxic effects typical of retinoid treatment, including skin rash, hypertriglyceridemia, headache, cheilitis, conjunctivitis, arthralgia, and myalgia.[29] Drug-related toxicity was graded according to the National Cancer Institute's Common Toxicity Criteria.[34]

The original study had been approved by the institutional review board of The M.D. Anderson Cancer Center and by the US Department of Health and Human Services. Our current study was also approved by the institutional review board at M.D. Anderson.

IGF-I and IGFBP-3 Measurements

For analysis of serum concentrations of IGF-I and IGFBP-3, blood samples were drawn from nonfasting subjects and collected in heparinized tubes that were transported immediately to the laboratory, where the samples were immediately centrifuged for 10 minutes at 4,000 $\times$ *g* and then stored at -80°C until the assays were performed. The serum concentration of IGF-I was measured by a specific radioimmunoassay (Diagnostic Systems Laboratories Inc, Webster, TX) with intra-assay and interassay coefficients of variation of less than 4% and 8%, respectively. To separate IGFs from their binding proteins, we mixed serum specimens with an acid-ethanol extraction buffer before measurement. The extraction procedure had been previously evaluated, and the efficiency of the extraction was identical to that for acid-column chromatography.[35] The IGFBP-3 concentration was also measured by a specific radioimmunoassay (Diagnostic Systems Laboratories Inc) with intra-assay and interassay coefficients of variation of less than 3.5% and 7.5%, respectively, and no cross-reaction with other

members of the IGFBP family. The assays were performed according to the instructions of the manufacturer and without knowledge of who the subject was. The molar ratio of IGF-I to IGFBP-3 was calculated as (0.130 × IGF-I concentration [ng/mL])/(0.036 × IGFBP-3 concentration [ng/mL]).

Statistical Analysis

The characteristics of the study subjects were compared pre–random assignment, according to sex or study group, by using Fisher's exact test for dichotomous characteristics and the Kruskal-Wallis test for quantitative characteristics. Because the distributions of serum concentrations of IGF-I and IGFBP-3 were skewed, the differences between groups were tested by using the Wilcoxon rank sum test. An overall treatment effect over time was determined by comparing the modulation (ie, the value at the subsequent visit minus the value at the baseline evaluation) in serum concentrations of IGF-I and IGFBP-3 and in the molar ratio of IGF-I to IGFBP-3 between the 9-*cis*-RA and placebo groups. All *P* values were determined by two-sided tests. Associations were considered statistically significant at *P* values less than .05. In the multivariate analysis, the variables of sex, age, smoking status, and body mass index (body weight in kg/height in m^2) were included in the model.

Subject Characteristics

The characteristics of eligible subjects were described in detail previously.[29] Of the 226 former smokers enrolled in the original chemoprevention trial, 149 were randomly assigned to placebo or 9-*cis*-RA treatments, and 113 of them completed 3 months of treatment. The characteristics of subjects assessable for our study are detailed in Table 1. Each treatment group was well balanced for sex, race, age, body mass index, and history of smoking. Blood samples from 111 of these subjects (52 women and 59 men; 56 from the 9-*cis*-RA group and 55 from the placebo group) at the baseline of the study, and from 84 (40 women and 44 men; 41 from the 9-*cis*-RA group and 43 from the placebo group) after 3 months of treatment were assessable for serum concentrations of IGF-I and IGFBP-3. The two treatment groups had comparable baseline mean serum concentrations of IGF-I and IGFBP-3 and similar molar ratios of IGF-I to IGFBP-3 (Table 2).

To determine whether subject characteristics affected the baseline serum concentrations of IGF-I or IGFBP-3, we evaluated the correlation between certain variables (eg, sex, race, age, body mass index, pack-years of smoking, and number of years since stopping smoking) and the baseline serum concentrations of IGF-I and IGFBP-3 and the molar ratio of IGF-I to IGFBP-3 (Table 3). The baseline serum concentration of IGF-I and the molar ratio of IGF-I to IGFBP-3 were significantly lower in women, whereas the IGFBP-3 concentration was slightly higher, though the difference did not reach statistical significance. Moreover, the serum concentration of IGF-I and the molar ratio of IGF-I to IGFBP-3 in women significantly decreased with increasing age (Fig 1A). Because serum concentrations of IGF-I are reduced in women treated with hormone replacement therapy (HRT),[36,37] we analyzed whether the changes in the baseline serum concentration of IGF-I and the baseline molar ratio of IGF-I to IGFBP-3 were associated with HRT use among women. Self-reported data for HRT use were available for 38 of the 52 women (Table 3). Overall, baseline serum concentrations IGF-I and molar ratios of IGF-I to IGFBP-3 concentrations were significantly lower in the HRT users than the non–HRT users (Fig 1B). Among HRT users, differences in the IGFBP-3 concentrations were not significantly different. The mean baseline serum concentrations of IGF-I and IGFBP-3, and the molar ratio of IGF-I to IGFBP-3 in the HRT users are summarized in Table 3. Race, body mass index, number of pack-years, and years since stopping smoking did not affect the serum concentrations of IGF-I and IGFBP-3 or the molar ratio of IGF-I to IGFBP-3 in the study population.

Effect of 9-cis-RA on IGF-I and IGFBP-3 Serum Concentrations and on the IGF-I to IGFBP-3 Molar Ratio

The primary end point of the original lung cancer chemoprevention trial was restoration of RARβ expression in the bronchial epithelium.[29] In the previous study, we demonstrated that, compared with the effect of placebo, the median change in receptor index was significantly different from placebo for 9-*cis*-RA but not for 13-*cis*-RA plus AT,[29] raising the possibility that 9-*cis*-RA has potential chemopreventive properties in former smokers.

In the current study, we evaluated the serum concentrations of the IGF axis in former smokers during treatment with 9-*cis*-RA. The modulations in mean serum concentrations of IGF-I and IGFBP-3 and in the molar ratio of IGF-I to IGFBP-3 in the two treatment groups during 3 months of treatment are illustrated in Figure 2. The mean changes in the placebo and 9-*cis*-RA groups are summarized in Table 4. Compared with the placebo group, the 9-*cis*-RA group exhibited a statistically significant modulation in the IGF axis. The mean changes from the study's baseline to the end of 3 months of treatment in the placebo and 9-*cis*-RA groups were as follows: IGF-I, 14.3 and −19.2, respectively; IGFBP-3, −175.1 and 196.6, respectively; and molar ratio of IGF-I to IGFBP-3, 0.05 and −0.06, respectively. These findings suggested that 9-*cis*-RA increases serum concentrations of IGFBP-3 and decreases serum concentrations of IGF-I, thus reducing the molar ratio of IGF-I to IGFBP-3.

To determine whether the differences in the serum concentrations of IGFBP3 between untreated and treated groups reflected differences at the tissue level, we also performed immunohistochemical analysis of IGFBP3, using the methodology described previously for lung cancer

Table 1. Characteristics of Subjects According to Treatment Group

Characteristic	Placebo (n = 61)		9-*cis*-RA (n = 52)		P*
	No.	%	No.	%	
Sex					
Male	37	60.7	27	51.9	.35
Female	24	39.3	25	48.1	
Race					
White	52	85.3	49	94.2	
African American	6	9.8	2	3.9	.35
Hispanic	3	4.9	1	1.9	
Asian	0	0.0	0	0.0	
Smoking-related cancer					
No	54	88.5	48	92.3	.54
Yes	7	11.5	4	7.7	
Age, years					
Mean	58.1		55.7		.12
SD	8.9		9.2		
Median	58.8		54.9		
Range	34.9-73.6		35.9-74.5		
BMI					
Mean	27.8		28.1		.92
SD	4.1		5.38		
Median	27.1		27.3		
Range	20.6-39.4		19.4-44.4		
Smoking years					
Mean	29.1		27.3		.39
SD	9.8		9.5		
Median	30		26		
Range	15-50		10-50		
PPD					
Mean	1.7		1.9		.23
SD	0.7		0.8		
Median	1.5		2		
Range	1-4		0.8-4		
Pack-years					
Mean	50.2		52.6		.94
SD	27.2		30.5		
Median	42.5		42		
Range	20-135		20-136		
Smoking quit years					
Mean	10.4		11.0		.56
SD	8.8		8.7		
Median	10.1		7.8		
Range	1.1-35.2		1.0-38.2		

Abbreviations: 9-*cis*-RA, 9-*cis*-retinoic acid; SD, standard deviation; BMI, body mass index; PPD, packs per day.
*The Wilcoxon rank-sum test was performed to test continuous variables between two treatment groups. The χ^2 test (for sex) and Fisher's exact test (for race and smoking-related cancer) were performed to test the association between two categorical variables.

samples,[20] in more than 90% of the cases. The intensity of IGFBP-3 expression in the normal and hyperplastic epithelial tissue samples was high, and differences between placebo– and 9-*cis*-RA–treated groups were not significant (data not shown). We suggest that the reason for the apparent discrepancy between the results of the plasma concentration analysis reported in this article and the tissue analysis is the higher sensitivity and dynamic range of the enzyme-linked immunosorbent assay for the plasma IGFBP3 and IGF1 compared with the limited dynamic range of the immunohistochemical analysis. In addition, the sources of IGF1 and IGFBP-3 in the blood include the liver and other tissues and is not expected to be directly related to expression in bronchial epithelial cells.

Correlation Between Changes in Tissue Level of RAR-β and Modulation of the IGF Axis Induced by 9-cis-RA

We further evaluated the association between the changes in serum concentrations of the IGF axis peptides

Table 2. The Baseline Serum Concentration of IGF-I, IGFBP-3, and IGF-I:IGFBP-3 Molar Ratio in the Study Population According to Treatment Group

	Placebo (n = 55)			9-*cis*-RA (n = 56)			
	Mean	SD	95% CI	Mean	SD	95% CI	*P**
IGF-I, ng/mL	208.8	123.3	175.4 to 242.1	236.0	117.8	204.4 to 267.5	.87
IGFBP-3, ng/mL	2,416.5	826.2	2,193.2 to 2,639.9	2,415.5	636.2	2,245.1 to 2,585.9	.23
IGF-I:IGFBP-3	0.33	0.20	0.28 to 0.39	0.38	0.20	0.32 to 0.43	.22

Abbreviations: 9-*cis*-RA, 9-*cis*-retinoic acid; SD, standard deviation; IGFBP-3, insulin-like growth factor binding protein 3; IGF-I, insulin-like growth factor I.
*P was obtained from the Wilcoxon rank sum test.

and changes in the tissue expression level of RARβ during 9-*cis*-RA treatment. To determine the effect of treatment on loss of RARβ expression at any biopsy site, the subjects were grouped according to whether their biopsy samples were positive (ie, RARβ was detected in all six biopsy sites) or negative (ie, RARβ was not detected in at least one biopsy site) for RARβ expression, and the effects of treatment on RARβ expression was determined as a binary variable (ie, loss of RARβ expression at any biopsy site). The modulation of serum concentrations of IGF-I and IGFBP-3 and the molar ratio of IGF-I to IGFBP-3 were not significantly correlated with baseline RARβ expression (Fig 3A) or with the changes in tissue RARβ expression induced by 9-*cis*-RA (Fig 3B).

Our main finding in this analysis of data collected from a completed chemoprevention trial assessing the benefits of 9-*cis*-RA for former smokers was that the IGF axis can be modulated by 9-*cis*-RA in a population of former smokers. To our knowledge, this is the first report showing modulation of the IGF axis by 9-*cis*-RA in the setting of a chemoprevention trial.

Growing evidence supports an association between the IGF axis and the risk for lung cancer[8] and suggests that the development of agents targeting the IGF axis could be an effective strategy in chemoprevention of the disease. Therefore, retinoids, shown to regulate the IGF axis in vitro[22,38,39]

Table 3. Association Between Baseline IGF-I, IGFBP-3, and IGF-I:IGFBP-3 Molar Ratio and Subjects' Demographic Characteristics

	IGF-I			IGFBP-3			IGF-I:IGFBP-3		
Characteristic	Mean	SD	*P*	Mean	SD	*P*	Mean	SD	*P*
Sex									
Male (n = 59)	261.3	108.2	.0002	2,373.4	784.7	.52	0.43	0.19	< .0001
Female (n = 52)	178.5	120.1		2,464.4	674.2		0.28	0.19	
HRT									
HRT use (n = 23)	139.9	89.22	.004	2,331	770.6	.16	0.23	0.13	.009
No HRT use (n = 15)	282.9	139.8		2,523	556.4		0.43	0.25	
Race									
White (n = 98)	220.0	122.4	.51	2,439.1	732.2	.51	0.35	0.21	46
African American (n = 9)	261.6	107.4		2,356.3	740.0		0.39	0.06	
Hispanic (n = 4)	196.3	118.6		1,983.8	798.3		0.35	0.23	
Age, years									
< 60 (n = 71)	228.2	118.8	.47	2,353.6	658.3	.43	0.37	0.21	.22
≥ 60 (n = 40)	212.4	125.1		2,526.8	847.6		0.32	0.20	
BMI									
< 28 (n = 64)	235.1	117.4	.20	2,360.9	660.6	.51	0.38	0.20	.16
≥ 28 (n = 42)	206.7	129.8		2,483.4	854.0		0.33	0.22	
Pack-years									
< 40 (n = 46)	234.3	125.9	.39	2,388.9	624.2	.81	0.37	0.20	44
≥ 40 (n = 65)	214.2	117.3		2,435.2	805.6		0.35	0.20	
Years quit smoking									
< 10 (n = 61)	216.8	121.7	.60	2,434.8	770.0	.85	0.35	0.21	.89
≥ 10 (n = 50)	229.4	120.5		2,393.1	692.6		0.36	0.20	

NOTE. *P* was obtained from the Wilcoxon rank sum test.
Abbreviations: IGF-I, insulin-like growth factor-I; IGFBP-3, insulin-like growth factor binding protein-3; SD, standard deviation; BMI, body mass index.

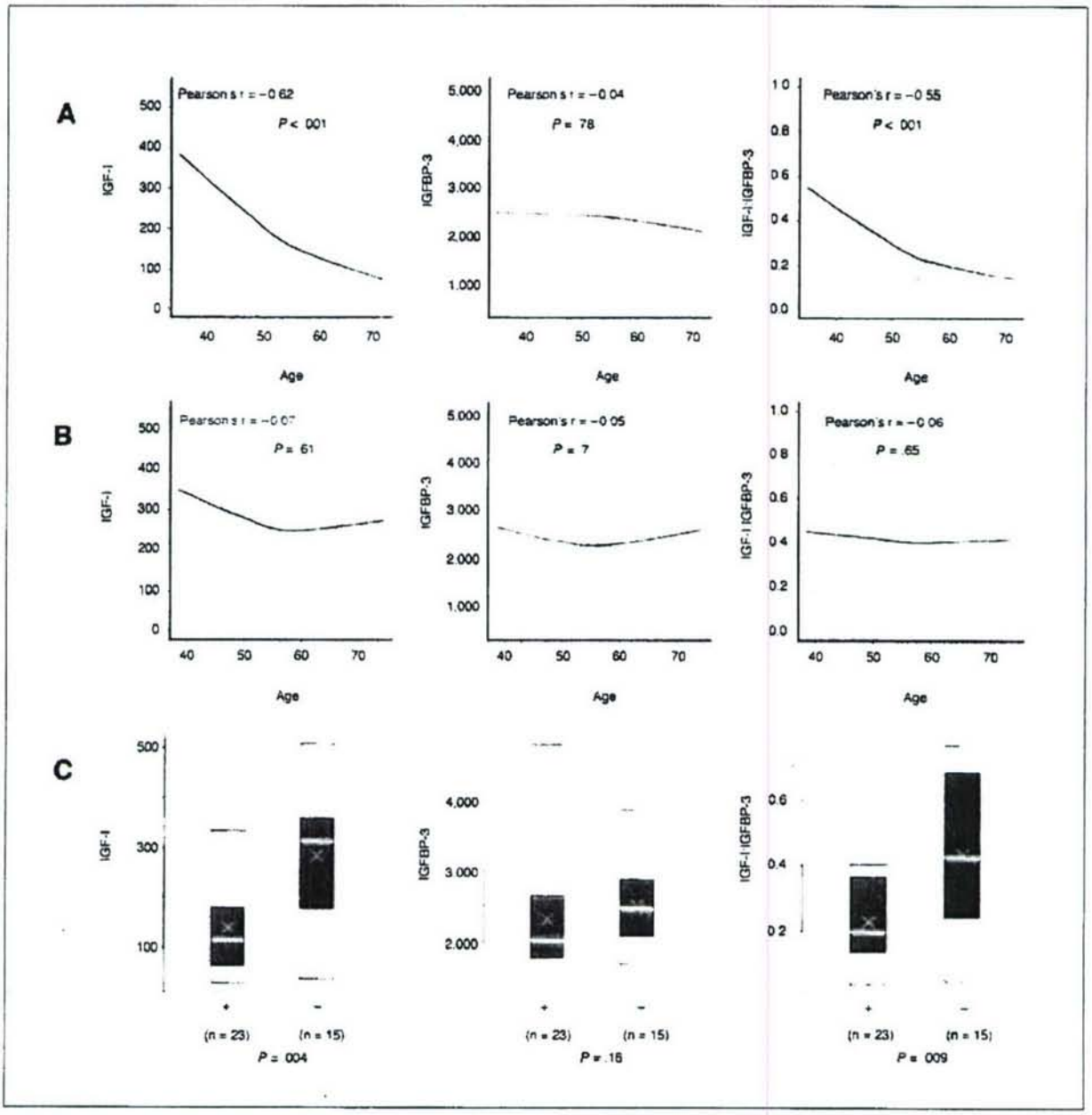

Fig 1. Effect of subject characteristics on the baseline serum concentrations of IGF-I and IGFBP-3 the molar ratio of IGF-I to IGFBP-3. Correlation between age and the baseline serum concentrations of IGF-1 (ng/mL) and IGFBP-3 (ng/mL) and the molar ratio of IGF-I to IGFBP-3 by increasing age in (A) female and (B) male subjects. (C) Effect of HRT use on the baseline serum concentrations of IGF-1 (ng/mL) and IGFBP-3 (ng/mL) and on the IGF-I to IGFBP-3 ratio. "+" indicates HRT use and "−" indicates no HRT use. IGF, insulin-like growth factor; IGFBP, IGF binding protein; HRT, hormone replacement therapy.

have a potential to exert chemopreventive activities. Indeed, several findings have demonstrated the potential use of retinoids as chemopreventive agents. For example, 9-*cis*-RA has shown antiproliferative activity against a broad range of neoplastic cells, including those from prostate cancer,[40] breast cancer,[41,42] leukemia and lymphoma,[43] lung cancer,[44] and head and neck cancer.[45] In vivo, 9-*cis*-RA has substantial anticarcinogenic activity in rat mammary glands[46,47] and rat colons.[48] More recently, the synthetic retinoid fenretinide has been shown to modulate circulating IGF-I and IGFBP-3 concentrations in breast cancer patients,[49,50] and the relative risk of a second breast cancer was 35% lower in premenopausal women treated with fenretinide than in those who received no treatment.[51] Thus, from the standpoint of directing future chemoprevention trials, our findings are important because we have

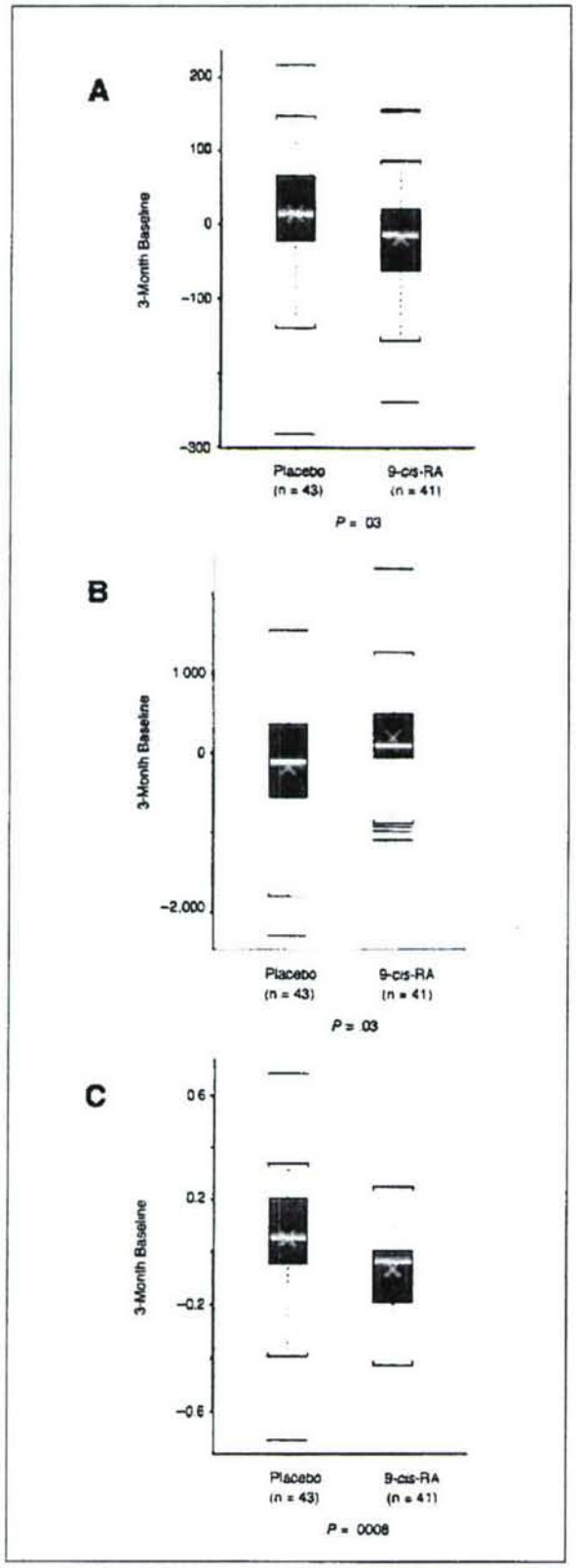

shown both that clinical trials targeting the IGF axis in former smokers are feasible and that 9-*cis*-RA can modulate the IGF axis in this population.

To determine whether the characteristics of subjects affected the baseline IGF axis, we evaluated many variables, such as sex, age, nutritional status, and growth hormone secretion level, which have all been shown to affect the serum concentrations of IGF-I.[52] The baseline serum level of IGF-I and the molar ratio of IGF-I to IGFBP-3 were significantly lower in women than in men. Estrogen is most likely responsible for the sex-related difference in the serum concentration of IGF-I. Endogenous estrogens have been shown to directly regulate circulating IGF-I synthesis[53] and oral administration of estrogen decreases IGF-I serum concentrations.[54,55] In our study, 38 of the 52 women took HRT during the treatment period, and the serum concentrations of IGF-I were significantly lower for HRT users than for non-HRT users. Therefore, the significant difference in serum concentrations of IGF-I and the molar ratio of IGF-I to IGFBP-3 might have resulted from the HRT. The role of estrogen in regulating the IGF-I level is further supported by the recent finding that the IGF-I concentrations of women using HRT were significantly lower than those of women not using HRT.[37] Studies have suggested that HRT use is associated with a decreased risk for several types of cancer, including lung cancer, through decreases in the production of IGF-I.[56,57] Therefore, if a high level of IGF-I is a putative risk factor for lung cancer, HRT use appears to lower IGF-I concentrations, thereby decreasing lung cancer risk.

We also observed that baseline serum concentrations of IGF-I and the molar ratio of IGF-I to IGFBP-3 were significantly decreased with increasing age in women. Duration of HRT use is also likely responsible for the age-related difference in the serum concentration of IGF-I in a female population because older women may conceivably have used HRT for a longer time. The decrease in IGF-I concentrations with aging has been described many times,[49,58,59] and may be due in part to decreased growth hormone levels.[60] In normal subjects, the interaction between growth hormone

Fig 2. Effect of 9-*cis*-retinoic acid (9-*cis*-RA) on the modulation of the IGFBP-3 concentration, IGF-I concentration, and the IGF-I to IGFBP-3 ratio after the 3 months of treatment. The distributions of serum concentrations of IGF-I and IGFBP-3 and of the IGF-I to IGFBP-3 ratio are presented using box plots. The top and bottom edges of the box portion of the plots represent the 75th and 25th percentiles, respectively, of the distributions. The vertical bars extend to the 90th and 10th percentiles. The *P* value was obtained by using the Wilcoxon rank sum test comparing baseline values and the modulation of IGFBP-3 concentration, IGF-I concentration, and the IGF-I to IGFBP-3 ratio between the 9-*cis*-RA and placebo groups. After 3 months of treatment with 9-*cis*-RA, the serum level of IGF-I and the IGF-I to IGFBP-3 ratio were significantly lower ($P = .03$ and $P < .01$, respectively) in the group receiving 9-*cis*-RA than in the placebo group, whereas the serum level of IGFBP-3 was significantly higher ($P = .03$). X, variables; horizontal line, medians of the variables; IGF, insulin-like growth factor; IGFBP, IGF binding protein.

Table 4. Modulation of Serum Concentration of IGF-I, IGFBP-3, and IGF-I:IGFBP-3 Molar Ratio in the Study Population According to Treatment Group

	Placebo (n = 43)				9-*cis*-RA (n = 41)				
	Mean	SD	Median	Range	Mean	SD	Median	Range	*P**
IGF-I (ng/mL)	14.3	85.0	14.5	−282.4-216.5	−19.2	78.3	−14.7	−238.9-156.1	.03
IGFBP-3 (ng/mL)	−175.1	790.9	−109.7	−2,277.2-1,548.9	196.6	657.5	100.1	−1,099.4-2,325.7	.03
IGF-I:IGFBP-3†	0.05	0.2	0.06	−0.7-0.7	−0.06	0.2	−0.03	−0.4-0.3	.0008

Abbreviations: 9-*cis*-RA, 9-*cis*-retinoic acid; SD, standard deviation; IGFBP-3, insulin-like growth factor binding protein 3; IGF-I, insulin-like growth factor I.
**P* comparing the differences between the baseline and the 3rd month values were obtained from the Wilcoxon rank sum test.
†IGF-I:IGFBP-3 = 0.13 IGF-I/0.036 IGFBP3.

and its specific hepatic receptor stimulates expression of the *IGF-I* gene and the release of the IGF-I polypeptide.[52] Therefore, it is likely that the concentration of IGF-I declines with age, as do secretions of growth hormone. However, we have not observed a significant correlation between the age of the study population in men and serum concentrations of IGF-I and IGFBP-3 or the molar ratio of IGF-I to IGFBP-3 in our study.

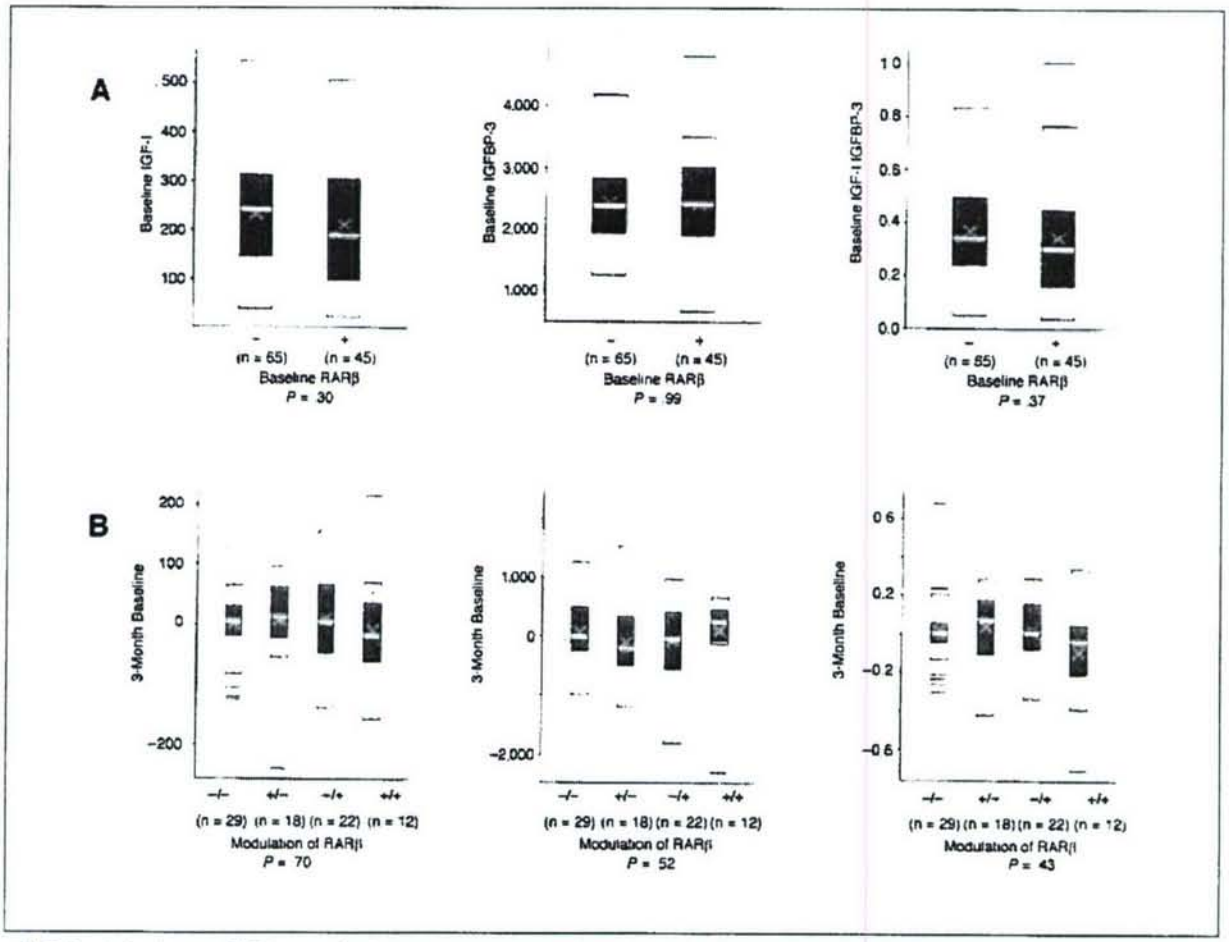

Fig 3. Correlation between RARβ expression in tissue and modulation of the IGF-axis. (A) A Wilcoxon rank sum test was performed to test the statistical significance of the changes in the median RARβ expression in tissues from baseline to after 3 months of treatment. (B) Kruskal-Wallis test was performed comparing the modulations in the median IGFBP-3 concentration, IGF-I concentration, and IGF-I to IGFBP-3 ratio from baseline to 3 months after treatment with the modulation in median RARβ expression in tissue. Subjects were grouped according to their levels of RARβ expression at baseline and at 3 months after treatment (+/+, +/−, −/+, −/−), "+" indicates that RARβ was detected in all six biopsy sites; "−" indicates that RAR-β was not detected in at least one biopsy site. The number of subjects with each combination of RARβ expression is given. RARβ, retinoic acid receptor; IGF, insulin-like growth factor; IGFBP, IGF binding protein.

Growth hormone deficiency is also associated with a decreased muscle mass and increased body fat,[61] and it has been hypothesized that low IGF-I concentrations are associated with high body fat, weight gain over time, and high body mass index.[62] This hypothesis was supported by a study of Swedish men and women, which showed an inverse association between IGF-I concentrations and body mass index.[53] However, we have not observed such correlation between IGF-I and body mass index, similar to the Rancho Bernardo study.[59]

The effects of smoking on serum concentrations of IGF-I are unclear. A positive association between IGF-I concentrations and pack-years of smoking and a negative association between pack-years or the number of cigarettes/d and concentrations of IGFBP-3 have been shown.[63] However, an inverse association between IGF-I concentrations and smoking has been also reported among men, although not among women.[53] Recently, Holmes et al[58] showed that lower serum concentrations of IGF-I are significantly associated with smoking. In our study subjects, we observed a very modest decrease in IGF-I concentrations and an increase in IGFBP-3 concentrations associated with pack-years. However, smoking history generally did not affect the serum concentrations of IGF-I and IGFBP-3 or the molar ratio of IGF-I to IGFBP-3.

We observed that subjects in the 9-*cis*-RA group had a significant decrease in their IGF-I serum concentration, an increase in their IGFBP-3 serum concentration, and a decrease in the molar ratio of IGF-I to IGFBP-3 compared with subjects in the placebo group. The magnitude of the 9-*cis*-RA–induced changes in the IGF axis was moderate. This may be a consequence of the substantial interindividual variability in concentrations of 9-*cis*-RA and IGFs, which is at least in part genetically driven.[33] Given the potential therapeutic activity of both exogenous growth hormone and IGF-I against heart failure[64] and the long-term positive association between the decline in serum IGF-I concentrations and aging,[65] a moderate yet durable effect of 9-*cis*-RA on the IGF axis may be desirable in a preventive context.

Although the exact mechanisms underlying the modulation of the IGF axis by 9-*cis*-RA are unclear, several in vitro results suggest the ability of retinoids to regulate the IGF axis; retinoids have been shown to regulate the expression of IGFBPs[22,23,66]; likewise, IGFs have been shown to modulate the cellular response of RAs, and vice versa.[24] The induction of IGFBP-3 expression is activated by retinoids. We previously demonstrated that all-*trans*-RA increases *IGFBP-3* expression at a transcriptional level through a RAR-α-dependent signaling pathway.[22] It is well known that the cellular effects of RAs are mediated by RXRs and RARs. 9-*cis*-RA is a ligand for both RXRs and RARs, but its affinity for RXRs is 40-fold higher than for RARs. On the other hand, RA is primarily a ligand for RARs and only activates RXRs at high concentrations.[67] Recently, the vitamin D receptor has been identified in the *IGFBP-3* promoter, and RXR has been shown to be required for 1,25-dihydroxyvitamin D_3–induced gene transcription.[68] Therefore, treatment with 9-*cis*-RA could lead to there being available ligand for activation of both the RAR:RXR and the VDR:RXR heterodimeric complex, so that *IGFBP-3* gene transcription could be efficiently activated.

Given the inverse association between estrogen and serum IGF-I concentrations, the ability of 9-*cis*-RA to regulate type 1 17β-hydroxysteroid dehydrogenases,[69] which catalyzes the conversion of estrone and 17β-estradiol, could increase the level of 17β-estradiol, the physiologically significant molecule of estrogen, and thereby decrease IGF-I concentrations. The ability of estrogens to increase the expression of vitamin D receptors in vitro[70] may also contribute to decreased concentrations of IGF-I by inducing IGFBP-3 expression.[71] Additional work will be necessary to investigate the mechanism that mediates the regulation of the IGF axis by 9-*cis*-RA in former smokers.

Because 9-*cis*-RA treatment increased the tissue expression of RARβ, we also explored the correlation between tissue levels of RARβ and serum concentrations of the IGF axis. However, we did not find any significant correlation between the modulation of the serum concentrations of IGF-I or IGFBP-3 and RARβ expression in the tissue. These findings provide evidence that the mechanisms involved in 9-*cis*-RA–mediated gene expression are diverse and complex.

In conclusion, we are the first to show that 3 months of treatment with 9-*cis*-RA decreased the serum level of IGF-I and the molar ratio of IGF-I to IGFBP-3 and increased the serum level of IGFBP-3 in former smokers. These effects may contribute to the chemopreventive benefit of 9-*cis*-RA to former smokers. Despite these promising findings, enthusiasm for the use of 9-*cis*-RA as a chemopreventive agent for lung cancer could be tempered by the toxic effects of the agent.[29] Although there were no serious side effects such as cardiovascular problems, pancreatitis, or death in the subjects treated with 9-*cis*-RA in our previous prevention study, and only one patient with grade 4 hypertriglyceridemia stopped 9-*cis*-RA treatment, it would be better to develop newer agents that are related to 9-*cis*-RA but that do not have the toxic effects of 9-*cis*-RA. Because 9-*cis*-RA can activate both RARs and RXRs and because the toxicities are thought to be mediated by RAR-RXR heterodimers, it had been suggested that "pure" RXR selective synthetic retinoids may exert the beneficial effects of retinoids without the toxicities. Indeed, a group of RXR-selective retinoids ("rexinoids") has demonstrated efficacy with fewer adverse effects in patients with NSCLC in early clinical trials.[72] Therefore, whether rexinoids regulate the IGF axis and thereby reduce lung cancer risk would be a worthwhile topic for future chemoprevention trials in former smokers. In addition, because Ras-mediated signaling pathways may participate in the development of resistance to IGFBP-3,[73] the combination

of RXR-selective agonists and inhibitors of the Ras-mediated signaling pathway could also be considered. Clearly, additional work will be necessary to determine whether the modulation of the IGF axis by 9-*cis*-RA correlates with the ability to reduce lung cancer risk in former smokers. In addition, further investigation into the role of serum concentrations of IGF-I and IGFBP-3 as surrogate biomarkers in determining the chemopreventive effects of retinoids are warranted.

Authors' Disclosures of Potential Conflicts of Interest

The authors indicated no potential conflicts of interest.

1. Khuri FR, Herbst RS, Fossella FV: Emerging therapies in non-small-cell lung cancer. Ann Oncol 12:739-744, 2001
2. Parkin DM, Pisani P, Ferlay J: Estimates of the worldwide incidence of 25 major cancers in 1990. Int J Cancer 80:827-841, 1999
3. Ginsberg RJ, Vokes EE, Kenneth R: Non-small cell lung cancer, in DeVita VT Jr, Hellman S, Rosenberg SA (eds): Cancer: Principles and Practice of Oncology (ed 6). Philadelphia, PA, Lippincott Williams & Wilkins, 2001, pp 925-983
4. Mattson ME, Pollack ES, Cullen JW. What are the odds that smoking will kill you? Am J Public Health 77:425-431, 1987
5. Wistuba II, Lam S, Behrens C, et al: Molecular damage in the bronchial epithelium of current and former smokers. J Natl Cancer Inst 89:1366-1373, 1997
6. Sekido Y, Fong KM, Minna JD: Progress in understanding the molecular pathogenesis of human lung cancer. Biochim Biochim Biophys Acta 1378:21-59, 1998
7. Burns DM: Primary prevention, smoking, and smoking cessation: Implications for future trends in lung cancer prevention. Cancer 89: 2506-2509, 2000
8. Ibrahim YH, Yee D: Insulin-like growth factor-I and cancer risk. Growth Horm IGF Res 14:261-269, 2004
9. Butt AJ, Firth SM, Baxter RC: The IGF axis and programmed cell death. Immunol Cell Biol 77:256-262, 1999
10. Lopez T, Hanahan D: Elevated levels of IGF-1 receptor convey invasive and metastatic capability in a mouse model of pancreatic islet tumorigenesis. Cancer Cell 1:339-353, 2002
11. Samani AA, Chevet E, Fallavollita L, et al: Loss of tumorigenicity and metastatic potential in carcinoma cells expressing the extracellular domain of the type 1 insulin-like growth factor receptor. Cancer Res 64:3380-3385, 2004
12. Yu H, Spitz MR, Mistry J, et al: Plasma levels of insulin-like growth factor-I and lung cancer risk: A case-control analysis. J Natl Cancer Inst 91:151-156, 1999
13. Wu X, Tortolero-Luna G, Zhao H, et al: Serum levels of insulin-like growth factor I and risk of squamous intraepithelial lesions of the cervix. Clin Cancer Res 9:3356-3361, 2003
14. Pollak M: Insulin-like growth factors (IGFs) and prostate cancer. Epidemiol Rev 23:59-66, 2001
15. Lukanova A, Lundin E, Toniolo P, et al: Circulating levels of insulin-like growth factor-1 and risk of ovarian cancer. Int J Cancer 101:549-554, 2002
16. Zhao H, Grossman HB, Spitz MR, et al: Plasma levels of insulin-like growth factor-1 and binding protein-3, and their association with bladder cancer risk. J Urol 169:714-717, 2003
17. Kaaks R, Toniolo P, Akhmedkhanov A, et al: Serum C-peptide, insulin-like growth factor (IGF)-I, IGF binding proteins, and colorectal cancer risk in women. J Natl Cancer Inst 92:1592-1600, 2000
18. Chang YS, Wang L, Mao L, et al: Mechanisms underlying lack of insulin like-growth factor binding protein-3 expression in NSCLC cells. Oncogene 23:6569-6580, 2004
19. Chang YS, Wang L, Liu D, et al: Correlation between IGFBP-3 promoter methylation and prognosis of patients with stage I non-small cell lung cancer. Clin Cancer Res 8:3669-3675, 2002
20. Chang YS, Gong K, Sun S, et al: Clinical significance of IGFBP-3 expression in stage I non-small cell lung cancer. Clin Cancer Res 8:3796-3802, 2002
21. Lee HY, Chun KH, Liu B, et al: Insulin-like growth factor binding protein-3 inhibits the growth of non-small cell lung cancer. Cancer Res 62:3530-3537, 2002
22. Han G-R, Dohi DF, Lee H-Y, et al: All-trans-retinoic acid increases transforming growth factor-β2 and insulin-like growth factor binding protein-3 expression through a retinoic acid receptor-β-dependent signaling pathway. J Biol Chem 272:13711-13716, 1997
23. Fontana JA, Burrows-Mezu A, Clemmons DR, et al: Retinoid modulation of insulin-like growth factor-binding proteins and inhibition of breast carcinoma proliferation. Endocrinology 128:1115-1122, 1991
24. Bentel JM, Lebwohl DE, Cullen KJ, et al: Insulin-like growth factors modulate the growth inhibitory effects of retinoic acid on MCF-7 breast cancer cells. J Cell Physiol 165:212-221, 1995
25. Nagy L, Thomazy VA, Heyman RA, et al: Retinoid-induced apoptosis in normal and neoplastic tissues. Cell Death Differ 5:11-19, 1998
26. Hansen LA, Sigman CC, Andreola F, et al: Retinoids in chemoprevention and differentiation therapy. Carcinogenesis 21:1271-1279, 2000
27. Mangelsdorf DJ, Evans RM: The RXR heterodimers and orphan receptors. Cell 83:841-850, 1995
28. Marchetti MN, Samplo E, Bun H, et al: In vitro metabolism of three major isomers of retinoic acid in rats: Intersex and interstrain comparison. Drug Metab Dispos 25:637-646, 1997
29. Kurie JM, Lotan R, Lee JJ, et al: Treatment of former smokers with 9-cis-retinoic acid reverses loss of retinoic acid receptor-βexpression in the bronchial epithelium: Results from a randomized placebo-controlled trial. J Natl Cancer Inst 95:206-214, 2003
30. Seewaldt VL, Johnson BS, Parker MB, et al: Expression of retinoic acid receptor beta mediates retinoic acid-induced growth arrest and apoptosis in breast cancer cells. Cell Growth Differ 6:1077-1088, 1995
31. Juul A, Dalgaard P, Blum W, et al: Serum levels of insulin-like growth factor (IGF)-binding protein-3 (IGFBP-3) in healthy infants, children, and adolescents: The relation to IGF-I, IGF-II, IGFBP-1, IGFBP-2, age, sex, body mass index, and pubertal maturation. J Clin Endocrinol Metab 80:2534-2542, 1995
32. Zi X, Zhang J, Agarwal R, et al: Silibinin up-regulates insulin-like growth factor-binding protein 3 expression and inhibits proliferation of androgen-independent prostate cancer cells. Cancer Res 60:5617-5620, 2000
33. Miller VA, Rigas JR, Benedetti FM, et al: Initial clinical trial of the retinoid receptor pan agonist 9-cis retinoic acid. Clin Cancer Res 6:471-475, 1996
34. National Cancer Institute: Common toxicity criteria, version 2.0. http://ctep.cancer.gov/forms/CTCv20_4-30-992.pdf
35. Baxter RC, Martin JL: Radioimmunoassay of growth hormone-dependent insulin-like growth factor binding protein in human plasma. J Clin Invest 78:1504-1512, 1986
36. Campagnoli C, Biglia N, Altare F, et al: Differential effects of oral conjugated estrogens and transdermal estradiol on insulinlike growth factor 1, growth hormone and sex hormone binding globulin serum levels. Gynecol Endocrinol 7:251-258, 1993
37. Schabath MB, Wu X, Sellin RV, et al: Hormone replacement therapy and lung cancer risk: A case-control analysis. Clin Cancer Res 10:113-123, 2004
38. Zhou Y, Mohan S, Linkhart TA, et al: Retinoic acid regulates insulin-like growth factor-binding protein expression in human osteoblast cells. Endocrinology 137:975-983, 1996
39. Gabbitas B, Canalis E: Retinoic acid regulates the expression of insulin-like growth factors I and II in osteoblasts. J Cell Physiology 172:253-264, 1997
40. Blutt SE, Allegretto EA, Pike JW, et al: 1,25-Dihydroxyvitamin D3 and 9-*cis*-retinoic acid act synergistically to inhibit the growth of LNCaP prostate cells and cause accumulation of cells in G1. Endocrinology 138:1491-1497, 1997
41. Rubin M, Fenig E, Rosenauer A, et al: 9-*cis*-Retinoic acid inhibits growth of breast cancer cells and down-regulates estrogen receptor RNA and protein. Cancer Res 54:6549-6556, 1994
42. Gottardis MM, Lamph WW, Shalinsky DR, et al: The efficacy of 9-*cis*-retinoic acid in experimental models of cancer. Breast Cancer Res Treat 38:85-96, 1996
43. Lutzky J, Vujicic M, Yamanishi DT, et al: Antiproliferative effects of all-*trans*-retinoic acid (tRA) and 9-*cis*-retinoic acid (9-cisRA) on human

lymphoid cell lines. Proc Am Assoc Cancer Res 34:292, 1993 (abstr 1738)

44. Guzey M, Demirpence E, Criss W, et al: Effects of retinoic acid (all-*trans* and 9-*cis*) on tumor progression in small-cell lung carcinoma. Biochem Biophys Res Commun 242:369-375, 1998

45. Giannini F, Maestro R, Vukosavljevic T, et al: All-*trans*, 13-*cis*, and 9-*cis* retinoic acids induce a fully reversible growth inhibition in HNSCC cell lines: Implications for *in vivo* retinoic acid use. Int J Cancer 70:194-200, 1997

46. Anzano MA, Byers SW, Smith JM, et al: Prevention of breast cancer in the rat with 9-*cis*-retinoic acid as a single agent and in combination with tamoxifen. Cancer Res 54:4614-4617, 1994

47. Anzano MA, Peer CW, Smith JM, et al: Chemoprevention of mammary carcinogenesis in the rat: Combined use of raloxifene and 9-*cis*-retinoic acid. J Natl Cancer Inst 88:123-125, 1996

48. Zheng Y, Kramer PM, Olson G, et al: Prevention by retinoids of azoxymethane-induced tumors and aberrant crypt foci and their modulation of cell proliferation in the colon of rats. Carcinogenesis 18:2119-2125, 1997

49. Decensi A, Johansson H, Miceli R, et al: Long-term effects of fenretinide, a retinoic acid derivative, on the insulin-like growth factor system in women with early breast cancer. Cancer Epidemiol Biomarkers Prev 10:1047-1053, 2001

50. Torrisi R, Parodi S, Fontana V, et al: Effect of fenretinide on plasma IGF-I and IGFBP-3 in early breast cancer patients. Int J Cancer 76:787-790, 1998

51. Veronesi U, De Palo G, Marubini E, et al: Randomized trial of fenretinide to prevent second breast malignancy in women with early breast cancer. J Natl Cancer Inst 91:1847-1856, 1999

52. Le Roith D: Seminars in medicine of the Beth Israel Deaconess Medical Center: Insulin-like growth factors. N Engl J Med 336:633-640, 1997

53. Landin-Wilhelmsen K, Wilhelmsen L, Lappas G, et al: Serum insulin-like growth factor I in a random population sample of men and women: Relation to age, sex, smoking habits, coffee consumption and physical activity, blood pressure and concentrations of plasma lipids, fibrinogen, parathyroid hormone and osteocalcin. Clin Endocrinol (Oxf) 41:351-357, 1994

54. Helle SI, Omsjo IH, Hughes SC, et al: Effects of oral and transdermal oestrogen replacement therapy on plasma levels of insulin-like growth factors and IGF binding proteins 1 and 3: a cross-over study. Clin Endocrinol (Oxf) 45:727-732, 1996

55. Raudaskoski T, Knip M, Laatikainen T: Plasma insulin-like growth factor-I and its binding proteins 1 and 3 during continuous non-oral and oral combined hormone replacement therapy. Menopause 5:217-222, 1998

56. Janne PA, Mayer RJ: Chemoprevention of colorectal cancer. N Engl J Med 342:1960-1968, 2000

57. Grodstein F, Newcomb PA, Stampfer MJ: Postmenopausal hormone therapy and the risk of colorectal cancer: A review and meta-analysis. Am J Med 106:574-578, 1999

58. Holmes MD, Pollak MN, Hankinson SE: Lifestyle correlates of plasma insulin-like growth factor I and insulin-like growth factor binding protein 3 concentrations. Cancer Epidemiol Biomarkers Prev 11:862-867, 2002

59. Goodman-Gruen D, Barrett-Connor E: Epidemiology of insulin-like growth factor-I in elderly men and women: The Rancho Bernardo Study. Am J Epidemiol 146:970-976, 1997

60. Bondy CA, Underwood LE, Clemmons DR, et al: Clinical uses of insulin-like growth factor I. Ann Intern Med 120:593-601, 1994

61. Sonksen PH, Salomon F, Cuneo R: Metabolic effects of hypopituitarism and acromegaly. Horm Res 36:27-31, 1991 (suppl 1)

62. Harris T, Kiel D, Roubenoff R, et al: Association of insulin-like growth factor-I with body composition, weight history, and past health behaviors in the very old: The Framingham Heart Study. J Am Geriatr Soc 45:133-139, 1997

63. Kaklamani VG, Linos A, Kaklamani E, et al: Age, sex, and smoking are predictors of circulating insulin-like growth factor 1 and insulin-like growth factor-binding protein 3. J Clin Oncol 17:813-817, 1999

64. Fazio S, Sabatini D, Capaldo B, et al: A preliminary study of growth hormone in the treatment of dilated cardiomyopathy. N Engl J Med 334:809-814, 1996

65. Janssen JA, Stolk RP, Pols HA, et al: Serum free IGF-I, total IGF-I, IGFBP-1 and IGFBP-3 levels in an elderly population: Relation to age and sex steroid levels. Clin Endocrinol (Oxf) 48:471-478, 1998

66. Woodward TL, Turner JD, Hung HT, et al: Inhibition of cellular proliferation and modulation of insulin-like growth factor binding proteins by retinoids in a bovine mammary epithelial cell line. J Cell Physiol 167:488-499, 1996

67. Heyman RA, Mangelsdorf DJ, Dyck JA, et al: 9-*cis* Retinoic acid is a high affinity ligand for the retinoid X receptor. Cell 68:397-406, 1992

68. Pathrose P, Barmina O, Chang CY, et al: Inhibition of 1,25-dihydroxyvitamin D3-dependent transcription by synthetic LXXLL peptide antagonists that target the activation domains of the vitamin D and retinoid X receptors. J Bone Miner Res 17:2196-2205, 2002

69. Piao Y-S, Peltoketo H, Jouppila A, et al: Retinoic acids increase 17β-hydroxysteroid dehydrogenase type 1 expression in JEG-3 and T47D cells, but the stimulation is potentiated by epidermal growth factor, 12-O-tetradecanoylphorbol-13-acetate, and cyclic adenosine 3', 5'-monophosphate only in JEG-3 cells. Endocrinology 138:898-904, 1997

70. Smirnoff P, Liel Y, Gnainsky J, et al: The protective effect of estrogen against chemically induced murine colon carcinogenesis is associated with decreased CpG island methylation and increased mRNA and protein expression of the colonic vitamin D receptor. Oncol Res 11:255-264, 1999

71. Boyle BJ, Zhao XY, Cohen P, et al: Insulin-like growth factor binding protein-3 mediates 1α,25-dihydroxyvitamin D_3 growth inhibition in the LNCaP prostate cancer cell line through p21/WAF1. J Urol 165:1319-1324, 2001

72. Rizvi NA, Marshall JL, Dahut W, et al: A phase I study of LGD1069 in adults with advanced cancer. Clin Cancer Res 5:1658-1664, 1999

73. Lee H-Y, Moon HJ, Chun K-H, et al: Effects of insulin-like growth factor binding protein-3 and farnesyltransferase inhibitor SCH66336 on Akt expression and apoptosis in non–small-cell lung cancer cells. J Natl Cancer Inst 96:1536-1548, 2004

BIOMETRICS 62, 986–995
December 2006

DOI: 10.1111/j.1541-0420.2006.00579.x

A Generalized Response Surface Model with Varying Relative Potency for Assessing Drug Interaction

Maiying Kong and J. Jack Lee*

Department of Biostatistics and Applied Mathematics, University of Texas, M. D. Anderson Cancer Center, Unit 447, 1515 Holcombe Boulevard, Houston, Texas 77030, U.S.A.
**email:* jjlee@mdanderson.org

SUMMARY. When multiple drugs are administered simultaneously, investigators are often interested in assessing whether the drug combinations are synergistic, additive, or antagonistic. Based on the Loewe additivity reference model, many existing response surface models require constant relative potency and some of them use a single parameter to capture synergy, additivity, or antagonism. However, the assumption of constant relative potency is too restrictive, and these models using a single parameter to capture drug interaction are inadequate to describe the phenomenon when synergy, additivity, and antagonism are interspersed in different regions of drug combinations. We propose a generalized response surface model with a function of doses instead of one single parameter to identify and quantify departure from additivity. The proposed model can incorporate varying relative potencies among multiple drugs as well. Examples and simulations are given to demonstrate that the proposed model is effective in capturing different patterns of drug interaction.

KEY WORDS: Additivity; Antagonism; Dose–response curve; Dose–response surface; Interaction index; Loewe additivity model; Synergy.

1. Introduction

Studies of interactions among biologically active agents, such as drugs, carcinogens, or environmental pollutants, have become increasingly important in many branches of biomedical research (Suhnel, 1998). An effective and accurate evaluation of drug interaction for in vitro and/or in vivo studies can help to determine whether a combination therapy should be further investigated in clinical trials.

The literature supports the notion that the Loewe additivity model can be considered as the "gold standard" to define drug interactions (Berenbaum, 1989; Greco, Bravo, and Parsons, 1995). Based on the Loewe additivity model, we focus on applying the response surface method (RSM) to study drug interaction. The RSM, which involves an estimation of the $(n + 1)$-dimensional response surface in n drug combinations, can take all of the information present in the full dose-effect data set for n drugs to give a complete picture of drug interactions over all possible drug combinations. In addition, the RSM can be used to determine the optimal combination therapy. Many examples of the RSM (e.g., Finney, 1971; Greco, Park, and Rustum, 1990; Plummer and Short, 1990) used a single parameter to capture synergy, additivity, or antagonism. These approaches are valid if only either synergy, additivity, or antagonism exists throughout the whole surface. They are inadequate to describe the presence of pockets of local synergy or local antagonism when they are interspersed in different regions of drug combinations. White et al. (2004) proposed a nonlinear mixture response surface approach based on the assumption that the combination doses at each fixed ratio follow the median effect model (Chou and Talalay, 1984), and the parameters in the median effect model are assumed to be polynomials of the ratio. The resulting models capture synergy, additivity, or antagonism exclusively based on the 50% maximal effect isoboles. However, at a fixed ratio, the combination doses of two drugs do not necessarily yield the same mode of drug interactions as that at 50% maximal effect. For example, Savelev et al. (2003) showed that the combinations of 1,8-cineole and α-pinene at the fixed ratio 11:1 are synergistic for higher combination doses and additive for lower combination doses. To address this issue, we propose a generalized response surface (GRS) model for two drugs. Instead of using one single parameter, we construct a function of the doses of two drugs to capture synergy, additivity, and antagonism without assuming any fixed patterns of drug interactions. The model contains a rich class of dose–response relationships and allows the drug interaction patterns to be determined by the observed data.

Before we proceed, let us recall a widely used model that provides a dose–response curve for a single agent: Chou and Talalay's (1984) median effect equation,

$$E = \frac{\left(\frac{d}{D_m}\right)^m}{1 + \left(\frac{d}{D_m}\right)^m}. \quad (1)$$

Here d is the dose of a drug, D_m is the median effective dose of a drug, and m is a slope parameter depicting the shape

© 2006, The International Biometric Society

of the dose–response curve. All these dose–response curves can be rewritten as Y, a monotone function of E, having a linear relationship with $\log d$. For example, the median effect equation has the form

$$Y = \log \frac{E}{1-E} = m(\log d - \log D_m). \tag{2}$$

All the families described by Suhnel (1998), excluding the Weibull family, can take such form by establishing a linear relationship between a monotone transformation of E and $\log d$. Tallarida (2000, Chapter 2) pointed out that, in many settings, the data points in the mid range (say between 20% and 80% of the maximum effect) typically display a nearly linear trend between the response and the $\log d$ when responses are measured on a continuous scale. For quantal response data, Finney (1971) and Govindarajulu (2001) pointed out that the probit- or logistic-transformed response usually exhibits a linear relationship with $\log d$. Consequently, we assume that the response or transformed response follows a linear function of $\log d$ for each of the two drugs when acting alone. Without loss of generality, we denote the dose–response curve as $Y = \beta_0 + \beta_1 \log d$.

Suhnel (1998) explicitly derived the combined additive effect of two drugs under the Loewe additivity model and made the assumption that the slopes β_1 are the same for both drugs. Finney (1971) proposed an additivity model for two drugs as $Y = \beta_0 + \beta_1 \log(d_1 + \rho d_2)$ for the combination dose (d_1, d_2), where ρ is the relative potency of drug 2 versus drug 1 and is assumed to be a constant. The constant ρ again implies that the two dose–response curves have the same slope. To construct a generalized model, we would first loosen the parallel assumption by allowing a varying relative potency. Next, we propose the use of a quadratic function of two doses instead of one single parameter to depict different patterns of drug interactions. The proposed model can be considered as a generalization of Finney's model (1971) and the model derived by Plummer and Short (1990). We will describe our proposed model in Section 2, relate this new model to isoboles and interaction indices in Section 3, state how to make inference on drug combinations in Section 4, and give simulations and examples to illustrate how the new approach performs in Section 5. The last section is devoted to discussion.

2. Derivation of the Generalized Response Surface Model

Recall the Loewe additivity model (Loewe and Muischnek, 1926; Berenbaum, 1989; Greco et al., 1995)

$$\frac{d_1}{D_{y,1}} + \frac{d_2}{D_{y,2}} = 1, \tag{3}$$

where d_1, d_2 are doses of drug 1 and drug 2 in the mixture eliciting an effect y, and $D_{y,1}$ and $D_{y,2}$ are the respective single-agent doses of drug 1 and drug 2 that elicit the effect y. One can obtain the predicted additive effect based on the Loewe additivity model providing that the dose–effect curves for each of the two drugs are known. Suppose that the dose–effect curves are $F_1(D_1)$ for drug 1 and $F_2(D_2)$ for drug 2, then the predicted effect, say y, can be obtained by solving equation (3) after replacing $D_{y,1}$ by $F_1^{-1}(y)$ and $D_{y,2}$ by $F_2^{-1}(y)$, where F_i^{-1} is the inverse function of $F_i (i = 1, 2)$. If the observed effect at (d_1, d_2) is more than or less than the predicted effect, the combination dose (d_1, d_2) is correspondingly synergistic or antagonistic.

Note that the above additive equation (3) can be rewritten as

$$d_1 + d_2 \frac{D_{y,1}}{D_{y,2}} = D_{y,1}. \tag{4}$$

Denote $\frac{D_{y,1}}{D_{y,2}}$ as $\rho(y)$, which is the relative potency of drug 2 versus drug 1, meaning that 1 unit of drug 2 has the same effect as $\rho(y)$ units of drug 1. Grabovsky and Tallarida (2004) addressed the issue that the relative potency may vary. The nonparallel dose–effect curves introduced by Suhnel (1998) can also be interpreted as the varying relative potency. When the relative potency varies, finding a method to transform the combination dose (d_1, d_2) into the equivalent doses of drug 1 or drug 2 requires careful investigation. In the following derivation, we uphold the Loewe additivity model regardless of the shape of the dose–effect curve associated with each single drug. We expound the interpretation of the varying relative potency, its correct usage, and the relationship of various quantities in equation (4) in the Appendix. From the Appendix, it follows that the additive y-isobole is a straight line $\overline{PQ}$, which connects $P = (D_{y,1}, 0)$ and $Q = (0, D_{y,2})$ (Figure 1, panel A). Each drug combination (d_1, d_2) on the y-isobole shares the same relative potency $\rho(y)$, and its equivalent amount dose is $d_1 + \rho(y)d_2$ in terms of drug 1, or $\rho(y)^{-1}d_1 + d_2$ in terms of drug 2. On the other hand, the combination doses on different additive isoboles may have different relative potencies as shown in Figure 1, panel B.

In this article, we construct a GRS model which incorporates the varying relative potency. We assume that the log(dose)–response curves are linear. Without loss of generality, the model derivation begins with the assumptions of a constant relative potency and a log(dose)–effect curve for drug 1:

$$Y_1 = \beta_0 + \beta_1 \log D_{Y_1,1}. \tag{5}$$

Subsequently, the predicted additive effect of the combination can be written as $Y = \beta_0 + \beta_1 \log(d_1 + \rho d_2)$, where ρ is a constant relative potency parameter. In order to capture synergy, additivity, or antagonism, Finney (1971, Section 11.5) suggested a model of the form

$$Y = \beta_0 + \beta_1 \log\left(d_1 + \rho d_2 + \kappa (d_1 \rho d_2)^{\frac{1}{2}}\right). \tag{6}$$

Here the additional term $(d_1 \rho d_2)^{\frac{1}{2}}$ is the geometric mean of d_1 and ρd_2, and κ is the synergy-antagonism parameter with $\kappa = 0$ corresponding to additivity, $\kappa > 0$ to synergy, and $\kappa < 0$ to antagonism.

Plummer and Short (1990) extended model (6) to a case in which the relative potency ρ may be varying while keeping the same formulation as (6). Let us assume that the log(dose)–effect curve for drug 2 is

$$Y_2 = \alpha_0 + \alpha_1 \log D_{Y_2,2}. \tag{7}$$

The question is: what form should the relative potency take under the log(dose)–effect curves (5) for drug 1 and (7) for drug 2? Let $Y_1 = Y_2 = y$, we have $\beta_0 + \beta_1 \log D_{y,1} = \alpha_0 + \alpha_1 \log D_{y,2}$. Then, $\beta_1 \log \frac{D_{y,1}}{D_{y,2}} = \alpha_0 - \beta_0 + (\alpha_1 - \beta_1) \log D_{y,2}$.

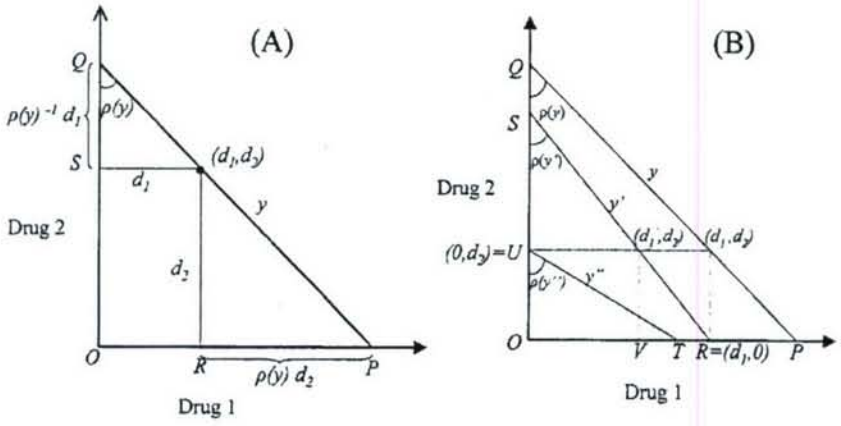

Figure 1. Relative potency and equivalent doses. $\overline{PQ}$ is an additive isobole, $P = (D_{y,1}, 0)$, $Q = (0, D_{y,2})$. The relative potency of drug 2 versus drug 1 is defined as $\rho(y) = \frac{D_{y,1}}{D_{y,2}}$. Under additive assumption the effect at (d_1, d_2) is the same as the effect of drug 1 alone at $d_1 + \rho(y)d_2$, and also the same as the effect of drug 2 alone at $\rho(y)^{-1}d_1 + d_2$ (panel A). Panel B shows that given drug 2 at dose d_2, its equivalent drug 1 dose may change when different amounts of drug 1 are added. Here $y = F_1(D_{y,1}) = F_2(D_{y,2})$, $y' = F_1(d_1)$, and $y'' = F_2(d_2)$. The equivalent amount of drug 1 doses of d_2 at combination doses (d_1, d_2), (d_1', d_2), and $(0, d_2)$ are $\rho(y)d_2(=\text{length}(\overline{RP}))$, $\rho(y')d_2(=\text{length}(\overline{VR}))$, and $\rho(y'')d2(=\text{length}(\overline{OT}))$, respectively.

Thus, the relative potency can be written as $\rho(y) = \frac{D_{y,1}}{D_{y,2}} = \exp(\frac{\alpha_0 - \beta_0}{\beta_1} + \frac{\alpha_1 - \beta_1}{\beta_1}\log D_{y,2})$. Introducing two parameters $\gamma_1(= \frac{\alpha_0 - \beta_0}{\beta_1})$ and $\gamma_2(= \frac{\alpha_1 - \beta_1}{\beta_1})$, we can write

$$\rho(y) = \exp(\gamma_1 + \gamma_2 \log D_{y,2}). \tag{8}$$

Here $D_{y,2}$ is the amount of the drugs in terms of drug 2, that is, $D_{y,2} = \rho(y)^{-1}d_1 + d_2$, which produces the same effect as the combination (d_1, d_2) under the additive assumption. Note that given one of the two, $D_{y,2}$ and y are uniquely determined, so we may suppress y to obtain the relative potency at combination dose (d_1, d_2) by solving $\rho = \exp(\gamma_1 + \gamma_2 \log D_2)$ subject to $D_2 = \rho^{-1}d_1 + d_2$.

Plummer and Short's model incorporates the varying relative potency. However, the model is inadequate to describe the phenomena when synergy and antagonism are interspersed in different regions of the drug combinations. To overcome this limitation, we propose the GRS model of the following form,

$$Y = \beta_0 + \beta_1 \log\left(d_1 + \rho d_2 + f(d_1, d_2; \gamma, \kappa)(d_1\rho d_2)^{\frac{1}{2}}\right) \tag{9}$$

using $f(d_1, d_2; \gamma, \kappa)$ to capture local synergy, local additivity, or local antagonism. In this article we take

$$f(d_1, d_2; \gamma, \kappa) = \kappa_0 + \kappa_1 d_1^{\frac{1}{2}} + \kappa_2(\rho d_2)^{\frac{1}{2}} + \kappa_3 d_1 + \kappa_4 \rho d_2 + \kappa_5(d_1\rho d_2)^{\frac{1}{2}}, \tag{10}$$

where f is a function of d_1 and d_2 with parameters γ's capturing the varying relative potency ρ as described above and κ's being the coefficients of the quadratic function.

Our main considerations for using the term $f(d_1, d_2; \gamma, \kappa)(d_1\rho d_2)^{\frac{1}{2}}$ are: (i) the marginal dose–effect curves are easily obtained and are impacted as little as possible by this extra term, and (ii) the function f can have enough flexibility to capture the departure from the predicted additivity effect, $\beta_0 + \beta_1 \log(d_1 + \rho d_2)$. For the first consideration, we used the factor $(d_1\rho d_2)^{\frac{1}{2}}$, and for the second consideration, we adopted the complete quadratic form of $d_1^{\frac{1}{2}}$ and $(\rho d_2)^{\frac{1}{2}}$ for $f(d_1, d_2; \gamma, \kappa)$. Extensive search and simulations show that the proposed model parameterization is reasonable and appropriate. One caveat is that the current parameterization may contain more parameters than necessary; therefore, model selection procedures need to be developed.

The following equations demonstrate how the GRS model captures different patterns of drug interaction: for each fixed effect level y, setting $d_2 = 0$ in (9), we obtain $D_{y,1} = \exp(\frac{y - \beta_0}{\beta_1})$; setting $d_1 = 0$, we obtain $D_{y,2} = \rho^{-1}\exp(\frac{y - \beta_0}{\beta_1})$; and the combination dose (d_1, d_2) satisfies $\exp(\frac{y - \beta_0}{\beta_1}) = d_1 + \rho d_2 + f(d_1, d_2; \gamma, \kappa)(d_1\rho d_2)^{\frac{1}{2}}$. Dividing both sides by $\exp(\frac{y - \beta_0}{\beta_1})$ and rearranging the equality, the interaction index, $\frac{d_1}{D_{y,1}} + \frac{d_2}{D_{y,2}}$, could be written as

$$\begin{aligned}
&\text{Interaction index} \\
&= \frac{d_1}{D_{y,1}} + \frac{d_2}{D_{y,2}} = \frac{d_1}{\exp\left(\frac{y - \beta_0}{\beta_1}\right)} + \frac{d_2}{\rho^{-1}\exp\left(\frac{y - \beta_0}{\beta_1}\right)} \\
&= 1 - \frac{f(d_1, d_2; \gamma, \kappa)(d_1\rho d_2)^{\frac{1}{2}}}{\exp\left(\frac{y - \beta_0}{\beta_1}\right)} \\
&= \left[1 + \frac{f(d_1, d_2; \gamma, \kappa)(d_1\rho d_2)^{\frac{1}{2}}}{d_1 + \rho d_2}\right]^{-1}.
\end{aligned} \tag{11}$$

From (11), the polynomial function $f(d_1, d_2; \gamma, \kappa)$ being greater than, equal to, or less than 0 corresponds to the interaction index being less than, equal to, or greater than 1, and consequently, this combination is synergistic, additive, or antagonistic, respectively.

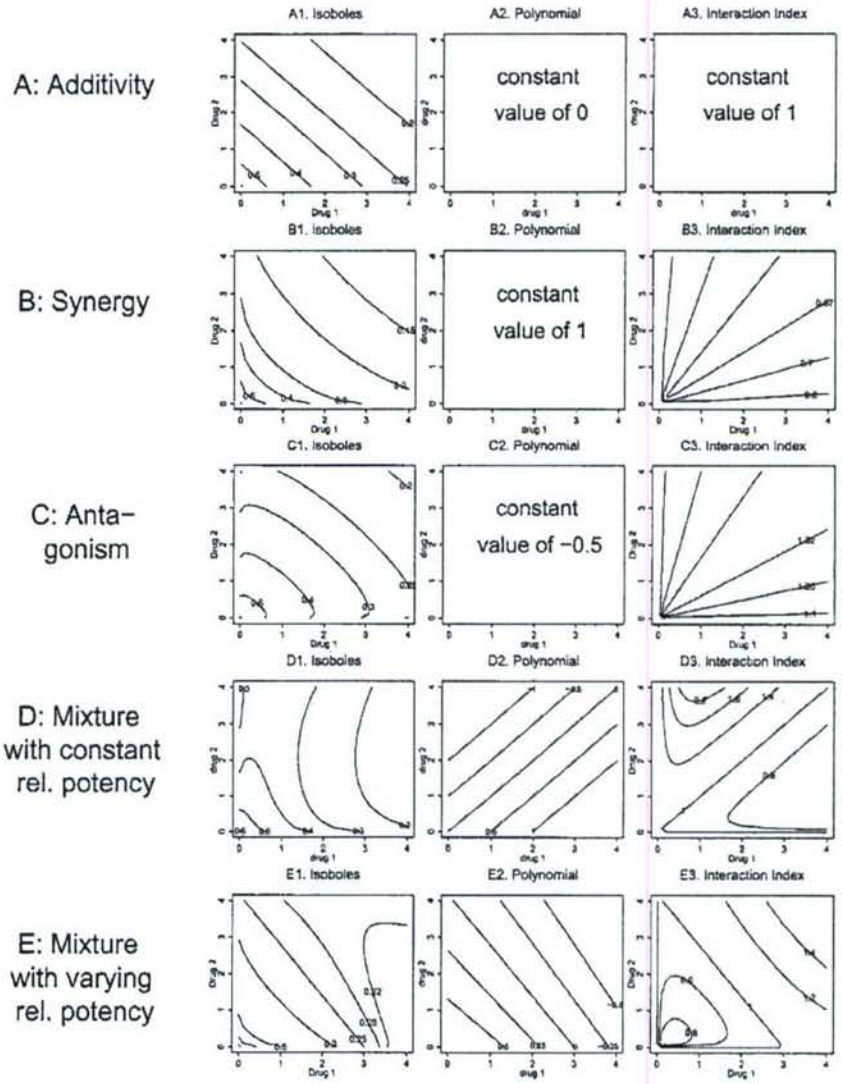

Figure 2. Contour plots of the response surfaces (i.e., isoboles), contour plots of the polynomial function $f(d_1, d_2; \gamma, \kappa)$, and contour plots of the interaction indices under different parameters. For all panels, $\beta_0 = 0$, $\beta_1 = -1$. For panels A, B, and C, $\kappa_0 = 0$, 1, and -0.5, respectively, while $\gamma_1 = \gamma_2 = 0$, $\kappa_i = 0$ for $i = 1, \ldots, 5$. Parameters in panel D are the same as in panel A except $\kappa_3 = 0.5$ and $\kappa_4 = -0.5$. In panel E we set $\gamma_1 = 0.1$, $\gamma_2 = -0.4$, $\kappa_0 = 0.9$, $\kappa_3 = \kappa_4 = -0.3$, and $\kappa_1 = \kappa_2 = \kappa_5 = 0$.

3. Relating the GRS Model to Isoboles and Interaction Indices

Recall that an isobole consists of all the drug combinations which elicit the same effect y. So, each curve in the contour plot of the response surface (9) can be viewed as an isobole. To better understand the proposed GRS model, we examine the relationship between the contour plots of the response surface, the polynomial function, and the interaction index. Chou and Talalay's (1984) median effect equation (2) is used to model the dose–effect curve for each single drug. We begin by taking the simplest case that the two dose–effect curves are the same with the slope being -1 and the median effective dose being 1, which yields $\beta_0 = \gamma_1 = \gamma_2 = 0$, $\beta_1 = -1$, and $\rho = 1$. In this special case the relative potency is constant, and the model conforms to equation (6). This model can be represented in the GRS model (9) by taking $\kappa_i = 0\,(i = 1, \ldots, 5)$ with different values of κ_0 in $f(d_1, d_2; \gamma, \kappa)$. In Figure 2, panels A, B, and C illustrate the cases for $\kappa_0 = 0$, 1, $-$ 0.5, respectively. In panel A, the contour plot of the response surface shows that the isoboles are straight lines (subpanel A1); $f(d_1, d_2; \gamma, \kappa)$ is a constant at 0 (subpanel A2); and the interaction index is a constant at 1 (subpanel A3). All three subpanels indicate that the combination doses are additive. In panel B, the contour plot of the response surface shows that the isoboles are concave down (subpanel B1); $f(d_1, d_2; \gamma, \kappa)$ is a constant at 1 (subpanel B2); and the interaction indices are less than 1 (subpanel B3). All three subpanels indicate that the combination doses are synergistic. Similarly, subpanel C1 shows that the

isoboles are concave up, subpanel C2 shows $f(d_1, d_2; \gamma, \kappa) = -0.5$, and subpanel C3 shows that the interaction indices are greater than 1, indicating that the combination doses are antagonistic. These special cases of our proposed model with $\kappa_i = 0$ $(i = 1, \ldots, 5)$ use a single parameter κ_0 to capture synergy, additivity, or antagonism and they reduce to Finney's model and Plummer and Short's model. Beyond these three special cases, the proposed model can be used more broadly, in particular when synergy and antagonism appear in different combination doses. We construct a case in panel D by setting $\kappa_0 = \kappa_1 = \kappa_2 = 0$, $\kappa_3 = 0.5$, $\kappa_4 = -0.5$, and $\kappa_5 = 0$, that is, $f(d_1, d_2; \gamma, \kappa) = 0.5d_1 - 0.5d_2$. The contour plot of the response surface is shown in subpanel D1. The contour plot of the polynomial function forms straight lines at a 45° angle (subpanel D2). The diagonal line $0.5d_1 - 0.5d_2 = 0$ separates the space into two parts. In the area below this 45° diagonal line, the polynomial is positive and the interaction index is less than 1 (subpanel D3), indicating that the combination doses in this area are synergistic. On the other hand, in the area above this 45° diagonal line, the polynomial is negative and the interaction index is greater than 1, indicating that the combination doses in this area are antagonistic. Furthermore, to show the varying relative potency, we set $\gamma_1 = 0.1$, $\gamma_2 = -0.4$ with $\kappa_0 = 0.9$, $\kappa_3 = -0.3$, and $\kappa_4 = -0.3$ (panel E). The isobole with effect level 0.25 is a straight line (subpanel E1), the corresponding polynomial is a constant at 0 (subpanel E2), and the interaction index is a constant at 1 (subpanel E3), indicating that all the combination doses on this line are additive. The isoboles with effect levels greater than 0.25 are concave down, the corresponding polynomial is positive, and the interaction index is less than 1, indicating that the combination doses in these regions are synergistic. In contrast, the isoboles with effect levels less than 0.25 are concave up, the corresponding polynomial is negative, and the interaction index is greater than 1, indicating that the combination doses in the other areas are antagonistic.

4. Statistical Consideration of the GRS Model

First we may consider whether the new model (9)-(10) provides a significant improvement of Plummer and Short's model by testing $H_0: \kappa_1 = \kappa_2 = \kappa_3 = \kappa_4 = \kappa_5 = 0$ against $H_1: \kappa_i \neq 0$ for any $i (i = 1, \ldots, 5)$ using the F-statistics (Gallant, 1987):

$$F = \frac{(\mathrm{RSS}_{\mathrm{P-S}} - \mathrm{RSS}_{\mathrm{full}})/q}{\mathrm{RSS}_{\mathrm{full}}/(n-p)} \tag{12}$$

with $q = 5$ and $n - p$ degrees of freedom. Here n is the number of observations and $p = 10$ is the number of parameters in model (9)-(10). $\mathrm{RSS}_{\mathrm{full}}$ is the residual sum of squares of our GRS model, and $\mathrm{RSS}_{\mathrm{P-S}}$ is the residual sum of squares of Plummer and Short's model. Rejecting H_0 suggests that Plummer and Short's model does not provide adequate fit to the data. On the other hand, failing to reject H_0 suggests that Plummer and Short's model is sufficient and there is no need to add more terms to the model. Note that the F-test requires that the responses on Y-scale are normally distributed. One should check the normality assumption, for example, applying the Q–Q plot to the residuals to examine whether the assumption is reasonable. If not, proper transformation should be sought.

The true model may include only a few terms in the GRS model (9)-(10). To avoid overparameterization, we remove the unnecessary terms by using the Akaike information criterion (AIC) (Venables and Ripley, 2002) and a backward elimination procedure. For the backward elimination procedure, a constraint is added that no lower-order terms can be removed until after the corresponding higher-order terms are removed. Here, AIC = $-2 \times$ maximized log likelihood $+ 2p$, which can be written as AIC = $n\log(\mathrm{RSS}/n) + 2p + C(n)$ under the normality assumption for the response Y. For a data set, the number of observations, n, remains constant, so, comparing AIC values under different parameterization is the same as comparing the sum of the first two terms, which is referred to as AIC later. To remove the unnecessary terms, we first fit the full model, calculate AIC, and then remove the parameter with the smallest absolute t-value among γ, β, and the higher-order terms of κ's in f if the parameter has a p-value greater than the level of significance α, say, $\alpha = 0.10$ (Hocking, 1976). We repeat the procedure, refit the reduced model, calculate the AIC for the reduced model, and check the t-values until either all the remaining parameters among γ, β, and the higher-order terms κ's in f have p-values smaller than α or when the AIC value increases.

As described in Section 3, the different patterns of drug interactions could be detected by observing the sign and magnitude of the polynomial function $f(d_1, d_2; \gamma, \kappa)$. Because the parameters γ and κ in the polynomial are estimated, their asymptotic properties follow the standard results from a nonlinear regression. For each combination dose (d_1, d_2), the variance of the estimated polynomial $f(d_1, d_2; \gamma, \kappa)$ can be approximated by $\widehat{\mathrm{Var}}_f = (\frac{\partial f}{\partial(\gamma,\kappa)})' \Sigma (\frac{\partial f}{\partial(\gamma,\kappa)})|_{(\gamma,\kappa)=(\hat{\gamma},\hat{\kappa})}$, where

$$\frac{\partial f}{\partial(\gamma,\kappa)} = \left(\frac{\partial f}{\partial\gamma_1}, \frac{\partial f}{\partial\gamma_2}, \frac{\partial f}{\partial\kappa_0}, \frac{\partial f}{\partial\kappa_1}, \frac{\partial f}{\partial\kappa_2}, \frac{\partial f}{\partial\kappa_3}, \frac{\partial f}{\partial\kappa_4}, \frac{\partial f}{\partial\kappa_5}\right)'$$

$$= \left(\frac{\partial f}{\partial\rho}\frac{\partial\rho}{\partial\gamma_1}, \frac{\partial f}{\partial\rho}\frac{\partial\rho}{\partial\gamma_2}, 1, d_1^{\frac{1}{2}}, (\rho d_2)^{\frac{1}{2}}, d_1, \rho d_2, (d_1\rho d_2)^{\frac{1}{2}}\right)'$$

with $\frac{\partial f}{\partial\rho} = \frac{1}{2}\kappa_2(\frac{d_2}{\rho})^{\frac{1}{2}} + \kappa_4 d_2 + \frac{1}{2}\kappa_5(\frac{d_1 d_2}{\rho})^{\frac{1}{2}}$, $\frac{\partial\rho}{\partial\gamma_1} = \frac{\rho^2(d_2 + d_1\rho^{-1})}{\rho(d_2+d_1\rho^{-1})+\gamma_2 d_1}$, and $\frac{\partial\rho}{\partial\gamma_2} = \frac{\rho^2(d_2+d_1\rho^{-1})}{\rho(d_2+d_1\rho^{-1})+\gamma_2 d_1}\log(d_2 + d_1\rho^{-1})$. Σ is the estimated covariance matrix of the parameters $(\gamma_1, \gamma_2, \kappa_0, \kappa_1, \kappa_2, \kappa_3, \kappa_4, \kappa_5)$. Thus, we may construct $(1 - \alpha) \times 100\%$ lower and upper confidence surfaces for $f(d_1, d_2; \gamma, \kappa)$:

$$f_{l,u}(d_1, d_2) = \hat{f}(d_1, d_2) \mp t_{\frac{\alpha}{2}, n-p}\sqrt{\widehat{\mathrm{Var}}_f(d_1, d_2)},$$

where $t_{\frac{\alpha}{2}, n-p}$ is the upper $\frac{\alpha}{2}$ percentile of a t-distribution with $n - p$ degrees of freedom. The intercepts of the lower and upper confidence surfaces of $f(d_1, d_2; \gamma, \kappa)$ with the dose plane form a bound which embraces the curve $f(d_1, d_2; \gamma, \kappa) = 0$. The combination doses beyond the bound with positive polynomial values are synergistic. Conversely, the combination doses beyond the other side of the bound with negative polynomial values are antagonistic. Inside the bound, the drug combinations are considered additive because the responses are not significantly different from the predicted effect based on the additive model. When the final model is a subset of the full model, a similar approach can be used to construct the confidence bound for $f(d_1, d_2, \gamma, \kappa) = 0$ in the final model.

Table 1
Simulation results from fitting the full model and the true model with $\sigma = 0.1$

	Set 1 $f(d_1, d_2; \gamma, \kappa) = 0.5d_1 - 0.5d_2$							Set 2 $f(d_1, d_2; \gamma, \kappa) = 0.9 - 0.3d_1 - 0.3\rho d_2$						
		Full model			True model				Full model			True model		
Parameters	True value	Est.	SE	CR	Est.	SE	CR	True value	Est.	SE	CR	Est.	SE	CR
β_0	0	0.002	0.044	0.950				0	0.002	0.043	0.957			
β_1	−1	−0.999	0.034	0.951	−1.000	0.020	0.954	−1.0	−0.999	0.033	0.956	−0.999	0.031	0.959
γ_1	0	0.002	0.062	0.957				0.1	0.102	0.062	0.958	0.100	0.041	0.953
γ_2	0	0.002	0.046	0.952				−0.3	−0.299	0.040	0.955	−0.299	0.038	0.952
κ_0	0	0.003	0.324	0.946				0.9	0.901	0.553	0.953	0.900	0.138	0.949
κ_1	0	−0.001	0.478	0.956				0	0.018	0.577	0.952			
κ_2	0	0.004	0.499	0.942				0	0	0.850	0.948			
κ_3	0.5	0.515	0.227	0.946	0.502	0.049	0.944	−0.3	−0.298	0.195	0.958	−0.298	0.047	0.945
κ_4	−0.5	−0.500	0.188	0.933	−0.500	0.022	0.963	−0.3	−0.293	0.366	0.958	−0.297	0.063	0.955
κ_5	0	−0.013	0.236	0.953				0	−0.017	0.312	0.950			

Est. = parameter estimate; SE = standard error; CR = coverage rate.

In medical research and its applications, the inferences should be made considering both clinical and statistical significance. Although the above inferences on synergy and antagonism are primarily based on statistical significance, the importance of clinical significance, that is, the magnitude of drug interaction to be considered clinically meaningful, should also be considered. Chou and Hayball (1996) recommended that the synergy, antagonism, and additivity at a combination dose should be made based on whether interaction index at this combination is less than 0.9, greater than 1.1, or in between. Our method provides a more rigorous way to assess statistical significance and also provides a venue for gauging the magnitude of clinical significance.

5. Simulation and Data Analysis

5.1 *Simulation*

We performed simulation studies to examine the finite-sample properties of the estimates of the proposed model. We took two sets of parameters, as shown in Figure 2, panel D (set 1) and panel E (set 2). The corresponding response surface models are

$$\text{Set 1: } Y = \log\frac{E}{1-E} = -\log\left(d_1 + d_2 + (0.5d_1 - 0.5d_2)(d_1 d_2)^{\frac{1}{2}}\right) + \epsilon$$

and

$$\text{Set 2: } Y = \log\frac{E}{1-E} = -\log\left(d_1 + \rho d_2 + (0.9 - 0.3d_1 - 0.3\rho d_2)(d_1\rho d_2)^{\frac{1}{2}}\right) + \epsilon$$

with $\rho = \exp(0.1 - 0.3 \log D_2)$, where $\epsilon \sim N(0, \sigma^2)$. For each model we generated 1000 random samples with $\sigma = 0.1$, and d_1 and d_2 taking values among (0, 0.1, 0.5, 1, 2, 4). The sample size in each simulation run was $6 \times 6 = 36$. We fitted each random sample to the full model and then the true model (i.e., only fitting the nonzero parameters), and obtained the estimated parameters and their corresponding standard errors (SE). For each parameter, we constructed the 95% confidence interval and observed whether the true parameter lies in the confidence interval. We report the averages of the estimated parameters, SE, and the coverage rate of the confidence intervals for the 1000 random samples in Table 1. We conclude that (1) the parameters are very well estimated; (2) the coverage rates are close to the nominal 95% coverage; (3) in the full model, the standard errors of β_0, β_1, γ_1, and γ_2 are close to half of $\sigma(=0.1)$, while the SE of $\kappa_i (i = 0, \ldots, 5)$ are two- to eightfold of σ. In the true model, the standard errors for β's, γ's, and κ's are all with similar magnitude, ranging from 0.020 to 0.063 with an exception of $\hat{\kappa}_0$ in set 2 (SE = 0.138). These facts reflect that including unnecessary parameters increases the uncertainty of estimating all parameters, especially those in the quadratic function f. Therefore, it is important to develop an appropriate procedure to remove unnecessary parameters. A parsimonious model can increase the accuracy of the estimated parameters; hence, it provides a better estimator for the dose–response relationship.

We also performed simulated case studies to examine whether the estimation and the backward elimination procedure described in Section 4 can recover the true dose–response function, that is, all the zero parameters are removed, the 95% confidence bounds for $f = 0$ have proper coverage rates, and the contours of the fitted response surfaces are similar to the underlying response surface. These simulations showed that the estimation and the backward elimination procedure work well (data not shown).

5.2 *Data Analysis*

We analyzed data sets from cell lines in a study conducted by Dr. Reuben Lotan and his colleagues at M. D. Anderson Cancer Center. The study aimed to evaluate the efficacy of combination therapy with two novel agents, SCH66336 and 4-HPR, in a number of squamous cell carcinoma cell lines (unpublished data). Cell lines of human squamous cell carcinoma were treated with SCH66336 and 4-HPR separately and in combination. After 6 hours, the proportions of surviving cells were calculated. To illustrate, we present the results for the cell line UMSCC22B, after treating with SCH66336 at

Table 2
Fractions of cells surviving (UMSCC22B) *treated by single and combination doses of* SCH66336 *and* 4-HPR

SCH66336 dose (μM)	4-HPR dose (μM)				
	0	0.1	0.5	1	2
0	1	0.7666	0.5833	0.5706	0.4934
0.1	0.6701	0.6539	0.4767	0.5171	0.3923
0.5	0.6289	0.6005	0.4919	0.4625	0.3402
1	0.5577	0.5102	0.4541	0.3551	0.2851
2	0.455	0.4203	0.3441	0.3082	0.2341
4	0.3755	0.3196	0.2978	0.2502	0.1578

doses ranging from 0 to 4 μM and 4-HPR at doses ranging from 0 to 2 μM, alone and in combination, respectively. The corresponding fractions of cells surviving at each combination dose are shown in Table 2.

We analyzed these data sets using different methods. We calculated the interaction indices and their associated confidence intervals at the combination doses at the fixed ratio 1:1 by first fitting the respective dose–effect curves for SCH66336 and 4-HPR. We concluded that the combination doses (0.1, 0.1) and (0.5, 0.5) are additive, and the combination doses (1, 1) and (2, 2) are synergistic. The contour plot of the raw data is shown in Figure 3, panel A. Based on Plummer and Short's model, the combinations are synergistic ($\hat{\kappa} = 2.146$ with SE = 1.102). The contour plot, interaction indices, and residual plot of the fitted response surface of Plummer and Short's model are shown in Figure 3, panels B1, B2, and B3, respectively. The contour plot in panel B1 differs from the raw data contour plot in panel A. We fitted the data to our proposed full model, and found that the contour plot of the fitted response surface (panel C1) is more similar to the raw data contour plot. The contour plot of the polynomial function $f(d_1, d_2; \gamma, \kappa)$ is shown in panel C2, where the dotted curve is the upper boundary of the 95% confidence bound for $f(d_1, d_2; \gamma, \kappa) = 0$, and the lower boundary is below the illustrated region. The combination doses above the dotted line are synergistic. Panel C3 shows the contour plot of the interaction indices, and panel C4 shows the residual plot of the full model. We used the aforementioned backward elimination procedure with an order constraint to remove γ_2, κ_4, and β_0 sequentially, and the corresponding AIC values were -106.28, -106.39, and -106.72, respectively. The backward elimination procedure stopped when AIC increased. The results of the final model are shown in panels D1–D4. Panel D2 shows that the combination doses above the confidence bound are synergistic, inside the bound are additive, and below the bound are antagonistic. The residual plots show that the full model (panel C4) and the final model (panel D4) provide better fit for the data than Plummer and Short's model

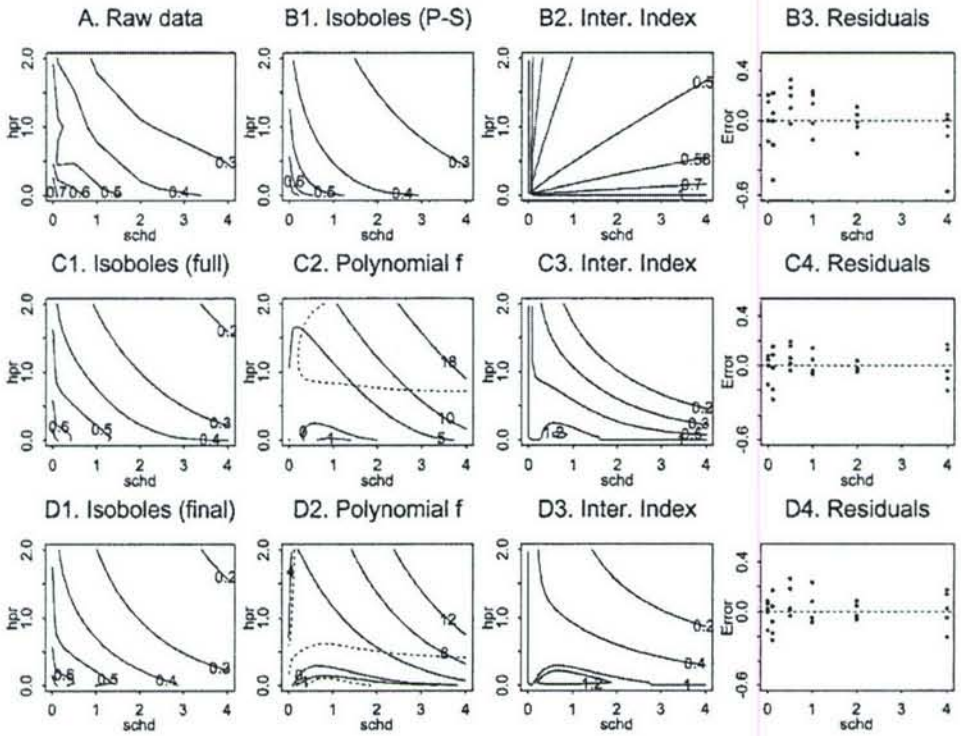

Figure 3. Results for cell line UMSCC22B: panel A is the contour plot of the raw data; panels B1–B3 show the results from Plummer and Short's model; panels C1–C4 show the results from the proposed full model; panels D1–D4 show the results from the final model. The dotted line in panel C2 is the upper boundary of the 95% confidence bound for $f(d_1, d_2; \gamma, \kappa) = 0$, and the lower boundary is out of the dose range. The two dotted lines in panel D2 are the two boundaries of a 95% confidence bound for $f(d_1, d_2; \gamma, \kappa) = 0$.

Table 3
The estimated parameters and their standard errors of different models for the data set shown in Table 2

		β_0	β_1	γ_1	γ_2	κ_0	κ_1	κ_2	κ_3	κ_4	κ_5	RSE
P-S	Est.	0.099	−0.473	−0.083	0.120	2.146						0.227
model	SE	0.093	0.062	0.292	0.259	1.102						
Full	Est.	0.088	−0.354	−0.339	0.148	5.735	−14.104	−5.539	7.114	5.283	7.021	0.143
model	SE	0.064	0.046	0.289	0.242	3.510	6.668	8.230	3.743	6.593	5.446	
Final	Est.		−0.384	−0.575		3.220	−12.368	1.195	5.492		8.250	0.143
model	SE		0.035	0.212		2.268	5.169	3.672	2.682		5.126	

P-S model = Plummer and Short's model; Est. = parameter estimate; SE = standard error; RSE = residual standard error.

(panel B3). The results from the final model are consistent with the results achieved by directly calculating the interaction indices and their associated confidence intervals.

In this example, $RSS_{P-S} = 1.238$, $RSS_{full} = 0.390$, and $n = 29$ (the model automatically assumed the fraction of cell survival being 1 at the combination dose $d_1 = d_2 = 0$ and this observation did not participate in the calculation). The Q–Q plots (not shown) indicated that the normality holds for the responses on Y-scale, therefore the F-test can be carried out. The F-statistic was 8.250 with degrees of freedom (5, 19), corresponding to $p < 0.003$. Hence, we rejected H_0 at $\alpha = 0.05$, that is, the new model (9)-(10) provides a significant improvement of Plummer and Short's model. The estimated parameters and their standard errors for Plummer and Short's model, the full model, and the final model are listed in Table 3. The residual standard error (RSE), which is an estimate of σ, is shown in the last column in Table 3 for each model. Figure 3 and Table 3 indicate that the final model fits the data as well as the full model, and the precisions on parameter estimation in the final model were improved over the full model. We conclude that the proposed model and procedure work well for this data set.

6. Discussion and Further Extension

One important contribution of this article is that the proposed model can incorporate varying relative potency. Although varying relative potency has been investigated by Tallarida (2000) and Grabovsky and Tallarida (2004), their interpretations resulted in inconsistent predicted additive effects for combination doses (Jonker et al., 2005). In the Appendix, we expound a method to correctly incorporate varying relative potency to predict the additive effect based on the Loewe additivity model. Using the proposed varying relative potency formulation, one can extend the additive response surface for k ($k \geq 2$) drug combinations as follows:

$$Y = \beta_0 + \beta_1 \log(d_1 + \rho_2 d_2 + \cdots \rho_k d_k), \qquad (13)$$

where $\rho_i = \exp(\gamma_{i0} + \gamma_{i1} \log D_1)$ $(i = 2, \ldots, k)$ is the relative potency of drug i versus drug 1, and D_1 is the amount of drug 1 having an equivalent effect to that of the combination $(d_1, \ldots, d_k)$ under the additive assumption. D_1 can be obtained by solving the following equation:

$$d_1 + \rho_2 d_2 + \cdots + \rho_k d_k = D_1.$$

Here γ_{i0} and γ_{i1} are uniquely determined by the two dose–effect curves for drug 1 and drug i $(i = 2, \ldots, k)$. The additive response surface model constructed this way is consistent with the Loewe additivity model.

In this article, we assume that the effect or transformed effect has a linear relationship with $\log d$. Although a broad class of dose–effect models satisfies this assumption, there are still some exceptions. One important exception is that the logit transform of the effect has a linear relationship with the dose, say $\log \frac{E}{1-E} = \alpha_0 + \alpha_1 d$. In that case, the relative potency for the two drugs is constant, and the additive response for the two drugs can be predicted by $\log \frac{E}{1-E} = \alpha_0 + \alpha_1 d_1 + \alpha_2 d_2$ (Carter et al., 1988). One can still use a quadratic function of d_1 and d_2 to detect different patterns of drug interactions by adding the product of the quadratic function and $(d_1 d_2)^{\frac{1}{2}}$ to the above model.

Suhnel (1990) used bivariate splines to fit dose–response data. The determination of drug interaction was based on the visualization of whether the contours of the response surface (i.e., isoboles) were concave up or concave down. The approach did not give any summary measure on drug interaction. Kelly and Rice (1990) used a monotone spline-based procedure to fit marginal dose–response curves first, then predicted the additive effect of the combination dose based on the Loewe additivity model. Extrapolation beyond the observed dose range is dangerous in this spline-based approach and, therefore, this approach has limited usage. Tan et al. (2003) proposed an optimal experimental design in the sense that it reduces the variability in modeling synergy while allocating the doses to minimize the sample size and to extract maximum information on the joint action of the compounds. The method uses a nonparametric function to detect drug interactions. Semiparametric approaches, as the format (9) or the format given by Tan et al. (2003), which combine parametric marginal dose–response curves with a nonparametric function to detect different patterns of drug interaction, provide logical extension to the current model and are appropriate topics for future research.

Acknowledgements

This research was supported in part by grants from the National Cancer Institute CA16672, CA97007, and CA91844, and the Department of Defense W81XWH-04-1-0142 and W81XWH-05-2-0027. The authors are thankful to the reviewers for their constructive comments, to Dr Reuben Lotan for providing the data, and to Lee Ann Chastain for editorial assistance.

References

Berenbaum, M. C. (1989). What is synergy? *Pharmacological Reviews* **41,** 93–141.

Carter, W. H., Jr., Gennings, C., Staniswalis, J. G., Cambell, E. D., and White, K. L., Jr. (1988). A statistical approach to the construction and analysis of isobolograms. *Journal of American College Toxicology* **7,** 963–973.

Chou, T. C. and Hayball, M. (1996). *CalcuSyn for Windows: Multiple-Drug Dose-Effect Analyzer and Manual.* Cambridge, U.K.: Biosoft.

Chou, T. C. and Talalay, P. (1984). Quantitative analysis of dose-effect relationships: The combined effects of multiple drugs or enzyme inhibitors. *Advances in Enzyme Regulation* **22,** 27–55.

Finney, D. J. (1971). *Probit Analysis.* Cambridge, U.K.: Cambridge University Press.

Gallant, A. R. (1987). *Nonlinear Statistical Models.* New York: Wiley.

Govindarajulu, Z. (2001). *Statistical Techniques in Bioassay.* Basel: Karger.

Grabovsky, Y. and Tallarida, R. J. (2004). Isobolographic analysis for combinations of a full and partial agonist: Curved isoboles. *Journal of Pharmacology and Experimental Therapeutics* **310,** 981–986.

Greco, W. R., Park, H. S., and Rustum, Y. M. (1990). Application of a new approach for the quantitation of drug synergy to the combination of cis-diamminedichloroplatinum and 1-β-D-arabinofuranosylcytosine. *Cancer Research* **50,** 5318–5327.

Greco, W. R., Bravo, G., and Parsons, J. C. (1995). The search of synergy: A critical review from a response surface perspective. *Pharmacological Reviews* **47,** 331–385.

Hocking, R. R. (1976). The analysis and selection of variables in linear regression. *Biometrics* **32,** 1–49.

Jonker, D. M., Visser, S. A. G., Van der Graaf, P. H., Voskuyl, R. A., and Danhof, M. (2005). Towards a mechanism-based analysis of pharmacodynamic drug-drug interactions in vivo. *Pharmacology and Therapeutics* **106,** 1–18.

Kelly, C. and Rice, J. (1990). Monotone smoothing with application to dose-response curves and the assessment of synergism. *Biometrics* **46,** 1071–1085.

Loewe, S. and Muischnek, H. (1926). Effect of combinations: Mathematical basis of problem. *Archives of Experimental Pathology and Pharmacology* **11,** 313–326.

Plummer, J. L. and Short, T. G. (1990). Statistical modeling of the effects of drug combinations. *Journal of Pharmacological Methods* **23,** 297–309.

Savelev, S., Okello, E., Perry, N. S. L., Wilkins, R. M., and Perry, E. K. (2003). Synergistic and antagonistic interactions of anticholinesterase terpenoids in *Salvia lavandulaefolia* essential oil. *Pharmacology, Biochemistry and Behavior* **75,** 661–668.

Suhnel, J. (1990). Evaluation of synergism or antagonism for the combined action of antiviral agents. *Antiviral Research* **13,** 23–40.

Suhnel, J. (1998). Parallel dose-response curves in combination experiments. *Bulletin of Mathematical Biology* **60,** 197–213.

Tallarida, R. J. (2000). *Drug Synergy and Dose-Effect Data Analysis.* Boca Raton, Florida: Chapman Hall/CRC Press.

Tan, M., Fang, H., Tian, G., and Houghton, P. J. (2003). Experimental design and sample size determination for testing synergism in drug combination studies based on uniform measures. *Statistics in Medicine* **22,** 2091–2100.

Venables, W. N. and Ripley, B. D. (2002). *Modern Applied Statistics with S,* 4th edition. New York: Springer-Verlag.

White, D. B., Faessel, H. M., Slocum, H. K., Khinkis, L., and Greco, W. R. (2004). Nonlinear response surface and mixture experiment methodologies applied to the study of synergy. *Biometrical Journal* **46,** 56–71.

Received July 2005. *Revised February* 2006. *Accepted February* 2006.

Appendix

Varying Relative Potency and Its Application

Figure 1, panel A shows that for each fixed effect y, as long as the dose–effect curves for each drug are known, $D_{y,1}$ and $D_{y,2}$ will be known and fixed, thus the relative potency defined by $\frac{D_{y,1}}{D_{y,2}}$ is fixed. Any combination dose (d_1, d_2) on the line $\overline{PQ}$ connecting $P(=(D_{y,1}, 0))$ and $Q(=(0, D_{y,2}))$ has the same relative potency, and d_2 units of drug 2 is equivalent to $\rho(y)d_2$ units of drug 1. Therefore the combination dose (d_1, d_2) is equivalent to $d_1 + \rho(y)d_2$ units of drug 1, which is exactly $D_{y,1}$, and the predicted effect is $F_1(d_1 + \rho(y)d_2)$, which is $F_1(D_{y,1})$. Similarly, for any combination dose (d_1, d_2) on the line $\overline{PQ}$, d_1 units of drug 1 is equivalent to $\rho(y)^{-1}d_1$ units of drug 2, thus the combination dose (d_1, d_2) is equivalent to $\rho(y)^{-1}d_1 + d_2$ units of drug 2, which is $D_{y,2}$. Consequently, the predicted effect is $F_2(\rho^{-1}(y)d_1 + d_2)$, that is, $F_2(D_{y,2})$. Hence, the predicted effect either by $F_1(d_1 + \rho(y)d_2)$ or by $F_2(\rho(y)^{-1}d_1 + d_2)$ is the same.

We then pay special attention to the fact that, for a given dose d_2 of drug 2, its equivalent amount of drug 1 may be different depending on the existing amount of drug 1 due to a varying relative potency. For example, suppose from the two marginal dose–effect curves we learn that the effects of drug 1 at doses $D_{y,1}$, d_1, and $D_{y'',1}$ are the same as the effects of drug 2 at doses $D_{y,2}$, $D_{y',2}$, and d_2, respectively. When two drugs are used, the three corresponding additive isoboles (Figure 1, panel B) are $\overline{PQ}$ connecting $P = (D_{y,1}, 0)$ and $Q = (0, D_{y,2})$, $\overline{RS}$ connecting $R = (d_1, 0)$ and $S = (0, D_{y',2})$, and $\overline{TU}$ connecting $T = (D_{y'',1}, 0)$ and $U = (0, d_2)$. All the combinations on $\overline{PQ}$ share the relative potency $\rho(y)$, all the combinations on $\overline{RS}$ share the relative potency $\rho(y')$, and all the combinations on $\overline{TU}$ share the relative potency $\rho(y'')$. Thus, in terms of drug 1 the equivalent dose of d_2 in the combinations (d_1, d_2), (d_1', d_2), and $(0, d_2)$ will be $\rho(y)d_2$, $\rho(y')d_2$, and $\rho(y'')d_2$, which can be illustrated by the length of $\overline{RP}$, $\overline{VR}$, and $\overline{OT}$, respectively. Here $y = F_1(D_{y,1}) = F_2(D_{y,2})$, $y' = F_1(d_1)$, and $y'' = F_2(d_2)$. Grabovsky and Tallarida (2004) proposed a model to

incorporate the varying relative potency, but they interpret the relative potency as $\rho(y'')$ at all three combinations, namely, (d_1, d_2), (d_1', d_2), and $(0, d_2)$. Consequently, the equivalent amount of drug 1 will be the dose of drug 1 plus $\rho(y'')d_2$ no matter the dose of drug 1. Their interpretation may result in two inconsistent additive effects, say $F_1(d_1 + \rho(y'')d_2)$ and $F_2(\rho(y')^{-1}d_1 + d_2)$ (Jonker et al., 2005), and curved additive isoboles (Grabovsky and Tallarida, 2004). Therefore, their approach is questionable. On the other hand, when combinations of two drugs are additive with varying relative potency, our formulation shows straight line isoboles, which are consistent with the Loewe additivity model.

Cellular FLICE-Inhibitory Protein Down-regulation Contributes to Celecoxib-Induced Apoptosis in Human Lung Cancer Cells

Xiangguo Liu,[1] Ping Yue,[1] Axel H. Schönthal,[2] Fadlo R. Khuri,[1] and Shi-Yong Sun[1]

[1]Department of Hematology and Oncology, Winship Cancer Institute, Emory University School of Medicine, Atlanta, Georgia and [2]Department of Molecular Microbiology and Immunology, University of Southern California, Los Angeles, California

Abstract

The cyclooxygenase-2 (COX-2) inhibitor celecoxib is an approved drug in the clinic for colon cancer chemoprevention and has been tested for its chemopreventive and therapeutic efficacy in various clinical trials. Celecoxib induces apoptosis in a variety of human cancer cells including lung cancer cells. Our previous work has shown that celecoxib induces death receptor 5 expression, resulting in induction of apoptosis and enhancement of tumor necrosis factor–related apoptosis-inducing ligand (TRAIL)–induced apoptosis in human lung cancer cells. In the current study, we further show that celecoxib down-regulated the expression of cellular FLICE-inhibitory protein (c-FLIP), a major negative regulator of the death receptor–mediated extrinsic apoptotic pathway, through a ubiquitin/proteasome–dependent mechanism independent of COX-2 in human lung cancer cells. Overexpression of c-FLIP, particularly $FLIP_L$, inhibited not only celecoxib-induced apoptosis but also apoptosis induced by the combination of celecoxib and TRAIL. These results thus indicate that c-FLIP down-regulation also contributes to celecoxib-induced apoptosis and enhancement of TRAIL-induced apoptosis, which complements our previous finding that the extrinsic apoptotic pathway plays a critical role in celecoxib-induced apoptosis in human lung cancer cells. Collectively, we conclude that celecoxib induces apoptosis in human lung cancer cells through activation of the extrinsic apoptotic pathway, primarily by induction of death receptor 5 and down-regulation of c-FLIP. (Cancer Res 2006; 66(23): 11115-9)

Introduction

Celecoxib, a marketed anti-inflammatory and anti-pain drug, is being tested in clinical trials for its chemopreventive and therapeutic effects against a broad spectrum of epithelial malignancies, including lung cancers, either as a single agent or in combination with other agents. The antitumor activity of celecoxib is thought to be associated with its ability to induce apoptosis in a variety of cancer cells (1). The molecular mechanism underlying celecoxib-mediated apoptosis remains largely uncharacterized, although it seems to be associated with inactivation of Akt, induction of endoplasmic reticulum stress involving up-regulation of CCAAT/enhancer-binding protein-homologous protein (CHOP)/GADD153 and increase in Ca^{2+} levels, or down-regulation of the antiapoptotic protein survivin (2). There are two major apoptotic pathways: the extrinsic death receptor–mediated pathway and the intrinsic mitochondria-mediated pathway, with truncated Bid protein accounting for the cross-talk between the two pathways (3). Our previous results have shown that celecoxib induces apoptosis in non–small-cell lung cancer cell lines primarily through the activation of the extrinsic death receptor pathway (4).

The cellular FLICE-inhibitory protein (c-FLIP) plays a key role in negatively regulating the extrinsic apoptotic pathway through inhibition of caspase-8 activation (5). c-FLIP has multiple splice variants, and two main forms have been well characterized: c-FLIP short form ($c\text{-}FLIP_S$) and long form ($c\text{-}FLIP_L$; ref. 5). It has been well documented that elevated c-FLIP expression protects cells from death receptor–mediated apoptosis, whereas down-regulation of c-FLIP by chemicals or small interfering RNA (siRNA) sensitizes cells to death receptor–mediated apoptosis (5). Moreover, overexpression of c-FLIP also protects cells from apoptosis induced by cancer therapeutic agents such as etoposide and cisplatin (6–8). In the present study, we show for the first time that celecoxib, in addition to up-regulating death receptor 5, down-regulates c-FLIP expression, which contributes to celecoxib-induced apoptosis in non–small-cell lung cancer cells. This further confirms and expands our previous finding that celecoxib induces apoptosis in non–small-cell lung cancer cell lines primarily through the activation of the extrinsic death receptor pathway (4).

Materials and Methods

Reagents. Celecoxib, other nonsteroidal anti-inflammatory drugs, and antibodies against caspases were the same as previously described (4). 2,5-Dimethyl-celecoxib was synthesized as previously described (9). Human recombinant tumor necrosis factor–related apoptosis-inducing ligand (TRAIL) was purchased from PeproTech, Inc. (Rocky Hill, NJ). Mouse monoclonal anti-FLIP antibody (NF6) was purchased from Alexis Biochemicals (San Diego, CA). MG132 and SP600125 were purchased from Sigma Chemicals (St. Louis, MO) and Biomol (Plymouth Meeting, PA), respectively.

Cell lines and cell culture. The human non–small-cell lung cancer cell lines used in this study were purchased from the American Type Culture Collection (Manassas, VA) and cultured as previously described (4). H157-V and H157-AS cell lines, in which retroviral vector and antisense cyclooxygenase-2 (COX-2) were stably transfected, respectively (10), were kindly provided by Dr. S.M. Dubinett.

Western blot analysis. Preparation of whole-cell protein lysates and the procedures for the Western blotting were previously described (4).

Immunoprecipitation. A549-$FLIP_L$-2 cells, which stably express $FLIP_L$, were transfected with hemagglutinin-ubiquitin plasmid using FuGENE 6 transfection reagent (Roche Diagnostics Corp., Indianapolis, IN) following the manufacturer's instruction. After 24 hours, the cells were treated with celecoxib or MG132 plus celecoxib for 4 hours and then were lysed for immunoprecipitation of Flag-$FLIP_L$ with Flag M2 monoclonal antibody (Sigma Chemicals) as previously described (11), followed by the detection of ubiquitinated $FLIP_L$ by Western blotting with antihemagglutinin antibody (Abgent, San Diego, CA).

Note: Supplementary data for this article are available at Cancer Research Online (http://cancerres.aacrjournals.org/).

F.R. Khuri and S-Y. Sun are Georgia Cancer Coalition Distinguished Cancer Scholars.

Requests for reprints: Shi-Yong Sun, Winship Cancer Institute, Emory University School of Medicine, 1365-C Clifton Road Northeast, C3088, Atlanta, GA 30322. Phone: 404-778-2170; Fax: 404-778-5520; E-mail: shi-yong.sun@emoryhealthcare.org.

©2006 American Association for Cancer Research.

doi:10.1158/0008-5472.CAN-06-2471

Silencing of COX-2 expression with siRNA. Stealth COX-2 siRNA that targets the sequence 5′-GCAGGCAGATGAAATACCAGTCTTT-3′ and Stealth control siRNA (12) were synthesized by Invitrogen (Carlsbad, CA). The transfection of siRNA was conducted as previously described (12).

Generation of lentiviral c-FLIP expression constructs and establishment of stable lines that overexpress c-FLIP. *c-FLIP$_L$* and *c-FLIP$_S$* coding regions were amplified by PCR using plasmids containing full-length cDNAs of *FLIP$_L$* and *FLIP$_S$*, respectively, which were provided by Dr. J. Tschopp. The amplified fragments were then ligated into the pT-easy vector (Promega, Madison, WI) following the manufacturer's protocol as pT-easy-FLIP$_L$ and pT-easy-FLIP$_S$, respectively, using the following primers: FLIP$_L$ sense, 5′-GACTAGTGCCGCCACCATGGATTACAAAGACGATGACG-3′; FLIP$_L$ antisense, 5′-CGGGCCCTTATGTGTAGGAGAGGATAAGTTTC-3′; FLIP$_S$ sense, 5′-GACTAGTGCCGCCACCATGTCTGCTGAAGTCATCCAT-CAGG-3′; and FLIP$_S$ antisense, 5′-CGGGCCCTCACATGGAACAATTTC-CAAG-3′. Both pLenti-DcR1 (a lentiviral vector harboring the *DcR1* gene, which was constructed using the pLenti6/V5 Directional TOPO Cloning kit purchased from Invitrogen) and pT-easy-FLIP$_L$ or pT-easy-FLIP$_S$ were cut with *Spe*I and *Apa*I restriction enzymes. The released fragment containing *c-FLIP$_L$* or *c-FLIP$_S$* gene was then cloned into the digested pLenti6/V5 vector and the resultant constructs were named pLenti-Flag-FLIP$_L$ and pLenti-FLIP$_S$, respectively. In this study, we used pLenti-LacZ as a vector control, which was included in the pLenti6/V5 Directional TOPO Cloning kit.

Lentiviral production and titer determination were previously described (12). For infection, the viruses were added to the cells at a multiplicity of infection of 10 with 10 μg/mL polybrene. For transient expression, cells were infected and then subjected to initial selection with 50 μg/mL blasticidin beginning at 24 hours after infection. Five days later, the cells were used for the given experiments. For stable expression, cell clones were picked after a 2-week selection with 50 μg/mL blasticidin postinfection and screened for FLIP expression by Western blotting with c-FLIP antibody. The clones with the highest levels of FLIP expression were used in the experiment.

Detection of apoptosis. Apoptosis was evaluated by Annexin V staining using Annexin V-PE apoptosis detection kit purchased from BD Biosciences (San Jose, CA) following the manufacturer's instructions. We also detected caspase activation by Western blotting (as described above) as an additional indicator of apoptosis.

Results and Discussion

Because c-FLIP levels are modulated by many cancer therapeutic agents, we were interested in determining whether celecoxib altered c-FLIP expression levels. Thus, we treated several non–small-cell lung cancer cell lines with increasing concentrations of celecoxib and then assessed c-FLIP levels. As presented in Fig. 1*A*, the expression levels of both FLIP$_L$ and FLIP$_S$ in these cell lines were reduced by celecoxib in a concentration-dependent manner after a 16-hour incubation. We noted that FLIP$_S$ levels were decreased after treatment with 10 μmol/L celecoxib, whereas FLIP$_L$ levels were reduced by relatively high concentrations of celecoxib (e.g., ≥25 μmol/L), suggesting that FLIP$_S$ is somewhat more sensitive to modulation by celecoxib than FLIP$_L$. The down-regulation of both FLIP$_L$ and FLIP$_S$ occurred as early as 3 hours and was sustained up to 48 hours after celecoxib treatment (Fig. 1*B*). We noted that the reduction of c-FLIP, particularly FLIP$_L$, at the late time points (e.g., 24 and 48 hours) was not as strong as that at the early time points (e.g., 3 and 6 hours). Nevertheless, these results clearly indicate that celecoxib down-regulates c-FLIP expression in human non–small-cell lung cancer cells, which represents an early event during celecoxib-induced apoptosis. We next determined whether other nonsteroidal anti-inflammatory drugs, including SC58125, NS-398, sulindac sulfide, and Dup697, down-regulated c-FLIP expression. As presented in Fig. 1*C*, these agents, particularly at 75 μmol/L, decreased the levels of both FLIP$_L$ and FLIP$_S$, albeit with weaker activity than celecoxib, which, at 50 μmol/L, effectively reduced c-FLIP levels. Thus, we conclude that other COX-2 inhibitors down-regulate c-FLIP expression as well.

c-FLIP is known to be regulated by a ubiquitin-proteasome mechanism (13, 14), and certain cancer therapeutic agents stimulate down-regulation of c-FLIP expression through this mechanism (13). To determine whether celecoxib induces proteasome-mediated c-FLIP degradation, we examined the effects of celecoxib on c-FLIP expression in the absence and presence of the proteasome inhibitor MG132 in A549 cells. As shown in Fig. 2*A*, MG132 at concentrations of ≥10 μmol/L abrogated the ability of celecoxib to reduce both FLIP$_L$ and FLIP$_S$, suggesting that celecoxib down-regulates c-FLIP through proteasome-mediated protein degradation. We also noted that MG132 alone did not increase the levels of FLIP$_L$ but strikingly increased the levels of FLIP$_S$, suggesting that FLIP$_S$ is more prone to proteasome-mediated

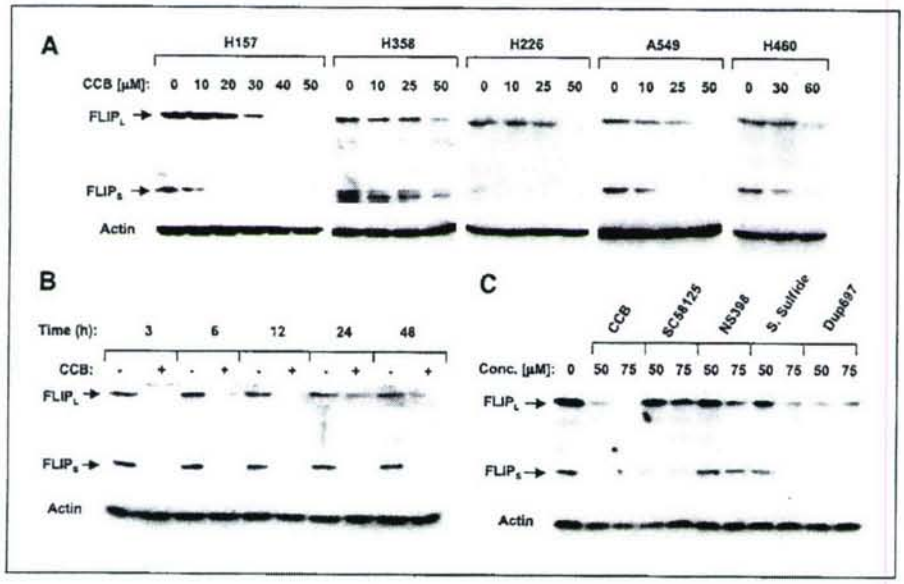

Figure 1. Down-regulation of c-FLIP expression by celecoxib (*A* and *B*) and other nonsteroidal anti-inflammatory drugs (*C*) in human non–small-cell lung cancer cells. *A*, the indicated cell lines were treated with the given concentrations of celecoxib (*CCB*) for 16 hours. *B*, H157 cells were treated with 50 μmol/L celecoxib for the indicated times. *C*, H157 cells were treated with the given concentrations of the indicated nonsteroidal anti-inflammatory drugs for 7 hours. Whole-cell protein lysates were prepared from the aforementioned treatments for detection of the given proteins using Western blot analysis, with actin serving as a loading control.

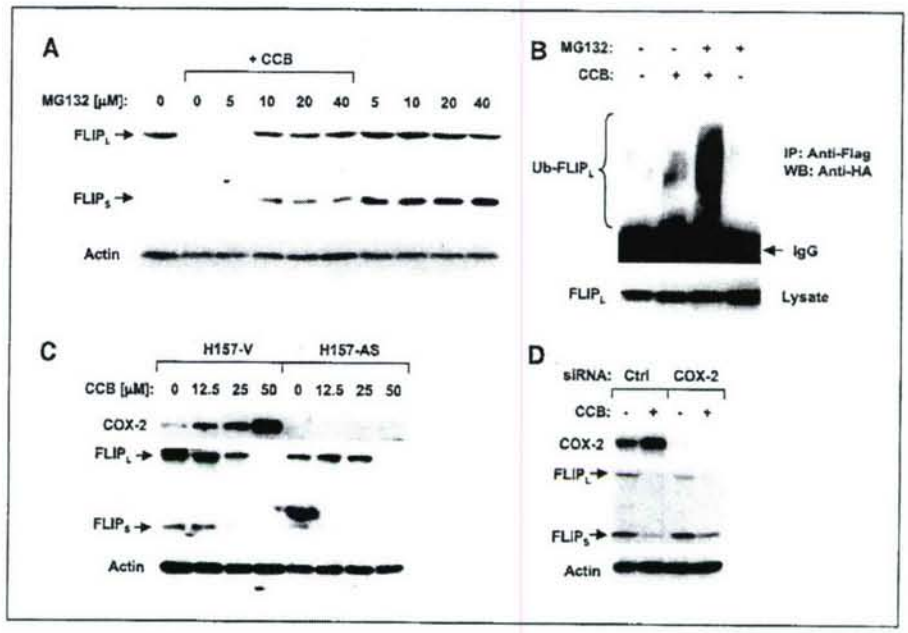

Figure 2. Celecoxib down-regulates c-FLIP through ubiquitin/proteasome–mediated protein degradation (*A* and *B*) independent of COX-2 (*C* and *D*). *A*, A549 cells were pretreated with the indicated concentrations of MG132 for 30 minutes and then cotreated with 50 μmol/L celecoxib (CCB) for another 4 hours. *B*, A549-FLIP$_L$-2 cells were transfected with hemagglutinin-ubiquitin plasmid using FuGENE 6 transfection reagent for 24 hours. The cells were then pretreated with 20 μmol/L MG132 for 30 minutes and then cotreated with 50 μmol/L celecoxib for 4 hours. *C*, H157-V (vector-control) and H157-AS (antisense COX-2) paired cell lines were treated with the given concentrations of celecoxib for 16 hours. *D*, A549 cells were transfected with control (*Ctrl*) or COX-2 siRNA for 48 hours and then treated with 50 μmol/L celecoxib for 16 hours. Whole-cell protein lysates were then prepared from the aforementioned treatments for detection of the given proteins by Western blot analysis (*A*, *C*, and *D*), with actin serving as the loading control, or immunoprecipitation (*IP*) with antihemagglutinin antibody followed by Western blotting (*WB*) for detection of ubiquitinated FLIP$_L$ (*Ub-FLIP$_L$*; *B*).

degradation, which is consistent to the recent findings by Poukkula et al. (14). Moreover, we examined the effects of celecoxib on overall proteasome activity and c-FLIP ubiquitination. Celecoxib did not increase proteasome activity (data not shown). However, it increased the levels of ubiquitinated c-FLIP, particularly in the presence of MG132 (Fig. 2*B*), indicating that celecoxib increases c-FLIP ubiquitination. Collectively, we suggest that celecoxib down-regulates c-FLIP levels through a ubiquitin-proteasome mechanism.

A recent study has shown that c-jun NH_2-terminal kinase (JNK) activation modulates FLIP$_L$ degradation (15). We then determined whether celecoxib down-regulates c-FLIP through a JNK-dependent mechanism. Celecoxib indeed increased the levels of phosphorylated c-Jun (p-c-Jun), an indicator of JNK activation, and decreased the levels of both FLIP$_L$ and FLIP$_S$. The JNK inhibitor SP600125 at concentrations up to 30 μmol/L abrogated celecoxib-induced c-Jun phosphorylation, but failed to block down-regulation of either FLIP$_L$ or FLIP$_S$ by celecoxib (Supplementary Fig. S1). Considering these findings and the fact that JNK does not modulate FLIP$_S$ turnover (15) whereas celecoxib down-regulates the levels of both FLIP$_L$ and FLIP$_S$ (Fig. 1), we conclude that celecoxib induces a JNK-independent degradation of c-FLIP.

It is well known that celecoxib is a specific COX-2 inhibitor. However, many studies show that celecoxib induces apoptosis independent of COX-2 inhibitory activity (2). To determine whether celecoxib decreases c-FLIP levels through its COX-2 inhibitory activity, we compared the modulatory effects of celecoxib on c-FLIP between H157 cells stably transfected with a retroviral vector harboring antisense COX-2 (H157-AS) and vector control cells (H157-V). As shown in Fig. 2*C*, the basal levels of COX-2 in H157 cell were reduced compared with H157-V cells. Interestingly, we found that celecoxib, albeit a COX-2 inhibitor, actually increased COX-2 protein levels in a concentration-dependent manner in H157-V cells; this effect was abolished in H157-AS cells. Together, these results validate the cell system in which COX-2 expression is inhibited due to the expression of antisense COX-2. In both cell lines, celecoxib still effectively reduced levels of FLIP$_L$ and FLIP$_S$, indicating that celecoxib modulates c-FLIP levels regardless of the presence of COX-2. Some nonsteroidal anti-inflammatory drugs were reported to induce COX-2 expression (16, 17). However, the inducing effect of celecoxib on COX-2 expression has not been reported. Currently, it is unclear what the implications of COX-2 induction are in celecoxib-mediated anticancer activity.

Moreover, we used siRNA to knockdown COX-2 expression in A549 cells and then examined its effect on celecoxib-induced c-FLIP down-regulation. Transfection of COX-2 siRNA inhibited not only the basal levels of COX-2 but also celecoxib-mediated COX-2 induction. However, it did not alter the effect of celecoxib on reduction of c-FLIP (Fig. 2*D*), furthering the notion that celecoxib down-regulates c-FLIP expression levels irrespective of COX-2 expression. In addition, we examined the effect of 2,5-dimethyl-celecoxib, a derivative of celecoxib completely lacking COX-2 inhibitory activity (9), on c-FLIP expression and found that 2,5-dimethyl-celecoxib still decreased c-FLIP levels, albeit with more potency than celecoxib (Supplementary Fig. S2). This result again suggests that celecoxib reduces c-FLIP levels independent of its COX-2-inhibitory activity. Collectively, we conclude that celecoxib down-regulates c-FLIP expression independent of COX-2.

To determine the involvement of c-FLIP down-regulation in celecoxib-induced apoptosis, we used a lentiviral expression system to enforce expression of c-FLIP in non–small-cell lung cancer cell lines and then analyzed its effect on celecoxib-induced caspase activation and apoptosis. Taking advantage of a lentiviral expression system that can achieve both transient and stable gene expression, we first transiently expressed FLIP$_L$ or FLIP$_S$ in H1792 cells. By Western blotting, we could detect high levels of ectopic FLIP$_L$ or FLIP$_S$ (Fig. 3*A*). Celecoxib induced cleavage of caspase-8, caspase-3, and poly(ADP-ribose) polymerase in lacZ-infected control cells, evidenced by the decrease in the levels of their pro-forms and the increase in the amounts of their cleaved bands. However, these effects were inhibited or diminished in cells infected with c-FLIP, particularly FLIP$_L$ (Fig. 3*A*). Consistently, we detected 34% apoptotic cells in lacZ-infected cells, but only 17% and 26% apoptosis in cells infected with FLIP$_L$ and FLIP$_S$,

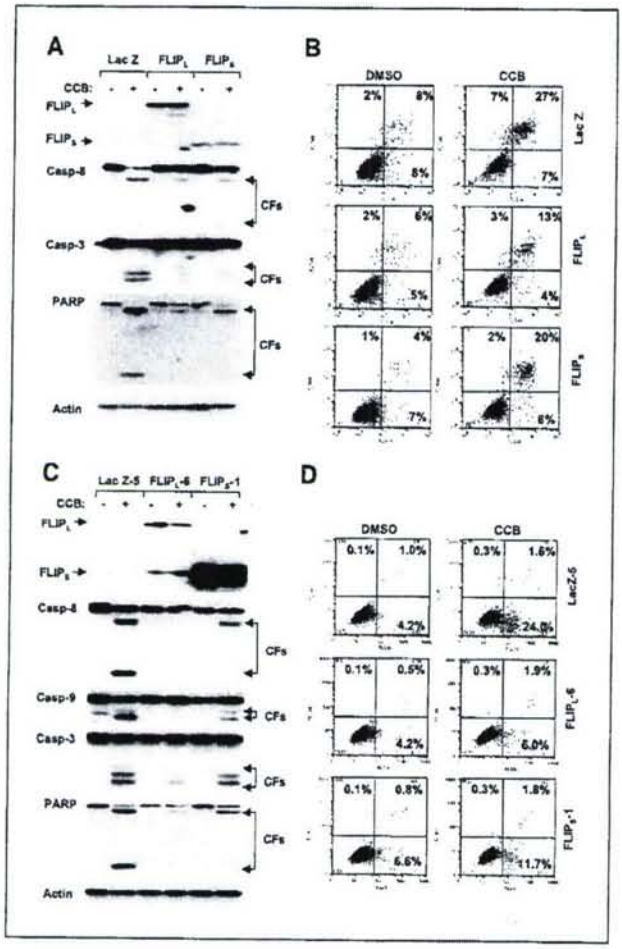

Figure 3. Both transient (*A* and *B*) and stable (*C* and *D*) overexpression of exogenous c-FLIP protect cells from celecoxib-induced caspase activation (*A* and *C*) and apoptosis (*B* and *D*) in human lung cancer cell lines. *A* and *B*, H1792 cells were infected with lentiviruses carrying lacZ, FLIP$_L$, and FLIP$_S$. After a brief selection with blasticidin for 5 days, the cells were treated with DMSO or 50 μmol/L celecoxib (CCB). Twenty-four hours later, the cells were subjected to preparation of whole-cell protein lysates and subsequent Western blot analysis for detection of caspase activation (*A*) or harvested for detection of apoptosis by Annexin V staining-flow cytometry (*B*). *C* and *D*, H157 stable transfectants expressing lacZ, FLIP$_L$, and FLIP$_S$ were treated with DMSO or 50 μmol/L celecoxib. Twenty-four hours later, the cells were subjected to preparation of whole-cell protein lysates and subsequent Western blot analysis for detection of caspase activation (*C*) or harvested for detection of apoptosis by Annexin V staining-flow cytometry (*D*). *CFs*, cleaved forms. Note that the endogenous levels of FLIP$_L$ and FLIP$_S$ proteins are not visible in these Western blots due to the short exposure times required to visualize the highly overexpressed exogenous forms of these proteins. In the Annexin V staining assay, the percent positive cells in the top right and bottom right quadrants were added to yield the total of apoptotic cells.

respectively, by Annexin V staining (Fig. 3*B*). Thus, these results show partial protective effects of c-FLIP, particularly FLIP$_L$, on celecoxib-induced apoptosis.

Following this study, we further established stable cell lines from H157 cells that expressed ectopic FLIP$_L$ or FLIP$_S$ and examined their responses to celecoxib-induced apoptosis. By Western blot analysis, we detected the expression of ectopic FLIP$_L$ and FLIP$_S$ in H157-FLIP$_L$-6 and H157-FLIP$_S$-1 transfectants, respectively (Fig. 3*C*), indicating the successful expression of ectopic FLIP$_L$ or FLIP$_S$ in H157 cells. Celecoxib treatment strongly increased amounts of cleaved forms of caspase-8, caspase-9, caspase-3, and poly(ADP-ribose) polymerase in the control H157-lacZ-5 cells; however, these effects were abrogated or diminished in either H157-FLIP$_L$-6 or H157-FLIP$_S$-1 cells. Accordingly, celecoxib caused 25.6% apoptosis in H157-lacZ-5 cells, but only 7.9% and 13.5% apoptosis in H157-FLIP$_L$-6 and H157-FLIP$_S$-1 transfectants, respectively (Fig. 3*D*). These results thus indicate that stable overexpression of c-FLIP, particularly, FLIP$_L$, protects cells from celecoxib-induced apoptosis. Taken together, we conclude that down-regulation of c-FLIP contributes to celecoxib-induced apoptosis. Because c-FLIP is a key regulatory protein that inhibits death receptor–mediated apoptosis (5), these findings further support our notion that the extrinsic apoptotic pathway plays a important role in celecoxib-induced apoptosis, at least in human non–small-cell lung cancer cells as previously shown (4). In agreement with our finding, a recent study has shown that celecoxib activates the death receptor–mediated apoptosis in hepatocellular carcinoma cells (18).

We previously reported that celecoxib in combination with TRAIL augmented the induction of apoptosis in human non–small-cell lung cancer cells (4). To determine whether down-regulation of c-FLIP also contributes to synergy between celecoxib and TRAIL on apoptosis induction, we examined the effects of enforced overexpression of c-FLIP on celecoxib-mediated enhancement of TRAIL-induced apoptosis in two non–small-cell lung cancer cell lines. To this end, we further established H460 transfectants that overexpressed ectopic FLIP$_L$ and FLIP$_S$ (Fig. 4*A*), in addition to the aforementioned H157 cells. In the two tested cell lines (i.e., H157 and H460), the combination of celecoxib and TRAIL induced more than additive effects on induction of apoptosis compared with each single agent in lacZ-infected control cells evaluated by Annexin V staining; however, these effects were either abrogated or

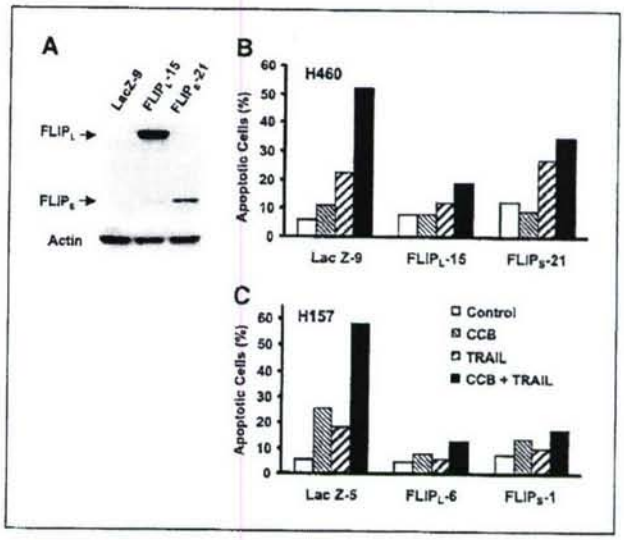

Figure 4. Overexpression of exogenous c-FLIP protects cells from induction of apoptosis by the combination of celecoxib (CCB) and TRAIL in H460 (*A* and *B*) and H157 (*C*) human lung cancer cell lines. *A* and *B*, the indicated H460 stable transfectants were treated with DMSO, 50 μmol/L celecoxib alone, 3 ng/mL TRAIL alone, or celecoxib and TRAIL combination for 24 hours (*B*). The expression of ectopic FLIP$_L$ and FLIP$_S$ was detected by Western blot analysis (*A*). *C*, the indicated H157 stable transfectants expressing lacZ, FLIP$_L$, and FLIP$_S$, as shown in Fig. 3, were treated with DMSO, 50 μmol/L celecoxib alone, 4 ng/mL TRAIL alone, or celecoxib and TRAIL combination for 24 hours. At the end of the aforementioned treatments (*B* and *C*), the cells were harvested for detection of apoptosis by Annexin V staining-flow cytometry.

inhibited in cells overexpressing c-FLIP, particularly $FLIP_L$ (Fig. 4*B* and *C*). For example, the combination of celecoxib and TRAIL caused ~58% apoptosis in H157-lacZ-5 cells, but only 13% apoptosis in H157-$FLIP_L$-6 cells and 17% apoptosis in H157-$FLIP_S$-1 cells (Fig. 4*C*). Thus, these results collectively show that down-regulation of c-FLIP also contributes to celecoxib-mediated enhancement of TRAIL-induced apoptosis.

We noted that the concentrations (≥10 μmol/L) required for celecoxib to down-regulate c-FLIP are higher than clinically achievable peak plasma concentrations (3.2-5.6 μmol/L) of celecoxib in humans after oral administration of a single dose of 800 mg (19). Given that celecoxib has been developed and marketed mainly for treatment of arthritis and pain, but not primarily for anticancer purposes, it is conceivable that this drug might be suboptimal for inclusion in the therapy of advanced cancers, such as non–small-cell lung cancer cells. In this regard, it might be beneficial to consider streamlined celecoxib derivatives that are optimized for anticancer applications, and some promising efforts have indeed been made in this direction. Certain novel non-COX-2 inhibitory celecoxib derivatives show better activity than celecoxib in inducing apoptosis and inhibiting the growth of tumors (9, 20), further emphasizing the need to explore and understand the underlying molecular mechanisms by which these drugs exert their proapoptotic, antitumor potential. In this regard, our finding that celecoxib and its COX-2-inactive derivative 2,5-dimethyl-celecoxib down-regulate c-FLIP provides a novel aspect of this process and is important for understanding the molecular mechanisms by which these drugs induce apoptosis. We noted that 2,5-dimethyl-celecoxib, which is more potent than celecoxib in down-regulating c-FLIP, was also more potent than celecoxib in decreasing cell survival and inducing apoptosis in human non–small-cell lung cancer cells,[3] suggesting that there is a inverse relationship between down-regulation of c-FLIP and induction of apoptosis by celecoxib and its derivatives. Therefore, we may consider modulation of c-FLIP as a screening tool for the development of novel celecoxib derivatives with better anticancer efficacy.

In conclusion, the present study shows for the first time that celecoxib down-regulates c-FLIP expression in human non–small-cell lung cancer cells; this down-regulation accounts for celecoxib-mediated induction of apoptosis and enhancement of TRAIL-induced apoptosis. These results complement our previous finding that the death receptor–mediated extrinsic apoptotic pathway plays a critical role in celecoxib-induced apoptosis in human lung cancer cells.

Acknowledgments

Received 7/7/2006; revised 9/27/2006; accepted 10/20/2006.

Grant support: Winship Cancer Institute faculty start-up research fund (S-Y. Sun), the Georgia Cancer Coalition Distinguished Cancer Scholar award (S-Y. Sun), and Department of Defense VITAL grant W81XWH-04-1-0142 (S-Y. Sun for Project 4).

The costs of publication of this article were defrayed in part by the payment of page charges. This article must therefore be hereby marked *advertisement* in accordance with 18 U.S.C. Section 1734 solely to indicate this fact.

We thank Dr. Steven M. Dubinett (University of California at Los Angeles, Los Angeles, CA) for providing cell lines expressing antisense COX-2, Dr. Jürg Tschopp (University of Lausanne, Lausanne, Switzerland) for c-FLIP cDNAs, and Dr. Ceshi Chen (Albany Medical College, Albany, NY) for hemagglutinin-ubiquitin plasmid.

[3] Our unpublished data.

References

1. Thun MJ, Henley SJ, Patrono C. Nonsteroidal anti-inflammatory drugs as anticancer agents: mechanistic, pharmacologic, and clinical issues. J Natl Cancer Inst 2002;94:252–66.
2. Schonthal AH. Antitumor properties of dimethyl-celecoxib, a derivative of celecoxib that does not inhibit cyclooxygenase-2: implications for glioma therapy. Neurosurg Focus 2006;20:E21.
3. Hengartner MO. The biochemistry of apoptosis. Nature 2000;407:770–6.
4. Liu X, Yue P, Zhou Z, Khuri FR, Sun SY. Death receptor regulation and celecoxib-induced apoptosis in human lung cancer cells. J Natl Cancer Inst 2004;96:1769–80.
5. Wajant H. Targeting the FLICE inhibitory protein (FLIP) in cancer therapy. Mol Interv 2003;3:124–7.
6. Kamarajan P, Sun NK, Chao CC. Up-regulation of FLIP in cisplatin-selected HeLa cells causes cross-resistance to CD95/Fas death signalling. Biochem J 2003;376:253–60.
7. Longley DB, Wilson TR, McEwan M, et al. c-FLIP inhibits chemotherapy-induced colorectal cancer cell death. Oncogene 2006;25:838–48.
8. Abedini MR, Qiu Q, Yan X, Tsang BK. Possible role of FLICE-like inhibitory protein (FLIP) in chemo-resistant ovarian cancer cells *in vitro*. Oncogene 2004; 23:6997–7004.
9. Kardosh A, Wang W, Uddin J, et al. Dimethyl-celecoxib (DMC), a derivative of celecoxib that lacks cyclooxygenase-2-inhibitory function, potently mimics the anti-tumor effects of celecoxib on Burkitt's lymphoma *in vitro* and *in vivo*. Cancer Biol Ther 2005; 4:571–82.
10. Dohadwala M, Luo J, Zhu L, et al. Non-small cell lung cancer cyclooxygenase-2-dependent invasion is mediated by CD44. J Biol Chem 2001;276:20809–12.
11. Chen C, Sun X, Ran Q, et al. Ubiquitin-proteasome degradation of KLF5 transcription factor in cancer and untransformed epithelial cells. Oncogene 2005;24: 3319–27.
12. Liu X, Yue P, Khuri FR, Sun SY. Decoy receptor 2 (DcR2) is a p53 target gene and regulates chemosensitivity. Cancer Res 2005;65:9169–75.
13. Kim Y, Suh N, Sporn M, Reed JC. An inducible pathway for degradation of FLIP protein sensitizes tumor cells to TRAIL-induced apoptosis. J Biol Chem 2002;277:22320–9.
14. Poukkula M, Kaunisto A, Hietakangas V, et al. Rapid turnover of c-FLIPshort is determined by its unique C-terminal tail. J Biol Chem 2005;280:27345–55.
15. Chang L, Kamata H, Solinas G, et al. The E3 ubiquitin ligase itch couples JNK activation to TNFα-induced cell death by inducing c-FLIP(L) turnover. Cell 2006;124: 601–13.
16. Paik JH, Ju JH, Lee JY, Boudreau MD, Hwang DH. Two opposing effects of non-steroidal anti-inflammatory drugs on the expression of the inducible cyclooxygenase. Mediation through different signaling pathways. J Biol Chem 2000;275:28173–9.
17. Pang L, Nie M, Corbett L, Knox AJ. Cyclooxygenase-2 expression by nonsteroidal anti-inflammatory drugs in human airway smooth muscle cells: role of peroxisome proliferator-activated receptors. J Immunol 2003;170: 1043–51.
18. Kern MA, Haugg AM, Koch AF, et al. Cyclooxygenase-2 inhibition induces apoptosis signaling via death receptors and mitochondria in hepatocellular carcinoma. Cancer Res 2006;66:7059–66.
19. Niederberger E, Tegeder I, Vetter G, et al. Celecoxib loses its anti-inflammatory efficacy at high doses through activation of NF-κB. FASEB J 2001;15:1622–4.
20. Zhu J, Song X, Lin HP, et al. Using cyclooxygenase-2 inhibitors as molecular platforms to develop a new class of apoptosis-inducing agents. J Natl Cancer Inst 2002;94: 1745–57.

[Cancer Biology & Therapy 6:1, e1-e8, EPUB Ahead of Print: http://www.landesbioscience.com/journals/cbt/abstract.php?id=3555; January 2007]; ©2007 Landes Bioscience

Research Paper

PPARγ Ligands Enhance TRAIL-induced Apoptosis through DR5 Upregulation and c-FLIP Downregulation in Human Lung Cancer Cells

Wei Zou
Xiangguo Liu
Ping Yue
Fadlo R. Khuri
Shi-Yong Sun*

Department of Hematology and Oncology; Winship Cancer Institute; Emory University School of Medicine; Atlanta, Georgia USA

*Correspondence to: Shi-Yong Sun; Winship Cancer Institute, Emory University School of Medicine; 1365-C Clifton Road, C3088; Atlanta, Georgia 30322 USA; Tel.: 404.778.2170; Fax: 404.778.5520; Email: shi-yong.sun@emoryhealthcare.org

Original manuscript submitted: 10/06/06
Manuscript accepted: 10/29/06

This manuscript has been published online, prior to printing for Cancer Biology & Therapy, Volume 6, Issue 1. Definitive page numbers have not been assigned. The current citation is: Cancer Biol Ther 2007; 6(1):
http://www.landesbioscience.com/journals/cbt/abstract.php?id=3555
Once the issue is complete and page numbers have been assigned, the citation will change accordingly.

KEY WORDS

PPARγ ligands, death receptor 5, c-FLIP, TRAIL, apoptosis, lung cancer cells

ACKNOWLEDGEMENTS

We thank Dr. Jürg Tschopp (University of Lausanne, Switzerland) for c-FLIP cDNAs. S-Y. Sun and F. Khuri are Georgia Cancer Coalition Distinguished Cancer Scholars. This work is supported in part by the Georgia Cancer Coalition Distinguished Cancer Scholar award (to S-Y. Sun) and Department of Defense VITAL grant W81XWH-04-1-0142 (to S-Y. Sun for Project 4).

ABSTRACT

Peroxisome proliferator-activated receptor γ (PPARγ) ligands are potential chemopreventive agents. Many studies have shown that PPARγ ligands induce apoptosis in various types of cancer cells including lung cancer cells. Some PPARγ ligands have been shown to downregulate c-FLIP expression and thus enhance tumor necrosis factor-related apoptosis-inducing ligand (TRAIL)-induced apoptosis in some cancer cell lines. In the current study, we further show that PPARγ ligands induced the expression of death receptor 5 (DR5) and increased DR5 distribution at the cell surface in addition to reducing c-FLIP levels in human lung cancer cells. These agents cooperated with TRAIL to enhance induction of apoptosis in human lung cancer cells. Both overexpression of c-FLIP and knockdown of DR5 abrogated PPARγ ligand's ability to enhance TRAIL-induced apoptosis. Thus, it appears that not only c-FLIP downregulation but also DR5 upregulation contribute to PPARγ ligand-mediated enhancement of TRAIL-induced apoptosis in human lung cancer cells. Both the PPARγ antagonist GW9662 and silencing PPARγ expression failed to diminish PPARγ ligand-induced DR5 upregulation or c-FLIP downregulation, indicating that PPARγ ligands modulate that expression of DR5 and c-FLIP through a PPARγ-independent mechanism. Collectively, we conclude that PPARγ ligands exert PPARγ-independent effects on inducing DR5 expression and downregulating c-FLIP levels, leading to enhancement of TRAIL-induced apoptosis.

INTRODUCTION

Tumor necrosis factor-related apoptosis-inducing (TRAIL) is a soluble protein that induces apoptosis upon binding to death receptor 4 (DR4, also named TRAIL-R1) or death receptor 5 (DR5, also named TRAIL-R2, TRICK2, or Killer/DR5). TRAIL preferentially induces apoptosis in transformed or malignant cells, demonstrating potential as a tumor-selective apoptosis-inducing cytokine for cancer treatment.[1,2] Importantly, many small molecules including traditional chemotherapeutic agents are able to augment TRAIL-induced apoptosis in multiple types of cancer cells including lung cancer cells. Thus, TRAIL shows a strong potential as a cancer therapeutic agent and is being tested in phase I clinical trials.

There are several key components that modulate TRAIL-induced apoptosis. One such component is death receptor 5, which is one of the apoptotic death receptors that compose of a cysteine-rich extracellular domain and cytoplasmic death domain.[3] DR5 locates at the cell surface, becomes activated or oligomerized (trimerized) upon binding to its ligand TRAIL, and then signals apoptosis through caspase-8-mediated rapid activation of caspase cascades.[3,4] Another important protein involved in TRAIL signaling is cellular FLICE-inhibitory protein (c-FLIP; also called Casper/I-FLICE/FLAME-1/CASH/CLARP/MRIT), which is the major negative regulator of TRAIL/death receptor-induced apoptosis.[5,6] c-FLIP binds to Fas-associated death domain (FADD) and caspase-8 at the death-inducing signaling complex (DISC), and thereby inhibits death receptor-mediated apoptosis.[7] c-FLIP has multiple splice variants, and two main forms have been well characterized: c-FLIP short form (c-FLIP$_S$) and c-FLIP long form (c-FLIP$_L$).[5,6] It has been well documented that elevated c-FLIP expression protects cells from death receptor-mediated apoptosis in various cell types, whereas downregulation of c-FLIP by chemicals or siRNA sensitizes cells to death receptor-mediated apoptosis.[5,6] Both DR5 and c-FLIP are subjected to modulation by certain cancer therapeutic agents. Generally speaking, agents that either upregulate DR5 expression and/or downregulates c-FLIP levels often exhibit activity in enhancing TRAIL induced apoptosis.[8]

Peroxisome proliferator-activated receptor γ (PPARγ) ligands are potential cancer chemopreventive and therapeutic agents.[9,10] Many preclinical studies have shown that PPARγ ligands induces growth arrest and apoptosis in various types of cancer cells including lung cancer cells in vitro and inhibit tumor growth and carcinogenesis in animal models.[9,11,12] Moreover, these agents can be combined with other agents to exhibit enhanced anticancer activity.[13,14] Some PPARγ ligands have been shown to downregulate c-FLIP expression and thus enhance TRAIL-induced apoptosis in certain types of cancer cell lines.[15,16] In contrast to c-FLIP, the studies on the modulation of PPARγ ligands on DR5 expression have generated conflicting results. The PPARγ agonists 15-deoxy-$\Delta^{12,14}$-prostaglandin J_2 (15d-PGJ_2) and troglitazone, but not pioglitazone and rosiglitazone, were shown to induce DR5 expression.[16,17] However, 15d-PGJ_2 was not shown to have such an effect in a different study.[15] Moreover, it is not clear whether DR5 upregulation is involved in enhancement of TRAIL-induced apoptosis by PPARγ ligands.

In the current study, we investigated the modulatory effects of synthetic PPARγ ligands on the TRAIL/death receptor-mediated apoptotic pathway in human lung cancer cells. In addition to down-regulation of c-FLIP, we, for the first time, demonstrate that PPARγ ligands also induce DR5 expression in various lung cancer cell lines. Like c-FLIP downregulation, DR5 upregulation also contributes to enhancement of TRAIL-induced apoptosis by PPARγ ligands.

MATERIALS AND METHODS

Reagents. Troglitazone, pioglitazone and rosiglitazone were purchased from LKT Laboratories Inc (St. Paul, MN). Cigolitazone and GW1929 were purchased from Tocris (Ellisville, MO). WY14363 was purchased from Biomol (Plymouth Meeting, PA). CDDO was provided by Dr. M. B. Sporn (Dartmouth Medical School, Hanover, NH). These agents were dissolved in dimethyl sulfoxide (DMSO) at a concentration of 10 mM or 100 mM, and aliquots were stored at -80°C. Stock solutions were diluted to the desired final concentrations with growth medium just before use. Soluble recombinant human TRAIL was purchased from PeproTech Inc (Rocky Hill, NJ). Rabbit polyclonal anti-DR5 antibody was purchased from ProSci Inc (Poway, CA). Mouse monoclonal anti-caspase-3 was purchased from Imgenex (San Diego, CA). Rabbit polyclonal anti-caspase-9, anti-caspase-8, and anti-PARP antibodies were purchased from Cell Signaling Technology, Inc. (Beverly, MA). Mouse monoclonal anti-FLIP antibody (NF6) was purchased from Alexis Biochemicals (San Diego, CA). Rabbit polyclonal anti-β-actin antibody was purchased from Sigma Chemical Co. (St. Louis, MO).

Cell lines and cell cultures. All lung cancer cell lines used in this study were purchased from the American Type Culture Collection (Manassas, VA). These cell lines were grown in monolayer culture in RPMI 1640 medium supplemented with glutamine and 5% fetal bovine serum (FBS) at 37°C in a humidified atmosphere consisting of 5% CO_2 and 95% air.

Establishment of stable cell lines that overexpress c-$FLIP_L$ or c-$FLIP_S$. c-$FLIP_L$ and c-$FLIP_S$ coding regions were amplified by PCR using plasmids containing full length cDNAs of $FLIP_L$ and $FLIP_S$, respectively, which were provided by Dr. J. Tschopp (University of Lausanne, Switzerland).[7] The amplified fragments were then ligated into the pT-easy vector (Promega, Madison WI) following the manufacturer's protocol as pT-easy-$FLIP_L$ and pT-easy-$FLIP_S$, respectively, using the primers: c-$FLIP_L$ sense, 5'-GACTAGTGCCGCCACCATGGATTACAAAGACGATGACG-3', and $FLIP_L$ antisense, 5'-CGGGCCCTTATGTGTAGGAGAGGATAAGTTTC-3'. c-$FLIP_S$ sense, 5'-GACTAGTGCCGCCACCATGTCTGCTGAAGTCATCCATCAGG-3' and c-$FLIP_S$ antisense, 5'-CGGGCCCTCACATGGAACAATTTCCAAG -3'. Both pLenti-DcR1 (a lentiviral vector harboring the DcR1 gene, which was constructed using the pLenti6/V5 Directional TOPO Cloning kit purchased from Invitrogen) and pT-easy-$FLIP_L$ or pT-easy-$FLIP_S$ were cut with *Spe*I and *Apa*I restriction enzymes. The released fragment containing c-$FLIP_L$ or c-$FLIP_S$ gene was then cloned into the digested pLenti6/V5 vector and the resultant constructs were named pLenti-Flag-$FLIP_L$ and pLenti-$FLIP_S$, respectively. In this study, we used pLenti-Lac Z as a vector control, which was included in the pLenti6/V5 Directional TOPO Cloning kit. Lentiviral production and titer determination were done following the manufacturer's instruction. To establish stable cell lines, A549 cells were infected with the lentiviruses at ten of multiplicity of infection (MOI) with 10 μg/mL polybrene. After a two-week selection using 50 μg/mL blasticidin post infection, the survival clones were picked up and screened for c-FLIP expression by Western blotting using c-FLIP antibody. The clones with the highest levels of c-FLIP expression were used in the experiment.

Cell survival assay. Cells were seeded in 96-well cell culture plates and treated on the second day with the indicated agents. At the end of treatment, cell number was estimated by the sulforhodamine B (SRB) assay as previously described.[18] The cell survival was presented as percentage of control as calculated by using the equation: $At/Ac \times 100$, where At and Ac represent the absorbance in treated and control cultures, respectively.

Western blot analysis. The procedures for preparation of whole-cell protein lysates and Western blot analysis were the same as described previously.[19,20]

Detection of cell surface DR5. In this study, cell surface DR5 expression was analyzed using flow cytometry. The procedure for direct antibody staining and subsequent flow cytometric analysis of cell surface protein was described previously.[21] The mean fluorescence intensity (MFI) that represents antigenic density on a per cell basis was used to represent DR5 expression level. Phycoerythrin (PE)-conjugated mouse anti-human DR5 monoclonal antibody (DJR2-4) and PE mouse IgG1 isotype control (MOPC-21/P3) were purchased from eBioscience (San Diego, CA).

Detection of caspase activation and apoptosis. Caspase activation and their substrate cleavage were detected by Western blot analysis as described above. Apoptosis was detected by estimating sub-G_1 population as described previously.[22] In addition, the amounts of cytoplasmic histone-associated DNA fragments (mononucleosome and oligonucleosomes) formed during apoptosis were also measured using a Cell Death Detection ELISA^{Plus} kit (Roche Molecular Biochemicals, Indianapolis, IN) according to the manufacturer's instructions.

Silencing of DR5 expression using small interfering RNA (siRNA). High purity control (nonsilencing) and DR5 siRNA oligos were described previously[20] and synthesized from Qiagen (Valencia, CA). The transfection of siRNA was conducted in a 24-well plate (1 μg/well) using RNAiFect^{TM} transfect reagent purchased from Qiagen following the manufacturer's instruction. Forty-eight hours after the transfection, cells were treated with a PPARg ligand alone, TRAIL alone and their combination. Gene silencing effect was evaluated by Western blot analysis and apoptosis was measured as described above.

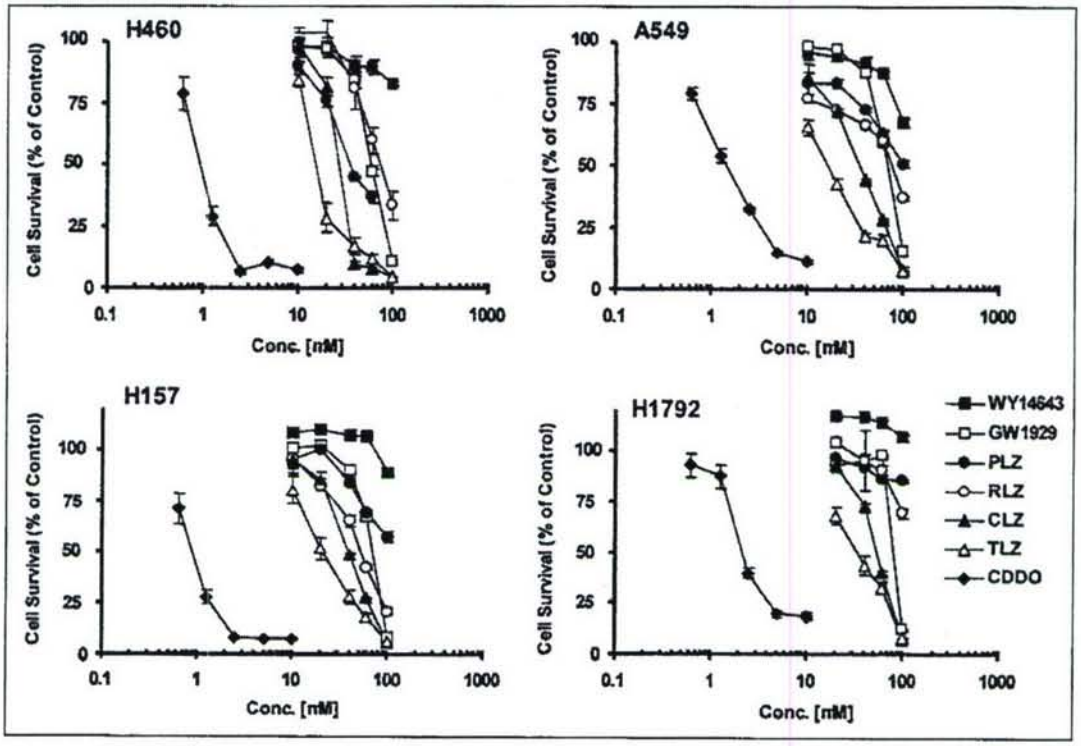

Figure 1. Effects of various PPARγ ligands on the growth of human lung cancer cells. The indicated cell lines were seeded in 96-well cell culture plates. On the second day, the cells were treated with different concentrations ranging from 0.5 to 100 μM of the given PPARγ ligands and WY14643 which is a PPARα ligand. After three days, the cells were fixed and subjected to estimation of cell number using the sulforhodamine B (SRB) assay. Each data value is a mean ± SD of four replicates. PLZ, pioglitazone; RLZ, rosiglitazone; CLZ, ciglitazone; TLZ, troglitazone

RESULTS

PPARγ ligands inhibit the growth of human lung cancer cells. To determine the concentration ranges or potencies of individual PPARγ ligands that effectively inhibit the growth of human lung cancer cells, we treated four lung cancer cell lines with several PPARγ ligands for three days and then evaluated their effects on the growth of the given cell lines. As presented in Figure 1, WY14643, a PPARα ligand, even at a concentration of 100 μM had minimal effects on decreasing the survival of four lung cancer cell lines tested, whereas all PPARγ ligands at the tested concentrations ranges effectively decreased cell survival at least in one of the tested cell lines albeit with various degrees. Among these ligands, CDDO stood out to be the most potent with IC_{50}s of 0.5–2 μM. Pioglitizone and roglitizone showed the weakest activity in decreasing the survival of the lung cancer cell lines with IC_{50}s' ranging from 40 μM to > 100 μM. Cigolitazone, troglitazone and GW1929 were in between with IC50s ranging from 15 μM to 100 μM. Therefore, we chose to use cigolitazone, troglitazone and GW1929 in our following experiments.

PPARγ ligands cooperate with TRAIL to induce apoptosis in human lung cancer cells. To determine whether the combination of a PPARγ ligand with TRAIL exhibits enhanced effects on induction of apoptosis in human lung cancer cells as observed in other types of cancer cell lines, we first examined the effects of PPARγ ligands on the survival of human lung cancer cells in the presence of TRAIL. As presented in Figure 2A, the addition of low doses of TRAIL, which itself minimally decreased cell survival (no more that 20%), greatly enhanced the effects of either of the tested PPARγ ligands (i.e., troglitazone, cigolitizone and GW1929) in the lung cancer cell lines tested. For example, troglitazone alone at 50 μM and TRAIL alone at 20 ng/ml decreased the survival of A549 cells by approximately 20%, whereas their combination decreased cell survival by >75%. Thus, it appears that the combination of a PPARγ ligand with TRAIL exhibits enhanced effects on decreasing the survival of lung cancer cells.

Following the cell survival study, we analyzed apoptosis in cells exposed to the combination of a PPARγ ligand and TRAIL. The single agent of the given PPARγ ligands or TRAIL at the concentrations tested caused minimal apoptosis (<15%). However, the combination of TRAIL with either PPARγ ligand tested induced apoptosis in >40% of cells (Fig. 1B). In agreement, we detected minimal cleaved forms of caspase-8, caspase-9, caspase-3 and PARP from cells treated with TRAIL or the PPARγ ligands tested alone under the tested conditions by Western blot analysis. However, we easily detected the cleaved forms from cells exposed to the respective combinations of TRAIL with PPARγ ligands (Fig. 2C). Collectively, these results clearly show that PPARγ ligands cooperate with TRAIL to enhance induction of apoptosis in human lung cancer cells.

PPARγ ligands induces DR5 expression in addition to downregulation of c-FLIP expression. It has been documented that some PPARγ ligands decrease c-FLIP expression, which contributes to enhancement of TRAIL-induced apoptosis by PPARγ ligands in certain types of cancer cells.[15] Thus, we examined effects of PPARγ ligands on c-FLIP expression in human lung cancer cells. The three PPARγ ligands trgolitizone, cigolitazone and GW1929 decreased the levels of both $FLIP_L$ and $FLIP_S$ in a dose-dependent manner in A549 cells (Fig. 3A). The downregulation of c-FLIP occurred after 6 h treatment with the given ligands (Fig. 3B), indicating that

c-FLIP downregulation is an early event induced by PPARγ ligands. Downregulation of c-FLIP expression by PPARγ ligands occurred not only in A549 cells as described, but also in other lung cancer cells (e.g., H157, H460, and H1792) as presented in (Fig. 3C). Therefore, it appears that downregulation of c-FLIP by PPARγ ligands commonly occurs in human lung cancer cells.

DR5 is also a key protein involved in TRAIL-mediated apoptosis and is susceptible to modulation by certain small molecules. Therefore, we were interested in determining whether PPARγ ligands modulate DR5 expression. To this end, we treated A549 cells with different concentrations of trglitizone, cigolitazone or GW1929 for 12 h and then detected DR5 expression in these cells by Western blot analysis. Similar to modulation of c-FLIP expression, all three ligands increased DR5 expression in a concentration-dependent maner. These ligands even at 25 μM were able to upregulate DR5 expression (Fig. 3A). Similar to c-FLIP downregulation, DR5 expression was increased after 6 h exposure to the ligands (Fig. 3B), indicating that DR5 upregulation is also an early event induced by PPARγ ligands. These ligands increased DR5 expression in other lung cancer cell lines as well (Fig. 3C), indicating that induction of DR5 by PPARγ ligands is also a common event in lung cancer cells. Because DR5 is a cell surface protein, we further analyzed DR5 distribution on the cell surface in cells treated with different PPARγ ligands. As presented in Figure 3D, these ligands increased the mean fluorescent intensity (MFI) of DR5 staining in both H1792 and A549 cells, indicating that PPARγ ligands increase cell surface DR5 levels in addition to upregulating the total levels of DR5.

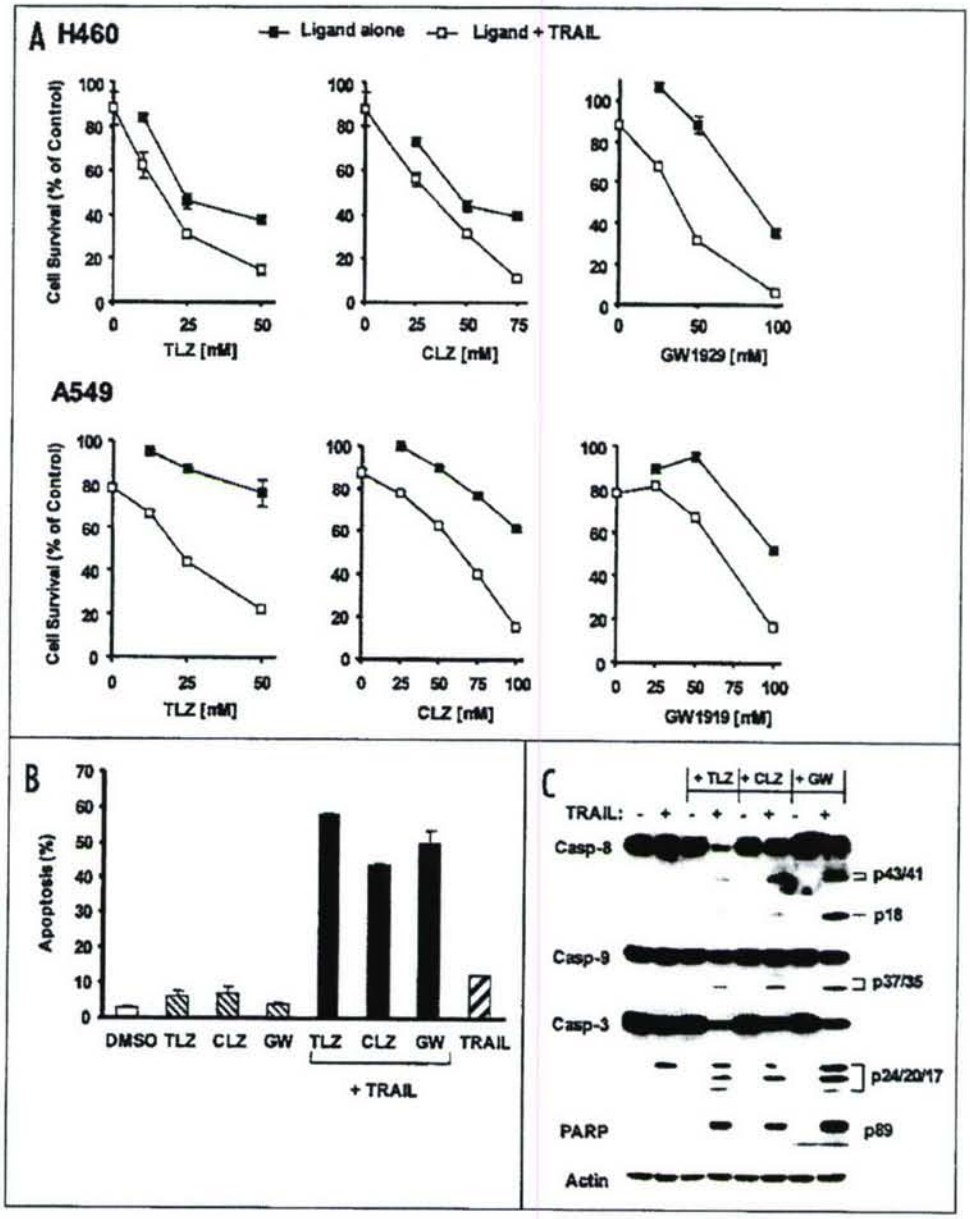

Figure 2. Effects of PPARγ ligands in combination with TRAIL on cell survival (B) and apoptosis (B and C) in human lung cancer cells. (A) H460 and A549 cell lines were seeded in 96-well plates. On the second day, the cells were treated with the indicated concentrations of troglitazone (TLZ), ciglitazone (CLZ), or GW1929 alone, 20 ng/ml TRAIL alone, and the combination of TRAIL with the respective PPARγ ligand. After 24 h, the cells were fixed and subjected to estimation of cell number using the SRB assay. Each data value is a mean ± SD of four replicates. (B and C) A549 cells were treated with 50 μM of the indicated PPARγ ligands alone, 20 ng/ml TRAIL alone and their respective combinations. After 24 h (B) or 12 h (C), the cells were harvested for detection of apoptosis by analyzing sub-G_1 population using flow cytometry (B) or for detection of activation of the indicated caspases using Western blot analysis (C). Each column in (B) is the mean ± SD of duplicate determinations. Casp, caspase.

Small interfering RNA (SiRNA)-mediated silencing of DR5 expression confers resistance to induction of apoptosis by the combination of a PPARγ ligand and TRAIL. To determine whether DR5 upregulation contributes to cooperative induction of apoptosis by the combination of a PPARγ ligand and TRAIL, we used DR5 siRNA to silence DR5 expression and then examined its impact on the apoptosis-inducing effect of the combination. The result in Figure 4A demonstrates the successful silencing the expression of DR5. The combination of troglitazone and TRAIL was much more potent than each single agent in decreasing the levels of uncleaved forms of caspase-8 and caspase-3 or increasing the levels of cleaved form of caspase-9 and PARP (Fig. 4B) and in increasing DNA fragment levels (Fig. 4C) in control siRNA-transfected A549 cells. These effects were all diminished in the cells transfected with DR5 siRNA (Fig. 4B and C). Thus, these results demonstrate that DR5 upregulation contributes to enhanced induction of apoptosis by the combination of a PPARγ) ligand and TRAIL.

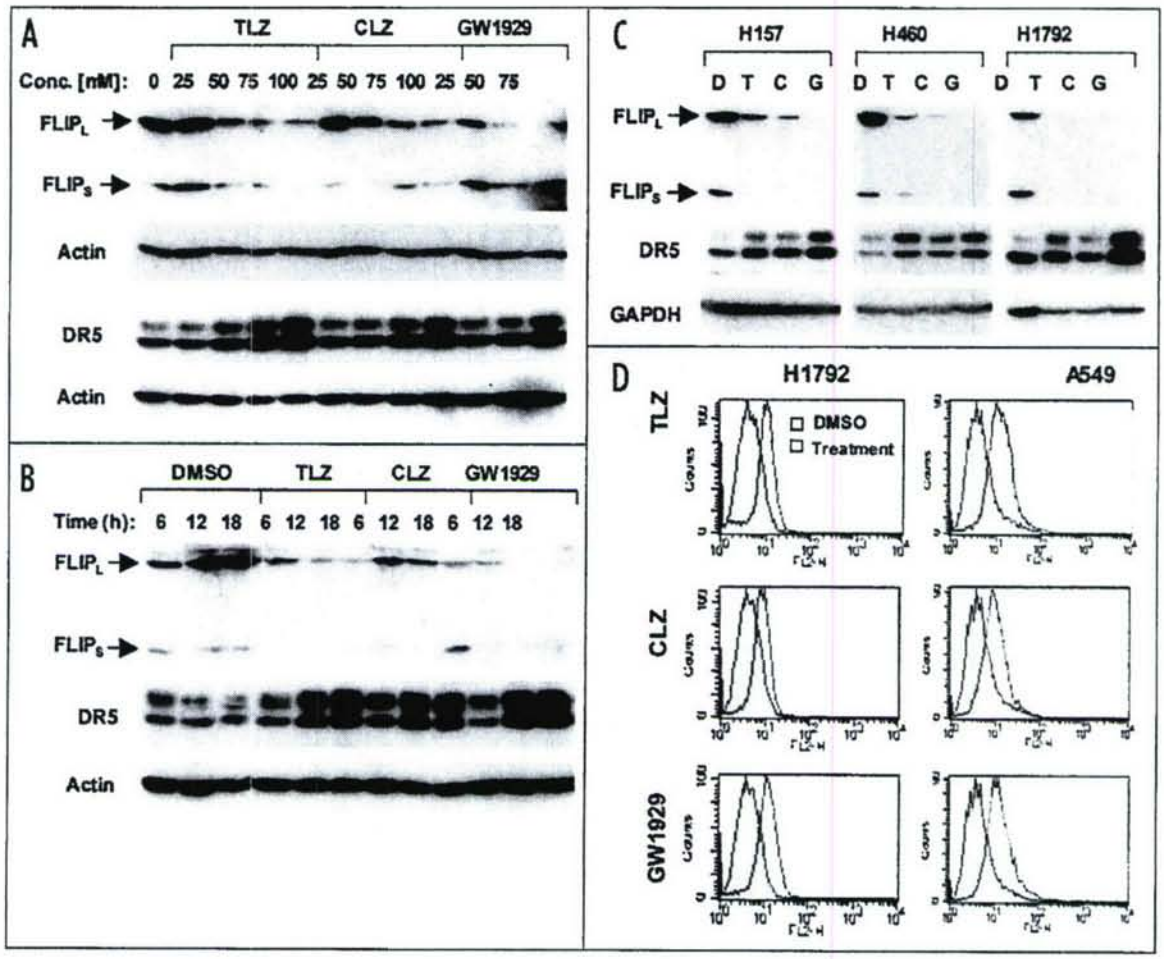

Figure 3. PPARγ ligands increase DR5 expression in addition to downregulation of c-FLIP expression (A–C) and increase cell surface DR5 (D) in human lung cancer cells. (A and B) A549 cells were treated with the indicated concentrations of troglitazone (TLZ), ciglitazone (CLZ) or GW1929 for 12 h (A) or 50 μM of the agents for the indicated times (B). Whole-cell protein lysates were then prepared from aforementioned treatments for detection of DR5, c-FLIP and actin using Western blot analysis. (C) The indicated lung cancer cell lines were treated with DMSO (D), 50 μM of troglitazone (T), ciglitazone (C) or GW1929 (G) for 12 h and then subjected to preparation of whole-cell protein lysates and subsequent Western blot analysis for the indicated proteins. (D) Both H1792 and A549 cell lines were exposed to 50 μM of the indicated PPARγ ligands for 12 h. The cells were then harvested, stained with PE-conjugated DR5 antibody, and analyzed by flow cytometry.

Enforced c-FLIP overexpression protects cells from induction of apoptosis by the combination of a PPARγ ligand and TRAIL. To determine the involvement of c-FLIP downregulation in enhancement of TRAIL-induced apoptosis by PPARγ ligands, we established A549 stable cell lines that overexpress Lac Z (serves as a control), $FLIP_L$ or $FLIP_s$ as presented in Figure 5A. In agreement with aforementioned results, the combination of troglitazone and TRAIL exhibited enhanced induction of apoptosis compared to each single agent in Lac Z-2 and Lac Z-9 cell lines. This effect was inhibited in all cell lines expressing either $FLIP_L$ or $FLIP_S$, particularly in cell lines expressing $FLIP_L$ (Fig. 5A). Consistently, apoptosis induced by TRAIL alone was also inhibited in c-FLIP-overexpressing cell lines (Fig. 5A). Results in (Fig. 5B) shows representative expression levels of $FLIP_L$ (i.e., $FLIP_L$-2) and $FLIP_S$ ($FLIP_S$-8) in the given cell lines. In agreement with induction of apoptosis, the combination of troglitazone and TRAIL strongly induced cleavage of both caspase-8 and PARP in Lac Z-2 cells, but only minimally in $FLIP_S$-8 cells and in $FLIP_L$-2 cells (Fig. 5B). Collectively, these results clearly show that overexpression of c-FLIP protects cells from induction of apoptosis by the combination of TRAIL with a PPARγ ligand. In another words, downregulation of c-FLIP contributes to enhanced induction of apoptosis by the combination of a PPARγ ligand and TRAIL.

PPARγ ligands modulate the expression of DR5 and c-FLIP independently of PPARγ. To determine whether PPARγ plays a role in mediating the modulation of DR5 or c-FLIP expression by PPARγ ligands, we compared the effects of troglitazone on the expression of DR5 and c-FLIP in the absence and presence of the PPARγ antagonist GW9662. As presented in Figure 6A, the presence of GW9662 at 50 μM and the maximal tolerated dose of 75 μM failed to impair the ability of troglitazone to induce DR5 or downregulate c-FLIP expression in both A549 and H1792 cells. Moreover, we silenced the expression of PPARγ and then examined its impact on PPARγ ligand-induced DR5 upregulation and c-FLIP downregulation. As shown in Figure 6B, transfection of PPARγ) siRNA into A549 cells substantially decreased the levels of PPARγ. However, both troglitazone and GW1929 induced DR5 expression and decreased c-FLIP levels in both control siRNA- and PPARγ siRNA transfected cells with comparable degrees, indicating that silencing of PPARγ expression does not affect the effects of PPARγ ligands on modulation of DR5 and c-FLIP. Token together, we conclude that PPARγ

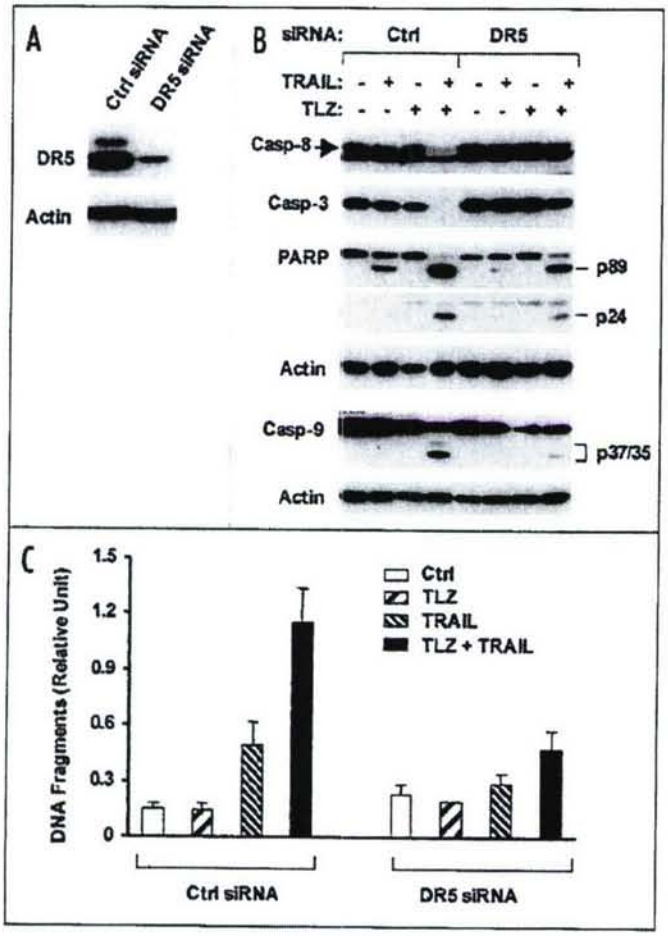

Figure 4. Silencing of DR5 expression by DR5 siRNA (A) attenuates caspase activation (B) and apoptosis (C) induced by the combination of troglitazone (TLZ) and TRAIL. A549 cells were seeded in a 24-well cell culture plate and on the second day transfected with control (Ctrl) or DR5 siRNA. Forty hours later, the cells were treated with 50 μM TLZ, 20 ng/ml TRAIL and their combination. After 12 h (A and B) or 24 h (C), the cells were harvested for preparation of whole-cell protein lysates and subsequent Western blot analysis (A and B) or for detection of DNA fragmentation using an ELISA kit. Each column (C) represents the mean ± SD of triplicate determinations.

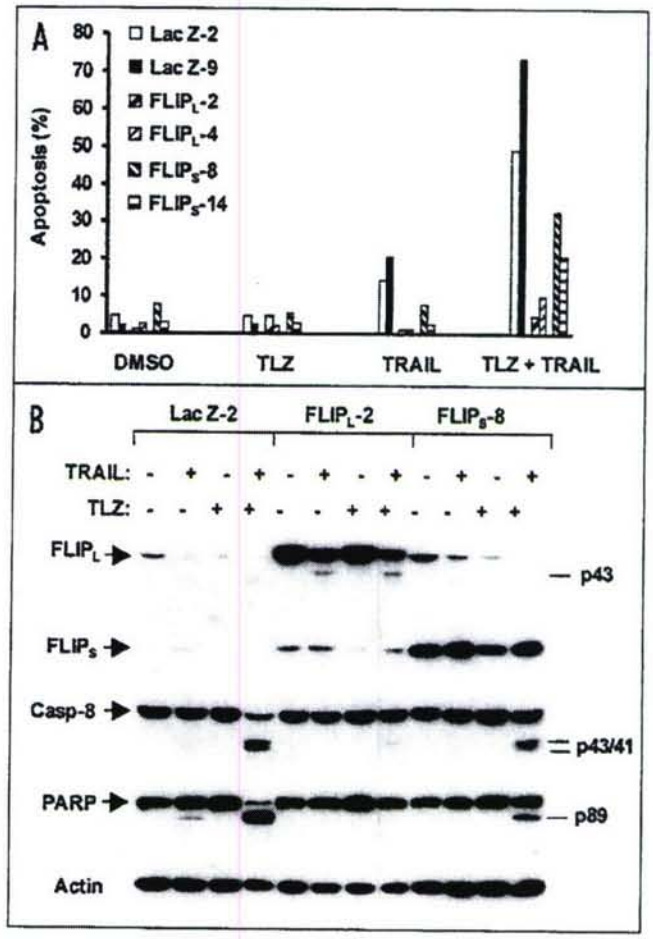

Figure 5. Enforced c-FLIP expression protects cells from induction of apoptosis (A) and caspase activation (B) by the combination of troglitazone (TLZ) and TRAIL. The indicated A549 cell lines expressing lac Z (control), FLIP$_L$ or FLIP$_S$ were treated with DMSO, 50 μM TLZ alone, 10 ng/ml TRAIL alone and the combination of TLZ and TRAIL, respectively. After 24 h (A) or 12 h (B), the cells were harvested and subjected to detection of apoptotic cells by analyzing sub-G$_1$ population using flow cytometry (A) or detection of caspase activation using Western blot analysis (B).

ligands modulate the expression of DR5 and c-FLIP independently of PPARγ.

DISCUSSION

Enhancement of TRAIL-induced apoptosis by PPARγ ligands has been documented in certain types of cancer cell lines including glioma, neuroblastoma, breast, ovarian, prostate and colon cancer cells in vitro[15,16,23,24] and in breast cancer in vivo.[24] Our current study confirms and extends this finding in human lung cancer cells. PPARγ ligands alone in general have weak apoptosis-inducing activity as demonstrated in our study (Fig. 1). However, the presence of a low dose of TRAIL can result in enhanced or synergistic induction of apoptosis in various types of cancer cells by previous studies[15,16,23,24] and our current finding. Given that some PPARγ ligands are marketed drugs for treatment of type II diabetes, these findings warrant the clinical testing of the combination of a PPARγ ligand with TRAIL as an effective cancer therapeutic regimen.

Downregulation of c-FLIP, survivin and cyclin D3 or induction of p21$^{waf1/cip1}$ has been documented to account for the mechanisms by which PPARγ ligands enhance TRAIL-induced apoptosis.[15,16,23,24] Among these mechanisms, downregulation of c-FLIP by PPARγ ligands and its role in sensitizing cancer cells to TRAIL-induced apoptosis were extensively studied.[15,16] In agreement with these findings, we also found that PPARγ ligands such as troglitazone, cigolitazone and GW1929 decreased the levels of both FLIP$_L$ and FLIP$_S$ in human lung cancer cells (Fig. 3). Moreover, we demonstrate that downregulation of c-FLIP contributes to enhancement of TRAIL-induced apoptosis by PPARγ ligands because enforced expression of exogenous c-FLIP (either FLIP$_L$ or FLIP$_S$) inhibited induction of apoptosis by the combination of TRAIL with troglitazone (Fig. 5). Taken together, it appears that c-FLIP downregulation is an important mechanism accounting for PPARγ ligand-mediated enhancement of TRAIL-induced apoptosis in human cancer cells.

By far, the few reports on the modulation of DR5 expression by PPARγ ligands have conflicting results.[15-17] Moreover, the involvement of DR5 modulation in PPARγ ligand-mediated enhancement of TRAIL-induced apoptosis in cancer cells has not been addressed.

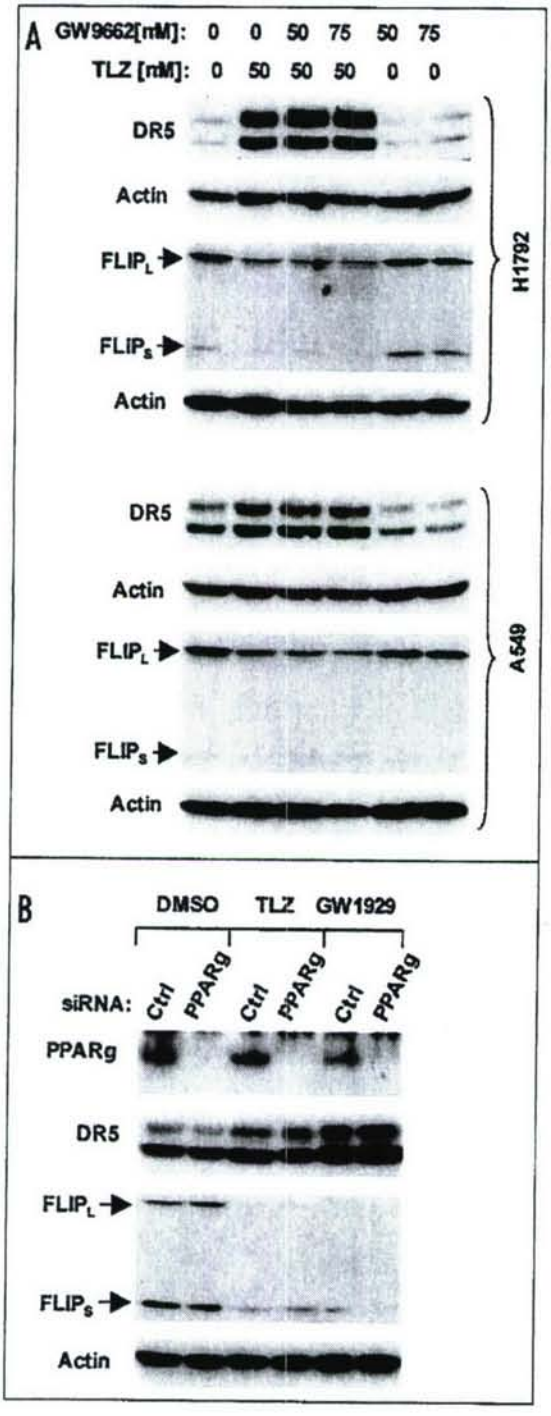

Figure 6. Effects of the PPARγ antagonist GW9662 (A) and the silencing of PPARγ expression (B) on PPARγ ligand-induced modulation of DR5 and c-FLIP expression. A, The indicated cell lines were pretreated with the given doses of GW9662 and then cotreated with 50 μM troglitazone (TLZ). After 12 h, the cells were subjected to preparation of whole-cell protein lysates and subsequent Western blot analysis. B, A549 cells were transfected with control (Ctrl) or PPARγ siRNA. After 48 h, the cells were treated with DMSO control, 50 μM TLZ or GW1929. Twelve hours later, the cells were harvested for preparation of whole-cell protein lysates and subsequent Western blot analysis.

In this study, we clearly show that several PPARγ ligands including troglitazone, cigolitazone and GW1929 induced DR5 expression while downregulating c-FLIP levels in multiple human lung cancer cell lines (Fig. 3), indicating that both DR5 upregulation and c-FLIP reduction are concurrent events in cells exposed to PPARγ ligands. By siRNA-mediated silencing of DR5 expression, we found that the enhanced induction of apoptosis including caspase activation and DNA fragmentation by the combination of troglitazone and TRAIL was substantially attenuated. Thus, we conclude that DR5 upregulation also contributes to cooperative induction of apoptosis by the combination of a PPARγ ligand and TRAIL. This should be the first demonstration for the involvement of DR5 upregulation in sensitization of cancer cells to TRAIL-induced apoptosis by PPARγ ligands.

The downregulation of c-FLIP by PPARγ ligands was documented to be independent of PPARγ,[15] as was the induction of DR5 by 15d-PGJ$_2$.[17] In our study, the presence of a PPARγ antagonist or siRNA-mediated silencing of PPARγ expression failed to inhibit the modulation of either DR5 or c-FLIP expression by PPARγ ligands (Fig. 6). Thus, we conclude that PPARγ ligands induce DR5 and downregulate c-FLIP expression independently of PPARγ in human lung cancer cells.

In summary, we demonstrate that PPARγ ligands enhance TRAIL-induced apoptosis in human lung cancer cells. In addition to downregulation of c-FLIP, PPARγ ligands also upregulate DR5 expression, both of which contribute to PPARγ ligand-mediated enhancement of TRAIL-induced apoptosis. Thus, our findings extend our understanding on the mechanisms by which PPARγ ligands sensitize cancer cells to TRAIL-induced apoptosis.

References

1. Almasan A, Ashkenazi A. Apo2L/TRAIL: Apoptosis signaling, biology, and potential for cancer therapy. Cytokine Growth Factor Rev 2003; 14:337-48.
2. Kelley SK, Ashkenazi A. Targeting death receptors in cancer with Apo2L/TRAIL. Curr Opin Pharmacol 2004; 4:333-9.
3. Ashkenazi A, Dixit VM. Death receptors: Signaling and modulation. Science 1998; 281:1305-8.
4. Wajant H, Gerspach J, Pfizenmaier K. Tumor therapeutics by design: Targeting and activation of death receptors. Cytokine Growth Factor Rev 2005; 16:55-76.
5. Wajant H. Targeting the FLICE Inhibitory Protein (FLIP) in cancer therapy. Mol Interv 2003; 3:124-7.
6. Kataoka T. The caspase-8 modulator c-FLIP. Crit Rev Immunol 2005; 25:31-58.
7. Irmler M, Thome M, Hahne M, Schneider P, Hofmann K, Steiner V, Bodmer JL, Schroter M, Burns K, Mattmann C, Rimoldi D, French LE, Tschopp J. Inhibition of death receptor signals by cellular FLIP. Nature 1997; 388:190-5.
8. Sun SY. Chemopreventive agent-induced modulation of death receptors. Apoptosis 2005; 10:1203-10.
9. Sporn MB, Suh N, Mangelsdorf DJ. Prospects for prevention and treatment of cancer with selective PPARgamma modulators (SPARMs). Trends Mol Med 2001; 7:395-400.
10. Rumi MA, Ishihara S, Kazumori H, Kadowaki Y, Kinoshita Y. Can PPAR gamma ligands be used in cancer therapy? Curr Med Chem Anticancer Agents 2004; 4:465-77.
11. Koeffler HP. Peroxisome proliferator-activated receptor gamma and cancers. Clin Cancer Res 2003; 9:1-9.
12. Li MY, Lee TW, Yim AP, Chen GG. Function of PPARgamma and its ligands in lung cancer. Crit Rev Clin Lab Sci 2006; 43:183-202.
13. Chang TH, Szabo E. Enhanced growth inhibition by combination differentiation therapy with ligands of peroxisome proliferator-activated receptor-gamma and inhibitors of histone deacetylase in adenocarcinoma of the lung. Clin Cancer Res 2002; 8:1206-12.
14. Avis I, Martinez A, Tauler J, Zudaire E, Mayburd A, Abu-Ghazaleh R, Ondrey F, Mulshine JL. Inhibitors of the arachidonic acid pathway and peroxisome proliferator-activated receptor ligands have superadditive effects on lung cancer growth inhibition. Cancer Res 2005; 65:4181-90.
15. Kim Y, Suh N, Sporn M, Reed JC. An inducible pathway for degradation of FLIP protein sensitizes tumor cells to TRAIL-induced apoptosis. J Biol Chem 2002; 277:22320-9.
16. Schultze K, Bock B, Eckert A, Oevermann L, Ramacher D, Wiestler O, Roth W. Troglitazone sensitizes tumor cells to TRAIL-induced apoptosis via down-regulation of FLIP and Survivin. Apoptosis 2006.
17. Nakata S, Yoshida T, Shiraishi T, Horinaka M, Kouhara J, Wakada M, Sakai T. 15-Deoxy-Delta12,14-prostaglandin J(2) induces death receptor 5 expression through mRNA stabilization independently of PPARgamma and potentiates TRAIL-induced apoptosis. Mol Cancer Ther 2006; 5:1827-35.

18. Sun SY, Yue P, Dawson MI, Shroot B, Michel S, Lamph WW, Heyman RA, Teng M, Chandraratna RA, Shudo K, Hong WK, Lotan R. Differential effects of synthetic nuclear retinoid receptor-selective retinoids on the growth of human nonsmall cell lung carcinoma cells. Cancer Res 1997; 57:4931-9.
19. Sun SY, Yue P, Wu GS, El-Deiry WS, Shroot B, Hong WK, Lotan R. Mechanisms of apoptosis induced by the synthetic retinoid CD437 in human nonsmall cell lung carcinoma cells. Oncogene 1999; 18:2357-65.
20. Liu X, Yue P, Zhou Z, Khuri FR, Sun SY. Death receptor regulation and celecoxib-induced apoptosis in human lung cancer cells. J Natl Cancer Inst 2004; 96:1769-80.
21. Sun SY, Yue P, Hong WK, Lotan R. Induction of Fas expression and augmentation of Fas/Fas ligand-mediated apoptosis by the synthetic retinoid CD437 in human lung cancer cells. Cancer Res 2000; 60:6537-43.
22. Sun SY, Yue P, Shroot B, Hong WK, Lotan R. Induction of apoptosis in human nonsmall cell lung carcinoma cells by the novel synthetic retinoid CD437. J Cell Physiol 1997; 173:279-84.
23. Goke R, Goke A, Goke B, El-Deiry WS, Chen Y. Pioglitazone inhibits growth of carcinoid cells and promotes TRAIL-induced apoptosis by induction of p21waf1/cip1. Digestion 2001; 64:75-80.
24. Lu M, Kwan T, Yu C, Chen F, Freedman B, Schafer JM, Lee EJ, Jameson JL, Jordan VC, Cryns VL. Peroxisome proliferator-activated receptor gamma agonists promote TRAIL-induced apoptosis by reducing survivin levels via cyclin D3 repression and cell cycle arrest. J Biol Chem 2005; 280:6742-51.

Multiple Oncogenic Changes (*K-RAS*^{V12}, p53 Knockdown, *Mutant EGFRs, p16* Bypass, Telomerase) Are Not Sufficient to Confer a Full Malignant Phenotype on Human Bronchial Epithelial Cells

Mitsuo Sato,[1] Melville B. Vaughan,[4] Luc Girard,[1] Michael Peyton,[1] Woochang Lee,[1] David S. Shames,[1] Ruben D. Ramirez,[1,2,6] Noriaki Sunaga,[1] Adi F. Gazdar,[1,3] Jerry W. Shay,[4] and John D. Minna[1,2,5]

[1]Hamon Center for Therapeutic Oncology Research and Departments of [2]Internal Medicine, [3]Pathology, [4]Cell Biology, and [5]Pharmacology, The University of Texas Southwestern Medical Center; and [6]Dallas Veterans Administration Medical Center, Dallas, Texas

Abstract

We evaluated the contribution of three genetic alterations (p53 knockdown, *K-RAS*^{V12}, and *mutant EGFR*) to lung tumorigenesis using human bronchial epithelial cells (HBEC) immortalized with telomerase and Cdk4-mediated p16 bypass. RNA interference p53 knockdown or oncogenic *K-RAS*^{V12} resulted in enhanced anchorage-independent growth and increased saturation density of HBECs. The combination of p53 knockdown and K-RAS^{V12} further enhanced the tumorigenic phenotype with increased growth in soft agar and an invasive phenotype in three-dimensional organotypic cultures but failed to cause HBECs to form tumors in nude mice. Growth of HBECs was highly dependent on epidermal growth factor (EGF) and completely inhibited by EGF receptor (EGFR) tyrosine kinase inhibitors, which induced G_1 arrest. Introduction of EGFR mutations E746-A750 del and L858R progressed HBECs toward malignancy as measured by soft agar growth, including EGF-independent growth, but failed to induce tumor formation. Mutant EGFRs were associated with higher levels of phospho-Akt, phospho–signal transducers and activators of transcription 3 [but not phospho-extracellular signal-regulated kinase (ERK) 1/2], and increased expression of *DUSP6/MKP-3* phosphatase (an inhibitor of phospho-ERK1/2). These results indicate that (*a*) the HBEC model system is a powerful new approach to assess the contribution of individual and combinations of genetic alterations to lung cancer pathogenesis; (*b*) a combination of four genetic alterations, including human telomerase reverse transcriptase overexpression, bypass of p16/RB and p53 pathways, and mutant K-RAS^{V12} or mutant EGFR, is still not sufficient for HBECs to completely transform to cancer; and (*c*) EGFR tyrosine kinase inhibitors inhibit the growth of preneoplastic HBEC cells, suggesting their potential for chemoprevention. (Cancer Res 2006; 66(4): 2116-28)

Introduction

Human lung cancer develops as a multistep process, usually occurring because of years of smoking-related tobacco exposure that results in specific proto-oncogene and tumor suppressor gene alterations in lung epithelial cells (1). In fact, the majority of lung cancers have many such changes (1). Identifying the minimal and most crucial set of changes required for lung tumorigenesis and the effect each of these alterations has on the carcinogenic process is vital to develop the best targets for early detection and therapeutic intervention. To address this issue, an *in vitro* model system using human bronchial epithelial cells (HBEC) was recently developed to assess the contribution of specific genetic alterations to lung cancer progression (2, 3). We accomplished this by overexpressing Cdk4 to abrogate the p16/Rb cell cycle checkpoint pathway and ectopic expression of human telomerase reverse transcriptase (hTERT) to bypass replicative senescence, allowing us to develop a series of immortalized HBEC lines without using viral oncoproteins. These HBECs have epithelial morphology, express epithelial markers, are able to differentiate into mature airway cells in organotypic cultures, have minimal genetic changes, and do not exhibit a transformed phenotype (2, 3). We have HBEC lines that are derived from patients with a variety of smoking histories, with and without lung cancer, which also allows us to explore interindividual variation in the tumor formation process.

Two of the genetic alterations that occur almost universally in human lung cancer, inactivation of the p16/pRb pathway and expression of hTERT, were used for establishment of immortalized HBECs and so are already present. The pRb pathway ($p16^{INK4a}$-cyclinD1-Cdk4-pRB pathway) is a key cell cycle regulator at the G_1-S phase transition. Absence of expression or structural abnormality of Rb protein is seen in >90% of small-cell lung cancers (SCLC) and loss of p16 protein expression by several mechanisms, including methylation or homozygous deletion of *p16*^{INK4a}, is seen in >70% of non-SCLC (NSCLC), both of which result in the inactivation of this pathway (1, 4, 5). Expression of high levels of telomerase is almost universal in lung cancer (1). hTERT is the key determinant of the enzymatic activity of human telomerase and its transcriptional control is a major contributor to the regulation of telomerase activity in many types of human cells (6–10). Because of the central role of the pRb pathway and telomerase expression, we initially evaluated the contribution of ectopically expressing Cdk4 and hTERT on lung cancer development. However, we found that such cells, although immortal and clonable, did not show anchorage-independent growth or an ability to form tumors *in vivo* (2). Other investigators and our group had also immortalized HBECs but these were made using viral oncoproteins, such as human papillomavirus E6/E7 or SV40 large T antigen with or without hTERT (2, 11, 12). These oncoproteins are known to cause

Requests for reprints: John D. Minna, Hamon Center for Therapeutic Oncology Research NB8.206, The University of Texas Southwestern Medical Center at Dallas, 6000 Harry Hines Boulevard, Dallas, TX 75390-8593. Phone: 214-648-4900; Fax: 214-648-4940; E-mail: John.Minna@UTsouthwestern.edu.

©2006 American Association for Cancer Research.

doi:10.1158/0008-5472.CAN-05-2521

malignant transformation through their ability to inactivate Rb and/or p53, as well as provide multiple other functions, which are not characterized. These "other functions" make it difficult to estimate the importance of added genetic or epigenetic changes in HBECs immortalized by viral oncoproteins.

Thus, we designed the current study to determine if the HBECs were genetically tractable and to analyze the effect of additional genetic alterations frequently observed in lung cancer on tumorigenic transformation of HBECs. First, we introduced two well-known genetic alterations seen in lung cancer, one of which is the loss of p53 function, which is observed in 90% of SCLCs and 50% of NSCLCs (1). The other is oncogenic K-RAS, which is frequently seen in NSCLCs (~30%), especially in adenocarcinomas but probably never in SCLCs (1, 13, 14). Furthermore, we introduced a mutant epidermal growth factor (EGF) receptor (EGFR) that has recently been reported in NSCLCs and shown to be correlated with tumor sensitivity to the EGFR tyrosine kinase inhibitors (15, 16). We report here that HBECs immortalized by overexpression of Cdk4 and hTERT and subsequently manipulated to have oncogenic K-RAS, knockdown of p53, or mutant EGFR have acquired part, but not all, of the malignant phenotype by the combination of these genetic alterations. These partially progressed lung epithelial cells show that more changes are needed for the full malignant phenotype. In addition, we have found that these preneoplastic cells are exquisitely sensitive to EGFR inhibition.

Materials and Methods

Cells and culture conditions. The HBEC3 (HBEC3-KT) immortalized normal HBEC line was established by introducing mouse Cdk4 and hTERT into normal HBECs obtained from a 65-year-old woman without cancer (2). NSCLC, NCI-H441, NCI-H358, NCI-H1299, and NCI-H2122 cell lines were obtained from Hamon Center Collection (University of Texas Southwestern Medical Center). HBEC3 was cultured with K-SFM (Life Technologies, Gaithersburg, MD) medium containing 50 μg/mL bovine pituitary extract (Life Technologies) with or without 5 ng/mL EGF (Life Technologies). These cells are resistant to G418 due to the neomycin-resistant gene introduced with the Cdk4 expression vector and to puromycin due to the puromycin-resistant gene introduced with the hTERT expression vector.

Viral vector construction and viral transduction. We used the pSUPER vector (OligoEngine, Seattle, WA) of Brummelkamp et al. (17, 18) as the basis for generating small interfering RNA for stable p53 knockdown. To generate pSUPER.retro-zeocin (pSRZ), *Sac*II and *Eco*RI sites were introduced into zeocin-resistant gene fragment amplified from pVgRXR (a gift from Dr. Preet Chaudhary) and the fragment was cloned into pSUPER.retro using *Sac*II and *Eco*RI sites, resulting in the replacement of the puromycin-resistant gene with a zeocin-resistant gene. To generate pSRZ-p53 for p53 knockdown, *Eco*RI- and *Hin*dIII-digested inserts from pSUPER-p53 (OligoEngine; ref. 18) was cloned into the same sites of pSRZ. pBabe-hyg and an oncogenic K-RAS^{V12}, pBabe-hyg-KRAS2-V12, vectors were provided by Dr. Michael White (The University of Texas Southwestern Medical Center, Dallas, TX). To produce viral-containing medium, 293T cells were transiently transfected with viral vector together with pVpack-VSVG and pVpack-GP vectors (Stratagene, La Jolla, CA). Forty-eight hours after the transfection, supernatant of the 293T cells was harvested and passed through a 0.45 μm filter and the viral supernatant was frozen at −80°C. The supernatant was used for infection after adding 4 μg/mL polybrene (Sigma, St. Louis, MO). Forty-eight hours after the infection, drug selection for infected cells was started with 12.5 μg/mL zeocin (Invitrogen, Carlsbad, CA) or 18 μg/mL hygromycin (Clontech, Palo Alto, CA) and continued for 7 to 11 days. HBEC3 cells were infected with four different combinations of the two retroviral vectors: (*a*) pSRZ and pBabe-hyg (vector control); (*b*) pSRZ-p53 and pBabe-hyg; (*c*) pSRZ and pBabe-hyg-KRAS2-V12; and (*d*) pSRZ-p53 and pBabe-hyg-K-RAS2-V12.

To introduce wild and mutant EGFRs into HBEC3 cells, we used the pLenti6/directional TOPO cloning kit. Full-length fragment of wild-type EGFR was amplified from pcDNA3.1-EGFR-wt (a gift from Dr. Joachim Herz, University of Texas Southwestern Medical Center) and cloned into pLenti6/directional TOPO vector according to the instructions of the manufacturer (pLenti-wt-EGFR). The L858R mutation was introduced into pLenti-wt-EGFR by using site-directed mutagenesis kit (Stratagene). The full length of E746-A750 del mutation was amplified from cDNA from HCC827 NSCLC cell line (19) and cloned into pLenti6/directional TOPO vector. Correct sequences were confirmed by sequencing for all vectors. Viral transduction was done following the instructions of the manufacturer. Briefly, the 293FT cells were transiently transfected with viral vector together with viral power (Invitrogen). Forty-eight hours after the transfection, supernatant of the 293FT cells was harvested and passed through a 0.45 μm filter, and frozen at −80°C. The supernatant was used for infection after adding 4 μg/mL polybrene (Sigma). Forty-eight hours after the infection, drug selection for infected cells was started with 5 μg/mL blasticidin (Invitrogen) and continued for 7 days.

Western blot analysis. Preparation of total cell lysates and Western blotting were done as described previously (20). Primary antibodies used were mouse monoclonal anti-p53 (Santa Cruz, Santa Cruz, CA), mouse monoclonal anti-p21 (BD Transduction Laboratories, Lexington, KY), mouse monoclonal anti-K-RAS (Santa Cruz), mouse monoclonal anti-EGFR (BD Transduction Laboratories), rabbit polyclonal anti-phospho-EGFR-Tyr^{1068} (Y1068), rabbit polyclonal anti-phospho-EGFR-Tyr^{845} (Y845), rabbit polyclonal anti-phospho-EGFR-Tyr^{992} (Y992), rabbit polyclonal anti-phospho-EGFR-Tyr^{1045} (Y1045; Cell Signaling, Beverly, MA), rabbit polyclonal anti-MEK1/2 (Cell Signaling), rabbit polyclonal anti-phospho-MEK1/2 (Cell Signaling), rabbit polyclonal anti–extracellular signal-regulated kinase (ERK) 1 (Cell Signaling), rabbit polyclonal anti-phospho-ERK1 (Cell Signaling), rabbit polyclonal anti-Akt (Cell Signaling), rabbit polyclonal anti-phospho-Akt (Thr^{308}), rabbit polyclonal anti-phospho-Akt (Ser^{473}), mouse monoclonal anti-phospho-signal transducers and activators of transcription (STAT) 3 (Tyr^{705}; Cell Signaling), poly(ADP-ribose) polymerase (PARP; Cell Signaling), and mouse monoclonal antiactin (Sigma) antibodies. Actin protein levels were used as a control for adequacy of equal protein loading. Antirabbit or antimouse antibody (1:2,000 dilution: Amersham, Piscataway, NJ) was used as the second antibody.

Immunofluorescence staining. Cells were washed with PHEM [60 mmol/L PIPES, 25 mmol/L HEPES, 10 mmol/L EGTA, and 1 mmol/L $MgCl_2$ (pH 7.4)] solution, and fixed in 3% paraformaldehyde for 10 minutes at 37°C in PHEM. After additional washes with PBS, the cells were permeabilized with 0.1% Triton in PBS for 10 minutes, blocked with 3% gelatin/3% bovine serum albumin (BSA)/0.2% Tween 20 for 1 hour at 37°C, and incubated with mouse polyclonal anti-p63 antibody (BD Transduction Laboratories) and rhodamine phalloidin (Molecular Probes, Eugene, OR) in gelatin/BSA blocking solution for 16 hours at 4°C. The cells were then incubated with the Alexa Fluor 568 anti-mouse IgG (H + L; Molecular Probes) secondary antibody for 1 hour at 37°C. Finally, cells were stained with 0.5 μg/mL Hoechst 33258 and examined in a fluorescence microscope.

RNA extraction and reverse transcription-PCR/RFLP analysis. We modified previously reported reverse transcription-PCR (RT-PCR)/RFLP method designed to distinguish mutated from wild-type *K-RAS* alleles (21). Total RNA was extracted using RNeasy mini kit (Qiagen, Valencia, CA). Four micrograms of total RNA were reverse transcribed with Superscript II First-Strand Synthesis using oligo-dTMP primer system (Invitrogen). PCR amplification was carried out with 3,704 K-RASTN sense (GACTGAATAT-AAACTTGTGGTAGTTGGACCT) and 3,672 K-RAS-RT-R antisense (5-TCC-TCTTGACCTGCTGTGTCG-3) primers, creating *Bst*NI restriction patterns that distinguished mutated from wild-type *K-RAS* alleles. PCR reactions were done in a 25 μL reaction mixture containing 1.5 mmol/L $MgCl_2$, 187.5 μmol/L of each deoxynucleotide triphosphate, 10 pmol of each primer, and 1.25 units of HotStar Taq DNA Polymerase (Qiagen). Cycling conditions were one incubation of 15 minutes at 95°C, followed by 35 cycles of a 20-second denaturation at 94°C, 60-second annealing at 58°C, and 90-second extension at 72°C, and a final elongation at 72°C for 7 minutes. PCR products were cut with *Bst*NI, electrophoresized on 1% agarose gel with

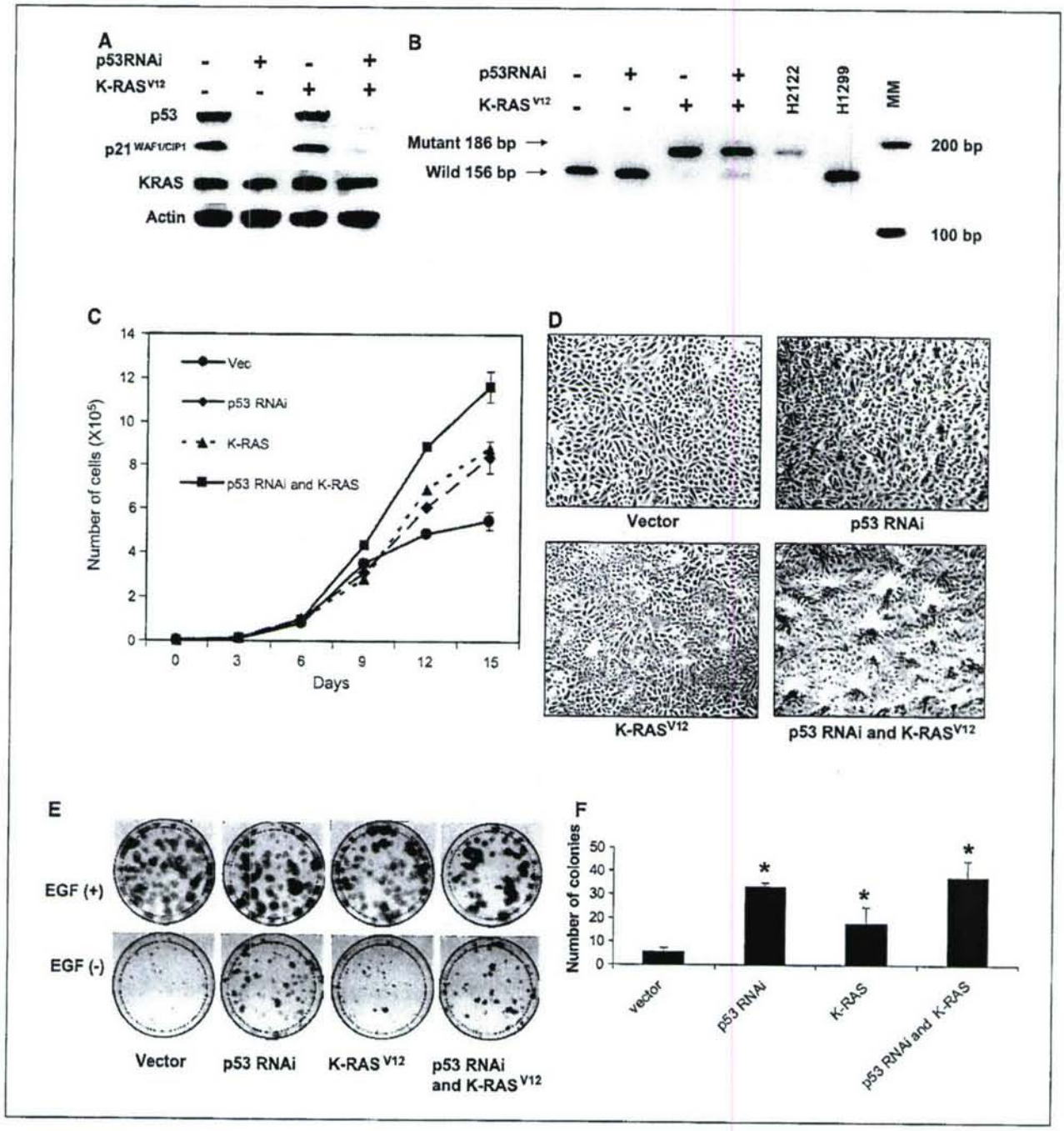

Figure 1. Characterization of p53 knocked down and K-RAS^{V12}–expressing HBEC3 cells. *A*, Western blots showing the suppression of p53, p21$^{WAF1/CIP1}$, and K-RAS in p53RNAi-, mutant K-RAS^{V12}–, and p53RNAi and mutant K-RAS^{V12}–expressing HBEC3 cells. p53 and p21$^{WAF1/CIP1}$ are clearly knocked down in p53RNAi-expressing cells, whereas the expression levels of K-RAS in K-RAS^{V12}–transfected and p53RNAi and K-RAS^{V12}–transfected HBEC3 cells approximate that of vector alone–transfected HBEC3 cells. *B*, RFLP analysis of K-RAS cDNA showing mutant K-RAS^{V12} transcripts are predominantly expressed in mutant K-RAS^{V12}–expressing and p53RNAi and mutant K-RAS^{V12}–expressing HBEC3 cells. H2122 and H1299 are used as positive controls for mutant K-RAS^{V12} and wild-type K-RAS, respectively. Brummelkamp et al. (18) reported a new vector system, named pSUPER, which generated small interfering RNAs in mammalian cells to functionally inactivate p53. Subsequently, they developed a retroviral version of pSUPER, named pSUPER.ret (pRS), to obtain stable knockdowns and showed stable and specific knockdown of oncogenic K-RAS^{V12} (17). To see the long-term effect of p53 inactivation, we used the pSUPER.ret system for p53 knockdown. Because a puromycin-resistant gene in pRS was already integrated in HBEC3 in the process of introducing Cdk4, we developed pRS-zeocin vector (pSRZ) by replacing the puromycin-resistant gene in pRS vector with a zeocin-resistant gene. Subsequently, the published p53 target small interfering RNA sequence was cloned into pSRZ (17, 18), yielding pSRZ-p53 vector. *C*, increased saturation density in p53 RNAi and mutant K-RAS^{V12}–expressing HBECs. HBEC3 cells (2,000) were cultured in triplicate 12-well plates and counted every 3 days. ●, vector–expressing HBEC3 cell; ◆, p53RNAi-expressing HBEC3 cells; ▲, mutant K-RAS^{V12}–expressing HBEC3 cells; ■, p53RNAi and mutant K-RAS^{V12}–expressing HBEC3 cells. *D*, cells were grown as described in (*C*) and pictures were taken on day 12. *E*, liquid colony formation assay for vector-, p53RNAi-, mutant K-RAS^{V12}–, and p53RNAi and mutant K-RAS^{V12}–expressing HBEC3 cells in the presence or absence of EGF (5 ng/mL). A total of 200 cells were plated per dish and cultured for 2 weeks before staining with methylene blue. *F*, quantitation of the number of colonies in the absence of EGF. *Columns*, mean of three independent experiments; *bars*, SD. *, $P < 0.01$, one-way ANOVA with Bonferroni's posttest.

Table 1. Tumorigenicity assay in nude mice for HBEC3 cells

Cell line	No. nude mice injected	No. cells per mouse	Observation period (d)	Percentage of tumors
NCI-H358	10	5×10^6	90	100
NCI-H441	5	5×10^6	61	100
NCI-H1299	40	5×10^6	17-38	100
HBEC3				
Nontreated	5	1×10^7	90	0
K-RAS^{V12}	5	5×10^6	90	0
p53RNAi	5	5×10^6	90	0
p53RNAi and K-RAS^{V12}	5	5×10^6	90	0
p53RNAi and K-RAS^{V12} With Matrigel	5	2.5×10^6	90	0
p53 RNAi and EGFR-L858R	5	2.5×10^6	90	0

ethidium bromide, and visualized by UV. NCI-H2122 cell line containing a endogenous mutant K-RAS at codon 12 was used as a control for *K-RAS^{V12}* allele, and NCI-H1299 cell was used as a control for the wild-type *K-RAS* allele.

***In vitro* and *in vivo* cell growth assays.** To determine growth curves, cells were cultured in triplicate wells in 12-well plates and counted every 3 days. Liquid colony formation assays were done as previously described (22). Briefly, 200 viable cells were plated in triplicate 100 mm plates and were cultured in K-SFM medium supplemented with 50 μg/mL bovine pituitary extract with or without 5 ng/mL EGF. To measure the effect of gefitinib or erlotinib, 1 μmol/L of each drug was added to the medium and the medium was replaced every 3 days. Surviving colonies were counted 14 days later after staining with methylene blue. For soft agar growth assays, 1,000 viable cells were suspended and plated in 0.37% Sea Kem agar (FMC, Philadelphia, PA) in K-SFM medium supplemented with 20% of fetal bovine serum and 50 μg/mL bovine pituitary extract with or without 5 ng/mL EGF in triplicate 12-well plates, and were layered over a 0.50% agar base in the same medium as the one used for suspending the cells. To measure

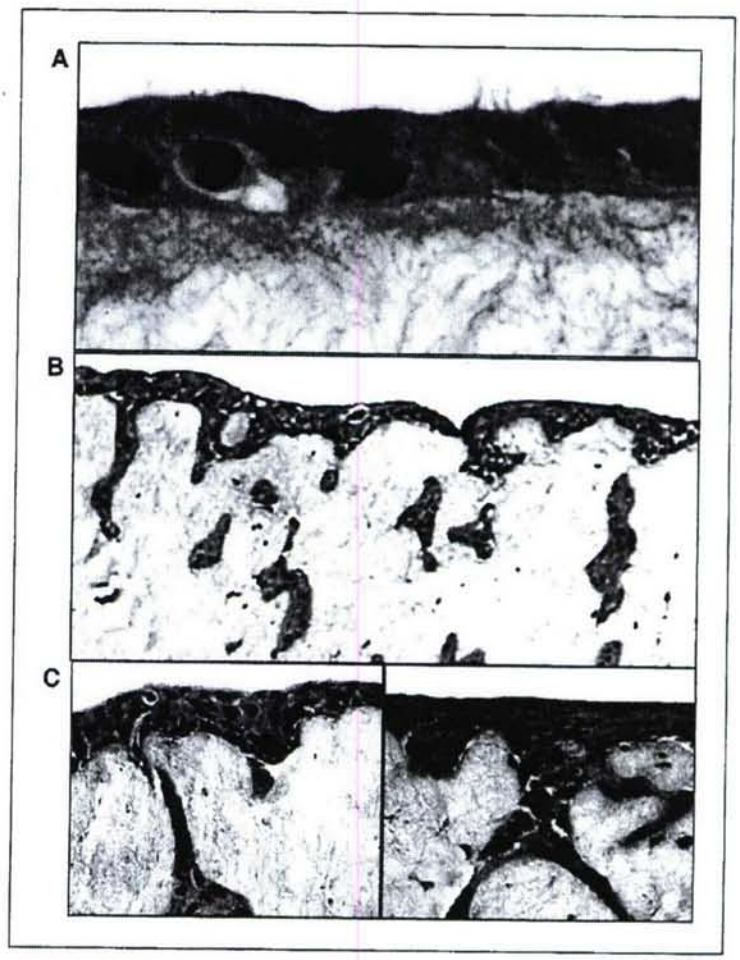

Figure 2. Effect of p53 knock down and mutant K-RAS^{V12} on three-dimensional organotypic culture of HBEC3 cells. *A*, stained paraffin cross-sections of organotypic cultures of HBEC3 cells showed that they formed a confluent layer of cells on the upper surface of the culture with the presence of cilia-like structures. Low-magnification (*B*) and high-magnification (*C*) p53RNAi and mutant K-RAS^{V12}–expressing HBEC3 cells showed a histologic change similar to metaplasia and dysplasia and they invaded into the fibroblast and collagen underlayer.

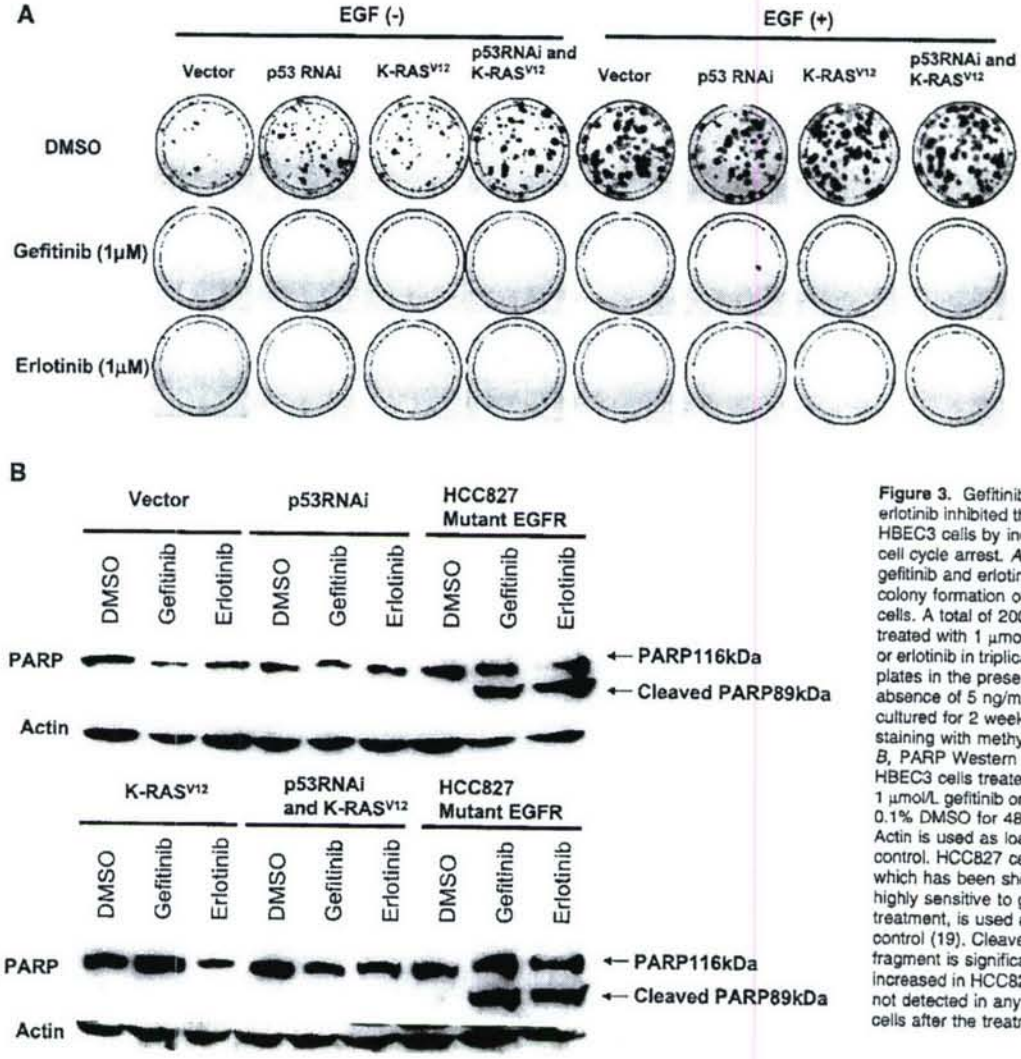

Figure 3. Gefitinib and erlotinib inhibited the growth of HBEC3 cells by inducing G_1 cell cycle arrest. *A*, effect of gefitinib and erlotinib on liquid colony formation of HBEC3 cells. A total of 200 cells were treated with 1 μmol/L gefitinib or erlotinib in triplicate 100 mm plates in the presence or the absence of 5 ng/mL EGF and cultured for 2 weeks before staining with methylene blue. *B*, PARP Western blot for HBEC3 cells treated with 1 μmol/L gefitinib or erlotinib or 0.1% DMSO for 48 hours. Actin is used as loading control. HCC827 cell line, which has been shown to be highly sensitive to gefitinib treatment, is used as positive control (19). Cleaved 89 kDa fragment is significantly increased in HCC827 cells but not detected in any of HBEC3 cells after the treatment.

the effect of gefitinib or erlotinib, 1 μmol/L of each drug was drug added to agar base layer. The number of microscopically visible colonies (>50 cells) was counted 4 weeks later. *In vivo* tumorigenicity was evaluated by injection of cells in nude mice. Male BALB/c nude (*nu/nu*) 3- to 6-week-old mice (Charles River Laboratories, Wilmington, DE) were irradiated on day 0 of the experiment in groups of five animals by a 5-minute exposure to 350 cGy from a cesium source. The next day, each mouse was given an injection s.c. on its flank 0.25×10^7 to 1×10^7 viable HBEC3 cells in 0.2 mL PBS containing different combinations of ectopically introduced genes. Coinjection of Matrigel (BD Bioscience, San Jose, CA) was also tested for HBEC3 cells expressing p53 RNA interference (RNAi) and K-RAS^{V12}. Mice were monitored every 2 to 3 days for tumor size. All animal care was in accord with institutional guidelines and approved Institutional Animal Care and Research Advisory Committee protocols. The NSCLC, NCI-H358, NCI-H441, and NCI-H1299 cell lines (5×10^6 cells) were used as positive controls.

Three-dimensional organotypic culture assay. Cultures were established as previously described for skin equivalents (23) except that airway fibroblasts were used in place of skin cells. Briefly, type I collagen and IMR90 fibroblasts were mixed and were allowed to polymerize. The collagen gels were released and incubated for a period of 4 to 10 days to allow the fibroblasts to contract the gels, creating a "submucosa." Cloning rings were then placed atop the gels and HBEC cells were plated into the rings at a concentration of $2 \times 10^5/cm^2$. After allowing the cells to attach for 4 hours, the rings were removed and organotypic cultures submerged for 4 days in keratinocyte feeder layer medium containing ascorbic acid, then emerged to the air-liquid interface for up to 28 days in culture, after which time the cultures were harvested, fixed, and prepared for histology. Organotypic cultures were immersed in 10% neutral buffered formalin overnight at 4°C followed by dehydration, paraffin embedding, and thin sectioning; 5 and 10 μM sections were then rehydrated and stained with H&E to view overall morphology (http://www.protocol-online.org/prot/Histology/Staining/). Stained slides were then viewed using an Axioscop-2 or Axioplan-2E microscope (Carl Zeiss, Thornwood, NY; www.zeiss.com) and photographed with Hamamatsu ORCA monochrome charge-coupled device camera (Hamamatsu, Bridgewater, NJ; www.hamamatsu.com).

Cell cycle analysis. Cells were harvested 48 hours after the treatment of 1 μmol/L gefitinib, erlotinib, or 0.1% DMSO, fixed with 70% ethanol, treated with 5 mg/mL RNase A (Roche Molecular Biochemicals), stained with 50 μg/mL propidium iodide, and analyzed by flow cytometry for DNA synthesis and cell cycle status [FACSCalibur instrument, (Becton Dickinson) with FlowJo software].

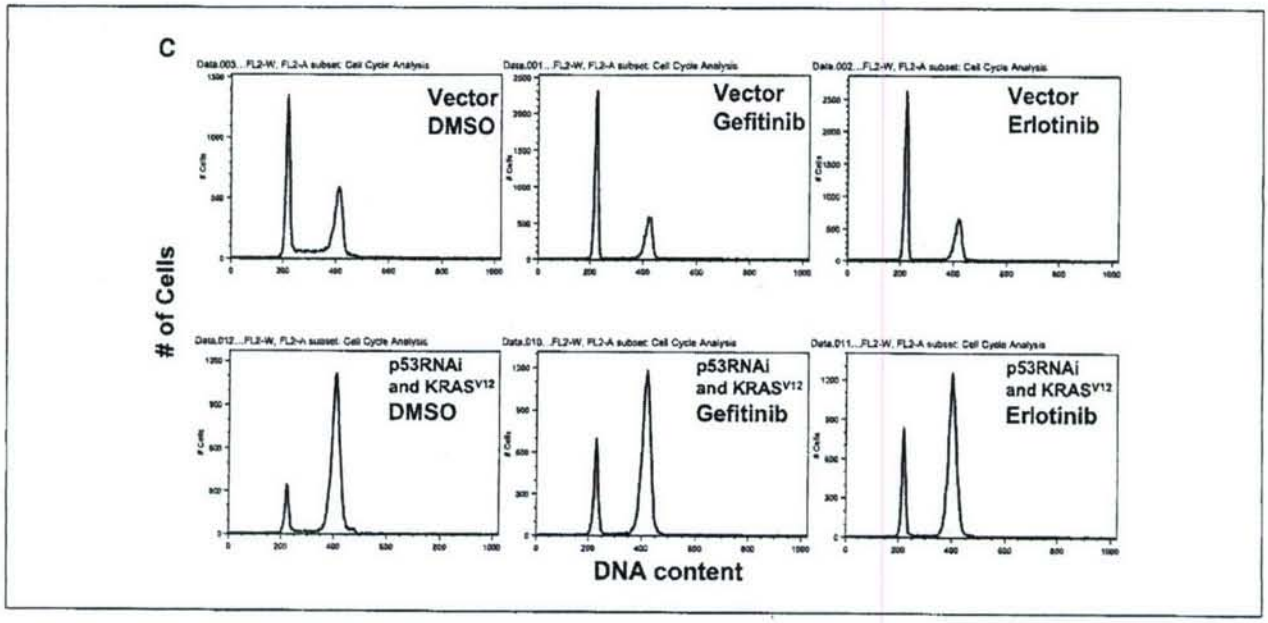

Figure 3 *Continued. C,* FACS profiles of vector (control) or p53 RNAi and mutant K-RAS^{V12}–expressing HBEC3 cells treated with 1 μmol/L of gefitinib or erlotinib or 0.1% DMSO for 48 hours. Cells were harvested after the treatment, stained with propidium iodide, and analyzed by using the flow cytometer. *X axis,* DNA content; *Y axis,* cell number. The fractions of cells in G_1 phase are significantly increased in both vector and the combined HBEC3 p53 knock down and mutant K-RAS cells, with the reduction of S-phase cells after the treatment of gefitinib or erlotinib. Compared with vector cells treated with DMSO, the combined HBEC3 p53 knockdown and mutant K-RAS cells treated with DMSO show a significant increase in G_2-M phase cells.

Microarray analysis. RNAs were labeled and hybridized to Affymetrix HG-U133-Plus2 GeneChips according to the protocol of the manufacturer (http://www.affymetrix.com). This array contains 54,675 genes (29,180 unique genes). Microarray analysis was done using Affymetrix MicroArray Suite 5.0 and in-house Visual Basic software MATRIX 1.26.

Real-time RT-PCR for DUSP6/MKP-3. The expression of *DUSP6/MKP-3* was analyzed by quantitative real-time RT-PCR. Primers were designed to ensure a single 107 bp amplicon using the standard Taqman assay-on-demand PCR protocol with a 10-minute hot start. Products were resolved on 2% agarose (Sigma). A probe sequence was designed using Primer-Express software (Applied Biosystems). The probe was labeled with TAMRA (quencher) and FAM (reporter) and synthesized by Integrated DNA Technologies. To establish the efficiency of this assay, we used a 5-fold serial dilution of cDNA over six concentrations. These samples were run on the Gene Amp 7700 Sequence Detection System (Applied Biosystems) in triplicate. The resultant curve had a slope of −3.396 and R^2 coefficient of 0.9939. For quantitative analysis of *DUSP6/MKP-3*, we used *GAPDH* (Applied Biosystems assay-on-demand) as an internal reference gene to normalize input cDNA. Quantitative real-time RT-PCR was done in a reaction volume of 25 μL, including 1 μL cDNA. We used the comparative C_t method to compute relative expression values.

Statistical analyses. For comparison of saturation density and colony formation between the different genetically manipulated cell strains, we used one-way ANOVA with Bonferroni's *post hoc* test correction and for comparisons of the effect of EGFR on growth the Mann-Whitney *U* test.

Results

RNAi-mediated p53 knockdown and K-RAS^{V12} introduction in HBEC3s. We used retroviral vector–mediated RNAi technology to generate HBEC3 clones stably knocked down for p53. HBEC3-expressing Cdk4 and hTERT cells were infected with pSRZ-p53 (see Materials and Methods and Fig. 1 caption), selected with zeocin, and tested for p53 and p21^{WAF1} protein expression. Western blot analysis showed clear suppression of p53 and p21^{WAF1} (Fig. 1*A*). Next, we introduced mutant K-RAS^{V12} into pSRZ-expressing and pSRZ-p53-expressing HBEC3 cells using pBabe-hyg-KRAS2-V12 retroviral vector followed by hygromycin selection. Western blot analysis showed that the expression levels of K-RAS in K-RAS^{V12}–transfected and p53RNAi and K-RAS^{V12}–transfected HBEC3 cells approximated that of vector alone–transfected HBEC3 cells (Fig. 1*A*). Because antibodies that recognize only wild or mutant K-RAS are not available, we did RT-PCR/RFLP analysis to distinguish between K-RAS^{V12} and wild-type K-RAS mRNA expression. The analysis revealed that mutant K-RAS^{V12} transcripts were the predominant form expressed in the K-RAS^{V12}–transfected HBEC3 alone or with p53 RNAi cells (Fig. 1*B*), indicating that most of the K-RAS protein expressed in HBEC3 cells infected with pBabe-hyg-KRAS2-V12 was the mutant form. We also did immunocytochemistry of p63 (a stem cell marker) and found that mutant K-RAS and/or p53 knockdown did not alter the p63 expression levels of HBEC3 cells (data not shown).

p53 knockdown and K-RAS^{V12} introduction into HBEC3s increase saturation density. We assessed the effect of p53 knockdown and expression of mutant K-RAS^{V12} on cell growth and found no significant difference in growth rate in the exponential growth phase between p53RNAi-expressing, K-RAS^{V12}-expressing, p53RNAi and K-RAS^{V12}–expressing, and vector-expressing HBEC3 cells. However, p53RNAi-expressing ($P < 0.01$), K-RAS^{V12}–expressing ($P < 0.01$), and p53RNAi and K-RAS^{V12}–expressing ($P < 0.001$) HBEC3 cells achieved significantly higher final saturation densities in confluent cultures compared with vector-transfected control (in all cases here and below using one-way ANOVA with Bonferroni's *post hoc* test; Fig. 1*C* and *D*). Also, the final density of the combined p53RNAi and K-RAS^{V12}–expressing HBEC3 cells was significantly higher than that of HBEC3 cells with either p53 knockdown ($P < 0.01$) or mutant K-RAS^{V12} ($P < 0.01$) alone (Fig. 1*C* and *D*). We conclude from these studies that introduction of these

Table 2. Soft agar colony formation assay for HBEC3 cells treated with gefitinib or erlotinib

	HBEC3			
	Vector	p53RNAi	K-RASV12	p53RNAi and K-RASV12
EGF(+)				
DMSO	1.3 ± 0.47	11 ± 1.6	5.7 ± 1.2	23 ± 2.1
Gefitinib (1 μmol/L)	0	0	0	0
Erlotinib (1 μmol/L)	0	0	0	0
EGF(−)				
DMSO	0	0	0	1.3 ± 0.94
Gefitinib (1 μmol/L)	0	0	0	0
Erlotinib (1 μmol/L)	0	0	0	0

NOTE: Number of colonies after 14 days are shown as average ± SD. HBEC3 cells (1,000) were plated in agar and treated with 1 μmol/L gefinitib or erlotinib in triplicate 12-well plates for up to 2 weeks in the presence or the absence of EGF and colonies (50-100 cells) were counted.

genetic changes produced part of the malignant phenotype, increased saturation density.

p53 knockdown and K-RAS^{V12} introduction permits anchorage-independent growth and partial bypass of EGF dependence. HBEC3 cells are able to form colonies in liquid medium but not in soft agar (i.e., they do not display anchorage-independent growth). We then tested the p53 and K-RAS^{V12}–manipulated variants to see if they had acquired this ability. In addition, because HBEC3 cells express robust levels of EGFR (Fig. 4*A*) and EGF is in the K-SFM synthetic medium, we tested the dependence of colony formation in liquid and semisolid medium on EGF. Supplementation of EGF dramatically enhanced liquid colony formation in all HBEC3 cells (Fig. 1*E*). In liquid colony formation in the presence of EGF, no significant difference in the number of colonies was seen between p53RNAi-expressing, K-RAS^{V12}–expressing, p53RNAi and K-RAS^{V12}–expressing, and vector-expressing HBEC3 cells. In contrast, there were significant differences in the number of colonies in the absence of EGF between these four strains (Fig. 1*F*). In the absence of EGF, p53RNAi-expressing (5.9 fold, $P < 0.001$) and p53RNAi and K-RAS^{V12}–expressing (6.6-fold, $P < 0.001$) HBEC3 cells formed a markedly increased number of colonies compared with vector control, whereas K-RAS^{V12}–expressing HBEC3 cells formed significantly increased (3.2-fold, $P < 0.001$) number of colonies compared with vector control (in all cases here and below using one-way ANOVA with Bonferroni's *post hoc* test; Fig. 1*F*). In the presence of EGF, p53RNAi-expressing, K-RAS^{V12}–expressing, and p53RNAi and K-RAS^{V12}–expressing HBEC3 cells formed significantly increased number of soft agar colonies compared with vector control, 7.3-fold ($P < 0.001$), 6.7-fold ($P < 0.001$), and 16.5-fold ($P < 0.001$), respectively, whereas in the absence of EGF, p53 RNAi and p53RNAi and K-RAS^{V12}–expressing HBEC3 cells formed very few colonies (Fig. 4*C*). We conclude from these studies that introduction of these genetic changes led to anchorage-independent growth and both oncogenic K-RAS or p53 knockdown led to partial bypass of dependence on EGF. However, the cells still remain dependent on EGF signaling to express this anchorage-independent growth although an unexpected finding was the ability of p53 knockdown to partially alleviate this EGF dependence.

p53 knockdown and expression of mutant K-RAS^{V12} does not give a full malignant phenotype. In tumorigenicity assays, none of HBEC3 derivatives formed s.c. tumors in nude mice. Because Matrigel (BD Bioscience) accelerates tumor growth when coinjected with cells in athymic mice (24), we injected HBEC3 cells expressing p53 RNAi and K-RAS^{V12} together with Matrigel. However, even with Matrigel, the HBEC3 cells expressing p53 RNAi and

Table 3. Effect of gefitinib and erlotinib on cell cycle progression in HBEC3 cells

	Nontreated (DMSO)			Gefitinib/erlotinib		
	G_1	S	G_2-M	G_1	S	G_2-M
Vector	45.4 ± 0.2	27.5 ± 6.0	28.7 ± 3.9	76.6 ± 5.6*	2.6 ± 0.5†	28.0 ± 2.0
p53RNAi	41.4 ± 2.9	27.6 ± 3.7	31.0 ± 4.5	69.5 ± 0.2*	7.4 ± 2.8*	27.0 ± 3.4
K-RAS^{V12}	49.5 ± 6.3	31.7 ± 10.6	17.8 ± 12.2	81.4 ± 4.6*	7.7 ± 2.4	16.6 ± 2.8
p53RNAi and K-RAS^{V12}	12.9 ± 3.2	11.8 ± 6.2	73.7 ± 3.8	25.6 ± 4.8*	5.3 ± 1.2	70.8 ± 3.7

NOTE: Data are percentages (mean ± SD). Averaged values of three independent experiments are shown. Watson Pragmatic algorithm was used to calculate each cell cycle distribution. Because the algorithm contains approximations, the total of each distribution is not exactly 100%.

*$P < 0.01$ in comparison with the respective control.

†$P < 0.05$ in comparison with the respective control.

K-RAS^{V12} did not form tumors. In contrast, tests of 5×10^6 NSCLC, NCI-H358, NCI-H441, and NCI-H1299 cells reproductively formed progressively growing nude mouse xenograft tumors in the 17- to 90-day observation period (Table 1). We conclude from these studies that even with these gain-of-function and loss-of-function manipulations, a full malignant phenotype is not achieved (*in vivo* tumor formation).

Oncogenic manipulation leads to an invasive phenotype in a three-dimensional organotypic culture assay. To evaluate the effect of oncogenic manipulation in HBEC3s on their ability to differentiate and to invade, we did three-dimensional organotypic culture. HBEC3 cells only expressing hTERT and Cdk4 cells formed a confluent layer of cells on the upper surface of a fibroblast and collagen gel under layer and developed both ciliated (Fig. 2*A*) and mucous-producing cell types. In stark contrast, the cells expressing hTERT, Cdk4, K-RAS^{V12}, and p53 RNAi showed histologic change similar to metaplasia/dysplasia and they invaded into the fibroblast and collagen gel similar to cancer cells invading into the submucosal layer (Fig. 2*B* and *C*). We conclude from these studies that p53 knockdown and K-RAS^{V12} are additive in malignant transformation leading to the development of anchorage-independent growth and the ability to invade in a three-dimensional culture system.

Gefitinib and erlotinib inhibit proliferation and colony formation of HBEC3 cells by inducing G_1 cell cycle arrest. The dependency of HBEC3 cell on EGF signaling prompted us to investigate the effect of tyrosine kinase inhibitors, gefitinib and erlotinib, on cell proliferation in mass culture and colony formation of these cells. Both gefitinib and erlotinib at 1 μmol/L completely inhibited the mass culture proliferation of all HBEC3 cells both in the presence and the absence of EGF (data not shown). Gefitinib or erlotinib at 1 μmol/L also completely inhibited both anchorage-dependent and anchorage-independent colony formation in all HBEC3 cells (Fig. 3*A*; Table 2). Thus, although oncogenic manipulation partially relieved EGF dependence, EGF tyrosine kinase inhibitors remain potent inhibitors of HBEC growth. To investigate the mechanisms of this growth inhibition by tyrosine kinase inhibitors, we did apoptosis and cell cycle analyses. Western blot for PARP cleavage, an indicator of caspase-mediated apoptosis, showed that cleaved 89 kDa fragment was not detected in any of HBEC3 cells treated with tyrosine kinase inhibitors but was significantly increased in HCC827 EGFR mutant cells after the treatment with tyrosine kinase inhibitors for 48 hours (Fig. 3*B*). Cell cycle analysis also did not show sub-G_1 DNA fractions indicative of apoptosis in HBEC3 cells treated with tyrosine kinase inhibitors. Instead, the cell cycle analysis showed increase in the fraction of cells in G_1 phase in all the HBEC3 cells treated with either of the drugs, with reduction of S-phase cells (Fig. 3*C*; Table 3). These results suggest that growth inhibition for HBEC3 cells by tyrosine kinase inhibitors is mainly caused by G_1 cell cycle arrest and not apoptosis. Comparing the results of fluorescence-activated cell sorting (FACS) analysis for the control cells treated with DMSO, we found that the combined HBEC3 p53 knockdown and mutant K-RAS cells showed a significantly increase in G_2-M phase cells compared with either manipulation alone, suggesting dramatic cell cycle deregulation results from this oncogenic combination (Fig. 3*C*; Table 3).

Effect of K-RAS^{V12} and EGF supplementation on expression of phospho-EGFR, phospho-MEK, phospho-ERK, and phospho-Akt. We measured the expression of phosphorylated and total EGFR, mitogen-activated protein kinases (MAPK), and Akt proteins in the HBEC3 cells in the presence and absence of EGF. Addition of EGF resulted in massive induction of phospho-EGFR, a slight induction of phospho-ERK, and a modest induction of phospho-Akt^{Thr308} in all HBEC3 cells (Fig. 4*A*). In the absence of EGF, two immunoreactive phospho-MEK1/2 bands were detected whereas the faster migrating band was not detected in the presence of EGF, representing a shift to the hyper phosphorylated form (Fig. 4*A*). Surprisingly, introduction of K-RAS^{V12} did not show a significant effect on phosphorylation of MAPKs in the presence or absence of EGF but led to a slight increased phospho-Akt^{Thr308} in the absence of EGF (Fig. 4*A*). Also, surprisingly, both phospho-MEK1/2 and phospho-ERK were down-regulated in p53RNAi and K-RAS^{V12}–expressing HBEC3 cells compared with the other three cell lines in the absence of EGF (Fig. 4*A*).

Tyrosine kinase domain mutant EGFRs enhanced anchorage-independent growth of HBEC3 cells. EGFR with mutations in the tyrosine kinase domain have been discovered in lung cancers predominantly arising in never smokers (25). These mutant EGFRs are suspected as having oncogenic properties. To determine if mutant EGFRs commonly found in lung cancer (E746-A750, L858R) have oncogenic ability, we evaluated the tumorigenicity of wild-type and mutant EGFR transfected HBEC3s by soft agar colony formation assays. In the absence of EGF, E746-A750 del expressing HBEC3 cells formed significantly increased number of colonies compared with wild type–expressing cells in both p53 wild-type ($P < 0.001$ by Mann-Whitney U test) and p53 knocked down cells ($P < 0.01$ by Mann-Whitney U test), whereas L858R mutant-expressing HBEC3 cells increased the number of colonies only in p53 knocked down cells ($P < 0.001$ by Mann-Whitney U test; Fig. 4*C*). In contrast to p53 RNAi and mutant K-RAS–expressing HBEC3s that formed very few number of colonies (2.7 ± 2.0 of 1,000) in the absence of EGF, the E746-A750 del mutant transfectants formed substantial number of colonies even in the absence of EGF (Fig. 4*C*), suggesting that E746-A750 del mutant reduced the EGF dependence of HBEC3s in terms of anchorage-independent growth. Of interest, the L858R mutant only showed this independence when p53 was removed by knockdown (Fig. 4*C*). Again, in these p53 knocked down HBEC3s carrying a control vector (used for EGFR introduction), the cells remained dependent on EGF for soft agar growth. These results indicate that both types of mutant EGFRs possess oncogenic properties compared with wild-type EGFR. They also provide functional differences between the deletion and missense EGFR mutants, including differences in p53 interaction. We also did nude mice injection assays for p53 knocked down HBEC3s carrying L858R mutant, which formed the most number of colonies in the absence of EGF (Fig. 4*C*). However, they did not form tumor in nude mice (Table 1).

Introduction of both wild-type and mutant EGFR into HBEC3s resulted in constitutive activation of EGFR. Phosphorylation level of EGFR was evaluated by Western blotting with four (Y845, Y992, Y1045, and Y1068) phosphorylation-specific antibodies. To reduce the background for Western blotting, cells were first starved in the medium without bovine pituitary extract and EGF for 24 hours before harvest. In the absence of exogenous EGF, we found EGFR mutants and wild-type EGFR to exhibit induced levels of phosphorylated EGFR, suggesting the existence of autocrine ligands stimulating EGFR (Fig. 4*B*). In p53 wild-type cells, wild-type EGFR showed phosphorylation of Y845, Y992, and Y1068 to a lesser extent than when mutant EGFRs were present (Fig. 4*B*). In contrast, in p53 knocked down cells, such a difference

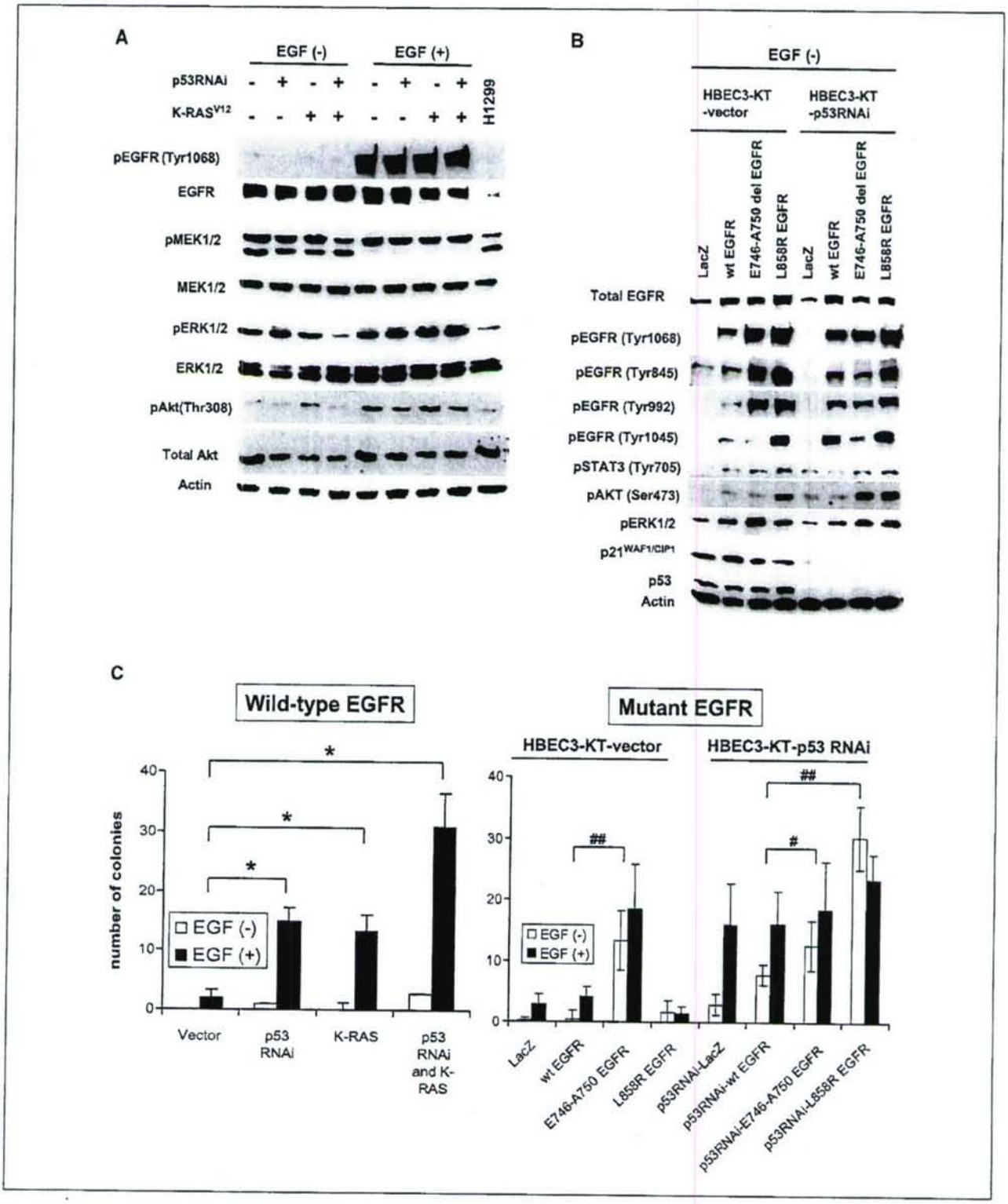

Figure 4. Transduction analysis for oncogenically manipulated HBEC3 cells. *A*, effect of K-RAS^{V12} and EGF supplementation on expression of phospho-EGFR, phospho-MEK, phospho-ERK, and phospho-Akt. HBEC3 cells were grown in the presence or absence of 5 ng/mL EGF and were immunoblotted to detect phospho-EGFR (*pEGFR*), EGFR, phospho-MEK1/2 (*pMEK1/2*), MEK1/2, phospho-ERK (*pERK*), ERK, phospho-Akt (*pAkt*; Thr^{308}), and Akt. Actin was used as loading control. *B*, effect of wild-type and mutant EGFR introduction on expression of phospho-EGFRs, phospho-STAT3, phospho-ERK, and phospho-Akt in HBEC3 cells. Wild type– or mutant EGFR–introduced HBEC3 cells were grown in the absence of EGF and were immunoblotted to detect phospho-EGFRs (Y1068, Y1045, Y992, and Y845), EGFR, phospho-STAT3, phospho-Akt (Y473), and phospho-ERK. Actin was used as loading control. *C*, soft agar colony formation assay for oncogenically manipulated HBEC3 cells. A total 1,000 of each HBEC3 cell strains were plated in agar and 4 weeks later microscopically visible colonies were counted. *Columns*, mean of three independent experiments; *bars*, SD. *, $P < 0.01$, one-way ANOVA with Bonferroni's posttest, #, $P < 0.01$, Mann-Whitney test; ##, $P < 0.001$, Mann-Whitney test.

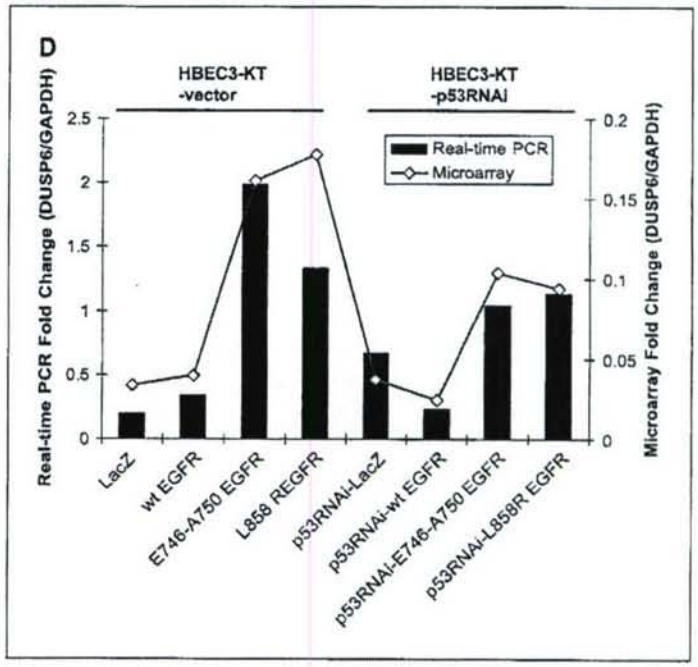

Figure 4 *Continued. D*, microarray analysis and real-time PCR validation for *DUSP6/MKP-3* gene. *Columns*, fold changes of the mRNA levels of *DUSP6/MKP-3* gene relative to those of *GAPDH* gene in HBEC3 cells transfected with wild-type or mutant EGFR.

was not seen (Fig. 4*B*). This result suggests that the activation of wild-type EGFR might be suppressed by p53. Interestingly, the Y1045 site was highly phosphorylated in L858R transfectants but not in E746-A750 del transfectant (Fig. 4*B*), indicating that Y1045 is unique in distinguishing between the two types of EGFR mutations (Fig. 4*B*).

AKT and STAT3 were phosphorylated at higher level in mutant EGFRs than wild-type EGFR. The EGFR L858R mutant showed increased level of phosphorylated Akt and STAT3 in both p53 wild-type and p53 knocked down cells, whereas the EGFR E746-A750 del mutant showed increased level of phosphorylated Akt only in p53 knocked down cells and slightly increased level of phosphorylated STAT3 in both p53 wild-type and p53 knocked down cells (Fig. 4*B*). By contrast, no significant difference in phosphorylated ERK was seen between wild-type and mutant EGFRs (Fig. 4*B*). These results suggest that mutant EGFRs selectively transduces signals through Akt and STAT3, which is consistent with previously reported data (26).

***DUSP6/MKP-3* gene was up-regulated in mutant EGFR transfected HBEC3 cells.** Microarray analysis for HBEC3 cells transfected with wild-type or mutant EGFRs shows that mRNA of DUSP6/MKP-3, whose protein is a dual-specificity phosphatase that dephosphorylate the active form of ERK (27, 28), is significantly up-regulated in mutant EGFR transfectants compared with wild-type and vector-transfected cells (Fig. 4*D*). Real-time PCR analysis for DUSP6/MKP-3 also showed this result (Fig. 4*D*).

Discussion

We have taken HBECs immortalized using overexpression of Cdk4 (to circumvent p16-mediated cell culture growth arrest) and hTERT (to prevent telomere erosion) and genetically manipulated them by stably knocking down p53, expressing oncogenic K-RAS^{V12} and mutant EGFR, alone or in combination. The results show that these additional genetic changes, commonly found in human lung cancer, progress the HBEC3 cells part, but not all, of the way toward malignancy. The human cells exhibit higher saturation density, anchorage-independent growth, invade in an organotypic culture assay but do not form tumors in mouse xenografts. Although, in general, the cells remain dependent on EGF, p53 knockdown and mutant EGFR reduce this EGF dependence. In addition, their growth and ability to form colonies in liquid and semisolid medium is dramatically reduced by EGFR-directed tyrosine kinase inhibitors. These studies indicate that more than four genetic alterations are required for the full cancer transformation of HBECs.

Several studies have reported that introduction of oncogenes, such as K-RAS or HRAS and c-myc, result in malignant transformation of HBECs (29–31). However, until the present study, there has not been immortalized cell lines with wild-type p53 function. (Prior studies were done with viral oncoprotein immortalized cells abrogating p53 function; refs. 11, 12, 29, 30, 32.) In the present study, we have shown that >90% inhibition of p53 protein in immortalized HBECs enhances the clonal and soft agar colony formation and results in partial loss of contact inhibition, indicating that loss of p53 function contributes importantly to the malignant progression of HBECs. In addition, the combination of p53 knockdown and oncogenic K-RAS^{V12} enhanced these changes further, suggesting these two genetic alterations have additive effects on tumorigenicity. Taken together, these results show that this model system provides a powerful new approach to assess the contribution of individual genetic alterations in HBECs in the malignant process.

RAS was first identified as an oncogene by virtue of its ability to overcome cell-to-cell contact inhibition of proliferation and this ability has been well documented in many types of cells (33, 34). In the present study, not only oncogenic K-RAS^{V12} but also p53 knockdown resulted in partial loss of contact inhibition and the combination of them enhanced this ability. Recently, Meerson et al. (35) reported results consistent with this finding. They showed that p53 knockdown in WI38 human embryonic lung fibroblasts

reduced density-dependent inhibition of growth by abolishing G_1 phase arrest. Although density-dependent inhibition of growth is a complex phenomenon and its precise mechanism is not well understood, this phenomenon is thought to be indicative of tumorigenic potential. Thus, their results and ours suggest that p53 may function as a tumor suppressor even when the cells are not under stresses, such as genotoxic damage and irradiation. Recently, other studies also reported that p53 function is involved in regulating cell motility and adhesion (36, 37).

It is unclear how the mutant K-RAS transfected HBECs preferentially express the mutant compared with wild-type *K-RAS* allele. These cells express mutant K-RAS mRNA predominantly without changing the total K-RAS protein levels, suggesting that wild-type K-RAS expression is suppressed at the transcriptional level in these cells. The mechanism of transcriptional regulation of K-RAS has not been fully elucidated and we are unable to explain the mechanism of this observation. However, the hypothesis that oncogenic RAS inhibits the transcription of wild-type RAS is compatible with our observations. Because the tumor suppressor function of wild-type K-RAS has been shown in mice, one possibility is that mutant RAS exerts its oncogenic ability in part by suppressing the expression of wild-type RAS. This hypothetical function of oncogenic RAS seems very attractive in terms of better understanding the mechanism of oncogenic RAS, and thus it will be of interest to further investigate these findings.

Previous studies have found high levels of EGFR expression in both immortalized and nonimmortalized HBECs (38). EGF supplementation also results in a slight increase of growth rate at normal cell density in HBECs (38). Several studies have shown the existence of an EGFR autocrine loop involving EGF, transforming growth factor-α, and amphiregulin in HBECs (39, 40). In addition, tobacco smoke induces proliferation of primary HBEC through an EGFR autocrine loop mediated by tumor necrosis factor-α–converting enzyme and amphiregulin, suggesting tobacco smoke induction of the EGFR autocrine loop in lung cancer pathogenesis (41). In the present study, we found that HBEC3 cells expressed high level of EGFR that was stimulated to phospho-EGFR with EGF whereas their colony-forming ability in both liquid and soft agar was highly dependent on EGF supplementation. Signal transduction studies in HBEC3 cells suggest that this may in part be due to the up-regulation of the Akt pathway. With p53 knockdown and K-RAS oncogenic manipulation, the EGF dependence was partially relieved, suggesting the potential for autocrine growth factor production. Thus, previous studies and our results suggest that EGF autocrine loop may play an important role in cell proliferation and tumorigenic progression of HBECs.

Gefitinib (Iressa) and erlotinib (Tarceva) are orally available tyrosine kinase inhibitors that target EGFR (42–45). Gefitinib has been approved as a third-line therapy for NSCLC patients. Erlotinib has been shown to be active and well tolerated in patients with NSCLC, providing survival benefit (46). Although these drugs are being developed as anticancer drugs, recent studies have shown that gefitinib inhibits cell proliferation in immortalized normal or precancerous breast cells, supporting its role as a chemopreventive agent (47). Because we found robust expression of EGFR in HBEC3 cells and their high dependency of growth on EGF, we considered the possibility that tyrosine kinase inhibitors are also effective in oncogenically manipulated HBEC3 cells. We observed that 1 μmol/L gefitinib or erlotinib dramatically inhibited both anchorage-dependent and anchorage-independent cell growth of HBEC3 cells. Apoptosis and cell cycle analyses showed that this inhibition was caused mainly by not apoptosis but G_1 cell cycle arrest, which is consistent with previous papers reporting that gefitinib and erlotinib induce G_1 cell cycle arrest in several types of cells (48–52). These results provide part of a preclinical rationale for the development of these drugs for the prevention of human lung cancer. It is important to point out that the concentrations used in the present studies are actually achieved in patients with current standard drug practices (53, 54). In addition, interestingly, we found that G_2-M fraction significantly increase with the combination of p53 knock down and mutant K-RAS cells compared with either oncogenic manipulation alone. We speculate that in the presence of intact p53 function, cell cycle progression induced by mutant K-RAS in HBECs is suppressed by the ability of p53 to induce G_1 arrest, whereas in the absence of p53, mutant K-RAS exerts its ability to progress the cell cycle from G_1 to S phases, resulting in significantly increased G_2-M phase fraction. Consistent with this hypothesis, one paper showed that ectopic expression of mutant N-RAS impaired the G_1 and G_2 cell cycle arrest only in p53-defective cells (55). In addition, it will be interesting to see whether similar types of cell cycle deregulation are also found when mutant EGFR is combined with loss of p53 function in these cells.

Introduction of tyrosine kinase domain EGFR mutants enhanced anchorage-independent growth of HBEC3s, providing evidence of their oncogenic properties. In addition, signal transduction analysis showed that they stimulated Akt and STAT3 but not Erk1/Erk2 signals, consistent with previously reported results (26). Our discovery of DUSP6/MKP-3 mRNA up-regulation in mutant EGFR transfectants provides an explanation for this. Because DUSP6/MKP-3 protein is a dual-specificity phosphatase that dephosphorylates the active form of ERK (27, 28), it is possible that Erk1/Erk2 phosphorylation in EGFR mutant cells is down-regulated by DUSP6/MKP-3. In addition, the findings that Akt and STAT3 were not highly phosphorylated in HBECs that showed robust level of phosphorylated EGFR suggests that a negative feedback regulatory pathway may be activated for Akt and STAT3 as well, and that the mutant EGFRs bypass this regulation.

Although p53 knockdown, K-RAS^{V12}, and mutant EGFR progress HBEC3 cells toward malignancy, the manipulated cells are not fully malignant. What additional genetic alterations are required for full malignant transformation in HBEC3 cells? For this question, there may be a clue from recent work of Hahn et al., who showed that defined genetic alterations, including the early region of the SV40 genome, the *hTERT* gene, and an oncogenic allele of H-ras, resulted in malignant transformation in human embryonic epithelial and fibroblast cells (56). By precisely analyzing the early region of SV40, they have shown that small T antigen, which is transcribed from the early region together with large T antigen, may play an important role in carcinogenesis. Small T antigen has been shown to bind and to target phosphatase 2A (PP2A), which regulates the RAS/MAPK cascade. Our unpublished studies have shown no mutation but frequent loss of PP2A expression in lung cancer, raising the possibility that PP2A is involved in lung carcinogenesis. Thus, a next step would be to inactivate PP2A in HBEC3 cells in addition to p53 knockdown and K-RAS^{V12}. It will also be of interest to introduce other genetic alterations observed in lung cancer, such as MYC family overexpression, FHIT inactivation, RASSF1A inactivation, and PTEN inactivation. Although we used a previously reported target sequence for p53 knockdown, which has also been used in several papers (17, 18, 57) and has no other BLAST hits, we are unable to completely exclude the possibility that off-target effects might affect our phenotypic analysis.

In conclusion, we have shown that using the immortalized HBEC model, p53 knockdown, K-RAS^{V12}, and mutant EGFR in the presence of p16 bypass and human telomerase contribute to lung cancer tumorigenesis, but additional genetic alterations are required for full malignant transformation of HBECs. In addition, we note that p53 knockdown relaxes the dependence on EGF in the presence of both wild-type and mutated EGFR. However, these oncogenically manipulated HBEC cells remain highly dependent on EGFR signaling for expression of key portion of the malignant phenotype. This dependence along with activated EGFR in bronchial preneoplasia suggests the use of EGFR inhibition by tyrosine kinase inhibitors as chemoprevention agents for lung cancer.

Acknowledgments

Received 7/18/2005; revised 11/22/2005; accepted 12/14/2005.

Grant support: Lung Cancer Specialized Programs of Research Excellence grants P50CA75907, CA71618, and NO1-CN-43301; Department of Defense VITAL grant W81XWH041014202PP; the Gillson Longenbaugh Foundation, and a NASA Specialized Center of Research (NSCOR) NNJ05HD36G.

The costs of publication of this article were defrayed in part by the payment of page charges. This article must therefore be hereby marked *advertisement* in accordance with 18 U.S.C. Section 1734 solely to indicate this fact.

References

1. Sekido Y, Fong KM, Minna JD. Molecular genetics of lung cancer. Annu Rev Med 2003;54:73–87.
2. Ramirez RD, Sheridan S, Girard L, et al. Immortalization of human bronchial epithelial cells in the absence of viral oncoproteins. Cancer Res 2004;64:9027–34.
3. Vaughan MB, Ramirez RD, Wright WE, Minna JD, Shay JW. A three-dimensional model of differentiation of immortalized human bronchial epithelial cells. Differentiation. In press 2006.
4. Geradts J. Abrogation of the RB-p16 tumor suppressor pathway in human lung cancer. Methods Mol Med 2003; 74:89–99.
5. Kaye FJ. RB and cyclin dependent kinase pathways: defining a distinction between RB and p16 loss in lung cancer. Oncogene 2002;21:6908–14.
6. Horikawa I, Barrett JC. Transcriptional regulation of the telomerase hTERT gene as a target for cellular and viral oncogenic mechanisms. Carcinogenesis 2003;24: 1167–76.
7. Meyerson M, Counter CM, Eaton EN, et al. hEST2, the putative human telomerase catalytic subunit gene, is up-regulated in tumor cells and during immortalization. Cell 1997;90:785–95.
8. Nakamura TM, Morin GB, Chapman KB, et al. Telomerase catalytic subunit homologs from fission yeast and human. Science 1997;277:955–9.
9. Nakayama J, Tahara H, Tahara E, et al. Telomerase activation by hTRT in human normal fibroblasts and hepatocellular carcinomas. Nat Genet 1998;18:65–8.
10. Kilian A, Bowtell DD, Abud HE, et al. Isolation of a candidate human telomerase catalytic subunit gene, which reveals complex splicing patterns in different cell types. Hum Mol Genet 1997;6:2011–9.
11. Reddel RR, Ke Y, Gerwin BI, et al. Transformation of human bronchial epithelial cells by infection with SV40 or adenovirus-12 SV40 hybrid virus, or transfection via strontium phosphate coprecipitation with a plasmid containing SV40 early region genes. Cancer Res 1988;48: 1904–9.
12. Lundberg AS, Randell SH, Stewart SA, et al. Immortalization and transformation of primary human airway epithelial cells by gene transfer. Oncogene 2002; 21:4577–86.
13. Barbacid M. ras genes. Annu Rev Biochem 1987;56: 779–827.
14. Bos JL. ras oncogenes in human cancer: a review. Cancer Res 1989;49:4682–9.
15. Paez JG, Janne PA, Lee JC, et al. EGFR mutations in lung cancer: correlation with clinical response to gefitinib therapy. Science 2004;304:1497–500.
16. Pao W, Miller V, Zakowski M, et al. EGF receptor gene mutations are common in lung cancers from "never smokers" and are associated with sensitivity of tumors to gefitinib and erlotinib. Proc Natl Acad Sci U S A 2004; 101:13306–11.
17. Brummelkamp TR, Bernards R, Agami R. Stable suppression of tumorigenicity by virus-mediated RNA interference. Cancer Cell 2002;2:243–7.
18. Brummelkamp TR, Bernards R, Agami R. A system for stable expression of short interfering RNAs in mammalian cells. Science 2002;296:550–3.
19. Amann J, Kalyankrishna S, Massion PP, et al. Aberrant epidermal growth factor receptor signaling and enhanced sensitivity to EGFR inhibitors in lung cancer. Cancer Res 2005;65:226–35.
20. Sato M, Girard L, Sekine I, et al. Increased expression and no mutation of the Flap endonuclease (FEN1) gene in human lung cancer. Oncogene 2003;22:7243–6.
21. Nishikawa T, Maemura K, Hirata I, et al. A simple method of detecting K-ras point mutations in stool samples for colorectal cancer screening using one-step polymerase chain reaction/restriction fragment length polymorphism analysis. Clin Chim Acta 2002; 318:107–12.
22. Burbee DG, Forgacs E, Zochbauer-Muller S, et al. Epigenetic inactivation of RASSF1A in lung and breast cancers and malignant phenotype suppression. J Natl Cancer Inst 2001;93:691–9.
23. Vaughan MB, Ramirez RD, Brown SA, Yang JC, Wright WE, Shay JW. A reproducible laser-wounded skin equivalent model to study the effects of aging *in vitro*. Rejuvenation Res 2004;7:99–110.
24. Fridman R, Giaccone G, Kanemoto T, Martin GR, Gazdar AF, Mulshine JL. Reconstituted basement membrane (Matrigel) and laminin can enhance the tumorigenicity and the drug resistance of small cell lung cancer cell lines. Proc Natl Acad Sci U S A 1990;87: 6698–702.
25. Shigematsu H, Lin L, Takahashi T, et al. Clinical and biological features associated with epidermal growth factor receptor gene mutations in lung cancers. J Natl Cancer Inst 2005;97:339–46.
26. Sordella R, Bell DW, Haber DA, Settleman J. Gefitinib-sensitizing EGFR mutations in lung cancer activate anti-apoptotic pathways. Science 2004;305:1163–7.
27. Muda M, Boschert U, Dickinson R, et al. MKP-3, a novel cytosolic protein-tyrosine phosphatase that exemplifies a new class of mitogen-activated protein kinase phosphatase. J Biol Chem 1996;271:4319–26.
28. Groom LA, Sneddon AA, Alessi DR, Dowd S, Keyse SM. Differential regulation of the MAP, SAP and RK/p38 kinases by Pyst1, a novel cytosolic dual-specificity phosphatase. EMBO J 1996;15:3621–32.
29. Reddel RR, Ke Y, Kaighn ME, et al. Human bronchial epithelial cells neoplastically transformed by v-Ki-ras: altered response to inducers of terminal squamous differentiation. Oncogene Res 1988;3:401–8.
30. Ura H, Bonfil RD, Reich R, et al. Expression of type IV collagenase and procollagen genes and its correlation with the tumorigenic, invasive, and metastatic abilities of oncogene-transformed human bronchial epithelial cells. Cancer Res 1989;49:4615–21.
31. Yoakum GH, Lechner JF, Gabrielson EW, et al. Transformation of human bronchial epithelial cells transfected by Harvey ras oncogene. Science 1985;227: 1174–9.
32. Reddel RR, Salghetti SE, Willey JC, et al. Development of tumorigenicity in simian virus 40-immortalized human bronchial epithelial cell lines. Cancer Res 1993; 53:985–91.
33. Hurlin PJ, Fry DG, Maher VM, McCormick JJ. Morphological transformation, focus formation, and anchorage independence induced in diploid human fibroblasts by expression of a transfected H-ras oncogene. Cancer Res 1987;47:5752–7.
34. Kinch MS, Clark GJ, Der CJ, Burridge K. Tyrosine phosphorylation regulates the adhesions of ras-transformed breast epithelia. J Cell Biol 1995;130:461–71.
35. Meerson A, Milyavsky M, Rotter V. p53 mediates density-dependent growth arrest. FEBS Lett 2004;559: 152–8.
36. Alexandrova A, Ivanov A, Chumakov P, Kopnin B, Vasiliev J. Changes in p53 expression in mouse fibroblasts can modify motility and extracellular matrix organization. Oncogene 2000;19:5826–30.
37. Sablina AA, Chumakov PM, Kopnin BP. Tumor suppressor p53 and its homologue p73α affect cell migration. J Biol Chem 2003;278:27362–71.
38. Tsao MS, Zhu H, Viallet J. Autocrine growth loop of the epidermal growth factor receptor in normal and immortalized human bronchial epithelial cells. Exp Cell Res 1996;223:268–73.
39. Plowman GD, Green JM, McDonald VL, et al. The amphiregulin gene encodes a novel epidermal growth factor-related protein with tumor-inhibitory activity. Mol Cell Biol 1990;10:1969–81.
40. Cook PW, Mattox PA, Keeble WW, et al. A heparin sulfate-regulated human keratinocyte autocrine factor is similar or identical to amphiregulin. Mol Cell Biol 1991; 11:2547–57.
41. Lemjabbar H, Li D, Gallup M, Sidhu S, Drori E, Basbaum C. Tobacco smoke-induced lung cell proliferation mediated by tumor necrosis factor α-converting enzyme and amphiregulin. J Biol Chem 2003;278:26202–7.
42. Glover KY, Perez-Soler R, Papadimitradopoulou VA. A review of small-molecule epidermal growth factor receptor-specific tyrosine kinase inhibitors for development for non-small cell lung cancer. Semin Oncol 2004; 31:83–92.
43. Perez-Soler R. The role of erlotinib (Tarceva, OSI 774) in the treatment of non-small cell lung cancer. Clin Cancer Res 2004;10:4238–40s.
44. Ciardiello F, Caputo R, Bianco R, et al. Antitumor effect and potentiation of cytotoxic drugs activity in human cancer cells by ZD-1839 (Iressa), an epidermal growth factor receptor-selective tyrosine kinase inhibitor. Clin Cancer Res 2000;6:2053–63.
45. Wakeling AE, Guy SP, Woodburn JR, et al. ZD1839 (Iressa): an orally active inhibitor of epidermal growth factor signaling with potential for cancer therapy. Cancer Res 2002;62:5749–54.
46. Perez-Soler R, Chachoua A, Hammond LA, et al. Determinants of tumor response and survival with erlotinib in patients with non-small-cell lung cancer. J Clin Oncol 2004;22:3238–47.
47. Lu C, Speers C, Zhang Y, et al. Effect of epidermal growth factor receptor inhibitor on development of estrogen receptor-negative mammary tumors. J Natl Cancer Inst 2003;95:1825–33.
48. Di Gennaro E, Barbarino M, Bruzzese F, et al. Critical role of both p27KIP1 and p21CIP1/WAF1 in the antiproliferative effect of ZD1839 ("Iressa"), an epidermal growth factor receptor tyrosine kinase inhibitor, in head and neck squamous carcinoma cells. J Cell Physiol 2003;195:139–50.
49. Sgambato A, Camerini A, Faraglia B, et al. Targeted inhibition of the epidermal growth factor receptor-tyrosine kinase by ZD1839 ("Iressa") induces cell-cycle arrest and inhibits proliferation in prostate cancer cells. J Cell Physiol 2004;201:97–105.

50. Shintani S, Li C, Mihara M, et al. Gefitinib ("Iressa", ZD1839), an epidermal growth factor receptor tyrosine kinase inhibitor, up-regulates p27KIP1 and induces G_1 arrest in oral squamous cell carcinoma cell lines. Oral Oncol 2004;40:43–51.
51. Chang GC, Hsu SL, Tsai JR, et al. Molecular mechanisms of ZD1839-induced G_1-cell cycle arrest and apoptosis in human lung adenocarcinoma A549 cells. Biochem Pharmacol 2004;68:1453–64.
52. Chinnaiyan P, Huang S, Vallabhaneni G, et al. Mechanisms of enhanced radiation response following epidermal growth factor receptor signaling inhibition by erlotinib (Tarceva). Cancer Res 2005;65: 3328–35.
53. Zhang W, Siu LL, Moore MJ, Chen EX. Simultaneous determination of OSI-774 and its major metabolite OSI-420 in human plasma by using HPLC with UV detection. J Chromatogr B Analyt Technol Biomed Life Sci 2005; 814:143–7.
54. Ranson M, Wardell S. Gefitinib, a novel, orally administered agent for the treatment of cancer. J Clin Pharm Ther 2004;29:95–103.
55. Agapova LS, Ivanov AV, Sablina AA, et al. P53-dependent effects of RAS oncogene on chromosome stability and cell cycle checkpoints. Oncogene 1999;18: 3135–42.
56. Hahn WC, Dessain SK, Brooks MW, et al. Enumeration of the simian virus 40 early region elements necessary for human cell transformation. Mol Cell Biol 2002;22:2111–23.
57. Duursma A, Agami R. p53-Dependent regulation of Cdc6 protein stability controls cellular proliferation. Mol Cell Biol 2005;25:6937–47.

Dimethyl-celecoxib, a derivative of the COX-2 inhibitor celecoxib that lacks COX-2 inhibitory activity, sensitizes human lung cancer cells to tumor necrosis factor-related apoptosis-inducing ligand (TRAIL) through induction of DR5 and downregulation of c-FLIP. Shuzhen Chen,[1] Xiangguo Liu,[1] Ping Yue,[1] Axel H. Schönthal,[2] Fadlo R. Khuri,[1] and Shi-Yong Sun.[1] [1]*Winship Cancer Institute, Emory University School of Medicine, Atlanta, Georgia and* [2]*University of Southern California, Los Angeles, California.*

The cyclooxygenase-2 (COX-2) inhibitor, celecoxib, exhibits anticancer activity in both preclinical studies and clinical practice. However, celecoxib has relatively weak apoptosis-inducing activity and modest cancer therapeutic efficacy. Therefore, efforts have been made to develop derivatives of celecoxib with superior anticancer activity. Dimethyl-celecoxib (DMC) is just such a derivative which lacks COX-2-inhibitory activity. Several preclinical studies have demonstrated that DMC has better apoptosis-inducing activity than celecoxib albeit with undefined mechanisms and exhibits anticancer activity in animal models. In this study, we examined the effects of DMC on the growth of human lung cancer cells as well as its cooperative effect with tumor necrosis factor-related apoptosis-inducing ligand (TRAIL) on induction of apoptosis and the underlying mechanisms. By comparing the effects of DMC and celecoxib on the growth of a group of human lung cancer cell lines, we found that DMC decreased cell survival with IC_{50}s ranging from 10 μM to 20 μM, whereas celecoxib did so with IC_{50}s ranging between 20 and 30 μM, indicating that DMC is more effective than celecoxib in decreasing the survival of lung cancer cells. When cells were treated with the combination of DMC and TRAIL, enhanced or synergistic effects in reduction of cell survival and induction of apoptosis including activation of caspases were observed in comparison with the effects in cells exposed to each agent alone. To understand the mechanisms underlying this synergy, we also analyzed the effects of DMC on modulation of several apoptosis-related genes. We found that DMC rapidly increased DR5 levels and reduced c-FLIP (both $FLIP_L$ and $FLIP_S$) levels starting from 2 h post treatment while having limited effects on modulating the levels of other proteins including DR4, Bcl2, Bcl-X_L and Bax. Importantly, enforced expression of $FLIP_L$ or silencing of DR5 expression using DR5 small interfering RNA (siRNA) abrogated the enhanced effects on induction of apoptosis by the combination of DMC and TRAIL, indicating that both DR5 upregulation and c-FLIP reduction contribute to cooperative induction of apoptosis by the combination of DMC and TRAIL. Collectively, we conclude that DMC sensitizes TRAIL-induced apoptosis in human lung cancer cells via induction of DR5 and downregulation of c-FLIP. (Supported by GCC Distinguished Cancer Scholar award and DOD grant W81XWH-04-1-0142-VITAL)

c-Jun N-terminal kinase (JNK)-independent c-FLIP downregulation contributes to induction of apoptosis by the novel synthetic triterpenoid methyl-2-cyano-3, 12-dioxooleana-1, 9-dien-28-oate (CDDO-Me) in human lung cancer cells.

Wei Zou,[1] Shuzhen Chen,[1] Xiangguo Liu,[1] Ping Yue,[1] Michael B. Sporn,[2] Fadlo R. Khuri,[1] and Shi-Yong Sun.[1]

[1]*Winship Cancer Institute, Emory University School of Medicine, Atlanta, Georgia and* [2]*Dartmouth Medical School, Hanover, New Hampshire.*

The novel synthetic triterpenoid methyl-2-cyano-3, 12-dioxooleana-1, 9-dien-28-oate (CDDO-Me) induces apoptosis of cancer cells, enhances tumor necrosis factor-related apoptosis-inducing ligand (TRAIL)-induced apoptosis, and exhibits potent anticancer activity in animal models with a favorable pharmacokinetic profile. Thus, CDDO-Me is being tested in Phase I clinical trials. In an effort to understand the mechanism by which CDDO-Me induces apoptosis, particularly in human lung cancer cells, we previously demonstrated that CDDO-Me induces apoptosis in human lung cancer cells involving c-Jun N-terminal kinase (JNK)-dependent upregulation of death receptor 5 (DR5) expression. In the current work, we further show that CDDO-Me downregulates the levels of c-FLIP, a major inhibitor of death receptor-mediated caspase-8 activation, which contributes to induction of apoptosis by CDDO-Me in human lung cancer cells. CDDO-Me rapidly and potently decreased c-FLIP levels including both long ($FLIP_L$) and short ($FLIP_S$) forms of c-FLIP in multiple human lung cancer cell lines. The presence of the proteasome inhibitor MG132, but not the JNK inhibitor SP600125 or JNK siRNA, prevented CDDO-Me-induced c-FLIP reduction. Thus, CDDO-Me induces proteasome-dependent c-FLIP degradation independently of JNK activation. Importantly, overexpression of c-FLIP (e.g., $FLIP_L$) in both A549 and H157 cell lines protected cells from CDDO-Me-induced apoptosis, indicating that c-FLIP downregulation is involved in CDDO-Me-initiated apoptosis. Given our previous finding that CDDO-Me induces apoptosis involving DR5 upregulation, we collectively conclude that the activation of the extrinsic apoptotic pathway via DR5 induction and c-FLIP downregulation plays a pivotal role in CDDO-Me-induced apoptosis in human lung cancer cells. (Supported by GCC Distinguished Cancer Scholar award and DOD grant W81XWH-04-1-0142-VITAL)

American Association for Cancer Research | SAVING LIVES THROUGH RESEARCH

97th Annual Meeting 2006

ABSTRACT SUBMITTER

Print this Page for Your Records Close Window

Control/Tracking Number: 06-AB-6978-AACR
Activity: Abstract Submission
Current Date/Time: 11/14/2005 7:20:24 PM

Existence of clonal and subclonal outgrowths in the bronchial epithelium and stroma of current smokers

Short Title:
Clonal outgrowth in smokers

Author Block: *Tao Lu, Ignacio I. Wistuba, Walter N. Hittelman.* UT MD Anderson Cancer Center, Houston, TX

The identification of individuals at high risk for lung cancer is critical for individualized clinical management and is important for the identification of suitable subjects for chemoprevention trials. Using chromosome in situ hybridization (CISH) technology, we previously demonstrated the presence of chromosomal instability and multifocal clonal/subclonal outgrowths in the bronchial epithelium of current and former smokers. We also verified the presence of these clonal/subclonal outgrowths in normal-appearing bronchial epithelium in lung cancer resections using fluorescence inter-simple sequence repeat PCR (FISSR-PCR) analysis, a DNA fingerprinting methodology. To evaluate and compare FISSR-PCR and CISH technologies for accessing genetic instability and clonal/subclonal outgrowth, we subjected frozen bronchial biopsies obtained prior to entry onto a chemoprevention trial to FISSR-PCR analysis from sixteen (16) current smokers without lung cancer. The group of biopsies from these same individuals have previously been analyzed by CISH and exhibited a wide range of chromosomal changes. Multiple regions (i.e., 1-4 areas each) of bronchial epithelium and stroma were microdissected, and purified genomic DNA was analyzed by FISSR-PCR using three sets of primers ($(CA)_8RG$, $(CA)_8RY$, and $(AGC)_4Y$), providing a maximum of 350 informative DNA bands of varying lengths. Overall, we detected from 0 to 55 total band changes per microdissected epithelial region (median = 1.6 per 100 DNA bands). Different regions within the same bronchial biopsies showed both common and distinct DNA band changes, suggesting subclonal variations even within a single biopsy. We also detected from 0-20 total band changes per microdissected stromal region (median = 1.0 per 100 DNA bands), suggesting the presence of clonal outgrowths even in the stroma. Interestingly, bronchial biopsies with high clonal frequencies showed increased clonal

change in the associated stroma (p =0.04, two-tailed chi square). Importantly, bronchial biopsies from individuals showing high clonal changes by FISSR-PCR also showed evidence of high clonal change by CISH ($R^2 = 0.3$). These results confirm the existence of clonal/subclonal outgrowths in both the bronchial epithelium and stroma of smokers. With future improvements in microdissection, automated genomic DNA extraction, and DNA sequencing, FISSR-PCR has potential to be a sensitive method with high dynamic range to detect clonal/subclonal outgrowths in lung tissue. Such a methodology may be of use in identifying individuals at high risk for developing lung cancer. Supported in part by DAMD17-02-1-0706, NIH/NCI CA-91844, and EDRN NCI CA-86390.
Author Disclosure Block: **T. Lu**, None; **I.I. Wistuba**, None; **W.N. Hittelman**, None.

Submitted to AACR, 2006.

Analysis of *EGFR* Abnormalities in the Sequential Pathogenesis and Progression of Lung Adenocarcinoma.

Ximing Tang, Marileila Varella-Garcia, Ana Carolina Xavier, Xiaoqing Bi, Natalie Ozburn, Waun Ki Hong, Ignacio I. Wistuba. Departments of Thoracic/Head and Neck Medical Oncology and Pathology, UT-MD Anderson Cancer Center, Houston, TX, and University of Colorado Cancer Center, Aurora, CO.

EGFR tyrosine kinase (TK) domain mutations, increased gene copy number and protein overexpression have been associated to lung cancer pathogenesis and correlated with response to EGFR TK inhibitors in lung adenocarcinoma. However, the sequence of these molecularly abnormal events in the pathogenesis and progression of lung adenocarcinoma is unknown. To elucidate this question, we performed a detailed mapping analysis correlating in the same tissue sites *EGFR* mutation, gene copy number and protein immunohistochemistry (IHC) expression in 94 formalin-fixed tissue sites comprising normal bronchial/bronchiolar epithelium (NBE; N=22), primary tumor (PT; N=43) and metastasis (MT; N=29) histologies obtained from 9 surgically resected *EGFR* mutant (exons 19 and 21) lung adenocarcinomas. *EGFR* mutation analysis was performed by PCR and direct sequencing from DNA extracted from precisely microdissected tissues. *EGFR* gene copy number analysis was performed using FISH, and high level of polysomy and gene amplification were considered as increased copy number. Semi-quantitative IHC expression analysis of cytoplasmic and cell membrane EGFR and phosphorylated EGFR (p-EGFR) was performed. *EGFR* mutation was found in 18% (4/22) NBE, 91% (39/43) PT and 86% (25/29) MT sites. Low genomic gain was found in 8 NBE sites (37%), but increased copy number was not detected. Of interest, the 4 *EGFR* mutant NBE sites exhibited normal gene copy number. No difference in the frequency of *EGFR* increased copy number was found comparing PT (39/43, 93%) and MT (25/29, 86%) sites. *EGFR* mutation frequency (89% vs. 41%; $P<0.0000$) and mutant to wild-type ratio mean (1.04 vs. 0.49, $P<0.0001$) in the sequencing chromatograms were significantly higher in tissue sites with increased copy number than areas with normal or low genomic gain. *EGFR* mutation heterogeneity, with two or more mutant genotypes in the same tumor case, was found in 4 out of 9 (44%) PT cases, and this phenomenon was not observed in corresponding MTs. *EGFR* copy number heterogeneity was more frequent in PT than MT; however, significant copy number progression from PT to MT was not observed. Although no correlation was found between EGFR IHC and *EGFR* mutation or copy number status, significantly higher levels of EGFR and p-EGFR IHC expression were detected in mutant MT compared to PT sites ($P= 0.005$ to <0.0001). Our findings indicate that *EGFR* mutation precedes genomic gain in the sequential pathogenesis of lung adenocarcinoma. In tumor specimens, there was strong correlation between *EGFR* mutation and increased copy number. The heterogeneity of *EGFR* mutation and gene copy number in primary tumor, but not in metastasis, and the increased expression of total and p-EGFR IHC in metastasis sites are probably associated to tumor progression and could have clinical implications when these abnormalities are searched in small clinical specimens. Supported by grants W81XWH0410142 and W81XWH0520027.

Annual Meeting 2007
ABSTRACT SUBMITTER
American Association for Cancer Research

Print this Page for Your Records Close Window

Control/Tracking Number: 07-AB-4637-AACR
Activity: Abstract Submission
Current Date/Time: 11/28/2006 5:55:43 PM

Increased genetic instability and metastases from spontaneous murine lung adenocarcinomas with K-ras and p53 R172HΔg mutations

Short Title:
genetic instability and lung tumor

Author Block: *Tao Lu, Shuling Zheng, Jonathan M. Kurie, Guillermina Lozano, Walter N. Hittelman.*
UT M.D. Anderson Cancer Ctr., Houston, TX

Abstract:
Lung adenocarcinomas spontaneously occur in mice with a latent K-ras G12D mutation but do not metastasize. Mice carrying a p53 R172HΔg mutation have previously been shown to exhibit a relatively high metastatic rate compared to p53 +/- mice, suggesting a gain-of-function mechanism. Our unpublished results show that when K-ras G12D mice were crossed with p53 R172HΔg mice, lung adenocarcinomas developed with high metastatic potential, more closely mimicking the metastatic nature of human lung cancer. To better understand the underlying driving force for a more aggressive tumor phenotype in the K-ras G12D/p53 R172HΔg mice, we compared the degree of clonal genetic heterogeneity in normal lung tissue, primary lung tumors, and metastases between K-ras G12D mice on a wild type p53 (n=2 mice) versus on a p53 R172HΔg (n=9 mice) versus on a p53 +/- (n=2 mice) background. The relative number of clonal genetic changes was determined using fluorescence inter-simple sequence repeat PCR (FISSR-PCR), a DNA fingerprinting technique where individual DNA band gains or losses indicate clonal and subclonal changes. Genomic DNA was purified from isolated normal lung tissue, primary lung tumor and metastatic organ sites, was subjected to FISSR-PCR and the band patterns were compared to that derived from normal uninvolved tissue. The frequencies of band changes were enumerated and normalized to the number of changed bands per 100 bands analyzed. In K-ras G12D mice, the lung adenocarcinomas showed slightly increased clonal change when compared to histologically normal adjacent lung tissue in the same mice (i.e., 1.2 ± 0.3 band changes/100 bands versus 0.9 ± 0.5 band changes/100 bands, respectively). In contrast, while normal appearing lung tissue from K-ras G12D/p53 R172HΔg mice showed similar low levels of clonal change to K-ras G12D mice (0.7 ± 0.2 band changes/100 bands), primary lung tumors from K-ras G12D/p53 R172HΔg mice showed significantly increased clonal change (3.7 ± 2.8 band changes/100 bands). Strikingly, metastatic lesions in K-ras G12D/p53 R172HΔg mice showed an even higher degree of clonal change (7.2 ± 5.1 band changes/100 bands). These results show that the p53 R172HΔg mutation background leads to increased genetic instability and clonal outgrowth in the lungs of mice carrying the K-ras G12D mutation, associated with higher grade tumors with increased

metastatic potential. Because the normal appearing lung tissue of K-ras G12D and K-ras G12D/p53 R172HΔg mice showed similar low levels of genetic instability, these results also suggest that it is the combination of K-ras and p53 R172HΔg mutations that confer enhanced genetic instability, clonal outgrowth, and an increased rate of malignant progression. Supported in part by DAMD17-02-1-0706, NIH/NCI CA-91844, EDRN NCI CA-86390 and DAMD17-01-1-0689.

Author Disclosure Block: **T. Lu**, None; **S. Zheng**, None; **J.M. Kurie**, None; **G. Lozano**, None; **W.N. Hittelman**, None.

Additional Disclosures (Complete):

The presenter of this abstract will discuss commercial products, devices, or technology in this presentation, as outlined below. : No - [Type "none" in the first box below]

1. Generic Name: : None

I anticipate discussing an OFF-LABEL use of a commercial product/device in this educational activity. : No - [Type "none" in the box below]

If you selected "Yes" above, you must indicate the product/device and describe its intended use in the box below. If you selected "No" above, you must type "none" in the box below: : None

Investigational Use (Not approved by the FDA for any purpose):

I anticipate discussing an INVESTIGATIONAL use of a commercial product/device in this educational activity. : No - [Type "none" in the box below]

If you selected "Yes" above, you must indicate the product/device and describe its intended use in the box below. If you selected "No" above, you must type "none" in the box below: : None

I agree with the declaration statement above. : True

Name: : Tao Lu

Date [mm/dd/yyyy]: : 11/27/2006

Category and Subclass (Complete): TB01-01 Mouse models of human cancer

Primary Organ Site (Complete):

Organ Site Classification: : **Applicable.** My abstract does refer to a specific primary organ site/tumor type as indicated below.

Primary Organ Site: : Lung cancer: non-small cell

Keywords/ Indexing (Complete): Lung cancer ; Genetic instability ; Metastases ; Mouse models

Chemical Structure Disclosure (Complete): NOT APPLICABLE. No chemical structures were used to generate the data in this abstract.

Sponsor (Complete):

2007 Travel Awards (Complete):

Payment (Complete): Your credit card order has been processed on Tuesday 28 November 2006 at 10:12 AM.

Status: Complete

Submitted to AACR, 2006.

Analysis of *EGFR* Abnormalities in the Sequential Pathogenesis and Progression of Lung Adenocarcinoma.

Ximing Tang, Marileila Varella-Garcia, Ana Carolina Xavier, Xiaoqing Bi, Natalie Ozburn, Waun Ki Hong, Ignacio I. Wistuba. Departments of Thoracic/Head and Neck Medical Oncology and Pathology, UT-MD Anderson Cancer Center, Houston, TX, and University of Colorado Cancer Center, Aurora, CO.

EGFR tyrosine kinase (TK) domain mutations, increased gene copy number and protein overexpression have been associated to lung cancer pathogenesis and correlated with response to EGFR TK inhibitors in lung adenocarcinoma. However, the sequence of these molecularly abnormal events in the pathogenesis and progression of lung adenocarcinoma is unknown. To elucidate this question, we performed a detailed mapping analysis correlating in the same tissue sites *EGFR* mutation, gene copy number and protein immunohistochemistry (IHC) expression in 94 formalin-fixed tissue sites comprising normal bronchial/bronchiolar epithelium (NBE; N=22), primary tumor (PT; N=43) and metastasis (MT; N=29) histologies obtained from 9 surgically resected *EGFR* mutant (exons 19 and 21) lung adenocarcinomas. *EGFR* mutation analysis was performed by PCR and direct sequencing from DNA extracted from precisely microdissected tissues. *EGFR* gene copy number analysis was performed using FISH, and high level of polysomy and gene amplification were considered as increased copy number. Semi-quantitative IHC expression analysis of cytoplasmic and cell membrane EGFR and phosphorylated EGFR (p-EGFR) was performed. *EGFR* mutation was found in 18% (4/22) NBE, 91% (39/43) PT and 86% (25/29) MT sites. Low genomic gain was found in 8 NBE sites (37%), but increased copy number was not detected. Of interest, the 4 *EGFR* mutant NBE sites exhibited normal gene copy number. No difference in the frequency of *EGFR* increased copy number was found comparing PT (39/43, 93%) and MT (25/29, 86%) sites. *EGFR* mutation frequency (89% vs. 41%; $P<0.0000$) and mutant to wild-type ratio mean (1.04 vs. 0.49, $P<0.0001$) in the sequencing chromatograms were significantly higher in tissue sites with increased copy number than areas with normal or low genomic gain. *EGFR* mutation heterogeneity, with two or more mutant genotypes in the same tumor case, was found in 4 out of 9 (44%) PT cases, and this phenomenon was not observed in corresponding MTs. *EGFR* copy number heterogeneity was more frequent in PT than MT; however, significant copy number progression from PT to MT was not observed. Although no correlation was found between EGFR IHC and *EGFR* mutation or copy number status, significantly higher levels of EGFR and p-EGFR IHC expression were detected in mutant MT compared to PT sites ($P= 0.005$ to <0.0001). Our findings indicate that *EGFR* mutation precedes genomic gain in the sequential pathogenesis of lung adenocarcinoma. In tumor specimens, there was strong correlation between *EGFR* mutation and increased copy number. The heterogeneity of *EGFR* mutation and gene copy number in primary tumor, but not in metastasis, and the increased expression of total and p-EGFR IHC in metastasis sites are probably associated to tumor progression and could have clinical implications when these abnormalities are searched in small clinical specimens. Supported by grants W81XWH0410142 and W81XWH0520027.

Submitted to AACR, 2006

"Field" Defect Abnormalities in Lung Adenocarcinoma: *KRAS* vs. *EGFR* Mutant Tumors.

Ximing Tang, Xiaoqing Bi, Natalie Ozburn, Waun Ki Hong, Ignacio I. Wistuba. Departments of Thoracic/Head and Neck Medical Oncology and Pathology, UT-MD Anderson Cancer Center, Houston, TX.

Lung adenocarcinoma is characterized by diagnosis at advanced stages, and new strategies for early diagnosis are needed. Although little is known about the histological precursors and the molecular events preceding the development of lung adenocarcinoma, at least 2 molecular pathways have been suggested: *KRAS* and *EGFR* mutation; the latter associated to non-smoking and East Asian ethnicity. We recently reported that *EGFR* mutations were detected in histologically normal bronchial/bronchiolar epithelium (NBE) in 43% of patients with *EGFR* mutant lung adenocarcinomas (Cancer Res 65: 7568-72, 2005), indicating that this mutation represents an early "field" event in the pathogenesis of this neoplasm. To further investigate the molecular abnormalities in the lung respiratory epithelium "field" in lung adenocarcinoma patients, we performed a detailed mapping analysis of *KRAS* and *EGFR* mutations in NBE adjacent to mutant and wild-type tumors. In NBE sites we correlated *EGFR* mutation status with immunohistochemical (IHC) expression of EGFR and TTF-1 (a marker for lung terminal respiratory cell differentiation) proteins. We selected 191 NBE sites from 50 surgically resected lung adenocarcinomas, including 12 *KRAS* mutant, 24 *EGFR* mutant (12, East Asian ethnicity), and 14 wild-type tumors. *KRAS* (codons 12 and13) and *EGFR* (exons 19 and 21) mutation analysis was performed by PCR-sequencing using DNA extracted from microdissected tissue. Semi-quantitative IHC expression analysis of EGFR, phosphorylated EGFR (p-EGFR) and TTF-1 was performed. Our main findings were: a) No *KRAS* mutation was detected in 61 NBE sites obtained from 12 *KRAS* mutant and 11 wild-type tumors. b) Examining more cases than the previously published, similar frequency of *EGFR* mutation in NBE by patients (12/24, 50%) and by epithelial site (22/73, 30%) were detected in *EGFR* mutant adenocarcinomas. However, now we found *EGFR* mutation in 6 (11%) NBE sites from 3 (12%) patients with *EGFR* wild-type tumors. d) Previously the same type of *EGFR* mutation was detected comparing NBE and corresponding tumor; however, now we identified 5 NBE sites from 3 East Asian patients demonstrating different mutation pattern than their corresponding tumors. e) No correlation between EGFR and p-EGFR expression and *EGFR* mutation was detected in NBE, and, interestingly, 13/21 (62%) of *EGFR* mutant NBE sites did not expressed TTF-1. Our findings indicate that in lung adenocarcinoma a "field" defect phenomenon is observed in respiratory epithelium for *EGFR* mutation, but not for *KRAS* mutation. We have extended our recently published findings by detecting *EGFR* mutation in NBE of a small subset of East Asian patients with wild-type tumors, and by detecting some cases with different mutation patterns comparing NBE and corresponding tumor. The finding that most *EGFR* mutant NBE lacked TTF-1 expression suggests that terminal respiratory epithelial cells may not be the only cell type affected by *EGFR* mutation. Supported by grant W81XWH0410142.

Submitted to AACR, 2007.

Caveolin-1 Gene Methylation is a Field Effect Phenomenon in Lung Cancer Patients

Ximing Tang, Natalie Ozburn, Ignacio I. Wistuba. UT MD Anderson Cancer Center, Houston, Texas 77030

Caveolin-1 (Cav-1), an essential structural constituent of caveolae that plays an important role in cellular process such as transport and signaling, has been implicated in the development of several cancers, including lung. Reduction and absence of Cav-1 expression has been reported in almost all small cell lung cancers (SCLC) and a subset of non-small cell lung cancers (NSCLC), mostly due to gene promoter methylation. Although several studies have provided information on the molecular characterization of NSCLC premalignant changes, they have been poorly documented for SCLCs. For lung cancer, molecular changes commence in histologically normal epithelium as field effect phenomenon. To better understand the role of *CAV1* gene in the early pathogenesis of lung cancers we investigated gene methylation and protein immunohistochemical (IHC) expression in the lung respiratory field by examining histologically normal respiratory epithelia adjacent to lung tumors. We studied formalin-fixed surgically resected tumor specimens from 100 lung cancers, including 40 SCLCs and 60 NSCLCs (48 adenocarcinomas, AC; 12 squamous cell carcinomas, SCC). For *CAV1* methylation analysis we extracted DNA from 202 precisely microdissected tissue sites, including 101 tumors and 101 normal epithelia (79 small bronchi and 22 bronchioles). Among normal epithelial sites, 30 were located inside tumors (INE), 60 closed to tumors (<1mm, ONE), and 11 distant to tumors (DNE). The DNA was undergone methylation specific polymerase chain reaction for assessing *CAV1* methylation and the results were confirmed by sequencing. Cav-1 protein IHC expression was studied in the same tumoral and epithelial sites examined for methylation. A high level of *CAV1* methylation rate was detected in tumors, being more frequent in SCLC (100%) compared to AC (49%) and SCC (50%). NSCLCs, but not SCLCs, demonstrated heterogeneity in *CAV1* methylation in 6 cases in which multiple tumor sites were examined. *CAV1* methylation was also frequently detected in histologically normal respiratory epithelia adjacent to lung tumors, without differences in methylation frequency by lung tumor histology (SCLC 64%, AC 69% and SCC 63%), and type (bronchi 65% and bronchioles 66%) and location (INE 67%, ONE 66% and DNE 64%) of respiratory structures examined. Gene methylation was highly correlated with protein expression in tumor (90%) and normal epithelium (95%) tissue sites. Our findings indicate that *CAV1* methylation is a frequent molecular abnormality in lung tumors, especially SCLC. The finding of high frequency of Cav-1 abnormalities in normal bronchial and bronchiolar epithelia adjacent to lung cancers suggests that *CAV1* may be involved in the early pathogenesis of lung cancer as field effect phenomenon (Supported by grant VITAL W81XWH-04-1-0142).

The 2006 AACR, Abstract #2849

Oncogenic manipulation and biologic selection for complete tumorigenic transformation of immortalized normal human bronchial epithelial cells

Mitsuo Sato, Woochang Lee, Luc Girard, Ruben D. Ramirez, David S. Shames, Adi F. Gazdar, Jerry W. Shay and John D. Minna
UT Southwestern Medical Center, Dallas, TX

Purpose: To develop an *in vitro* model system to study the multi-step pathogenesis of lung cancer. Introduction: We established a series of cdk4/hTERT-immortalized human bronchial epithelial cell lines (HBECs) which can be genetically manipulated, are able to differentiate into mature airway cells in organotypic cultures, but do not form colonies in soft agar or tumors in nude mice. Previously, we observed that combinations of p53 knockdown with mutant *EGFR* or with physiological levels of oncogenic $KRAS^{V12}$ progressed HBECs part but not all of the way towards malignancy. These cells form colonies in soft agar, but fail to form tumors in nude mice. In the present study we evaluated various combinations of oncogenic manipulation, higher levels of expression of oncogenic $KRAS^{V12}$, and the biologic behavior of clones selected to grow to large size in soft agar. Methods: HBEC3 immortalized with cdk4 and hTERT was engineered with various vectors systems to have stable: p53 knockdown (with shRNA); PTEN knockdown; express oncogenic $KRAS^{V12}$ at physiologic or 10 fold higher; express mutant EGFR (deletion and missense mutants). These were made alone and in combination. These and selected colonies were then tested for soft agar colony formation and subcutaneous and orthotopic tumor formation in nude mice. Results: Without oncogenic manipulation soft agar colony forming efficiency (CFE) was <~0.1%. With various oncogenic manipulations including higher expression of $KRAS^{V12}$ alone soft agar colony CFEs were ~3%, and the combination of higher $KRAS^{V12}$ and p53 knockdown increased CFE to 8%. None of these were tumorigenic. However, the combination of higher $KRAS^{V12}$ and p53 knockdown but not high $KRAS^{V12}$ alone led to development of a subset of very large soft agar colonies (~0.1-0.2%). These large colonies were isolated and found to have CFE of 10~15% with large colony numbers increased 10 fold. 5 of the large colonies were expanded and tested for tumorgenicity and 2 were capable of forming subcutaneous and orthotopic (bronchus) tumors. Of interest one was an adenocarcinoma and the other was a squamous cell carcinoma. In addition, the adenocarcinoma expressed high levels of $KRAS^{V12}$ and the squamous carcinoma expressed normal levels of $KRAS^{V12}$. Conclusion: Multiple oncogenic changes found in lung cancer (telomerase expression, p16 bypass, p53 ablation, mutant EGFR, oncogenic KRAS) introduced into HBECs are still not capable of full oncogenic transformation. However, a subset of cells selected for the ability to form large colonies in soft agar are capable of tumor formation and tend to differentiate into two non-small cell lung cancer phenotypes (adenocarcinoma and squamous cell cancer). The expression, genetic, and epigenetic changes as well as the stem cell like characteristics of these subsets of cells are being investigated to delineate the key final steps in lung cancer pathogenesis. This study was supported in part by the Department of Defense VITAL program (W81XWH-04-1-0142)

The 2006 AACR, Abstract #3582

Protein profiles of lung tumorigenesis using immmobilized metal ion adsorption chromatography

Hening Ren, David Hawke, Zuo M Chu and Li Mao
UT MD Anderson Cancer Center, Houston, TX

Understanding the molecular process of lung cancer development is important for development of novel diagnostic, preventive, and therapeutic strategies. Proteomics is a promissing approache to extend such understanding. One of the major limitations of this approache is the inability to reveal and identify lower abundant proteins. Fractionation and enrichment of cancer proteome is a logic step in expanding the application of proteomics in tumor classification and biomarker discovery. Immobilized metal ion adsorption chromatography (IMAC), also know as metal chelate affinity chromatography (MCAC), selectively enrich proteins with exposed surface histidine, cysteine, and tryptophan. To test the utility of IMAC in protein marker identification, we performed IMAC enrichment using proteins extracted from 4 lung cancer cell lines and 4 immortalized human bronchia epithelia (HBE) cell lines, followed by 2-dimensional electrophoresis (2DE) of the enriched proteins. Using this strategy, we observed substantially more proteins differentially presented between the two groups of cell lines. More than 100 such proteins were revealed when a broad range (pH 3-10) isoelectric focusing condition was used. The identities of 33 of the protein spots were further characterized by tandem mass spectrometry. Many of the proteins were low abundant proteins. Among them, stratifin, thioredoxin peroxidase, and guanine monophosphate synthetase, have transcript abundance ranging from 0.3% to 5% of the abundance of the actin transcript in lung tissues. Our results demonstrate a utility of IMAC-2DE approach in proteomics analysis of tumorigenic processes. (Supported by Department of Defense grant W81XWH-04-1-0142)

The 2006 AACR, Abstract #2864

Detecting low-abundant proteins in human plasma proteome by using multi-lectin affinity chromatography and two-dimensional gel electrophoresis

Hidetoshi Kawaguchi, Hening Ren, Wenhua Lang, Zuoming Chu, You-Hong Fan and Li Mao
University of Texas M.D. Anderson Cancer Center, Houston, TX

Glycosylation is one of the most common post-translational protein modifications and plays a fundamental role in a diverse set of biologic processes. These plasma glycoproteins can be enriched using lectins, which bind to specific sugar structures. To determine the utility of a multi-lectin column, we analyzed two independent sets of plasma samples, each consisting of 400µl mixture of plasma from five healthy controls. Captured proteins in the column were released sequentially using inhibitory carbohydrates and collected stepwise. The total glycoprotein bound to the column was 10.9% of total plasma proteins including 2.3% to jacalin, 3.7% to ConA, and 4.9% to WGA. Therefore, this column provides 20-44 folds enrichment of plasma glycoproteins in each fractionation. We further performed two-dimensional gel electrophoresis (2-DE) and generated reproducible profiles of enriched plasma glycoproteins. Several major plasma proteins, such as albumin, transferrin, immunoglobulin G, and α1-antitrypsin, were largely removed by the enrichment strategy. In the areas of high molecular weight proteins on the 2-DE gels, substantially more protein spots were visible in the sample with enrichment than its un-enriched counterpart (289 spots vs. 117 for WGA fractionation as an example). Our results demonstrate that the multi-lectin affinity-2-DE approach can help visualize lower-abundant plasma proteins and may improve the identification of plasma protein markers. This strategy has potential to be used to identify plasma protein markers associated with diseases, such as cancer. (Supported in part by Department of Defense grants DAMD17-01-1-01689-1 and W81XWH-04-1-0142; National Cancer Institute grants CA91844 and CA106451)

APPENDIX 3

Protocols

PROTOCOL

A Phase IIb Vanguard Study Characterizing the Occurrence of Recurrent or Second Primary Tumors in Patients with a Prior History of a Definitively Treated Stage I/II Head and Neck or Non-Small Cell Lung Cancer who are Current or Former Smokers

TABLE OF CONTENTS

TABLE OF CONTENTS (CONT)

TABLE OF CONTENTS (cont)

1.0 Objectives

Patients who have surgically resected early stage head and neck and lung cancer are at significant risk for developing recurrent or second primary tumors (SPTs). Patients who continue to smoke (current smokers) and even those who have quit smoking (former smokers) have an increased risk of developing another tumor. Adjuvant therapy trials with radiation or chemotherapy have been controversial and these modalities are not considered to be the current standard of care in these high-risk patients. The outcomes of large scale chemoprevention trials have been uniformly disappointing. Novel biologic agents are beginning to be tested in the adjuvant or maintenance setting, but data is still early. Biologic agents in the metastatic setting for lung cancer have been disappointing and have yet to show a survival benefit in any treatment setting.

Follow-up measures such as CXR and sputum as screening or after surgical resection in these high risk patients have failed in preventing or detecting early recurrence or SPTs. Development of a risk model with intermediate biomarkers to predict risk is needed to help improve survival. Furthermore, treatment interventions in the adjuvant setting are needed in order to improve disease-free survival. To test this hypothesis we will perform a clinical characterization and biomarker-based clinical trial in patients with definitively treated stage I/II NSCLC and head and neck squamous cell carcinoma (HNSCC). We propose to study these high-risk patients in a comprehensive clinical trial "Vanguard Trial" which will closely follow patients with imaging, tissue and serologic markers. Also, we will study a series of biologic agents in the adjuvant setting.

Specific Aim 1: To assess the smoking-related disease-free survival in patients who are current or former smokers with a prior definitively-treated stage I/II lung or head and neck cancer.

Rationale: Patients who are current or former smokers and with a history of a prior early stage cancer at high risk for recurrence or SPTs. There are no standard interventions which have been proven to help reduce the risk or cancer occurrence. We plan to enroll patients into a vanguard trial and aggressively follow their post-surgical course with radiographic imaging, tissue (bronchial epithelium) and serum molecular markers, and autofluorescence bronchoscopy using a light-induced fluorescence endoscope (LIFE).

Specific Aim 2: To develop a risk model to help predict the likelihood of lung cancer development both imaging and biomarker based in this high-risk population.

Rationale: Patients with a history of a prior stage I/II head and neck or lung cancer who have had surgical resection are at high risk for recurrence or SPTs. There are no standard interventions which have been proven to help reduce the risk or cancer occurrence. Patients will have aggressive post-operative follow-up with analysis including frequent serologies, bronchial specimens and CT scanning. Trends in these multiple biomarkers would be analyzed and used to develop a predictive model.

We plan to enroll patients into one of four concurrent biologic adjuvant trials with targeted agents. These will be conducted as separate studies under the backdrop of the Vanguard trial. The primary endpoints will be histologic change as well as multiple secondary endpoints including safety/toxicity and biomarker modulation.

2.0 Significance and Background

2.1 Lung Cancer and Head and Neck Cancer

Lung cancer is the leading cause of cancer-related death among men and women in the United States (1). An estimated 159,900 Americans died of lung cancer in 2003. In recent years, the incidence of lung cancer has begun to decline among men (1). However, smoking-related lung cancer has continued to increase among women, surpassing even breast cancer as the leading cause of death among women (2). Despite aggressive treatment, the five-year survival rate for lung cancer remains approximately 15% (1). These grim facts point out to need for a radical change in our approach to lung cancer.

Head and neck squamous cell carcinoma (HNSCC) is the 5th leading cause of cancer incidence and the 6th leading cause of cancer death. Per year in the United States, there are approximately 40,400 new cancer cases and 12,300 cancer deaths (1). It is strongly associated with tobacco and alcohol use. In early stage disease (stage I and II) curative measures can be undertaken with surgery and radiation therapy. Treatment options for advanced or recurrent disease remain limited as advanced disease (stage III and IV) has a less than 30% cure rate. Prevention of recurrence and second primary tumors has been studied in patients with early HNSCC. No standard therapies exist as phase II trials have failed to demonstrate a survival advantage in phase III trials thus far. Many of these patients will develop SPTs in the lung as tobacco use is prevalent in about 85% of cases. Because of the poor survival in patients who develop lung cancer, the National Cancer Institute's Division of Cancer Prevention and Control has set prevention as the primary strategy in the control of lung cancer.

2.2 Smoking cessation and lung cancer prevention

Prevention of smoking and smoking cessation deserves a prominent place in the National Cancer Institute's programs to reduce mortality from cancer. Massive campaigns to educate the public about the hazards of cigarette smoking have resulted in a substantial reduction in the percentage of adults who smoke in the United States. Recent estimates suggest that approximately 50% of adults are former smokers (about 44 million people in the United States) (2, 3). Despite the reduction in lung cancer risk observed with smoking cessation (2), several studies have demonstrated that former smokers still have a higher lung cancer risk than non-smokers (4-6). Even ten years after smoking cessation, the risk remains significantly elevated for men (7). Former smokers account for a large proportion of lung cancers in this country and the current smoking trends indicate that the percentage is increasing. it appears that former

smokers will account for a growing percentage of all lung cancer cases. Thus, the risk of lung cancer in former smokers poses a substantial long-term health threat in this country. Strikingly, 50% of new lung cancer cases are among former smokers, a population numbering roughly 46 million people in the United States (8). Strategies to prevent lung cancer deaths in former smokers include early detection and chemoprevention.

Methods of early detection are now critical in lung cancer treatment. Screening techniques analyzing sputum cytology, chest x-rays and more recently, spiral computed tomography (CT) scans have been studied. Recent studies have specifically tested the efficacy of screening individuals at high risk with spiral CT scanning (9-11). These results, while provocative, are not yet definitive, and debate continues as to whether they are sufficient to mandate broad lung cancer screening programs. A study reported in 1999 used low-dose helical CT to screen 1,000 asymptomatic smokers or former smokers, who smoked at least one pack of cigarettes a day for 10 years, or two packs per day for 5 years. All were age 60 or older. All participants received chest x-rays and CT scans. CT detected from 1-6 non-calcified pulmonary nodules in 23% patients while CXR detected nodules in 7%. 27 of the 233 CT lesions were diagnosed as tumor whereas 7 of the 68 CXR lesions were malignant. 23 of the 27 CT tumors were diagnosed as stage I. Although this study shows potential promise in the use of CT for screening, additional trials will be needed before routine CT scanning can be deemed cost effective (11).

2.3 Chemoprevention

The past ten years has revealed the potential of chemoprevention in the reduction of mortality associated with common epithelial cancers. Tamoxifen was effective in primary prevention of breast cancers in high-risk women at high risk (12). Non-steroidal anti-inflammatory drugs (NSAIDs) reduced the risk of colorectal cancer in participants with familial adenomatous polyposis (12). Retinoids decreased the incidence of second primary tumors in participants with a prior squamous cell carcinoma of the head and neck (12). In contrast, the results of lung cancer chemoprevention trials have been disappointing. Several large-scale chemoprevention trials have been performed, including the Euroscan Trial, the Physicians Health Study, the Alpha-Tocopherol and Beta-Carotene (ATBC) trial, and the Beta-Carotene and Retinol Efficacy Trial (CARET), which involved thousands of active smokers followed for over ten years. These studies demonstrated no protective effect of treatment on lung cancer incidence (13-15). In fact, beta-carotene treatment appeared to act as a co-carcinogen, enhancing lung cancer incidence in active smokers. The failure of these large-scale clinical trials has taught us an important lesson; it may be premature to embark on large-scale trials that involve thousands of participants and cost millions of dollars prior to demonstrating the efficacy of a chemopreventive agent in small, biomarker-based clinical trials. Supporting a biomarker-based approach to predicting the efficacy of specific lung cancer chemopreventive agents, no effect was found of 13-*cis* retinoic acid on bronchial metaplasia and dysplasia in current smokers (16), which is similar to the outcome of the retinoid-based large-scale chemoprevention trials described above. Based on the data

outlined above, smoking cessation and primary prevention of smoking remain the most proven measures to prevent primary lung cancer. Patients who have had prior definitively treated tobacco-related cancers, primarily head and neck and lung cancers, are at higher risk (20-40%) for recurrence or second-primary tumors. No traditional therapies have proven effective to prevent lung cancer in this setting. Clearly, further strategies such as development of a model to assess risk and integration of biologic agents are needed.

2.4 Bronchial Histology

The highest risk of lung cancer occurs in patients with bronchial dysplasia. The presence of bronchial epithelial abnormalities is clearly linked to smoking. Several series have shown that these preneoplastic lesions arise from normal to hyperplasia to squamous metaplasia and then from mild to moderate and severe dysplasia, followed by carcinoma *in situ* and ultimately invasive squamous cell cancer (17, 18). A standard histologic classification system of preneoplastic lesions has therefore been established.

The highest risk of lung cancer occurs in subjects with dysplastic lesions and we have selected a patient population expected to have a high rate of dysplasia on bronchial biopsy. Currently, histologic assessment remains the gold standard since there are no definitive intermediate biomarkers for lung cancer development. We have previously shown that metaplasia index is not an optimal biomarker. However, histologic changes uncommonly regress spontaneously and are highly correlated with a number of intermediate biomarkers (19).

Over the past 5 years, a number of advancements have been made in the detection of bronchial premalignancy and early stage lung cancer using molecular and radiologic techniques. Molecular studies have shown that approximately 30% of lung adenocarcinomas contain mutated K-*ras* (20), and these mutations can be detected in premalignant bronchial biopsies (20). Bronchial washings and sputum samples, which contain cells shed from peripheral sites in the lung are other potential methods of screening participants for the presence of premalignant or malignant cells. Recently developed techniques based on polymerase chain reaction (PCR) and *in situ* hybridization technologies can detect molecular abnormalities in cells shed into stool, sputum, and urine with a sensitivity that far exceeds that of standard cytologic techniques (21-23). We have discovered evidence of clonal outgrowths in the bronchial epithelium of smokers and former smokers using molecular techniques that can detect DNA methlyation at CpG islands in the promoter regions of specific genes, chromosomal aneuploidy, and loss-of-heterozygosity at putative tumor suppressor loci (24). Fluorescence bronchoscopy, studied in smokers at high risk for lung cancer, found a unique lesion consisting of capillary blood vessels adjacent to and juxtaposed to squamous bronchial epithelium that was metaplastic or dysplastic (25). Hirsch et al. reported a majority of patients could be diagnosed solely on the results of LIFE if they had at least one biopsy with moderate or severe dysplasia. LIFE was statistically significantly more sensitive than WLB for detecting moderate dysplasia or worse. Angiogenic squamous dysplasia (ASD) was found to have markedly elevated

proliferative activity as well as some loss of heterozygosity at chromosome 3p. ASD was found in 54 of 158 high-risk smoking patients without carcinoma and 6 of 10 patients with squamous carcinoma. In nonsmokers, 0 of 16 had the presence of ASD. This suggests that ASD may represent an early, premalignant stage of bronchial carcinogenesis associated with increased lung cancer risk, even beyond that associated with standard histology.

2.5 Molecular Targets and Lung Cancer

As our understanding of cellular signaling pathways and their interactions with other signals broadens and their role in carcinogenesis progress, different biomarkers continued to be measured in order to predict outcome in epithelial cancers. HER2 in breast cancer is an example of a biomarker which predicts poor survival (26). Other biomarkers which may serve as prognostic variables in lung cancer as well as other epithelial cancers include epidermal growth factor receptor (EGFR), ras, vascular endothelial growth factor (VEGF), fhit and p53 (27-37). Development of targeted agents which disrupt various cellular signals may help disrupt the cellular growth pathways and in turn preventing development of carcinoma. Studies in the metastatic setting have demonstrated single-agent activity in some of these agents, however no difference in survival has been recorded (38). Several trials with single-agent biologic treatment are ongoing in definitively-treated patients.

2.6 Adjuvant Therapy for Lung Cancer

Based on the data outlined above, smoking cessation and primary prevention of smoking remain the most proven measures to prevent primary lung cancer. However, despite surgical treatment of early stage lung cancer (stage I/II), only 40-70% of patients are alive at 5 years. Additionally, patients who have had prior definitively treated tobacco-related cancers, primarily head and neck and lung cancers, are at higher risk (20-40%) for recurrence or second-primary tumors during their lifetime. No therapies have proven effective to prevent lung cancer in this setting.

Radiation therapy given after complete surgical resection was one of the earliest forms of adjuvant therapy explored. As reported in the PORT meta-analysis (39), 2,128 patients from several trials were compared. Results showed a detrimental effect of post-operative radiotherapy on survival with an absolute reduction of 7% at 2 years. Subgroup analysis suggested that this occurred in the N0-1 disease subgroup and not in the N2 group. As various surgical and radiotherapy techniques were used, randomized trials are still needed to further clarify the role of radiotherapy, especially in those patients with N2 disease.

Chemotherapy has been tested as adjuvant therapy in resected early stage primary lung cancers in multiple trials. Earlier trials prior to 1980 of single-agent chemotherapy as adjuvant therapy with alkylating agents failed to show a survival benefit and in fact, showed a detrimental effect on survival. A recent meta-analysis of all randomized trials over a 26 year period showed that the absolute risk of death was reduced by 3% at 2

years and 5% at 5 years for patients who had been treated with a cisplatin-containing regimen as opposed to surgical resection (40-45, 49).

2.7 Rationale

Most patients with diagnosed lung cancer present in advanced stages including III and IV. Therapies for these patients are more difficult and translate into a poor 5 year survival rate (stage III 10-30%, stage IV <1%). However, about 25% of patients who are initially diagnosed with lung cancer are stage I or II. A majority of these patients undergo curative surgery. The 5 year survival for these early stage lung cancer patients is only 30-70%. This is extremely disappointing and so studies have been conducted to look at adjuvant therapy. Modalities such as adjuvant radiotherapy or chemotherapy have proven to be of no benefit or minimal at best. No standard of care for these potentially curable early stage resected patients has been established. Primary screening studies for prevention of lung cancer have failed to demonstrate a survival benefit including CXR and sputum screening. CT scan screening studies are underway but it will be many years before conclusions can be made. Controversies lie with what criteria make a patient high-risk for development of lung cancer as these patients are the most likely to benefit from any intervention to impede carcinogenesis.

We propose a Vanguard comprehensive multidisciplinary study which will focus on the characterization of recurrence and second-primary tumors in a high-risk patient cohort. These patients will have had prior smoking exposure as well as a definitively surgically treated head and neck squamous cell or non-small cell lung cancer. Some of these patients will have the presence of ground glass lesions (GGLs) and those may protend an even worse prognosis. Patients will be followed with multiple modalities including radiographic (computed tomography), bronchoscopic (LIFE), and serological. By obtaining bronchial and serum samples at specific timepoints, we hope to define a risk model which may be able to predict those patients who may have a higher propensity to develop a recurrent or new lung cancer. By utilizing a biomarker based approach and complementing with radiographic and bronchoscopic, development of a risk model of lung cancer will transform how we approach these patients and define a new standard of follow-up and risk assessment to ultimately improve survival.

3.0 Study Design and Overview

The main objective of this phase IIb study is to determine the smoking-related disease free survival in patients at high risk for developing a recurrent or SPT of the lung.

We plan to enroll patients into the "Vanguard trial". Upon enrollment, they will be assigned a study ID number. Patients will then be offered further participation in an optional adjuvant biologic trial that will coincide with this Vanguard trial. If patients decide to participate, then they will be enrolled in both the vanguard trial as well as the adjuvant biologic trial. Patients may choose not to participate in the adjuvant biologic trial, but can still participate in the "Vanguard Trial." Patients will be consented by the

treating physician and the research nurse. Witnesses will be clinic nurses or other members present during the informed consent interview process. Patients may request information and decide to enroll at a later date. Follow-up will occur through the research nurse.

Once enrolled into the adjuvant biologic trial, patients will be randomized in a 2:1 fashion to receive the biologic drug or follow-up only. Patients will receive treatment for 12 months with follow-up for 36 months afterwards. The details of this protocol are outlined as a separate protocol. There are four sequentially run bioadjuvant trials planned with 60 patients in each trial.

In the Vanguard Trial, patients with stage I or II HNSCC or NSCLC after definitive local therapy who have no evidence of disease will be followed for a total of 48 months. Patients will be evaluated with spiral CT, fluorescent bronchoscopy, and serum samples at specific time periods during the study (see schema).

Patients will be seen and enrolled in the Thoracic/Head and Neck Medical Oncology clinics. Patients may be referred from the surgical clinics or from outside referring physicians. Research nurses will promote awareness of the protocol and facilitate enrollment. MDACC sees about 2700 new patients and consults annually in the head and neck and lung cancer clinics.

3.1 Subject Identification

A unique master subject ID will be assigned to each individual participating the study. The subject ID will consist of 5 digits in the format of GG-NNN where GG is the group ID for the institution and NNN is the accession number within the institution. The unique master ID will be assigned by the central statistical coordinating center at M.D. Anderson. A password protected secured file will be created to store the cross reference list between the master ID and confidential patient information such as name, birth date, hospital number, and social security number (if available), etc. Master ID will be used throughout the trial and in database for patient identification purpose. Confidential patient information will be used only when it is necessary such as in patient care setting.

3.2 Subject Assignment in Bioadjuvant Trials

The eligibility criteria for the bioadjuvant trials are the same as in the vanguard study. Patients enrolled in the vanguard study will be given an opportunity to participate a bioadjuvant study. Consenting patients will then be randomized into the active or placebo group with a 2:1 ratio. Random permuted block with varying block size (such as 3 or 6) will be used to achieve the purpose of random allocation while maintain the balance of treatment assignment.

3.3 Study Schema

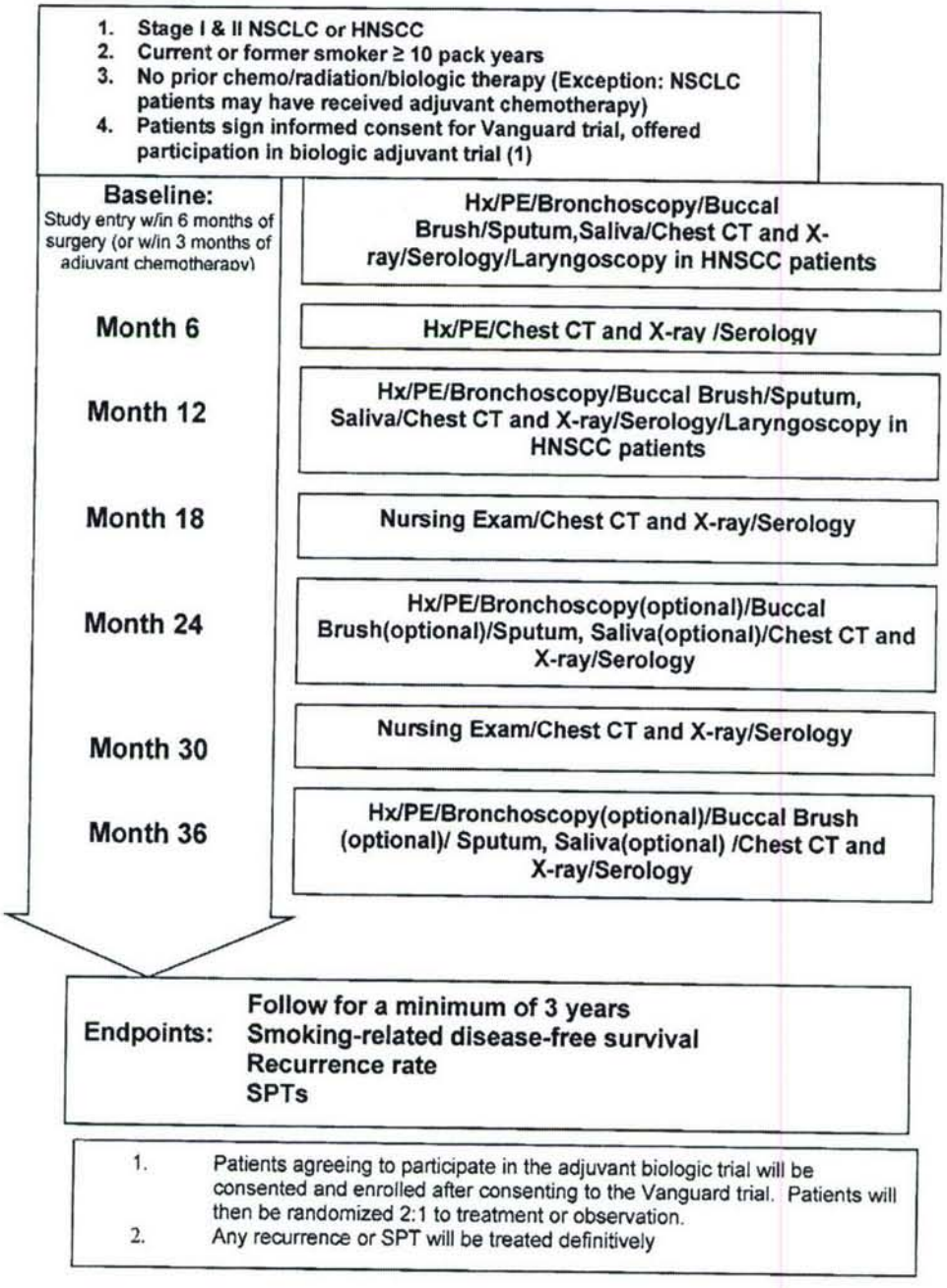

4.0 Patient Eligibility

4.1 Inclusion criteria

1. Patients with either: a) histologically proven stage I, II, IIIa NSCLC who have undergone a complete surgical resection of the primary tumor **OR** b) stage I or II HNSCC who have undergone definitive local treatment (surgery or radiation therapy).
2. HNSCC patients: Definitive local treatment $\leq$ 12 months prior to trial enrollment. NSCLC patients: Surgery $\leq$ 12 months prior to trial enrollment.
3. No evidence residual cancer
4. Smoking history of at least 10 pack years. May be current or former smoker.
5. Performance status of 0-2 (Zubrod, appendix E)
6. Age $\geq$ 18 years.
7. Patients must have no contraindications for undergoing bronchoscopy.
8. Patients must have no active pulmonary infections.
9. Participants must not be taking oral non-steroidal anti-inflammatory drugs on a regular basis.
10. Participants must have the following blood levels: total granulocyte count >1500; platelet count > 100,000; total bilirubin $\leq$ 1.5 mg. %; and creatinine $\leq$ 1.5 mg %.
11. Participants must complete the pretreatment evaluation and must consent to bronchoscopy and to endobronchial biopsy for biomarker studies.
12. All subjects who agree to participate will be given a written and verbal explanation of the study requirements and a consent form that must be signed prior to registration. Subjects will be informed that (a) they must be willing to take biopsies through bronchoscopy and give blood samples at the specified times, (b) they must schedule and keep the specified follow-up visits with their physicians and the study clinics, and (c) side effects and health risks may occur, as described in the informed consent form.
13. Subject must be considered legally capable of providing his or her own consent for participation in this study.
14. HNSCC patients only: Must have no contraindications for undergoing laryngoscopy.

4.2 Exclusion Criteria

1. History of radiation therapy to the chest. For those patients with head and neck cancer who received radiation, no more than 10% of the lung volume (apices) may be included.
2. History of systemic chemotherapy. Exception: NSCLC patients may have had up to 4 cycles of platinum-based doublet therapy.
3. Pregnant or breast-feeding (a negative pregnancy test within 72 hours of enrollment for women with child-bearing potential is required).
4. Participants with active pulmonary infections or recent history of pulmonary infection (within one month).
5. Participants with acute intercurrent illness.

6. Participants requiring chronic ongoing treatment with NSAIDs. (Casual or non-prescribed use of NSAIDs is permitted as long as their use does not exceed one week at a time).
7. Participants with history of stroke, uncontrolled hypertension, and/or uncontrolled angina pectoris.
8. Patients may not take high dose antioxidants (vitamins E or C) during the study period. "High dose" will be determined by the study investigators.
9. Patients may not take high dose synthetic or natural Vitamin A derivatives (> 10,000 IU per day).
10. History of biologic therapy.

5.0 Treatment Plan

Patients who meet the eligibility criteria will be enrolled into the Vanguard Trial and followed for a total of 36 months. Patients who are entered into the adjuvant biologic trial will be followed on a similar schedule. All patients will undergo radiographic, bronchoscopic and serologic procedures at specific time periods during the study.

We anticipate this study will be activated in August, 2004 and will be completed in August, 2008.

5.1 Severe Dysplasia/Carcinoma in Situ

Any participants found to have severe dysplasia or carcinoma in situ at initial or subsequent bronchoscopy will be strongly encouraged to undergo additional bronchoscopies at 6-month intervals. Any participant discovered to have invasive carcinoma at any time during the study will be referred for appropriate intervention (CIS pathway Appendix B).

5.2 Smoking Cessation Program

Any participant who is a current smoker will be offered participation in a smoking cessation program.

5.3 Patient Recruitment

MD Anderson Cancer Center: Patients will be recruited for this study by working closely with thoracic surgeons and head and neck surgeons. Representatives from Thoracic/Head & Neck Medical Oncology (i.e., the principal and co-principal investigators, the research nurse) will attend the weekly surgical conferences to identify potential subjects. In addition, the research nurse will review patient lists from the Surgical, Thoracic, and Head & Neck Clinics as well as lists of patients who were screened unsuccessfully for other protocols. This study will also be publicized by brochures in the Thoracic and Head & Neck Clinics and on the MDACC website.

6.0 Study Evaluations

6.1 Pre-Study Evaluations

Unless otherwise noted, labs, physical exams, imaging studies, and the laryngoscopy are to be performed within 4 weeks of beginning participation in this study.

6.1.1 Signed informed consent
6.1.2 Medical history including smoking history (duration and intensity)
6.1.3 Physical exam: including height, weight, Zubrod performance status assessment. Vital signs including pulse, blood pressure, temperature
6.1.4 Bronchoscopy
6.1.5 Buccal brushing
6.1.6 Sputum and saliva sample
6.1.7 Serum sample for biomarkers
6.1.8 Serum chemistry and electrolytes to include: BUN, creatinine, total bilirubin, SGPT, alkaline phosphatase, albumin
6.1.9 Hematology to include: CBC with automated differential and platelet count
6.1.10 Chest x-ray
6.1.11 CT scan of chest
6.1.12 Laryngoscopy for patients with prior head and neck cancers
6.1.13 PT
6.1.14 Pregnancy test (urine or serum) for women of childbearing potential only.

6.2 Treatment Evaluations while on study

The participant will be observed on the Vanguard trial for a minimum of 36 months. Treatment evaluations will consist of the following study activities:

6.2.1 Medical history and physical exam at months 6,12, 18, 24, 30, and 36. (The exams at 18 and 30 months will be nursing visits).
6.2.2 Bronchoscopy at months 12, 24 (optional), and 36 (optional). Assessment of histology and biomarkers will be performed in the tissue biopsy at the same time. If an intercurrent illness coincides with a time period where bronchoscopy is scheduled, the bronchoscopy will be delayed 30 days or until resolution of the illness.
6.2.3 Buccal brushing at months 12, 24 (optional), and 36 (optional).
6.2.4 Sputum and saliva sample at months 12, 24 (optional), and 36 (optional).
6.2.6 Serum chemistry and electrolytes to include BUN, creatinine, SGPT, total bilirubin, alkaline phosphatase, albumin at months 6, 12, 18, 24, 30 and 36. After 36 months, the participant will have assessments every 12 months for as long as s/he remains observed on the study.
6.2.7 Hematology to include: CBC with automated differential and platelet count at month 6, 12, 18, 24, 30 and 36. After 36 months, the participant will have assessments every 12 months for as long as s/he remains observed on the study.

6.2.8 Serum samples for biomarkers will be collected at months 6, 12, 18, 24, 30 and 36. After 36 months, the participant will have assessments every 12 months for as long as s/he remains observed on the study.
6.2.9 Chest x-ray at 6, 12, 18, 24, 30 and 36 months.
6.2.10 Chest CT at 6, 12, 18, 24, 30 and 36 months. If an intercurrent illness coincides with a time period where CT is scheduled, the CT will be delayed 30 days or until resolution of the illness.
6.2.11 Head neck exam with laryngoscopy at 12 months for patients with prior head and neck cancer.
6.2.12 Pregnancy test (serum or urine) will be conducted if a participant suspects she is pregnant.
6.2.13 PT at 12, 24, and 36 months.

6.3 Long-term follow-up

All participants will be followed until approximately 36 months after study enrollment at which time repeat testing and assessment will be done including optional bronchoscopy. Participants will then be followed with physical exams at 6 month intervals until the study is completed. Every 12 months (i.e., month 48, month 60, etc.) the physical exam will be done by a physician. The other physical exams will be done by a registered nurse. Follow-up will continue for at least one year after the final participant enrolled completes a 36 month evaluation or a maximum follow-up of 6 years.

6.4 Early withdrawal

Early withdrawal is defined as a participant who is unable to continue participation on the study, participant refusal, or noncompliance. The following study activities will be completed at early withdrawal or at the end of study.

6.4.1 Medical history including documentation of smoking status
6.4.2 Physical exam
6.4.3 Radiologic/ (optional) bronchoscopic assessment with tissue/sputum/washings samples
6.4.4 Serum chemistry and electrolytes to include: BUN, creatinine, total bilirubin, SGPT, alkaline phosphatase, and albumin.
6.4.5 Hematology to include: CBC with automated differential and platelet count
6.4.6 Serum collection for biomarker studies
6.4.7 Record for concomitant medications.
6.4.8 Monitor for adverse events.

7.0 Study Procedures/Tests

7.1 Bronchoscopy

Bronchoscopies will be performed at baseline and at months 12, 24 (optional) and 36 (optional) while participating in the study. White-light alone or white light and

autofluorescence modalities may be used, both are preferred. Any carcinoma in situ found during the series of bronchoscopies will be documented and treated with ablation (see Appendix B).

1. Bronchoscopy: Study subjects will undergo autofluorescence and white-light bronchoscopy after being NPO in regard to solid food for a minimum of six hours and NPO for oral medications and small amounts of liquids for two hours prior to the procedure. The participant will be monitored with continuous electro-cardiographic, respiratory, and oximetric monitoring, with intermittent blood pressure monitoring. A complete endobronchial inspection will be performed and suspicious areas under white-light and autofluorescence bronchoscopy will be identified and recorded for subsequent biopsies and brushings. Specimens will be used to analyze biomarkers, genomic and proteomic studies and histologic assessment.
2. Bronchial secretions collection: During the bronchoscopy procedure, after the bronchoscope has passed beyond the vocal cords, a trap will be placed in the suction line and bronchial secretions will be suctioned, collected and saved until the initiation of endobronchial biopsy and brushing procedures. Additional normal saline may be instilled on each side of the bronchial tree until a minimum volume of 15 ml. is retrieved. These liquids are saved for cytological and biological marker analyses.
3. Bronchoalveolar lavage: Following collection of bronchial secretions, the bronchoscope will be wedged in the right middle lobe or lingular orifice. Three 20 ml aliquots of sterile saline will be sequentially instilled, retrieved by gentle suction, pooled, and placed on ice for later analysis and storage. The volume of recovered effluent will be recorded.
4. Endobronchial biopsies: Biopsies will be taken from six predetermined sites even if they appear normal under white light or autofluorescence bronchoscopy: main carina, carinas at both upper lobe orifices, carina at right middle lobe orifice, carina between RB 9 and RB 10 and carina between LB 9 and LB10. Biopsies will also be taken from any additional sites that appear abnormal under white light and/or autofluorescence bronchoscopy. If a biopsy cannot be obtained at an abnormal site, then a brushing alone of that site will be performed. If possible, biopsies will be taken in such a fashion that not all of a potential marker lesion is removed. On followup bronchoscopies, the six predetermined sites and the sites that had histologic dysplasia determined to be mild or greater will be re-biopsied. One or more biopsy may be cultured to obtain respiratory epithelial cells. Depending on participant tolerance and operator discretion, endobronchial biopsies may be terminated at any time; however, an attempt will be made to biopsy between 6 and 12 sites on each participant. Additional sites may be biopsied if deemed clinically indicated, but more than 12 endobronchial biopsies will not be routinely taken. Bronchial brushings may be performed based on patient tolerance and yield of biopsies.
5. Bronchial brushings: Following completion of each biopsy, a bronchial brushings will be taken from the region adjacent to the biopsy site. Bronchial brushings will therefore be obtained from the six predetermined carinas (main carina, carinas at both upper lobe orifices, carina at right middle lobe orifice, carina between RB 9 and RB 10 and carina between LB 9 and LB10). Brushings will also be taken from any

additional sites that appear abnormal under white light and/or autofluorescence bronchoscopy. A brushing alone will be performed at any an abnormal site that cannot be biopsied. On followup bronchoscopies, the six predetermined sites and the sites that had histologic dysplasia determined to be mild or greater will be re-brushed.

6. Bronchial washings: Following the collection of bronchial secretions and bronchoalveolar lavage, the trap in the suction line will be changed. Any bronchial secretions will be suctioned, collected, and saved until the completion of the procedure and withdrawal of the bronchoscope above the vocal cords. Additional normal saline may be instilled on each side of the bronchial tree until a minimum volume of 15 ml. is retrieved. These liquids are saved for cytological and biological marker analyses.

7.2 Repeat Bronchoscopy

All evaluable study participants will have repeat bronchoscopies with biopsies, brushes, and washes at months 12, 24 (optional) and 36 (optional) while participating in the study. Biopsy, brush, and wash samples will be obtained from the same sites sampled in the initial bronchoscopy. New abnormal areas detected by bronchoscopy will also be biopsied. Histologic assessment will be performed to determine whether malignant changes have occurred during the time period.

7.3 Sputum Samples

All registered participants will undergo sputum collection prior to bronchoscopy at baseline and months 12, 24 (optional) and 36 (optional) while participating in the study. Sputum samples will be analyzed cytologically, and specimens will be stored for biomarker studies.

7.4 Buccal Brushings

All registered participants will undergo buccal brushings from the inner left cheek at baseline and months 12, 24 (optional) and 36 (optional) while participating in the study to investigate evidence for tobacco-induced histologic and genetic alterations. This procedure may be found to serve as a surrogate marker of damage incurred in the bronchial tree.

7.5 Saliva

All registered participants will have saliva collected at baseline and months 12, 24 (optional) and 36 (optional) while participating in the study to investigate evidence for tobacco-induced histologic and genetic alterations and biomarker studies.

7.6 Serologies

All registered participants will have serum collected at baseline and month 6, 12, 18, 24, 30 and 36 while participating in the study. Serum will be stored and analyzed for biomarker, genomic and proteomic studies as well as gene expression profiles.

8.0 Investigational Centers

Patients will be seen and enrolled at the University of Texas M. D. Anderson Cancer Center, Department of Thoracic/Head and Neck Medical Oncology clinics, Houston, TX. Additional study sites include: 1) Eisenhower Army Medical Center, Fort Gordon, GA, 2) Conemaugh Memorial Medical Center, Johnstown, PA, 3) The Methodist Hospital, Houston, TX. Laboratory studies will also be performed at each of these sites. Additional sites may be added throughout the study.

8.1 Investigator Contact Information

Principal Investigator:

Waun Ki Hong, MD
University of Texas M.D. Anderson Cancer Center
1515 Holcombe Blvd., Unit 432
Houston, TX 77030
Phone: 713-792-6363
Fax: 713-792-1220
e-mail: whong@mdanderson.org

Co-Principal Investigator:

Edward Kim, MD
University of Texas M.D. Anderson Cancer Center
1515 Holcombe Blvd., Unit 432
Houston, TX 77030
Phone: 713-792-6363
Fax: 713-792-1220
e-mail: edkim@mdanderson.org

8.2 Investigator Contact Information for Additional Sites

Eisenhower Army Medical Center:

Col. Kenneth Fink, USA
Chief, Hematology/Oncology Service
Department of the Army
Dwight David Eisenhower Army Medical Center
Fort Gordon, GA 30905
706-787-2527

Conemaugh Memorial Medical Center:

Ibrahim Sbeitan, M.D.

Conemaugh Memorial Medical Center
1086 Franklin Street
Johnstown, PA 15905-4398
814-534-9165

The Methodist Hospital:

Hector A. Preti, M.D.
6560 Fannin, Suite 2202
Scurlock Tower
Houston, TX 77030
(713) 795-0933

9.0 Criteria for Discontinuation on Study

Patients will be removed from the study for any of the following reasons:

1. Patient requests to withdraw
2. Unwilling or unable to comply with study requirements
3. Identification or recurrent or new cancer
4. Unrelated intercurrent illness that will affect assessment of clinical status to a significant degree as determined by the principal investigator or the treating physician
5. The treating physician or investigator must discontinue study if he/she thinks that the patient's health or well-being is threatened by continuation on study.

Appropriate safety monitoring will continue until the patient is discharged from the study. Patients withdrawn from the study will be followed for survival. The reason for and date of the discontinuation will be obtained.

If a patient is non-compliant or lost to follow-up, the research nurse or his/her designee will make three attempts to call the patient over the period of one month. These attempts will be documented. If the research nurse or his/her designee is unable to make contact with either the patient or a family member after three phone calls, then a letter will be sent to the patient's last known address.

10.0 Adverse Events

10.1 Assessment of Adverse Event Severity & Relationship to Study

All serious adverse events (defined below), whether or not deemed study-related or expected, must be reported by the Principal Investigator or designee to the HSRRB and/or USAMRMC, Human Research Protection Office within 24 hours (one working day) by telephone. A written report must follow as soon as possible, which includes a full description of the event and any sequelae. This includes serious adverse events that occur any time after the inclusion of the subject in the study (defined as the time when the subject signs the informed consent) up to 30 days after the subject completed or discontinued the

study. The subject is considered completed either after the completion of the last visit or contact (e.g., phone contact with the Investigator or designee). Discontinuation is the date a subject and/or Investigator determines that the subject can no longer comply with the requirements for any further study visits or evaluations (e.g., the subject is prematurely discontinued from the study). An adverse event temporarily related to participation in the study should be documented whether or not considered to be related to the test article. This definition includes intercurrent illnesses and injuries and exacerbations of preexisting conditions. Include the following in all IND safety reports: Subject identification number and initials; associate investigator's name and name of MTF; subject's date of birth, gender, and ethnicity; test article and dates of administration; signs/symptoms and severity; date of onset; date of resolution or death; relationship to the study drug; action taken; concomitant medication(s) including dose, route, and duration of treatment, and date of last dose.

A serious adverse event is any event that is: fatal; life-threatening (life-threatening is defined as the patient was at immediate risk of death from the adverse event as it occurred); significantly or permanently disabling; or requires in-patient hospitalization.

Important medical events that may not result in death, be life-threatening, or require hospitalization may be considered a serious adverse drug experience when, based upon appropriate medical judgment, they may jeopardize the patient or subject and may require medical or surgical intervention to prevent one of the outcomes listed in this definition. In addition, laboratory value changes may require reporting.

Reports of all serious adverse events must be communicated to the appropriate Institutional Review Board (IRB) or ethical review committee and/or reported in accordance with local laws and regulations.

10.2 Procedures for Reporting Serious Adverse Events

Serious and/or unexpected adverse events are submitted in writing to the M.D. Anderson Cancer Center Institutional Office of Protocol Research (OPR) within 10 working days of the adverse experience. Unexpected fatal or life-threatening experiences are phoned immediately to the Office of Protocol Research (713-792-2933). A follow up written report is submitted to OPR within 10 working days. The form for communication to OPR of all serious adverse events is appended to this plan.

Reports of all serious adverse events must be communicated to the appropriate Institutional Review Board (IRB) or ethical review committee and/or reported in accordance with local laws and regulations. Adverse experiences that are both serious and unexpected will be immediately reported by telephone to the USAMRMC, Human Research Protection Office (301-619-2165) and send information by facsimile to 301-619-7803. A written report will follow the initial telephone call within 3 working days. Address the written report to the U.S. Army Medical Research and Material Command, ATTN: MCMR-HRPO, 504 Scott Street, Fort Detrick, Maryland 21702-5012.

For all protocols conducted at M.D. Anderson Cancer Center, the Principal Investigator is responsible for submitting adverse event reports to the Institutional IRB and the HSRRB and/or USAMRMC, Human Research Protection Office on an ongoing basis. Adverse event reports are submitted to the Institutional Office of Protocol Research (OPR), where they are entered into PDMS and forwarded to the designated IRB vice chairperson for review. Attached to each adverse event report is a listing of all prior adverse events submitted for that protocol. Any comments, questions or changes the IRB requests to the protocol as a result of this review are conveyed to the principal investigator. The investigator response and protocol modification process is monitored by the IRB vice-chairperson and OPR support staff. The vice chairperson presents the report on adverse event review to the full committee at the next IRB meeting.

An adverse event report compilation is provided once annually to the M.D. Anderson Cancer Center IRB. Comments, questions or other considerations from the IRB are conveyed to the principal investigator for evaluation, discussion and implementation.

10.3 Reporting of Subject Death

The death of any subject during the study or within 30 days of study completion (as defined above), regardless of the cause, must be reported within 24 hours by telephone, to the principal investigator and/or study coordinator and the HSRRB and/or USAMRMC, Deputy for Human Research Protection Office. A full written report must follow as soon as possible. If an autopsy is performed, the report must be provided to the Sponsor.

Reports of all **serious adverse events, including deaths,** must be communicated to the appropriate Institutional Review Board or ethical review committee and/or reported in accordance with local law and regulations.

10.4 Known Adverse Events Relating to the Underlying Clinical Condition

These will be reported on the chart and in the study case report forms.

11.0 Statistical Considerations Statistical Considerations

In this proposed vanguard trial, we will provide comprehensive risk assessment and screenings for current and former smokers with definitively-treated stage I/II lung or head and neck cancer. The main goals are (1) to characterize the patterns of failure including recurrence, smoking related second primary tumor (SPT), and disease-specific death; (2) to identify high-risk individuals; and (3) to evaluate the prognostic significance of molecular and diagnostic markers such as the ground glass lesions (GGL).

The target accrual is to enroll 350 patients over three years. It is expected that we will recruit 70% lung cancer patients and 30% head/neck cancer patients. In both groups, approximately 60% will be former smokers and 40% current smokers. The primary endpoint of the study is smoking-related disease-free survival (S-DFS) defined as time from

registration to the development of recurrence, smoking related SPT, or disease-specific death, whichever occurs first. The rate and pattern of each and overall failure will be computed and summarized. Kaplan-Meier survival curves will be constructed with 95% confidence intervals. Point estimates and Greenwood variance estimators for the smoking related disease-free survival rates at each year of follow-up will also be computed.

Based on our prior two large, multi-center chemoprevention trials (one in lung cancer and one in head/neck cancer with similar eligibility criteria), we estimate the smoking related progression or death rate is 9.2% per year (5-Year S-DFS = 62%) and 6.2% per year (5-Year S-DFS = 73%) in the lung cancer and head/neck cancer patients, respectively. We estimate 70% of our lung cancer patients (n=172) will receive adjuvant chemotherapy with 5-year S-DFS of 67%; equivalent to an annual smoking related progression or death rate of 7.8%. Under the exponential model, it is expected that the progression or death rate for the whole group will be (0.21 x 9.2%) + (0.49 x 7.8%) + (0.3 x 6.2%) = 7.6% per year. This is equivalent to 1-year, 3-year, and 5-year S-DFS of 92%, 79%, and 67%, respectively.

We performed power calculations to detect the significance of a prognostic factor with 3 years of accrual plus three additional years of follow-up and a total of 350 patients. The log-rank test will be used and a two-sided 5% error rate is assumed throughout. If we divide the group by the median of a prognostic factor, it will result in a 50%-50% split between the low-risk and high-risk group. With the overall S-DFS rate holding at 7.6% and an assumption of a hazard ratio of 2, the corresponding annual event rates are 5.2% and 10% for the low-risk and high-risk groups, respectively. Based on the above assumptions, we will have 92% power to detect a hazard ratio of 2.

We also performed power calculations by varying the ratio of patients in the high-risk: low-risk groups and by varying the hazard ratio. The overall event rate remains at 7.6% per year. Statistical power figures are summarized in the following table.

Nhigh-risk :Nlow-risk	Hazard Ratio		
	1.75	2.00	2.25
1:1	79%	92%	97%
1:2	80%	92%	97%
1:3	75%	89%	96%
1:4	71%	86%	94%

With a total of 350 patients, we will have 86% to 92% power to identify a prognostic factor with a hazard ratio of 2 when the high-risk proportion ranges from 20% to 50%. The statistical power will reach 79% if the hazard ratio is 1.75 and 97% if a hazard ratio is 2.25 with equal proportion of high-risk and low-risk patients.

As mentioned in the study design earlier, we expect 280 (80% of all patients) patients will participate in four sequentially planned, biologic agent trials. The remaining 70 patients will be untreated. The relative short-term treatment duration (12 months) may or may not alter

the clinical endpoints. Comparisons will be made between various biologic agent groups and no-treatment groups in terms of S-DFS and other endpoints. If differences are found, the biologic agent groups will be treated separately. Otherwise, they will be combined to evaluate the prognostic effect of other risk factors. Secondary analyses will also be performed to evaluate the clinical outcomes among various groups. Specifically, of 70 patients in each of the 4 sequential trials, 20 patients will be randomized into the control group and 50 patients will be randomized to receive active treatment. Therefore, we will have 20x4 + 70 = 150 patients in the vanguard study who will not receive any active agents. Control patients will be analyzed to test for any trial-specific difference or time trend and will be combined if no differences are found among the various control groups. Clinical outcomes between each of the active biologic agent groups can be compared with the combined control group. With 50 patients in each biologic agent study and 150 patients in the control group, we will have 62%, 74%, and 82% power to detect a hazard ratio of 2.5, 3.0, and 3.5, respectively. Hierarchical Bayes models can be applied to evaluate the similarity or difference among various groups across all trials (46, 47).

In addition, the Cox proportional hazard regression model will be applied to incorporate all potential prognostic variables including biomarkers and treatment to evaluate their effect on the time-to-event outcomes. Transformation to the variables will be applied whenever appropriate to enhance the model fitting. The proportional hazard assumption will be evaluated graphically and analytically, and regression diagnostics (e.g., martingale and Shoenfeld residuals) will be examined to ensure that the models are appropriate (48). Violations of the proportional hazards assumption will be addressed by use of time-dependent covariates or extended Cox models. The possibility of co-linearity will be reduced through the careful initial assessment of correlations among all study covariates.

Other than the possibility of receiving the optional 12 months of biologic agents, there is no treatment in the vanguard trial. Consequently, no interim analysis or early stopping rule is planned in the vanguard study. All data will be prospective acquired to evaluate the effectiveness of screening modalities, to identify prognostic factors and high-risk individuals, and to evaluate the short-term and long-term effect of the therapy. All the study results will be carefully assembled and thoroughly analyzed. The study findings will help us identifying efficacious agents and their combinations, effective screening strategies, endpoints, and relevant study population for a future large-scale, definitive, prevention study.

12.0 Concomitant Medications

- All concomitant medications will be recorded.
- The best supportive care and treatment will be given to each participant (antibiotics, transfusions, diet, etc.)
- No concurrent investigational agents will be permitted.
- No concurrent antineoplastic agents or hormonal anticancer therapy will be permitted.
- No concurrent radiotherapy will be permitted.

- Participants taking cyclooxygenase inhibitors, lipoxygenase inhibitors, NSAIDs, and steroids will be encouraged to refrain from taking, if possible, while on study and at least 4 weeks prior to enrollment.
- Other Concomitant Treatment
- Systemic retinoids and herbal medicines or remedies (including green tea) must be discontinued before entry into the trial and are not allowed during the trial. Patients may not be taking high-dose vitamin A within 30 days of study entry.

Other medication, which is considered necessary for the participant's safety and well being, may be given at the discretion of the investigator(s).

13.0 Methods for Biomarker Analysis

All samples will be processed and stored via the pathology department. Then, the samples will be distributed to specific investigators for studies including biomarkers of apoptosis and cell proliferation, gene expression profiling, genomics, proteomics, and other specified biomarkers of intermediate response.

14.0 Study Administration and Investigator Obligations

14.1 Replacement of Subjects

Participants who withdraw from the study prior to completion of the study treatments for reasons other than serious adverse events, unacceptable toxicity or progressive disease will be defined as dropouts and will be replaced. Replacement participants will be assigned the next sequential number.

14.2 Protocol Compliance

The attending physician and oncology research nurse will evaluate each participant at the initial clinic visit to determine whether the participant qualifies for the study and at each clinic visit thereafter to determine readiness for bronchoscopic procedures. All required interim and pretreatment data will be available to them for evaluation.

14.3 Institutional Review Board

This study must have the approval of a properly constituted Hospital Ethics Committee, Regional Ethics Committee, or other Institutional Review Board (IRB).

The investigator must also report all serious and medically significant adverse events to the IRB or Ethics Committee, as well as the USAMRMC, Human Research Protection Office (see section 10.1).

14.4 Informed Consent

All study participants must sign and date an informed consent form prior to study participation. The investigator will be responsible for designing the consent form using appropriate National or Regional Guidelines (equivalent to the American Federal Guidelines Federal Register July 27, 1981, or 21 CRF Part 50, or International Committee on Harmonization-Good Clinical Practice).

The informed consent form must be approved by the IRB or Ethics Committee. State and local laws, and/or institutional requirements may require the disclosure of additional information on the informed consent form.

A copy of the informed consent form will be given to the participant. The investigator will keep each participant's signed informed consent form on file for inspection by a regulatory authority at any time.

14.5 Record Retention

The investigator and other appropriate study staff will be responsible for maintaining all documentation relevant to the study. Such documentation includes:

- Case Report Forms—must be legible, accurate, and up-to-date.
- Copies of all Serious AE reporting forms faxed to the USAMRMC, Human Research Protection Office.
- Participant Files—should substantiate the data entered in the CRFs with regard to laboratory data, participant histories, treatment regimens, etc.
- Participant Exclusion Log—should record the reason any participant was screened for the study and found to be ineligible.
- Drug Dispensing Log—should record the total amount of study drug received and returned to sponsor, and the amount distributed and returned or destroyed. This information must agree with the information entered in the CRFs.
- Informed Consent Forms—completed consent forms from each participant must be available and verified for proper documentation.
- Informed Consent Log—must identify all participants who signed an Informed Consent Form so that the participants can be identified by audit.

The Investigator must keep on file protocols, amendments, IRB approvals, all copies of Form FDA 1572, all correspondence, and any other documents pertaining to the conduct of the study for a minimum of two (2) years after notification by USAMRMC, Human Research Protection Office of either FDA approval or discontinuation of the IND.

14.6 Case Report Forms

Data recorded on Case Report Forms (CRFs) must be legible and complete. CRFs will be completed on a timely basis. The individual making the correction on the CRF must initial and date the correction. The investigator must review all final and corrected CRFs. Corrected copies of CRFs will be filed with the corresponding original.

If a subject's medical record is needed, it will be requested by the Principal Investigator or Co-Principal Investigator. The requesting investigator (i.e., either the PI or co-PI) will assume responsibility for medical record abstraction, which will be performed by an oncology research nurse and the PI or co-PI. The PI and co-PI are medical oncologists.

14.7 Study Monitoring

The University of Texas M.D. Anderson Cancer Center will monitor the study investigators in the Department of Thoracic/Head and Neck Oncology, once a year or at appropriate intervals to assure satisfactory enrollment rate, data recording, and protocol adherence. The frequency of monitoring may vary depending on enrollment rate and the quality of data collected. The investigator and staff are expected to cooperate and provide all relevant study documentation in detail at each site visit on request for review. M.D. Anderson Cancer Center will randomly monitor and/or audit the other participating sites at appropriate intervals to assure satisfactory protocol adherence and enrollment.

14.7.1 Medical Monitoring

The medical monitor will review all serious and unexpected adverse events associated with this protocol and provide an unbiased written report of the event within ten (10) calendar days of the initial report. The medical monitor should be a qualified physician, other than the principal investigator, not associated with the protocol, able to provide medical care for research volunteers for conditions that may arise during the conduct of the study, and who will monitor the volunteers during the conduct of the study. The medical monitor is required to review all serious and unexpected adverse events (per ICH definitions) associated with the protocol and provide an unbiased written report of the initial report. At a minimum the medical monitor should comment on the outcomes of the adverse event (AE) and relationship of the AE to the test article. The medical monitor should also indicate whether he/she concurs with the details of the report provided by the study investigator. Reports for events determined by either the investigator or medical monitor to be possibly or definitely related to participation and reports of events resulting in death should be promptly forwarded to the HSRRB.

The medical monitor for this study will be Aman U. Buzdar, MD:

Aman U. Buzdar, M.D.
University of Texas M.D. Anderson Cancer Center
Department of Breast Medical Oncology
1515 Holcombe Blvd. - 424
Houston, Texas 77030 USA
Phone: 713- 792-2817
Fax: (713) 794-4385
email: abuzdar@mdanderson.org

The medical monitor will forward reports to the U.S. Army Research and Material Command, ATTN: MCMR-HRPO, 504 Scott Street, Fort Detrick, Maryland, 21702-5012.

14.8 Termination of Study

The HSRRB and/or USAMRMC, Human Research Protection Office and M. D. Anderson will retain the right to terminate the study and remove all study materials from the study site at any time. Specific instances that may precipitate such termination are as follows:

- Unsatisfactory participant enrollment with regard to quality or quantity
- Deviation from protocol requirements, without prior approval from HSRRB and M. D. Anderson.
- Inaccurate and/or incomplete data recording on a recurrent basis
- The incidence and/or severity of adverse drug events in this or other studies indicating a potential health hazard caused by the treatment

14.9 Study Amendments

The investigator will only alter the protocol to eliminate apparent immediate hazards to the participant. If preliminary or interim statistical analysis indicated that the experimental design, dosages parameters, or selection of participants should be modified, these changes will be described in an amendment to be approved by the institution's and other appropriate review committees after consultation with the statistician and Study Chairman. Any amendments cannot be enacted unless approved by the HSRRB and/or USAMRMC, Human Research Protection Office. All revisions made to protocols previously approved by the IRB will be submitted to the IRB for approval prior to implementation of the revision. If the IRB decides to disapprove a research activity, it shall include in its written notification a statement of the reasons for its decision and give the investigator an opportunity to respond in person or in writing. No changes to the protocol will be initiated unless also approved by the Human Subjects Research Review Board.

14.10 Ethical and Legal Considerations

This study will undergo full approval in accordance with the human surveillance requirements of each institution. Blood samples will be obtained for the evaluations as described in the protocol. Tissue samples obtained at the time of prior surgeries will be reviewed before participant enrollment to confirm the participant's diagnosis. Measures will be taken to ensure confidentiality of participant information. Tissue samples will be collected prospectively during the trial. Data collected on paper forms will be stored in locked file cabinets with restricted access. Data collected on electronic media will be stored in computer files with restricted password access. All staff members in the study will be informed prior to employment and at regular intervals of the necessity for keeping all data confidential. Computers will not be accessible to the public and will be located in locked offices. Subjects will be assigned a separate study number to protect subject identification. No patient identifiers will be used in any publications of this research. Data will be maintained indefinitely. When the time comes to dispose of the data, all database files will be deleted.

14.11 Risks/Benefits

Participants will benefit from the educational information provided, including counseling on alcohol and smoking cessation, from the regular follow-up procedures required, and from the blood analyses (i.e., electrolytes, liver function tests, complete blood count, and platelet count). Participants will also benefit from the close comprehensive follow-up after their surgery including additional imaging tests. Participants may benefit from development of a risk model and adjuvant therapy with biologic compounds.

Participants will undergo several invasive procedures (i.e., bronchoscopies) that do have associated risks. These risks will be explained completely prior to consenting of the participant. The following table summarizes risks associated with this study and the steps that will be taken to minimize these risks:

Procedure	Risks	How risks will be reduced
Bronchoscopy with bronchoalveolar lavage, bronchial washings, bronchial brushings, and bronchial biopsies	➢ Coughing ➢ Bleeding ➢ Collapsed lung ➢ Minor sore throat ➢ Mild fever ➢ May cause breathing problems similar to asthma ➢ Bronchitis ➢ Pneumonia ➢ Sedatives given during procedure can decrease breathing function and/or level of oxygen in blood. ➢ May have allergic reaction to sedatives or anesthetics	➢ Presedation assessment to identify particular risk factors ➢ Use of conscious sedation and topical anesthesia to minimize discomfort and cough. ➢ Establish adequate preprocedure bleeding parameters ➢ Monitoring of level of consciousness, cardiovascular and gas exchange parameters during procedure and recovery.
Buccal sample	➢ Pain ➢ Discomfort ➢ Irritation ➢ Bleeding	➢ Brushings on inner cheek performed lightly while patient is under conscious sedation
Laryngoscopy	➢ Discomfort ➢ Gagging ➢ Reaction to topical anesthesia ➢ Nasal irritation ➢ Nasal bleeding	➢ Topical anesthesia will be used to reduce discomfort and gagging ➢ Exams will be performed by experienced personnel

Participants will not be financially responsible for any study-related tests outside of accepted standard of care follow-up.

14.12 Gender and Minority Inclusion

Women and minorities will be actively recruited to participate in the trial. However, since only 42% of lung cancer participants and 22% of laryngeal cancer participants are female, we expect to have more male than female subjects on the study. We expect that the ethnic

distribution of the enrolled participants will reflect the local ethnic mixture of each institution's surrounding community.

14.13 Subject Records

HSRRB and/or USAMRMC, Human Research Protection Office, M.D. Anderson or their representatives may have access to subject records.

14.14 Publication Statement

Data will be reviewed by the collaborating biostatistician prior to publication. HSRRB and/or USAMRMC, Human Research Protection Office will have 30 days to review all definitive publications, such as manuscripts and book chapters, and a minimum of 10-15 days to review all abstracts.

14.15 Conflict of Interest

It is the policy of M.D. Anderson that individuals responsible for the design, conduct, or reporting of all research activities will follow established guiding principles that govern disclosure, reporting, and management of potential conflicts of interest. Full disclosure of financial relationships in research is required.

If a faculty member serves as a PI for a study, he or she cannot hold stock or options in the study sponsor or be on the sponsor's Board of Directors. In addition, the faculty member cannot receive consultant fees in excess of $10,000 per year over the previous 36 months from a study sponsor.

In exceptional circumstances, the President of M.D. Anderson may grant permission to a faculty member to serve as a study PI even if he or she has a financial interest in the study sponsor. If this occurs, it will be stated in the informed consent document that the patient signs.

The informed consent document will also identify any co-investigators with a financial interest in a study sponsor. The informed consent document will also identify any M.D. Anderson and University of Texas System interests in a study sponsor.

Patients shall have access to lists of all faculty with financial interests in trials on which they are enrolled.

14.16 Roles and Responsibilities of Key Study Personnel

Dr. Waun Ki Hong will serve as the Study Chairman for this protocol at M. D. Anderson Cancer Center. He will assume primary responsibility for the study.

Dr. Edward Kim will serve as Study Co-Chairman of this protocol at M. D. Anderson Cancer Center. He will coordinate and supervise all aspects of the clinical trial, and preparation of results for presentations and publication.

Dr. Jack Roth will perform lung resections and identify patients eligible for the Vanguard trial at M. D. Anderson Cancer Center.

Dr. Rodolfo Morice will perform bronchoscopies for patients enrolled at M. D. Anderson Cancer Center.

Dr. Carlos Jimenez will assist with bronchoscopies for patients enrolled in the clinical trial at M. D. Anderson Cancer Center.

Dr. Reginald Munden will perform CT scans for patients enrolled at M. D. Anderson Cancer Center.

Dr. Kenneth Fink will oversee the conduct of the clinical trial at Eisenhower Army Medical Center at Fort Gordon, GA. He will communicate with various departments, obtain referrals of potentially eligible patients, enrollment and follow up of patients, and will be the treating physician for patients entering the clinical trial. He will meet regularly with co-investigators and the Project Director to discuss the progress of the study. He will assist with data analysis and interpretation, and preparation of reports.

Dr. Daniel Lee will perform bronchoscopies for patients enrolled in the clinical trial at Eisenhower Army Medical Center. He will also assist in recruitment of eligible patients.

Dr. Yeini Thompson will serve as the Project Director for the clinical trial at Eisenhower Army Medical Center. She will coordinate and oversee all day-to-day aspects of the study to include IRB submission, screening, enrollment, and follow-up of patients, biologic sample management and shipping, data collection, and coordination and communication with the different departments within EAMC. She will ensure continuity of procedures and data procurement, and assist with the data analysis and preparation of reports and manuscripts.

Dr. Ibrahim Sbeitan will oversee the conduct of the clinical trial at Conemaugh Memorial Medical Center in Johnstown, PA.

Dr. Robert Pickerill will perform bronchoscopies for patients enrolled at Conemaugh Memorial Medical Center.

Dr. Gregory Rys will work with the Research Nurse to identify eligible patients and assist with follow-up and provide counseling.

Gaynelle Schmieder, RN, will identify eligible patients, schedule patients for collection of tissue and/or blood samples, coordinate the activities of oncologists/technicians, and be responsible for follow-up of patients.

Dr. Hector A. Preti will oversee the conduct of the clinical trial at The Methodist Hospital in Houston, TX.

Dr. Mario Gonzales will perform bronchoscopies for patients enrolled at The Methodist Hospital in Houston, TX.

Dr. Philip Cagle will identify eligible patients and assist with follow-up at The Methodist Hospital in Houston, TX.

15.0 References

1. Cancer Facts and Figures. *In:* American Cancer Society, Atlanta, GA, 1997.
2. U.S. Department of Health and Human Services. The Health Benefits of Smoking Cessation: A Report of the Surgeon General. DHHS Publication Number 90-8416, 1990.
3. Glynn, T. J., Manley, M. W., Mills, S. L., and Shopland, D. R. The United States National Cancer Institute and the science of tobacco control research. Cancer Detect Prev, *17:* 507-512, 1993.
4. Halpern, M. T., Gillespie, B. W., and Warner, K. E. Patterns of absolute risk of lung cancer mortality in former smokers. J Natl Cancer Inst, *85:* 457-464., 1993.
5. Lubin, J. H. and Blot, W. J. Lung cancer and smoking cessation: patterns of risk. J Natl Cancer Inst, *85:* 422-423., 1993.
6. Sobue, T., Yamaguchi, N., Suzuki, T., Fujimoto, I., Matsuda, M., Doi, O., Mori, T., Furuse, K., Fukuoka, M., Yasumitsu, T., and et al. Lung cancer incidence rate for male ex-smokers according to age at cessation of smoking. Jpn J Cancer Res, *84:* 601-607., 1993.
7. Risch, H. A., Howe, G. R., Jain, M., Burch, J. D., Holowaty, E. J., and Miller, A. B. Are female smokers at higher risk for lung cancer than male smokers? A case-control analysis by histologic type. Am J Epidemiol, *138:* 281-293., 1993.
8. Landis, S. H., Murray, T., Bolden, S., and Wingo, P. A. Cancer statistics, 1999. CA Cancer J Clin, *49:* 8-31, 31., 1999.
9. Fontana, R. S., Sanderson, D. R., Woolner, L. B., Taylor, W. F., Miller, W. E., Muhm, J. R., Bernatz, P. E., Payne, W. S., Pairolero, P. C., and Bergstralh, E. J. Screening for lung cancer. A critique of the Mayo Lung Project. Cancer, *67:* 1155-1164., 1991.
10. Fontana, R. S., Sanderson, D. R., Taylor, W. F., Woolner, L. B., Miller, W. E., Muhm, J. R., and Uhlenhopp, M. A. Early lung cancer detection: results of the initial (prevalence) radiologic and cytologic screening in the Mayo Clinic study. Am Rev Respir Dis, *130:* 561-565., 1984.
11. Henschke, C. I., McCauley, D. I., Yankelevitz, D. F., Naidich, D. P., McGuinness, G., Miettinen, O. S., Libby, D. M., Pasmantier, M. W., Koizumi, J., Altorki, N. K., and Smith, J. P. Early Lung Cancer Action Project: overall design and findings from baseline screening. Lancet, *354:* 99-105., 1999.
12. Hong, W. K. and Sporn, M. B. Recent advances in chemoprevention of cancer. Science, *278:* 1073-1077., 1997.
13. Hennekens, C. H., Buring, J. E., Manson, J. E., Stampfer, M., Rosner, B., Cook, N. R., Belanger, C., LaMotte, F., Gaziano, J. M., Ridker, P. M., Willett, W., and Peto, R. Lack of effect of long-term supplementation with beta carotene on the incidence of malignant neoplasms and cardiovascular disease. N Engl J Med, *334:* 1145-1149., 1996.
14. Omenn, G. S., Goodman, G. E., Thornquist, M. D., Balmes, J., Cullen, M. R., Glass, A., Keogh, J. P., Meyskens, F. L., Valanis, B., Williams, J. H., Barnhart, S., and Hammar, S. Effects of a combination of beta carotene and vitamin A on lung cancer and cardiovascular disease. N Engl J Med, *334:* 1150-1155., 1996.

15. The effect of vitamin E and beta carotene on the incidence of lung cancer and other cancers in male smokers. The Alpha-Tocopherol, Beta Carotene Cancer Prevention Study Group. N Engl J Med, *330:* 1029-1035., 1994.
16. Lee, J. S., Lippman, S. M., Benner, S. E., Lee, J. J., Ro, J. Y., Lukeman, J. M., Morice, R. C., Peters, E. J., Pang, A. C., Fritsche, H. A., Jr., and et al. Randomized placebo-controlled trial of isotretinoin in chemoprevention of bronchial squamous metaplasia. J Clin Oncol, *12:* 937-945., 1994.
17. Nasiell M. The general appearance of the bronchial epithelium in bronchial carcinoma: a histopathological study with some cytological viewpoints. *Acta Cytol* 1963;8: 97-106.
18. Saccomanno G, Archer VE, Auerbach O, Saunders RP and Brennan LM. Development of carcinoma of the lung as reflected in exfoliated cells. *Cancer* 1974;33: 256-270.
19. Hirsch FR, Bunn PA, Miller YE, Kelly K, Kennedy TC, Bremnes RM, Prindiville S, Sclafani R, Franklin WA. Intermediate Biomarker Profile for Lung Cancer Chemoprevention Trials. Proc Amer Soc Clin Onc 2001, 1286 [abstract].
20. Ohsima S, Shimizu Y and Takahama M. Detection of c-Ki-*ras* gene mutation in paraffin sections of adenocarcinoma and atypical bronchioloalveolar cell hyperplasia of human lung. *Virchows Archiv* 1994;424: 129-134.
21. Sidransky D, Tokino T, Hamilton SR, Kinzler KW, Levin B, Frost P and Vogelstein B. Identification of *ras* oncogene mutations in the stool of patients with curable colorectal tumors. *Science* 1992;256: 102-105.
22. Mao L, Hruban RH, Boyle JO, Tockman M and Sidransky D. Detection of oncogene mutations in sputum precedes diagnosis of lung cancer. *Cancer Res,* 1994;5: 1634-1637.
23. Hruban RH, van der Riet P, Erozan YS and Sidransky D. Brief report: molecular biology and the early detection of carcinoma of the bladder-the case of Hubert H. Humphrey. *N Engl J Med* 1994; 330: 1276-1278.
24. Mao L, Lee JS, Kurie JM, Fan YH, Lippman SM, Lee JJ, Ro JY, Broxson A, Yu R, Morice RC, Kemp BL, Khuri FR, Walsh GL, Hittelman WN and Hong WK. Clonal genetic alterations in the lungs of current and former smokers. *J Natl Cancer Inst* 1997;89: 857-62.
25. Keith RL, Miller YE, Gemmill RM, et al. Angiogenic Squamous Dysplasia in Bronchi of Individuals at High Risk for Lung Cancer. *Clin Cancer Res* 2000 May 6(5):1616-25.
26. Mai GF, Zheng H, Luo RC, et al: Association of progesterone receptor and HER2 expressions with the survival time of patient with breast cancer. Di Yi Jun Yi Da Xue Xue Bao 2003 Apr;23(4):372-4
27. Kanematsu T, Yano S, Uehara H, et al: Phosphorylation, but not overexpression, of epidermal growth factor receptor is associated with poor prognosis of non-small cell lung cancer patients. Oncol Res 2003;13(5):289-98
28. Camp RL, Dolled-Filhart M, King BL, et al: Quantitative Analysis of Breast Cancer Tissue Microarrays Shows That Both High and Normal Levels of HER2 Expression Are Associated with Poor Outcome. Cancer Res 2003 Apr 1;63(7):1445-8

29. Tsutsui S, Ohno S, Murakami S, et al: Prognostic value of the combination of epidermal growth factor receptor and c-erbB-2 in breast cancer. Surgery 2003 Feb;133(2):219-21
30. Kruger S, Weitsch G, Buttner H, et al: Overexpression of c-erbB-2 oncoprotein in muscle-invasive bladder carcinoma: relationship with gene amplification, clinicopathological parameters and prognostic outcome. Int J Oncol 2002 Nov;21(5):981-7
31. Fuchs IB, Loebbecke M, Buhler H, et al: HER2 in brain metastases: issues of concordance, survival, and treatment. J Clin Oncol 2002 Oct 1;20(19):4130
32. Nagler RM, Kerner H, Laufer D, et al: Squamous cell carcinoma of the tongue: the prevalence and prognostic roles of p53, Bcl-2, c-erbB-2 and apoptotic rate as related to clinical and pathological characteristics in a retrospective study. Cancer Lett 2002 Dec 5;186(2):137-50
33. Knosel T, Yu Y, Stein U, et al: Overexpression of c-erbB-2 protein correlates with chromosomal gain at the c-erbB-2 locus and patient survival in advanced colorectal carcinomas. Clin Exp Metastasis 2002;19(5):401-7
34. Selvaggi G, Scagliotti GV, Torri V, et al: HER-2/neu overexpression in patients with radically resected nonsmall cell lung carcinoma. Impact on long-term survival. Cancer 2002 May 15;94(10):2669-74
35. Carbognani P, Tincani G, Crafa P, et al: Biological markers in non-small cell lung cancer. Retrospective study of 10 year follow-up after surgery. J Cardiovasc Surg (Torino) 2002 Aug;43(4):545-8
36. Takizawa S, Nakagawa S, Nakagawa K, et al: Abnormal Fhit expression is an independent poor prognostic factor for cervical cancer. Br J Cancer 2003 Apr 22;88(8):1213-6
37. Wang C, Van Rijnsoever M, Grieu F, et al: Prognostic Significance of Microsatellite Instability and Ki-RAS Mutation Type in Stage II Colorectal Cancer. Oncology 2003;64(3):259-65
38. Kris MG, Natale RB, Herbst RS, et al: A phase II trial of ZD1839 ('Iressa') in advanced non-small cell lung cancer (NSCLC) patients who had failed platinum- and docetaxel-based regimens (IDEAL 2). *Proc Am Soc Clin Oncol.* 2002;21. Abstract 1166.
39. PORT Meta-analysis Trialists Group: Postoperative radiotherapy in non-small cell lung cancer: Systematic review and meta-analysis of individual patient data from nine randomized controlled trials. Lancet 352:257-263, 1998.
40. Holmes EC, Gail M: Surgical adjuvant therapy for stage II and stage III adenocarcinoma and large cell undifferentiated carcinoma. J Clin Oncol 4:710-715, 1986.
41. Feld R, Rubenstein L, Thomas PA: Adjuvant chemotherapy with cyclophosphamide, doxorubicin, and cisplatin in patients with completely resected stage I non-small cell lung cancer. The Lung Cancer Study Group. J Natl Cancer Inst 85:299-306, 1993.
42. Niiranen A, Niitamo-Korhonen S, Kouri M, et al: Adjuvant chemotherapy after radical surgery for non-small cell lung cancer: A randomized study. J Clin Oncol 10:1927-1932, 1992.

43. Wada H, Hitomi S, Teramatsu T: Adjuvant chemotherapy after compete resection in non-small cell lung cancer. West Japan Study Group for Lung Cancer Surgery. J Clin Oncol 14:1048-1054, 1996.
44. Ohta M, Tsuchiya R, Shimoyama M, et al: Adjuvant chemotherapy for completely resected stage III non-small cell lung cancer. The Japan Clinical Oncology Group. J Thorac Cardiovasc Sur 106:703-708, 1993.
45. Non-Small Cell Lung Cancer Collaborative Group: Chemotherapy in non-small cell lung cancer: A meta-analysis using updated data on individual patients from 52 randomized clinical trials. Br Med J 311:899-909, 1995.
46. Gustafson, P. (1998), ``Flexible Bayesian modelling for survival data", Lifetime Data Analysis, 4 , 281-299.
47. Gustafson, P. (1997), ``Large hierarchical Bayesian analysis of multivariate survival data", Biometrics, 53 , 230-242.
48. Grambsch, P.M., Therneau, T.M. (1994): "Proportional hazards test and diagnostics based on weighted residuals," Biometrika 81:515-526.
49. Le Chevalier, T. et al. Results of the Randomized International Adjuvant Lung Cancer Trial (IALT): cisplatin-based chemotherapy (CT) vs no CT in 1867 patients (pts) with resected non-small cell lung cancer (NSCLC). Proc Am Soc Clin Oncol. 2003:22. Abstract 6.

Appendix - A.

Appendix Subtitle:

Guidelines for Filing Reports of Adverse Experiences at M. D. Anderson Cancer Center

21 CFR 312.32

Serious Adverse Experience (SAE) –Any adverse drug experience occurring at any dose that results in any of the following outcomes:

- Death
- A life-threatening adverse drug experience – any adverse experience that places the patient, in the view of the initial reporter, at immediate risk of death from the adverse experience as it occurred. It does not include an adverse experience that, had it occurred in a more severe form, might have caused death.
- Inpatient hospitalization or prolongation of existing hospitalization
- A persistent or significant disability/incapacity – a substantial disruption of a person's ability to conduct normal life functions.
- A congenital anomaly/birth defect.

Important medical events that may not result in death, be life-threatening, or require hospitalization may be considered a serious adverse drug experience when, based upon appropriate medical judgment, they may jeopardize the patient or subject and may require medical or surgical intervention to prevent one of the outcomes listed in this definition. Examples of such medical events include allergic bronchospasm requiring intensive treatment in an emergency room or at home, blood dyscrasias or convulsions that do not result in inpatient hospitalization, or the development of drug dependency or drug abuse.

Unexpected Adverse Drug Experience - Any adverse drug experience, the specificity or severity of which is not consistent with the current investigator brochure; or, if an investigator brochure is not required or available, the specificity or severity of which is not consistent with the risk information described in the general investigational plan or elsewhere in the current application, as amended. Unexpected, as used in this definition, refers to an adverse drug experience that has not been previously observed (e.g., included in the investigator brochure) rather than from the perspective of such experience not being anticipated from the pharmacological properties of the pharmaceutical product.

MDA Policy and Procedure for reporting of adverse experiences (Includes both commercial and investigational drugs):

- All clinical protocols should include a list of the expected and anticipated events or hospitalizations relating to the study regimen. If an expected or anticipated event is documented in the protocol, then it does not have to be reported as an SAE. (Example: Expected Grade 4 mylosuppression needs only to be reported as part of the study results)
- All events falling under the definition of serious adverse event that are not listed in the protocol as being expected or anticipated, and occurring within 30 days following the last treatment date, must be reported to the sponsor within the specified time frame stated in the protocol.
- All deaths with possible, probable or definite attribution to the study drug, device, or intervention must have a written report submitted to the Institutional Review Board (IRB) via OPR within one working day (24 hours) of knowledge of the event.
- All serious adverse events other than that stated above must have a written report submitted to the Institutional Review Board (IRB) via OPR within 5 working days of knowledge of the event.
- If necessary, the sponsor is then required to notify the Food and Drug Administration (FDA) within 7 calendar days.
- All unexpected adverse experiences that are classified as Grade 4 must be reported by following the guidelines listed above.
- Known reactions classified as Grades 1-3 do not need to be reported. However, these toxicities should be submitted as part of the study results.

Adverse Experience Reporting Forms:

Attached is the MDACC severe adverse event reporting form. This form should be utilized if MDACC is the sponsor, the study is a non-sponsored study, or the sponsor does not provide an appropriate reporting form.

If the study sponsor requires a protocol specific SAE form to be completed, then that form may be use for IRB submission as long as the MDACC protocol number and patient medical record number is written at the top of the front page.

External Adverse Experiences / Safety Reports

All external adverse events/safety reports received from the sponsor should be submitted to the IRB through the Office of Protocol Research. The "External Adverse Event Report" can be located under section 1 of the OPR Forms Manual, and should be utilized as the cover sheet for this submission.

IRB Approval Date: 7/3/2002

Appendix - B.

Appendix Subtitle: Carcinoma In Situ Pathway

There is no standard approach to the management of CIS at present. Approaches have ranged from surgical resection to close followup. CIS may be found at the edge of an invasive carcinoma or may occur as a small isolated focus of a few epithelial cells that would be completely removed by a biopsy. The major safety issue related to CIS is that an invasive carcinoma may exist in an adjacent area that the biopsy did not sample. CIS is a rare lesion and it is not likely that enough CIS lesions will be found in the study for statistical analysis of response to the chemopreventive agents.

As there are a wide range of approaches to the treatment of CIS and as this is dependent on the bronchoscopic appearance of the lesion, we believe that the final decision regarding therapy, if any, should be left to the bronchoscopist and primary physician.

If a **CIS** lesion is found on a bronchoscopy at baseline, we would recommend:
1) Follow-up bronchoscopy within one month with repeat inspection of the area of the CIS and multiple biopsies to insure that an invasive carcinoma was not missed.
2) A CT scan with attention to the area of the CIS lesion.
If there is question of **invasive carcinoma** on either follow up bronchoscopy or CT, then the participant should be managed directly according to the preferences of the participant and primary physician.

If **no CIS** lesion is found on the repeat bronchoscopy, then the participant is to be continued on study.

If a **persistent CIS** lesion is found on repeat bronchoscopy, then the management should be directed as follows:

1) Repeat bronchoscopy in 1 month.
If CIS present, definitive treatment of lesion. Patient continues to remain on study.

Appendix - C.

Appendix Subtitle:

Common Terminology Criteria for Adverse Events v3.0 (CTCAE)

Publish Date: June 10, 2003

Click On Link » 🖹 « To access Document

Appendix - D.

Appendix Subtitle:

Prioritization List

Prioritization List

Thoracic Protocol Prioritization List
As of May 9th, 2003

The University of Texas MD Anderson Cancer Center
Prioritization List for Current Thoracic Center Research Protocols
713-792-6363

Protocol Number/Title (RI/Nurse/Regulatory Contact)*	Patient Accrual	Recent Accrual	Data Management	Budget Status
I. Locally Advanced Resectable NSCLC				
A. Superior Sulcus Tumors				
1. ID92-038 (Ritsuko Komaki, MD /Deitra Mooring, RN, Ted Henderson, RN): Combined Modality Therapy, Surgery then Chemo-XRT	32/47 (10 of 31 inevaluable)	1-Feb-02 1-Apr-02 3-May 02	Radiology dept.	Radiology dept.
B. Stage IIIA NSCLC*				
C. Stage I, Ib, II and Selected IIIA*				
1. ID99-400 (Putnam, MD/Katherine Pisters, MD/ Faye Martin, RN): A Randomized Phase III Trial Surgery Alone or Surgery Plus Preoperative Paclitaxel/ Carboplatin in Clinical Stage Ib (T2NO), II (T2-2N1, T3NO) and Selected IIIa (T3N1) NSCLC	20/100	1-June-02 2-July-02 1-Sept-02 1-Dec-02	Surgery dept.	Surgery Budget
2. ACOSOG-Z0030 (Ara Vaporciyan, MD/ Faye Martin, RN): Randomized Trial of Mediastinal Lymph Node Sampling versus Complete Lymphadenectomy During Pulmonary Resection in the Patient with NO or N1 (less than hilar) Non-Small Cell Carcinoma	2/30	2-Apr-03	Thoracic & Cardiovascular	ACOSOG
3. ACOSOG-Z0040 (David C. Rice, MD/A.J. Sarabia, RN): A Prospective Study of the Prognostic Significance of Occult Metastases in the Patient with Resectable Non- Small Cell Lung Carcinoma	1/120	1-Apr-03	Thoracic & Cardiovascular	ACOSOG

Thoracic Protocol Prioritization List
As of May 9th, 2003

Protocol Number/Title (PI/Nurse/Regulatory Contact)	Patient Accrual	Research Activity	Data Management	Budget Status
D. Adjuvant Treatment for Resected NSCLC				
3. RTOG96-16 (Roy Herbst, MD, PhD/Putnam, MD/ Jeanne Riddle, RN/Andrew Bouquard): Post-Op adjuvant Chemo Taxol/Carbo vs. Observation. Stage Ib	2/30	1-Mar-98 1-Dec-00	MDACC	
*T3N1 patients are candidates for both b and c protocols. The small overlap group can be triaged at the discretion of each individual physician.				
II. Locally Advanced, Unresectable NSCLC				
A. Good Performance Status				
1. ID99-303 (Charles Lu, MD/ Li-Ling Hwang, RN/Andrew Bouquard): Phase II Study of AE-941 in Addition to Combined Modality Treatment (Chemo/XRT) for Locally Advanced Unresectable NSCLC (shark cartilage)	237/756 MDACC (186 MDACC+ CCOP)	3-Dec-02 11-Jun-03 4-Feb-03 7-Mar-03 9-Apr-03	RTOG as of Jan 3rd Contracted data outside due to backlog of CRFs	We will receive a portion of the RTOG funding plus additional money from pharmaceutical company.
2. RTOGL-0017 (Ralph Zinner, MD/Deidre Mooring, RN/Li-Ling Hwang, RN) A Phase I Study of Gemcitabine, Carboplatin or Gemcitabine, Paclitaxel and Radiation therapy Followed by Adjuvant Chemotherapy for Patients with Favorable Prognosis Inoperable Stage IIIA/B Non-Small Cell Lung Cancer	***ON HOLD***			
B. Poor Performance Status				
1. ID00-346 (Zhongxing Liao, MD /TBA): Phase I/II	33/80	1-Sept-02 1-Dec-02	Radiation Dept.	

Thoracic Protocol Prioritization List
As of May 9th, 2005

Protocol Number/Title (PI/Nurse/Regulatory Contact)	Patient Accrual	Recent Accrual	Data Management	Budget Status
Radiation with Celebrex for pts with unfavorable Performance Status Inoperable/Unresectable NSCLC		2-Jan-03 ~~1-Apr-03~~		
III. Recurrent or Metastatic NSCLC – No Prior Chemotherapy *All patients should be tested for EGFR*				
1. DM02-107 (George R. Blumenschein, Jr., MD, Pam Lee, RN/Andrew Bouquard): Randomized Phase III Trial Comparing Targretin Capsules/ Carboplatin/Paclitaxel Versus Carboplatin/Paclitaxel in Chemotherapy-Naïve Patients with Advanced or Metastatic Non-Small Cell Lung Cancer	37/40	2-Dec-02 5-Jan-03 1-Feb-03 1-Mar-03 ~~1-Apr-03~~	MDACC	
2. DM02-149 (George R. Blumenschein, Jr., MD/Carmen Summey, RN/Leslie Hardy): A Phase III Randomized Study of Lonafarnib in Combination with Paclitaxel and Carboplatin vs. Placebo in Combination with Paclitaxel and Carboplatin in Patients with Non-small Cell Lung Cancer (P01901-Amendment 1)	15/48	CORe		
3. DM02-141 (Ralph Zinner, MD/Rebecca Zentgraf, RN/Leslie Hardy): A Phase I Evaluation of Oral CI-1033 in Combination Paclitaxel and Carboplatin as First-Line Chemotherapy in Patients With Advanced Non-Small Cell Lung Cancer or Ovarian Cancer	4/10	CORe		
4. 2003-0401 (Yun Oh, MD, and Roy Herbst, MD, PhD): Randomized, Placebo-Controlled, Double-Blind, Phase 2 Study of Gemcitabine-Cisplatin Combined with Two Different Doses of LY293111 or Placebo in Patients with Stage IIIB or IV Non-Small Cell Lung Cancer.	/30			

Thoracic Protocol Prioritization List
As of May 9th, 2003

Protocol Number/Title (PI/Nurse/Regulatory Contact)	Patient Accrual	Recent Accrual	Data Management	Budget Status
IV. Recurrent or Metastatic NSCLC – With One Prior Chemotherapy Regimen				
1. TD02-294 (Roy Herbst, MD, PhD/ Cathy Henceroth, RN/ Leslie Hardy):A Randomized, Double-Blind, Multicenter, Phase II Study to Assess the Safety, Tolerability, and Efficacy of ZD6474 in Combination With Docetaxel (Taxotere®) in Subjects With locally Advanced or Metastatic Non-small Cell Lung Cancer	5/40	2-Jan-03 3-Apr-03		Invoiced for initial payment.
2. DM02-396 (Vali Papadimitrakopoulou, MD/ Lisa King, RN/ Leslie Hardy): A Phase 1-2a Dose-ranging Study of TLK286 in combination with Docetaxel (Taxotere) in Platinum- resistant Non-Small Cell Lung Cancer.	11/28	3-Jan-03 2-Feb-03 2-Mar-03 1-Apr-03		
3. TD01-595 (Roy Herbst, MD, PhD/Patricia Degen, RN/Leslie Hardy): Randomized Study of Docetaxel Versus Docetaxel Plus Genasense™ (Bcl-2 Antisense Oligonucleotide) in Patients with Previously Treated Non-Small Cell Lung Cancer (Genta)	29/40	2-Dec-02 3-Feb-03 3-Mar-03 1-Apr-03	MDACC	
4. DM02-409 (Edward Kim, MD/Pam Lee, RN/Leslie Hardy): A Randomized Phase II/III Study Comparing Two Combination Modalities of IV HMR 1275 (Flavopiridol) and IV Docetaxel (Taxotere®) with IV Docetaxel (Taxotere®) Alone in Patients with Non-small Cell Lung Cancer (NSCLC) Previously Treated with Platinum-based Chemotherapy	1/21	1-Apr-03		
5. 2003-0396 (Edward Kim/TBA/Leslie Hardy): An open label, Phase Ib/II, EPO906 Dose Escalation trial in Patients with Non-Small Cell Lung Cancer	/10			
6. DM02-663 (Frank Fossella, MD/ Rebecca Zenigra/ Leslie Hardy): A Randomized, Multicenter, Open-Label, Phase 2 Study of VELCADE plus Docetaxel in Previously Treated Patients with Advanced Non-Small Cell Lung Cancer (M34102-048.)	1/30	CORe		

Thoracic Protocol Prioritization List
As of May 9th, 2003

Protocol Number/Title/PI/Nurse/Regulatory Contact)	Patient Accrual	Recent Accrual	Data Management	Budget Status
7. ID00-123 (Charles Lu, MD and Jack Roth, MD/ A.J Sarabia, RN/Betsi Thompson): Phase I Study of IV DOTAP: Chol-Fus 1 Liposome Complex in Patients with Advanced NSCLC previously treated with chemo.	/30	Activated	*Thoracic & Cardiovascular*	*Surgery*
Recurrent or Metastatic NSCLC w/o Taxotere				
1. ID02-225 (Papadimitrakopoulou, MD/Lisa King, RN/Leslie Hardy): Phase II Study of TLK286 Admin. Weekly in Advanced NSCLC	24/30	3-Nov-02 1-Dec-02 3-Jan-03 1-Feb-03	Contracted Out	Recently invoiced for additional payments.
Unlimited Prior Therapy (no prior EGFR)				
1. ID01-604 (Roy Herbst, MD, PhD/Ted Henderson, RN /Betsi Thompson): A Phase I/II, Multidose, Multicenter Clinical Trial to Evaluate the Safety and Efficacy of the Combination of Recombinant Humanized Monoclonal Anti-VEGF Antibody rhuMAb VEGF (Avastin™) and the EGFR Tyrosine Kinase Inhibitor OSI-774 (Tarceva™) for Locally Advanced or Metastatic Non-Squamous Cell Non-Small Cell Lung Cancer (NSCLC) in Patients Who Have Been Previously Treated	21/48	3-Jan-03 1-Feb-03 5-Mar-03 2-Apr-03		Payments up-to-date
V. Recurrent or Metastatic NSCLC –With ≥ 2 Prior Chemotherapy Regimen				
A. Biopsiable Disease				
B. Non-Biopsiable Disease Unlimited Prior Therapy (w/ Prior EGFR)				
1. ID01-326 (Vali Papadimitrakopoulou, MD/Pat Degen, RN/Andrew Bouquard): A Phase I Study To Determine The	19/40	1-Dec-02 1-Jan-03 4-Feb-03	MDACC	Recently invoiced for $97,809.00

Thoracic Protocol Prioritization List
As of May 9th, 2003

	Protocol Number/Title (PI/Nurse/Regulatory Contact)	Patient Accrual	Recent Accrual	Data Management	Budget Status
	Safety and Pharmacokinetics of BMS-387032 Given Every Three Weeks In Patients With Metastatic Refractory Solid Tumors Bristol-Myers Squibb Protocol No. CA174-001		1-Mar-03 2-Apr-03		
2.	ID01-575 (Roy S. Herbst, MD, PhD & Hai T. Tran, PharmD/Cathy Henceroth, RN/Leslie Hardy): Phase I, Open-Label, Multicenter, Dose-Escalation Study of the Tyrosine Kinase Inhibitor of VEGFR-2, AG013736 in Patients with Advanced Solid Tumors	9/30	1-July-02 1-Nov-02 1-Jan-03 3-Mar-03	MDACC	
3.	ID02-660 (Roy Herbst, MD, PhD/ Cathy Henceroth, RN/ Leslie Hardy): Continuing access to the Tyrosine Kinase Inhibitor of VEGF-2, AG013736 (A406) for Patients Previously Receiving AG013736 in Clinical Trials	1/30	1-Mar-03		
4.	DM01-180 (Edward Kim, MD Carmen Summey, RN/Leslie Hardy): Phase I Study of Continuous Oral Administration of SCH 66336 and IV Docetaxel as Second Line Treatment in Patients with Advanced Solid Tumors	12/24	1-Jan-02 2-Feb-02 1-Mar-02 1-May-02	MDACC	
5.	ID02-759 (Edward Kim, MD/Lisa King, RN and Colleen Jones, RN/Andrew Bouquard) A Phase II, Open Label Non-Randomized, Multicenter Single Agent Study of Intravenous SDX-102 for the Treatment of Patients w/ MTAP-Deficient Cancer	***Screening patients***			
VI.	**Small Cell Lung Cancer – No Prior Chemotherapy**				
A.	**Extensive Disease**				
1.	ID00-433 (Bonnie Glisson, MD/Beverly Peeples, RN & Beena Varghese, RN/Betsi Thompson): Pilot Trial of Weekly Etoposide/Cisplatin/Irinotecan/G-CSF for Patients with Small Cell Lung Cancer	26/40	1-Nov-02 1-Dec-02 1-Jan-03 2-Mar-03	MDACC	Payments up to date.
2.	ID01-576 (Bonnie Glisson, MD/Beverly Peeples, RN &	3/15	1-Oct-02		

Thoracic Protocol Prioritization List
As of May 9th, 2003

Protocol Number/Title (PI/Nurse/Regulatory Contact)	Patient Accrual	Recent Accrual	Data Management	Budget Status
Beena Varghese, RN/Betsi Thompson): Phase I Trial of Imatinib Mesylate (Gleevec), Cisplatin, and Irinotecan for Patients with Small Cell Lung Cancer		1-Jan-03 1-Feb-03	MDACC	Received initial payment.
VII. Small Cell Lung Cancer – With Prior Chemotherapy				
1. ID01-032 (Frank Fossella, MD/Rebecca Zentgraf, RN/Andrew Bouquard): A Phase I, Open-Label Dose Escalation Study of Weekly Dosing With BB-10901, followed by a Phase II Efficacy Expansion	26/82	1-Aug-02 1-Sept-02 1-Oct-02 1-Apr-03	Contracted out	Amended contract for Phase II portion.
VIII. Malignant Mesothelioma				
A. Operable Disease				
1. 2003-0339 (Katherine Pisters, MD and William Smythe, MD, Craig Stevens, MD): A Multicenter Phase II Trial of Neo-adjuvant Alimta plus Cisplatin followed by Surgery and Radiation for Pleural Mesothelioma.	/30			
2. ID01-318 (Roy Smythe, MD and Craig Stevens, MD, PhD/Janie Wilde, RN): A Phase I/II Study of Intensity Modulated Radiotherapy (IMRT) for Malignant Pleural Mesothelioma after Extrapleural Pneumonectomy	19/40	1-June-02 3-July-02 2-March-03 2-Apr-03	Surgery	Surgery Budget
B. Inoperable Disease				

Thoracic Protocol Prioritization List
As of May 9th, 2003

Protocol Number/Title (PI/Nurse/Regulatory Contact)	Patient Accrual	Recent Activity	Data Management	Budget Status
1. ID97-224 (Ralph Zinner, MD/ Pam Lee, RN/Betsi Thompson): Onconase + Doxorubicin vs Doxorubicin	20/30 CNPE	1-Dec-99 1-Oct-00 1-Jan-01 1-Aug-02	MDACC	
2. ID02-005 (Charles Lu, MD/Li-Ling Hwang, RN/Andrew Bouquard A Double Blind, Placebo Controlled, Randomized Phase II Trial Of Gemcitabine And Cisplatin With Or Without The VEGF Inhibitor Bevacizumab In Patients With Malignant Mesothelioma.	4/24	1-June-02 1-Sept-02 1-Jan-03 1-Apr-03	MDACC	Katarjan N01 Grant
3. ID02-759 (Edward Kim, MD/Lisa King, RN and Colleen Jones, RN/Andrew Bouquard) A Phase II, Open Label Non-Randomized, Multicenter Single Agent Study of Intravenous SDX-102 for the Treatment of Patients w/ MTAP-Deficient Cancer	***Screening patients***			
IX. Sarcomatous Pulmonary Metastases				
C. Pulmonary Metastases				
X. Esophageal Cancer				
1. ID02-256 (Stephen Swisher, MD/ Rhodette Fransico, RN): Phase I/II Multicenter, Single Arm Evaluation of Preoperative Chemoprevention plus TN Formde™ Prior to Esophagectomy for Locally Advanced respectable Esophageal Cancer	/30			

Thoracic Protocol Prioritization List
As of May 9th, 2005

Protocol Number/Title (PI/Nurse/Regulatory Contact)	Patient Accrual	Recent Accrual	Data Management	Budget Status
XI. Miscellaneous				
1. ID99-052 (Craig Stevens, MD, PhD and Roy Smythe, MD/TBA): A Feasibility Study to Measure Tumor Oxygenation in Human Non-small Cell Carcinomas	26/60	9-Apr-02 1-June-02 1-Aug-02 2-Jan-03	Surgery	
XII. Extended Access Iressa				
1. DM00-357 (Roy Herbst, MD, PhD/Rainell Schaerer, RN/Leslie Hardy): An Expanded Access Clinical Program with ZD1839 (IRESSA™) for Patients with Advanced Non-Small Cell Lung Cancer (NSCLC)	203/250	1-Dec-02 21-Feb-03 4-Apr-03	MDACC	No Funding
XIII. Chemoprevention				
1. ID00-230 (Jonathan Kurie, MD, Vanessa Ray, RN/Betsi Thompson): A Randomized, Double-Blind Study of the Biological Effects and Tolerability of Celecoxib as a Chemopreventive Agent in Current and Former Smokers	52/216	2-Dec-02 2-Jan-03 4-Feb-03 2-Apr-03	MDACC	Grant
2. 2003-0424/2003-0423 (Waun Ki Hong, MD/Edward Kim, MD) Vanguard Trial and Bioadjuvant Trial for Early Stage NSCLC	/240			Grant
3. ID01-307 (Reginald Munden, MD, DMD): Helical CT Screening for Lung Cancer in Patients Previously Treated for Laryngeal Cancer.	17/140	1-May-02 4-Nov-02 1-Dec-02	Radiology	Radiology Budget
4. ACRIN01-6654 (Reginald Munden, MD, DMD): Contempocary Screening for the Detection of Lung Cancer.	350/100		Radiology	Radiology Budget
XIV. New Studies Not Yet Open				
ID01-383 (Edward Kim, MD/RN TBA/Betsi Thompson): Phase III Trial of ZD1839, a Tyrosine Kinase Inhibitor, versus Placebo in Former/Current Smokers with a Previous History of Cancer	0/150	Approved: NOT YET ACTIVATED		

Thoracic Protocol Prioritization List
As of May 9th, 2003

Protocol Number/Title (PI/Nurse/Regulatory Contact)	Patient Accrual	Recent Accrual	Data Management	Budget Status
ID01-384 (Edward Kim, MD/RN TBA/Betsi Thompson): Phase III Trial of R115777, a Farnesyl Transferase Inhibitor, versus Placebo in Former/Current Smokers with a Previous History of Cancer		LCDCC SPORE Approved: NOT YET ACTIVATED		
ID03-0149 (Ritsuko Komaki, MD (Merrill Kies, MD/Lisa King RN/TBA): A Phase I Translational Study of Poly-L-Glutamate-Taxol (CT-2103) and Radiotherapy for Locally Advanced, Unresectable or Medically Inoperable Non-Small Cell Lung Carcinoma	/20	IRB Approved ***pending activation***		
ID02-144 (Edward Kim, MD/Nurse TBA/Betsi Thompson): A Phase II Study of Sertraline (Zoloft®), a Selective Serotonin-Reuptake Inhibitor, and Its Effect on the Quality of Life in Patients with Advanced Non-Small Cell Lung Cancer (NSCLC).	0/144	Submitted to CCOP		
ACOSOG-Z0060 (Stephen G. Swisher, MD and Homer Macapinlac, MD/TBA/TBA): The Utility of Positron Emission Tomography (PET) in Staging of Patients with Potentially Operable Carcinoma of the Thoracic Esophagus	/25		Thoracic & Cardiovascular	
ID03-0143 (George Blumenschein, MD/Beena Varghese, RN and Beverly Peeples, RN/ Leslie Hardy): "A Phase II of Triapine ® in Combination with Gemcitabine in Patients with Metastatic Non-Small Cell Lung Cancer"		***Waiting on activation***		
DM02-664 (Merrill Kies, MD/Michelle Purdom, RN/Leslie Hardy): "A Phase II Randomized, Open-Label Study of Single Agent CI-1033 in Patients with Advanced Non-Small Lung Cancer (Protocol A4161003) .	/24	***Waiting on drug shipment		
DM00-327(Jonathan Kurie, MD/ Beverly Peeples, RN and Beena Varghese,RN/ Andrew Bouquard): A Phase I/II, Multi-Center, Dose-Escalation, Pharmacokinetic, Safety, and Efficacy Study of Oral TAC-101 in Patients with Stage IV Non-Small Cell Lung Cancer		***Amendment being reviewed by IRB		

Updated on May 13, 2003

CURRENT RESEARCH STUDIES FOR HEAD AND NECK MEDICAL ONCOLOGY

The University of Texas M.D. Anderson Cancer Center □ 1515 Holcombe □ Houston, TX 77030
Thoracic/Head and Neck Medical Oncology □ Box 432 □ 713-792-6363

Protocol No.	Protocol Title Sponsor	Principal Investigator (Research Nurse)	Patient Accrual Currently Projected	Record Accrual	Date Activated	Priority	Data Support	Comments
	CHEMOPREVENTION							
ID98-017	Induction Biochemoprevention, Fenretinide vs Placebo for Laryngeal Dysplasia Hoffman-LaRoche, (NCI)	Hong/ Papadimitrakopoulou (Anthea Atwell)	30/100	2-Sep-02 2-Dec-02 1-Feb-03 1-Mar-03	11/98	1		
ID99-131	Clinical Protocol for a Phase II Double-Blind, Placebo-Controlled, Randomized Study of Celecoxib (SC-58635) in Oral Premalignant Lesions (Searle)	Papadimitrakopoulou (Anthea Atwell)	36/64	3-Nov-02 2-Dec-02 1-Jan-03 1-Feb-03	6/22/00	1		Study now covers all patient care costs.
ID98-087	Phase II Chemoprevention Trial with 4-HPR Oral Premalignant Lesions	Lippman/ Papadimitrakopoulou (Pat Cote)	6/35	3-Feb-03 1-Mar-03 1-Apr-03	11/19/02	2		Study pays for entire patient care.
ID01-155	Phase II Randomized Double-Blind, Placebo Controlled Dose Ranging Pilot of GTE for Chemoprevention of OPLs in High Risk Pts	Papadimitrakopoulou (Anthea Atwell)	1/27	1-Apr-03	10/14/02	3		amended contract
2003-0424/2003-0423	Vanguard Trial and Biadjuvant Trial for Patients with Early Stage HNSCC	Hong/Kim	/240					
	LOCALLY ADVANCED DISEASE PREVIOUSLY UNTREATED							
ID01-062	Phase II Study of Induction Chemotherapy Followed by Surgical Resection for Young Patients with Squamous Cell Carcinoma of the Oral Tongue and Floor of Mouth	Kies (Gracy Zachariah)	8/30	1-Dec-01 1-Jan-02 1-Nov-02 1-Feb-03	6/25/01	1	MDACC	First payment received.
RTOG H0129	A Phase III Trial of Concurrent Radiation and Chemotherapy for Advanced Head and Neck Carcinomas	Rosenthal (Brenda Brumfield)	21/160	4-Jan-03 5-Feb-03 2-Mar-03 1-Apr-03		1		
	LOCALLY ADVANCED DISEASE PREVIOUSLY UNTREATED – Adjuvant Therapy							

CURRENT RESEARCH STUDIES FOR HEAD AND NECK MEDICAL ONCOLOGY

The University of Texas M.D. Anderson Cancer Center ☐ 1515 Holcombe ☐ Houston, TX 77030
Thoracic/Head and Neck Medical Oncology ☐ Box 432 ☐ 713-792-6363

Protocol No.	Protocol Title Brief	Principal Investigator / (Research Nurse)	Patient Accrual Current / Projected	Recent Accrual	Date Activated	Priority	Data Support	Comments
ID96-252	Adjuvant Biologic Therapy (NCI)	Kim (Tess Francisco)	32/180	1-Nov 01 1-Dec 01 1-Oct-02 1-Mar-03	7/2000	1	MDACC	
RTOG H0024	Phase II Early Postoperative Paclitaxel Followed By Paclitaxel And Cisplatin Concurrent With Radiation Therapy For Resected, High-Risk Squamous Carcinoma Of The Head And Neck	Myers/Olsson (Gracy Zacharias)	16/60 National accrual 45/60	1-Nov-02 1-Dec-02 1-Feb-03 1-Apr-03	12/2001	2		Radiation budget
	LOCALLY ADVANCED DISEASE PREVIOUSLY UNTREATED – Larynx Only							
ID97-080	Phase II Study of Taxol, Cisplatin, and Mostamide followed by Surgery in Pts w/ Laryngeal Cancer Bristol Myers	Kies/Gallenwater (Katherine Gillaspy)	27/38	1-Jan 02 1-Apr 02 1-Oct-02 2-Feb-03	6/2/2097	1		Receive next payment with 28th patient.
	LOCALLY ADVANCED DISEASE PREVIOUSLY UNTREATED – Nasopharynx Only							
	RECURRENT/METASTATIC DISEASE – Chemotherapy							
	Front Line For Recurrence							
RTOG98-11	Phase II Study of Paclitaxel and Cisplatin in Combination with Split Course Concomitant Hyperfractionated Re-Irradiation in Patients with Recurrent Squamous Cell Cancer of the Head and Neck	Kies (Marites 'Tess' Francisco)	4/100 National Accrual	1-Dec 01 1-Feb 02 1-Apr 02 1-May 02	09/10/01	1	Radiation does	NCI GRANT
ID00-342 (T302)	A Phase III Multicenter Open-Label, Randomized Study to Compare the Effectiveness and Safety of Intratumoral Administration of RPR/INGN 201 in Combo w/Chemo Versus Chemotherapy Alone in	Clayman/Kies (Brenda Brumfield)	3/288	1-Mar 02 1-Aug 02 1-Jan-03	8/31/01	3	surgery	surgery

CURRENT RESEARCH STUDIES FOR HEAD AND NECK MEDICAL ONCOLOGY

The University of Texas M.D. Anderson Cancer Center □ 1515 Holcombe □ Houston, TX 77030
Thoracic/Head and Neck Medical Oncology □ Box 432 □ 713-792-6363

Protocol No.	Protocol Title Sponsor	Principal Investigator (Research Nurse)	Patient Accrual Current Projected	Recent Accrual	Date Activated	Priority	Data Support	Comments
	288 Patients with Recurrent Squamous Cell Carcinoma of the Head and Neck							
	Prior Treatment For Recurrence							
ID99-334	A Phase II Study Of Fenretinide In Recurrent And Metastatic Squamous Cell Carcinoma Of The Head And Neck (NCI)	Glisson (Tess Francisco)	10/35	1-Sep 01 1-Nov 01 2-Dec 01 1-Mar 02	8/15/00	1		
ID00-006 (T001)	A Phase III, Multi-Center, Open-Label, Randomized Study to Compare the Overall Survival and Safety of Bi-weekly Intratumoral Administration of RPRUNGN 201 Versus Weekly Methotrexate in 240 Patients with Refractory Squamous Cell Carcinoma of the Head and Neck	Clayman/Kies (Brenda Brumfield)	7/46	8-Dec 01 1-Jan 02 1-Feb 02 1-Dec-02 1-Jan-03	5/31/01	3	Surgery	Surgery
DM02-384	Phase II clinical Trial of Oral Suberoylanilide Hydroxamic Acid SAHA in Patients With Recurrent and/or Metastatic Head and Neck Cancer	Blumenschein/ Jong (Maritess Fransico)	10/37	1-Jan-03 1-Feb-03 2-Mar-03 2-Apr-03		2		Invoiced 3rd payment

CURRENT RESEARCH STUDIES FOR HEAD AND NECK MEDICAL ONCOLOGY

The University of Texas M.D. Anderson Cancer Center ◻ 1515 Holcombe ◻ Houston, TX 77030
Thoracic/Head and Neck Medical Oncology ◻ Box 432 ◻ 713-792-6363

Protocol No.	Protocol Title Sponsor	Principal Investigator (Research Nurse)	Patient Accrual Currently Protected	Recent Accrual	Date Activated	Priority	Data Support	Comments
DM03-0008	A Phase II Study of 250-mg ZD1839 Monotherapy in Recurrent or Metastatic or both Recurrent and Metastatic Squamous Cell Carcinoma of the Head and Neck	Glisson (TBA)	/83			4		IRB approved
	SKIN CANCER							
	NEW STUDIES – Not yet active							
ID01-456	4-HPR (N-4-(hydroxyphenyl) retinamide) as Induction Preoperative Therapy for Patients with Advanced Squamous Cell Carcinoma of the Skin (Skin P01)	Kim/Glisson (TBA)	/36					IRB approved
ID01-457	Farnesyltransferase Inhibitor SCH66336 as Induction Preoperative Therapy for Patients with Advanced Squamous Cell Carcinoma of the Skin (Skin P01)	Kim/Glisson (TBA)	/52					IRB approved
ID01-444	Phase III Chemoprevention Trial of ZD1839, a Tyrosine Kinase Inhibitor, versus Placebo in Subjects with Oral Preinvasive Lesions (SPORE)	Papadimitrakopoulou Martia (Anthea Atwell)	/109					IRB approved
ID01-450	A Randomized Phase II Study of SCH54031 in Surgically Resectable Squamous Cell Tumors of the Head and Neck (SPORE)	Herbst/Kies/Hyers/ Talpaz (Grace Zacharian)	/72					Ready for Activation
ID01-456	A Phase I study of Fenretinide in Combination with SCH66336, a Farnesyltransferase Inhibitor, in Patients with Advanced Head and Neck Cancer (SPORE)	Kim (Marites Fransico)	/36					IRB approved
ID02-468	A Phase II Study of OSI-774 in Combination with Cisplatin and Docetaxel in Metastatic or Recurrent Head and Neck Squamous Cell Cancer	Kim/Tsao Barbara Burke	/30					IND approved
ID02-282	A Phase II study of ZD1839 (IRESSA), epidermal growth factor receptor (EGFR) tyrosine inhibitor, in treatment of recurrent or metastatic squamous cell carcinoma of the skin.	Kim Barbara Burke						IND Approved
	Future Protocols							

CURRENT RESEARCH STUDIES FOR HEAD AND NECK MEDICAL ONCOLOGY

The University of Texas M.D. Anderson Cancer Center ◻ 1515 Holcombe ◻ Houston, TX 77030
Thoracic/Head and Neck Medical Oncology ◻ Box 432 ◻ 713-792-6363

Protocol No.	Protocol Title Sponsor	Principal Investigator (Research Nurse)	Patient Accrual Currently Protected	Recent Accrual	Date Activated	Priority	Data Support	Comments
	A phase II study of ZD1839 (IRESSA), epidermal growth factor receptor (EGFR) tyrosine kinase inhibitor in patients with advanced, recurrent or metastatic salivary gland cancer	Kies						
	Phase II Trial of Induction Therapy with C225 (ERBITUX) and Carboplatin/Paclitaxel Chemotherapy in Previously Untreated Patients With Advanced (Stage III-IV) Head & Neck Squamous Cell Carcinoma.	Kies						
	Phase I Trial of OSI-774 and Docetaxel with Concurrent Radiation for Locally Advanced SCCHN	Glisson						

Appendix - E.

Appendix Subtitle: Study Evaluations

Procedure	Baseline[6]	3 mos	6 mos	9 mos	12 mos	18 mos	24 mos	30 mos	36 mos	Long-term F/U
Informed consent	X									
Physical exam (by physician or nurse)	X		X		X		X		X	Every 12 mos
Nursing exam only						X		X		Every 6 mos[5]
Medical history	X		X		X	X	X	X	X	Every 6 mos
Cardiac risk assessment	X									
Bronchoscopy	X				X		X[7]		X[7]	
Sputum and saliva sample	X				X		X[7]		X[7]	
Buccal brush	X				X		X[7]		X[7]	
Hematology[1]	X		X		X	X	X	X	X	Every 12 mos
Serum chemistry, electrolytes[2]	X		X		X	X	X	X	X	Every 12 mos
Lipid profile	X									
PT	X				X		X		X	
Pregnancy test[3]	X									
Chest x-ray	X		X		X	X	X	X	X	
CT scan of chest	X		X		X	X	X	X	X	
Laryngoscopy[4]	X				X					
Biomarkers (serum)	X		X		X	X	X	X	X	Every 12 mos
Nursing Follow-up via phone		X		X						

[1] CBC with differential, platelets
[2] BUN, creatinine, total bilirubin, SGPT, alkaline phosphatase, albumin
[3] Women of child-bearing potential only. Serum or urine. Must be done within 72 hrs. prior to enrollment. Should be repeated any time pregnancy is suspected.
[4] Patients with prior head and neck cancer only
[5] Nursing only visit will occur when patient is not scheduled for a physician visit.
[6] Unless otherwise noted, labs, physical exams, imaging studies, and the laryngoscopy are to be performed within 4 weeks of beginning participation in this study.
[7] Optional

Appendix - F.

Appendix Subtitle: Research Informed Consent Process

The informed consent process is to ensure that individuals participating in clinical trials are informed about the study's purpose, the risks and benefits, alternative therapies, and voluntarily agree to participate. It is a process that should provide ample opportunity for the person obtaining informed consent and the participant to exchange information and answer questions. The process will also provide for updates to the informed consent, as the study requires. This policy is to assure study participants receive adequate information in the appropriate manner, timing and setting.

All areas of UTMDACC conducting clinical research are expected to comply with this standard procedure.

MDA Policy and Procedure:

The informed consent process begins when a potential research participant is initially contacted regarding a study by the investigator or his staff. Participants should not be approached about a potential protocol prior to that study being approved by the Institutional Review Board (IRB).

The attending physician shall be responsible for ensuring that the informed consent process is documented by the use of a written consent form approved by the IRB and signed by the participant or participant's legally authorized representative (unless this requirement is specifically waived by the IRB).

Upon activation, the informed consent document is imprinted with the "IRB Approved Consent" stamp. The stamp is signed and dated by the assigned protocol compliance specialists and distributed to the principal investigator. Additional copies must be made and distributed by the department. Consents that are submitted in PDOL will be available on-line following activation.

Only the most recent version of the informed consent document approved by the IRB should be used when addressing new patients. The date stamped on the informed consent document should correspond with the informed consent date in the Protocol Data Management System (PDMS) during the registration process, verifying that the correct version of the document has been signed. Consents for protocols that are available on-line through PDOL, will have the most recent revision date typed on the lower right-hand corner of the document.

Informed consent must be obtained prior to the initiation of any protocol-specific screening procedures that are not considered standard of care.

The informed consent document should be presented in a language that is understandable to the participant. The informed consent document will only be generated in the English language. For other languages, the research nurse should contact Language Assistance.

Informed consent will be obtained under circumstances that provide the participant or the participant's legally authorized representative sufficient opportunity to ask questions and

consider whether or not to participate. It should be clear that the subject has a right to withdraw from the study at any time.

If a participant chooses to withdraw consent for a study, the primary investigator must document that the participant is "withdrawing consent to participate in the study" in the chart.

Authority to obtain informed consent:

- The principal investigator, regardless of how his or her authority is delegated, remains ultimately responsible for the actions of those to whom he may delegate authority in obtaining the informed consent.

- The principal investigator may delegate authority to those individuals **who are licensed as physicians in the state of Texas** to obtain the legally effective informed consent of the participant for any study that involves drug therapy, surgery, or invasive procedures.

- Following a discussion between the physician and the patient, a research nurse/coordinator should review the protocol and informed consent document to ensure that the patient understands the protocol procedures and/or treatments. If the patient does not understand the research nurse/coordinator must notify the physician of the patient's concerns or lack of knowledge.

- Once all patient questions and concerns are addressed the physician or the research nurse/coordinator may obtain the actual signature on the informed consent document. It is important that the person obtaining the informed consent must have an adequate understanding of the scientific content of the protocol.

- The principal investigator may delegate authority to obtain informed consent to a **individual who is not a physician** in limited circumstances and only when involving protocols with no more than minimal risk and do not involve drug therapy, surgery or invasive procedures. An individual obtaining informed consent **who is not a physician** should be described in the body of the protocol as the person authorized to obtain informed consent.

- When informed consent is obtained, the person obtaining the consent from the participant or the participant's legally authorized representative must sign his or her name on the informed consent document where the investigator signs. By signing the document, the person obtaining consent certifies that the clinical research study has been fully discussed with the participant and that all requirements for obtaining informed consent have been followed.

Completing the informed consent document:

- Verify that the patient is being presented with the proper version of the informed consent document.

- Complete all blanks listed throughout the document, including name of treating physician.

- The participant or their authorized representative must sign and date three original informed consent documents.

- The principal investigator or collaborator must sign and date the same three original informed consent documents.

- A witness to the consent process must then sign and date the same three informed consent documents. Preferably, the witness should be someone who has no interest in the protocol. The participant's spouse, family member or friend would be the ideal witness. In the event that the participant is alone during the informed consent process, the clinic or research nurse/coordinator can sign as witness.

- An original signed informed consent document should be placed in the participant's medical record, one should be given to the participant and the third placed in the investigator's protocol file.

Documenting the Informed Consent Process:

The informed consent process must be documented in the progress notes of the medical record by the investigator or collaborator explaining the protocol. To verify that the consent process was completed correctly, the documentation should include:

- UTMDACC protocol number or name of the study,

- a brief statement explaining alternative treatment option discussed,

- a statement that the informed consent document was reviewed with the patient, including the risks and benefits of the study,

- a statement describing the patient's decision. Examples include:

  "Patient would like to be treated on study, informed consent signed and copy of original given to patient."

  "Patient wishes to take informed consent home to review with family, will follow up tomorrow with research nurse for additional questions and desired treatment plan"

  "Patient does not wish to participate in study at this time. Will treat off protocol with..."

- If the patient returns on a later date to sign the consent form a note should be placed in the chart on that day describing the interaction.

- A statement describing when the treatment is scheduled to begin.

Re-consenting:

- The informed consent document is considered valid for 30 days from the patient's signature date to begin treatment. If treatment has not begun within 30 days following the signature date listed on the informed consent document than the patient must be reassessed for protocol eligibility and a new consent document completed.

- If there is any material change in the patient's status after informed consent is obtained but before the treatment begins, the patient must be reassessed and the informed consent process should be repeated.

- Participants must be re-consented if there are changes in the informed consent related to safety and/or treatment

a. If the informed consent document is revised due to a serious safety issue, all participants actively receiving treatment will be notified in a timely manner.

b. Participants who are off study will be informed of any new serious adverse events by letter.

c. The participant's medical record must reflect the oral and/or written re-consent process including protocol number or title of study, the date the patient was notified of the change, and if applicable the date the new informed consent document was signed.

d. It is the responsibility of the principal investigator and the research staff to ensure that participants are informed of any changes that may influence their continued participation in a protocol.

Surrogate Decision Makers:

If an adult patient is incompetent or otherwise mentally or physically incapable of communication and **has completed an Advance Directive**, then the designated agent and the attending physician may make health care decisions for the patient.

If the patient is incompetent or otherwise mentally or physically incapable of communication, **has not completed an Advance Directive**, and does not have a legal guardian, then the attending physician and one person, if available, from one of the following categories, in the following priority, may make health care decisions for the patient:

- the spouse;
- the reasonably available adult children;
- the parents; or
- the patient's nearest living relative.

Celecoxib as Adjuvant Biologic Therapy in Patients with Early Stage Head and Neck and Lung Cancer

1.0 Objectives

Current and former smokers have been the focus of recently completed, large-scale lung cancer chemoprevention trials. The outcomes of these trials have been uniformly disappointing. Patients with previous tumors of the aerodigestive tract are at particular risk for second primaries of this area, including non-small cell lung cancer (NSCLC). Preclinical data suggest that celecoxib (celebrex) may have a chemopreventive effect in patients with NSCLC. To test this hypothesis we will perform a randomized biomarker-based clinical trial in patients with definitively treated NSCLC and head and neck squamous cell carcinoma (HNSCC), examining the effect of celecoxib treatment on biomarkers of lung cancer risk.

Specific Aim 1
Hypothesis: Patients with previously treated HNSCC or NSCLC with no evidence of disease will respond to the chemopreventive effects of celecoxib.
Aim: To examine the effect of celecoxib treatment on histological response (defined in Appendix H), markers of proliferation (Ki-67), and apoptosis. Secondary endpoints include time to second primary or recurrence and survival.

Specific Aim 2
Hypothesis: Current and former smokers tolerate treatment with celecoxib.
Aim: To examine the toxicity associated with celecoxib administration in patients with previously treated HNSCC or NSCLC.

2.0 Significance and Background

2.1 Lung cancer as a Significant Public Health Problem

Lung cancer is the leading cause of death from cancer among men and women in the United States, accounting for approximately 28% of deaths from cancer (1). An estimated 159,900 Americans died of lung cancer in 2003. In recent years, the incidence of lung cancer has begun to decline among men (1). However, smoking-related lung cancer has continued to increase among women, surpassing even breast cancer as the leading cause of death from cancer among women (2). Despite aggressive treatment, the five-year survival rate for lung cancer remains approximately 15% (1). These grim facts point out the need for a radical change in our approach to lung cancer. In response to this need, the National Cancer Institute's Division of Cancer Prevention and Control has set prevention as the primary strategy in the control of lung cancer.

2.2 Smoking Cessation and Lung Cancer Prevention

Prevention of smoking and smoking cessation have deservedly prominent places in the National Cancer Institute's programs to reduce deaths from cancer. As a result of massive campaigns to educate the public about the hazards of cigarette smoking, there has been a substantial reduction in the percentage of adults who smoke in the United States. Recent estimates suggest that approximately 50% of adults were once smokers

(about 44 million people in the United States) (2, 3). Despite the reduction in lung cancer risk observed with smoking cessation (2), several studies have demonstrated that former smokers still have a higher lung cancer risk than non-smokers (4-6). Even ten years after smoking cessation, the risk was still significantly elevated for men (7). As a consequence, former smokers account for a large proportion of lung cancers in this country. From the current smoking trends, it appears that former smokers will account for a growing percentage of all lung cancer cases. Thus, the risk of lung cancer in former smokers poses a substantial long-term health threat in this country. Strikingly, 50% of new lung cancer cases are among former smokers, a population numbering roughly 46 million people in the United States (8). Strategies to prevent lung cancer deaths in former smokers include early detection and chemoprevention.

Methods of early detection are now greatly important in lung cancer treatment. Screening techniques analyzing sputum cytology, chest x-rays and more recently, spiral computed tomography (CT) scans have been studied. Recent studies have specifically tested the efficacy of screening individuals at high risk with spiral CT scanning (9-11). The results, while provocative, are not yet definitive, and debate continues as to whether they are sufficient to mandate broad lung cancer screening programs. A study reported in 1999 used low-dose helical CT to screen 1,000 asymptomatic smokers or former smokers, who smoked at least one pack of cigarettes a day for 10 years, or two packs per day for 5 years. All were age 60 or older. All participants received chest x-rays and CT. CT detected from 1-6 non-calcified pulmonary nodules in 23% patients while CXR detected 7%. 27 of the 233 CT lesions were diagnosed as tumor whereas 7 of the 68 CXR lesions were malignant. 23 of the 27 CT tumors were diagnosed as stage I. Although this study shows potential promise in the use of CT for screening, additional trials will be needed before routine CT scanning can be deemed effective (11).

The past fifteen years have revealed the potential of chemoprevention in the reduction of mortality associated with common epithelial cancers. Tamoxifen was effective in primary prevention of breast cancers in women at high risk (12). Non-steroidal anti-inflammatory drugs (NSAIDs) reduced the risk of colorectal cancer in participants with familial adenomatous polyposis (12). Retinoids have in some studies decreased the incidence of second primary tumors (SPTs) in participants with a prior squamous cell carcinoma of the head and neck (HNSCC). A significant SPT reduction in stage I-IV HNSCC was seen with short-term, high-dose 13-cis retinoic acid (51). However, a study using low-dose, long-term 13-cis retinoic acid showed no benefit in overall survival, or SPT- or recurrence-free survival (52). In contrast, the results of lung cancer chemoprevention trials have been disappointing. Several large-scale chemoprevention trials have been performed, including the Euroscan Trial, the Physicians Health Study, the Alpha-Tocopherol and Beta-Carotene (ATBC) trial, and the Beta-Carotene and Retinol Efficacy Trial (CARET), which involved thousands of active smokers followed for over ten years. These studies demonstrated no protective effect of treatment on lung cancer incidence (13-15). In fact, beta-carotene treatment appeared to act as a co-carcinogen, enhancing lung cancer incidence in active smokers. The failure of these large-scale clinical trials has taught us an important lesson; it may be premature to

embark on large-scale trials that involve thousands of participants and cost millions of dollars prior to demonstrating the efficacy of a chemopreventive agent in small, biomarker-based clinical trials. Supporting a biomarker-based approach to predicting the efficacy of specific lung cancer chemopreventive agents, we found no effect of 13-*cis* retinoic acid on bronchial metaplasia and dysplasia in current smokers (16), which is similar to the outcome of the retinoid-based large-scale chemoprevention trials described above.

Based on the data outlined above, smoking cessation and primary prevention of smoking remain the most proven measures to prevent primary lung cancer. Patients who have had prior definitively treated tobacco-related cancers, primarily head and neck and lung cancers, are at higher risk (20-40%) for recurrence or second-primary tumors. No therapies have proven effective to prevent lung cancer in this setting.

2.3 Adjuvant Therapy for Lung Cancer

Despite surgical treatment of early stage lung cancer (stage I/II), only 40-70% of patients are alive at 5 years. Additionally, patients who have had prior definitively treated tobacco-related cancers, primarily head and neck and lung cancers, are at higher risk (20-40%) for recurrence or second-primary tumors during their lifetime. No therapies have proven effective to prevent lung cancer in this setting.

Radiation therapy given after complete surgical resection was one of the earliest forms of adjuvant therapy explored. As reported in the PORT meta-analysis, 2,128 patients from several trials were compared (17). Results showed a detrimental effect of post-operative radiotherapy on survival with an absolute reduction of 7% at 2 years. Subgroup analysis suggested that this occurred in the N0-1 disease subgroup and not in the N2 group. As various surgical and radiotherapy techniques were used, randomized trials are still needed to further clarify the role of radiotherapy, especially in those patients with N2 disease.

Chemotherapy has been tested as adjuvant therapy in resected early stage primary lung cancers in multiple trials. Earlier trials prior to 1980 of single-agent chemotherapy as adjuvant therapy with alkylating agents failed to show a survival benefit and in fact, showed a detrimental effect on survival. A recent meta-analysis of all randomized trials over a 26 year period showed that the absolute risk of death was reduced by 3% at 2 years and 5% at 5 years for patients who had been treated with a cisplatin-containing regimen as opposed to surgical resection (18-23, 50).

2.4 Cyclooxygenase and Cancer Prevention

Cyclooxygenase (COX) inhibitors are being studied in cancer treatment and prevention. There is an increasing body of evidence that non-steroidal anti-inflammatory drugs (NSAIDs) can prevent cancer in humans (24). Most of the epidemiological studies examining NSAIDs as chemopreventive agents have examined the roles of these agents in colorectal cancer. Both retrospective and prospective studies have shown that aspirin, sulindac, and celecoxib can prevent colon cancer and colorectal polyps in humans (25-28). In addition, a prospective study of 12,668 subjects showed that the

incidence of lung cancer, breast cancer, and colon cancer was lower in those who reported aspirin use (29). The exact mechanism of action of the NSAIDs in cancer prevention is unclear, although it is likely that the inhibition of cyclooxygenase-2 (COX-2) is at least partly responsible for their chemopreventive effects.

Most NSAIDs have pleiotropic biological effects, including the inhibition of cyclooxygenase. There are two identified cyclooxygenase enzymes, COX-1 and COX-2. Most tissues express COX-1 constitutively. COX-2 is inducible and increased levels are seen with inflammation and in many types of cancer, including NSCLC and HNSCC. Due to the NSAID side–effect of bleeding, which was attributed to COX-1 inhibition in platelets, selective COX-2 inhibitors were developed (e.g. celecoxib and rofecoxib). COX-2 inhibitors have been used in a variety of pre-clinical studies to examine the effect of COX-2 inhibition on a variety of tumor types, including NSCLC.

Examination of NSCLC tumor tissue from humans by immunohistochemistry, *in situ* hybridization for mRNA, or RT-PCR by several independent investigators has shown that COX-2 is frequently expressed in NSCLC and in premalignant lesions (30-33). COX-2 expression correlates with a worse prognosis, at least in those with early stage disease (34-36). In contrast, adjacent histologicaly normal epithelium as well as histologicaly normal epithelium from smokers without known cancer shows negligible COX-2 expression (37, 38).

Inhibition of COX-2 by genetic and pharmacological methods have led to decreased growth, decreased invasion, decreased angiogenesis, increased tumor lymphocyte infiltration, and increased apoptosis of NSCLC cancer cells *in vitro* and *in vivo* in human tumor xenografts in mice (39-46). Interestingly, there is significant data that suggests that the effects of NSAIDs and even selective COX-2 inhibitors may be independent of COX-2 inhibition (47-49). However, despite this controversy about mechanism, the biological effects of NSAIDs have been clearly seen in pre-clinical models of NSCLC by many independent investigators.

2.5 Rationale for Therapy with Celecoxib

Recent studies have been done in order to assess the effect of celecoxib in chemoprevention and treatment of non-small cell lung cancer (NSCLC). Celecoxib inhibited the growth of seven NSCLC cell lines in a time- and dose-dependent fashion, with an IC50 ranging from 20 to 30 μM. Celecoxib induced apoptosis at concentrations $\geq$50 μM. These effects of celecoxib appeared to be independent of COX-2 protein levels. Based on the clinical and pre-clinical data outlined above, chemopreventive trials for NSCLC using selective COX-2 inhibitors are well supported and have been proposed. These agents are well tolerated for sustained use with relatively few side effects and may have the added benefit of preventing multiple types of cancer (27-29). Thus, substantial preclinical and clinical data support the hypothesis that strategies to target COX-2 will be effective in lung cancer chemoprevention. These findings suggest that celecoxib may be useful for lung cancer chemoprevention, adjuvant therapy, and treatment.

2.6 Study Drug Information (see Appendix C) (53-55)

Celecoxib (marketed under the brand name of Celebrex) is an FDA approved drug for treatment of the symptoms of osteoarthritis and rheumatoid arthritis, and for the reduction in the number of adenomatous colorectal polyps in familial adenomatous polyposis (FAP), as an adjunct to usual care. Celecoxib is a specific inhibitor of the inducible form of the cyclooxygenase enzyme. It has approximately a 375-fold COX-2:COX-1 specificity ratio *in vitro*. Serious toxicities of celecoxib are uncommon and include gastrointestinal (GI) bleeding, allergic reactions, abnormalities in liver function tests, aggravated hypertension, and anemia.

Results from Three Cancer Prevention Clinical Trials, December, 2004:
Safety information from the following three cancer prevention trials was reported from the studies' Independent Data Safety Monitoring Boards:

1. Adenoma Prevention with Celebrex (APC) (National Cancer Institute)
2. Prevention of Spontaneous Adenomatous Polyps (PreSAP) trials (National Cancer Institute)
3. Alzheimer's Prevention study (ADAPT) (National Institute of Aging)

The following is a summary of the results of these three studies:

- The cancer prevention studies used the same cardiovascular review board (commissioned by the data safety monitoring boards of the two respective trials) to adjudicate the results and used the same analysis methods. Patients in the studies were treated for up to 4 years.
- In one of these studies (APC), but not the other (preSAP), celecoxib demonstrated a statistically significant increased cardiovascular risk over placebo.
- A third trial (ADAPT) compared celecoxib to either naproxen sodium or placebo in a group of patients at risk for Alzheimer's disease treated for up to 3 years. Preliminary safety data (not yet adjudicated) from this study indicate an increased cardiovascular risk with naproxen sodium but not with celecoxib relative to placebo.

Cross-sensitivity and/or related problems
Celecoxib may cause bronchoconstriction or anaphylaxis in aspirin-sensitive asthmatics, especially those with aspirin-induced nasal polyps, asthma, and other allergic reactions (the "aspirin triad").

Patients sensitive to other nonsteroidal anti-inflammatory drugs, aspirin, sulfonamides, or related compounds may be sensitive to celecoxib.

Potential drug interactions and/or related problems
The following celecoxib drug interactions and/or related problems have been selected

on the basis of their potential clinical significance. This list is not necessarily inclusive.

Angiotensin-converting enzyme (ACE) inhibitors: Concurrent use with celecoxib may decrease the antihypertensive effects of ACE inhibitors. There is also increased risk of renal failure in patients taking these medications

Antacids containing aluminum or magnesium: The administration of celecoxib with an aluminum– or magnesium–containing antacid has been reported to result in a 37% decrease in the peak plasma concentration and a 10% decrease in the area under the plasma concentration–time curve [AUC] of celecoxib.

Aspirin: Concurrent use with celecoxib may result in celecoxib-induced gastrointestinal ulceration or other gastrointestinal complications. Therefore, low-dose aspirin is recommended.

Diuretics, thiazide or Furosemide: Nonsteroidal anti-inflammatory drugs may decrease the natriuretic effects of diuretics, possibly by inhibiting renal prostaglandin synthesis. Also, the risk of renal failure is increased in patients taking these medications.

Fluconazole: In clinical trials, concurrent administration of fluconazole 200 mg daily resulted in a twofold increase in plasma concentration of celecoxib. The increase in plasma concentration of celecoxib was due to the inhibition of celecoxib metabolism via P450 2C9 by fluconazole. Therefore, if celecoxib is coadministered with fluconazole, the dose of celecoxib should be initiated at the lowest recommended dose.

Lithium: A 17% increase in the plasma concentration of lithium has been reported in patients receiving lithium 450 mg twice a day with celecoxib 200 mg twice a day compared with patients receiving lithium alone. Therefore, monitoring of lithium concentrations is recommended when treatment is initiated and when treatment with celecoxib is discontinued.

Warfarin: Clinical studies reported that celecoxib does not alter the anticoagulant effects of warfarin. Since patients receiving warfarin are at increased risk of bleeding complications, caution is recommended with concurrent use.
In addition, patients receiving celecoxib therapy who are known or suspected to be P450 2C9 poor metabolizers based on previous history may have abnormally high plasma levels of celecoxib due to reduced metabolic clearance. Therefore, celecoxib should be administered with caution in these patients.

Side/Adverse Effects
The following potential adverse events are considered to be more in frequency: edema, skin rash, upper respiratory tract infection.

The following potential adverse events are considered to be less in frequency or rare: bronchitis, dyspnea, gastritis, gastroenteritis, gastrointestinal bleeding or ulceration, allergic reactions, abnormalities in liver function tests, aggravated hypertension,

anemia, influenza-like symptoms, tachycardia, weight gain, back pain, diarrhea, dizziness, dyspepsia, flatulence, headache, insomnia, nausea, pharyngitis, rhinitis, sinusitis, stomach pain, anxiety, anorexia, arthralgia, asthenia, blurred vision, constipation, depression, dry mouth, dysphagia, esophagitis, fatigue, fever, hot flashes, increased sweating, nervousness, palpitations, paresthesias, somnolence, taste perversion, tendonitis, tinnitus, vertigo, vomiting.

3.0 Study Design and Overview

The primary objective of this phase IIb study is to determine the effect of celecoxib on bronchial histological change in patients at high risk for developing NSCLC. Other objectives are to determine if celecoxib is tolerable in this patient population and to examine effects on markers of proliferation and apoptosis and the incidence of second primary tumors and recurrences.

Patients with stage I or II HNSCC or NSCLC after definitive local therapy who have no evidence of disease will be treated with celecoxib for one year. Patients will be evaluated with spiral CT, fluorescent bronchoscopy, and serologies per the vanguard trial. Detailed description of the vanguard trial can be found in a separate protocol. All patients need to consent to the vanguard trial first before consenting to the current study. This celecoxib study is the first of the four sequentially planned biological adjuvant studies in conjunction with the vanguard study.

Clinical studies with celecoxib given as a single agent show that this medication is well tolerated with well-defined, toxicity profiles.

No specific demographic or gender groups will be targeted.

Patients will be consented by the treating physician and the research nurse. Witnesses will be clinic nurses or other members present during the informed consent interview process. Patients may request information and decide to enroll at a later date. Follow-up will occur through the research nurse.

4.0 Patient Eligibility

4.1 Inclusion criteria

1. Patients with either: a) histologically proven stage I, II, or IIIa NSCLC who have undergone a complete surgical resection of the primary tumor **OR** b) stage I or II HNSCC who have undergone definitive local treatment (surgery or radiation therapy).
2. HNSCC patients: Definitive local treatment $\leq$ 12 months prior to trial enrollment. NSCLC patients: Surgery $\leq$ 12 months prior to trial enrollment.
3. No evidence residual cancer
4. Smoking history of at least 10 pack years. May be current or former smoker.

5. Performance status of ≤ 2 (Zubrod, appendix E)
6. Age ≥ 18 years
7. Participants must have no contraindications for undergoing bronchoscopy.
8. Patients must have no active pulmonary infections.
9. Participants must not be taking oral non-steroidal anti-inflammatory drugs on a regular basis.
10. Participants must have the following blood levels: total granulocyte count >1500; platelet count > 100,000; total bilirubin ≤ 1.5 mg %; and creatinine ≤ 1.5 mg %.
11. Participants must complete the pretreatment evaluation and must consent to bronchoscopy and to endobronchial biopsy for biomarker studies.
12. All subjects who agree to participate will be given a written and verbal explanation of the study requirements and a consent form that must be signed prior to registration. Subjects will be informed that (a) they must be willing to take capsules daily for the duration of the trial, (b) they must be willing to take biopsies through bronchoscopy and give blood samples at the specified times, (c) they must schedule and keep the specified follow-up visits with their physicians and the study clinics, and (d) side effects and health risks may occur, as described in the informed consent form.
13. Participant must be enrolled in MDACC protocol #2003-0424 titled "A Phase IIb Vanguard Study Characterizing the Occurrence of Recurrent or Second Primary Tumors in Patients with a Prior History of a Definitively Treated Stage I/II Head and Neck or Non-Small Cell Cancer who are Current or Former Smokers."
14. Patients with prior head and neck cancer only: Participants must have no contraindications for undergoing laryngoscopy.
15. Subject must be considered legally capable of providing his or her own consent for participation in this trial.

4.2 Exclusion Criteria

1. History of radiation therapy to the chest. For those patients with head and neck cancer who received radiation, no more than 10% of the lung volume (apices) may be included.
2. History of systemic chemotherapy. Exception: NSCLC patients may have had up to 4 cycles of platinum-based doublet therapy.
3. Pregnant or breast-feeding (a negative pregnancy test within 72 hours of enrollment for women with child-bearing potential is required)
4. Participants with active gastric or duodenal ulcers or a history of ulcers requiring prophylactic H2 blockers.
5. Participants with active pulmonary infections or recent history of pulmonary infection (within one month).
6. Participants with acute intercurrent illness.
7. Participants requiring chronic ongoing treatment with NSAIDs. (Casual or non-prescribed use of NSAIDs is permitted as long as their use does not exceed one week at a time.)
8. Participants who are allergic to aspirin or sulfanamides.
9. Patients may not take high dose antioxidants (vitamins E or C) during the study period. "High dose" will be determined by the study investigators.

10. Patients may not take high dose synthetic or natural Vitamin A derivatives (> 10,000 IU per day).
11. History of biologic therapy
12. Women of childbearing potential and men with partners of childbearing potential who are not using an effective method of contraception. Use of contraception will be verified at office visits during first year on study.

In addition, the following exclusion criteria have been added to address the cardiovascular risk associated with celecoxib:

a. History of cardiovascular diseases that might include one of the following: myocardial infarction, angina, coronary angioplasty, congestive heart failure, stroke, or coronary bypass surgery.
b. Diagnosis of diabetes
c. History of deep venous thrombosis, pulmonary embolism, systemic lupus erythermatous, family history of protein S or C deficiencies, prior heparin-induced thrombocytopenia, or known Factor V Leiden mutation.
d. Family history of premature CAD. This is defined as individuals with either: 1) father with MI prior to age 55, or 2) mother with MI prior to age 60.

Patients will be enrolled from the Thoracic/Head and Neck Medical Oncology and Surgical Oncology clinics at M. D. Anderson and from respective clinics at the other sites. Research nurses will also identify candidates from the clinic rosters and promote awareness in the community through various media outlets.

Children, pregnant women, and breast-feeding women will not be enrolled into the study. Participants will be consented by procedures described in sections 3.0 and 13.4. The consent process and informed consent document will clearly state that patients are not required to participate in the study and that they may stop participation in the study at any time.

5.0 Treatment Plan

Patients who meet the eligibility criteria in section 4 will be randomly assigned in a 2.5:1 ratio to either: 1) treatment with celecoxib or 2) no treatment. Patients assigned to treatment will be treated for a total of 12 months. All patients will undergo a bronchoscopy and spiral CT at baseline. These studies will be repeated 12 months after baseline. The plan is to start treatment patients at dose level 0 and reduce the dose as outlined in section 6.3. There will be no dose escalation.

Patients will be followed for up to 3 years after the first 12 month period, for a total of up to 4 years.

Celecoxib will be administered in oral 200 or 400 mg capsules. Patients will take the celecoxib by mouth twice daily at least 8 hours apart. Prior to study entry, all NSCLC patients will be counseled on the risks and benefits of systemic chemotherapy as adjuvant therapy and recent trials that have been reported (i.e., International Adjuvant Lung Cancer Trial (IALT)) (50). Only NSCLC patients not wishing to receive adjuvant chemotherapy will be eligible for enrollment into this trial.

5.1 Severe Dysplasia/Carcinoma in Situ

Any participants found to have severe dysplasia or carcinoma in situ at initial or subsequent bronchoscopy will be strongly encouraged to undergo additional bronchoscopies at 6-month intervals. Any participant discovered to have invasive carcinoma at any time during the study will be referred for appropriate intervention (CIS pathway Appendix B).

5.2 Smoking Cessation Program

Any participant who is a current smoker will be offered participation in a smoking cessation program.

6.0 Study Activities

6.1 Pre-Study Evaluations (see Appendix I)

Unless otherwise noted, labs, physical exams, imaging studies, and the laryngoscopy are to be performed within 4 weeks of beginning participation in this study.

1. Signed informed consent
2. Medical history including smoking history (duration and intensity)
3. Physical exam: including height, weight, Zubrod performance status assessment. Vital signs including pulse, blood pressure, temperature
4. Bronchoscopy
5. Buccal brushing
6. Sputum and saliva sample
7. Serum sample for biomarkers
8. Serum chemistry and electrolytes to include: BUN, creatinine, total bilirubin, SGPT, alkaline phosphatase, albumin
9. Hematology to include: CBC with automated differential and platelet count
10. Chest x-ray
11. CT scan of chest
12. Laryngoscopy for patients with prior head and neck cancers
13. PT
14. Pregnancy test (urine or serum) for females of childbearing potential within 72 hours prior to enrollment
15. Lipid profile

The following steps will be taken in order to minimize the cardiovascular risk for study participants:

1. Patients with uncontrolled hypertension should receive treatment according to JNC-7 guidelines (appendix J) for their hypertension before beginning treatment on this study. The treating physician will consult with Cardiology regarding this treatment.
2. Uncontrolled hypercholesteremia [low-density lipoprotein cholesterol (LDL-C) > 130] needs to be controlled following the updated National Cholesterol Education Program Adult Treatment Panel III Guidelines (see Appendix K) prior to enrolling in the study. Hypercholesteremia treatment should continue during the entire period of celecoxib treatment on the protocol.
3. Patients who are currently taking low-dose aspirin (≤ 81 mg/day) or Plavix therapy will continue to do so. However, these patients will be informed that taking either low-dose aspirin or Plavix in combination with celecoxib may increase their risk of bleeding. Patients who experience bleeding diathesis during treatment will be removed from the protocol.
4. Patients with metabolic syndrome will be aggressively managed according to the National Cholesterol Education Program (NCEP) using ATP III Guidelines (see Appendix K). Information on the NCEP can be found at: http://www.nhlbi.nih.gov/about/ncep/index.htm

6.2 Treatment Evaluations while on study (see Appendix I)

The participant will be observed on the study for a total of 36 months. Treatment evaluations will include those as part of the Vanguard trial as well as additional testing for those enrolled on this adjuvant study including:

1. Patients randomized to receive celecoxib: Medical history and physical exam by a physician or nurse at 3, 6, and 12 months. Upon completion of celecoxib patients will be followed monthly until resolution of symptoms from study medications. A focused history and physical will be done to evaluate and document any symptoms of GI bleeding, vision changes, rash, headache, arthralgias, dyspepsia, or other symptoms. At each visit, patients will be evaluated for cardiac symptoms, including chest pain, shortness of breath, and palpitations. If a participant develops cardiac symptoms during the trial, s/he will be referred to the consulting cardiologist.

   Patients randomized to no treatment: Medical history and physical exam by a physician or nurse at months 6 and 12. Nursing follow-up by phone at months 3 and 9.

   All patients: Medical history and physical exam by physician at months 24 and 36. Medical history and nursing exam at months 18 and 30. After 36 months, the patient will have a medical history and physical exam every 6 months. The exam will be performed by a physician every 12 months after 36 months. The other physical exams will be performed by a nurse.

2. Bronchoscopy at months 12, 24 (optional), and 36 (optional). Assessment of histology and biomarkers will be performed in the tissue biopsy at the same time. If an intercurrent illness coincides with a time period where bronchoscopy is scheduled, the bronchoscopy will be delayed 30 days or until resolution of the illness.
3. Buccal brushing at months 12, 24 (optional), and 36 (optional).
4. Sputum and saliva sample at months 12, 24 (optional), and 36 (optional).
5. Serum chemistry and electrolytes to include BUN, creatinine, SGPT, total bilirubin, alkaline phosphatase, albumin at months 3 (patients randomized to celecoxib only), 6, 12, 18, 24, 30 and 36. After 36 months, the participant will have assessments every 12 months for as long as s/he remains observed on the study.
6. Hematology to include: CBC with automated differential and platelet count at month 3 (patients randomized to celecoxib only), 6, 12, 18, 24, 30 and 36. After 36 months, the participant will have assessments every 12 months for as long as s/he remains observed on the study.
7. Serum samples for biomarkers will be collected at months 3, 6, 12, 18, 24, 30 and 36. After 36 months, the participant will have assessments every 12 months for as long as s/he remains observed on the study.
8. Chest x-ray at 6, 12, 18, 24, 30 and 36 months.
9. Chest CT at 6, 12, 18, 24, 30 and 36 months.
10. Head neck exam with laryngoscopy at 12 months for those patients with prior head and neck cancer.

6.3 Dose modifications

All patients will start at dose level 0. There will be no planned dose escalation. The NCI Common Terminology Criteria for Adverse Events v3.0 (CTCAE) will be used (appendix F). Patients who experience any grade 2 or 3 toxicity will have medication held until resolution to grade 0-1 and then medication will be restarted at the next lower dose level. Patients who experience any grade 4 toxicity will have medication held until resolution to grade 0-1 and then medication will be restarted at the dose two levels below that at which the grade 4 toxicity occurred.

Dose Level	Celecoxib
0	600 mg QD
-1	400 mg QD
-2	200 mg QD
-3	Discontinue

6.4 Long Term Follow up

All participants will be followed until approximately 36 months after study enrollment at which time repeat testing and assessment will be done including optional bronchoscopy. Participants will then be followed at 6 month intervals until the study is completed. Participants will be followed for survival with an annual follow-up appointment and form to be completed for at least one year after final participant enrolled completes a 36

month evaluation or a maximum follow-up of 6 years. We plan to begin enrolling participants in this study in 5/05. We expect that participants will be followed until 4/10.

6.5 Early withdrawal

Early withdrawal is defined as a participant who is unable to continue participation on the study, participant refusal, or noncompliance. The following study activities will be completed at early withdrawal or at the end of study.

1. Medical history including documentation of smoking status
2. Physical exam
3. Radiologic/ (optional) bronchoscopic assessment with tissue/sputum/washings samples
4. Serum chemistry and electrolytes to include: BUN, creatinine, sodium, potassium, chloride, glucose, total bilirubin, SGPT, alkaline phosphatase, and albumin.
5. Hematology to include: CBC with automated differential and platelet count
6. Serum collection for biomarker studies
7. Record for concomitant medications.
8. Monitor for adverse events.

6.6 Study Procedures

Please refer to the Vanguard Protocol (MDACC protocol #2003-0424, titled "A Phase IIb Vanguard Study Characterizing the Occurrence of Recurrent or Second Primary Tumors in Patients with a Prior History of a Definitively Treated Stage I/II Head and Neck or Non-Small Cell Cancer who are Current or Former Smokers") for specific details of the trial procedures.

6.7 Handling and Dispensing of Celebrex™

Celebrex™ must be dispensed only from official study sites by authorized personnel according to local regulations. It should be stored in a secure area according to local regulations. It is the responsibility of the Investigator to ensure that study drug is only dispensed to study patients. Unless otherwise instructed by Pfizer in writing, the Institution will destroy any supplies of Celebrex™ that expire during this study. The Institution will destroy these materials in accordance with all applicable regulations and governmental guidelines and institutional policies.

7.0 Investigational Centers

Patients will be seen and enrolled at the University of Texas M. D. Anderson Cancer Center, Department of Thoracic/Head and Neck Medical Oncology clinics, Houston, TX. Additional study sites include: 1) Eisenhower Army Medical Center, Fort Gordon, GA, 2) Conemaugh Memorial Medical Center, Johnstown, PA, and 3) The Methodist

Hospital, Houston, TX. Laboratory studies will also be performed at each of these sites. Additional sites may be added throughout the study.

7.1 Investigator Contact Information

Principal Investigator:

Waun Ki Hong, MD
University of Texas M.D. Anderson Cancer Center
1515 Holcombe Blvd., Unit 432
Houston, TX 77030
Phone: 713-792-6363
Fax: 713-792-1220
e-mail: whong@mdanderson.org

Co-Principal Investigator:

Edward Kim, MD
University of Texas M.D. Anderson Cancer Center
1515 Holcombe Blvd., Unit 432
Houston, TX 77030
Phone: 713-792-6363
Fax: 713-792-1220
e-mail: edkim@mdanderson.org

8.0 Criteria for Discontinuation of Therapy

Patients will be removed from therapy for any of the following reasons:

1. Dose reduction to the –3 level (above)
2. Pregnancy or planned pregnancy
3. Patient requests to withdraw
4. Unwilling or unable to comply with study requirements
5. Identification of recurrent or new cancer
6. Unrelated intercurrent illness that will affect assessment of clinical status to a significant degree as determined by the principal investigator or the treating physician
7. The treating physician or investigator must discontinue therapy if he/she thinks that the patient's health or well-being is threatened by continuation of therapy.

If any safety parameters show a clinically significant change from baseline that warrants early termination of treatment, the patient will continue with the scheduled study-related procedures. Appropriate safety monitoring will continue until the patient is discharged from the study. Patients withdrawn from the study will be followed until resolution of toxicity. The reason for and date of the discontinuation will be obtained. The date of the last dose of study medication will also be obtained.

9.0 Adverse Events

9.1 Assessment of Adverse Event Severity & Relationship to Treatment

All serious adverse events (defined below), whether or not deemed drug-related or expected, must be reported by the Principal Investigator or designee to the HSRRB and/or USAMRMC, Human Research Protection Office within 24 hours (one working day) by telephone. A written report must follow as soon as possible, which includes a full description of the event and any sequelae. This includes serious adverse events that occur any time after the inclusion of the subject in the study (defined as the time when the subject signs the informed consent) up to 30 days after the subject completed or discontinued the study. The subject is considered completed either after the completion of the last visit or contact (e.g., phone contact with the Investigator or designee). Discontinuation is the date a subject and/or Investigator determines that the subject can no longer comply with the requirements for any further study visits or evaluations (e.g., the subject is prematurely discontinued from the study). An adverse event temporarily related to participation in the study should be documented whether or not considered to be related to the test article. This definition includes intercurrent illnesses and injuries and exacerbations of preexisting conditions.

Include the following in all IND safety reports: Subject identification number and initials; associate investigator's name and name of MTF; subject's date of birth, gender, and ethnicity; test article and dates of administration; signs/symptoms and severity; date of onset; date of resolution or death; relationship to the study drug; action taken; concomitant medication(s) including dose, route, and duration of treatment, and date of last dose.

A serious adverse event is any event that is: fatal; life-threatening (life-threatening is defined as the patient was at immediate risk of death from the adverse event as it occurred); significantly or permanently disabling; or requires in-patient hospitalization.

Important medical events that may not result in death, be life-threatening, or require hospitalization may be considered a serious adverse drug experience when, based upon appropriate medical judgment, they may jeopardize the patient or subject and may require medical or surgical intervention to prevent one of the outcomes listed in this definition. In addition, laboratory value changes may require reporting.

Reports of all serious adverse events must be communicated to the appropriate Institutional Review Board (IRB) or ethical review committee and/or reported in accordance with local laws and regulations.

9.2 Procedures for Reporting Serious Adverse Events

Serious and/or unexpected adverse events are submitted in writing to the M.D. Anderson Cancer Center Institutional Office of Protocol Research (OPR) within 10 working days of the adverse experience as described Appendix A. Unexpected fatal or life-threatening experiences are phoned immediately to the Office of Protocol Research

(713-792-2933). A follow up written report is submitted to OPR within 10 working days. The form for communication to OPR of all serious adverse events is appended to this plan.

Reports of all serious adverse events must be communicated to the appropriate Institutional Review Board (IRB) or ethical review committee and/or reported in accordance with local laws and regulations. Adverse experiences that are both serious and unexpected will be immediately reported by telephone to the USAMRMC, Human Research Protection Office (301-619-2165) and send information by facsimile to 301-619-7803. A written report will follow the initial telephone call within 3 working days. Address the written report to the U.S. Army Medical Research and Material Command, ATTN: MCMR-HRPO, 504 Scott Street, Fort Detrick, Maryland 21702-5012.

For all protocols conducted at M.D. Anderson Cancer Center, the Principal Investigator is responsible for submitting adverse event reports to the Institutional IRB and DoD on an ongoing basis. Adverse event reports are submitted to the Institutional Office of Protocol Research (OPR), where they are entered into PDMS and forwarded to the designated IRB vice chairperson for review. Attached to each adverse event report is a listing of all prior adverse events submitted for that protocol. Any comments, questions or changes the IRB requests to the protocol as a result of this review are conveyed to the principal investigator. The investigator response and protocol modification process is monitored by the IRB vice-chairperson and OPR support staff. The vice chairperson presents the report on adverse event review to the full committee at the next IRB meeting.

An adverse event report compilation is provided once annually to the M.D. Anderson Cancer Center IRB. Comments, questions or other considerations from the IRB are conveyed to the principal investigator for evaluation, discussion and implementation.

For all protocols conducted at M.D. Anderson Cancer Center, the Principal Investigator is responsible for submitting adverse event reports to the Institutional IRB on an ongoing basis. Adverse event reports are submitted to the Institutional Office of Protocol Research (OPR), where they are entered into PDMS and forwarded to the designated IRB vice chairperson for review. Attached to each adverse event report is a listing of all prior adverse events submitted for that protocol. Any comments, questions or changes the IRB requests to the protocol as a result of this review are conveyed to the principal investigator. The investigator response and protocol modification process is monitored by the IRB vice-chairperson and OPR support staff. The vice chairperson presents the report on adverse event review to the full committee at the next IRB meeting.

An adverse event report compilation is provided once annually to the M.D. Anderson Cancer Center IRB. Comments, questions or other considerations from the IRB are conveyed to the principal investigator for evaluation, discussion and implementation.

9.3 Reporting of Subject Death

The death of any subject during the study or within 30 days of study completion (as defined above), regardless of the cause, must be reported within 24 hours by telephone, to the principal investigator and/or study coordinator, and the HSRRB and/or USAMRMC, Human Research Protection Office. A full written report must follow as soon as possible. If an autopsy is performed, the report must be provided to the Sponsor.

Reports of all serious adverse events, including deaths, must be communicated to the appropriate Institutional Review Board or ethical review committee and/or reported in accordance with local law and regulations.

9.4 Known Adverse Events Relating to the Underlying Clinical Condition

These will be reported on the chart and in the study case report forms.

10.0 Statistical Considerations

A total of 70 patients will be recruited in this trial and randomized with a 2.5:1 ratio (via computerized central randomization) into active (celecoxib treatment) or the no-treatment control arm. The standard practice for these patients after definitive therapy is follow-up (no treatment). Therefore, it is ethical to randomize patients into the no-treatment control arm. All patients will receive comprehensive risk assessment and screenings as defined in the Vanguard Trial.

The primary endpoint of the study is histological response. Histological response is based on changes in baseline to 12 month assessment of biopsies taken during bronchoscopy at six sites (main carina, carinas at both upper lobe orifices, carina at right middle lobe orifice, carina between RB 9 and RB 10 and carina between LB 9 and LB10) in the lung. There are 3 critiera for establishing a response based upon a 1-7 score assigned to each biopsy including, 1) the average score of all biopsies decrease by 1, 2) the percentage of biopsies with moderate dysplasia or worse (score 5-8) decreases by 10%, and 3) the worst score improves by 1. A response is defined as an improvement in at least 2 of the 3 criteria. Progression is worsening in 2 or more of the 3 criteria. Otherwise, the histological response will be coded as no change. The proliferation marker Ki-67 will be used as a secondary endpoint to evaluate the efficacy of the biologic treatment. Other mechanism-based biomarkers such as apoptotic index will also be analyzed.

We will monitor efficacy and toxicity simultaneously using the method of Bryant and Day (Biometrics 1995) (56). Efficacy is based baseline to 12-month histological response as defined above. For purposes of toxicity, any grade 2 or higher adverse event will be counted. Unacceptable response is 10% and a 30% response rate would be considered sufficiently active to warrant further study of this regimen. A 10% and 40% grade II toxicity rate are considered acceptable and excessive, respectively. We assume one-sided 5% type I error rates for both efficacy and toxicity. With 50 patients treated and evaluated, we have 95% power to detect clinically meaningful improvement

in response to 30% at 12 months. The interim analysis will take place when 20 patients have been treated and are evaluable for response. If 2 or fewer responses are observed in the first 20 patients treated with acceptable toxicity, the protocol will stop accrual due to insufficient activity. Similarly, if 7 or more patients experience a grade 2 or higher adverse event with acceptable response, the protocol will stop accrual due to excessive toxicity. Otherwise, the protocol will continue accrual to a maximum of 50 patients. If 9 or more patients experience a response and 36 patients do not experience a grade 2 or higher adverse event in 50 patients treated and evaluated, then this treatment will be recommended for further clinical evaluation.

For detecting biomarker modulation on a continuous variable such as Ki-67, the paired-t test will be performed comparing the biomarker values before and after treatment. Transformations (e.g. natural log) will be performed if necessary to meet normality assumptions of the test. With 50 patients receiving the biologic treatment, we will be able to detect an effect size (expected mean difference divided by the standard deviation of the difference) of 0.404 with 80% power and two-sided 5% type I error rate.

For detecting biomarker modulation on a dichotomous variable, McNemar's test will be used to compare the status of a biomarker such as present/absence or high/low before and after treatment. Assume that p_{21} and p_{12} are the probability changing from absence to presence and from presence to absence for a biomarker. $p_{21} + p_{12}$ are the proportion of discordant pairs pre- and post-treatment. Further, $p_{11} + p_{12}$ is the proportion of concordant pairs (i.e., p_{11} = proportion positive pre- and post-treatment and p_{22}=proportion negative pre- and post-treatment). With 50 patients and two-sided 5% type I error rate, we will have 85% power detect a 25% change in modulation for p_{21} = 0.05 and p_{12} = 0.30 and 94% power to detect a 30% change for p_{21} = 0.05 and p_{12} = 0.35. The power computations are shown in the following table.

p_{21}	p_{12}	$p_{12} - p_{21}$	Power
0.05	0.30	0.25	85%
0.10	0.35	0.25	71%
0.05	0.35	0.30	94%
0.10	0.40	0.30	84%

We will also compare the treatment efficacy between the treatment arm and the control arm. We plan to treat 280 patients in four sequentially conducted bioadjuvant trials (70 patients each); each trial will have exactly the same eligibility criteria. We will randomize 20 patients into the control group in each of these four biologic-agent trials. We expect an additional 70 patients will choose to enroll in the vanguard (i.e. observation only) part of the umbrella trial. Therefore, we will have 20x4 + 70 = 150 control patients in the vanguard study who did not receive any active agents. Control patients will be analyzed to test for any trial-specific difference or time trend and will be combined if no difference is found among various control groups. Power calculations for two-sample t-test was performed with two-sided 5% type I error rate. With 50 in the biologic treatment arm and 20 (only control patients in this trial is used) or 150 (aggregate all the control patients together) in the control arm, we will have 80% power to detect standardized effect sizes

of 0.76 and 0.46 for continuous outcomes, respectively. For dichotomous outcomes, statistical power for detecting various differences is given in the following table. With 20 in the control arm and 50 in the active arm, we will have 80% power to detect a difference of histological response of 5% and 35%, respectively. Similarly, 85% of power can be achieved if the response rates are 10% and 45%, respectively. If we combined all no-treatment controls, we will be able to detect a 25% difference in the response rate with at least 92% power for no-treatment response rates from 5% to 20%.

Ncontrol	$P_1 - P_0$	P_0		
		0.05	0.10	0.20
20	0.30	80%	73%	65%
	0.35	91%	85%	79%
150	0.20	99%	94%	78%
	0.25	99%	99%	92%

11.0 Concomitant Medications

- All concomitant medications will be recorded.
- The best supportive care and treatment will be given to each participant (antibiotics, transfusions, diet, etc.)
- No concurrent investigational agents will be permitted.
- No concurrent antineoplastic agents or hormonal anticancer therapy will be permitted.
- No concurrent radiotherapy will be permitted.
- Participants taking cyclooxygenase inhibitors, lipoxygenase inhibitors, NSAIDs, and steroids will be encouraged to refrain from taking, if possible, while on study and at least 4 weeks prior to enrollment.
- Other Concomitant Treatment
- Systemic retinoids and herbal medicines or remedies (including green tea) must be discontinued before entry into the trial and are not allowed during the trial. Patients may not be taking high-dose vitamin A within 30 days of study entry.
- Other medication, which is considered necessary for the participant's safety and well being, may be given at the discretion of the investigator(s).

12.0 Methods for Biomarker Analysis

All samples will be processed and stored via the pathology department. Then, the samples will be distributed to specific investigators for studies including biomarkers of apoptosis and cell proliferation, gene expression profiling, genomics, proteomics, and other specified biomarkers of intermediate response.

13.0 Study Administration and Investigator Obligations

13.1 Replacement of Subjects

Participants who withdraw from the study prior to completion of the study treatments for reasons other than serious adverse events, unacceptable toxicity or progressive disease will be defined as dropouts and will be replaced. Replacement participants will be assigned the next sequential number.

13.2 Protocol Compliance

The attending physician and oncology research nurse will evaluate each participant at the initial clinic visit to determine whether the participant qualifies for the study and at each clinic visit thereafter to determine readiness for bronchoscopic procedures. All required interim and pretreatment data will be available to them for evaluation.

13.3 Institutional Review Board

This study must have the approval of a properly constituted Hospital Ethics Committee, Regional Ethics Committee, or other Institutional Review Board (IRB).

The investigator must also report all serious and medically significant adverse events to the IRB or Ethics Committee, NCI, sponsor, as well as the USAMRMC, Human Research Protection Office (see section 9.1).

13.4 Informed Consent

All study participants must sign and date an informed consent form prior to study participation. The investigator will be responsible for designing the consent form using appropriate National or Regional Guidelines (equivalent to the American Federal Guidelines Federal Register July 27, 1981, or 21 CRF Part 50, or International Committee on Harmonization-Good Clinical Practice).

The informed consent form must be approved by the IRB or Ethics Committee. State and local laws, and/or institutional requirements may require the disclosure of additional information on the informed consent form.

A copy of the informed consent form will be given to the participant. The investigator will keep each participant's signed informed consent form on file for inspection by a regulatory authority at any time.

13.5 Record Retention

- The investigator and other appropriate study staff will be responsible for maintaining all documentation relevant to the study. Such documentation includes:
- Case Report Forms—must be legible, accurate, and up-to-date.
- Copies of all Serious AE reporting forms faxed to the USAMRMC, Human Research Protection Office.
- Participant Files—should substantiate the data entered in the CRFs with regard to laboratory data, participant histories, treatment regimens, etc.

- Participant Exclusion Log—should record the reason any participant was screened for the study and found to be ineligible.
- Drug Dispensing Log—should record the total amount of study drug received and returned to supporter providing the study drug, and the amount distributed and returned or destroyed. This information must agree with the information entered in the CRFs.
- Informed Consent Forms—completed consent forms from each participant must be available and verified for proper documentation.
- Informed Consent Log—must identify all participants who signed an Informed Consent Form so that the participants can be identified by audit.

The Investigator must keep on file protocols, amendments, IRB approvals, all copies of Form FDA 1572, all correspondence, and any other documents pertaining to the conduct of the study for a minimum of two (2) years after notification by USAMRMC, Human Research Protection Office of either FDA approval or discontinuation of the IND.

13.6 Case Report Forms

Data recorded on Case Report Forms (CRFs) must be legible and complete. CRFs will be completed on a timely basis. The individual making the correction on the CRF must initial and date the correction. The investigator must review all final and corrected CRFs. Corrected copies of CRFs will be filed with the corresponding original.

If a subject's medical record is needed, it will be requested by the Principal Investigator or Co-Principal Investigator. The requesting investigator (i.e., either the PI or co-PI) will assume responsibility for medical record abstraction, which will be performed by an oncology research nurse and the PI or co-PI. The PI and co-PI are medical oncologists.

13.7 Study Monitoring

The University of Texas M.D. Anderson Cancer Center will monitor the study investigators in the Department of Thoracic/Head and Neck Oncology, once a year or at appropriate intervals to assure satisfactory enrollment rate, data recording, and protocol adherence. The frequency of monitoring may vary depending on enrollment rate and the quality of data collected. The investigator and staff are expected to cooperate and provide all relevant study documentation in detail at each site visit on request for review. Compliance will be measured by (1) self-reported records of pill-taking and (2) pill counts. M.D. Anderson Cancer Center will randomly monitor and/or audit the other participating sites at appropriate intervals to assure satisfactory protocol adherence and enrollment.

13.8 Termination of Study

The HSRRB and/or USAMRMC, Human Research and Protection and M. D. Anderson will retain the right to terminate the study and remove all study materials from the study site at any time. Specific instances that may precipitate such termination are as follows:

- Unsatisfactory participant enrollment with regard to quality or quantity
- Deviation from protocol requirements, without prior approval from HSRRB and M. D. Anderson.

- Inaccurate and/or incomplete data recording on a recurrent basis
- The incidence and/or severity of adverse drug events in this or other studies indicating a potential health hazard caused by the treatment

13.9 Study Amendments

The investigator will only alter the protocol to eliminate apparent immediate hazards to the participant. If preliminary or interim statistical analysis indicated that the experimental design, dosages parameters, or selection of participants should be modified, these changes will be described in an amendment to be approved by the institution's and other appropriate review committees after consultation with the statistician and Study Chairman. Any amendments cannot be enacted unless approved by the HSRRB and/or USAMRMC, Human Research Protection Office. All revisions made to protocols previously approved by the IRB will be submitted to the IRB for approval prior to implementation of the revision. If the IRB decides to disapprove a research activity, it shall included in its written notification a statement of the reasons for its decision and give the investigator an opportunity to respond in person or in writing. No changes to the protocol will be initiated unless also approved by the Human Subjects Research Review Board.

13.10 Ethical and Legal Considerations

This study will undergo full approval in accordance with the human surveillance requirements of each institution. Blood samples will be obtained for the evaluations as described in the protocol. Tissue samples obtained at the time of prior surgeries will be reviewed before participant enrollment to confirm the participant's diagnosis. Measures will be taken to ensure confidentiality of participant information. Tissue samples will be collected prospectively during the trial. Data collected on paper forms will be stored in locked file cabinets with restricted access. Data collected on electronic media will be stored in computer files with restricted password access limited to the principal investigator and study coordinators. All staff members in the study will be informed prior to employment and at regular intervals of the necessity for keeping all data confidential. Computers will not be accessible to the public and will be located in locked offices. Subjects will be assigned a separate study number to protect subject identification. No patient identifiers will be used in any publications of this research. Data will be maintained indefinitely. When the time comes to dispose of the data, all database files will be deleted.

13.11 Risks/Benefits

Participants will benefit from the educational information provided, including counseling on alcohol and smoking cessation, from the regular follow-up procedures required, and from the blood analyses (i.e., electrolytes, liver function tests, complete blood count, and platelet count). Participants will also benefit from the close comprehensive follow-up after their surgery including additional imaging tests. Participants may benefit from development of a risk model and adjuvant therapy with biologic compounds.

Participants will undergo several invasive procedures (bronchoscopies) which do have associated risks. These risks will be explained completely prior to consenting of the

participant. The following table summarizes risks associated with this study and the steps that will be taken to minimize these risks:

Procedure	Risks	How risks will be reduced
Bronchoscopy with bronchoalveolar lavage, bronchial washings, bronchial brushings, and bronchial biopsies	➢ Coughing ➢ Bleeding ➢ Collapsed lung ➢ Minor sore throat ➢ Mild fever ➢ May cause breathing problems similar to asthma ➢ Bronchitis ➢ Pneumonia ➢ Sedatives given during procedure can decrease breathing function and/or level of oxygen in blood. ➢ May have allergic reaction to sedatives or anesthetics	➢ Presedation assessment to identify particular risk factors ➢ Use of conscious sedation and topical anesthesia to minimize discomfort and cough. ➢ Establish adequate preprocedure bleeding parameters ➢ Monitoring of level of consciousness, cardiovascular and gas exchange parameters during procedure and recovery.
Buccal sample	➢ Pain ➢ Discomfort ➢ Irritation ➢ Bleeding	➢ Brushings on inner cheek performed lightly while patient is under conscious sedation
Laryngoscopy	➢ Discomfort ➢ Gagging ➢ Reaction to topical anesthesia ➢ Nasal irritation ➢ Nasal bleeding	➢ Topical anesthesia will be used to reduce discomfort and gagging ➢ Exams will be performed by experienced personnel

As described in section 2.6, results from the celecoxib adenoma prevention study show a statistically significant increased cardiovascular risk over placebo in patients receiving long-term treatment with celecoxib. Since the treatment on this study is limited to 12 months and since patients will be screened for pre-existing cardiac risk and monitored for any new cardiac symptoms, we do not anticipate that treatment with celecoxib will produce any serious or long-term health effects, although some toxicity (such as gastrointestinal toxicity) may be experienced. The cardiac risks and possible gastrointestinal toxicity will be clearly described in the informed consent form.

Subjects who are on low-dose aspirin regimens or Plavix® (clopidogrel bisulfate) therapy may be at increased risk of bleeding by taking celecoxib. However, as described in section 6.1, individuals who are on a low-dose aspirin regimen or Plavix therapy will be instructed to continue taking aspirin or Plavix. The increased risk of bleeding will be described in the informed consent.

Smokers are at increased risk of cardiovascular events. This will be described in the informed consent.

Subjects will benefit from the educational information provided, including counseling on alcohol and smoking cessation, from the regular follow-up procedures required, and from the blood analyses (i.e., complete blood count, platelet count). If celecoxib is found to modulate biomarkers of lung cancer risk, this information will be shared with

patients as soon as possible. In addition, the benefits to society will be substantial and may directly translate into a reduction of cancer morbidity and mortality. If celecoxib is not found to be effective, the trial will still be of value in providing prospective information on risk in this population and in allowing future research to focus on other potentially beneficial intervention initiatives.

Participants will not be financially responsible for any study-related tests outside of accepted standard of care follow-up.

13.12 Gender and Minority Inclusion

Women and minorities will be actively recruited to participate in the Vanguard trial. However, since only 42% of lung cancer participants and 22% of laryngeal cancer participants are female, we expect to have more male than female subjects on the study. We expect that the ethnic distribution of the enrolled participants will reflect the local ethnic mixture of each institution's surrounding community.

13.13 Subject Records

HSRRB and/or USAMRMC, Human Research Protection Office, M.D. Anderson or their representatives may have access to subject records as a part of their responsibility to protect human subjects in research.

13.14 Publication Statement

Data will be reviewed by the collaborating biostatistician prior to publication. HSRRB and/or USAMRMC, Human Research Protection Office will have 30 days to review all definitive publications, such as manuscripts and book chapters, and a minimum of 10-15 days to review all abstracts.

14.0 References

1. Cancer Facts and Figures. *In:* American Cancer Society, Atlanta, GA, 1997.
2. U.S. Department of Health and Human Services. The Health Benefits of Smoking Cessation: A Report of the Surgeon General. DHHS Publication Number 90-8416, 1990.
3. Glynn, T. J., Manley, M. W., Mills, S. L., and Shopland, D. R. The United States National Cancer Institute and the science of tobacco control research. Cancer Detect Prev, *17:* 507-512, 1993.
4. Halpern, M. T., Gillespie, B. W., and Warner, K. E. Patterns of absolute risk of lung cancer mortality in former smokers. J Natl Cancer Inst, *85:* 457-464., 1993.
5. Lubin, J. H. and Blot, W. J. Lung cancer and smoking cessation: patterns of risk. J Natl Cancer Inst, *85:* 422-423., 1993.
6. Sobue, T., Yamaguchi, N., Suzuki, T., Fujimoto, I., Matsuda, M., Doi, O., Mori, T., Furuse, K., Fukuoka, M., Yasumitsu, T., and et al. Lung cancer incidence rate for male ex-smokers according to age at cessation of smoking. Jpn J Cancer Res, *84:* 601-607., 1993.
7. Risch, H. A., Howe, G. R., Jain, M., Burch, J. D., Holowaty, E. J., and Miller, A. B. Are female smokers at higher risk for lung cancer than male smokers? A case-control analysis by histologic type. Am J Epidemiol, *138:* 281-293., 1993.
8. Landis, S. H., Murray, T., Bolden, S., and Wingo, P. A. Cancer statistics, 1999. CA Cancer J Clin, *49:* 8-31, 31., 1999.
9. Fontana, R. S., Sanderson, D. R., Woolner, L. B., Taylor, W. F., Miller, W. E., Muhm, J. R., Bernatz, P. E., Payne, W. S., Pairolero, P. C., and Bergstralh, E. J. Screening for lung cancer. A critique of the Mayo Lung Project. Cancer, *67:* 1155-1164., 1991.
10. Fontana, R. S., Sanderson, D. R., Taylor, W. F., Woolner, L. B., Miller, W. E., Muhm, J. R., and Uhlenhopp, M. A. Early lung cancer detection: results of the initial (prevalence) radiologic and cytologic screening in the Mayo Clinic study. Am Rev Respir Dis, *130:* 561-565., 1984.
11. Henschke, C. I., McCauley, D. I., Yankelevitz, D. F., Naidich, D. P., McGuinness, G., Miettinen, O. S., Libby, D. M., Pasmantier, M. W., Koizumi, J., Altorki, N. K., and Smith, J. P. Early Lung Cancer Action Project: overall design and findings from baseline screening. Lancet, *354:* 99-105., 1999.
12. Hong, W. K. and Sporn, M. B. Recent advances in chemoprevention of cancer. Science, *278:* 1073-1077., 1997.
13. Hennekens, C. H., Buring, J. E., Manson, J. E., Stampfer, M., Rosner, B., Cook, N. R., Belanger, C., LaMotte, F., Gaziano, J. M., Ridker, P. M., Willett, W., and Peto, R. Lack of effect of long-term supplementation with beta carotene on the incidence of malignant neoplasms and cardiovascular disease. N Engl J Med, *334:* 1145-1149., 1996.
14. Omenn, G. S., Goodman, G. E., Thornquist, M. D., Balmes, J., Cullen, M. R., Glass, A., Keogh, J. P., Meyskens, F. L., Valanis, B., Williams, J. H., Barnhart, S., and Hammar, S. Effects of a combination of beta carotene and vitamin A on lung cancer and cardiovascular disease. N Engl J Med, *334:* 1150-1155., 1996.

15. The effect of vitamin E and beta carotene on the incidence of lung cancer and other cancers in male smokers. The Alpha-Tocopherol, Beta Carotene Cancer Prevention Study Group. N Engl J Med, *330:* 1029-1035., 1994.
16. Lee, J. S., Lippman, S. M., Benner, S. E., Lee, J. J., Ro, J. Y., Lukeman, J. M., Morice, R. C., Peters, E. J., Pang, A. C., Fritsche, H. A., Jr., and et al. Randomized placebo-controlled trial of isotretinoin in chemoprevention of bronchial squamous metaplasia. J Clin Oncol, *12:* 937-945., 1994.
17. Postoperative radiotherapy in non-small-cell lung cancer: systematic review and meta-analysis of individual patient data from nine randomised controlled trials. PORT Meta-analysis Trialists Group. Lancet, *352:* 257-263., 1998.
18. Holmes, E. C. and Gail, M. Surgical adjuvant therapy for stage II and stage III adenocarcinoma and large-cell undifferentiated carcinoma. J Clin Oncol, *4:* 710-715., 1986.
19. Feld, R., Rubinstein, L., and Thomas, P. A. Adjuvant chemotherapy with cyclophosphamide, doxorubicin, and cisplatin in patients with completely resected stage I non-small-cell lung cancer. The Lung Cancer Study Group. J Natl Cancer Inst, *85:* 299-306., 1993.
20. Niiranen, A., Niitamo-Korhonen, S., Kouri, M., Assendelft, A., Mattson, K., and Pyrhonen, S. Adjuvant chemotherapy after radical surgery for non-small-cell lung cancer: a randomized study. J Clin Oncol, *10:* 1927-1932., 1992.
21. Wada, H., Hitomi, S., and Teramatsu, T. Adjuvant chemotherapy after complete resection in non-small-cell lung cancer. West Japan Study Group for Lung Cancer Surgery. J Clin Oncol, *14:* 1048-1054., 1996.
22. Ohta, M., Tsuchiya, R., Shimoyama, M., Sawamura, K., Mori, T., Miyazawa, N., Suemasu, K., Watanabe, Y., Tomita, M., and Terashima, M. Adjuvant chemotherapy for completely resected stage III non-small-cell lung cancer. Results of a randomized prospective study. The Japan Clinical Oncology Group. J Thorac Cardiovasc Surg, *106:* 703-708., 1993.
23. Chemotherapy in non-small cell lung cancer: a meta-analysis using updated data on individual patients from 52 randomised clinical trials. Non-small Cell Lung Cancer Collaborative Group. Bmj, *311:* 899-909., 1995.
24. Vainio, H. Chemoprevention of cancer: a controversial and instructive story. Br Med Bull, *55:* 593-599, 1999.
25. Giardiello, F. M., Hamilton, S. R., Krush, A. J., Piantadosi, S., Hylind, L. M., Celano, P., Booker, S. V., Robinson, C. R., and Offerhaus, G. J. Treatment of colonic and rectal adenomas with sulindac in familial adenomatous polyposis. N Engl J Med, *328:* 1313-1316., 1993.
26. Giovannucci, E., Egan, K. M., Hunter, D. J., Stampfer, M. J., Colditz, G. A., Willett, W. C., and Speizer, F. E. Aspirin and the risk of colorectal cancer in women. N Engl J Med, *333:* 609-614., 1995.
27. Steinbach, G., Lynch, P. M., Phillips, R. K., Wallace, M. H., Hawk, E., Gordon, G. B., Wakabayashi, N., Saunders, B., Shen, Y., Fujimura, T., Su, L. K., and Levin, B. The effect of celecoxib, a cyclooxygenase-2 inhibitor, in familial adenomatous polyposis. N Engl J Med, *342:* 1946-1952., 2000.
28. Thun, M. J., Namboodiri, M. M., and Heath, C. W., Jr. Aspirin use and reduced risk of fatal colon cancer. N Engl J Med, *325:* 1593-1596., 1991.

29. Schreinemachers, D. M. and Everson, R. B. Aspirin use and lung, colon, and breast cancer incidence in a prospective study. Epidemiology, *5:* 138-146., 1994.
30. Hida, T., Yatabe, Y., Achiwa, H., Muramatsu, H., Kozaki, K., Nakamura, S., Ogawa, M., Mitsudomi, T., Sugiura, T., and Takahashi, T. Increased expression of cyclooxygenase 2 occurs frequently in human lung cancers, specifically in adenocarcinomas. Cancer Res, *58:* 3761-3764., 1998.
31. Hosomi, Y., Yokose, T., Hirose, Y., Nakajima, R., Nagai, K., Nishiwaki, Y., and Ochiai, A. Increased cyclooxygenase 2 (COX-2) expression occurs frequently in precursor lesions of human adenocarcinoma of the lung. Lung Cancer, *30:* 73-81., 2000.
32. Watkins, D. N., Lenzo, J. C., Segal, A., Garlepp, M. J., and Thompson, P. J. Expression and localization of cyclo-oxygenase isoforms in non-small cell lung cancer. Eur Respir J, *14:* 412-418., 1999.
33. Wolff, H., Saukkonen, K., Anttila, S., Karjalainen, A., Vainio, H., and Ristimaki, A. Expression of cyclooxygenase-2 in human lung carcinoma. Cancer Res, *58:* 4997-5001., 1998.
34. Achiwa, H., Yatabe, Y., Hida, T., Kuroishi, T., Kozaki, K., Nakamura, S., Ogawa, M., Sugiura, T., Mitsudomi, T., and Takahashi, T. Prognostic significance of elevated cyclooxygenase 2 expression in primary, resected lung adenocarcinomas. Clin Cancer Res, *5:* 1001-1005., 1999.
35. Brabender, J., Park, J., Metzger, R., Schneider, P. M., Lord, R. V., Holscher, A. H., Danenberg, K. D., and Danenberg, P. V. Prognostic significance of cyclooxygenase 2 mRNA expression in non- small cell lung cancer. Ann Surg, *235:* 440-443., 2002.
36. Khuri, F. R., Wu, H., Lee, J. J., Kemp, B. L., Lotan, R., Lippman, S. M., Feng, L., Hong, W. K., and Xu, X. C. Cyclooxygenase-2 overexpression is a marker of poor prognosis in stage I non-small cell lung cancer. Clin Cancer Res, *7:* 861-867., 2001.
37. Hasturk, S., Kemp, B., Kalapurakal, S. K., Kurie, J. M., Hong, W. K., and Lee, J. S. Expression of cyclooxygenase-1 and cyclooxygenase-2 in bronchial epithelium and nonsmall cell lung carcinoma. Cancer, *94:* 1023-1031., 2002.
38. Soslow, R. A., Dannenberg, A. J., Rush, D., Woerner, B. M., Khan, K. N., Masferrer, J., and Koki, A. T. COX-2 is expressed in human pulmonary, colonic, and mammary tumors. Cancer, *89:* 2637-2645., 2000.
39. Berman, K. S., Verma, U. N., Harburg, G., Minna, J. D., Cobb, M. H., and Gaynor, R. B. Sulindac enhances tumor necrosis factor-alpha-mediated apoptosis of lung cancer cell lines by inhibition of nuclear factor-kappaB. Clin Cancer Res, *8:* 354-360., 2002.
40. Eli, Y., Przedecki, F., Levin, G., Kariv, N., and Raz, A. Comparative effects of indomethacin on cell proliferation and cell cycle progression in tumor cells grown in vitro and in vivo. Biochem Pharmacol, *61:* 565-571., 2001.
41. Williams, C. S., Tsujii, M., Reese, J., Dey, S. K., and DuBois, R. N. Host cyclooxygenase-2 modulates carcinoma growth. J Clin Invest, *105:* 1589-1594., 2000.

42. Tsubouchi, Y., Mukai, S., Kawahito, Y., Yamada, R., Kohno, M., Inoue, K., and Sano, H. Meloxicam inhibits the growth of non-small cell lung cancer. Anticancer Res, *20:* 2867-2872., 2000.
43. Hida, T., Kozaki, K., Muramatsu, H., Masuda, A., Shimizu, S., Mitsudomi, T., Sugiura, T., Ogawa, M., and Takahashi, T. Cyclooxygenase-2 inhibitor induces apoptosis and enhances cytotoxicity of various anticancer agents in non-small cell lung cancer cell lines. Clin Cancer Res, *6:* 2006-2011., 2000.
44. Stolina, M., Sharma, S., Lin, Y., Dohadwala, M., Gardner, B., Luo, J., Zhu, L., Kronenberg, M., Miller, P. W., Portanova, J., Lee, J. C., and Dubinett, S. M. Specific inhibition of cyclooxygenase 2 restores antitumor reactivity by altering the balance of IL-10 and IL-12 synthesis. J Immunol, *164:* 361-370., 2000.
45. Dohadwala, M., Luo, J., Zhu, L., Lin, Y., Dougherty, G. J., Sharma, S., Huang, M., Pold, M., Batra, R. K., and Dubinett, S. M. Non-small cell lung cancer cyclooxygenase-2-dependent invasion is mediated by CD44. J Biol Chem, *276:* 20809-20812., 2001.
46. El-Bayoumy, K., Rose, D. P., Papanikolaou, N., Leszczynska, J., Swamy, M. V., and Rao, C. V. Cyclooxygenase-2 expression influences the growth of human large and small cell lung carcinoma lines in athymic mice: impact of an organoselenium compound on growth regulation. Int J Oncol, *20:* 557-561., 2002.
47. Grosch, S., Tegeder, I., Niederberger, E., Brautigam, L., and Geisslinger, G. COX-2 independent induction of cell cycle arrest and apoptosis in colon cancer cells by the selective COX-2 inhibitor celecoxib. Faseb J, *15:* 2742-2744., 2001.
48. Song, X., Lin, H. P., Johnson, A. J., Tseng, P. H., Yang, Y. T., Kulp, S. K., and Chen, C. S. Cyclooxygenase-2, player or spectator in cyclooxygenase-2 inhibitor-induced apoptosis in prostate cancer cells. J Natl Cancer Inst, *94:* 585-591., 2002.
49. Waskewich, C., Blumenthal, R. D., Li, H., Stein, R., Goldenberg, D. M., and Burton, J. Celecoxib exhibits the greatest potency amongst cyclooxygenase (COX) inhibitors for growth inhibition of COX-2-negative hematopoietic and epithelial cell lines. Cancer Res, *62:* 2029-2033., 2002.
50. Le Chevalier, T. et al. Results of the Randomized International Adjuvant Lung Cancer Trial (IALT): cisplatin-based chemotherapy (CT) vs no CT in 1867 patients (pts) with resected non-small cell lung cancer (NSCLC). *Proc Am Soc Clin Oncol.* 2003:22. Abstract 6.
51. Hong WK, Lippman SM, Itri LM, Karp DD, Lee JS, Byers RM, Schantz SP, Kramer AM, Lotan R, Peters LJ, Dimery IW, Brown BW, Goepfert H. Prevention of second primary tumors with isotretinoin in squamous cell carcinoma of the head and neck. *N Engl J Med* 323:795-801, 1990.
52. Khuri, F. et al. Isotretinoin effects on head and neck cancer recurrence and second primary tumors *Proc Am Soc Clin Oncol* 2003:22. Abstract 359.
53. Celecoxib package insert (Searle-US), New 12/98, Rec 1/99.
54. Product Information: Celebrex ®, celecoxib. G.D.Searle, Chicago, IL (PI revised 10/2001) reviewed 12/2001.
55. Product Information: Celebrex ™, celecoxib. Searle Canada, Mississauga, Ontario, Canada (PI revised 4/2000) reviewed 12/2001

56. Bryant J. Day R. Incorporating toxicity considerations into the design of two-stage phase II clinical trials. *Biometrics. 51(4):1372-83, 1995 Dec.*

Appendix - A.

Appendix Subtitle:

Guidelines for Filing Reports of Adverse Experiences at M. D. Anderson Cancer Center

21 CFR 312.32

Serious Adverse Experience (SAE) –Any adverse drug experience occurring at any dose that results in any of the following outcomes:

- Death
- A life-threatening adverse drug experience – any adverse experience that places the patient, in the view of the initial reporter, at immediate risk of death from the adverse experience as it occurred. It does not include an adverse experience that, had it occurred in a more severe form, might have caused death.
- Inpatient hospitalization or prolongation of existing hospitalization
- A persistent or significant disability/incapacity – a substantial disruption of a person's ability to conduct normal life functions.
- A congenital anomaly/birth defect.

Important medical events that may not result in death, be life-threatening, or require hospitalization may be considered a serious adverse drug experience when, based upon appropriate medical judgment, they may jeopardize the patient or subject and may require medical or surgical intervention to prevent one of the outcomes listed in this definition. Examples of such medical events include allergic bronchospasm requiring intensive treatment in an emergency room or at home, blood dyscrasias or convulsions that do not result in inpatient hospitalization, or the development of drug dependency or drug abuse.

Unexpected Adverse Drug Experience - Any adverse drug experience, the specificity or severity of which is not consistent with the current investigator brochure; or, if an investigator brochure is not required or available, the specificity or severity of which is not consistent with the risk information described in the general investigational plan or elsewhere in the current application, as amended. Unexpected, as used in this definition, refers to an adverse drug experience that has not been previously observed (e.g., included in the investigator brochure) rather than from the perspective of such experience not being anticipated from the pharmacological properties of the pharmaceutical product.

MDA Policy and Procedure for reporting of adverse experiences (Includes both commercial and investigational drugs):

- All clinical protocols should include a list of the expected and anticipated events or hospitalizations relating to the study regimen. If an expected or anticipated event is documented in the protocol, then it does not have to be reported as an SAE. (Example: Expected Grade 4 mylosuppression needs only to be reported as part of the study results)

- All events falling under the definition of serious adverse event that are not listed in the protocol as being expected or anticipated, and occurring within 30 days following the last treatment date, must be reported to the sponsor within the specified time frame stated in the protocol.

- All deaths with possible, probable or definite attribution to the study drug, device, or intervention must have a written report submitted to the Institutional Review Board (IRB) via OPR within one working day (24 hours) of knowledge of the event.

- All serious adverse events other than that stated above must have a written report submitted to the Institutional Review Board (IRB) via OPR within 5 working days of knowledge of the event.

- If necessary, the sponsor is then required to notify the Food and Drug Administration (FDA) within 7 calendar days.

- All unexpected adverse experiences that are classified as Grade 4 must be reported by following the guidelines listed above.

- Known reactions classified as Grades 1-3 do not need to be reported. However, these toxicities should be submitted as part of the study results.

Adverse Experience Reporting Forms:

Attached is the MDACC severe adverse event reporting form. This form should be utilized if MDACC is the sponsor, the study is a non-sponsored study, or the sponsor does not provide an appropriate reporting form.

If the study sponsor requires a protocol specific SAE form to be completed, then that form may be use for IRB submission as long as the MDACC protocol number and patient medical record number is written at the top of the front page.

External Adverse Experiences / Safety Reports

All external adverse events/safety reports received from the sponsor should be submitted to the IRB through the Office of Protocol Research. The "External Adverse Event Report" can be located under section 1 of the OPR Forms Manual, and should be utilized as the cover sheet for this submission.

IRB Approval Date: 7/3/2002

Appendix - B.

Appendix Subtitle: Carcinoma In Situ Management

There is no standard approach to the management of CIS at present. Approaches have ranged from surgical resection to close followup. CIS may be found at the edge of an invasive carcinoma or may occur as a small isolated focus of a few epithelial cells that would be completely removed by a biopsy. The major safety issue related to CIS is that an invasive carcinoma may exist in an adjacent area that the biopsy did not sample. CIS is a rare lesion and it is not likely that enough CIS lesions will be found in the study for statistical analysis of response to the chemopreventive agents.

As there are a wide range of approaches to the treatment of CIS and as this is dependent on the bronchoscopic appearance of the lesion, we believe that the final decision regarding therapy, if any, should be left to the bronchoscopist and primary physician.

If a **CIS** lesion is found on a bronchoscopy at baseline, we would recommend:

1) Follow-up bronchoscopy within one month with repeat inspection of the area of the CIS and multiple biopsies to insure that an invasive carcinoma was not missed.
2) A CT scan with attention to the area of the CIS lesion.

If there is question of **invasive carcinoma** on either follow up bronchoscopy or CT, then the participant should be managed directly according to the preferences of the participant and primary physician.

If **no CIS** lesion is found on the repeat bronchoscopy, then the participant is to be continued on study.

If a **persistent CIS** lesion is found on repeat bronchoscopy, then the management should be directed as follows:

1) Repeat bronchoscopy in 1 month.

If CIS present, definitive treatment of lesion. Patient continues to remain on study.

Appendix - C.

Appendix Subtitle: Celecoxib Background Information

Appendix - C.

Appendix Subtitle: Celecoxib Background Information

CELECOXIB

OVERVIEW

- A. Celecoxib is a nonsteroidal anti-inflammatory drug, which selectively inhibits the enzyme, cyclo-oxygenase-2 (COX-2).
- B. DOSING INFORMATION: The recommended dose for osteoarthritis is 200 mg daily which may be given as a single dose or divided and given as 100 mg twice daily. The recommended dose for rheumatoid arthritis is 100 mg or 200 mg twice daily. The recommended dose for familial adenomatous polyposis is 400 mg twice daily. The recommended dose for acute pain and primary dysmenorrhea is 400 mg initially with an additional dose of 200 mg as needed on day 1, then 200 mg twice daily as needed on subsequent days.
- C. PHARMACOKINETICS: Celecoxib is 97% bound to plasma protein. Celecoxib is extensively metabolized in the liver via cytochrome P450 2C9 to 3 inactive metabolites; elimination is via the kidney (27%) and feces (57%). Less than 3% is eliminated as unchanged drug. The half-life is 11 hours.
- D. CAUTIONS: Common adverse effects include dyspepsia, diarrhea, and abdominal pain. Although the risk for ulcers and other serious gastrointestinal adverse effects is lower than for other NSAIDs, product labeling still includes warnings about the risk of ulceration, bleeding and perforation.
- E. CLINICAL APPLICATIONS: Celecoxib is indicated for the treatment of osteoarthritis, rheumatoid arthritis, acute pain including primary dysmenorrhea, and is also indicated for reducing the number of colon and rectal polyps in familial adenomatous polyposis (FAP). This treatment has NOT been shown to reduce the risk of gastrointestinal cancer or the need for FAP-associated surgeries and routine endoscopic surveillance.

Appendix - D.

Appendix Subtitle:

CCSG Checklist

(Cancer Center Support Grant -- NCI Core Grant)

Preclinical Drug Development

Was preclinical work to develop the therapy or methodology being tested in this protocol performed at UTMDACC or by UTMDACC faculty?
○ Yes ● No

Protocol Design and Biostatistics

Did you participate in the design of this study?
● Yes -- Completely
○ Yes -- Partially
○ No -- Sponsor Designed

Did an MDACC Biostatistician participate in the design of this study?
● Yes -- Completely
○ Yes -- Partially
○ No -- Sponsor provided biostatistical design

Financial Support and Use of the CTRC

How is the proposed trial to be financially supported?
○ Drug Only from Industry
○ Drug and Funding from Industry
● Grant
○ Unfunded
○ Donor Funds

Will the Clinical and Translational Research Center be used in this study?
○ Yes ● No

Laboratory Data

Will a UTMDACC investigator perform pharmacologic, molecular or other laboratory studies on patient specimens?
● Yes
○ No

What is the type of study?

○ Pharmacology and/or pharmacokinetics
○ Molecular and/or pharmacodynamics
● Other

Please Describe:
Genetic, biomarker studies

Appendix - E.

Appendix Subtitle:

ZUBROD'S PERFORMANCE STATUS SCALE

Grade	Scale
0	Fully active, able to carry on all pre-disease performance without restriction.
1	Ambulatory, capable of light or sedentary work. Restricted in physically strenuous activity.
2	Ambulatory, capable of all self-care, but not of work activities; up and about more than 50% of waking hours.
3	Capable of only limited self-care; confined to bed or chair more than 50% of waking hours.
4	Completely disabled. Cannot carry on any self-care. Totally confined to bed or chair.

Appendix - F.

Appendix Subtitle:

Common Terminology Criteria for Adverse Events v3.0 (CTCAE)

Publish Date: June 10, 2003

Click On Link ➢ 🖹 ➢ To access Document

Appendix - G.

Appendix Subtitle:

Prioritization List

2-6-04 submission Thoracic.d

2-6-04 submission Head & Neck List.

Appendix - H.

Appendix Subtitle: Histology Grading System

SCORE	HISTOLOGY
1	Normal
2	Reserve cell hyperplasia
3	Metaplasia
4	Mild dysplasia
5	Moderate dysplasia
6	Severe Dysplasia
7	Carcinoma in situ
8	Invasive cancer

Scoring System for Response

1) The average score of all biopsies (decrease by 1)

2) The percentage of biopsies with moderate dysplasia or worse (10% decrease)

3) The worst score (decrease by 1)

Response: **Improvement in 2 of 3 criteria**

No change: **No change in 2 of 3 criteria**

Improvement in 2 of 3 criteria with 1 worse

Progression: **Worsening in 2 of 3 criteria**

Appendix - I.

Appendix Subtitle: Study Activities

Study Activities for Patients Assigned to Celecoxib Treatment Arm

Procedure	Baseline[6]	3 mos	6 mos	12 mos	18 mos	24 mos	30 mos	36 mos	Long-term F/U
Informed consent	X								
Physical exam (by physician or nurse)	X	X	X	X		X		X	Every 12 mos
Nursing exam only[5]					X		X		Every 6 mos[5]
Medical history	X	X	X	X	X	X	X	X	Every 6 mos
Cardiac risk assessment	X								
Cardiac symptom assessment		X	X	X					
Bronchoscopy	X			X		X[7]		X[7]	
Sputum and saliva sample	X			X		X[7]		X[7]	
Buccal brush	X			X		X[7]		X[7]	
Hematology[1]	X	X	X	X	X	X	X	X	Every 12 mos
Serum chemistry, electrolytes[2]	X	X	X	X	X	X	X	X	Every 12 mos
Lipid profile	X								
PT	X			X		X		X	
Pregnancy test[3]	X	Repeat if pregnancy is suspected.							
Chest x-ray	X		X	X	X	X	X	X	
CT scan of chest	X		X	X	X	X	X	X	
Laryngoscopy[4]	X			X					
Biomarkers (serum)	X	X	X	X	X	X	X	X	Every 12 mos

[1] CBC with differential, platelets
[2] BUN, creatinine, total bilirubin, SGPT, alkaline phosphatase, albumin
[3] Women of child-bearing potential only. Serum or urine. Must be done within 72 hrs. prior to enrollment. Should be repeated any time pregnancy is suspected.
[4] Patients with prior head and neck cancer only
[5] Nursing only visit will occur when patient is not scheduled for a physician visit.
[6] Unless otherwise noted, labs, physical exams, imaging studies, and the laryngoscopy are to be performed within 4 weeks of beginning participation in this study.
[7] Optional

Study Activities for Patients Assigned to No Treatment Arm

Procedure	Baseline[6]	3 mos	6 mos	9 mos	12 mos	18 mos	24 mos	30 mos	36 mos	Long-term F/U
Informed consent	X									
Physical exam (by physician or nurse)	X		X		X		X		X	Every 12 mos
Nursing exam only						X		X		Every 6 mos[5]
Medical history	X		X		X	X	X	X	X	Every 6 mos
Cardiac risk assessment	X									
Bronchoscopy	X				X		X[7]		X[7]	
Sputum and saliva sample	X				X		X[7]		X[7]	
Buccal brush	X				X		X[7]		X[7]	
Hematology[1]	X		X		X	X	X	X	X	Every 12 mos
Serum chemistry, electrolytes[2]	X		X		X	X	X	X	X	Every 12 mos
Lipid profile	X									
PT	X				X		X		X	
Pregnancy test[3]	X									
Chest x-ray	X		X		X	X	X	X	X	
CT scan of chest	X		X		X	X	X	X	X	
Laryngoscopy[4]	X				X					
Biomarkers (serum)	X		X		X	X	X	X	X	Every 12 mos
Nursing Follow-up via phone		X		X						

[1] CBC with differential, platelets
[2] BUN, creatinine, total bilirubin, SGPT, alkaline phosphatase, albumin
[3] Women of child-bearing potential only. Serum or urine. Must be done within 72 hrs. prior to enrollment. Should be repeated any time pregnancy is suspected.
[4] Patients with prior head and neck cancer only
[5] Nursing only visit will occur when patient is not scheduled for a physician visit.
[6] Unless otherwise noted, labs, physical exams, imaging studies, and the laryngoscopy are to be performed within 4 weeks of beginning participation in this study.
[7] Optional

Appendix - J.

Appendix Subtitle: JNC-7 Report on Detection, Evaluation, and Treatment of High Blood Pressure

JNC-7.pdf

Reference Card From the Seventh Report of the Joint National Committee on Prevention, Detection, Evaluation, and Treatment of High Blood Pressure (JNC 7)

EVALUATION

Classification of Blood Pressure (BP)*

Category	SBP mmHg		DBP mmHg
Normal	<120	and	<80
Prehypertension	120–139	or	80–89
Hypertension, Stage 1	140–159	or	90–99
Hypertension, Stage 2	≥160	or	≥100

* See *Blood Pressure Measurement Techniques* (reverse side)
Key: SBP = systolic blood pressure DBP = diastolic blood pressure

Diagnostic Workup of Hypertension

- Assess risk factors and comorbidities.
- Reveal identifiable causes of hypertension.
- Assess presence of target organ damage.
- Conduct history and physical examination.
- Obtain laboratory tests: urinalysis, blood glucose, hematocrit and lipid panel, serum potassium, creatinine, and calcium. Optional: urinary albumin/creatinine ratio.
- Obtain electrocardiogram.

Assess for Major Cardiovascular Disease (CVD) Risk Factors

- Hypertension
- Obesity (body mass index ≥30 kg/m²)
- Dyslipidemia
- Diabetes mellitus
- Cigarette smoking
- Physical inactivity
- Microalbuminuria, estimated glomerular filtration rate <60 mL/min
- Age (>55 for men, >65 for women)
- Family history of premature CVD (men age <55, women age <65)

Assess for Identifiable Causes of Hypertension

- Sleep apnea
- Drug induced/related
- Chronic kidney disease
- Primary aldosteronism
- Renovascular disease
- Cushing's syndrome or steroid therapy
- Pheochromocytoma
- Coarctation of aorta
- Thyroid/parathyroid disease

U.S. DEPARTMENT OF HEALTH AND HUMAN SERVICES
National Institutes of Health
National Heart, Lung, and Blood Institute

TREATMENT

Principles of Hypertension Treatment

- Treat to BP <140/90 mmHg or BP <130/80 mmHg in patients with diabetes or chronic kidney disease.
- Majority of patients will require two medications to reach goal.

Algorithm for Treatment of Hypertension

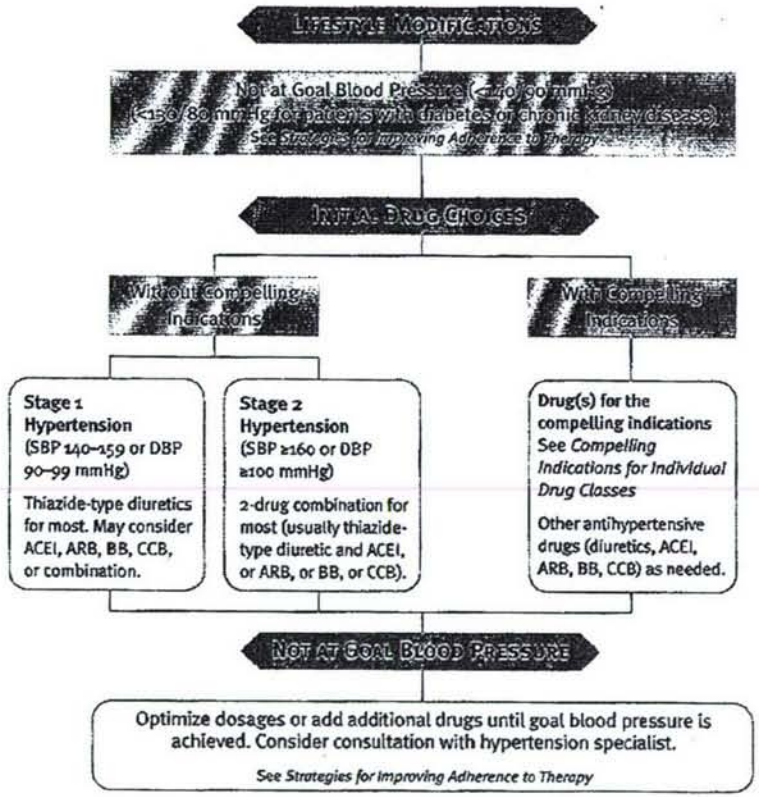

Blood Pressure Measurement Techniques

Method	Notes
In-office	Two readings, 5 minutes apart, sitting in chair. Confirm elevated reading in contralateral arm.
Ambulatory BP monitoring	Indicated for evaluation of "white coat hypertension." Absence of 10–20 percent BP decrease during sleep may indicate increased CVD risk.
Patient self-check	Provides information on response to therapy. May help improve adherence to therapy and is useful for evaluating "white coat hypertension."

Causes of Resistant Hypertension

- Improper BP measurement
- Excess sodium intake
- Inadequate diuretic therapy
- Medication
  - Inadequate doses
  - Drug actions and interactions (e.g., nonsteroidal anti-inflammatory drugs (NSAIDs), illicit drugs, sympathomimetics, oral contraceptives)
  - Over-the-counter (OTC) drugs and herbal supplements
- Excess alcohol intake
- Identifiable causes of hypertension (see reverse side)

Compelling Indications for Individual Drug Classes

Compelling Indication	Initial Therapy Options
• Heart failure	THIAZ, BB, ACEI, ARB, ALDO ANT
• Post myocardial infarction	BB, ACEI, ALDO ANT
• High CVD risk	THIAZ, BB, ACEI, CCB
• Diabetes	THIAZ, BB, ACEI, ARB, CCB
• Chronic kidney disease	ACEI, ARB
• Recurrent stroke prevention	THIAZ, ACEI

Key: THIAZ = thiazide diuretic, ACEI= angiotensin converting enzyme inhibitor, ARB = angiotensin receptor blocker, BB = beta blocker, CCB = calcium channel blocker, ALDO ANT = aldosterone antagonist

Strategies for Improving Adherence to Therapy

- Clinician empathy increases patient trust, motivation, and adherence to therapy.
- Physicians should consider their patients' cultural beliefs and individual attitudes in formulating therapy.

The National High Blood Pressure Education Program is coordinated by the National Heart, Lung, and Blood Institute (NHLBI) at the National Institutes of Health. Copies of the JNC 7 Report are available on the NHLBI Web site at http://www.nhlbi.nih.gov or from the NHLBI Health Information Center, P.O. Box 30105, Bethesda, MD 20824-0105; Phone: 301-592-8573 or 240-629-3255 (TTY); Fax: 301-592-8563.

Principles of Lifestyle Modification

- Encourage healthy lifestyles for all individuals.
- Prescribe lifestyle modifications for all patients with prehypertension and hypertension.
- Components of lifestyle modifications include weight reduction, DASH eating plan, dietary sodium reduction, aerobic physical activity, and moderation of alcohol consumption.

Lifestyle Modification Recommendations

Modification	Recommendation	Avg. SBP Reduction Range†
Weight reduction	Maintain normal body weight (body mass index 18.5–24.9 kg/m^2).	5–20 mmHg/10 kg
DASH eating plan	Adopt a diet rich in fruits, vegetables, and lowfat dairy products with reduced content of saturated and total fat.	8–14 mmHg
Dietary sodium reduction	Reduce dietary sodium intake to ≤100 mmol per day (2.4 g sodium or 6 g sodium chloride).	2–8 mmHg
Aerobic physical activity	Regular aerobic physical activity (e.g., brisk walking) at least 30 minutes per day, most days of the week.	4–9 mmHg
Moderation of alcohol consumption	Men: limit to ≤2 drinks* per day. Women and lighter weight persons: limit to ≤1 drink* per day.	2–4 mmHg

* 1 drink = 1/2 oz or 15 mL ethanol (e.g., 12 oz beer, 5 oz wine, 1.5 oz 80-proof whiskey).

† Effects are dose and time dependent.

U.S. DEPARTMENT OF HEALTH AND HUMAN SERVICES
National Institutes of Health
National Heart, Lung, and Blood Institute
National High Blood Pressure Education Program

NIH Publication No. 03-5231
May 2003

Appendix - K.

Appendix Subtitle: ATP III Guidelines for Treating Hypercholesteremia

ATP III guidelines.pd

ATP III Guidelines At-A-Glance Quick Desk Reference

Step 1

Determine lipoprotein levels–obtain complete lipoprotein profile after 9- to 12-hour fast.

ATP III Classification of LDL, Total, and HDL Cholesterol (mg/dL)

LDL Cholesterol – Primary Target of Therapy	
<100	Optimal
100-129	Near optimal/above optimal
130-159	Borderline high
160-189	High
≥190	Very high
Total Cholesterol	
<200	Desirable
200-239	Borderline high
≥240	High
HDL Cholesterol	
<40	Low
≥60	High

Step 2

Identify presence of clinical atherosclerotic disease that confers high risk for coronary heart disease (CHD) events (CHD risk equivalent):

- Clinical CHD
- Symptomatic carotid artery disease
- Peripheral arterial disease
- Abdominal aortic aneurysm.

Step 3

Determine presence of major risk factors (other than LDL):

Major Risk Factors (Exclusive of LDL Cholesterol) That Modify LDL Goals

Cigarette smoking

Hypertension (BP ≥140/90 mmHg or on antihypertensive medication)

Low HDL cholesterol (<40 mg/dL)*

Family history of premature CHD (CHD in male first degree relative <55 years; CHD in female first degree relative <65 years)

Age (men ≥45 years; women ≥55 years)

** HDL cholesterol ≥60 mg/dL counts as a "negative" risk factor; its presence removes one risk factor from the total count.*

- Note: In ATP III, diabetes is regarded as a CHD risk equivalent.

Step 4

If 2+ risk factors (other than LDL) are present without CHD or CHD risk equivalent, assess 10-year (short-term) CHD risk (see Framingham tables).
Three levels of 10-year risk:

- >20% — CHD risk equivalent
- 10-20%
- <10%

Step 5

Determine risk category:

- Establish LDL goal of therapy
- Determine need for therapeutic lifestyle changes (TLC)
- Determine level for drug consideration

LDL Cholesterol Goals and Cutpoints for Therapeutic Lifestyle Changes (TLC) and Drug Therapy in Different Risk Categories.

Risk Category	LDL Goal	LDL Level at Which to Initiate Therapeutic Lifestyle Changes (TLC)	LDL Level at Which to Consider Drug Therapy
CHD or CHD Risk Equivalents (10-year risk >20%)	<100 mg/dL	≥100 mg/dL	≥130 mg/dL (100-129 mg/dL: drug optional)*
2+ Risk Factors (10-year risk ≤20%)	<130 mg/dL	≥130 mg/dL	10-year risk 10-20%: ≥130 mg/dL 10-year risk <10%: ≥160 mg/dL
0-1 Risk Factor†	<160 mg/dL	≥160 mg/dL	≥190 mg/dL (160-189 mg/dL: LDL-lowering drug optional)

* *Some authorities recommend use of LDL-lowering drugs in this category if an LDL cholesterol <100 mg/dL cannot be achieved by therapeutic lifestyle changes. Others prefer use of drugs that primarily modify triglycerides and HDL, e.g., nicotinic acid or fibrate. Clinical judgment also may call for deferring drug therapy in this subcategory.*

† *Almost all people with 0-1 risk factor have a 10-year risk <10%, thus 10-year risk assessment in people with 0-1 risk factor is not necessary.*

Step 6

Initiate therapeutic lifestyle changes (TLC) if LDL is above goal.

TLC Features

- TLC Diet:
  - Saturated fat <7% of calories, cholesterol <200 mg/day
  - Consider increased viscous (soluble) fiber (10-25 g/day) and plant stanols/sterols (2g/day) as therapeutic options to enhance LDL lowering
- Weight management
- Increased physical activity.

Step 7

Consider adding drug therapy if LDL exceeds levels shown in Step 5 table:

- Consider drug simultaneously with TLC for CHD and CHD equivalents
- Consider adding drug to TLC after 3 months for other risk categories.

Drugs Affecting Lipoprotein Metabolism

Drug Class	Agents and Daily Doses	Lipid/Lipoprotein Effects		Side Effects	Contraindications
HMG CoA reductase inhibitors (statins)	Lovastatin (20-80 mg) Pravastatin (20-40 mg) Simvastatin (20-80 mg) Fluvastatin (20-80 mg) Atorvastatin (10-80 mg) Cerivastatin (0.4-0.8 mg)	LDL HDL TG	↓18-55% ↑5-15% ↓7-30%	Myopathy Increased liver enzymes	Absolute: • Active or chronic liver disease Relative: • Concomitant use of certain drugs*
Bile acid sequestrants	Cholestyramine (4-16 g) Colestipol (5-20 g) Colesevelam (2.6-3.8 g)	LDL HDL TG	↓15-30% ↑3-5% No change or increase	Gastrointestinal distress Constipation Decreased absorption of other drugs	Absolute: • dysbeta-lipoproteinemia • TG >400 mg/dL Relative: • TG >200 mg/dL
Nicotinic acid	Immediate release (crystalline) nicotinic acid (1.5-3 gm), extended release nicotinic acid (Niaspan®) (1-2 g), sustained release nicotinic acid (1-2 g)	LDL HDL TG	↓5-25% ↑15-35% ↓20-50%	Flushing Hyperglycemia Hyperuricemia (or gout) Upper GI distress Hepatotoxicity	Absolute: • Chronic liver disease • Severe gout Relative: • Diabetes • Hyperuricemia • Peptic ulcer disease
Fibric acids	Gemfibrozil (600 mg BID) Fenofibrate (200 mg) Clofibrate (1,000 mg BID)	LDL *(may be increased in patients with high TG)* HDL TG	↓5-20% ↑10-20% ↓20-50%	Dyspepsia Gallstones Myopathy	Absolute: • Severe renal disease • Severe hepatic disease

* *Cyclosporine, macrolide antibiotics, various anti-fungal agents, and cytochrome P-450 inhibitors (fibrates and niacin should be used with appropriate caution).*

Step 8

Identify metabolic syndrome and treat, if present, after 3 months of TLC.

Clinical Identification of the Metabolic Syndrome – Any 3 of the Following:

Risk Factor	Defining Level
Abdominal obesity*	Waist circumference†
Men	>102 cm (>40 in)
Women	>88 cm (>35 in)
Triglycerides	≥150 mg/dL
HDL cholesterol	
Men	<40 mg/dL
Women	<50 mg/dL
Blood pressure	≥130/≥85 mmHg
Fasting glucose	≥110 mg/dL

* *Overweight and obesity are associated with insulin resistance and the metabolic syndrome. However, the presence of abdominal obesity is more highly correlated with the metabolic risk factors than is an elevated body mass index (BMI). Therefore, the simple measure of waist circumference is recommended to identify the body weight component of the metabolic syndrome.*

† *Some male patients can develop multiple metabolic risk factors when the waist circumference is only marginally increased, e.g., 94-102 cm (37-39 in). Such patients may have a strong genetic contribution to insulin resistance. They should benefit from changes in life habits, similarly to men with categorical increases in waist circumference.*

Treatment of the metabolic syndrome

- Treat underlying causes (overweight/obesity and physical inactivity):
  - Intensify weight management
  - Increase physical activity.

- Treat lipid and non-lipid risk factors if they persist despite these lifestyle therapies:
  - Treat hypertension
  - Use aspirin for CHD patients to reduce prothrombotic state
  - Treat elevated triglycerides and/or low HDL (as shown in Step 9).

Step 9

Treat elevated triglycerides.

ATP III Classification of Serum Triglycerides (mg/dL)

<150	Normal
150-199	Borderline high
200-499	High
≥500	Very high

Treatment of elevated triglycerides (≥150 mg/dL)

- Primary aim of therapy is to reach LDL goal
- Intensify weight management
- Increase physical activity
- If triglycerides are ≥200 mg/dL after LDL goal is reached, set secondary goal for non-HDL cholesterol (total − HDL) 30 mg/dL higher than LDL goal.

Comparison of LDL Cholesterol and Non-HDL Cholesterol Goals for Three Risk Categories

Risk Category	LDL Goal (mg/dL)	Non-HDL Goal (mg/dL)
CHD and CHD Risk Equivalent (10-year risk for CHD >20%)	<100	<130
Multiple (2+) Risk Factors and 10-year risk ≤20%	<130	<160
0-1 Risk Factor	<160	<190

If triglycerides 200-499 mg/dL after LDL goal is reached, consider adding drug if needed to reach non-HDL goal:

- intensify therapy with LDL-lowering drug, or
- add nicotinic acid or fibrate to further lower VLDL.

If triglycerides ≥500 mg/dL, first lower triglycerides to prevent pancreatitis:

- very low-fat diet (≤15% of calories from fat)
- weight management and physical activity
- fibrate or nicotinic acid
- when triglycerides <500 mg/dL, turn to LDL-lowering therapy.

Treatment of low HDL cholesterol (<40 mg/dL)

- First reach LDL goal, then:
- Intensify weight management and increase physical activity
- If triglycerides 200-499 mg/dL, achieve non-HDL goal
- If triglycerides <200 mg/dL (isolated low HDL) in CHD or CHD equivalent consider nicotinic acid or fibrate.

Estimate of 10-Year Risk for Men

(Framingham Point Scores)

Age	Points
20-34	-9
35-39	-4
40-44	0
45-49	3
50-54	6
55-59	8
60-64	10
65-69	11
70-74	12
75-79	13

Total Cholesterol	Points				
	Age 20-39	Age 40-49	Age 50-59	Age 60-69	Age 70-79
<160	0	0	0	0	0
160-199	4	3	2	1	0
200-239	7	5	3	1	0
240-279	9	6	4	2	1
≥280	11	8	5	3	1

	Points				
	Age 20-39	Age 40-49	Age 50-59	Age 60-69	Age 70-79
Nonsmoker	0	0	0	0	0
Smoker	8	5	3	1	1

HDL (mg/dL)	Points
≥60	-1
50-59	0
40-49	1
<40	2

Systolic BP (mmHg)	If Untreated	If Treated
<120	0	0
120-129	0	1
130-139	1	2
140-159	1	2
≥160	2	3

Point Total	10-Year Risk %
<0	< 1
0	1
1	1
2	1
3	1
4	1
5	2
6	2
7	3
8	4
9	5
10	6
11	8
12	10
13	12
14	16
15	20
16	25
≥17	≥ 30

10-Year risk _____%

Estimate of 10-Year Risk for Women

(Framingham Point Scores)

Age	Points
20-34	-7
35-39	-3
40-44	0
45-49	3
50-54	6
55-59	8
60-64	10
65-69	12
70-74	14
75-79	16

Total Cholesterol	Points				
	Age 20-39	Age 40-49	Age 50-59	Age 60-69	Age 70-79
<160	0	0	0	0	0
160-199	4	3	2	1	1
200-239	8	6	4	2	1
240-279	11	8	5	3	2
≥280	13	10	7	4	2

	Points				
	Age 20-39	Age 40-49	Age 50-59	Age 60-69	Age 70-79
Nonsmoker	0	0	0	0	0
Smoker	9	7	4	2	1

HDL (mg/dL)	Points
≥60	-1
50-59	0
40-49	1
<40	2

Systolic BP (mmHg)	If Untreated	If Treated
<120	0	0
120-129	1	3
130-139	2	4
140-159	3	5
≥160	4	6

Point Total	10-Year Risk %
< 9	< 1
9	1
10	1
11	1
12	1
13	2
14	2
15	3
16	4
17	5
18	6
19	8
20	11
21	14
22	17
23	22
24	27
≥25	≥ 30

10-Year risk _____%

U.S. DEPARTMENT OF HEALTH AND HUMAN SERVICES
Public Health Service
National Institutes of Health
National Heart, Lung, and Blood Institute

NIH Publication No. 01-3096
May 2001

Erlotinib as Adjuvant Biologic Therapy in Patients with Early Stage Head and Neck and Lung Cancer

1.0 Objectives

Current and former smokers have been the focus of recently completed, large-scale lung cancer chemoprevention trials. The outcomes of these trials have been uniformly disappointing. Patients with previous tumors of the aerodigestive tract are at particular risk for second primaries of this area, including non-small cell lung cancer (NSCLC). Preclinical data suggest that erlotinib (tarceva) may have a chemopreventive effect in patients with NSCLC. To test this hypothesis we will perform a randomized biomarker-based clinical trial in patients with definitively treated NSCLC and head and neck squamous cell carcinoma (HNSCC), examining the effect of erlotinib treatment on biomarkers of lung cancer risk.

Primary Objective
- To examine the effect of erlotinib treatment on histological response (defined in Appendix D), markers of proliferation (Ki-67), and apoptosis in patients with previously treated HNSCC or NSCLC with no evidence of disease.

Secondary Objectives:
- To determine time to second primary or recurrence and survival.
- To examine the toxicity associated with erlotinib administration in patients with previouslytreated HNSCC or NSCLC.

2.0 Significance and Background

2.1 Lung cancer as a Significant Public Health Problem

Lung cancer is the leading cause of death from cancer among men and women in the United States, accounting for approximately 28% of deaths from cancer. An estimated 159,900 Americans died of lung cancer in 2003. In recent years, the incidence of lung cancer has begun to decline among men (Cancer Facts and Figures, 1997). However, smoking-related lung cancer has continued to increase among women, surpassing even breast cancer as the leading cause of death from cancer among women (U.S. Dept of Health and Human Services, 1990). Despite aggressive treatment, the five-year survival rate for lung cancer remains approximately 15%. These grim facts point out the need for a radical change in our approach to lung cancer. In response to this need, the National Cancer Institute's Division of Cancer Prevention and Control has set prevention as the primary strategy in the control of lung cancer.

2.2 Smoking Cessation and Lung Cancer Prevention

Prevention of smoking and smoking cessation have deservedly prominent places in the National Cancer Institute's programs to reduce deaths from cancer. As a result of massive campaigns to educate the public about the hazards of cigarette smoking, there has been a substantial reduction in the percentage of adults who smoke in the United States. Recent estimates suggest that approximately 50% of adults were once smokers (about 44 million people in the United States) (U.S. Dept of Health and Human Services, 1990, Glyn 1993). Despite the reduction in lung cancer risk observed with smoking cessation, several studies have demonstrated that former smokers still have a higher lung cancer risk than non-smokers (Halpern 1993, Lubin 1993, Sobue 1993). Even ten years after smoking cessation, the risk was still significantly elevated for men (Risch 1993). As a consequence, former smokers account for a large proportion of lung cancers in this country. From the current smoking trends, it appears that former smokers will account for a growing percentage of all lung cancer cases. Thus, the risk of lung cancer in former smokers poses a substantial long-term health threat in this country. Strikingly, 50% of new lung cancer cases are among former smokers, a population numbering

roughly 46 million people in the United States (Landis 1999). Strategies to prevent lung cancer deaths in former smokers include early detection and chemoprevention.

Methods of early detection are now greatly important in lung cancer treatment. Screening techniques analyzing sputum cytology, chest x-rays and more recently, spiral computed tomography (CT) scans have been studied. Recent studies have specifically tested the efficacy of screening individuals at high risk with spiral CT scanning (Fontana 1991, Fontana 1984, Henschke 1999). The results, while provocative, are not yet definitive, and debate continues as to whether they are sufficient to mandate broad lung cancer screening programs. A study reported in 1999 used low-dose helical CT to screen 1,000 asymptomatic smokers or former smokers, who smoked at least one pack of cigarettes a day for 10 years, or two packs per day for 5 years. All were age 60 or older. All participants received chest x-rays and CT. CT detected from 1-6 non-calcified pulmonary nodules in 23% patients while CXR detected 7%. 27 of the 233 CT lesions were diagnosed as tumor whereas 7 of the 68 CXR lesions were malignant. 23 of the 27 CT tumors were diagnosed as stage I. Although this study shows potential promise in the use of CT for screening, additional trials will be needed before routine CT scanning can be deemed effective (Henschke 1999).

The past fifteen years have revealed the potential of chemoprevention in the reduction of mortality associated with common epithelial cancers. Tamoxifen was effective in primary prevention of breast cancers in women at high risk. Non-steroidal anti-inflammatory drugs (NSAIDs) reduced the risk of colorectal cancer in participants with familial adenomatous polyposis (Hong 1997). Retinoids have in some studies decreased the incidence of second primary tumors (SPTs) in participants with a prior squamous cell carcinoma of the head and neck (HNSCC). A significant SPT reduction in stage I-IV HNSCC was seen with short-term, high-dose 13-cis retinoic acid (Hong 1991). However, a study using low-dose, long-term 13-cis retinoic acid showed no benefit in overall survival, or SPT- or recurrence-free survival (Khuri 2003). In contrast, the results of lung cancer chemoprevention trials have been disappointing. Several large-scale chemoprevention trials have been performed, including the Euroscan Trial, the Physicians Health Study, the Alpha-Tocopherol and Beta-Carotene (ATBC) trial, and the Beta-Carotene and Retinol Efficacy Trial (CARET), which involved thousands of active smokers followed for over ten years. These studies demonstrated no protective effect of treatment on lung cancer incidence (Hennekens 1996, Omenn 1996, ATBC 1994). In fact, beta-carotene treatment appeared to act as a co-carcinogen, enhancing lung cancer incidence in active smokers. The failure of these large-scale clinical trials has taught us an important lesson; it may be premature to embark on large-scale trials that involve thousands of participants and cost millions of dollars prior to demonstrating the efficacy of a chemopreventive agent in small, biomarker-based clinical trials. Supporting a biomarker-based approach to predicting the efficacy of specific lung cancer chemopreventive agents, we found no effect of 13-*cis* retinoic acid on bronchial metaplasia and dysplasia in current smokers (Lee 1994), which is similar to the outcome of the retinoid-based large-scale chemoprevention trials described above.

Based on the data outlined above, smoking cessation and primary prevention of smoking remain the most proven measures to prevent primary lung cancer. Patients who have had prior definitively treated tobacco-related cancers, primarily head and neck and lung cancers, are at higher risk (20-40%) for recurrence or second-primary tumors. No therapies have proven effective to prevent lung cancer in this setting.

2.3 Adjuvant Therapy for Lung Cancer

Despite surgical treatment of early stage lung cancer (stage I/II), only 40-70% of patients are alive at 5 years. Additionally, patients who have had prior definitively treated tobacco-related

cancers, primarily head and neck and lung cancers, are at higher risk (20-40%) for recurrence or second-primary tumors during their lifetime. No therapies have proven effective to prevent lung cancer in this setting.

Radiation therapy given after complete surgical resection was one of the earliest forms of adjuvant therapy explored. As reported in the PORT meta-analysis, 2,128 patients from several trials were compared (PORT 1998). Results showed a detrimental effect of post-operative radiotherapy on survival with an absolute reduction of 7% at 2 years. Subgroup analysis suggested that this occurred in the N0-1 disease subgroup and not in the N2 group. As various surgical and radiotherapy techniques were used, randomized trials are still needed to further clarify the role of radiotherapy, especially in those patients with N2 disease.

Chemotherapy has been tested as adjuvant therapy in resected early stage primary lung cancers in multiple trials. Earlier trials prior to 1980 of single-agent chemotherapy as adjuvant therapy with alkylating agents failed to show a survival benefit and in fact, showed a detrimental effect on survival. A recent meta-analysis of all randomized trials over a 26 year period showed that the absolute risk of death was reduced by 3% at 2 years and 5% at 5 years for patients who had been treated with a cisplatin-containing regimen as opposed to surgical resection (Holmes 1986, Feld 1993, Nilranen 1992, Wada 1996, Ohta 1993, NSCLC Collaborative Group 1995, LeChevalier 2003).

2.4 Epidermal Growth Factor Receptor (EGFR) and Cancer Prevention

The epidermal growth factor receptor is involved in the regulation of cellular differentiation and proliferation and is overexpressed in a variety of malignancies including NSCLC (Baselga and Arteaga, 2005; Herbst and Bunn, 2003). In some but not all studies of subjects with non-small cell lung cancer, EGFR detected by immunohistochemistry has been associated with a shortened survival (Brabender et al., 2001; Rusch et al., 1997). Many inhibitors of EGFR have been developed, including erlotinib (OSI-774; Tarceva™), gefitinib (ZD1839; Iressa™), and are presently being tested in phase II and III clinical trials (Baselga et al., 2001; Kris et al., 2003; Perez-Soler et al., 2004; Shepherd et al., 2005; Thatcher et al., 2005) These agents targeted against EGFR are well tolerated and have demonstrated single agent activity in phase II and III clinical trials in subjects with advanced NSCLC previously treated with systemic chemotherapy. In general, the side effects of EGFR inhibitors show less than 5% grade 3 and 4 toxicity including predominately rash and diarrhea. Unlike in many chemotherapy trials, subjects seldom discontinue these agents for toxicity (Fukuoka et al., 2003; Kris et al., 2003; Perez-Soler et al., 2004; Shepherd et al., 2005; Thatcher et al., 2005).

2.5 Rationale for Therapy with Erlotinib

The epidermal growth factor receptor is an important target in cancer cell biology. Erlotinib has proven efficacy in patients with NSCLC refractory to chemotherapy with a good safety profile (Shepherd 2005). Additionally, erlotinib is being studied in other treatment settings including as adjuvant therapy in NSCLC. Based on the clinical and pre-clinical data outlined above, erlotinib seems to be an excellent drug to test in the chemopreventive setting in high-risk patients. Thus, substantial preclinical and clinical data support the hypothesis that strategies to target EGFR will be effective in lung cancer chemoprevention. These findings suggest that erlotinib may be useful for lung cancer chemoprevention, adjuvant therapy, and treatment.

2.6 Study Drug Information

2.6.1 Erlotinib Background

Erlotinib (Tarceva™; OSI-774), a quinazoline, is an orally active, potent, selective inhibitor of the EGFR (HER-1) tyrosine kinase. An overview of selected non-clinical and clinical information is presented here; complete details are available in the OSI-774 Investigator Brochure.

2.6.1.1. Nonclinical Pharmacology

Erlotinib directly and reversibly inhibits the human EGFR tyrosine kinase with an IC_{50} of 2 nM (0.79 ng/mL) in an in vitro enzyme assay and reduces EGFR autophosphorylation in intact tumor cells with an IC_{50} of 20 nM (7.9 ng/mL). This potent inhibition is selective for the EGFR tyrosine kinase both in assays assessing the effects of erlotinib on a variety of other isolated tyrosine kinases and in cellular bioassays designed to isolate this functional pathway. Erlotinib is designed to inhibit EGF-dependent proliferation of cells at submicromolar concentrations and blocks cell cycle progression in the G1 phase. Oral administration of OSI-774 in mice results in a >70% reduction in EGFR (HER-1) autophosphorylation in human xenografts. Marked growth inhibition of HN5 (head and neck carcinoma) and A431 (squamous cell carcinoma) xenografts in nude mice has been demonstrated.

Data on drug exposure and anti-tumor responses in human tumor xenograft models (HN5 and A431) were analyzed in order to estimate the plasma concentration of erlotinib associated with anti-tumor activity. Based on these efficacy models, the minimum steady-state plasma concentration targeted for clinical activity in humans is projected to be 500 ng/mL.

2.6.1.2 Nonclinical Toxicology

Toxicology studies have been performed in mice, rats (up to 6 months), dogs (up to 1 year), and monkeys (1 week). Treatment-related effects observed in at least one species or study included effects on the cornea (atrophy, ulceration), skin (follicular degeneration and inflammation, redness, and alopecia), ovary (atrophy), liver (necrosis), kidney (papillary necrosis and tubular dilatation), gastrointestinal tract (delayed gastric emptying and diarrhea), and embryo-fetal toxicity. Red blood cell parameters were decreased, and white blood cells (primarily neutrophils) were increased. There were treatment-related increases in ALT, AST and bilirubin; increases in bilirubin were likely caused by a treatment-related impairment of bilirubin metabolism.

2.6.1.3 Summary of Phase I Findings

Phase I trials of erlotinib have explored both schedule and dose to evaluate the safety, tolerability, and pharmacokinetic profile of the compound. A number of pharmacokinetic trials in healthy subjects have been conducted, along with three classic Phase I trials in patients with advanced cancer. The single-agent maximum tolerated dose (MTD) was estimated to be 150 mg administered once daily. The primary toxicities consisted of diarrhea, rash, nausea, headache, emesis, and fatigue. The only dose-limiting toxicity was diarrhea. This event was dose related and was generally controlled with the addition of loperamide therapy and treatment with erlotinib doses of < 200 mg/day. The appearance of the rash seen in the clinical trials of erlotinib conducted in healthy subjects and cancer subjects has been similar. It was only loosely dose related and was seen commonly at doses of > 25 mg/day. The rash was variable in onset, duration, and severity. The mechanistic basis of the rash remains uncertain; histopathologic examination of biopsies of the rash demonstrated polymorphonuclear leukocyte infiltration and mild epidermal hyperproliferation. In some cases, the rash improved despite continued dosing, and in general, it gradually resolved without sequelae following erlotinib discontinuation. The rash did not result in study discontinuation in cancer subjects in either of the Phase I trials. In the phase I study, 50% of patients developed rash and 86% diarrhea at the recommended phase II dose of 150 mg daily (Hidalgo et al., 2001).

Based on the ocular changes observed in the 12-month toxicology study in dogs, screening and follow-up ophthalmologic examinations were instituted in the Phase I and II trials in cancer subjects. In the weekly dosing study (Study 248-005), the only reported erlotinib–related ocular event was an episode of mild watery eyes. In the daily dosing study (Study 248-004), 1 subject experienced moderate corneal edema/keratitis attributed to wearing contact lenses, although an influence of erlotinib was not discounted. The event resolved with temporary discontinuation of both erlotinib and contact lens use; there was no recurrence of symptoms with erlotinib rechallenge in the absence of continued use of contact lenses. No increased incidence of ocular toxicity related to erlotinib treatment compared to placebo was noted in the randomized phase III trial of carboplatin/paclitaxel +/- erlotinib (see investigator's brochure).

2.6.1.4 Human Pharmacokinetic Studies
Review of the pharmacokinetic profiles from Studies 248-005 and 248-004 (see Investigator Brochure) revealed dose-related increases in exposure to erlotinib. Exposure to the active metabolite (OSI-420) represented ~10% of the parent compound, with an inter-subject variability in exposure of ~2-fold. Repetitive daily dosing resulted in drug accumulation. The target average plasma concentration for clinical efficacy (500 ng/mL) was achieved at doses of ≥ 100 mg in both the daily (Study 248-004) and weekly (Study 248-005) dosing studies. At the recommended dose of 150 mg/day, the accumulation ratio was 2.5±1.2, minimum plasma steady-state concentrations averaged 1,200±0.62 ng/mL, which is above the IC_{50} (7.86 ng/mL) required to inhibit EGFR in intact tumor cells. The half-life with the recommended 150 mg/day dosing was 24.1 hours.

2.6.1.5 Phase II Trials: Studies in Subjects with Advanced Cancer
The 150 mg/day dose of erlotinib selected for all subsequent trials was based on pharmacokinetic parameters as well as the safety and tolerability profile of this dose level in Phase I trials in advanced, heavily pretreated cancer subjects. Three Phase II trials of the safety, tolerability, and antitumor activity of erlotinib have been conducted in subjects with advanced, refractory malignancies, including NSCLC, squamous cell carcinoma of the head and neck, and ovarian carcinoma. Subjects in each of these studies received 150 mg/day of erlotinib. Dose reductions were allowed in the case of intolerance. Diarrhea was treated with loperamide therapy and/or dose reduction. Rash was treated with a variety of agents, including oral and topical antibiotics, corticosteroids, and other agents. Available data from the two reported Phase II trials in NSCLC and head and neck cancer demonstrate objective response rate of 4%–12% (Perez-Soler et al., 2004; Soulieres et al., 2004).

2.6.1.6 Non–Small Cell Lung Carcinoma.
Study 248-1007 enrolled 57 subjects at five centers with progressive, recurrent NSCLC previously treated with a platinum-based chemotherapy regimen. Erlotinib was administered at a daily dose of 150 mg. In this study, enrolled subjects had measurable tumors that expressed at least minimal levels of EGFR (HER-1) as detected by immunohistochemical (IHC) analysis. All 57 subjects were evaluable for antitumor response. Eight subjects (12.3%) achieved an objective response (1 complete response, 7 partial responses; 6 were confirmed at Week 12 and beyond). The median and 1 year survivals were 8.4 months and 40% respectively (Perez-Soler et al., 2004). A relationship between response and the degree of EGFR (HER-1) over expression has not been established. Rash was observed in 75% of enrolled subjects.

A phase II study of single agent erlotinib in 80 subjects ≥ 70 years of age with previously untreated advanced NSCLC has completed accrual within the Dana Farber Partners Cancer Care. Sixty-six are evaluable for response and outcome. The results from the study thus far demonstrate a response rate of 12% (8/66) with an additional 48% (32/66) of subjects achieving

stable disease at 2 months after starting treatment. All 8 of the responders have adenocarcinoma. Three of the 5 patients with a partial response who had tumors available for study had a mutation of EGFR. Two of the 14 with stable disease had a mutation of EGFR. The median survival of the elderly patients with NSCLC treated with single agent erlotinib was 10 months.

2.6.1.7 Response to Treatment with Erlotinib

There has been *in vitro* information generated to show both gefitinib and erlotinib downregulate the EGFR receptor and the downstream kinase molecules in sensitive NSCLC cell lines sensitive to 20 nM-5 nM gefitinib and erlotinib (Amann et al., 2005; Arao et al., 2004; Engelman et al., 2005; Tracy et al., 2004) The NSCLC cell lines that are growth inhibited by gefitinib and erlotinib also undergo downregulation of the phorpho-EGFR, phosphor-Akt, and phosphor-Erk pathways. In addition, gefitinib and erlotinib inhibit the binding of EGFR to ErbB-3 in NSCLC cell lines sensitive to these agents(Engelman et al., 2005). The NSCLC cell lines with mutations of EGFR also undergo apoptosis when treated with both gefitinib and erlotinib(Amann et al., 2005; Tracy et al., 2004).

3.0 Study Design and Overview

The primary objective of this phase IIb study is to determine the effect of erlotinib in patients with previously treated HNSCC or NSCLC with no evidence of disease. Other objectives are to determine if erlotinib is tolerable in this patient population and to examine effects on markers of proliferation and apoptosis and the incidence of second primary tumors and recurrences.

Patients with stage I or II HNSCC or NSCLC after definitive local therapy who have no evidence of disease will be treated with erlotinib for one year. Patients will be evaluated with spiral CT, fluorescent bronchoscopy, and serologies per the vanguard trial. Detailed description of the vanguard trial can be found in a separate protocol. All patients need to consent to the vanguard trial first before consenting to the current study. This erlotinib study is the second sequentially planned biological adjuvant studies in conjunction with the vanguard study.

Clinical studies with erlotinib given as a single agent show that this medication is well tolerated with well-defined, toxicity profiles.

No specific demographic or gender groups will be targeted.

Patients will be consented by the treating physician and the research nurse. Witnesses will be clinic nurses or other members present during the informed consent interview process. Patients may request information and decide to enroll at a later date. Follow-up will occur through the research nurse.

4.0 Patient Eligibility

4.1 Inclusion criteria

1. Patients with either: a) histologically proven stage I, II, or IIIA NSCLC who have undergone a complete surgical resection of the primary tumor **OR** b) stage I or II HNSCC who have undergone definitive local treatment (surgery or radiation therapy).
2. HNSCC patients: Definitive local treatment $\leq$ 12 months prior to trial enrollment.

NSCLC patients: Surgery ≤ 12 months prior to trial enrollment.

3. No evidence of residual cancer
4. Smoking history of at least 10 pack years. May be current or former smoker.
5. Performance status of ≤ 2 (Zubrod, appendix C)
6. Age ≥ 18 years
7. Participants must have no contraindications for undergoing bronchoscopy.
8. Patients must have no active pulmonary infections.
9. Participants must not be taking oral non-steroidal anti-inflammatory drugs on a regular basis.
10. Participants must have the following blood levels: total granulocyte count >1500; platelet count > 100,000; total bilirubin ≤ 1.5 mg %; and creatinine ≤ 1.5 mg %.
11. Participants must complete the pretreatment evaluation and must consent to bronchoscopy and to endobronchial biopsy for biomarker studies.
12. All subjects who agree to participate will be given a written and verbal explanation of the study requirements and a consent form that must be signed prior to registration. Subjects will be informed that (a) they must be willing to take capsules daily for the duration of the trial, (b) they must be willing to take biopsies through bronchoscopy and give blood samples at the specified times, (c) they must schedule and keep the specified follow-up visits with their physicians and the study clinics, and (d) side effects and health risks may occur, as described in the informed consent form.
13. Participant must be enrolled in MDACC protocol #2003-0424 titled "A Phase IIb Vanguard Study Characterizing the Occurrence of Recurrent or Second Primary Tumors in Patients with a Prior History of a Definitively Treated Stage I/II Head and Neck or Non-Small Cell Cancer who are Current or Former Smokers."
14. Patients with prior head and neck cancer only: Participants must have no contraindications for undergoing laryngoscopy.
15. Subject must be considered legally capable of providing his or her own consent for participation in this trial.

4.2 Exclusion Criteria

1. History of radiation therapy to the chest. For those patients with head and neck cancer who received radiation, no more than 10% of the lung volume (apices) may be included.
2. History of prior EGFR treatment
3. Pregnant or breast-feeding (a negative pregnancy test within 72 hours of enrollment for women with child-bearing potential is required)
4. Participants with active gastric or duodenal ulcers or a history of ulcers requiring prophylactic H2 blockers.
5. Participants with active pulmonary infections or recent history of pulmonary infection (within one month).
6. Participants with acute intercurrent illness.
7. Participants requiring chronic ongoing treatment with NSAIDs. (Casual or non-prescribed use of NSAIDs is permitted as long as their use does not exceed one week at a time.)
8. Participants with history of stroke, uncontrolled hypertension and/or uncontrolled angina pectoris.
9. Patients may not take high dose antioxidants (vitamins E or C) during the study period. "High dose" will be determined by the study investigators.
10. Patients may not take high dose synthetic or natural Vitamin A derivatives (> 10,000 IU per day).
11. History of biologic therapy

12. Women of child-bearing potential must agree to use adequate contraception (hormonal or barrier method of birth control; abstinence) prior to study entry and for the duration of study participation. Childbearing potential will be defined as women who have had menses within the past 12 months, who have not had tubal ligation or bilateral oophorectomy. Should a woman become pregnant or suspect that she is pregnant while participating in this study, she should inform her treating physician immediately. The patient, if a man, agrees to use effective contraception or abstinence.
13. The patient has dysphagia. A patient who is unable to swallow intact capsules must be able to swallow capsules dissolved in water.
14. The patient has active gastrointestinal disease or a disorder that alters gastrointestinal motility or absorption (i.e., lack of integrity of the gastrointestinal tract such as a significant surgical resection of the stomach or small bowel).

Patients will be enrolled from the Thoracic/Head and Neck Medical Oncology and Surgical Oncology clinics at M. D. Anderson. Research nurses will also identify candidates from the clinic rosters and promote awareness in the community through various media outlets.

Children, pregnant women, and breast-feeding women will not be enrolled into the study. Participants will be consented by procedures described in sections 3.0 and 14.4. The consent process and informed consent document will clearly state that patients are not required to participate in the study and that they may stop participation in the study at any time.

5.0 Treatment Plan

Patients who meet the eligibility criteria in section 4 will be randomly assigned in a 2:1 ratio to either: 1) treatment with erlotinib or 2) no treatment. Patients assigned to treatment will be treated for a total of 12 months. All patients will undergo a bronchoscopy and spiral CT at baseline. These studies will be repeated 12 months after baseline. The plan is to start treatment patients at dose level 0 and reduce the dose as outlined in section 6.3. There will be no dose escalation.

Patients will be followed for up to 3 years after the first 12 month period, for a total of up to 4 years.

Erlotinib will be administered in oral 150 mg tablets. Patients will take the erlotinib by mouth once daily.

5.1 Severe Dysplasia/Carcinoma in Situ

Any participants found to have severe dysplasia or carcinoma in situ at initial or subsequent bronchoscopy will be strongly encouraged to undergo additional bronchoscopies at 6-month intervals. Any participant discovered to have invasive carcinoma at any time during the study will be referred for appropriate intervention (CIS pathway Appendix A).

5.2 Smoking Cessation Program

Any participant who is a current smoker will be offered participation in a smoking cessation program.

5.3 IND

Since erlotinib is approved by the FDA for locally advanced or metastatic non-small cell lung cancer (after failure of prior chemotherapy), the FDA has determined that this study is exempt from IND regulations, and therefore, an IND is not required to conduct the investigation.

6.0 Study Activities

6.1 Pre-Study Evaluations (see Appendix E)

Unless otherwise noted, labs, physical exams, imaging studies, and the laryngoscopy are to be performed within 4 weeks of beginning participation in this study.

1. Signed informed consent
2. Medical history including smoking history (duration and intensity)
3. Physical exam: including height, weight, Zubrod performance status assessment. Vital signs including pulse, blood pressure, temperature
4. Bronchoscopy
5. Buccal brushing
6. Sputum and saliva sample
7. Serum sample for biomarkers
8. Serum chemistry and electrolytes to include: BUN, creatinine, total bilirubin, SGPT, alkaline phosphatase, albumin
9. Hematology to include: CBC with automated differential and platelet count
10. Chest x-ray
11. CT scan of chest
12. Laryngoscopy for patients with prior head and neck cancers
13. PT
14. Pregnancy test (urine or serum) for females of childbearing potential within 72 hours prior to enrollment

6.2 Treatment Evaluations while on study (see Appendix E)

The participant will be observed on the study for a total of 36 months. Treatment evaluations will include those as part of the Vanguard trial as well as additional testing for those enrolled on this adjuvant study including:

1. Patients randomized to receive erlotinib: Medical history and physical exam by a physician at 3, 6, and 12 months. Medical history and nursing exam every 3 months during each of the first 12 months in which a physician exam is not scheduled. Upon completion of erlotinib patients will be followed monthly until resolution of symptoms from study medications. A focused history and physical will be done to evaluate and document any symptoms of GI bleeding, vision changes, rash, headache, arthralgias, dyspepsia, or other symptoms.
   Patients randomized to no treatment: Medical history and physical exam by a physician at months 6 and 12. Nursing follow-up by phone at months 3 and 9.
   All patients: Medical history and physical exam by physician at months 24 and 36. Medical history and nursing exam at months 18 and 30. After 36 months, the patient will have a medical history and physical exam every 6 months. The exam will be performed by a physician every 12 months after 36 months. The other physical exams will be performed by a nurse.

2. Bronchoscopy at month 12, 24 (optional), 36 (optional). Assessment of histology and biomarkers will be performed in the tissue biopsy at the same time. If an intercurrent illness coincides with a time period where bronchoscopy is scheduled, the bronchoscopy will be delayed 30 days or until resolution of the illness.
3. Buccal brushing at month 12, 24 (optional), 36 (optional).
4. Sputum and saliva sample at month 12, 24 (optional), 36 (optional).
5. Serum chemistry and electrolytes to include BUN, creatinine, SGPT, total bilirubin, alkaline phosphatase, albumin at months 3 (patients randomized to erlotinib only), 6, 12,18, 24, 30 and 36. After 36 months, the participant will have assessments every 12 months for as long as s/he remains observed on the study.
6. Hematology to include: CBC with automated differential and platelet count at month 3 (patients randomized to erlotinib only), 6, 12, 18, 24, 30 and 36. After 36 months, the participant will have assessments every 12 months for as long as s/he remains observed on the study.
7. Serum samples for biomarkers will be collected at months 3, 6, 12, 18, 24, 30 and 36. After 36 months, the participant will have assessments every 12 months for as long as s/he remains observed on the study.
8. Chest x-ray at 6, 12, 18, 24, 30 and 36 months.
9. Chest CT at 6, 12, 18, 24, 30 and 36 months.
10. Head neck exam with laryngoscopy at 12 months for those patients with prior head and neck cancer.

6.3 Dose modifications

All patients will start at dose level 0. There will be no planned dose escalation. The NCI Common Terminology Criteria for Adverse Events v3.0 (CTCAE) will be used (Appendix H).

Dose Level 0	Dose Level -1	Dose Level -2	Dose Level -3
150 mg/day	100 mg/day	50 mg/day	Off Study

6.3.1 Treatment of Erlotinib Toxicity and Dose Modification:

Toxicity grading is based on NCI Common Terminology Criteria for Adverse Events (v3.0) (http://ctep.cancer.gov/forms/CTCAEv3.pdf) and a treatment algorithm for the most common toxicities, diarrhea and skin rash is outlined in Table 6.1.

Management of a tolerable Grade 2 or 3 rash should include continuation of erlotinib at the current dose and symptomatic management. Because secondary bacterial infections are common and can lead to more serious complications, topical or systemic antibiotics may be considered. Anecdotally, topical or a short course of systemic corticosteroids can be helpful. If skin rash is intolerable, dose reduction should occur as described above. When skin toxicity improves by at least one grade level, the dose may be re-escalated as tolerated. In Phase II trials, this approach enabled dose re-escalation for the majority of patients requiring dose reduction for skin toxicity. Patients experiencing Grade 4 skin toxicity should be discontinued from study treatment.

For Grade 1 or 2 diarrhea, early intervention should include continuation of erlotinib at the current dose and initiation of loperamide therapy as described in Table 6.1. Grade 2

diarrhea that persists over 48–72 hours, despite optimal medical management, should be managed by dose reduction according to Table 6.1. Patients experiencing Grade 3 diarrhea should interrupt erlotinib until resolution to Grade ≤1 and re-start at a reduced dose according to table above. Patients should be maintained at the reduced dose without attempt at dose re-escalation. Patients experiencing Grade 4 diarrhea should be discontinued from study treatment.

Patients who experience Grade 3 fatigue should be managed with a dose reduction of 150mg to 100mg. Patients who experience Grade 4 fatigue should be discontinued from study.

Other serious adverse events or Grade 3 or 4 adverse events considered to be related to study drug should be managed with dose interruption until resolution of the event (Grade 1). Other serious adverse events or Grade 3 or 4 adverse events not resolving in 2 weeks will result in patient discontinuation. Patients may be rechallenged with study drug at the same dose level if the criteria for rechallenge are met. If the adverse event recurs after rechallenge, the patient should be withdrawn from the study.

Although quite rare, interstitial lung disease (ILD) can be life threatening. Therefore, patients should be monitored closely for symptoms consistent with ILD, such as new onset dyspnea without an obvious cause. In the event that ILD is suspected, erlotinib treatment should be discontinued and the patient should receive appropriate medical management. Although there is no proven therapy, systemic corticosteroids are often provided. Erlotinib should not be restarted in those patients suspected of having drug-related ILD. See Table 6.1 for management guidelines, including erlotinib dose interruption.

Table 6.1

Dosage Modification Criteria and Guidelines for Management of Erlotinib-Related Toxicities

NCI-CTCAE (v 3.0) Grade	Erlotinib Dose Modification	Guideline for Management
Diarrhea		
Grade 1	None	Consider loperamide (4 mg at first onset, followed by 2 mg q 2–4 hours until free of diarrhea for 12 hours)
Grade 2	None (Dose reduction of erlotinib is necessary if diarrhea persists over 48–72 hours despite optimal medical management)	Loperamide (4 mg at first onset, followed by 2 mg q 2–4 hours until diarrhea free for 12 hours)
Grade 3	Interrupt then dose reduce erlotinib. Erlotinib should not be re-escalated.	Interrupt erlotinib until resolution to Grade ≤1, and restart at next reduced dose
Grade 4	Discontinue study treatment.	
Pulmonary Events if possibly ILD		
All Grades	Temporarily interrupt erlotinib pending the diagnostic evaluation. If the pulmonary adverse event is assessed as related to erlotinib, discontinue the patient from study treatment.	Unexplained dyspnea, either new or progressive, should be aggressively evaluated.
Rash		
Tolerable rash (Grade 2 or 3)	None	Any of the following: minocycline [a], topical tetracycline, topical clindamycin, topical silver sulfadiazine, diphenhydramine, oral prednisone (short course) at discretion of investigator
Intolerable rash (Grade 2 or 3)	Consider interruption and or dose reduction if unresponsive to symptomatic management. Re-escalation is allowed.	Manage as described above
Grade 4	Discontinue study treatment.	Manage as described above

[a] Recommended dose: 200 mg po bid (loading dose) followed by 100 mg po bid for 7–10 days.

All subjects will be evaluable for toxicity if they have received any study drug. Safety parameters will include description of toxic deaths, premature withdrawals from treatment for toxicity reasons, description of adverse events, serious adverse events (SAE), and evaluation of toxicity.

6.4 Long Term Follow up

All participants will be followed until approximately 36 months after study enrollment at which time repeat testing and assessment will be done including bronchoscopy. Participants will then be followed at 6 month intervals until the study is completed. Participants will be followed for survival with an annual follow-up appointment and form to be completed for at least one year after final participant enrolled completes a 36 month evaluation or a maximum follow-up of 6 years. We plan to begin enrolling participants in this study in 12/06. We expect that participants will be followed until 8/12.

6.5 Early withdrawal

Early withdrawal is defined as a participant who is unable to continue participation on the study, participant refusal, or noncompliance. The following study activities will be completed at early withdrawal or at the end of study.

1. Medical history including documentation of smoking status
2. Physical exam
3. Radiologic/bronchoscopic assessment with tissue/sputum/washings samples
4. Serum chemistry and electrolytes to include: BUN, creatinine, sodium, potassium, chloride, glucose, total bilirubin, SGPT, alkaline phosphatase, and albumin.
5. Hematology to include: CBC with automated differential and platelet count
6. Serum collection for biomarker studies
7. Record for concomitant medications.
8. Monitor for adverse events.

6.6 Study Procedures

6.6.1 Bronchoscopy

Bronchoscopies will be performed at baseline and at months 12, 24 (optional) and 36 (optional) while participating in the study. White-light alone or white light and autofluorescence modalities may be used, both are preferred. Any carcinoma in situ found during the series of bronchoscopies will be documented and treated with ablation (see Appendix A).

1. Bronchoscopy: Study subjects will undergo autofluorescence and white-light bronchoscopy after being NPO in regard to solid food for a minimum of six hours and NPO for oral medications and small amounts of liquids for two hours prior to the procedure. The participant will be monitored with continuous electro-cardiographic, respiratory, and oximetric monitoring, with intermittent blood pressure monitoring. A complete endobronchial inspection will be performed and suspicious areas under white-light and autofluorescence bronchoscopy will be identified and recorded for subsequent biopsies and brushings. Specimens will be used to analyze biomarkers, genomic and proteomic studies and histologic assessment.
2. Bronchial secretions collection: During the bronchoscopy procedure, after the bronchoscope has passed beyond the vocal cords, a trap will be placed in the suction

line and bronchial secretions will be suctioned, collected and saved until the initiation of endobronchial biopsy and brushing procedures. Additional normal saline may be instilled on each side of the bronchial tree until a minimum volume of 15 ml. is retrieved. These liquids are saved for cytological and biological marker analyses.

3. Bronchoalveolar lavage: Following collection of bronchial secretions, the bronchoscope will be wedged in the right middle lobe or lingular orifice. Three 20 ml aliquots of sterile saline will be sequentially instilled, retrieved by gentle suction, pooled, and placed on ice for later analysis and storage. The volume of recovered effluent will be recorded.
4. Endobronchial biopsies: Biopsies will be taken from six predetermined sites even if they appear normal under white light or autofluorescence bronchoscopy: main carina, carinas at both upper lobe orifices, carina at right middle lobe orifice, carina between RB 9 and RB 10 and carina between LB 9 and LB10. Biopsies will also be taken from any additional sites that appear abnormal under white light and/or autofluorescence bronchoscopy. If a biopsy cannot be obtained at an abnormal site, then a brushing alone of that site will be performed. If possible, biopsies will be taken in such a fashion that not all of a potential marker lesion is removed. On followup bronchoscopies, the six predetermined sites and the sites that had histologic dysplasia determined to be mild or greater will be re-biopsied. One or more biopsy may be cultured to obtain respiratory epithelial cells. Depending on participant tolerance and operator discretion, endobronchial biopsies may be terminated at any time; however, an attempt will be made to biopsy between 6 and 12 sites on each participant. Additional sites may be biopsied if deemed clinically indicated, but more than 12 endobronchial biopsies will not be routinely taken. Bronchial brushings may be performed based on patient tolerance and yield of biopsies.
5. Bronchial brushings: Following completion of each biopsy, a bronchial brushings will be taken from the region adjacent to the biopsy site. Bronchial brushings will therefore be obtained from the six predetermined carinas (main carina, carinas at both upper lobe orifices, carina at right middle lobe orifice, carina between RB 9 and RB 10 and carina between LB 9 and LB10). Brushings will also be taken from any additional sites that appear abnormal under white light and/or autofluorescence bronchoscopy. A brushing alone will be performed at any an abnormal site that cannot be biopsied. On followup bronchoscopies, the six predetermined sites and the sites that had histologic dysplasia determined to be mild or greater will be re-brushed.
6. Bronchial washings: Following the collection of bronchial secretions and bronchoalveolar lavage, the trap in the suction line will be changed. Any bronchial secretions will be suctioned, collected, and saved until the completion of the procedure and withdrawal of the bronchoscope above the vocal cords. Additional normal saline may be instilled on each side of the bronchial tree until a minimum volume of 15 ml. is retrieved. These liquids are saved for cytological and biological marker analyses.

6.6.2 Repeat Bronchoscopy

All evaluable study participants will have repeat bronchoscopies with biopsies, brushes, and washes at months 12, 24 (optional) and 36 (optional) while participating in the study. Biopsy, brush, and wash samples will be obtained from the same sites sampled in the initial bronchoscopy. New abnormal areas detected by bronchoscopy will also be biopsied. Histologic assessment will be performed to determine whether malignant changes have occurred during the time period.

6.6.3 Sputum Samples

All registered participants will undergo sputum collection prior to bronchoscopy at baseline and months 12, 24 (optional) and 36 (optional) while participating in the study. Sputum samples will be analyzed cytologically, and specimens will be stored for biomarker studies.

6.6.4 Buccal Brushings

All registered participants will undergo buccal brushings from the inner left cheek at baseline and months 12, 24 (optional) and 36 (optional) while participating in the study to investigate evidence for tobacco-induced histologic and genetic alterations. This procedure may be found to serve as a surrogate marker of damage incurred in the bronchial tree.

6.6.5 Saliva

All registered participants will have saliva collected at baseline and months 12, 24 (optional) and 36 (optional) while participating in the study to investigate evidence for tobacco-induced histologic and genetic alterations and biomarker studies.

6.6.6 Serologies

All registered participants will have serum collected at baseline and month 6, 12, 18, 24, 30 and 36 while participating in the study. Serum will be stored and analyzed for biomarker, genomic and proteomic studies as well as gene expression profiles.

7.0 Investigational product description

Erlotinib (OSI-774, Tarceva™) is supplied by OSI Pharmaceuticals, Melville, NY, in partnership with Genentech. Erlotinib is FDA approved for treatment of locally advanced or metastatic non-small cell lung cancer after the failure of at least one prior chemotherapy regimen.

7.1 Drug Accountability

All study drug required for completion of the study will be provided by OSI Pharmaceuticals, Inc. The recipient will acknowledge receipt of the drug by returning the drug receipt form indicating shipment content and condition. Damaged supplies will be replaced. Study drug accountability records should be maintained by the site in accordance with the regulations.

The original drug supply request of erlotinib will be submitted to Genentech along with the form "Approval for Drug Re-Supply", indicating which personnel will be able to submit drug re-supply requests. All subsequent drug re-supply requests will be directly submitted to OSI-Pharmaceuticals from the site.

At the time of study closure, the unused, used and expired study drug will be destroyed at the site per Institutional SOPs, or returned to the OSI-Pharmaceutical Drug Depot.

7.2 Formulation, Packaging and Storage

Erlotinib oral tablets are conventional, immediate-release tablets containing erlotinib as the hydrochloride salt. In addition to the active ingredient, erlotinib, tablets contain lactose, hydrous microcrystalline cellulose, sodium starch glycolate, sodium lauryl sulfate, and magnesium stearate. Study drug for daily oral administration will be supplied as 25, 100, and 150 mg

tablets of erlotinib, in white, high-density polyethylene (HDPE) bottles with child-resistant closures and should be stored at temperatures between 15°C and 30°C (59°F and 86°F). For further details, see the erlotinib Investigator Brochure.

7.3 Preparation and Administration

Tablets should be taken preferably in the morning one hour prior or two hours after a meal with up to 200 mL of water. Subjects who are unable to swallow tablets may dissolve the tablets in distilled water for administration. If a subject forgets to take a dose, the last missed dose should be taken as soon as the subject remembers, as long as it is at least 12 hours before the next dose is due to be taken. The daily treatment schedule will be resumed the next day with the subject taking their scheduled dose at their usual time. In subjects who have emesis and are unable to retain erlotinib for 30 minutes or longer, every attempt should be made to obtain control of nausea and vomiting. The dose of erlotinib may be repeated if emesis occurs within 30 minutes of taking the tablet.

7.4 Pretreatment Medications

Although no pre-medication is necessary prior to taking erlotinib, pre-medication will be allowed if needed.

7.5 Warnings and Precautions of Erlotinib Administration

Based upon clinical experience to date, the following adverse effects may be associated with erlotinib administration: The primary toxicities consist of diarrhea, rash, nausea, vomiting, stomatitis, headache, and fatigue. The only dose-limiting toxicity observed to date is diarrhea. This event is dose-related and is generally controlled with the addition of loperamide therapy, starting doses of erlotinib of < 200 mg/day, and dose reductions.
Rash occurred in 75% of erlotinib-treated NSCLC patients enrolled in BR.21. A papular, pustular rash manifesting most often on the face and upper trunk was common across all studies, but rash was rarely the cause of study drug discontinuation. The rash may be associated with erythema, pain, pruritus, dryness, and less commonly, stomatitis, keratitis and nailbed changes. Wearing of contact lenses while receiving erlotinib therapy is not recommended. The incidence of diarrhea in BR.21 was 54% of erlotinib-treated NSCLC patients. The median time to onset of skin rash was 8 days and median time to occurrence of first diarrheal symptom was 9 days.

There have been infrequent reports of serious (including fatal) interstitial lung disease (ILD) in patients receiving erlotinib for treatment of NSCLC or other advanced solid tumors. In Study BR.21, the incidence of ILD (0.8%) was the same in the placebo and erlotinib groups. The overall incidence in erlotinib-treated patients from all studies (including uncontrolled studies and studies with concurrent chemotherapy) is approximately 0.6%. Included in this rate of ILD are reported diagnoses of pneumonitis, interstitial pneumonia, interstitial lung disease, obliterative bronchiolitis, pulmonary fibrosis, acute respiratory distress syndrome, and lung infiltration, irrespective of investigator assessed causality. Most of the cases were associated with confounding or contributing factors such as concomitant/prior chemotherapy, prior radiotherapy, preexisting parenchymal lung disease, metastatic lung disease, or pulmonary infections. Reversible renal impairment has been reported in association with dehydration associated with nausea, vomiting, and diarrhea. There have been rare reports of renal failure in patients receiving erlotinib in combination with platinum-containing chemotherapy regimens. Febrile neutropenia has been reported in patients receiving concomitant chemotherapy.

Erlotinib is both protein bound (92%–95%) and metabolized by hepatic cytochromes CYP3A4 and CYP3A5 and pulmonary cytochrome CYP1A1. Therefore, a potential for drug–drug interaction exists when erlotinib is co-administered with drugs that are highly protein bound or that are CYP3A4 inhibitors/inducers.

Co-administration of erlotinib with an inhibitor of CYP3A4 metabolism (ketoconazole, 200 mg po BID for 5 days) resulted in increased exposure to erlotinib as measured by an 86% increase in median erlotinib AUC and a 69% increase C_{max}, compared with administration of erlotinib alone. Induction of CYP3A4 metabolism by a known enzyme inducer (rifampin, 600 mg po QD for 7 days) resulted in a 69% decrease in the median erlotinib AUC, compared with administration of erlotinib alone. However, the effect of rifampin on C_{max} was negligible.

International normalized ratio (INR) elevations and/or bleeding events have been reported in some cancer patients taking warfarin while on erlotinib.

Additional rare side effects have included: interstitial pneumonitis, gastrointestinal irritation including gastrointestinal perforation, increased risk of gastrointestinal bleeding when combined with NSAIDS, stomatitis, anorexia, alopecia, pruritis, myalgias, bone pain, cough, dyspnea, and ocular changes. For complete details of these rare side effects please see the IND safety reports and erlotinib Investigator's brochure.

7.6 Concomitant Medications and Therapy

Information on concomitant medications will be collected on this study. Medications for supportive care will be allowed as needed to treat nausea, pain, fever, rash, diarrhea, etc. Granulocyte growth factors (GCSF or GMCSF) will not be given routinely. Although this drug rarely causes hematologic toxicity, these agents can be administered only in the presence of febrile neutropenia (defined as ANC<1000 cells/μL and oral temperature >38.5°C) or grade IV neutropenia lasting more than 4 days. Erythropoietin can be administered for anemia at the discretion of the treating physician. Commercial suppliers of growth factors will be utilized. The use of growth factors (GSCF, GMCSF and erythropoietin) will be according to ASCO guidelines (Ozer et al., 2000). The use of bisphosphanates for the purposes of treating bone metastases can be administered at the discretion of the treating physician.

Other chemotherapeutic agents or investigational medications will not be allowed.

Systemic steroids are discouraged for the treatment of skin toxicities. Subjects who are taking steroids for reasons other than skin toxicity at trial entry may continue treatment.

Other medication, which is considered necessary for the subject's safety and well being, may be given at the discretion of the investigator(s).

There are potential interactions between erlotinib and CYP3A4 inhibitors and CYP3A4 promoters. Although caution and careful monitoring are recommended when use of these compounds are necessary, usage does not exclude subjects from participating in this trial (see Appendix F for a list of CYP3A4 inhibitors).

Because of the potential for drug-drug interaction between erlotinib and warfarin, subjects in this study who are receiving concomitant warfarin therapy will have INR results obtained at screening and during treatment as follows: weekly for the first 5 weeks and then at each cycle.

If surgery is considered necessary for the subject, whenever possible, at least 7 days should elapse after the last dose of erlotinib before surgery is performed.

If radiation therapy is considered necessary for the subject at any point during this study, then this will be considered progressive disease and the subject will be removed from the study.

For additional guidance for concomitant medications, please refer to section 12.

8.0 Investigational Centers

Patients will be seen and enrolled at the University of Texas M. D. Anderson Cancer Center, Department of Thoracic/Head and Neck Medical Oncology clinics, Houston, TX. Additional sites may be added throughout the study.

8.1 Investigator Contact Information

Principal Investigator:

Waun Ki Hong, MD
University of Texas M.D. Anderson Cancer Center
1515 Holcombe Blvd., Unit 432
Houston, TX 77030
Phone: 713-792-6363
Fax: 713-796-8655
e-mail: whong@mdanderson.org

Co-Principal Investigator:

Edward Kim, MD
University of Texas M.D. Anderson Cancer Center
1515 Holcombe Blvd., Unit 432
Houston, TX 77030
Phone: 713-792-6363
Fax: 713-792-1220
e-mail: edkim@mdanderson.org

9.0 Criteria for Discontinuation of Therapy

Patients will be removed from therapy for any of the following reasons:

1. Dose reduction to the –3 level (above)
2. Pregnancy or planned pregnancy
3. Patient requests to withdraw
4. Unwilling or unable to comply with study requirements
5. Identification of recurrent or new cancer
6. Unrelated intercurrent illness that will affect assessment of clinical status to a significant degree as determined by the principal investigator or the treating physician
7. The treating physician or investigator must discontinue therapy if he/she thinks that the patient's health or well-being is threatened by continuation of therapy.

If any safety parameters show a clinically significant change from baseline that warrants early termination of treatment, the patient will continue with the scheduled study-related procedures. Appropriate safety monitoring will continue until the patient is discharged from the study. Patients withdrawn from the study will be followed until resolution of toxicity. The reason for and date of the discontinuation will be obtained. The date of the last dose of study medication will also be obtained.

10.0 Adverse Events

10.1 Assessment of Adverse Event Severity & Relationship to Treatment

All serious adverse events (defined below), whether or not deemed drug-related or expected, must be reported by the Principal Investigator or designee to the HSRRB and/or USAMRMC, Human Research Protection Office within 24 hours (one working day) by telephone. A written report must follow as soon as possible, which includes a full description of the event and any sequelae. This includes serious adverse events that occur any time after the inclusion of the subject in the study (defined as the time when the subject signs the informed consent) up to 30 days after the subject completed or discontinued the study. The subject is considered completed either after the completion of the last visit or contact (e.g., phone contact with the Investigator or designee). Discontinuation is the date a subject and/or Investigator determines that the subject can no longer comply with the requirements for any further study visits or evaluations (e.g., the subject is prematurely discontinued from the study). An adverse event temporarily related to participation in the study should be documented whether or not considered to be related to the test article. This definition includes intercurrent illnesses and injuries and exacerbations of preexisting conditions.

Include the following in all safety reports: Subject identification number and initials; associate investigator's name and name of MTF; subject's date of birth, gender, and ethnicity; test article and dates of administration; signs/symptoms and severity; date of onset; date of resolution or death; relationship to the study drug; action taken; concomitant medication(s) including dose, route, and duration of treatment, and date of last dose.

A serious adverse event is any event that is: fatal; life-threatening (life-threatening is defined as the patient was at immediate risk of death from the adverse event as it occurred); significantly or permanently disabling; or requires in-patient hospitalization.

Important medical events that may not result in death, be life-threatening, or require hospitalization may be considered a serious adverse drug experience when, based upon appropriate medical judgment, they may jeopardize the patient or subject and may require medical or surgical intervention to prevent one of the outcomes listed in this definition. In addition, laboratory value changes may require reporting.

Reports of all serious adverse events must be communicated to the appropriate Institutional Review Board (IRB) or ethical review committee and/or reported in accordance with local laws and regulations.

10.2 Procedures for Reporting Serious Adverse Events

Serious and/or unexpected adverse events are submitted in writing to the M.D. Anderson Cancer Center Institutional Office of Protocol Research (OPR) within 10 working days of the adverse experience as described Appendix G. Unexpected fatal or life-threatening experiences are phoned immediately to the Office of Protocol Research (713-792-2933). A follow up written

report is submitted to OPR within 10 working days. The form for communication to OPR of all serious adverse events is appended to this plan.

Reports of all serious adverse events must be communicated to the appropriate Institutional Review Board (IRB) or ethical review committee and/or reported in accordance with local laws and regulations. Adverse experiences that are both serious and unexpected will be immediately reported by telephone to the USAMRMC, Human Research Protection Office (301-619-2165) and send information by facsimile to 301-619-7803. A written report will follow the initial telephone call within 3 working days. Address the written report to the U.S. Army Medical Research and Material Command, ATTN: MCMR-HRPO, 504 Scott Street, Fort Detrick, Maryland 21702-5012.

For all protocols conducted at M.D. Anderson Cancer Center, the Principal Investigator is responsible for submitting adverse event reports to the Institutional IRB and DoD on an ongoing basis. Adverse event reports are submitted to the Institutional Office of Protocol Research (OPR), where they are entered into PDMS and forwarded to the designated IRB vice chairperson for review. Attached to each adverse event report is a listing of all prior adverse events submitted for that protocol. Any comments, questions or changes the IRB requests to the protocol as a result of this review are conveyed to the principal investigator. The investigator response and protocol modification process is monitored by the IRB vice-chairperson and OPR support staff. The vice chairperson presents the report on adverse event review to the full committee at the next IRB meeting.

An adverse event report compilation is provided once annually to the M.D. Anderson Cancer Center IRB. Comments, questions or other considerations from the IRB are conveyed to the principal investigator for evaluation, discussion and implementation.

For all protocols conducted at M.D. Anderson Cancer Center, the Principal Investigator is responsible for submitting adverse event reports to the Institutional IRB on an ongoing basis. Adverse event reports are submitted to the Institutional Office of Protocol Research (OPR), where they are entered into PDMS and forwarded to the designated IRB vice chairperson for review. Attached to each adverse event report is a listing of all prior adverse events submitted for that protocol. Any comments, questions or changes the IRB requests to the protocol as a result of this review are conveyed to the principal investigator. The investigator response and protocol modification process is monitored by the IRB vice-chairperson and OPR support staff. The vice chairperson presents the report on adverse event review to the full committee at the next IRB meeting.

An adverse event report compilation is provided once annually to the M.D. Anderson Cancer Center IRB. Comments, questions or other considerations from the IRB are conveyed to the principal investigator for evaluation, discussion and implementation.

10.3 Reporting of Subject Death

The death of any subject during the study or within 30 days of study completion (as defined above), regardless of the cause, must be reported within 24 hours by telephone, to the principal investigator and/or study coordinator, and the HSRRB and/or USAMRMC, Human Research Protection Office. A full written report must follow as soon as possible. If an autopsy is performed, the report must be provided to the Sponsor.

Reports of all serious adverse events, including deaths, must be communicated to the appropriate Institutional Review Board or ethical review committee and/or reported in accordance with local law and regulations.

10.4 Known Adverse Events Relating to the Underlying Clinical Condition

These will be reported on the chart and in the study case report forms.

11.0 Statistical Considerations

A total of 70 patients will be recruited in this trial and randomized with a 2.5:1 ratio (via computerized central randomization) into active (erlotinib treatment) or the no-treatment control arm. The standard practice for these patients after definitive therapy is follow-up (no treatment). Therefore, it is ethical to randomize patients into the no-treatment control arm. All patients will receive comprehensive risk assessment and screenings as defined in the Vanguard Trial.

The primary endpoint of the study is histological response. Histological response is based on changes in baseline to 12 month assessment of biopsies taken during bronchoscopy at six sites (main carina, carinas at both upper lobe orifices, carina at right middle lobe orifice, carina between RB 9 and RB 10 and carina between LB 9 and LB10) in the lung. There are 3 critiera for establishing a response based upon a 1-7 score assigned to each biopsy including, 1) the average score of all biopsies decrease by 1, 2) the percentage of biopsies with moderate dysplasia or worse (score 5-8) decreases by 10%, and 3) the worst score improves by 1. A response is defined as an improvement in at least 2 of the 3 criteria. Progression is worsening in 2 or more of the 3 criteria. Otherwise, the histological response will be coded as no change. The proliferation marker Ki-67 will be used as a secondary endpoint to evaluate the efficacy of the biologic treatment. Other mechanism-based biomarkers such as apoptotic index will also be analyzed.

We will monitor efficacy and toxicity simultaneously using the method of Bryant and Day (Biometrics 1995) (56). Efficacy is based baseline to 12-month histological response as defined above. For purposes of toxicity, any grade 2 or higher adverse event will be counted. Unacceptable response is 10% and a 30% response rate would be considered sufficiently active to warrant further study of this regimen. A 10% and 40% grade II toxicity rate are considered acceptable and excessive, respectively. We assume one-sided 5% type I error rates for both efficacy and toxicity. With 50 patients treated and evaluated, we have 95% power to detect clinically meaningful improvement in response to 30% at 12 months. The interim analysis will take place when 20 patients have been treated and are evaluable for response. If 2 or fewer responses are observed in the first 20 patients treated with acceptable toxicity, the protocol will stop accrual due to insufficient activity. Similarly, if 7 or more patients experience a grade 2 or higher adverse event with acceptable response, the protocol will stop accrual due to excessive toxicity. Otherwise, the protocol will continue accrual to a maximum of 50 patients. If 9 or more patients experience a response and 36 patients do not experience a grade 2 or higher adverse event in 50 patients treated and evaluated, then this treatment will be recommended for further clinical evaluation.

For detecting biomarker modulation on a continuous variable such as Ki-67, the paired-t test will be performed comparing the biomarker values before and after treatment. Transformations (e.g. natural log) will be performed if necessary to meet normality assumptions of the test. With 50 patients receiving the biologic treatment, we will be able to detect an effect size (expected mean

difference divided by the standard deviation of the difference) of 0.404 with 80% power and two-sided 5% type I error rate.

For detecting biomarker modulation on a dichotomous variable, McNemar's test will be used to compare the status of a biomarker such as present/absence or high/low before and after treatment. Assume that p_{21} and p_{12} are the probability changing from absence to presence and from presence to absence for a biomarker. $p_{21} + p_{12}$ are the proportion of discordant pairs pre- and post-treatment. Further, $p_{11} + p_{12}$ is the proportion of concordant pairs (i.e., p_{11} = proportion positive pre- and post-treatment and p_{22}=proportion negative pre- and post-treatment). With 50 patients and two-sided 5% type I error rate, we will have 85% power detect a 25% change in modulation for $p_{21} = 0.05$ and $p_{12} = 0.30$ and 94% power to detect a 30% change for $p_{21} = 0.05$ and $p_{12} = 0.35$. The power computations are shown in the following table.

p_{21}	p_{12}	$p_{12} - p_{21}$	Power
0.05	0.30	0.25	85%
0.10	0.35	0.25	71%
0.05	0.35	0.30	94%
0.10	0.40	0.30	84%

We will also compare the treatment efficacy between the treatment arm and the control arm. We plan to treat 280 patients in four sequentially conducted bioadjuvant trials (70 patients each); each trial will have exactly the same eligibility criteria. We will randomize 20 patients into the control group in each of these four biologic-agent trials. We expect an additional 70 patients will choose to enroll in the vanguard (i.e. observation only) part of the umbrella trial. Therefore, we will have 20x4 + 70 = 150 control patients in the vanguard study who did not receive any active agents. Control patients will be analyzed to test for any trial-specific difference or time trend and will be combined if no difference is found among various control groups. Power calculations for two-sample t-test was performed with two-sided 5% type I error rate. With 50 in the biologic treatment arm and 20 (only control patients in this trial is used) or 150 (aggregate all the control patients together) in the control arm, we will have 80% power to detect standardized effect sizes of 0.76 and 0.46 for continuous outcomes, respectively. For dichotomous outcomes, statistical power for detecting various differences is given in the following table. With 20 in the control arm and 50 in the active arm, we will have 80% power to detect a difference of histological response of 5% and 35%, respectively. Similarly, 85% of power can be achieved if the response rates are 10% and 45%, respectively. If we combined all no-treatment controls, we will be able to detect a 25% difference in the response rate with at least 92% power for no-treatment response rates from 5% to 20%.

		P_0		
Ncontrol	$P_1 - P_0$	0.05	0.10	0.20
20	0.30	80%	73%	65%
	0.35	91%	85%	79%
150	0.20	99%	94%	78%
	0.25	99%	99%	92%

12.0 Concomitant Medications

- All concomitant medications will be recorded.

- The best supportive care and treatment will be given to each participant (antibiotics, transfusions, diet, etc.)
- No concurrent investigational agents will be permitted.
- No concurrent antineoplastic agents or hormonal anticancer therapy will be permitted.
- No concurrent radiotherapy will be permitted.
- Participants taking cyclooxygenase inhibitors, lipoxygenase inhibitors, NSAIDs (except aspirin at ≤ 81 mg a day), and steroids will be encouraged to refrain from taking, if possible, while on study and at least 4 weeks prior to enrollment.
- Other Concomitant Treatment
- Systemic retinoids and herbal medicines or remedies (including green tea) must be discontinued before entry into the trial and are not allowed during the trial. Patients may not be taking high-dose vitamin A within 30 days of study entry.
- Other medication, which is considered necessary for the participant's safety and well being, may be given at the discretion of the investigator(s).

13.0 Methods for Biomarker Analysis

All samples will be processed and stored via the pathology department. Then, the samples will be distributed to specific investigators for studies including biomarkers of apoptosis and cell proliferation, gene expression profiling, genomics, proteomics, and other specified biomarkers of intermediate response.

14.0 Study Administration and Investigator Obligations

14.1 Replacement of Subjects

Participants who withdraw from the study prior to completion of the study treatments for reasons other than serious adverse events, unacceptable toxicity or progressive disease will be defined as dropouts and will be replaced. Replacement participants will be assigned the next sequential number.

14.2 Protocol Compliance

The attending physician and oncology research nurse will evaluate each participant at the initial clinic visit to determine whether the participant qualifies for the study and at each clinic visit thereafter to determine readiness for bronchoscopic procedures. All required interim and pretreatment data will be available to them for evaluation.

14.3 Institutional Review Board

This study must have the approval of a properly constituted Hospital Ethics Committee, Regional Ethics Committee, or other Institutional Review Board (IRB).

The investigator must also report all serious and medically significant adverse events to the IRB or Ethics Committee, NCI, sponsor, as well as the USAMRMC, Human Research Protection Office (see section 9.1).

14.4 Informed Consent

All study participants must sign and date an informed consent form prior to study participation. The investigator will be responsible for designing the consent form using appropriate National or Regional Guidelines (equivalent to the American Federal Guidelines Federal Register July 27, 1981, or 21 CRF Part 50, or International Committee on Harmonization-Good Clinical Practice).

The informed consent form must be approved by the IRB or Ethics Committee. State and local laws, and/or institutional requirements may require the disclosure of additional information on the informed consent form. For a detailed description of the UTMDACC Research Informed Consent Process please refer to Appendix J.

A copy of the informed consent form will be given to the participant. The investigator will keep each participant's signed informed consent form on file for inspection by a regulatory authority at any time.

14.5 Record Retention

- The investigator and other appropriate study staff will be responsible for maintaining all documentation relevant to the study. Such documentation includes:
- Case Report Forms—must be legible, accurate, and up-to-date.
- Copies of all Serious AE reporting forms faxed to the USAMRMC, Human Research Protection Office.
- Participant Files—should substantiate the data entered in the CRFs with regard to laboratory data, participant histories, treatment regimens, etc.
- Participant Exclusion Log—should record the reason any participant was screened for the study and found to be ineligible.
- Drug Dispensing Log—should record the total amount of study drug received and returned to supporter providing the study drug, and the amount distributed and returned or destroyed. This information must agree with the information entered in the CRFs.
- Informed Consent Forms—completed consent forms from each participant must be available and verified for proper documentation.
- Informed Consent Log—must identify all participants who signed an Informed Consent Form so that the participants can be identified by audit.

The Investigator must keep on file protocols, amendments, IRB approvals, all copies of Form FDA 1572, all correspondence, and any other documents pertaining to the conduct of the study for a minimum of two (2) years after notification by USAMRMC, Human Research Protection Office of either FDA approval or discontinuation of the IND.

14.6 Case Report Forms

Data recorded on Case Report Forms (CRFs) must be legible and complete. CRFs will be completed on a timely basis. The individual making the correction on the CRF must initial and date the correction. The investigator must review all final and corrected CRFs. Corrected copies of CRFs will be filed with the corresponding original.

If a subject's medical record is needed, it will be requested by the Principal Investigator or Co-Principal Investigator. The requesting investigator (i.e., either the PI or co-PI) will assume responsibility for medical record abstraction, which will be performed by an oncology research nurse and the PI or co-PI. The PI and co-PI are medical oncologists.

14.7 Study Monitoring

Study Investigators and appointed research Study Investigators and appointed research staff will oversee the study conduct to assure satisfactory enrollment rate, data recording, and protocol adherence at MDACC as well as participating sites. The investigator and staff are expected to cooperate and provide all relevant study documentation in detail at each site visit on request for review.

The medical monitor will review all serious and unexpected adverse events associated with this protocol and provide an unbiased written report of the event within ten (10) calendar days of the initial report. The medical monitor should be a qualified physician, other than the principal investigator, not associated with the protocol, able to provide medical care for research volunteers for conditions that may arise during the conduct of the study, and who will monitor the volunteers during the conduct of the study. The medical monitor is required to review all serious and unexpected adverse events (per ICH definitions) associated with the protocol and provide an unbiased written report of the initial report. At a minimum the medical monitor should comment on the outcomes of the adverse event (AE) and relationship of the AE to the test article. The medical monitor should also indicate whether he/she concurs with the details of the report provided by the study investigator. Reports for events determined by either the investigator or medical monitor to be possibly or definitely related to participation and reports of events resulting in death should be promptly forwarded to the HSRRB.

The medical monitor for this study will be Aman U. Buzdar, MD:

Aman U. Buzdar, M.D.
University of Texas M.D. Anderson Cancer Center
Department of Breast Medical Oncology
1515 Holcombe Blvd. - 424
Houston, Texas 77030 USA
Phone: 713- 792-2817
Fax: (713) 794-4385
email: abuzdar@mdanderson.org

The medical monitor will forward reports to the U.S. Army Research and Material Command, ATTN: MCMR-HRPO, 504 Scott Street, Fort Detrick, Maryland, 21702-5012.

14.8 Termination of Study

The HSRRB and/or USAMRMC, Human Research Protection Office and M. D. Anderson will retain the right to terminate the study and remove all study materials from the study site at any time. Specific instances that may precipitate such termination are as follows:

- Unsatisfactory participant enrollment with regard to quality or quantity
- Deviation from protocol requirements, without prior approval from HSRRB and M. D. Anderson.
- Inaccurate and/or incomplete data recording on a recurrent basis
- The incidence and/or severity of adverse drug events in this or other studies indicating a potential health hazard caused by the treatment

14.9 Study Amendments

The investigator will only alter the protocol to eliminate apparent immediate hazards to the participant. If preliminary or interim statistical analysis indicated that the experimental design, dosages parameters, or selection of participants should be modified, these changes will be described in an amendment to be approved by the institution's and other appropriate review committees after consultation with the statistician and Study Chairman. Any amendments cannot be enacted unless approved by the HSRRB and/or USAMRMC, Human Research Protection Office. All revisions made to protocols previously approved by the IRB will be submitted to the IRB for approval prior to implementation of the revision. If the IRB decides to disapprove a research activity, it shall included in its written notification a statement of the reasons for its decision and give the investigator an opportunity to respond in person or in

writing. No changes to the protocol will be initiated unless also approved by the Human Subjects Research Review Board.

14.10 Protocol Deviations and Violations

In the event of a protocol deviation and/or violation, the principal investigator will notify the Institutional Review Board, U.S. Army Medical Research and Materiel Command, Human Subjects Research Review Board (HSRRB), M.D. Anderson, and the study Medical Monitor (Aman U. Buzdar, M.D.). This notification will occur as soon as the deviation is identified and will be included in the annual review and final study report. For a detailed description of the procedure for submission of protocol deviations and violations refer to Appendix K.

14.11 Ethical and Legal Considerations

This study will undergo full approval in accordance with the human surveillance requirements of each institution. Blood samples will be obtained for the evaluations as described in the protocol. Tissue samples obtained at the time of prior surgeries will be reviewed before participant enrollment to confirm the participant's diagnosis. Measures will be taken to ensure confidentiality of participant information. Tissue samples will be collected prospectively during the trial. Data collected on paper forms will be stored in locked file cabinets with restricted access. Data collected on electronic media will be stored in computer files with restricted password access limited to the principal investigator and study coordinators. All staff members in the study will be informed prior to employment and at regular intervals of the necessity for keeping all data confidential. Computers will not be accessible to the public and will be located in locked offices. Subjects will be assigned a separate study number to protect subject identification. No patient identifiers will be used in any publications of this research. Data will be maintained indefinitely. When the time comes to dispose of the data, all database files will be deleted, patient identifiers will be removed from all paper forms and documents will be shredded.

14.12 Risks/Benefits

Participants will benefit from the educational information provided, including counseling on alcohol and smoking cessation, from the regular follow-up procedures required, and from the blood analyses (i.e., electrolytes, liver function tests, complete blood count, and platelet count). Participants will also benefit from the close comprehensive follow-up after their surgery including additional imaging tests. Participants may benefit from development of a risk model and adjuvant therapy with biologic compounds.

Participants will undergo several invasive procedures (bronchoscopies) which do have associated risks. These risks will be explained completely prior to consenting of the participant. The following table summarizes risks associated with this study and the steps that will be taken to minimize these risks:

Procedure	Risks	Measures to Minimize Risks
Complete History and Physical Exam, Including blood chemistries and Pregnancy test	Identification of previously unknown condition	Qualified Health Care provider to evaluate potential subject.
Venipuncture	Pain, bleeding, clotting, bruising at the injection	Included in consent form.

	site, and rarely infection.	Qualified health care worker with experience in phlebotomy.
Erlotinib (Tarceva®)	Rash, diarrhea, fatigue, nausea, vomiting, abdominal pain, headache, stomatitis, anorexia, alopecia, pruritis, myalgias, bone pain, cough dyspnea, elevated liver enzymes, interstitial lung dz, ocular changes. Warfarin drug interactions Other Drug interactions which may require dosage adjustments (e.g. azole antifungals, barbituates etc). Caution advised in combination with NSAIDS due to risk of GI bleed Contraindicated in subjects with hypersensitivity to components/drug or class Unanticipated risks	Close monitoring of participant by qualified staff. Dose of erlotinib may be reduced and/or stopped in the event of toxic side effects Experienced clinical research center with well qualified staff familiar with this patient population. INR results obtained at screening and during treatment for subjects receiving warfarin Included in consent form Reporting and monitoring mechanism in place for SAE/AE or Unanticipated problems
Bronchoscopy with bronchoalveolar lavage, bronchial washings, bronchial brushings, and bronchial biopsies	Pain, irritation, minor sore throat, mild fever, coughing, bleeding, pneumothorax. May cause breathing problems similar to asthma; Bronchitis, Pneumonia Sedatives given during procedure can	Risks fully addressed in protocol and ICF. Establish adequate pre-procedure bleeding parameters Use of conscious sedation and topical anesthesia to minimize discomfort and cough. Well trained well qualify medical professionals and rescue meds at beside. Pre-sedation assessment to identify particular

	decrease breathing function and/or level of oxygen in blood. May have allergic reaction to sedatives or anesthetics. Increase risk of bleeding in participants on warfarin. Also in subjects who may be on other anti-coagulants or ASA.	risk factors Monitoring of level of consciousness, cardiovascular and gas exchange parameters during procedure and recovery. Advise patients of discontinuation of anticoagulants for an adequate period of time prior to the procedure
CT-guided Core Tumor Biopsy	Pain, Discomfort Bleeding and rarely infection. Coughing Collapsed lung (pneumothorax) Sedatives given during procedure can decrease breathing function and/or level of oxygen in blood. May have allergic reaction to sedatives or anesthetics Increase risk of bleeding in participants on warfarin. Also in subjects who may be on other anti-coagulants or ASA.	Risks fully addressed in protocol and ICF. Establish adequate pre-procedure bleeding parameters Use of conscious sedation and topical anesthesia to minimize discomfort and cough. Well trained well qualify medical professionals and rescue meds at beside. Pre-sedation assessment to identify particular risk factors Monitoring of level of consciousness, cardiovascular and gas exchange parameters during procedure and recovery. Advise patients of discontinuation of anticoagulants for an adequate period of time prior to the procedure
Buccal sample	Pain Discomfort Irritation Bleeding	Brushings on inner cheek performed lightly while patient is under conscious sedation
Laryngoscopy	Discomfort Gagging Reaction to topical anesthesia	Topical anesthesia will be used to reduce discomfort and gagging Exams will be performed by experienced

	Nasal irritation Nasal bleeding	personnel
X-rays, and CT or MRI scans	Radiation exposure	These diagnostic tests are medically necessary to monitor the patient; however, however, low risk of radiation exposure as part of participation in the study.
Collection of data	Breach of Patient privacy and confidentiality	Patient assigned unique code Restricted access to research records Investigators trained in Human Subjects Protection

Participants will not be financially responsible for any study-related tests outside of accepted standard of care follow-up.

14.13 Gender and Minority Inclusion
Women and minorities will be actively recruited to participate in the Vanguard trial. However, since only 42% of lung cancer participants and 22% of laryngeal cancer participants are female, we expect to have more male than female subjects on the study. We expect that the ethnic distribution of the enrolled participants will reflect the local ethnic mixture of each institution's surrounding community.

14.14 Subject Records
HSRRB and/or USAMRMC, Human Research Protection Office, M.D. Anderson or their representatives may have access to subject records as a part of their responsibility to protect human subjects in research.

14.15 Publication Statement
Data will be reviewed by the collaborating biostatistician prior to publication. HSRRB and/or USAMRMC, Human Research Protection Office will have 30 days to review all definitive publications, such as manuscripts and book chapters, and a minimum of 10-15 days to review all abstracts.

15.0 References

The effect of vitamin E and beta carotene on the incidence of lung cancer and other cancers in male smokers. The Alpha-Tocopherol, Beta Carotene Cancer Prevention Study Group. N Engl J Med, *330:* 1029-1035., 1994.

Baselga, J., and Arteaga, C. Critical update and emerging trends in epidermal growth factor receptor targeting in cancer. J Clin Oncol. 2005 Apr 10;23(11):2445-59. Epub 2005 Mar 7. Review.

Baselga J, Yano S, Giaccone G, et al: Initial results from a phase II trial of ZD1839 (Iressa) as second- and third-line monotherapy for patients with advanced non-small cell lung cancer (IDEAL-1). Proceedings AACR-NCI-EORTC International Conference, 2001 630A(abstract).

Brabender, J., Danenberg, KD., Metzger R, et al. Epidermal growth factor receptor and HER2-neu mRNA expression in non-small cell lung cancer Is correlated with survival. Clin Cancer Res. 2001 Jul;7(7):1850-5.

Cancer Facts and Figures. *In:* American Cancer Society, Atlanta, GA, 1997.
U.S. Department of Health and Human Services. The Health Benefits of Smoking Cessation: A Report of the Surgeon General. DHHS Publication Number 90-8416, 1990.

Feld, R., Rubinstein, L., and Thomas, P. A. Adjuvant chemotherapy with cyclophosphamide, doxorubicin, and cisplatin in patients with completely resected stage I non-small-cell lung cancer. The Lung Cancer Study Group. J Natl Cancer Inst, *85:* 299-306., 1993.

Fontana, R. S., Sanderson, D. R., Woolner, L. B., Taylor, W. F., Miller, W. E., Muhm, J. R., Bernatz, P. E., Payne, W. S., Pairolero, P. C., and Bergstralh, E. J. Screening for lung cancer. A critique of the Mayo Lung Project. Cancer, *67:* 1155-1164., 1991.

Fontana, R. S., Sanderson, D. R., Taylor, W. F., Woolner, L. B., Miller, W. E., Muhm, J. R., and Uhlenhopp, M. A. Early lung cancer detection: results of the initial (prevalence) radiologic and cytologic screening in the Mayo Clinic study. Am Rev Respir Dis, *130:* 561-565., 1984.

Glynn, T. J., Manley, M. W., Mills, S. L., and Shopland, D. R. The United States National Cancer Institute and the science of tobacco control research. Cancer Detect Prev, *17:* 507-512, 1993.

Halpern, M. T., Gillespie, B. W., and Warner, K. E. Patterns of absolute risk of lung cancer mortality in former smokers. J Natl Cancer Inst, *85:* 457-464., 1993.

Hennekens, C. H., Buring, J. E., Manson, J. E., Stampfer, M., Rosner, B., Cook, N. R., Belanger, C., LaMotte, F., Gaziano, J. M., Ridker, P. M., Willett, W., and Peto, R. Lack of effect of long-term supplementation with beta carotene on the incidence of malignant neoplasms and cardiovascular disease. N Engl J Med, *334:* 1145-1149., 1996.

Henschke, C. I., McCauley, D. I., Yankelevitz, D. F., Naidich, D. P., McGuinness, G., Miettinen, O. S., Libby, D. M., Pasmantier, M. W., Koizumi, J., Altorki, N. K., and Smith, J. P. Early Lung

Cancer Action Project: overall design and findings from baseline screening. Lancet, *354:* 99-105., 1999.

Herbst, RS, Bunn, P. Targeting the epidermal growth factor receptor in non-small cell lung cancer. Clin Cancer Res. 2003 Dec 1;9(16 Pt 1):5813-24. Review.

Holmes, E. C. and Gail, M. Surgical adjuvant therapy for stage II and stage III adenocarcinoma and large-cell undifferentiated carcinoma. J Clin Oncol, *4:* 710-715., 1986.

Hong, W. K. and Sporn, M. B. Recent advances in chemoprevention of cancer. Science, *278:* 1073-1077., 1997.

Hong WK, Lippman SM, Itri LM, Karp DD, Lee JS, Byers RM, Schantz SP, Kramer AM, Lotan R, Peters LJ, Dimery IW, Brown BW, Goepfert H. Prevention of second primary tumors with isotretinoin in squamous cell carcinoma of the head and neck. *N Engl J Med* 323:795-801, 1990.

Khuri, F. et al. Isotretinoin effects on head and neck cancer recurrence and second primary tumors *Proc Am Soc Clin Oncol* 2003:22. Abstract 359.

Kris M, Natale RB, Herbst RS, et al: A phase II trial of ZD1839 (Iressa) in advanced non-small cell lung cancer (NSCLC) patients who had failed platinum- and docetaxel-based regimens (IDEAL 2). Proc Am Soc Clin Oncol, 2002 1166 (abstract)

Le Chevalier, T. et al. Results of the Randomized International Adjuvant Lung Cancer Trial (IALT): cisplatin-based chemotherapy (CT) vs no CT in 1867 patients (pts) with resected non-small cell lung cancer (NSCLC). *Proc Am Soc Clin Oncol.* 2003:22. Abstract 6.

Lee, J. S., Lippman, S. M., Benner, S. E., Lee, J. J., Ro, J. Y., Lukeman, J. M., Morice, R. C., Peters, E. J., Pang, A. C., Fritsche, H. A., Jr., and et al. Randomized placebo-controlled trial of isotretinoin in chemoprevention of bronchial squamous metaplasia. J Clin Oncol, *12:* 937-945., 1994.

Landis, S. H., Murray, T., Bolden, S., and Wingo, P. A. Cancer statistics, 1999. CA Cancer J Clin, *49:* 8-31, 31., 1999.

Lubin, J. H. and Blot, W. J. Lung cancer and smoking cessation: patterns of risk. J Natl Cancer Inst, *85:* 422-423., 1993.

Niiranen, A., Niitamo-Korhonen, S., Kouri, M., Assendelft, A., Mattson, K., and Pyrhonen, S. Adjuvant chemotherapy after radical surgery for non-small-cell lung cancer: a randomized study. J Clin Oncol, *10:* 1927-1932., 1992.

Chemotherapy in non-small cell lung cancer: a meta-analysis using updated data on individual patients from 52 randomised clinical trials. Non-small Cell Lung Cancer Collaborative Group. Bmj, *311:* 899-909., 1995.

Ohta, M., Tsuchiya, R., Shimoyama, M., Sawamura, K., Mori, T., Miyazawa, N., Suemasu, K., Watanabe, Y., Tomita, M., and Terashima, M. Adjuvant chemotherapy for completely resected stage III non-small-cell lung cancer. Results of a randomized prospective study. The Japan Clinical Oncology Group. J Thorac Cardiovasc Surg, *106:* 703-708., 1993.

Omenn, G. S., Goodman, G. E., Thornquist, M. D., Balmes, J., Cullen, M. R., Glass, A., Keogh, J. P., Meyskens, F. L., Valanis, B., Williams, J. H., Barnhart, S., and Hammar, S. Effects of a combination of beta carotene and vitamin A on lung cancer and cardiovascular disease. N Engl J Med, *334:* 1150-1155., 1996.

Perez-Soler, R. Determinants of tumor response and survival with erlotinib in patients with non--small-cell lung cancer. J Clin Oncol. 2004 Aug 15;22(16):3238-47.

Postoperative radiotherapy in non-small-cell lung cancer: systematic review and meta-analysis of individual patient data from nine randomised controlled trials. PORT Meta-analysis Trialists Group. Lancet, *352:* 257-263., 1998.

Risch, H. A., Howe, G. R., Jain, M., Burch, J. D., Holowaty, E. J., and Miller, A. B. Are female smokers at higher risk for lung cancer than male smokers? A case-control analysis by histologic type. Am J Epidemiol, *138:* 281-293., 1993.

Rusch, V., Klimstra, D., Venkatraman, E., et al. Overexpression of the epidermal growth factor receptor and its ligand transforming growth factor alpha is frequent in resectable non-small cell lung cancer but does not predict tumor progression. Clin Cancer Res. 1997 Apr;3(4):515-22.

Shepherd, F et al. Erlotinib in previously treated non-small-cell lung cancer. N Engl J Med. 2005 Jul 14;353(2):123-32.

Sobue, T., Yamaguchi, N., Suzuki, T., Fujimoto, I., Matsuda, M., Doi, O., Mori, T., Furuse, K., Fukuoka, M., Yasumitsu, T., and et al. Lung cancer incidence rate for male ex-smokers according to age at cessation of smoking. Jpn J Cancer Res, *84:* 601-607., 1993.

Thatcher, N, Chang, A, et al. Gefitinib plus best supportive care in previously treated patients with refractory advanced non-small-cell lung cancer: results from a randomised, placebo-controlled, multicentre study (Iressa Survival Evaluation in Lung Cancer). Lancet. 2005 Oct 29-Nov 4;366(9496):1527-37.

Wada, H., Hitomi, S., and Teramatsu, T. Adjuvant chemotherapy after complete resection in non-small-cell lung cancer. West Japan Study Group for Lung Cancer Surgery. J Clin Oncol, *14:* 1048-1054., 1996.

Appendix - A.

Appendix Subtitle: Carcinoma In Situ Pathway

There is no standard approach to the management of CIS at present. Approaches have ranged from surgical resection to close followup. CIS may be found at the edge of an invasive carcinoma or may occur as a small isolated focus of a few epithelial cells that would be completely removed by a biopsy. The major safety issue related to CIS is that an invasive carcinoma may exist in an adjacent area that the biopsy did not sample. CIS is a rare lesion and it is not likely that enough CIS lesions will be found in the study for statistical analysis of response to the chemopreventive agents.

As there are a wide range of approaches to the treatment of CIS and as this is dependent on the bronchoscopic appearance of the lesion, we believe that the final decision regarding therapy, if any, should be left to the bronchoscopist and primary physician.

If a **CIS** lesion is found on a bronchoscopy at baseline, we would recommend:
1) Follow-up bronchoscopy within one month with repeat inspection of the area of the CIS and multiple biopsies to insure that an invasive carcinoma was not missed.
2) A CT scan with attention to the area of the CIS lesion.
If there is question of **invasive carcinoma** on either follow up bronchoscopy or CT, then the participant should be managed directly according to the preferences of the participant and primary physician.

If **no CIS** lesion is found on the repeat bronchoscopy, then the participant is to be continued on study.

If a **persistent CIS** lesion is found on repeat bronchoscopy, then the management should be directed as follows:

1) Repeat bronchoscopy in 1 month.
If CIS present, definitive treatment of lesion. Patient continues to remain on study.

Appendix - B.

Appendix Subtitle:

Protocol Checklist

This information is being collected for internal use and for M.D. Anderson (MDACC) to provide required summary reports to the National Cancer Institute (NCI) on clinical protocol development.

What is the type of study?

○ Phase I
● Phase II or Phase I/II
○ Phase III
○ Laboratory
○ Observational
○ Behavioral
○ Other

CCSG Program

Which Cancer Center Support Grant (CCSG) - NCI Core Grant Program does this protocol relate to?
Lung Cancer

Who initiated this protocol?

● MDACC Investigator
○ NCI/NIH
○ Industry

Role of MDACC Principal Investigator (Check all that apply)

☒ Major role in writing the protocol
☒ Assisted in design of the study
☒ Study Principal Investigator (including anticipated first-author)
☐ Study Co-Principal Investigator (including anticipated co-author)
☐ Participation only (justification for M.D. Anderson participation only is required)
☐ Other

Administrative Department

Thoracic / Head & Neck Medical Oncology

Preclinical Drug Development

Was preclinical work to develop the therapy or methodology being tested in this protocol performed at UTMDACC or by UTMDACC faculty?
○ Yes ● No

Protocol Design and Biostatistics

Did you participate in the design of this study?
● Yes -- Completely
○ Yes -- Partially
○ No -- Sponsor Designed
○ No prospective statistical design in this trial

Did an MDACC Biostatistician participate in the design of this study?
● Yes -- Completely
○ Yes -- Partially
○ No -- Sponsor provided biostatistical design
○ No prospective statistical design in this trial

Financial Support and Use of the CTRC

How is the proposed trial to be financially supported?

Type of Funding:
☐ NCI
☐ NIH (other than NCI)
☒ DOD
☐ Other peer reviewed funding (e.g. NSF or ACS etc.)
☒ Industry
☐ Departmental Funds
☐ Donor Funds
☐ Unfunded
☐ Not known at this time
☐ Other:

Source of Agent/Device:
☐ NCI
☐ NIH (other than NCI)
☐ DOD
☒ Industry
☐ Departmental Funds
☐ Commercially available
☐ Not known at this time
☐ Other:

List any device(s) which will be used (if applicable):

Use of the CTRC

Will the Clinical and Translational Research Center be used in this study?
○ Yes ● No

Laboratory Data

Will a UTMDACC investigator perform pharmacologic, molecular or other laboratory studies on patient specimens?
● Yes ○ No

What type of tissues will be used?
☒ Blood
☒ Tumor
☐ Normal

What is the type of study?
☐ Pharmacology and/or pharmacokinetics
☐ Molecular and/or pharmacodynamics
☒ Other

Please Describe:
Genetic, biomarker studies

Biological Markers

Are Biological Markers being evaluated in this trial?
● Yes ○ No

The marker(s) are being evaluated in (check all that apply):
☒ Blood
☒ Tumor Tissue
☐ Normal Tissue
☐ Urine
☐ Other

The marker(s) are being evaluated to predict (check all that apply):
☒ Response or resistance to treatment in the trial
☒ Time to disease progression
☒ Duration of overall survival
☐ Development of cancer in an individual without cancer and no previously defined heightened risk
☐ Development of cancer in an individual without cancer and a previously defined heightened risk (e.g. pre-cancerous condition family history genetic abnormality)
☐ Other:

Will the marker(s) being evaluated be used to modify treatment during the conduct of this trial?
○ Yes ● No

Additional Information

Enter any additional information here.

Appendix - C.

Appendix Subtitle:

ZUBROD'S PERFORMANCE STATUS SCALE

Grade	Scale
0	Fully active, able to carry on all pre-disease performance without restriction.
1	Ambulatory, capable of light or sedentary work. Restricted in physically strenuous activity.
2	Ambulatory, capable of all self-care, but not of work activities; up and about more than 50% of waking hours.
3	Capable of only limited self-care; confined to bed or chair more than 50% of waking hours.
4	Completely disabled. Cannot carry on any self-care. Totally confined to bed or chair.

Appendix - D.

Appendix Subtitle: Histology Grading System

SCORE	HISTOLOGY
1	Normal
2	Reserve cell hyperplasia
3	Metaplasia
4	Mild dysplasia
5	Moderate dysplasia
6	Severe Dysplasia
7	Carcinoma in situ
8	Invasive cancer

Scoring System for Response

1) The average score of all biopsies (decrease by 1)

2) The percentage of biopsies with moderate dysplasia or worse (10% decrease)

3) The worst score (decrease by 1)

Response: **Improvement in 2 of 3 criteria**

No change: **No change in 2 of 3 criteria**

Improvement in 2 of 3 criteria with 1 worse

Progression: **Worsening in 2 of 3 criteria**

Appendix - E.

Appendix Subtitle: Study Activities

Study Activities for Patients Assigned to Erlotinib Treatment Arm

Procedure	Baseline[6]	3 mos	6 mos	12 mos	18 mos	24 mos	30 mos	36 mos	Long-term F/U
Informed consent	X								
Physical exam (by physician or nurse)	X	X	X	X		X		X	Every 12 mos
Nursing exam only[5]					X		X		Every 6 mos[3]
Medical history	X	X	X	X	X	X	X	X	Every 6 mos
Cardiac risk assessment	X								
Cardiac symptom assessment		X	X	X					
Bronchoscopy	X			X		X[7]		X[7]	
Sputum and saliva sample	X			X		X[7]		X[7]	
Buccal brush	X			X		X[7]		X[7]	
Hematology[1]	X	X	X	X	X	X	X	X	Every 12 mos
Serum chemistry, electrolytes[2]	X	X	X	X	X	X	X	X	Every 12 mos
Lipid profile	X								
PT	X			X		X		X	
Pregnancy test[3]	X	Repeat if pregnancy is suspected.							
Chest x-ray	X		X	X	X	X	X	X	
CT scan of chest	X		X	X	X	X	X	X	
Laryngoscopy[4]	X			X					
Biomarkers (serum)	X	X	X	X	X	X	X	X	Every 12 mos

[1] CBC with differential, platelets
[2] BUN, creatinine, total bilirubin, SGPT, alkaline phosphatase, albumin
[3] Women of child-bearing potential only. Serum or urine. Must be done within 72 hrs. prior to enrollment. Should be repeated any time pregnancy is suspected.
[4] Patients with prior head and neck cancer only
[5] Nursing only visit will occur when patient is not scheduled for a physician visit.
[6] Unless otherwise noted, labs, physical exams, imaging studies, and the laryngoscopy are to be performed within 4 weeks of beginning participation in this study.
[7] Optional

Study Activities for Patients Assigned to No Treatment Arm

Procedure	Baseline[6]	3 mos	6 mos	9 mos	12 mos	18 mos	24 mos	30 mos	36 mos	Long-term F/U
Informed consent	X									
Physical exam (by physician or nurse)	X		X		X		X		X	Every 12 mos
Nursing exam only						X		X		Every 6 mos[5]
Medical history	X		X		X	X	X	X	X	Every 6 mos
Cardiac risk assessment	X									
Bronchoscopy	X				X		X[7]		X[7]	
Sputum and saliva sample	X				X		X[7]		X[7]	
Buccal brush	X				X		X[7]		X[7]	
Hematology[1]	X		X		X	X	X	X	X	Every 12 mos
Serum chemistry, electrolytes[2]	X		X		X	X	X	X	X	Every 12 mos
Lipid profile	X									
PT	X				X		X		X	
Pregnancy test[3]	X									
Chest x-ray	X		X		X	X	X	X	X	
CT scan of chest	X		X		X	X	X	X	X	
Laryngoscopy[4]	X				X					
Biomarkers (serum)	X		X		X	X	X	X	X	Every 12 mos
Nursing Follow-up via phone		X		X						

[1] CBC with differential, platelets
[2] BUN, creatinine, total bilirubin, SGPT, alkaline phosphatase, albumin
[3] Women of child-bearing potential only. Serum or urine. Must be done within 72 hrs. prior to enrollment. Should be repeated any time pregnancy is suspected.
[4] Patients with prior head and neck cancer only
[5] Nursing only visit will occur when patient is not scheduled for a physician visit.
[6] Unless otherwise noted, labs, physical exams, imaging studies, and the laryngoscopy are to be performed within 4 weeks of beginning participation in this study.
[7] Optional

Appendix - F.

Appendix Subtitle: CYP3A4 Index of interactions

CYP3A4 substrates: potential drug-drug interaction

Alprazolam
buspirone
carbamazepine
cyclosporine
erythromycin
felodipine
HIV protease inhibitors
lovastatin *(not pravastatin)*
nifedipine
quinidine
simvastatin
terfenadine
astemizole
calcium channel blockers
cisapride
doxorubicin
etoposide
fentanyl
ifosphamide
midazolam
pimozide
quinine
tacrolimus
triazolam

CYP3A4 inhibitors: can increase concentration of co-administered drug => potentially leading to toxicities

cimetidine
danazol
fluconazole *(large doses)*
HIV protease inhibitors
ketoconazole
miconazole
omeprazole
ritonavir
cyclosporine
diltiazem
grapefruit juice
itraconazole
macrolides (*not azithromycin)*
nefazadone
quinidine
verapamil

CYP3A4 inducers: can decrease concentration of co-administered drug => potentially decrease efficacy

carbamazepine
rifabutin
rifampin
ritonavir

Appendix - G.

Appendix Subtitle:

IRB Approval Date: 12/17/2003

SUBMITTING INTERNAL AND EXTERNAL ADVERSE EVENTS TO THE MDACC INSTITUTIONAL REVIEW BOARD

45 CFR § 46.109(e) An IRB shall conduct continuing review of research covered by this policy at intervals appropriate to the degree of risk, but not less than once per year, and shall have authority to observe or have a third party observe the consent process and the research.

45 CFR § 46.111(6) When appropriate, the research plan makes adequate provision for monitoring the data collected to ensure the safety of subjects.

21 CFR § 56.108(a) Follow written procedures: (1) For conducting its initial and continuing review of research and for reporting its findings and actions to the investigator and the institution; (2) for determining which projects require review more often than annually and which projects need verification from sources other than the investigator that no material changes have occurred since previous IRB review; (3) for ensuring prompt reporting to the IRB of changes in research activity; and (4) for ensuring that changes in approved research, during the period for which IRB approval has already been given, may not be initiated without IRB review and approval except where necessary to eliminate apparent immediate hazards to the human subjects. **(b)** Follow written procedures for ensuring prompt reporting to the IRB, appropriate institutional officials, and the Food and Drug Administration of: (1) Any unanticipated problems involving risks to human subjects or others.

21 CFR § 56.111(6) Where appropriate, the research plan makes adequate provision for monitoring the data collected to ensure the safety of subjects.

21 CFR § 312.32

Serious Adverse Experience (SAE) –Any adverse drug experience occurring at any dose that results in any of the following outcomes:

- Death
- A life-threatening adverse drug experience – any adverse experience that places the patient, in the view of the initial reporter, at immediate risk of death from the adverse experience as it occurred. It does not include an adverse experience that, had it occurred in a more severe form, might have caused death.

- Inpatient hospitalization or prolongation of existing hospitalization
- A persistent or significant disability/incapacity – a substantial disruption of a person's ability to conduct normal life functions.
- A congenital anomaly/birth defect.

Important medical events that may not result in death, be life-threatening, or require hospitalization may be considered a serious adverse drug experience when, based upon appropriate medical judgment, they may jeopardize the patient or subject and may require medical or surgical intervention to prevent one of the outcomes listed in this definition. Examples of such medical events include allergic bronchospasm requiring intensive treatment in an emergency room or at home, blood dyscrasias or convulsions that do not result in inpatient hospitalization, or the development of drug dependency or drug abuse.

Unexpected Adverse Drug Experience - Any adverse drug experience, the specificity or severity of which is not consistent with the current investigator brochure; or, if an investigator brochure is not required or available, the specificity or severity of which is not consistent with the risk information described in the general investigational plan or elsewhere in the current application, as amended. Unexpected, as used in this definition, refers to an adverse drug experience that has not been previously observed (e.g., included in the investigator brochure) rather than from the perspective of such experience not being anticipated from the pharmacological properties of the pharmaceutical product.

MDA Policy: The IRB requires that Principal Investigators (PI) promptly report adverse events. The PI is responsible for determining attribution for both internal as well as external adverse events. The IRB will review protocol safety information in the informed consent document and request modifications on a continuous basis throughout the year during the review of adverse events. This policy should be utilized for both commercial and investigational drugs.

- All clinical protocols should include a list of the expected and anticipated events or hospitalizations relating to the study regimen. If an expected or anticipated event is documented in the protocol, then it does not have to be reported as an SAE. (Example: Expected Grade 4 myelosuppression needs only to be reported as part of the study results)
- All events falling under the definition of serious adverse event that are not listed in the protocol as being expected or anticipated, and occurring within 30 days following the last treatment date, must be reported to the sponsor within the specified time frame stated in the protocol.
- All deaths with possible, probable or definite attribution to the study drug, device, or intervention must have a written report submitted to the Institutional Review Board (IRB) via the Office of Protocol Research (OPR) within one working day (24 hours) of knowledge of the event.

- All serious adverse events other than that stated above must have a written report submitted to the Institutional Review Board (IRB) via OPR within 5 working days of knowledge of the event.
- If necessary, the sponsor is then required to notify the Food and Drug Administration (FDA) within 7 calendar days.
- All unexpected adverse experiences that are classified as Grade 4 must be reported by following the guidelines listed above.
- Known reactions classified as Grades 1-3 do not need to be reported. However, these toxicities should be submitted as part of the study results.

Procedure:

- Multiple events may be reported on one form as long as all events occurred in one patient around a particular time.
- The PI is responsible for determining attribution for both internal as well as external adverse events.
- The PI is responsible for completing the PI section on both the internal and external events form. The sections that must be completed by the PI are clearly indicated on both the internal and external adverse events forms. The PI may delegate completion of the remaining information on the form to a member of the research team, but the PI may not abdicate the supervision. The PI is still responsible for all information submitted on the forms.
- Follow-up reports must be submitted in the absence of the initial report.
- Checking the box marked "follow-up report" and signing the form is not acceptable if material information related to that event is included in the documents submitted to the PI by the sponsor or other entity.
- The **risks section of the informed consent document** must be submitted with the internal and external adverse event form. OPR will return the form if it is submitted without the risks section of the informed consent document.

Serious Adverse Event Reporting/Internal:

The attached Internal Adverse Event Reporting form should be used for submissions to OPR. If the study sponsor requires a protocol specific SAE form to be completed, then the attached Addendum must be completed for IRB submission.

External Adverse Event Reporting/Safety Reports:

All external adverse events/safety reports received from the sponsor should be submitted to the IRB through OPR. The attached External Adverse Event Summary should be utilized as the coversheet for the submission.

Approved by UTMDACC IRB#3 on December 17, 2003

Appendix - H.

Appendix Subtitle:

Common Terminology Criteria for Adverse Events v3.0 (CTCAE)

Publish Date: June 10, 2003

Click On Link ➤ 🖹 ◄ To access Document

Appendix - I.

Appendix Subtitle:

Prioritization List

02 Prioritization List for IRB Submission Only (Head & Neck) 11.0

15 Prioritization List for IRB Submission Only November 1, :

Head & Neck Protocol Prioritization List
As of November 1, 2006

CURRENT RESEARCH STUDIES FOR HEAD AND NECK MEDICAL ONCOLOGY

The University of Texas M.D. Anderson Cancer Center □ 1515 Holcombe □ Houston, TX 77030
Thoracic/Head and Neck Medical Oncology □ Box 432 □ 713-792-6363

Protocol No.	Protocol Title/ Sponsor	Principal Investigator (Research Nurse)	Patient Accrual Current/ Projected	Recent Accrual	Date Activated	Priority	Comments
	CHEMOPREVENTION						
ID00-193 (p53 trial)	Clinical Protocol for Wildtype p53 Gene Induction in Premalignancies of Squamous Epithelium of the Oral Cavity and Oral Pharynx via An Adenoviral Vector, INGN 201 (Ad5CMV-p53)(**SPORE**)	Clayman (Shirley Taylor)	4/20 MDACC 4/51 National	1-Oct-03 1-Apr-04 1-Feb-05 1-Oct-05	06/25/03	1	U. of Chicago only other site- not yet open due to regulatory issues.
ID01-155	Phase II Randomized Double-Blind, Placebo Controlled Dose Ranging Pilot of GTE for Chemoprevention of OPLs in High Risk Pts	Papadimitrakopoulou (Nancy Shinn)	32/36 MDACC	2-Jan-06 1-Apr-06 1-May-06	10/14/02	2	
2003-0824	Erlotinib Prevention of Oral Cancer (EPOC)	Papadimitrakopoulou (Jeanne Riddle)	0/90 MDACC 0/160 National			1	
2005-0485	Phase IIA Trial of Rosiglitazone (AVANDIA) for Oral Leukoplakia	Papadimitrakopoulou (Nancy Shinn)	0/6 MDACC x/25 National		07/12/06	2	
	LOCALLY ADVANCED DISEASE PREVIOUSLY UNTREATED						
2003-1049	Phase I evaluation of Erlotinib and Docetaxel with Concomitant Boost radiation for Locoregionally Advanced Squamous Cell Carcinoma of the Head and Neck	Glisson (Kathy Gillaspy)	5/27 MDACC	1-Apr-05 1-Jun-05 1-Aug-05 2-Jan-06	04/12/05	1	
RTOG0522	A Randomized Phase III Trial of Concurrent Accelerated Radiation and Cisplatin Versus Concurrent Accelerated Radiation, Cisplatin, and Cetuximab (C225) [Followed by Surgery for Selected Patients] for Stage III and IV Head and Neck Carcinomas	Rosenthal (Patricia Grossman/ Kathy Gillaspy)	3/75 MDACC 24/700 National	**3-Jun-06**	04/19/06	2	
SWOG S0011	Phase II Trial of Surgery with Perioperative INGN 201 (Ad5CMV-p53) Gene Therapy Followed by Chemoradiotherapy for Advanced, Resectable Squamous Cell Carcinoma of the Oral Cavity and Oropharynx	Hanna/Sabichi (Arsenio J. Sarabia)	0/12 MDACC x /60 National		03/07/05	3	Study closing due to poor accrual rate.
	ADJUVANT THERAPY						
2003-0424	A Phase IIb Vanguard Study Characterizing the Occurrence of Recurrent or Second Primary Tumors in Patients with a Prior History of a Definitively Treated Stage I/II **Head and Neck** or Non-Small Cell Lung Cancer who are Current or Former Smokers	Hong/Kim (Cindy Duron)	29/250 MDACC 30/350 National	1-Jan-06 1-Feb-06 2-Mar-06 3-Apr-06 **3-Jun-06**	8/25/04	1	

Head & Neck Protocol Prioritization List
As of November 1, 2006

Protocol No.	Protocol Title Sponsor	Principal Investigator (Research Nurse)	Patient Accrual Current/ Projected	Recent Accrual	Date Activated	Priority	Comments
2004-0104	Celecoxib as Adjuvant Biological Therapy in Patients with Early Stage Head and Neck and Lung Cancer **(Note: All patients in 2004-0104 must also be enrolled in 2003-0424.)**	Kim (Cindy Duron)	1/50 MDACC 1/70 National	1-Mar-06	09/29/05	1	
2006-0946	Erlotinib as Adjuvant Biologic Therapy in Patients w/Early Stage Head & Neck and Lung Cancer **(Note: All patients in 2004-0104 must also be enrolled in 2003-0424.)**	Kim (Cecilia Duron)	/50 MDACC /70 National			1	

Head & Neck Protocol Prioritization List
As of November 1, 2006

Protocol No.	Protocol Title / Sponsor	Principal Investigator (Research Nurse)	Patient Accrual Current/ Projected	Recent Accrual	Date Activated	Priority	Comments
	POST OP-HIGH RISK						
RTOG 0234	(Post OP High Risk) A PH II Randomized Trial of surgery followed by Chemoradiotherapy Plus C225 (Cetuximab) for Advanced Squamous Cell Carcinoma of the Head and Neck	Myers/Kies (Mary Jo Reyes Kathy Gillaspy)	12/100 MDACC 176/230 Nat'l	1-Feb-06 1-Mar-06 2-Apr-06 2-May-06 1-Jun-06	09/27/04	1	
	LOCALLY ADVANCED DISEASE PREVIOUSLY UNTREATED – Nasopharynx Only						
	RECURRENT/METASTATIC DISEASE – Chemotherapy						
2006-0950	A Phase II Trial of Cetuximab and Bevacizumab in Patients with Recurrent or Metastatic Head and Neck Cancer	Kies (Anne Meschwitz)	10/48			1	
	Front Line For Recurrence						
2004-0844	An Exploratory, Randomised, Double-Blind Study to Assess the Effects of AZD2171 and Gefitinib Alone or In Combination on Tumours and Biomarkers in Patients With Previously Untreated Non-Small Cell Lung Cancer (NSCLC) Evaluated Prior to Standard Therapy, or Patients with Metastatic or Recurrent Head and Neck Cancer (HNC)	Heymach (Justina Price)	0/30 MDACC 6/60 Internat'l	1-Mar-06 1-May-06	07/27/05	1	MDACC and 1 site in Spain. (1 Screen failure, 1 failure to complete study)
ID02-668	A Phase II Study of OSI-774 in Combination with Cisplatin and Docetaxel in Metastatic or Recurrent Head and Neck Squamous Cell Cancer	Kim/Tsao (Barbara Burke)	45/50 MDACC	2-Jan-06 1-Feb-06 2-Mar-06 1-Apr-06 1-May-06 2-Jun-06	01/28/04	2	
	Prior Treatment For Recurrence						

Head & Neck Protocol Prioritization List
As of November 1, 2006

2003-1027	Phase Ib/II Study of ABT-510 (Thrombospondin) in Patients with Advanced Head and Neck Cancer	Kim (Jeanne Riddle)	2/37 MDACC	2-Jun-05	04/21/05	1	
2005-0082	A Phase I Dose Escalation Study of Pemetrexed in Patients with Advanced Head and Neck Squamous Cell Cancer	Kim (Raquel Ayuste)	18/50 MDACC	1-Jan-06 2-Feb-06 3-Mar-06 2-May-06 2-Jun-06	09/12/05	2	1st cohort complete 2nd cohort begun 7.11.06
ID00-006 (T301)	A Phase III, Multi-Center, Open-Label, Randomized Study to Compare the Overall Survival and Safety of Bi-weekly Intratumoral Administration of RPR/INGN 201 Versus Weekly Methotrexate in 240 Patients with Refractory Squamous Cell Carcinoma of the Head and Neck	Clayman/Kies (Jeanne Riddle)	16/48 MDACC x /240 National	1-Apr-03 1-Jun-03 1-Jan-04 1-Aug-04	08/31/01	3	Study open to collect data. Plans to close in August.

Protocol No.	Protocol Title Sponsor	Principal Investigator (Research Nurse)	Patient Accrual Current/ Projected	Recent Accrual	Date Activated	Priority	Comments
	SALIVARY GLAND CANCER						
2004-0089	Phase II Study of ZD1839 (IRESSA®), Epidermal Growth Factor (EGFR) Tyrosine Kinase Inhibitor in Patients with Advanced, Recurrent or Metastatic Salivary Gland Cancer" (IRUSIRES0198)	Blumenschein (Barbara Burke)	35/80 MDACC	1-May-05 2-Oct-05 1-Feb-06 2-Apr-06	05/20/04	1	
	SKIN CANCER						
ID02-282	A phase II study of ZD1839 (IRESSA), epidermal growth factor receptor (EGFR) tyrosine kinase inhibitor, in treatment of recurrent or metastatic squamous cell carcinoma of the skin	Kim/Glisson (Raquel Ayuste)	23/40 MDACC	1-Feb-06 2-Mar-06 1-Apr-06 1-May-06	05/05/04	1	
2004-0204	A phase II Study of ZD1839 and Radiation in Patients with Squamous Cell Carcinoma of the Skin	Weber (Mary Jo Reyes)	7/35 MDACC 8/63 National	2-Aug-05 1-Sep-05 1-Nov-05 2-Mar-06	04/08/05	1	
	THYROID						
2003-0308	Phase II Study of Decitabine in Patients with Metastatic Papillary Thyroid Cancer or Follicular Thyroid Cancer Unresponsive to Radioiodine (NCI)	Sherman (Mary Jean-Klein/ Anne Meschwitz)	4/10 MDACC 6 /37 National	3-Aug-04 1-Jun-05 1-July-05 1-Mar-06	05/03/04	1	
2004-0059	Phase II Study of Bortezomib in Metastatic Papillary Thyroid Carcinoma or Follicular Thyroid Carcinoma	Sherman/Glisson (Mary Jean Klein/ Anne Meschwitz)	4/12 MDACC 11/37 National	1-Jan-05 1-Jun-05 2-May-06	12/22/04	2	
2004-0606	Phase II study of the Anti-Angiogenesis Agent AG-013736 in Patients with Metastatic Thyroid Cancer who are Refractory to or not Suitable Candidates for 131 I Treatment	Kies (Jeanne Riddle)	5/12 MDACC 60/60 National	4-Mar-06 1-May-06	02/10/06		Stage I CNPE, waiting for responders.

Head & Neck Protocol Prioritization List
As of November 1, 2006

Protocol No.	Protocol Title Sponsor	Principal Investigator (Research Nurse)	Patient Accrual Current/ Projected	Recent Accrual	Date Activated	Priority	Comments
	NEW STUDIES – Not yet active (↓)						
2006-0213	A Phase II Trial of Cetuximab and Bevacizumab in Patients With Recurrent or Metastatic Head and Neck Cancer	Kies (TBA)	0/x MDACC x/48 National				**Waiting to submit to CRC pending IRB approval from Pittsburg site.**
2006-0492	An Open Label, Multi-Center, Phase I Study To Assess The Maximum Tolerated Dose of ZD6474 (ZACTIMA) Given Concomitantly with Radiation Therapy or Concomitantly with Weekly Cisplatin Chemotherapy and Radiation Therapy in Patients with Previously Untreated, Unresected, Stage II-IV Head and Neck Squamous Cell Carcinoma	Papadimitrakopoulou (TBA)	0/16 MDACC x/48 National				**Submitted to CRC 6-7-06.**
2006-0362	Phase II study of Imatinib Mesylate and Docetaxel in Patients with Metastatic or Recurrent Head and Neck Squamous Cell Cancer.	Anne Tsao (TBA)	0/58 MDACC				**IRB Meeting on July 19, 2006**

Concepts in Development:

Dr. Kim—Carbo Alimta/ Front line recurrence

Dr. Kim—Pre-Op Tarceva/ Prior treatment for recurrence (or locally advanced disease previously untreated)

Dr.Lu—Abraxane

Dr Blumenschein—Carbo/Sorafinib / Frontline or first recurrence after definitive treatment

Dr Papa-ZD6474 + XRT with or without XRT/ locally advance unresectable / SPORE

Dr Papa-ZD6474 + Taxo/Carbo

Jody Garey PharmD –Aloxi (Anti-emetic)

Dr. Rosenthal – RTOG study - IMRT + Cisplatin with or without KGF

Current Thoracic Center Research MDACC PROTOCOL PRIORITY LIST

Priority	I. Locally Advanced Resectable NSCLC	Number	Phase	Title	Activated	Accrual	Recent Accruals	Principal Investigator Study Manager Regulatory Coordinator	Sponsor	Comments
1	A. Superior Sulcus Tumors	ID92-038	PH II	Phase II Study of Combined Modality Treatment for Resectable Non-Small Cell Superior Sulcus Tumors (SST)	10.11.93	MDACC 37/47	1-Mar-04 1-Aug-04 1-Sept-04 1-Jan-05	Ritsuko Komaki, MD /Cheryl Smith, RN& Rainell Schaerer	None	
	B.Stage IIIA NSCLC	RTOG-0412 /SWOG S0332	PH III	Phase III Randomized Trial of Preoperative Chemotherapy versus Preoperative Concurrent Chemotherapy and Thoracic Radiotherapy followed by surgical Resection and consolidation Chemotherapy in Favorable Prognosis Patients with Stage IIIA (N2) Non-Small cell Lung Cancer	04/25/06	MDACC 1/20 Nat'l 7/574	1-May-06	Vaporciyan, Ara,M.D./ Rhodette Francisco RN	RTOG	
	C. Stage I,Ib,II & Selected IIIA*									
1	D. Adjuvant Treatment for Resected NSCLC	2003-0424		Vangaurd Trial and Bioadjuvant Trial	08.25.04	MDACC 31/250 Nat'l x/350	3-April-06 3-Jun-06 1-Aug-06	Waun Ki Hong, MD/Edward Kim, MD/Cindy Duron, RN	US DOD	
2		2004-0104		(Celecoxib as Adjuvant Biologic Therapy in Patients with Early Stage Head and Neck and Lung Cancer	09.29.05	MDACC 1/50 Nat'l x/70	1-Mar-06	Waun Ki Hong, MD/ Cindy Duron RN/ Mellanie Price	US DOD	
		2006-0946		Erlotinib as Adjuvant Biologic Therapy in Patients with Early Stage Head and Neck and Lung Cancer		MDACC 1/50 Nat'l x/70				
3		2004-0221		A Pilot Study of Adjuvant Chemotherapy with Docetaxel, Cisplatin Followed by the EGFR Inhibitor Erlotinib (Tarceva) in Patients with Stage I, II and III Non-Small Cell Lung Cancer Following Definitive Surgical Resection	10.05.05	MDACC 1/40	1-Dec-05	Edward Kim, MD/ Richard Gonzales, RN/ Mellanie Price	MDACC/Aventis /Genentech	
	* T3N1 patients are candidates for both b and c protocols. The small overlap group can be triaged at the discretion of each individual physician									

Priority	II. Locally Advanced, Unresectable NSCLC	Number	Phase	Title	Activated	Accrual	Recent Accruals	Principal Investigator Study Manager Regulatory Coordinator	Sponsor	Comments
1	A. Good Performance Status	2003-0352	PH I	A Phase I Study of Concurrent CPT-11/Cisplatin and Celecoxib with Radiation Therapy for Patients with Unresectable Non-Small Cell Lung Cancer (NSCLC)	09.24.03	MDACC 13/40	2-Aug-04 1-Sept-04 2-Oct-04 1-Dec-04	Ritsuko Komaki, MD/Rainell Schaerer, RN and Cheryl Smith, RN	NCCN	
1	A1. PCI	RTOG 02-14	PH III	A Phase III Comparison of Prophylactic Cranial Irradiation Vs. Observation In Patients With Locally Advanced Non-Small Lung	04.23.03	MDACC 3/40	1-June 03 1-Jan-04 1-Feb-05	Thomas Guerrero, MD, PhD//Cheryl Smith RN	RTOG	
	B. Poor Performance Status									

Current Thoracic Center Research MDACC PROTOCOL PRIORITY LIST

Priority	IIIB Recurrent or Metastatic NSCLC No Prior Chemotherapy	Number		Title	Activated	Accrual	Recent Accruals	Principal Investigator / Study Manager / Regulatory Coordinator	Sponsor	Comments
1	Alternate with 2003-0635	2004-0844		An Exploratory, Randomised, Double-Blind Study to Assess the Effects of AZD2171 and Gefitinib Alone or In Combination on Tumours and Biomarkers in Patients With Previously Untreated Non-Small Cell Lung Cancer (NSCLC) Evaluated Prior to Standard Therapy, or Patients with Metastatic or Recurrent Head and Neck Cancer (HNC)	07.27.05	MDACC 1/30 Natl x/60	1-Mar-06 1-May-06 1-Aug-06	John Heymach, MD/ Rainell Schaerer, RN/ Alisha Thierry	Astrazeneca	
1	Alternate with 2004-0844	2003-0635	PH II	A Phase II Study of ZD6474 Alone and With Chemotherapy in Advanced NSCLC	1.19.06	MDACC 3/120	2-Mar-06 1-Apr-06	Vali Papadimitrakopoulou, MD/ Justina Price RN/ Mellanie Price	MDACC/NCI Grant	
2		2004-0690	PH I/II	An Open-label, Dose-Finding Study to Evaluate the Safety and Pharmacokinetics of AMG 706 with Carboplatin/Paclitaxel, AMG 705 with Panitumumab and AMG 706 with Panitumumab and Carboplatin/Paclitaxel in the treatment of subjects with advanced non-small cell lung cancer	01.10.05	MDACC 36/40 Natl x/85	4-Jan-06 2-Feb-06 1-Mar-06 2-April-06	George Blumenschein, MD/Christine Alden, RN and Michelle Langham RN /Brenda Coldman	Amgen Inc. & Immunex Corp.	Allows for brain metastases
3		2004-0664	PH Ib/II	A Phase 1b Dose Escalation/Phase 2 randomized, Non-Comparative Multiple Center, Open label study of CP-751, 871 in Combination with Paclitaxel and Carboplatin alone as First Line Treatment for Advanced NSCLC	09.13.05	MDACC 24/52 Natl x/192	3-Mar-06 2-Apr-06 3-May-06 4-Jun-06 3-Jul-06 1-Aug-06	Daniel Karp, MD/ Mary Rollins, RN/ Brenda Coldman	Pfizer Inc.	
4		2005-0818	PH I	Phase I Dose-Escalating, Open-label, Non-Placebo Controlled Study of BAY 43-9006 (sorafenib) in combination with Carboplatin, Paclitaxel and Bevacizumab in Previously Untreated Patients with Stage IIIB (with malignant pleural effusions) or Stage IV Non-Small Cell Lung Cancer (NSCLC)	5.9.06	MDACC 0/30 Natl x/60		George Blumenschein, MD/ Hanna Brewer/ Alisha Thierry	Bayer Healthcare Pharmaceuticals	
5		2005-0224	PH II	A Phase II Evaluation of Bevacizumab in Combination with Docetaxel and Carboplatin as Chemotherapy in Patients with Metastatic Non-Small Cell Lung Cancer.	12.5.05	MDACC 18/50	2-Apr-06 4-May-06 3-Jun-06 1-Jul-06 2-Aug-06	Edward S. Kim, MD/ Maria Cole RN / Mellanie Price	MDACC/ Genentech Inc	
6		2005-1009	PH II	A Phase 2 Randomized Study of Tarceva® (Erlotinib) as a Single Agent or Intercalated with Combination Chemotherapy in Patients with Newly Diagnosed Advanced Non-small Cell Lung Cancer who have Tumors with EGFR Protein Overexpression and/or Increased EGFR Gene Copy Numbers.	3.29.06	MDACC 2/10 Natl 31/140	1-April-06 1-May-06 1-Jun-06 3-Jul-06 1-Aug-06	Roy Herbst, MD,PhD/ Maria Cole, RN/ James Luca	OSI Pharmeceuticals	
7		SWOGS0536	Phase II	A Phase II Trial of Combination Carboplatin, Paclitaxel, Cetuximab and Bevacizumab (NSC-704865) Followed by Cetuximab and Bevacizumab in Patients with Advanced Non0Small Cell Lung cancer		MDACC x/20 Natl /90		Edward Kim	SWOG/NCI	
		2006-0894	Phase I	A two-step phase 1 study investigating the combination of RAD001 with carboplatin, paclitaxel and bevacizumab in non-small-cell lung cancer (NSCLC) patients not treated previously with systemic therapy		MDACC x/06 Natl x/30		Vali Papadimitrakopoulou, MD/ RN/ James Luca	Novartis	

Current Thoracic Center Research MDACC PROTOCOL PRIORITY LIST

Priority	IV. Recurrent or Metastatic NSCLC With One Prior Chemotherapy Regimen	Number	Title	Activated	Accrual	Recent Accruals	Principal Investigator/ Study Manager/ Regulatory Coordinator	Sponsor	Comments
1		2004-0690	PH I	An Open-label, Dose-Finding Study to Evaluate the Safety and Pharmacokinetics of AMG 706 with Carboplatin/Paclitaxel, AMG 706 with Panitumumab and AMG 706 with Panitumumab and Carboplatin/Paclitaxel in the treatment of subjects with advanced non-small cell lung cancer	01.10.05	MDACC 36/40 Nat'l x/85	4-Jan-06 2-Feb-06 1-Mar-06 2-April-06	G. Blumenschein, MD/ Michelle Langham, RN/ Brenda Coldman	Amgen Inc. & Immunex Corp.	Allows for brain metastases
2		2004-0726	PH II	Phase II Study of Imatinib Mesylate and Docetaxel in Pretreated Patients with Metastatic NSCLC	01.18.05	MDACC 21/50	1-Dec-05 1-Feb-06 1-April-06 1-May-06	Anne Tsao, MD/ Cindy Welch, RN/ Mellanie Price	Novartis	Allows for brain metastases
3		2005-0517	PH III	A phase III, randomized, placebo-controlled clinical trial to evaluate the efficacy of Bevacizumab in combination with Tarceva (Erlotinib) compared with Tarceva alone for treatment of advanced non-small cell lung cancer (NSCLC) after failure of standard first-	2.20.06	MDACC 2/15 Nat'l 234/650	1-Mar-06 1-May-06	Roy Herbst, MD/ Hannah Brewer, RN / Alisha Thierry	Genentech Inc.	
4		2004-0730	PH III	Randomized Phase III Study of Docetaxel or Pemetrexed with or without Cetuximab in Patients with Recurrent or Progressive Non-Small Cell Lung Cancer after Platinum-Based Therapy	03.10.05	MDACC 1/25 Nat'l >200/800	1-Jan-06	Edward Kim, MD/ Rainell Schaerer, RN/ Alisha Thierry	ImClone Systems, Inc	
5		2005-0796	PH II	Randomized, Double-Blind, Phase II study of Erlotinib with or without SU011248 in the treatment of Metastatic Non-Small Cell Lung Cancer	4.17.06	MDACC 6/12 Nat'l x/136	2-May-06 2-Jun-06 2-Jul-06	G. Blumenschein, MD/ Teresa Eddings, RN/ Brenda Coldman	Pfizer Inc.	
5a		2006-0951	N/A	A TREATMENT PROTOCOL FOR PATIENTS CONTINUING FROM A PRIOR SU011248 PROTOCOL	N/A	MDACC NA	N/A	G. Blumenschein, MD/ Teresa Eddings, RN/ Brenda Coldman	Pfizer Inc.	
6		2005-0238	PH II	An Open-Label, Non-Randomized, Multicenter, Three Stage, Phase II Study of S-1 as 2nd Line Therapy for Patients with Advanced Non-Small Cell Lung Cancer (StageIIIB/Stage IV)	07.15.05	MDACC 5/25 Nat'l x/95	1-Oct-05 2-Mar-06 1-Apr-06 1-Jun-06	Roy S. Herbst, MD, PhD/ Teresa Eddings ,RN/ James Luca	Taiho Pharma USA, Inc.	
7		2006-0134	PH III	A Phase III, Randomized, Double-Blinded, Multi-Center Study to Assess the Efficacy of Docetaxel (Taxotere) in Combination with ZD6474 (ZACTIMA) versus Docetaxel in Combination with Placebo in Patients with Locally Advanced or Metastatic (Stage IIIb – IV) Non-Small Cell Lung Cancer (NSCLC) after Failure of 1st Line Anti-Cancer Therapy	5.30.06	MDACC 1/16 Int'l 22/1200	1-Jul-06	Roy Herbst, MD, PhD/ Maria Cole, RN/ Alisha Thierry	Astrazeneca	
8		SWOGN0426	PH II	A Phase II Study of Pemetrexed Disodium (Alimta) Bevacizumab in Patients with Stage IIIB Pleural Effusion or Stage IV Non-Small Cell Lung Cancer (Second-Line Treatment)		MDACC 0/12 Nat'l x/42		Ralph Zinner, MD/ TBA, RN/ Faye Martin	NCCTG/SWOG	

Current Thoracic Center Research MDACC PROTOCOL PRIORITY LIST

Priority	V. POOR PERFORMANCE	Number	Title	Activated	Accrual	Recent Accruals	Principal Investigator/ Study Manager/ Regulatory Coordinator	Sponsor	Comments
1		2004-0957	PH II Single Agent Alimta in Poor Performance Status NSCLC	09.01.05	MDACC 16/70	2-Jan-06 3-Feb-06 1-Mar-06 5-April-06 3-Jul-06	Ralph Zinner, MD/ Justina Price,RN/ Mellanie Price	Eli Lilly and Company	

Priority	VI. Recurrent or Metastatic NSCLC </= 2 Prior Chemotherapy Regimens	Number	Title	Activated	Accrual	Recent Accruals	Principal Investigator/ Study Manager/ Regulatory Coordinator	Sponsor	Comments
1		2004-0937	PH I/II "A combined phase 1 and 2 study investigating the combination of RAD001 and erlotinib in patients with advanced NSCLC previously treated only with chemotherapy"	06.02.05	MDACC 16/20 Nat'l x/95	1-Oct-05 3-Nov-05 1-Jan-06 2-Feb-06	Vali Papadimitrakopoulou, MD/Mary Rollins, RN/Brenda	Novartis	Held for Amendment
2		2005-0408	PH II Open label, non-randomized, phase 2 Study investigating the effect of RAD001 monotherapy in patients with advanced NSCLC previously treated with either chemotherapy only or with chemotherapy and EGFR inhibitor(s)	08.01.05	MDACC 12/12 Nat'l /100	3-Oct-05 1-Dec-05 5-Jan-06 2-Feb-06 1-Jun-06	Vali Papadimitrakopoulou, MD/ Justina Price, RN/ Alisha Thierry	Novartis	CNPE 6.19.06
3		2004-0137	PH I A Phase I dose-Escalation Study of Intravenous MST- 997 Formulated in Polysorbate 80 Dilute Administered Weekly in Subjects with Advanced Malignant Solid Tumors	11.09.04	MDACC 13/36 National x/60	2-May-05 1-July-05 1-Aug-05 1-Feb-06	David Stewart, MD/ Rainell Schaerer, RN/ Brenda Coldman	Wyeth Pharmaceuticals	
4		2004-0367	PH I Phase I Trial of Motexafin Gadolinium (MGd) in Combination with Docetaxel and Cisplatin for Treatment of Non-Small Lung Cancer (NSCLC)	11.11.04	MDACC 22/36	2-Jan-06 2-Feb-06 1-Mar-06 2-Aug-06	David Stewart, MD/ Rainell Schaerer, RN/ Brenda Coldman	Pharmacyclics, Inc.	
5		2005-0796	PH II Randomized, Double-Blind, Phase II study of Erlotinib with or without SU011248 in the treatment of Metastatic Non-Small Cell Lung Cancer	4.17.06	MDACC 6/12 National x/136		G. Blumenschein, MD/ Teresa Eddings, RN/ Brenda Coldman	Pfizer Inc.	
6		2005-0873	PH II A multicenter, open label, single-arm, two-stage Phase II study of the efficacy and safety of AVE0005 (VEGF trap) administered intravenously every 2 weeks in subjects with platinum, taxane, and erlotinib-resistant advanced non-small cell lung adenocarcinoma	7.03.06	MDACC 3/10 National x/84	2-Jul-06 1-Aug-06	Roy Herbst, MD, PhD/ Cindy Welch, RN/ Brenda Coldman	Sanofi Aventis	
7		2006-0236	PH II A Phase II Trial of Bevacizumab in Combination with First or Second Line Therapy in Subjects with Treated Brain Metastases Due to Non-Squamous Non-Small Cell Lung Cancer	7.13.06	MDACC 1/10 National x/110	1-Jul-06	Yun Oh, MD/ Rainell Schaerer, RN/ James Luca	Genentech Inc.	

Current Thoracic Center Research MDACC PROTOCOL PRIORITY LIST

Priority	VII. Recurrent or Metastatic NSCLC – With at least one prior Chemotherapy Regimen & no limit to the number of prior chemotherapy regimens received)	Number	Title	Activated	Accrual	Recent Accruals	Principal Investigator/ Study Manager/ Regulatory Coordinator	Sponsor	Comments
1.		ID00-123 PH I	(Phase I Study of IV DOTAP: Chol-Fus 1 Liposome Complex in Patients with Advanced NSCLC previously treated with chemo.	03.11.03	MDACC 9/30	1-Sept-05 1-Aug-04 1-Dec-04 1-Jan-05	Charles Lu, MD and Jack Roth, MD/ Rhodette Francisco, RN/ Jan Jenkins	MDACC	Hold 2.16.05

Priority	VIII Advanced Solid Tumors	Number	Title	Activated	Accrual	Recent Accruals	Principal Investigator/ Study Manager/ Regulatory Coordinator	Sponsor	Comments
1		2005-0320 PH I	A Phase I Study of S-CKD602 in Patients With Advanced Small Cell Lung Cancer and Other Advanced Solid Tumors	09.16.05	MDACC 5/44 National 4/44	1-Mar-06 2-Apr-06 1-Jun-06 1-Jul-06	Glisson, Bonnie, MD/ Ashley White, RN/ Brenda Coldman	Alza Corp.	If another site participates MDACC will be less than 44 patients

Priority	IX. Bronchioalveolar	Number	Title	Activated	Accrual	Recent Accruals	Principal Investigator/ Study Manager/ Regulatory Coordinator	Sponsor	Comments

Priority	X. Small Cell Lung Cancer – No Prior Chemotherapy	Number	Number/ Title	Activated	Accrual	Recent Accruals	Principal Investigator/ Study Manager/ Regulatory Coordinator	Sponsor	Comments
1	A. Limited Disease	RTOG 0239 PH II	A Phase II Study of Accelerated High Dose Thoracic Irradiation with Concurrent Chemotherapy for Patients with Limited Small Cell Cancer	10.30.03	MDACC 12/30 National 71/71	1-Sept-04 1-Dec-04 1-Jun-05 1-Aug-05	Ritsuko Komaki, MD/ Rainell Schaerer,RN	Radiation Therapy Oncology	CNPE 5.26.06
1	B. Extensive Disease	ID00-433	Pilot Trial of Weekly Etoposide/Cisplatin/Irinotecan/ G-CSF for Patients With Small Cell Lung Cancer	04.03.01	51/62	2-Dec-05 1-Jan-06 1-Jun-06 1-Jul-06	Bonnie Glisson, MD/ Beverly Peeples, RN/ Alisha Thierry	Pharmacia Inc.	
2	B. Extensive Disease	2006-0297 PH III	Protocol H3E-MC-JMHO A Randomized Phase 3 Trial of ALIMTA® (Pemetrexed) and Carboplatin versus Etoposide and Carboplatin in Extensive-Stage Small Cell Lung Cancer		MDACC x/30 Nat'l x/1820		Frank Fossella, MD/ TBA, RN/ Brenda Coldman	Eli Lilly and Company	
3	B. Extensive Disease	2006-0793 PH Ib	A phase Ib study investigating the combination of RAD001 with cisplatin and etoposide in patients with extensive-stage small-cell lung cancer not previously treated with chemotherapy		MDACC x/6 Nat'l x/60		Vali Papadimitrakopoulou, MD/ TBA, RN/ James Luca	Novartis	

Current Thoracic Center Research MDACC PROTOCOL PRIORITY LIST

Priority	XI. Small Cell Lung Cancer – Without Prior Chemotherapy	Number	Phase	Title	Activated	Accrual	Recent Accruals	Principal Investigator/ Study Manager/ Regulatory Coordinator	Sponsor	Comments
1		SWOGS0435	PH II	A Phase II Trial of BAY 43-9006 (NSC-724772)) In Patients With Platinum-Treated Extensive Stage Small Cell Lung Cancer	1.26.06	MDACC 3/15 Natl x/80	3-Mar-06	Bonnie Glisson, MD/ Beverly Peeples RN/ Faye D. Martin	SWOG	
2		2005-0066	PH II	A Phase 2 Trial of Cloretazine (VNP40101M) for Patients with Relapsed or Refractory Small Cell Lung Cancer	09.02.05	MDACC 4/20 National 33/87	1-Feb-06 1-Mar-06 2-Jun-06	G. Blumenschein, MD/ Ashley White RN/ James Luca	Vion Pharmaceuticals, Inc.	
3		ID01-032	PH I	A Phase I, Open-Label Dose Escalation Study of Weekly Dosing With BB-10901, followed by a Phase II Efficacy Expansion	05.22.01	MDACC 33/59	1-Sept-04 3-Dec-04 1-May-05 1-Nov-05	Frank Fossella, MD/ Hannah Brewer, RN/ Brenda Coldman	Immunogen	

Priority	XII. Small Cell Lung Cancer – With Two Prior Chemotherapy	Number	Phase	Title	Activated	Accrual	Recent Accruals	Principal Investigator/ Study Manager/ Regulatory Coordinator	Sponsor	Comments
1		2005-0320	PH I	A Phase 1 Study of S-CKD602 in Patients With Advanced Small Cell Lung Cancer and Other Advanced Solid Tumors	09.16.05	MDACC 5/44 National 4/44	1- Mar-05 2-April-06 1-Jun-06 1-Jul-06	Glisson, Bonnie, MD/ Ashley White, RN/ Brenda Coldman	Alza Corp.	If another site participates MDACC will be less than 44 patients
2		2004-0557	PH I	A Phase I, Open Label, Dose Escalation Study of Daily Dosing with BB-10901	09.07.05	MDACC 4/12 National x/28	1-Oct-05 1-Nov-05 1-Dec-05 1-Jul-06	Frank Fossella, MD/ Hannah Brewer, RN/ Brenda Coldman	Immunogen	

Priority	XIII. Malignant Mesothelioma	Number	Phase	Title	Activated	Accrual	Recent Accruals	Principal Investigator/ Study Manager/ Regulatory Coordinator	Sponsor	Comments
		2005-0288	PH I		08.08.06	MDACC x/42		Anne Tsao, MD/ Cindy Welch, RN / Mellanie Price	MDACC/ Novartis Pharma	
1	A. Operable Disease									

Priority	XIV. Chemoprevention	Number	Phase	Title	Activated	Accrual	Recent Accruals	Principal Investigator/ Study Manager/ Regulatory Coordinator	Sponsor	Comments
1		ID00-230		A Randomized, Double-Blind Study of theBiological Effects and Tolerability of Celecoxib as a Chemopreventive Agent in Current and Former Smokers	11.12.01	MDACC 113/250	2-Mar-06 2-April-06 7-May-06 6-Jun-06 2-Aug-06	Jonathan Kurie, MD/ Chenrong Jiang, RN/ Mellanie Price	NIH Grant	

Current Thoracic Center Research MDACC PROTOCOL PRIORITY LIST										
Priority	XV. Unlimited Prior Therapy (Phase I – No Restrictions)	Number	Phase	Title	Activated	Accrual	Recent Accruals	Principal Investigator/ Study Manager/ Regulatory Coordinator	Sponsor	Comments
1		2004-0040	PH I	Phase I Study of Prolonged Low Dose Decitabine (5-AZA-DEOXYCYTIDINE, NSC # 127716) in Patients with Biopsiable Advanced Cancers Refractory to Standard Therapy	09.09.04	MDACC 27/36	2-Mar-06 1-Jun-06 3-Jul-06 2-Aug-06	David Stewart, MD/ Susan Pilat, RN	National Cancer Institute	Hold (For Protocol Amendment)
Priority	XVI. Neurosurgery	Number	Phase	Title	Activated	Accrual	Recent Accruals	Principal Investigator/ Study Manager/ Regulatory Coordinator	Sponsor	Comments
1		ID00-377	PH III	A Phase III Prospective Randomized Trial Comparing Radiosurgery with. Versus without Whole Brain Radiation Therapy for 1-3 Newly Diagnosed Brain Metastases	01.02.01	MDACC 101/152	1-Sept-05 1-Oct-05 1-Dec-05 2-Feb-06	Eric Chang, MD/ Leni Mathews, RN	None	

Appendix - J.

Appendix Subtitle: MDACC Research Informed Consent Process

Revised 9/18/06

Research Informed Consent Process

The informed consent process is to ensure that individuals participating in clinical trials are informed about the study's purpose, the risks and benefits, alternative therapies, and voluntarily agree to participate. It is a process that should provide ample opportunity for the person obtaining informed consent and the participant to exchange information and answer questions. The process will also provide for updates to the informed consent, as the study requires. This policy is to assure study participants receive adequate information in the appropriate manner, timing and setting.

All areas of UTMDACC conducting clinical research are expected to comply with this standard procedure.

MDA Policy and Procedure:

The informed consent process begins when a potential research participant is initially contacted regarding a study by the investigator or his staff. Participants should not be approached about a potential protocol prior to that study being approved by the Institutional Review Board (IRB).

The attending physician shall be responsible for ensuring that the informed consent process is documented by the use of a written consent form approved by the IRB and signed by the participant or participant's legally authorized representative (unless this requirement is specifically waived by the IRB).

Upon activation, each page of the informed consent document is imprinted with the "IRB Approved Consent" stamp. The stamp is signed and dated by the assigned protocol compliance specialists and distributed to the principal investigator. Additional copies must be made and distributed by the department. Consents that are submitted in PDOL will be available on-line following activation.

Only the most recent version of the informed consent document approved by the IRB should be used when addressing new participants. The date stamped on the informed consent document should correspond with the informed consent date in the Protocol Data Management System (PDMS)/Clinical Oncology Research System (CORe) during the registration process, verifying that the correct version of the document has been signed. Consents for protocols that are available on-line through PDOL, will have the most recent revision date typed on the lower right-hand corner of the document.

Informed consent must be obtained prior to the initiation of any protocol-specific screening procedures that are not considered standard of care.

The informed consent document should be presented in a language that is understandable to the participant. For other languages, please refer to the Policy on Consenting

Non-English Speaking Participants.

Informed consent will be obtained under circumstances that provide the participant or the participant's legally authorized representative sufficient opportunity to ask questions and consider whether or not to participate. It should be clear that the subject has a right to withdraw from the study at any time.

If a participant chooses to withdraw consent for a study, the primary investigator must document that the participant is "withdrawing consent to participate in the study" in the chart.

Authority to obtain informed consent:

- The principal investigator, regardless of how his or her authority is delegated, remains ultimately responsible for the actions of those to whom he may delegate authority in obtaining the informed consent.

- The principal investigator may delegate authority to those individuals **who are licensed as physicians in the state of Texas** to obtain the legally effective informed consent of the participant for any study that involves drug therapy, surgery, or invasive procedures.

- Following a discussion between the physician and the participant, a research nurse/coordinator should review the protocol and informed consent document to ensure that the participant understands the protocol procedures and/or treatments. If the participant does not understand the research nurse/coordinator must notify the physician of the participant's concerns or lack of knowledge.

- Once all participant's questions and concerns are addressed the physician or the research nurse/coordinator may obtain the actual signature on the informed consent document. It is important that the person obtaining the informed consent must have an adequate understanding of the scientific content of the protocol.

- The principal investigator may delegate authority to obtain informed consent to a **individual who is not a physician** in limited circumstances and only when involving protocols with no more than minimal risk and do not involve drug therapy, surgery or invasive procedures. An individual obtaining informed consent **who is not a physician** should be described in the body of the protocol as the person authorized to obtain informed consent.

- When informed consent is obtained, the person obtaining the consent from the participant or the participant's legally authorized representative must sign his or her name on the informed consent document where the investigator signs. By signing the document, the person obtaining consent certifies that the clinical research study has been fully discussed with the participant and that all requirements for obtaining informed consent have been followed.

Completing the informed consent document:

- Verify that the participant is being presented with the proper version of the informed consent document.

- The participant or their authorized representative must sign and date one original informed consent document.
- The principal investigator or treating physician must sign and date the same original informed consent document.
- An original signed informed consent document should be placed in the participant's medical record, a copy should be given to the participant and a copy placed in the investigator's protocol file.

Documenting the Informed Consent Process:

The informed consent process must be documented in the progress notes of the medical record by the investigator or collaborator explaining the protocol. To verify that the consent process was completed correctly, the documentation should include:

- UTMDACC protocol number or name of the study,
- a brief statement explaining alternative treatment option discussed,
- a statement that the informed consent document was reviewed with the participant, including the risks and benefits of the study,
- a statement describing the participant's decision. Examples include:

  "Participant would like to be treated on study, informed consent signed and copy of original given to participant."

  "Participant wishes to take informed consent home to review with family, will follow up tomorrow with research nurse for additional questions and desired treatment plan"

  "Participant does not wish to participate in study at this time. Will treat off protocol with..."

- If the participant returns on a later date to sign the consent form a note should be placed in the chart on that day describing the interaction.
- A statement describing when the treatment is scheduled to begin.

Re-consenting:

- The informed consent document is considered valid for 30 days from the participant's signature date to begin treatment. If treatment has not begun within 30 days following the signature date listed on the informed consent document then the participant must be reassessed for protocol eligibility and a new consent document completed.
- If there is any material change in the participant's status after informed consent is obtained but before the treatment begins, the participant must be reassessed and the informed

consent process should be repeated.

- Participants must be re-consented if there are changes in the informed consent related to safety and/or treatment.

a. If the informed consent document is revised due to a serious safety issue, all participants who are at risk for developing the toxicity should be notified in a timely manner.

b. Participants who are off study and considered to be at risk for developing the toxicity should be informed of any new serious safety issues by an IRB approved letter.

c. The participant's medical record must reflect the oral and/or written re-consent process including protocol number or title of study, the date the participant was notified of the change, and if applicable the date the new informed consent document was signed.

d. It is the responsibility of the principal investigator and the research staff to ensure that participants are informed of any changes that may influence their continued participation in a protocol.

Surrogate Decision Makers:

If an adult participant is incompetent or otherwise mentally or physically incapable of communication and **has completed an Advance Directive**, then the designated agent and the attending physician may make health care decisions for the participant.

If the participant is incompetent or otherwise mentally or physically incapable of communication, **has not completed an Advance Directive**, and does not have a legal guardian, then the attending physician and one person, if available, from one of the following categories, in the following priority, may make health care decisions for the participant:

- the spouse;
- the reasonably available adult children;
- the parents; or
- the participant's nearest living relative.

When a surrogate decision maker is utilized, a witness to the consent process must sign and date the informed consent document. Preferably, the witness should be someone who has no interest in the protocol. The participant's spouse, family member or friend would be the ideal witness. In the event that the participant's surrogate decision maker is alone during the informed consent process, the clinic or research nurse/coordinator can sign as witness. This information should be clearly documented in the medical record.

Appendix - K.

Appendix Subtitle: MDACC Policy Protocol Deviation and Protocol Violations

University of Texas M. D. Anderson Cancer Center Institutional Review Board Policy on Reporting Protocol Deviations and Protocol Violations

PURPOSE	It is the policy of The University of Texas M.D. Anderson Cancer Center Institutional Review Board (UTMDACC IRB) to comply with the regulations governing human subjects research to ensure that variations from approved research protocols are appropriately documented and communicated to the UTMDACC IRB.
POLICY STATEMENT	The purpose of this policy is to protect human subjects' safety by mandating that protocol violations and deviations be submitted to the IRB for review within a specific timeframe.
SCOPE	This policy applies to all human subjects research at (or conducted with) UTMDACC. Industry sponsored studies may have additional requirements beyond what is stipulated in this policy.
DEFINITIONS	**The Institutional Review Board (IRB)** – means any board, committee, or other group formally designated by an institution to review, to approve the initiation of, and to conduct periodic review of, biomedical research involving human subjects. The primary purpose of such review is to assure the protection of the rights and welfare of the human subjects
	Human subject - a living individual about whom an investigator conducting research obtains (1) data through intervention or interaction with the individual, or (2) identifiable protected health information
	Principal Investigator (PI)/Study Chair - the individual responsible for the conduct of the research study
	Research Team - co-investigators, collaborators, trainees, staff, and classified employees directly involved with the research
	Research Protocol/Study – a systematic investigation, including research development, testing and evaluation, designed to develop or contribute to generalizable knowledge
	Protocol Deviation- Noncompliance with the protocol that does not have a significant effect on the subject's rights, safety, welfare, and/or the integrity of the data. Deviations may be caused by the action of the subject, the investigator, the research staff, or natural events. **Examples:** <u>Informed Consent</u> *Consent form used was not current IRB-approved version at the time of subject registration (with administrative changes only).-

	*Consent form used did contain new information that would affect subject safety or subject participation on trial, but the subject was re-consented in a timely fashion (e.g., at their next scheduled appointment) or a plan to notify the subject of new safety information is submitted and approved by the IRB. Treatment and Procedures * Errors in dosing not affecting subject safety ▪Incorrect timing or scheduling of doses (error less than +/- 10%) ▪Incorrect timing or scheduling of doses that does not significantly affect subject safety ▪Additional agent/treatment/procedure used which is excluded by protocol that does not affect subject safety ▪Scheduled appointment is +/- 2 days from that defined in the protocol ▪Subject missed appointment due to factors not under control of the research team members. Adverse Events *Missing Expected Events not reported as required by protocol or institutional policy. Evaluations *Laboratory test performed off schedule (if not required for eligibility, treatment, dose modification, dose-limiting toxicity (DLT) determination, or to assess subject safety.)
	Protocol Violation- Changes to protocol procedures without prior approval of the IRB/Sponsor. These changes may have a significant effect on the subject's rights, safety, welfare, and/or the integrity of the data, and may cause an unanticipated problem to the subject or others. Violations may also significantly alter the clinical effectiveness of the treatment or the evaluation of its toxicity. **Examples:** Informed Consent * Consent form missing * Consent form not signed and dated by the subject * Original consent form signed after subject started on treatment * Consent form used was not current IRB-approved version at the time of subject registration and contained new information that would affect subject safety or subject participation on trial. (If subject was re-consented on correct IC/A in a timely fashion (e.g., at their next scheduled appointment), or a plan to notify the subject of new safety information is submitted and approved by the IRB, then it is considered a protocol deviation. * Consent form does not include updates or information required by IRB * No documentation of informed consent process in progress notes * Consent not obtained for optional procedures Eligibility * Review of documentation available at the time of the audit confirms subject did not meet all eligibility criteria as specified by the protocol * Unable to locate pre-study evaluations to confirm eligibility. Treatment and Procedures * Incorrect agent/treatment/procedure used * Additional agent/treatment/procedure used which is excluded by protocol

	* Errors in dosing ▪Incorrect timing or scheduling of doses (error greater than +/- 10%) ▪Incorrect scheduling of doses that affect subject safety * Dose modifications not followed per protocol or unjustified * Assessments for determining treatment modifications not completed as per protocol * Continuation of treatment that is potentially detrimental to subject <u>Disease Outcome and Response</u> * Tumor measurements/evaluation of status or disease not performed or documented adequately to assess baseline or interpret response * Documented response status cannot be verified <u>Adverse Events</u> * Serious or Unexpected Adverse Events not reported as required by protocol <u>Evaluations</u> * Diagnostic testing (e.g., labs or evaluations not completed and documented) that are required to determine eligibility, treatment, dose modification, dose-limiting toxicity (DLT) determination, or to assess subject safety * Other (i.e., data inconsistencies in case report forms)

INSTITUTIONAL REVIEW BOARD PROCEDURES

irb review guidelines	1.	The PI is responsible for ensuring that clear documentation is available in the medical record to describe all **protocol deviations** and corrective action taken. A log of all deviations should be maintained by the PI and kept in the PI's regulatory files. The deviation log must be submitted to the IRB, at least, quarterly for review. The IRB will issue an official notification letter to the PI acknowledging receipt of the deviation log. This notification letter should be kept in the PI's regulatory binder along with a copy of the deviation log. PI's should note that repetitive deviations may warrant a change to the protocol or the informed consent authorization (IC/A).
	2.	The PI is responsible for ensuring that all **protocol violations** are promptly reported to the IRB by completing the Protocol Violation Notification Form. When reporting violations to the IRB, the PI should include the corrective action that was taken to ensure the violation does not occur in the future. The IRB will issue an official notification letter to the PI acknowledging receipt of the Protocol Violation Notification Form. This notification letter should be kept in the PI's regulatory binder along with the completed Protocol Violation Notification Form.
POSSIBLE actions the irb may TAKE		Upon review of the Protocol Deviation Log or the Protocol Violation Notification Form, the IRB can require actions that may include but are not limited to:
		▪Close the protocol to new patient entry ▪Revision of the protocol or the IC/A to address the deviation or the violation

		•Notification of research subjects of the violation if it may have an impact on their safety or participation in the research •Assignment of the oversight of the protocol to an independent monitoring board (e.g., Data Safety and Monitoring Board or outside entity, if appropriate). •Accept the investigator's corrective action plan
Penalties for non-compliance		Failure to comply with this policy may result in temporary or permanent suspension of the research and/or the investigator's research privileges.
		In accordance with 45 CFR 46.113, any suspensions or terminations of approval will be reported promptly to the investigator, to the appropriate institutional officials, and possibly the federal department or agency head responsible for oversight or funding of the research.

REFERENCE:

21 CFR 56.108
21 CFR 56.109
21 CFR 56.111
ICH GCP 4.5

STRATEGIC VISION: From the following, please select the appropriate goal(s) applicable to this policy and identified in the 2005-2010 Strategic Vision:

Goal 2: Enhance the quality of existing research programs and develop priority programs for the future.